PRODUCED WATER IN THE UINTA BASIN, UTAH: EVALUATION OF RESERVOIRS, WATER STORAGE AQUIFERS, AND MANAGEMENT OPTIONS

Thomas C. Chidsey, Jr., Compiler and Editor

BULLETIN 138
UTAH GEOLOGICAL SURVEY
a division of
UTAH DEPARTMENT OF NATURAL RESOURCES
2017

Blank pages are intentional for printing purposes.

PRODUCED WATER IN THE UINTA BASIN, UTAH: EVALUATION OF RESERVOIRS, WATER STORAGE AQUIFERS, AND MANAGEMENT OPTIONS

Thomas C. Chidsey, Jr., Compiler and Editor

Cover photo: *Oil separation tanks and produced water evaporation pond, Monument Butte field, Uinta Basin, Utah. Photo by Ammon McDonald, Utah Division of Oil, Gas and Mining.*

ISBN: 978-1-55791-939-7

BULLETIN 138
UTAH GEOLOGICAL SURVEY
a division of
UTAH DEPARTMENT OF NATURAL RESOURCES
2017

STATE OF UTAH
Gary R. Herbert, Governor

DEPARTMENT OF NATURAL RESOURCES
Michael Styler, Executive Director

UTAH GEOLOGICAL SURVEY
Richard G. Allis, Director

PUBLICATIONS
contact
Natural Resources Map & Bookstore
1594 W. North Temple
Salt Lake City, UT 84116
telephone: 801-537-3320
toll-free: 1-888-UTAH MAP
website: mapstore.utah.gov
email: geostore@utah.gov

UTAH GEOLOGICAL SURVEY
contact
1594 W. North Temple, Suite 3110
Salt Lake City, UT 84116
telephone: 801-537-3300
website: geology.utah.gov

Although this product represents the work of professional scientists, the Utah Department of Natural Resources, Utah Geological Survey, makes no warranty, expressed or implied, regarding its suitability for a particular use. The Utah Department of Natural Resources, Utah Geological Survey, shall not be liable under any circumstances for any direct, indirect, special, incidental, or consequential damages with respect to claims by users of this product.

The Utah Geological Survey does not endorse any products or manufacturers. Reference to any specific commercial product, process, service, or company by trade name, trademark, or otherwise, does not constitute endorsement or recommendation by the Utah Geological Survey.

CONTENTS

LIST OF ACRONYMS AND ABBREVIATIONS ix

ABSTRACT xii

CHAPTER 1 Introduction 1
Thomas C. Chidsey, Jr.

CHAPTER 2 Stratigraphy and Depositional History 9
Thomas C. Chidsey, Jr., Taylor Boden, and Stephanie M. Carney

CHAPTER 3 Structural Setting 47
Thomas C. Chidsey, Jr., Stephanie M. Carney, and Taylor Boden

CHAPTER 4 Uinta Basin Reservoirs/Aquifers: Triassic-Jurassic Glen Canyon Group Through the Cretaceous Cedar Mountain and Dakota Formations 59
Craig D. Morgan and Stefan M. Kirby

CHAPTER 5 Uinta Basin Reservoirs/Aquifers: Upper Cretaceous Mancos Shale 127
Robert Ressetar

CHAPTER 6 Uinta Basin Reservoirs/Aquifers: Upper Cretaceous Mesaverde Group and Upper Paleocene to Lower Eocene Wasatch/Colton Formation 141
Peter J Nielsen and Rebekah W. Stimpson

CHAPTER 7 Uinta Basin Reservoirs/Aquifers: Eocene Green River Formation 189
Stephanie M. Carney and Michael D. Vanden Berg

CHAPTER 8 Summary of the Compiled Fluid Geochemistry Database for the Uinta Basin 217
Stefan M. Kirby

CHAPTER 9 Handling and Management of Water Produced From Oil and Gas Reservoirs in the Uinta Basin 231
David E. Tabet

CHAPTER 10 Conclusions and Recommendations 261
Thomas C. Chidsey, Jr., David E. Tabet, Michael D. Vanden Berg, Craig D. Morgan, Stefan M. Kirby, Peter J Nielsen, Stephanie M. Carney, Robert Ressetar, Rebekah W. Stimpson, and Taylor Boden

ACKNOWLEDGMENTS 266

REFERENCES 266

APPENDICES

APPENDIX A: Porosity and Permeability Measurements From Cores From the Lower Blue Gate Member of the Mancos Shale ..... attached

APPENDIX B: List of Wells Used in Calculations and Studies of the Mesaverde Group and Wasatch Formation ..... attached

APPENDIX C: Cations, Anions, Total Dissolved Solids, and Salinity Values From the Wasatch Formation, Mesaverde Group, and Mancos Shale ..... attached

APPENDIX D: Water Chemistry for the Wasatch/Colton Formation and the Mesaverde Group ..... attached

APPENDIX E: Zone Information Wasatch/Colton Formation and the Mesaverde Group ..... attached

APPENDIX F: Compiled Major Ion Chemistry for Produced Water and Groundwater in the Uinta Basin ..... attached

APPENDIX G: Summary Statistics for Major Ion Chemistry for Select Chemistry Samples ..... attached

PLATES

Plate 1. Compiled Geologic Map of the Uinta Basin, Utah

Plate 2. West-to-East Cross Section of the Wasatch/Colton Formation and the Mesaverde Group

Plate 3. North-to-South Cross Section of the Wasatch/Colton Formation and the Mesaverde Group

LIST OF ACRONYMS AND ABBREVIATIONS

ACTS – Anadarko Completion Technology System
APDs – Applications for Permit to Drill
API – American Petroleum Institute
BBC – Bill Barrett Corporation
bbls – barrels
BCF – billion cubic feet
BCFG – billion cubic feet of gas
BHT – bottom-hole temperature
BLM – Bureau of Land Management
BMSW – base of moderately saline water
BO – barrels of oil
BOPD – barrels of oil per day
BPD – barrels per day
BVW – bulk volume of water
BW – barrels of water
Ca/Na ratio – calcium/sodium ratio
CBM – coal-bed methane
CMKD – Cretaceous Cedar Mountain and Dakota Formations
CO_2 – carbon dioxide
CUP – conditional use permit
DEM – digital elevation model
DFZ – Duchesne fault and fracture zone
DOGM – Utah Division of Oil, Gas and Mining
DT – sonic log, Delta T
DWSP – drinking water source protection
ECS – Environmentally Clean Systems
EIS – Environmental Impact Statement
EOR – enhanced oil recovery
EPA – U.S. Environmental Protection Agency
Fm. – Formation
GAPI – gamma-ray measurements in American Petroleum Institute units
GCG/N – Glen Canyon Group/Nugget Sandstone
GIS – Geographic Information System
GMBU – Greater Monument Butte Unit
Gp. – Group
GWQPP – Ground Water Quality Protection Program
GOR – gas-oil ratio
GOS – Gas-Oil-Separation
GR – gamma-ray log
GRF – Green River Formation

HDPE – high-density polyethylene
IDW – Inverse Distance Weighting
IFP – initial flowing potential
IGT – Induced Gas-Flotation Tank
I-70 – Interstate 70
K-T boundary – Cretaceous-Tertiary boundary
LGS – liquids-gathering system
Ls. – Limestone
LSN – large-saline-nodule [facies]
Ma – million years ago
MB – thousand barrels
Mbr. – Member
mD – millidarcies
MCF – thousand cubic feet
MCFG – thousand cubic feet of gas
MCFGPD – thousand cubic feet of gas per day
mg/L – milligrams/liter
MMB – million barrels
MMBO – million barrels of oil
MMBW – million barrels of water
MMCF – million cubic feet
MMCFG – million cubic feet of gas
nD – nanodarcies
NGR – net-to-gross sand ratios
NOx – nitrogen oxides
NWIS – National Water Information System
OWR – oil-water ratio
PHIA – average porosity
PHIE – effective porosity
PHIS – sonic porosity
ppm – parts per million
RES – resistivity log
RESD – deep resistivity
R_F – retardation factor
RMCCS – Rocky Mountain Carbon Capture and Storage
R_{mf} – resistivity of mud filtrate
R_{mfft} – resistivity of mud filtrate at formation temperature
ROD – Record of Decision
ROSS – removal of oil and suspended solids
RPSEA – Research Partnership to Secure Energy for America
R_w – water resistivity
R_{we} – equivalent formation water resistivity

Sh. – Shale
SLBL&M – Salt Lake Base Line & Meridian
SP – spontaneous potential log
SPHIS – sonic porosity – sandstone
SPHIS_GAS – sonic porosity curve adjusted for gas
Ss. – Sandstone
ss. – sandstone
SSC – small-saline-crystal [facies]
SSP – static spontaneous potential
TCFG – trillion cubic feet of gas
TDS – total dissolved solids
TMDL – total maximum daily loads
TWT – two-way time
UBMBF – Uinta Basin-Mountain boundary fault
UBL&M – Uintah Base Line & Meridian
UDEQ – Utah Department of Environmental Quality
UDWQ – Utah Division of Water Quality
UGS – Utah Geological Survey
USGS – U.S. Geological Survey
UU – University of Utah
VOC – volatile organic compounds
V_{sh} – V-shale

ABSTRACT

Oil and gas fields in the Uinta Basin of eastern Utah produced nearly 30 million barrels of oil and 324 billion cubic feet of gas in 2015 from the Tertiary Wasatch and Green River Formations and several formations in the Upper Cretaceous Mesaverde Group. Nearly 103 million barrels of water was also produced with these hydrocarbons. The vast majority of the water production was from wells producing in tight-sand gas reservoirs. Over the past 10 years, even after the fall in gas prices in 2008, extensive drilling for lenticular, tight gas sands in the Wasatch and Mesaverde occurred in the eastern part of the basin, whereas large drilling programs, as part of expanding waterflood projects for oil in the Green River, continued in the south-central basin; over 1300 wells were permitted in 2014 (before oil prices collapsed). The environmentally sound disposal of produced water affects the economics of the hydrocarbon resource development in the basin and has become a topic of much public debate because produced water is the largest-volume waste stream associated with hydrocarbon production.

Managing produced water can be a significant cost fraction of the value of the hydrocarbons extracted. Thus, there is an economic incentive to minimize this waste stream, and/or reduce freshwater usage by treating and reusing produced water in hydrocarbon production applications. Balancing the water-use needs and produced-water disposal requirements associated with oil and gas production creates significant material handling challenges to both industry and regulators. These challenges are complicated by an operating environment where many individual producers of varying sizes exist within a field, each with differing water needs and production, and a production timescale of decades for the basin as wells play out and new ones are completed. Specific Uinta Basin water issues include water use/reuse for well drilling and completion (hydraulic fracturing), appropriate sites for disposal/reuse of water, development of systems to manage the produced-water streams, and differing challenges for gas versus oil producers, especially those who require water for use in waterflood programs in oil fields.

Current produced-water disposal practices in the Uinta Basin consist of (1) injection in deep wells, most below the base of a moderately saline aquifer in the Green River Formation, (2) storage and evaporation in lined disposal ponds, and (3) supplying water for flooding in enhanced-oil recovery programs. Uses for the produced water from Uinta Basin reservoirs include drilling mud formulation and hydraulic fracturing fluid for well completion. Potential uses include waterflooding for secondary recovery and future possible shale gas, oil shale, and tar sand production.

Our study consisted of three major components: (1) compilation and analysis of past and new information on the thickness, structure, depth, lithology, porosity, permeability, water quality, and temperature of all major oil and gas reservoir units and aquifers that store produced water or have the potential for water storage in the basin from the Tertiary down through the Upper Triassic–Lower Jurassic Glen Canyon Group, (2) statistical analysis of water production quantity and quality, and (3) evaluation of the existing infrastructure for produced-water management/reuse and recommendations for best management practices.

The “Birds Nest” aquifer in the upper Green River Formation is the most widespread and economically viable disposal unit in terms of depth, proximity to producing wells, and water quality. Statistical analysis of water production quantity and quality identified and forecasted volume trends. For example, the greatest need for water disposal results from drilling gas wells in the eastern part of the basin whereas water is needed for enhanced-oil recovery projects in the south-central basin. These needs will continue, based on predicted drilling trends once oil and gas prices recover from the 2015 collapse and as producing wells mature leading to increased water production. Thus, we suggest that excess produced water from gas wells, with appropriate water quality, could be transported to oil fields undergoing enhanced oil recovery. Produced water could also be used for the water component in hydraulic fracturing, required to produce from tight-gas sand reservoirs and from the tight-oil Uteland Butte limestone member of the Green River Formation.

CHAPTER 1:
INTRODUCTION

by

Thomas C. Chidsey, Jr.

CONTENTS

OVERVIEW 3
LOCATION AND GENERAL GEOLOGIC SETTING 4
BASIC PETROLEUM GEOLOGY AND OIL AND GAS DEVELOPMENT HISTORY 4
PURPOSE AND SCOPE 6

FIGURES

Figure 1.1. Oil and gas fields in the Uinta Basin of eastern Utah 3
Figure 1.2. Production in the Uinta Basin in comparison to the rest of the state in 2015 4
Figure 1.3. Eocene lake basins of the Rocky Mountain west 5
Figure 1.4. Uinta Basin cross section from southwest flank to the north-central part of the basin showing producing reservoirs, general facies, and widely recognized stratigraphic markers 6
Figure 1.5. Stratigraphic column from the surface down through Upper Triassic–Lower Jurassic Nugget section in the Uinta Basin showing major producing reservoirs and aquifers evaluated 7

CHAPTER 1:
INTRODUCTION

OVERVIEW

Utah ranked 11th in the United States in oil production and 10th in gas production in 2014 (Energy Information Administration, 2015). Oil and gas fields in the Uinta Basin of eastern Utah (figure 1.1) produced nearly 30 million barrels of oil (MMBO) and 324 billion cubic feet of gas (BCFG) in 2015 from the Tertiary Wasatch and Green River Formations and several formations in the Upper Cretaceous Mesaverde Group (Utah Division of Oil, Gas and Mining, 2016). Nearly 103 million barrels of water (MMBW) were also produced with these hydrocarbons. This production represents 80%, 76%, and 55% of the oil, gas, and water produced, respectively, in Utah (figure 1.2). The vast majority of the water production was from wells producing in tight-gas sand reservoirs. Over the past 10 years, even after the fall in gas prices in 2008, extensive drilling for lenticular, tight-gas sands in the Wasatch and Mesaverde occurred in the eastern part of the basin. Large drilling programs, as part of expanding waterflood projects (which use produced water from oil wells) for oil in the Green River, continued in the south-central basin in the Monument Butte–Brundage Canyon trend (figure 1.1) until oil prices dramatically fell beginning in 2014. Operators had also begun to target the Uteland Butte limestone member of the Green River in the central basin, successfully using long-reach horizontal wells.

Over 1300 wells were permitted in 2014 in the Uinta Basin (Utah Division of Oil, Gas and Mining, 2015), with 60% in the eastern part of the basin having tight gas-sands as the primary objectives. Many of these permitted wells will still be drilled when prices improve. Even with the collapse of oil prices and continued depressed gas prices, resulting in significantly reduced drilling activity in the basin, existing wells will mature and produce increasing amounts of water. As has been the case throughout the history of the petroleum industry, oil and gas prices will eventually rebound and exploration and development will undoubtedly return to pre-2014 and pre-2008 levels, respectively, in Utah's most prolific hydrocarbon-producing basin. Thus, the question this study sought to answer was: "What should be done with the produced water in the Uinta Basin?"

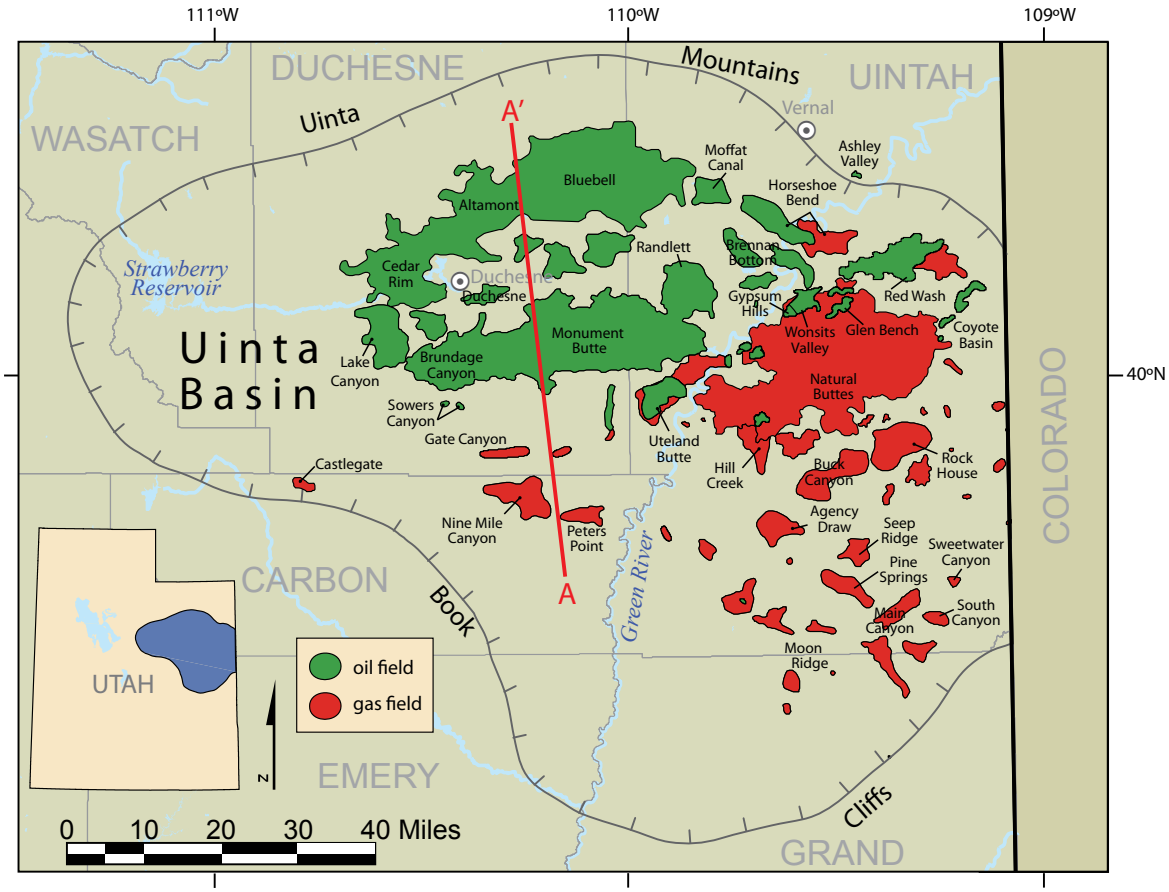

Figure 1.1. *Generalized outline of the Uinta Basin of eastern Utah showing oil and gas fields. Cross section A–A' shown on figure 1.4.*

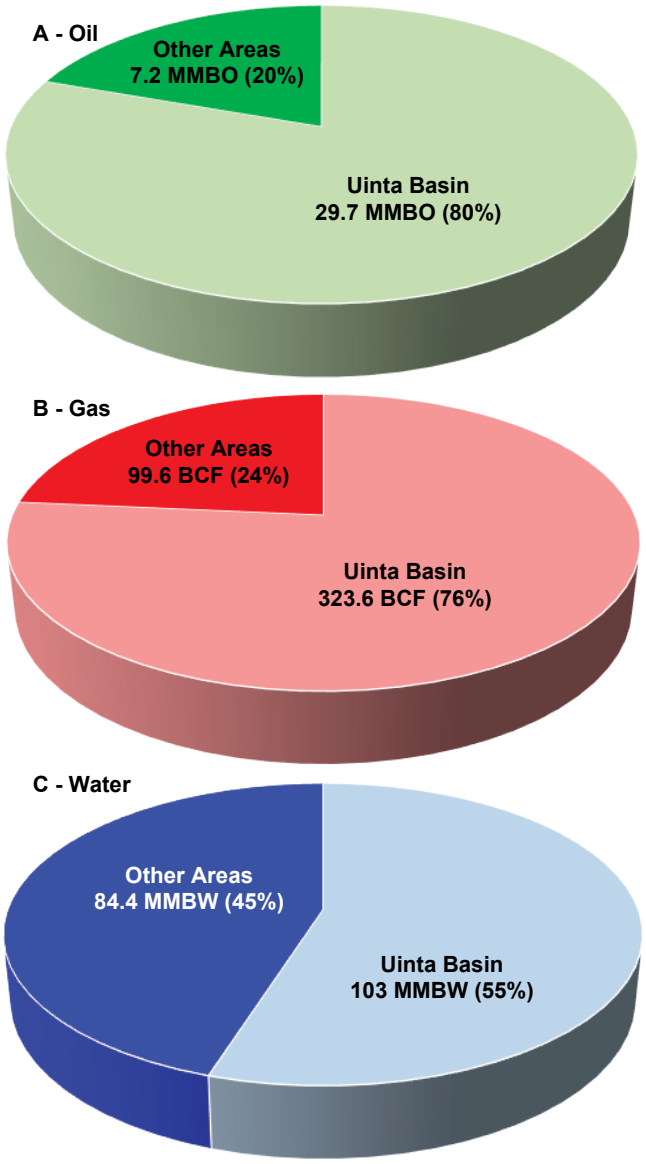

Figure 1.2. *Production in the Uinta Basin in comparison to the rest of the state in 2015 (Utah Division of Oil, Gas and Mining, 2016a).*

LOCATION AND GENERAL GEOLOGIC SETTING

The Uinta Basin is located in the northern Colorado Plateau geologic province. It extends west from the Colorado state line to about Strawberry Reservoir in north-central Utah and from the east-west trending Uinta Mountains south to the Book Cliffs. It is both a structural and topographic basin, dissected and drained by the Green River and its tributaries as part of the Colorado River system. The average elevation of the Uinta Basin is 5000 feet (1500 m) (Hamblin, 2004), and like most areas in eastern Utah it has a semi-arid climate with low humidity, hot and dry summers, and cold winters; the average annual precipitation is 9.2 inches (23.4 cm). Water availability in this semi-arid climate is, of course, a critical issue for agriculture, light industries, culinary use, and oil and gas development.

The Laramide orogeny, between latest Cretaceous and Eocene time, produced numerous basins and basement-cored uplifts in the Rocky Mountain states. The Uinta Basin is a major depositional and structural basin that subsided during the early Cenozoic along the southern flank of the Uinta Mountains. More than 10,000 feet (3000 m) of alluvial and lacustrine deposits filled the basin between the eroding Sevier highlands to the west and the rising Laramide-age Uinta Mountains, Uncompahgre uplift, and San Rafael Swell to the north, east, and south, respectively (Hintze and Kowallis, 2009). The Eocene Lake Uinta formed within the Uinta Basin and Colorado's Piceance Creek Basin (figure 1.3). At times of low water level, the Douglas Creek Arch separating the two basins was exposed, creating two distinct lakes.

The Uinta Basin is asymmetrical to the north, paralleling the east-west trending Uinta Mountains. The north flank dips 10° to 35° into the basin and is bounded by a large north-dipping, basement-involved thrust fault. The southern flank gently dips between 4° and 6° north-northwest from the Book Cliffs. Regional uplift of the Colorado Plateau occurred throughout the Cenozoic primarily due to the Laramide orogeny and isostatic rebound from massive erosion (Hunt, 1956; Lucchitta, 1979; Pederson and others, 2002). The drainage pattern on the plateau was disrupted 5 to 6 million years ago (Ma) by major normal faults along the Basin and Range transition zone, resulting in massive erosion removing several thousand feet of sedimentary rocks and the relatively rapid incision of the Colorado and Green Rivers and their tributaries (Lucchitta, 1989; Potochnik and Faulds, 1998). The result is the spectacular exposure of rocks as old as Cretaceous along the southern flank of the basin, ideal for reservoir/aquifer outcrop analog studies (plate 1).

BASIC PETROLEUM GEOLOGY AND OIL AND GAS DEVELOPMENT HISTORY

The Uinta Basin is the most productive petroleum province in Utah due to an ideal combination of depositional and structural events. During the Cretaceous, compressional forces of the Sevier orogeny produced highlands in western Utah and the Western Interior Seaway covered most of eastern Utah. Extensive coal-forming swamps and marshes developed near the coastline (Emery, Book Cliffs, and Sego coal fields) and fluvial- and wave-dominated deltas migrated eastward across the state as the sea gradually retreated. During the Paleocene and Eocene, Lakes Flagstaff and Uinta formed in the Uinta Basin where alluvial, marginal lacustrine, and open lacustrine sediments accumulated in an intertonguing relationship. Trapping mechanisms (figure 1.4) for hydrocarbons in these deposits include (1) fracture-enhanced stratigraphic pinchouts of lenticular sandstone beds updip along the south flank of the basin or across minor flexures or subtle, plunging anticlines with no four-way closure, (2) a reduction of fluid pressure and associated closing of fractures updip from the basin center, and (3) fractured "tight" shale and carbonate zones sealed by

Figure 1.3. *Eocene lake basins of the Rocky Mountain west. Lake Gosiute occupied the Green River and Washakie Basins in Wyoming, while Lake Uinta filled the Uinta and Piceance Creek Basins in Utah and Colorado. Modified from Vanden Berg (2011).*

unfractured shales or low-permeability marls (unconventional reservoirs). Cretaceous coal and shale and Eocene organic-rich lacustrine shale serve as hydrocarbon source rocks. Reservoirs consist mainly of (1) alluvial to deltaic channel and bar, fluvial-deltaic shoreface to shoreline, and eolian sandstone, (2) carbonate-flat dolomitized ostracod and pellet grainstone and packstone, and (3) coalbeds that produce methane (CBM) in the extreme southwest part of the Uinta Basin. The major producing units are the Eocene Uinta (gas) and Green River Formations (oil), Paleocene/Eocene Colton/Wasatch Formations (oil and gas [tight-gas sands]), Cretaceous Mesaverde Group (gas [tight-gas sands]), Ferron Sandstone Member of the Mancos Shale (CBM), Dakota Formation, Cedar Mountain Formation (gas [tight-gas sands]), and Jurassic Morrison, Entrada, and Wingate Formations (gas) (figure 1.5).

Utah's drilling history has fluctuated greatly due to periodic discoveries, oil and gas price trends, and changing exploration targets—the Uinta Basin is no exception. The first commercial oil discovery in the Uinta Basin was Roosevelt field (now part of Bluebell field, figure 1.1) in 1949; gas and oil were discovered at Ashley Valley field southeast of Vernal in 1925 and 1948, respectively, but the field is technically just outside of the basin. The Humble Oil Ute Tribal No. 1 well (section 21, T. 1 S., R. 1 E., Uinta Base Line & Meridian [UBL&M], Uintah County, American Petroleum Institute [API] No. 43-047-15550) had an initial flowing potential (IFP) of 1633 barrels of oil per day (BOPD) out of the Green River Formation. The opening of Bluebell field was followed by a number of major Green River oil discoveries: Red Wash (1951) (figure 1.1), Pleasant Valley (1952), Walker Hollow (1953), and Wonsits Valley (1962) among others (Hill and Bereskin, 1993). In 1952, gas was discovered in the Mesaverde Group with the completion of the Chapita Wells Unit No. 1 well (section 16, T. 9 S., R. 23 E., Salt Lake Base Line & Meridian [SLB&M], Uintah County, API No. 43-047-10095) for an IFP of 275 thousand cubic feet of gas per day (MCFGPD). In 1955, gas was discovered nearby in the Wasatch Formation with the completion of the Chapita Wells Unit No. 2 well (section 28, T. 9 S., R. 23 E., SLB&M, Uintah County, API No. 43-047-15050) for an IFP of 4618 MCFGPD. Ultimately, these and others gas discoveries in the area were merged to create what is now Utah's largest gas field—Natural Buttes (figure 1.1) with over 3.5 trillion cubic feet of gas (TCFG) produced (Utah Division of Oil, Gas and Mining, 2016c). Since then, significant tight-gas sand discoveries have spread throughout the eastern Uinta Basin. Along the southwest flank of the Uinta Basin, multiple Tertiary and Cretaceous gas reservoirs were discovered on a trend that began with Peters Point field (figure 1.1) in 1953. In the center of the basin, deep, fractured, overpressured Wasatch oil and gas production began with the Shell Oil Miles No. 1-35A4 well (section 35, T. 1 S., R. 4 W., UBL&M, Duchesne County, API No. 43-013-30029) that had an IFP of 1004 BOPD and 530 MCFGPD, opening the giant Altamont-Bluebell-Cedar Rim field trend in 1970 (figure 1.1), which has produced 345 MMBO and 620 BCFG (Utah Division of Oil, Gas and Mining, 2016c). In 1981, Monument Butte field in the south-central Uinta Basin (figure 1.1) was discovered with the completion of the Monument Butte Federal No. 1-35 (section 35, T. 8 S., R. 16 E., SLB&M, Duchesne County, API No. 43-013-30561) for an IFP of 37 BOPD in the Green River. The Green River oil discoveries of Antelope Creek and Brundage Canyon fields followed in 1983. The Monument Butte–Brundage Canyon trend has produced 125 MMBO and 415 BCFG (Utah Division of Oil, Gas and Mining, 2016c).

At the end of 2015, there were about 80 active oil and gas fields in the Uinta Basin (figure 1.1) and over 11,300 active wells. Average monthly production in 2015 was about 2.5 MMBO, 27 BCFG, and 8.6 MMBW (Utah Division of Oil, Gas and Mining, 2016a). State-of-the-art horizontal drilling technology, improved hydraulic fracturing techniques, and waterflood projects have collectively resulted in a continued boost in production rates and ultimate recovery from known fields and new discoveries in the Uinta Basin. Deeper exploration drilling in the eastern and southern Uinta Basin during the past five years has led to discoveries of substantial gas accumulations in Mesaverde, Entrada, and Wingate reservoirs

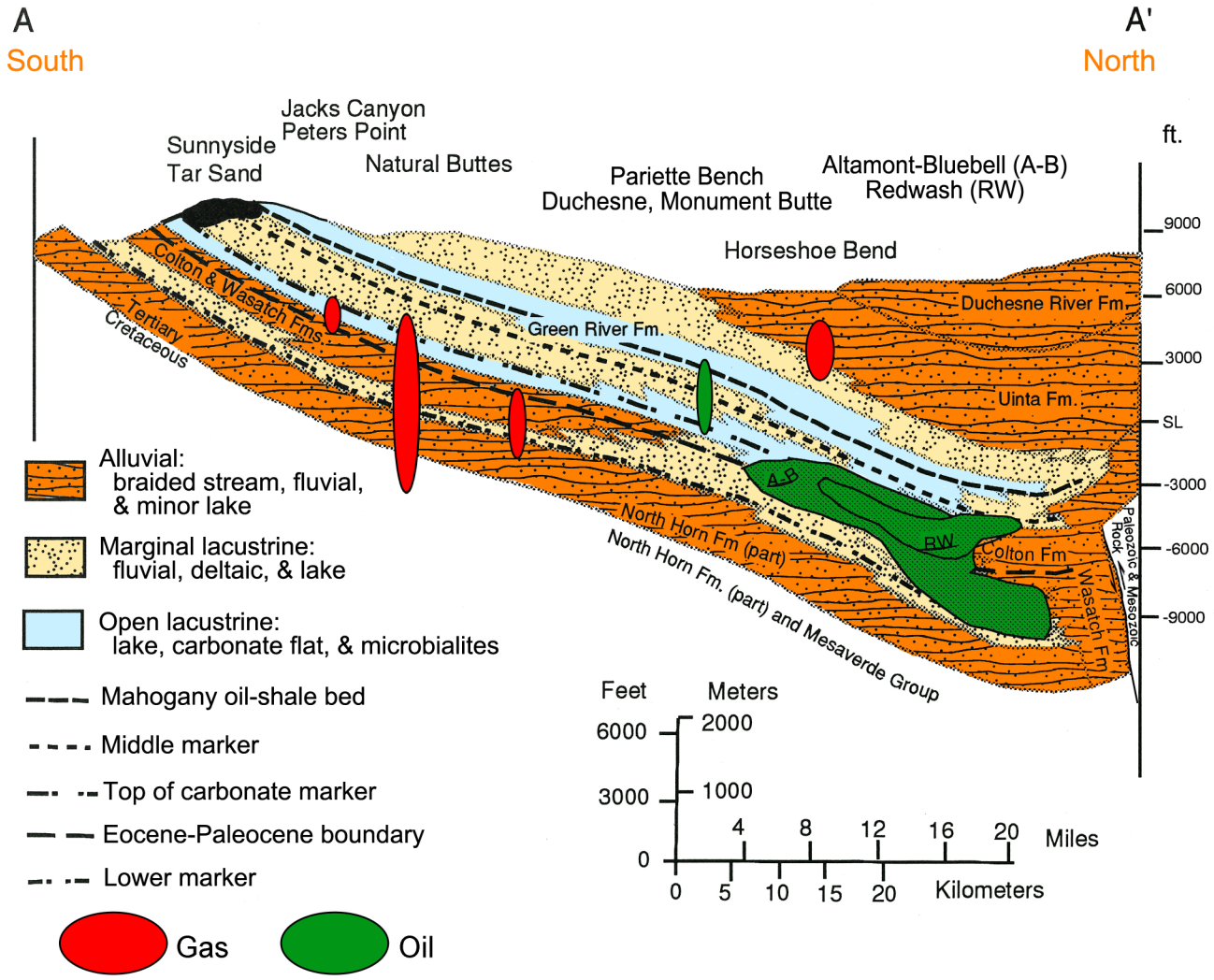

Figure 1.4. *Cross section extending from the southwest flank of the Uinta Basin (A) to the north-central part of the basin (A') showing producing reservoirs, general facies, and widely recognized stratigraphic markers. Also shown are major fields, some projected into the line of section. Location of cross section A–A' shown on figure 1.1. Modified from Fouch (1975) and Fouch and others (1992a).*

(e.g., Hill Creek field, Uintah County, figure 1.1). Interest in the Uinta Basin's oil shale and tar sand resources has also reawakened. Just to the southwest of the Uinta Basin proper, the development of CBM accumulations in the Ferron Sandstone, beginning with the discovery of Drunkards Wash field in 1992, has produced 1.3 TCFG (Utah Division of Oil, Gas and Mining, 2016c). Significant potential to yield CBM exists for other coal fields around the southern edge of the Uinta Basin, and the extent of deeper conventional and tight gas plays remains to be explored.

PURPOSE AND SCOPE

The environmentally sound production and disposal of produced water affects the economics of hydrocarbon resource development in the Uinta Basin. It has recently become a topic of much public debate because produced water is the largest-volume waste stream associated with tight-gas sand plays in the eastern Uinta Basin. Managing produced water can be a significant cost fraction of the value of the gas extracted, so there is an economic incentive to minimize this waste stream and/or generate revenue from treating and reusing produced water from tight-sand gas production in other applications.

Balancing the water-use needs and produced-water disposal requirements associated with oil and gas development creates significant material handling challenges to both industry and regulators in the Uinta Basin. Deciding how to manage large volumes of produced water, whether for disposal, reuse, or energy production, presents a number of major decision options. These challenges include understanding the variable chemistry of the produced water, determining the various quality needs of the potential reuses, managing transport from widely distributed sources to use or disposal facilities, optimizing treatment facility siting to minimize transport distances and account for the varying volume and quality of water produced over time, and identifying available disposal options for un-

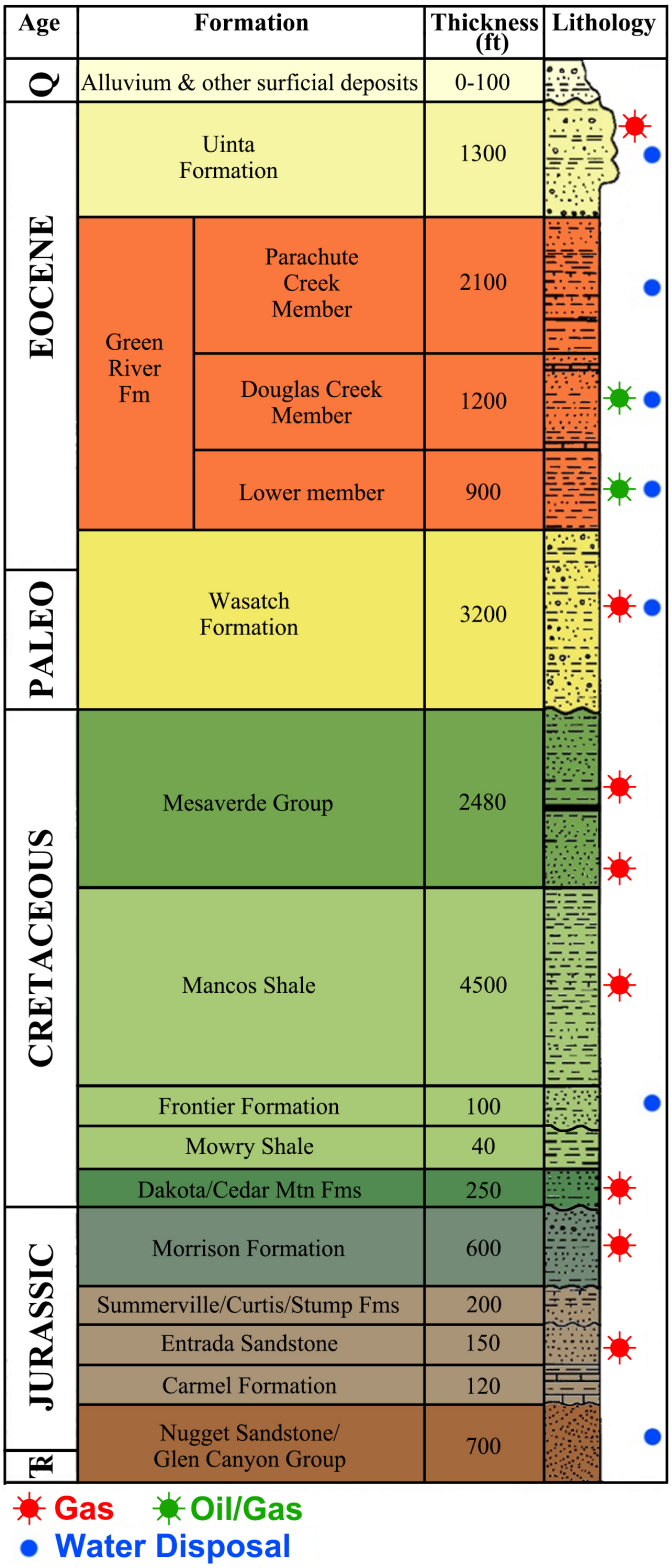

Figure 1.5. *Stratigraphic column from the surface down through the Upper Triassic–Lower Jurassic Nugget section in the Uinta Basin showing major producing reservoirs and aquifers evaluated in this study. Modified from Hintze and Kowallis (2009).*

usable produced water. They are further complicated by an operating environment where many individual producers of varying sizes exist within a field or the Uinta Basin, each with varying water needs and production, and a production timescale of decades for the basin as wells play out and new ones are completed. Specific Uinta Basin water issues include: water use/reuse for well drilling and completion (hydraulic fracturing), appropriate sites for disposal/reuse of water, development of systems to manage the produced water streams, and differing challenges for gas versus oil producers.

Current produced-water disposal practices in the Uinta Basin consist of (1) injection in deep wells, most below the base of a moderately saline aquifer in the Green River Formation, (2) storage and evaporation in lined disposal ponds, and (3) supplying water for flooding in enhanced oil recovery (EOR) programs. Potential uses for the produced water from producing formations in the basin include waterflooding for secondary recovery, drilling mud formulation, hydraulic fracturing fluid for well completion, and future use for possible oil shale production.

This study had three main objectives: (1) create basin-wide, produced-water management tools that integrate produced-water character, water disposal/reuse, and water transport to allow for quicker and more efficient regulatory and management decisions related to oil and gas developments in the Uinta Basin; (2) promote maximized produced-water reuse, which will minimize use of fresh water in unconventional tight-gas sand development and production; and (3) compile Uinta Basin produced-water management practices and suggest best practices. The study investigated the integrated management of water production and disposal in the Uinta Basin, across many producers, and with multiple reuse or disposal options. The study contained three major components:

1. Compilation and analysis within a geographic information system (GIS) format of past and new information on the thickness, structure, depth, porosity, permeability, and lithologic nature of all aquifer/reservoir units in the basin from the Tertiary down through the Upper Triassic–Lower Jurassic Nugget/Navajo Sandstone (figure 1.5); the regional variations in quality, flow direction, and temperature of water produced from the various reservoirs across the basin; the existing infrastructure for water management/reuse; and the location and geochemical and hydrological characteristics of aquifers used/proposed for disposal of produced water or concentrated brines.
2. Compilation and statistical analysis of water production quantity and quality for each discrete producing interval. The geostatistical characterization of the basin's produced-water streams from both oil and gas wells helped analyze the options for treatment, transportation, disposal, and alternative uses of produced water.
3. Evaluation of produced-water management practices and suggestions for best management practices.

Science-based decision-support models, such as outlined here, will help industry, particularly small producers, and regulators alike in making optimum management decisions, and provide sound scientific information to allay public concerns about the potential for drinking water contamination from hydraulic fracturing and production operations. The produced-water quantity and quality geostatistical models, and best practice suggestions provide a framework to address the divergent water uses and disposal interests of various stakeholders. The produced-water models for the various reservoirs in the basin allow stakeholders to evaluate the cause and effect of the timing and rate of oil and gas development drilling decisions on both their operations and those of other operators, allow the evaluation of water input and output impacts and their consequences, and ultimately allow an improved understanding of complex interactions typical of produced-water management systems. Decision-support models, built with components of estimates of water needs for drilling and fracture stimulation and options for treatment, distribution, disposal, and reuse of produced water, will allow efficient management and improved reuse of produced-water flows in a semi-arid region on a basin-wide scale (across the Uinta Basin), and potentially in other oil- and gas-producing areas of the U.S. Finally, we hope that this study will foster extensive collaboration among producers, users, regulators, and local water management interests, providing insight and information necessary for effective protection of alluvial aquifers, sustainable produced-water management, and potential for beneficial use of produced water.

This Utah Geological Survey (UGS) Bulletin covers research and results of the UGS's study of the geology, chemistry, and best practices related to produced water in the Uinta Basin. The Bulletin includes (1) descriptions of Uinta Basin reservoirs and aquifers, (2) statistical trends of Uinta Basin water quality, and (3) overviews of produced-water facilities and recommendations for best handling practices. Appendices provide the complete data compilations either collected or generated as part of this study. The UGS study also (1) evaluated the groundwater chemistry of shallow alluvial wells and springs in the Uinta Basin, (2) analyzed the sensitivity and vulnerability of the aquifers and springs in the Uinta Basin to potential contamination associated with energy resource development, and (3) investigated the reuse of produced water as a potential geothermal resource. These additional research topics were published as separate papers in the Utah Geological Association's Publication 44, *Geology of Utah's Uinta Basin and Uinta Mountains* (see Wallace, 2015; Wallace and others, 2015; and Hardwick and others, 2015; respectively).

CHAPTER 2:
STRATIGRAPHY AND DEPOSITIONAL HISTORY

by

Thomas C. Chidsey, Jr., Taylor Boden, and Stephanie M. Carney

CONTENTS

INTRODUCTION 13
UPPER TRIASSIC–JURASSIC ROCKS 13
Upper Triassic and Lower Jurassic Rocks 13
Wingate Sandstone 13
Kayenta Formation 16
Navajo/Nugget Sandstone 16
Middle and Upper Jurassic Rocks 17
Carmel and Arapien Formations 17
Entrada Sandstone 18
Curtis and Stump Formations 19
Summerville Formation 20
Morrison Formation 21
CRETACEOUS ROCKS 22
Lower and Lower Upper Cretaceous Rocks 22
Cedar Mountain Formation 22
Dakota Formation 24
Upper Cretaceous Rocks 24
Mowry Shale 25
Frontier Formation 26
Mancos Shale 26
Mesaverde Group 28
Star Point Sandstone 28
Blackhawk Formation 28
Castlegate Sandstone 30
Sego Sandstone 30
Neslen Formation 31
Farrer Formation 31
Price River Formation 33
Tuscher Formation 33
TERTIARY ROCKS 33
North Horn Formation 33
Flagstaff Limestone 35
Colton Formation 36
Wasatch Formation 36
Green River Formation 37
Uinta Formation 42
Duchesne River Formation 42
QUATERNARY DEPOSITS 43

FIGURES

Figure 2.1. Generalized geologic map of the Uinta Basin with simplified north-south cross section 14
Figure 2.2. Representative outcrop of Upper Triassic–Lower Jurassic Wingate Sandstone 15
Figure 2.3. Representative outcrop of Lower Jurassic Kayenta Formation 16
Figure 2.4. Representative outcrop of the Lower Jurassic Navajo Sandstone 17
Figure 2.5. Representative outcrop of Middle Jurassic Carmel Formation 18
Figure 2.6. Representative outcrop and facies of the Middle Jurassic Entrada Sandstone 19
Figure 2.7. Representative outcrop of the Middle Jurassic Curtis Formation 20
Figure 2.8. Representative outcrop of the Middle Jurassic Summerville Formation 21
Figure 2.9. Representative outcrop of the Salt Wash and Brushy Basin Members of the Upper Jurassic Morrison Formation 22
Figure 2.10. Representative outcrops of the Lower to lower Upper Cretaceous Cedar Mountain Formation 23
Figure 2.11. Typical exposures of Upper Cretaceous Dakota Formation 25
Figure 2.12. Representative outcrop of Upper Cretaceous Dakota, Mowry, and Frontier Formations 25

Figure 2.13. Chronostratigraphic chart for Late Cretaceous–Paleogene strata in the Book Cliffs–Wasatch Plateau region 26
Figure 2.14. Classic outcrop of the Tununk Member of the Mancos Shale..... 27
Figure 2.15. Tununk and Ferron Sandstone Members of the Mancos Shale in the San Rafael Swell..... 28
Figure 2.16. Blackhawk Formation outcrops in the Book Cliffs..... 29
Figure 2.17. Castlegate Sandstone outcrops in the Book Cliffs..... 30
Figure 2.18. Paleogeography of the Uinta Basin during late Campanian through Maastrichtian 31
Figure 2.19. Outcrop lower Sego Sandstone and Buck Tongue of the Mancos Shale, eastern Book Cliffs..... 32
Figure 2.20. Stratigraphic section in Sego Canyon, eastern Book Cliffs..... 32
Figure 2.21. Representative outcrop of Upper Cretaceous Price River Formation 34
Figure 2.22. Representative outcrop of Tuscher Formation and underlying Farrer Formation, eastern Book Cliffs..... 34
Figure 2.23. Representative outcrop of late Upper Cretaceous–early Paleocene North Horn Formation, Book Cliffs 35
Figure 2.24. Representative outcrop of Paleocene Flagstaff Limestone, Book Cliffs..... 36
Figure 2.25. Paleogeography of the Uinta Basin during Paleocene through Eocene 37
Figure 2.26. Representative outcrop of Paleocene-Eocene Colton Formation, Roan Cliffs 38
Figure 2.27. Paleocene-Eocene Wasatch Formation, Hells Hole area, southeastern Uinta Basin..... 38
Figure 2.28. General stratigraphy and major marker beds of the Green River Formation in the Uinta Basin 39
Figure 2.29. Representative outcrops of the Eocene Green River Formation 40
Figure 2.30. Generalized depositional setting for Lake Uinta..... 43
Figure 2.31. Badland topography formed in the Eocene Uinta Formation..... 44
Figure 2.32. Representative outcrop of the Eocene Duchesne River Formation..... 44

CHAPTER 2:
STRATIGRAPHY AND DEPOSITIONAL HISTORY

INTRODUCTION

Consolidated sedimentary rocks in the Uinta Basin were deposited intermittently over the past 540 million years and have a cumulative average thickness of about 22,000 feet (6700 m) (Hintze and Kowallis, 2009); however, rocks older than Cretaceous are not exposed in the basin. Exploratory drilling for hydrocarbons in the Uinta Basin has penetrated the entire stratigraphic section down to the Precambrian basement. Several major unconformities represent significant periods of erosion or non-deposition. Exposed strata in the Uinta Basin, including the Book Cliffs along the southern boundary and those rocks in the deep subsurface of the basin that outcrop in the San Rafael Swell to the southwest and eastern Uinta Mountains to the northeast, serve as outcrop reservoir and aquifer analogs which display changes in color, rock types, thicknesses, and weathering profiles representing various depositional environments and geologic processes, depending on their location within the region. In addition, relatively thin unconsolidated gravel, sand, silt, and clay are found in a variety of settings—the products of weathering, running water, wind, and mass wasting as the Uinta Basin is currently in a state of regional erosion. Figure 2.1 and plate 1 are generalized geologic maps showing the distribution of rock units across the Uinta Basin and surrounding areas.

This study focuses on (1) water produced from Uinta Basin oil- and gas-bearing formations, (2) Upper Triassic–Lower Jurassic to Tertiary aquifers either currently storing that water or having the potential to do so, and (3) Quaternary alluvial aquifers containing fresh water (figure 1.5). The stratigraphy and depositional history of Upper Triassic through Quaternary deposits in the Uinta Basin are discussed in general below.

UPPER TRIASSIC–JURASSIC ROCKS

Upper Triassic and Jurassic rocks in the Uinta Basin are shallow marine, marginal marine, and terrestrial sedimentary formations deposited between 205 and 145 million Ma, coeval with the breakup of the supercontinent Pangea (Blakey and Ranney, 2008). Hintze and Kowallis (2009) grouped the strata into three packages: Upper Triassic to Lower Jurassic rocks that are primarily eolian and fluvial sandstone; Middle Jurassic marine and marginal marine rocks that reflect a change in conditions as an epicontinental seaway advanced from and subsequently retreated to the north; and Upper Jurassic rocks composed of continental interior fluvial and lacustrine deposits.

Upper Triassic and Lower Jurassic Rocks

Three Upper Triassic to Lower Jurassic formations in the Uinta Basin are collectively called the Glen Canyon Group (figures 1.5 and 2.1, plate 1). In ascending order of deposition, they consist of the Triassic-Jurassic Wingate Sandstone, Jurassic Kayenta Formation, and Jurassic Navajo Sandstone (the three formations are equivalent to the Upper Triassic–Lower Jurassic Nugget Sandstone in the eastern Uinta Mountains just outside the basin boundary). This sequence is spectacularly exposed on the San Rafael Swell and consists of predominantly eolian and fluvial sandstones, which generally thicken southwestward across the Uinta Basin and Utah. The depositional limit of the Wingate and Kayenta Formations is near the central part of the Uinta Basin, and they are not present in the northern and northeastern parts of the basin, based on deep wells. The thickness of the Glen Canyon Group ranges between 700 and 1000 feet (200–300 m), where all three formations are present in the basin (Hintze and Kowallis, 2009). In the central and southern part of the Uinta Basin, the Wingate Sandstone conformably overlies the Triassic Chinle Formation, whereas in the north and northwest, the Nugget (Navajo) conformably overlies the Chinle. In outcrops and wells surrounding the Uinta Mountains, the Wingate and Kayenta Formations are not present, and thus the name Nugget Sandstone is applied to the predominately sandstone Upper Triassic to Lower Jurassic section (Sprinkel and others, 2011b).

Wingate Sandstone

The Wingate Sandstone, the basal formation of the Glen Canyon Group, is latest Triassic (Rhaetian) through the early part of Early Jurassic (early Sinemurian) in age. The Wingate consists of 300 to 440 feet (90–130 m) of very fine to fine-grained, laminated to thin-bedded, flat- and cross-stratified sandstone, which contains very sparse shaly and silty partings (Gualtieri, 1988; Hintze and Kowallis, 2009). It is light yellow-gray to orange-brown in color, weathering dark brown, and characteristically stained with dark-red-brown manganese oxide (desert varnish). The thick-bedded to massive Wingate forms sheer vertical to ledgey cliffs (figure 2.2), which are often jointed through the entire section.

The sandstone of the Wingate was deposited in a desert dune field (eolian erg) environment (Blakey and Ranney, 2008). The Wingate Sandstone contains only ichnofossils (mostly tracks from dinosaurs and other vertebrates) and no known ash beds; thus, dating has been difficult. Recent studies of dinosaur track sites elsewhere on the Colorado Plateau indicate that the lower Wingate is Triassic; other track sites show that

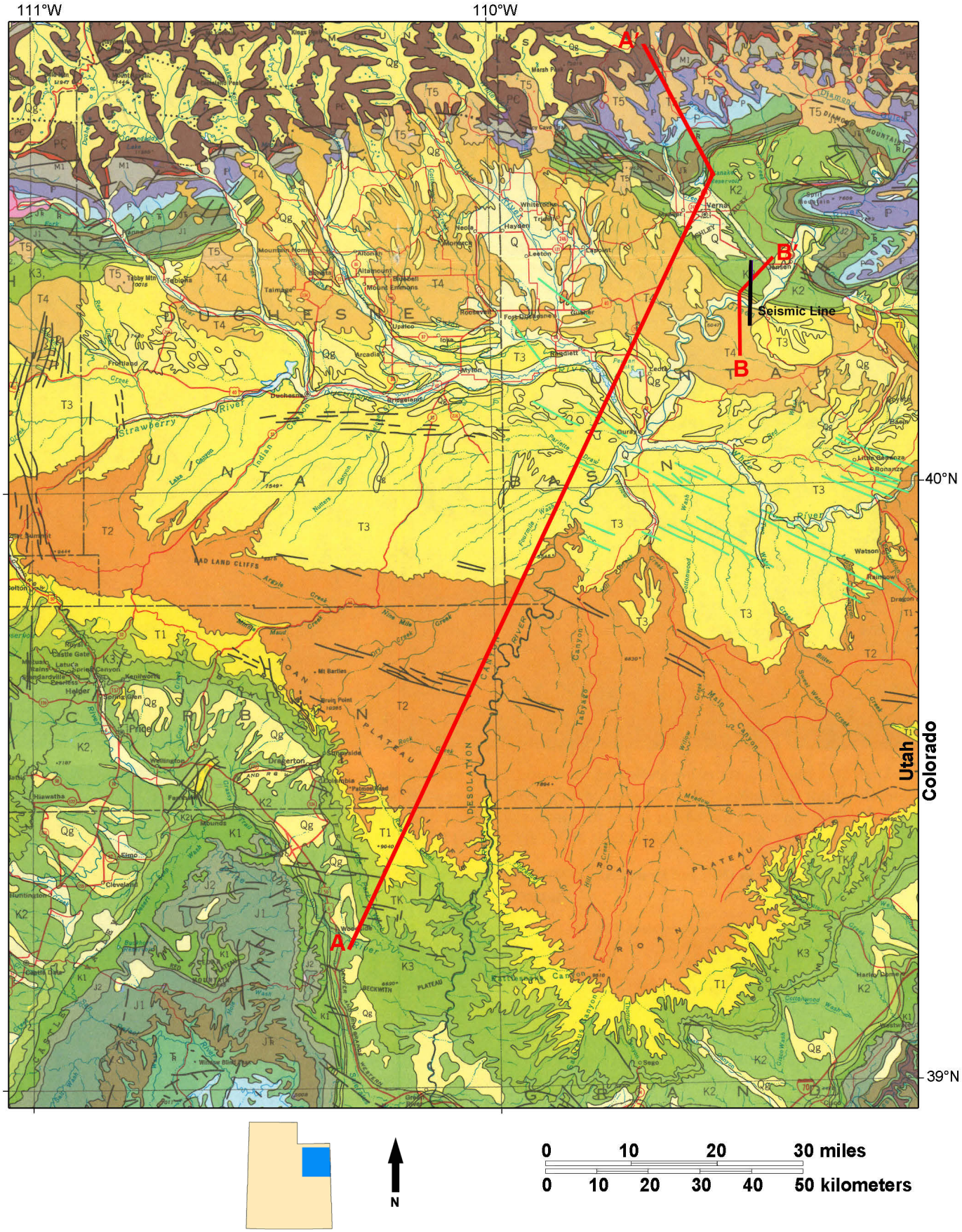

Figure 2.1. *Generalized geologic map of the Uinta Basin and surrounding areas with simplified north-south cross section A–A' (modified from Hintze, 1997). Seismic line shown on figure 3.3; cross section B–B' shown on figure 3.4.*

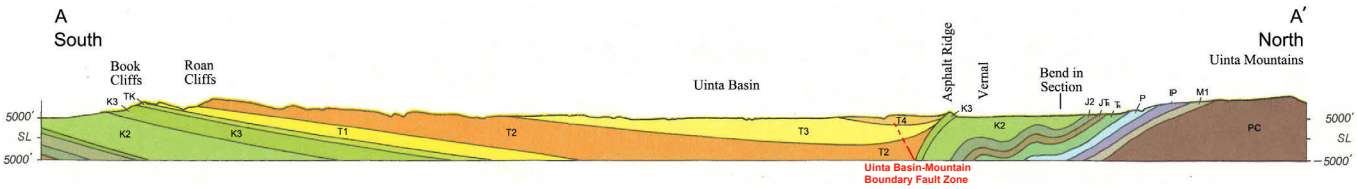

Explanation

Quaternary
- Q alluvium
- Qg glacial deposits

Tertiary
- T5 Browns Park Formation
- T4 Duchesne River Formation
- T3 Uinta Formation
- T2 Green River Formation
- T1 Flagstaff Limestone, Wasatch/Colton Formation
- TK North Horn Formation

Cretaceous
- K3 Mesaverde Group
- K2 Mowry Shale, Frontier Formation, Mancos Shale
- K1 Cedar Mountain Formation, Dakota Formation

Jurassic
- J2 Curtis/Stump Formation, Morrison Formation
- J1 Carmel/Arapien Formation, Entrada Sandstone
- JR Glen Canyon Group

Triassic
- TR Dinwoody Formation, Moenkopi Formation,Chinle Formation

Permian
- P Park City Formation

Pennsylvanian
- IP Weber Sandstone, Morgan Formation Round Valley Limestone

Mississippian
- M2 Doughnut Formation
- M1 Humbug Formation, Deseret Limestone, Madison Limestone

Cambrian
- C1 Lodore Sandstone

Precambrian
- PC Uinta Mountain Group

Gilsonite veins

Fault, dotted where concealed

Figure 2.1. *Continued*

Figure 2.2. *Eolian, cross-stratified Upper Triassic–Lower Jurassic Wingate Sandstone, Glen Canyon Group, northern San Rafael Swell; view to the northeast. Photograph by Michael Chidsey, Sqwak Productions Inc.*

the upper Wingate is Early Jurassic (Molina-Garza and others, 2003; Lockley and others, 2004; Lucas and others, 2005; Milner and Kirkland, 2006). Thus, the Triassic-Jurassic boundary lies within the Wingate (Sprinkel and others, 2011a).

Kayenta Formation

The Kayenta Formation (Sinemurian and Pliensbachian in age) is easy to distinguish from the underlying Wingate and overlying Navajo Sandstones. Whereas the formations above and below form large vertical cliffs, the Kayenta forms a series of ledges, small cliffs, and benches (figure 2.3). The Kayenta consists of 0 to 240 feet (0–73 m) of gray, pinkish-gray, and red interbedded fine- to coarse-grained partly micaceous sandstone, siltstone, and mudstone (Gualtieri, 1988; Hintze and Kowallis, 2009). The sandstone beds are thin to medium bedded, and flat- and cross-stratified (Gualtieri, 1998). The Kayenta has gradational contacts with the underlying Wingate Sandstone and overlying Navajo Sandstone (Doelling, 2002).

The Kayenta Formation was deposited in a sandy, braided fluvial environment, although the environment was arid. Perennial streams flowed west from the remaining Ancestral Rockies and the Appalachians farther to the east (Lynds and Hajek, 2006; Blakey and Ranney, 2008). Uplift of the Ancestral Rockies may have contributed locally to a slightly wetter climate, enhancing fluvial conditions during Kayenta deposition (Blakey and Ranney, 2008).

Navajo/Nugget Sandstone

The Navajo Sandstone (Pliensbachian and Toarcian in age) with its spectacular cross-stratification is perhaps the most well-known formation in Utah, where it forms the magnificent cliffs and canyons in Zion and other national parks, monuments, and recreational areas in the southern part of the state; it is equivalent to the upper (Lower Jurassic part) Nugget Sandstone in and north of the Uinta Basin. The Navajo in the San Rafael Swell ranges in thickness from 400 to 600 feet (120–180 m), pinching out to the east near the Colorado border. The Nugget ranges in thickness from 560 to 1300 feet (170–400 m) in the subsurface of Uinta Basin proper (Hintze and Kowallis, 2009). The Navajo/Nugget is light brown to light gray, thick-bedded to massive sandstone that is cross-stratified in large trough sets (figure 2.4). The sandstone beds are friable and composed of clean, fine- to medium-grained, frosted, subrounded to subangular, moderately to well-sorted quartz sand with minor amounts of feldspar and scattered heavy-mineral grains. The Navajo forms steep cliffs and rounded knolls and locally contains thin, lenticular, light-gray limestone beds. The Navajo Sandstone is separated from the overlying Middle Jurassic Carmel Formation by the J-1 unconformity (Pipiringos and O'Sullivan, 1978).

The sandstone of the Navajo and age-equivalent rocks represents one of the largest eolian deposits in all of geologic time (Kocurek and Dott, 1983) and was deposited in a coastal to

Figure 2.3. *Lenticular sandstone beds representing the sandy braided steam environment of the Lower Jurassic Kayenta Formation, Glen Canyon Group, northern San Rafael Swell; view to the south. Photograph by Michael Chidsey, Sqwak Productions Inc.*

Figure 2.4. Outcrop of the Lower Jurassic Navajo Sandstone displaying spectacular eolian trough cross-stratification representing multiple dune sets northern San Rafael Swell; view to the northeast. Soft-sediment deformation is common in the lower third of the outcrop. Dune foreset beds indicate paleowind directions were dominantly from the north and northwest. Photograph by Michael Chidsey, Sqwak Productions Inc.

inland desert dune field (erg) environment, which extended from present-day Wyoming to Arizona (Blakey and Ranney, 2008). In Early Jurassic time, Utah had an arid climate and lay 15° north of the equator (Smith and others, 1981). The erg was comparable to the Sahara desert in North Africa or the Alashan area of the Gobi desert in northern China. The eolian deposits included dunes, interdunes, and sand sheets. Navajo dunes were large (widths up to 2200 feet [670 m]) to small, straight-crested to sinuous, coalescing, transverse barchanoid ridges as suggested by the large-scale cross-stratification (Picard, 1975; Fryberger, 1990). Regional analyses of the mean dip of dune foreset beds indicate paleocurrent and paleowind directions were dominantly from the north and northwest (Kocurek and Dott, 1983; Peterson, 1988), as well displayed in the San Rafael Swell. A high paleo-water table produced oases; carbonate deposition occurred in ephemeral springs and lakes when they existed for relatively long periods of time.

Middle and Upper Jurassic Rocks

Middle and Upper Jurassic rocks found in, or exposed around, the Uinta Basin include the Carmel/Arapien, Entrada, Curtis/Stump, Summerville (Stump Formation equivalent), and Morrison Formations (figures 1.5 and 2.1, plate 1). The Carmel through Summerville Formations make up the San Rafael Group in the San Rafael Swell. Middle and Upper Jurassic rocks in the basin range from 680 to 3200 feet (200–980 m) thick (Hintze and Kowallis, 2009) and reflect a time of complex sedimentation resulting from the advance and retreat of a long, north-south oriented, narrow epicontinental seaway to the initial rise of highlands far to the west.

Carmel and Arapien Formations

The Carmel Formation (Bajocian through Callovian in age) is exposed in the San Rafael Swell and northward in the central and eastern parts of the Uinta Basin where it is divided into four members, which in ascending order are: Co-op Creek Limestone (or equivalent Judd Hollow), Crystal Creek, Paria River, and Winsor (figure 2.5). However, all four members are not always present within the San Rafael Swell. Members of the Carmel and other Middle Jurassic formations in the region have been mapped, measured, and described by Sprinkel and others (in preparation). Stratigraphically equivalent beds exposed along the western part of the south flank of the Uinta Mountains (near the town of Hanna), were redefined as the Arapien Formation by Spinkel and others (2011a) based on the mudstone-dominated lithofacies and gypsum in the upper member. They argued that these beds were more lithologically similar to the Twelvemile Canyon Member of the Arapien than the Leeds Creek and Giraffe Creek Members of the Twin Creek Limestone of northern Utah. Sprinkel and others (2011a), however, applied Twin Creek member names to members of the Arapien below the Twelvemile Canyon Member. Thus, the Arapien Formation consists of five members, which in ascending order are: Sliderock, Rich, Boundary Ridge, Watton Canyon, and Twelvemile Canyon. Consequently, the Arapien Formation is now mapped near Hanna and vicinity (Sprinkel, in review).

In general, the Carmel Formation consists of interbedded sandstone, siltstone, mudstone, and limestone with subordinate amounts of dolosiltite, doloarenite, calcarenite, and

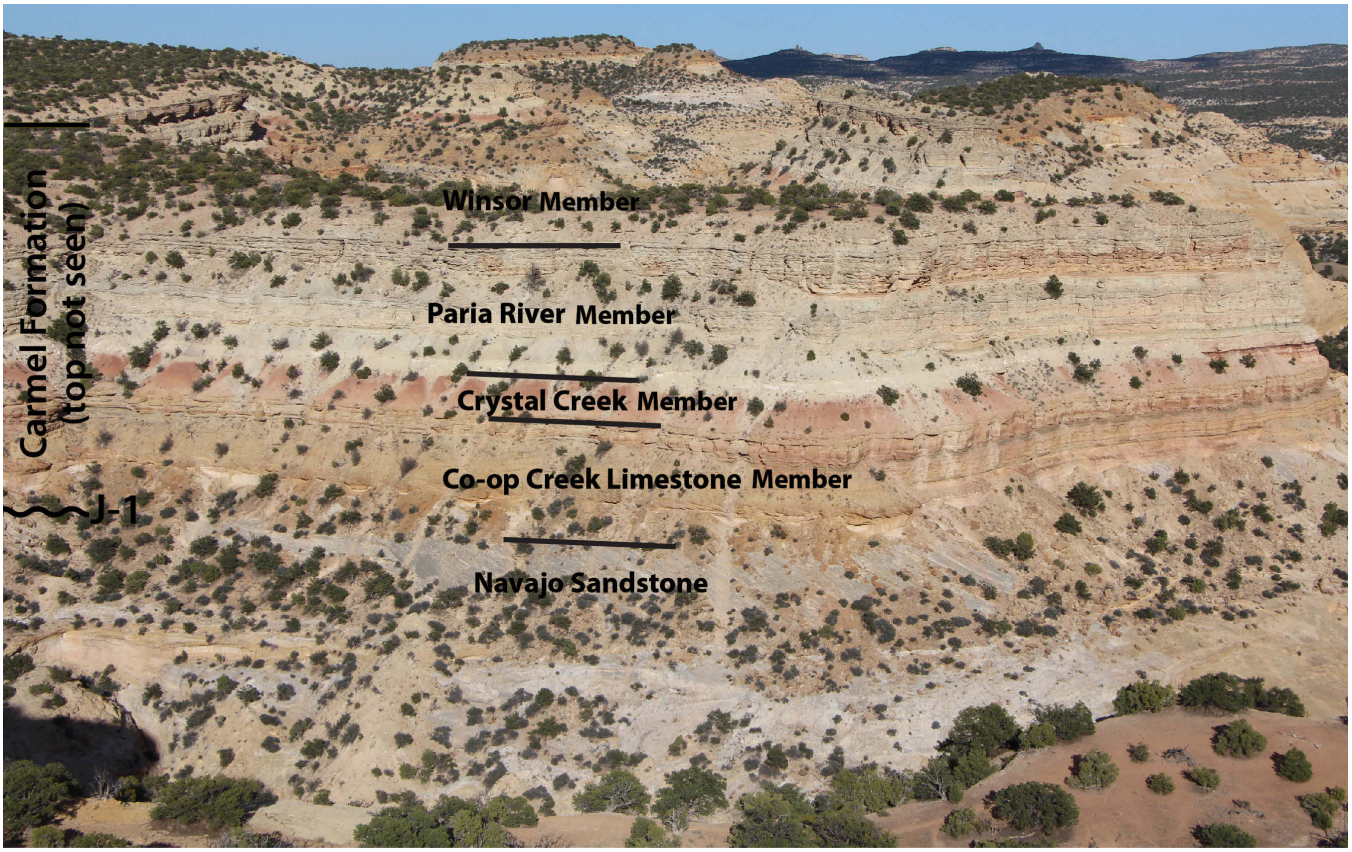

Figure 2.5. *Excellent exposure of Middle Jurassic Carmel Formation, San Rafael Group, west flank of the San Rafael Swell, Devils Canyon south of Interstate 70 (I-70); view to the east. The Co-op Creek, Crystal Creek, Paria River, and part of the Winsor Members are shown. The Carmel contact with the underlying Navajo Sandstone represents the J-1 unconformity. Photograph by Michael Chidsey, Sqwak Productions Inc.*

calcisiltite. Locally, the Paria and regionally the Winsor Members contain thick gypsum beds. These lithotypes are generally thin to medium bedded, forming blocky ledges (weathering into slabs and plates) and steep slopes. The lower Arapien Formation (Sliderock to Watton Canyon Members) consists mostly of thin- to medium-bedded, dense, micritic to grainstone-rich, and locally bioclastic to dolomitic limestone; oolitic beds are common in the Sliderock and Watton Canyon Members (Sprinkel and others, 2011a). The Twelvemile Canyon Member is a mixed mudstone, carbonate, and clastic unit interbedded with gypsum (anhydrite) and salt (salt is generally restricted to central Utah).

The Carmel and Arapien Formations were deposited during the transgression of the shallow marine Sundance Sea, which extended south from Canada along a narrow embayment or arm (called the Utah-Idaho trough) through northern, central, and southwestern Utah (Blakey and Ranney, 2008; Hintze and Kowallis, 2009). Shoreline fluctuations produced variations between restricted- and more open- to marginal-marine conditions, causing significant changes in deposition. This was especially the case along the eastern margin of the marine embayment, which is now exposed on the San Rafael Swell and along the south flank of the Uinta Mountains. The Carmel and Arapien Formations range from 0 to 1000 feet (0–300 m) in depositional thickness (Sprinkel and others, in preparation); however, the Arapien is tectonically thickened several thousand feet in the central Utah thrust belt.

Entrada Sandstone

Marine waters retreated northward out of Utah and the Entrada Sandstone was deposited on top of the Carmel Formation. The Entrada (Callovian in age) consists of 100 to 950 feet (30–290 m) of orange-brown, red-brown, or light brown sandstone, siltstone, mudstone, and subordinate oolitic limestone (figure 2.6A) (Gualtieri, 1988; Hintze and Kowallis, 2009). Red siltstone and silty sandstone are dominant in the basal part (Gualtieri, 1988). Sandstone beds are friable, porous, silty or very fine to fine grained with scattered coarse grains, poorly to moderately sorted, and cemented with calcite or iron oxide. A variety of sedimentary structures is found in the Entrada: ripple marks, mudcracks, rip-up clasts, trough cross-stratification, micro-cross-lamination, and soft-sediment deformation. Bedding is thin to very thick, forming earthy slopes and rounded ledges and cliffs. The Entrada Sandstone lies conformably above the Carmel Formation. It is separated from the overlying Curtis Formation by the regional J-3 unconformity of Pipiringos and O'Sullivan (1978).

Figure 2.6. *Two representative facies in the Middle Jurassic Entrada Sandstone, San Rafael Group.* ***A.*** *Orange-brown, red-brown, and light brown sandstone, siltstone, and mudstone, deposited in broad, mud-dominated intertidal and subtidal zones, supratidal sabkha mudflats and ponds; view to the northwest on west flank of the San Rafael Swell south of I-70.* ***B.*** *Mudstone and medium-grained, cross-stratified sandstone representing tidal flats and coastal dunes; view to the southeast on the east flank of the San Rafael Swell north of I-70. Photographs by Michael Chidsey, Sqwak Productions Inc.*

The Entrada Sandstone was deposited primarily in broad, mud-dominated intertidal (low to high) and subtidal zones, supratidal sabkha mudflats and ponds, and related erg-margin coastal dunes (Hicks and others, 2010; Herbst and Morris, 2011; Thomas H. Morris, Brigham Young University, written communication, December 2012). Associated shoreface, ooid shoal and bar, foreshore, tidal channel, and storm deposits are also present (Marino and Morris, 1996; Hicks and others, 2010). Coastal dunes encroached on the region from the east, while the remaining part of the Sundance Sea lay to the west and northwest. These eolian deposits are found along the eastern flank of the San Rafael Swell (figure 2.6B). Locally, the Entrada produces gas in the southeastern Uinta Basin.

Curtis and Stump Formations

The final Jurassic marine incursion deposited the Curtis/Stump Formation (Oxfordian in age [Wilcox, 2007]); along the southern flank of the Uinta Mountains the Curtis is the lower member of the Stump (Hintze and Kowallis, 2009). The

Curtis/Stump consists of 0 to 300 feet (0–90 m) of light gray-green, light gray, to light brown sandstone (sublitharenite, lithic arenite, and subarkose), siltstone, and claystone/shale (figure 2.7) with subordinate conglomerate and limestone (Smith, 1976; Witkind, 1988; Caputo and Pryor, 1991; Doelling, 2002, 2004). Sandstone is very fine to coarse grained, poorly to moderately sorted, subrounded to subangular, and quartzose. The green color is attributed to the presence of glauconite in the matrix, although it may be iron-chlorite clay instead (written communication to Mario V. Caputo from Richard Pollastro, U.S. Geological Survey, October 1987). Bedding is finely laminated to medium, forming cliffs, ledgy benches, and slopes. The contact with the overlying Summerville Formation is gradational and conformable.

The Curtis/Stump Formation was deposited in a shallow-shelf and marginal-marine environment (Blakey and Ranney, 2008). The lithofacies display the effects of low-energy, marine (normal wave base) conditions, and tidal currents in intertidal and subtidal zones with tidal channels, shoals, storm deposits, tidal flats, etc. (Smith, 1976; Caputo and Pryor, 1991; Currie and Reeder, 2002; Currie and others, 2005).

Summerville Formation

The Summerville Formation (Oxfordian) commonly appears like chocolate-colored pages of a book displayed in prominent buttes and mesas (figure 2.8); it is only present in the southernmost part of the Uinta Basin. The Summerville consists of 0 to 400 feet (0–120 m) of red-brown, light to medium brown siltstone, mudstone, sandstone, and white gypsum with subordinate claystone/shale and gray limestone (Stanton, 1976; Witkind, 1988; Caputo and Pryor, 1991; Doelling, 2002, 2004). Siltstone is the most common lithotype, present both as mottled regular bedded units or small lenses, and is composed of silt with abundant clay. Sandstone is very fine to fine grained and silty, and weathers into plates. Ripple marks are profuse throughout the Summerville. Bedding is laminar to medium, forming vertical cliffs and steep earthy slopes with a few smooth ledges. The Summerville Formation is separated from the overlying Morrison Formation by the regional J-5 unconformity of Pipiringos and O'Sullivan (1978).

The Summerville Formation was deposited in a broad, low-energy, muddy tidal flat/sabkha environment along an arid coastal

Figure 2.7. *Typical greenish colored, thin- to thick-bedded, shallow-shelf and marginal-marine sandstone of the Middle Jurassic Curtis Formation, San Rafael Group; west flank of the San Rafael Swell along I-70; view to the west. Person is standing on a thin sandstone bed containing trough cross-stratification, possibly representing a migrating sand bar. Photograph by Michael Chidsey, Sqwak Productions Inc.*

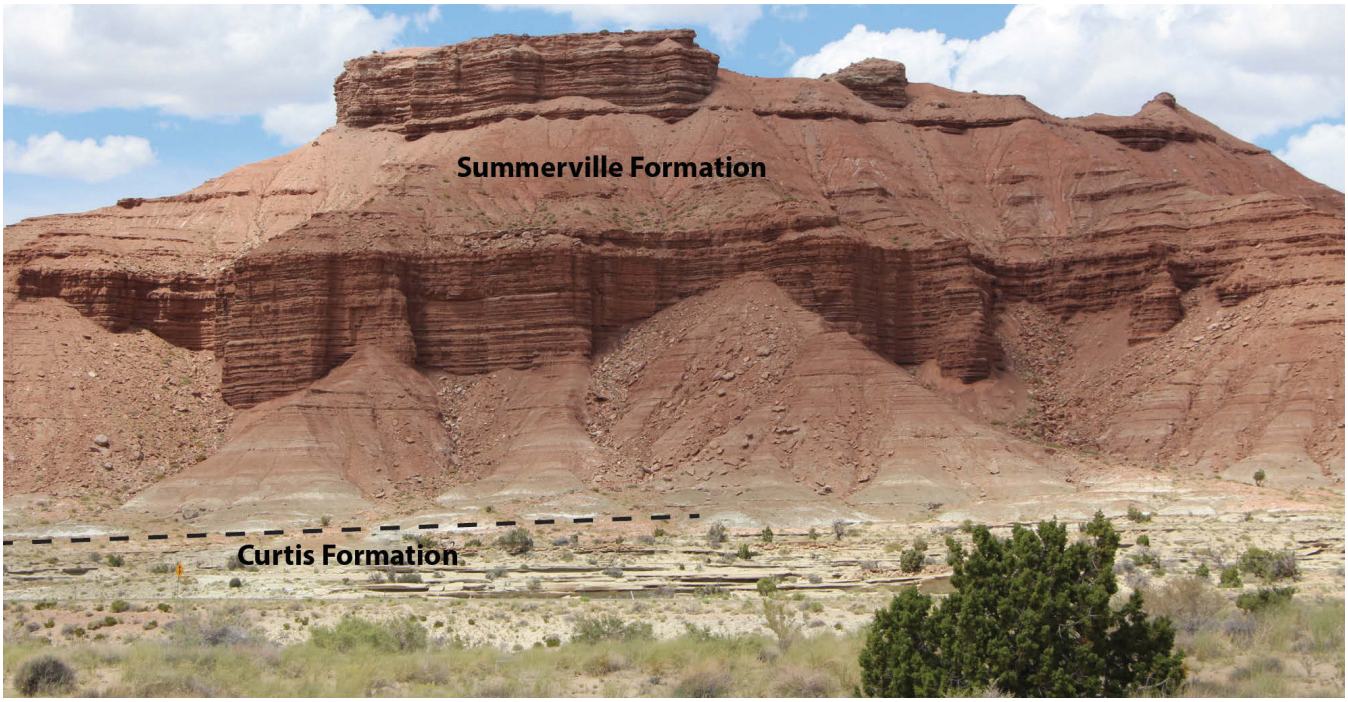

Figure 2.8. *Tidal-flat and sabkha siltstone, mudstone, and sandstone of the Middle Jurassic Summerville Formation, San Rafael Group, west flank of the San Rafael Swell along I-70; view to the north. The contact with the underlying Curtis Formation is conformable and gradational. Photograph by Michael Chidsey, Sqwak Productions Inc.*

plain during a supratidal stage of an upward-shallowing cycle (Stanton, 1976; Caputo and Pryor, 1991; Currie and others, 2005). These conditions were restricted, hypersaline, and evaporative; the narrow and receding sea was to the west and northwest of the San Rafael Swell. In eastern Utah, eolian environments occurred on a coastal plain (Blakey and Ranney, 2008).

Morrison Formation

The Morrison Formation (Upper Jurassic [Kimmeridgian through Tithonian] in age) is world famous for its dinosaur fossils from outcrops around the San Rafael Swell (figure 2.9) and the quarry at Dinosaur National Monument east of Vernal. The Morrison is divided into three members within the region, which in ascending order are: Tidwell, Salt Wash, and Brushy Basin. The Tidwell Member consists of lavender, maroon, red, red-brown, or light gray interbedded siltstone, shale, limestone (marl), sandstone, and gypsum. The Salt Wash Member consists of red, gray, purple, or brown mudstone and siltstone with few sandy limestone beds and light yellow-gray, light gray, or gray sandstone, conglomeratic sandstone, and conglomerate (Witkind, 1980, 1988; Doelling, 2002; Doelling and Kuehne, 2012). Sandstone beds are fine to coarse grained, subangular to well rounded, and arkosic or quartzose, and contain well-displayed trough cross-stratification. Conglomerate is composed of poorly sorted, subangular to well-rounded chert and quartzite ranging in size from pebbles to cobbles in a matrix of coarse quartz sand. The Brushy Basin Member produces the most colorful section of the Morrison, consisting of purple, green, red, yellow, maroon, bluish gray, gray, and white bands of claystone (often bentonitic/smectitic), mudstone, and siltstone interbedded with white, gray, and light brown sandstone with subordinate limestone and conglomerate (figure 2.9) (Witkind, 1980, 1988; Gualtieri, 1988; Doelling, 2002; Doelling and Kuehne, 2012). Brushy Basin strata form smooth, steep slopes composed of thin to thick color bands that are devoid of vegetation. The Brushy Basin is separated from the overlying Lower Cretaceous Cedar Mountain Formation by the K-0 unconformity, representing a time gap of 25 million years (Pipiringos and O'Sullivan, 1978; Hintze and Kowallis, 2009).

The 200- to 1500-foot-thick (60–460 m) Morrison Formation represents entirely continental deposition when mountains were rising far to the west in Nevada and westernmost Utah, and the last Jurassic inland sea had retreated to the northeast (Hintze and Kowallis, 2009). The regional structural setting was a back-bulge depozone of a foreland basin east of the thrust belt forebulge (DeCelles and Coogan, 2006). The Tidwell Member was deposited in fluvial, lacustrine (numerous lakes and ponds), and coastal-plain environments (Doelling and Kuehne, 2012). The Salt Wash Member was deposited in an anastomosing system of well-preserved braided or meandering rivers and streams on a broad floodplain (Doelling and others, 2010). These fluvial systems flowed in a general east-northeast direction from highlands in eastern Nevada and northern Arizona (Blakey and Ranney, 2008). The Brushy Basin Member was deposited by a northeast-flowing meandering river system (although individual channels flowed in different directions) on a floodplain that contained large lakes and ponds; the climate was hot and humid (Blakey and Ranney, 2008). Gas is produced from the upper Morrison in the southeastern Uinta Basin.

Figure 2.9. *Fluvial channel sandstone of the Salt Wash Member and pastel-colored floodplain mudstone and shale of the Brushy Basin Member, Upper Jurassic Morrison Formation, west flank of the San Rafael Swell along I-70; view to the northeast. Photograph by Michael Chidsey, Sqwak Productions Inc.*

CRETACEOUS ROCKS

During the Cretaceous, North America was divided into two large landmasses by the north-south oriented Cretaceous Interior Seaway, and part of the western shore was located in present-day eastern Utah. Cretaceous deposition in the Uinta Basin was controlled by the Sevier orogeny, which uplifted a north-south trending mountain belt in western Utah, and created a subsiding basin in eastern Utah that received some 15,000 feet (4600 m) of sedimentary outwash from the eroding mountain belt (Hintze and Kowallis, 2009). The mountain belt was composed of folded and thrust faulted Mesozoic, Paleozoic, and Precambrian rocks. Cretaceous deposits derived from these units consist of clastic rocks laid down along a coastal plain where coal-bearing non-marine sandstones and conglomerates interfinger with nearshore deposits and grade eastward into marine shale of the mid-continental Interior Seaway. This belt of coastal-plain facies shifted from west to east across the Uinta Basin in Cretaceous time. These facies reflect a balance between changing sediment supply from the advancing Sevier orogenic belt in western Utah and changes in accommodation space resulting from transgressions and regressions of the Cretaceous Interior Seaway in eastern Utah and from variations in tectonic subsidence (Armstrong, 1968; Hintze and Kowallis, 2009). In the Uinta Basin and surrounding areas, the Cretaceous section consists of (in ascending order): the Cedar Mountain Formation, Dakota Sandstone, Mowry Shale, Frontier Formation, Mancos Shale, and Mesaverde Group (figures 1.5 and 2.1).

Lower and Lower Upper Cretaceous Rocks

The Lower and lower Upper Cretaceous Cedar Mountain and Dakota Formations are significant producers of gas from tight sandstone reservoirs in the southeastern Uinta Basin. Productive units are typically lenticular, discontinuous fluvial sandstone beds that can be observed in outcrop reservoir analogs around the basin.

Cedar Mountain Formation

The Cedar Mountain Formation (Early to early Late Cretaceous [Barremian to early Cenomanian] in age [Doelling and Davis, 1989; Cifelli and others, 1997, 1999; Kirkland and others, 1998, 2016; Burton and others, 2006]) is divided into two members in the subsurface of the Uinta Basin: the basal Buckhorn Conglomerate and the Ruby Ranch. These members are exposed along the flanks of the San Rafael Swell and farther to the east, and in the Split Mountain area north of the basin (Currie and others, 2008, 2012) (figure 2.10). The Buckhorn, where present, is recognized in well logs in the Uinta Basin whereas the other members are generally not discernable. The contact between the Cedar Mountain and the Morrison is also difficult to recognize when the Buckhorn Conglomerate Member is absent and thus the two formations are mapped together in the subsurface. In San Rafael Swell outcrops, this situation places the Ruby Ranch Member of the Cedar Mountain over the Brushy Basin Member of the Morrison Formation—both create colorful, banded steep slopes and badland topography. However, the Cedar Mountain has (1) a more drab variegated color, (2) less smectite clay, (3) the presence of polished chert pebbles (gastroliths), (4) abundant carbonate nodules, and (5) a thick paleosol at the base (Kirkland and Madsen, 2007; Currie and others, 2008, 2012; Kirkland and others, 2016). The contact with the overlying Dakota Formation is an unconformity with varying relief depending on the presence or absence of the Buckhorn (Currie and others, 2008, 2012; Doelling and others, 2009; Kirkland and others, 2016).

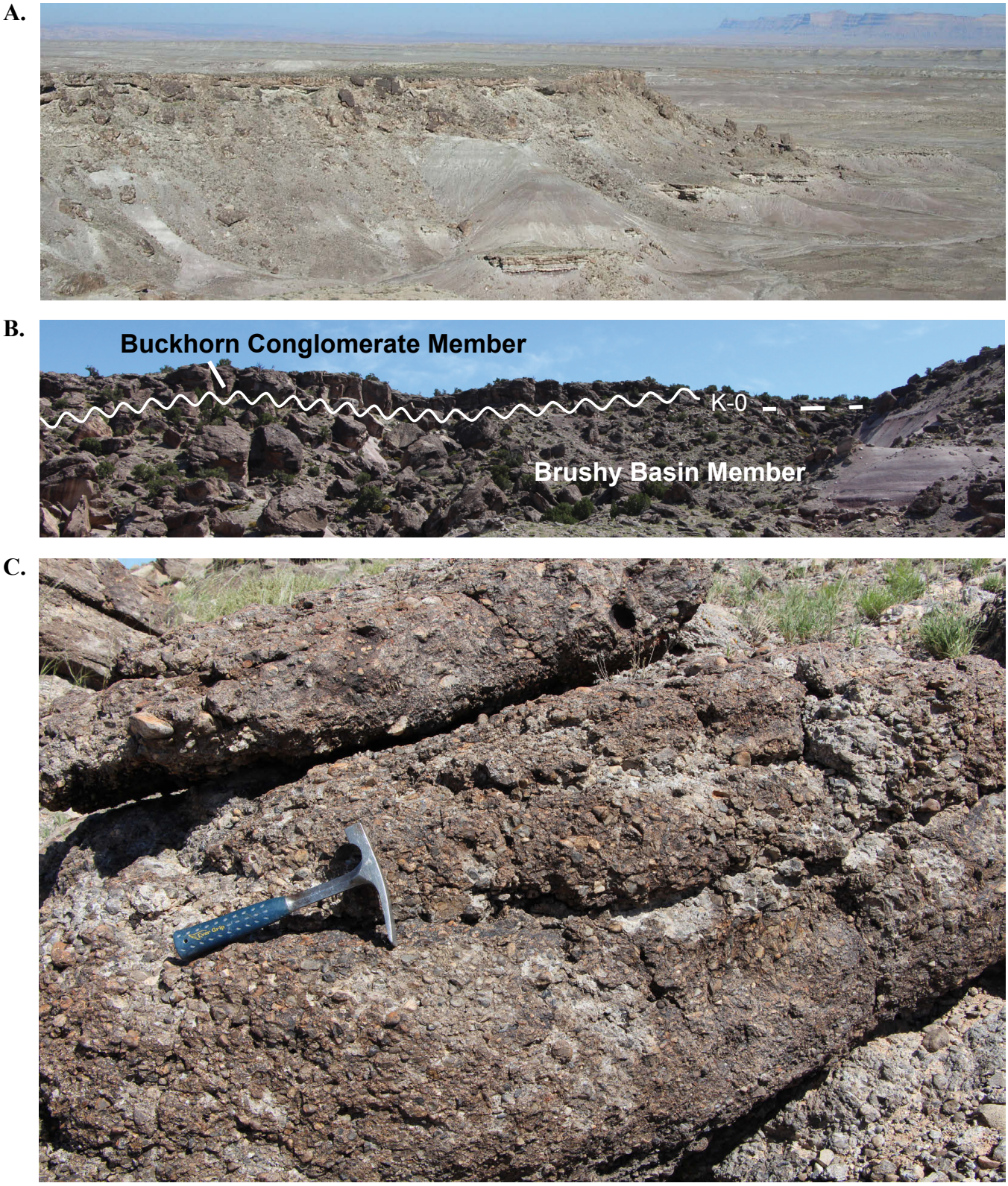

Figure 2.10. *Representative outcrops of the Lower to lower Upper Cretaceous Cedar Mountain Formation.* ***A.*** *Floodplain and fluvial channel deposits of the Ruby Ranch Member, southwest of Green River, Utah; view to the north. Photograph courtesy of David E. Eby, Eby Petrography & Consulting, Inc.* ***B.*** *Basal, and discontinuous, Buckhorn Conglomerate Member overlying the Brushy Basin Member of the Upper Jurassic Morrison Formation, west flank of the San Rafael Swell along I-70; view to the north. The contact is marked by the K-0 unconformity.* ***C.*** *Close-up of typical Buckhorn conglomerate consisting of pebbles and cobbles composed of poorly to moderately sorted, subangular to well-rounded clasts of white quartzite and black, brown, light brown, and light gray chert. Photographs B and C by Michael Chidsey, Sqwak Productions Inc.*

The Buckhorn Conglomerate Member (Barremian to Aptian) is discontinuous within the San Rafael Swell and Uinta Basin, ranging in thickness from 0 to 80 feet (0–24 m) (Hintze and Kowallis, 2009). It consists of gray to dark brown conglomerate to conglomeratic sandstone with subordinate amounts of sandstone and mudstone (figure 2.10B). Pebbles and cobbles are composed of poorly to moderately sorted, subangular to well-rounded clasts of white quartzite, and black, brown, light brown, and light gray chert (figure 2.10C). Conglomerate beds are either clast supported or supported by a matrix of clay or medium- to coarse-grained sandstone. Bedding is lenticular, thick to very thick, and trough cross-stratified; beds generally fine upward and form single cliffs or ledges.

The Ruby Ranch Member (Aptian to Albian) ranges in thickness from 60 to 130 feet (20–40 m) and consists of subtle bands of dark gray to dark purplish gray mudstone and tan to gray sandstone (figure 2.10A) (Doelling and others, 2009; Doelling and Kuehne, 2012; Kirkland and others, 2016). Mudstone is clayey and silty with local lenticular sandstone beds. Sandstone is fine grained to pebbly, poorly sorted, trough cross-stratified, and discontinuous, and usually occurs in the upper half of the section. The Ruby Ranch is medium to thick bedded, with mudstone forming steep, rounded slopes, whereas sandstone produces ledges and cliffs.

The Cedar Mountain Formation represents the continuation of continental deposition that began during the Late Jurassic. By Early Cretaceous time, the Sevier orogenic belt was emerging in western Utah (Armstrong, 1968). East-central Utah was the site of deposition in alluvial plains, fluvial channels, and floodplains (similar to the depositional environments of the Morrison Formation) in a back-bulge to foredeep setting; the climate was arid, becoming wetter during deposition of the upper section (Currie, 1998; DeCelles and Coogan, 2006). The Buckhorn Conglomerate was deposited in gravel-filled channels of a northeast-flowing fluvial system originating from the rising highlands to the west (Yingling, 1987; Currie, 1998). The Ruby Ranch Member was deposited in fluvial channel and floodplain environments. Sandstone beds represent levee, generally linear to low-sinuosity channel-fill, and point-bar deposits.

Dakota Formation

The Dakota Formation is time-transgressive in the study area and is considered to be Early Cretaceous (Albian) in the Uinta Basin (Sprinkel, 2007, 2009) and Late Cretaceous (Cenomanian) farther south (Gualtieri, 1988; Witkind, 1988). The Dakota, unlike other formations, is thin and not widespread in the San Rafael Swell, and within the Uinta Basin it is often mapped together with the underlying Cedar Mountain Formation. Hydrocarbon production from the two formations is often commingled. The Dakota ranges in thickness from 0 to 100 feet (0–30 m), consisting of light yellow, tan, yellow-brown, orange-gray, light tan-gray, or light brown sandstone, conglomeratic sandstone, conglomerate, shale, and coal, particularly east of the San Rafael Swell (Witkind, 1979, 1980, 1988; Doelling, 2002; Doelling and others, 2009; Kirschbaum and Schenk, 2011; Doelling and Kuehne, 2012). Sandstones are friable, quartzitic, fine to coarse grained, and moderately to well sorted. Conglomerates contain rounded to subrounded pebbles of chert and quartzite. Sandstones and conglomerates are thin to thick bedded, cross-stratified (trough and planar); some ripples and convolute bedding are also present. The upper part is lenticular sandstone, 5 to 12 feet (1.5–4 m) thick and encased in mudrock (Kirschbaum and Schenk, 2011). Shale beds are commonly the only rocks that represent the Dakota section. The Dakota weathers to form mound-like hills and discontinuous ridges or small cliffs (figures 2.11 and 2.12). The contacts with the conformably overlying Mancos or Mowry Shales are defined by the first appearance of deeper-water marine shales compared to those in the Dakota (Molenaar and Cobban, 1991; Doelling and others, 2009; Doelling and Kuehne, 2012).

In general, the Dakota Formation was deposited in swamps, beaches, bars, and marginal-marine environments associated with the approaching Cretaceous Interior Seaway from the northeast (Blakey and Ranney, 2008). The lower section is interpreted as a fluvial/braided stream system whereas the upper section of mud-encased lenticular sandstone was deposited in low-energy, anastomosed channels on an alluvial and coastal floodplain setting (Kirschbaum and Schenk, 2011).

Upper Cretaceous Rocks

Upper Cretaceous deposits reflect transgressive-regressive cycles associated with the western shore of the Cretaceous Interior Seaway, and contacts between formations are mostly gradational. The Dakota Formation is overlain by the Mowry Shale and Frontier Formation in the northern Uinta Basin and the region farther north. Above the Frontier in the north and the Dakota in the south, the massive and regionally extensive Mancos Shale epitomizes the various deposits resulting from the Cretaceous Interior Seaway on its western margin, and the influence of the Sevier orogenic belt in western Utah. The lower formations of the Upper Cretaceous Mesaverde Group interfinger with the upper part of the Mancos Shale. The Mesaverde is composed of at least four to six main formations, depending on its location in the Uinta Basin, which record several transgressive-regressive cycles and the eventual withdraw of the Cretaceous Interior Seaway (figure 2.13). The combined thickness of the Mancos and Mesaverde is nearly 8000 feet (2400 m) in the Uinta Basin. Deposition of these units took place from ~93 to 70 Ma as the shoreline of the seaway transgressed to the south and west, and then gradually regressed back to the east.

The tight sandstone beds within the formations of the Mesaverde Group are the major gas producer (along with the Tertiary Wasatch Formation, to be discussed later) in the east-

Figure 2.11. *Typical exposures of Upper Cretaceous Dakota Formation, west flank of the San Rafael Swell along I-70; view to the north. Photograph courtesy of Michael Chidsey, Sqwak Productions Inc.*

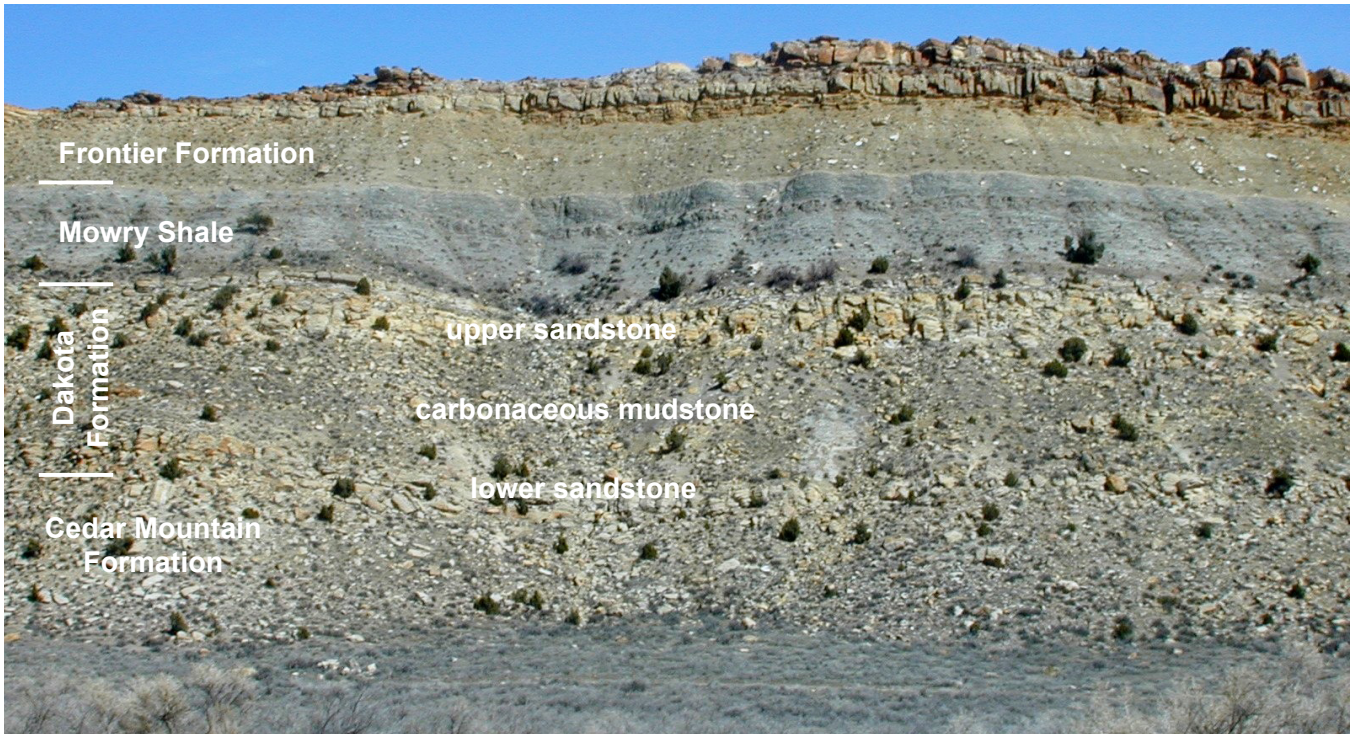

Figure 2.12. *Typical exposures of the brownish-colored Upper Cretaceous Dakota Formation, silver gray Mowry Shale, and overlying brownish slope and cliff of the Frontier Formation along U.S. 191 east of Steinaker Reservoir near Vernal, Utah; view to the east. The Dakota consists of basal and upper sandstone units separated by a middle carbonaceous mudstone. The Frontier consists of a lower slope-forming zone of calcareous shale and silty shale, and an upper part composed of fine-grained sandstone that forms the prominent cliff (from Sprinkel and others, 2012). Photograph by Doug Sprinkel, UGS.*

ern Uinta Basin. The coal beds in the Blackhawk and Neslen Formations in the Mesaverde are the source of much of the non-associated gas in the basin. The Mancos Shale is a secondary drilling target with shale-gas resource potential in the Uinta Basin.

Mowry Shale

The Mowry Shale (Cenomanian) is found in wells within the northeastern Uinta Basin and in outcrop around the eastern Uinta Mountains (as well as in the subsurface of the Green River Basin of southwestern and other regions of Wyoming). The Mowry is a thin (less than 70 feet [20 m] thick within the Uinta Basin [Hintze and Kowallis, 2009]), dark gray, fissile, siliceous shale that weathers characteristically silver-gray (figure 2.12). It also contains bentonite (ash) beds, with swelling clays, used to obtain radiometric ages. The Mowry forms slopes or strike valleys where shale chips in the soil are commonly the only evidence of its presence (Sprinkel, 2009; Gregson and others, 2010). In Wyoming, the Mowry is organic-rich and serves as a source rock for hydrocarbons in the thrust belt and elsewhere (Nixon, 1973). In the Uinta Basin area, the contact with the overlying Frontier Formation is an unconformity represented by a time gap of about 5 million years (Sprinkel, 2009).

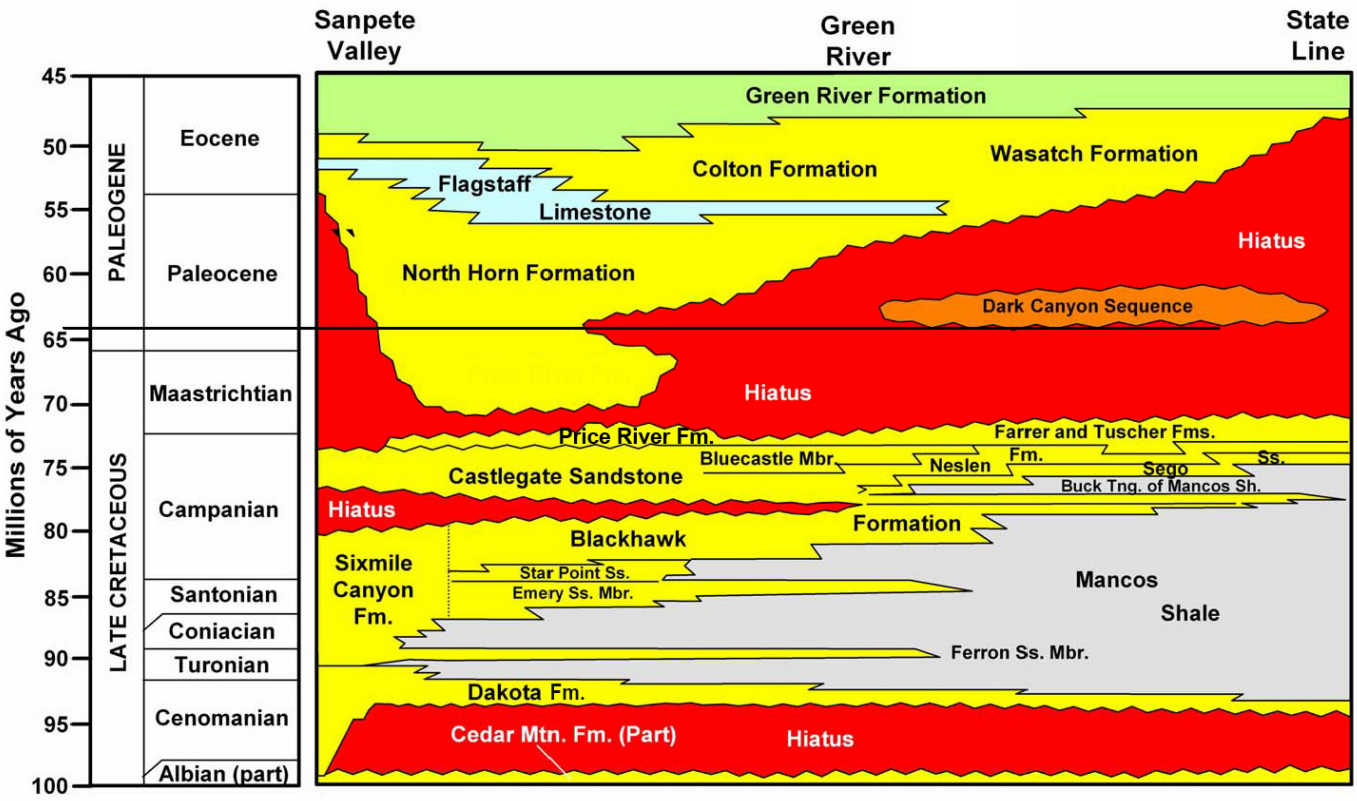

Figure 2.13. *Chronostratigraphic chart for Late Cretaceous–Paleogene strata in the Book Cliffs–Wasatch Plateau region (modified from Fouch and others, 1983; Franczyk and others, 1990a; White and others, 2008).*

The Mowry Shale was deposited in a shallow, open-marine environment during the westernmost transgression of the Cretaceous Interior Seaway. The Mowry contains abundant fish scales, as well as ammonites, bivalves, and shark teeth (Hansen and others, 1983).

Frontier Formation

The Frontier Formation (Turonian), like the Mowry Shale, is found in wells within the northeastern Uinta Basin and in outcrop (figure 2.12) around the eastern Uinta Mountains (as well as in the subsurface of the Green River Basin of southwestern and other regions of Wyoming where it is a major hydrocarbon producer). In the Utah area of Dinosaur National Monument, the Frontier ranges in thickness from 100 to 200 feet (30–60 m) (Hintze and Kowallis, 2009). It consists of upper and lower parts separated by a medial shale. The lower part is composed of soft, light to dark gray calcareous shale, silty shale, and siltstone with some minor limestone beds and coal; it forms slopes and saddles. The upper part is light brown to light greenish-gray, fine-grained sandstone that forms prominent cliffs. It is thin to very thick bedded, containing cross-stratification and ripple marks (Hansen and others, 1983; Sprinkel, 2009; Gregson and others, 2010).

The Frontier Formation was deposited in nearshore marine and coastal swamp environments as the sea temporarily regressed to the east (Gregson and others, 2010). As evidence of this nearshore environment, the Frontier contains bivalves, ammonites, gastropods, and petrified wood (Hansen and others, 1983). The Ferron Sandstone Member of the Mancos Shale is the approximate stratigraphic equivalent of the Frontier and is found on the south and west edges of the Uinta Basin.

Mancos Shale

The Upper Cretaceous (Turonian to Campanian) Mancos Shale produces a drab, barren landscape (figure 2.14). The thickness of the Mancos exceeds 5000 feet (1500 m) in certain places within the Uinta Basin (Hintze and Kowallis, 2009). The Mancos is divided into as many as eight formal and informal units along the west flank of the San Rafael Swell and in the Uinta Basin. However, most units do not occur throughout the study area, so a single outcrop or wellbore will not encounter them all. In approximate ascending order the units are: Tununk, Ferron Sandstone/Juana Lopez, lower Blue Gate, Emery Sandstone, Prairie Canyon/Mancos B, upper Blue Gate, and Buck Tongue. The Ferron interfingers with the Juana Lopez Member to the east where much of the sandstone has pinched out. The Emery and the somewhat younger Prairie Canyon Member in the Book Cliffs and the Mancos B zone in the subsurface of the Uinta Basin divide the Blue Gate into informal lower and upper members. The Prairie Canyon/Mancos B are coeval with the lower Blackhawk Formation of the Mesaverde Group to the west. The Buck Tongue, the uppermost unit of the Mancos, is a marine shale that thins

Figure 2.14. *Classic outcrop of the basal Tununk Member of the Mancos Shale composed of soft and deeply weathered slopes and low, rounded hills devoid of vegetation, and small vertical cliffs, west flank of the San Rafael Swell near I-70; view to the northwest. Photograph by Michael Chidsey, Sqwak Productions Inc.*

and pinches out to the west, interfingering with the Mesaverde Group, as exposed in the eastern Book Cliffs and identified in the subsurface of the eastern Uinta Basin.

The basal Tununk (early Turonian) and Blue Gate Members (Turonian-Campanian), and Buck Tongue (Campanian) have very similar characteristics. They consist of light to dark gray, medium to dark brown or black shale, shaley siltstone, and mudstone. Shale is fissile, breaking into thin, platy fragments. Some shale beds are bentonitic, providing regional correlation markers. Bedding is indistinct or even, thin, and laminated with a few siliceous zones that create small ledges. However, for the most part these members are soft and deeply weathered, forming slopes and low, rounded hills devoid of vegetation (figures 2.14 and 2.15). They contain marine fossils including bivalves, cephalopods, fish scales, and a few shark teeth.

The Ferron Sandstone (Turonian) is spectacularly exposed along the west flank of the San Rafael Swell (figure 2.15) where it consists of yellow-gray, light brown, to white sandstone and siltstone, gray sandy to black carbonaceous shale, and coal. Sandstone is very fine to medium grained, poorly to moderately sorted, with subrounded to angular clasts. Sedimentary structures in sandstone that determine facies include ripples, channel scours, soft-sediment deformation to contorted bedding, cross-stratification (trough, swaley, and hummocky), and planar beds. Many beds contain rooted zones, a variety of burrows, or intense bioturbation. Bedding in sandstone is thin or lenticular to very thick, forming vertical cliffs, whereas siltstone, shale, and coal create recesses and slopes. Coal beds are persistent but lenticular and often burned (due to spontaneous combustion or lightning strikes), leaving "clinker" zones with red oxidation staining. To the east, the Juana Lopez Member is a light to dark gray, organic-rich, thin- to medium-bedded, heterolithic zone of shale and shaly siltstone.

The low cliff-forming Emery Sandstone (Santonian) is divided into lower and upper sandstone units, which are separated by a middle shale unit (Witkind, 1988). The lower and upper units consist of light brown to yellowish-brown, thin- to medium-bedded, locally cross-stratified, very fine grained quartzose sandstone. The middle unit consists of light gray to gray, thin- and even-bedded shale and shaly siltstone. The Prairie Canyon Member (or Mancos B) (Santonian-Campanian) consists of thinly interbedded and interlaminated, very fine grained to fine-grained sandstone, siltstone, and claystone (Hettinger and Kirschbaum, 2002) and separates the Blue Gate into the upper and lower members in the central and eastern parts of the Uinta Basin. The Mancos B is a correlative to the Prairie Canyon Member and major gas producer in Colorado.

The shale members of the Mancos Shale were deposited in shallow, open-marine environments during major and rapid western transgressions of the Cretaceous Seaway. The Ferron Sandstone exposed along the west flank of the San Rafael Swell was deposited in fluvial-dominated and wave-modified

Figure 2.15. *The Tununk and Ferron Sandstone Members of the Upper Cretaceous Mancos Shale along the west flank of the San Rafael Swell near I-70; view to the east. Photograph by Michael Chidsey, Sqwak Productions Inc.*

deltaic environments that prograded eastward into the Cretaceous Interior Seaway. The alluvial to lower delta or coastal plain of the Ferron contained meander belts, swamps and peat bogs, levees, crevasse splays/overbanks, bays, distributary channels, mouth bars, and shoreface facies. To the east, the Juana Lopez and Prairie Canyon Members may represent offshore bars produced by longshore drift or sand plumes that accumulated on the shallow-marine shelf.

Mesaverde Group

The Upper Cretaceous Mesaverde Group (Campanian-Maastrichtian) represents clastic deltaic packages that prograded east and interfinger with the upper Mancos Shale (figure 2.13) (Cole and others, 2008) and with later coastal to alluvial-plain deposits as the Cretaceous Interior Seaway finally withdrew farther to the east. The Mesaverde Group ranges between 600 and about 4000 feet (180–1200 m) thick in and around the Uinta Basin (Hintze and Kowallis, 2009) and is spectacularly exposed in the Book Cliffs along the southern margin of the basin. In the western Books Cliffs, the Mesaverde consists of, in ascending order, the Star Point, Blackhawk, Castlegate, and Price River Formations. In the eastern Book Cliffs, near the state line, and the eastern Uinta Basin, including the Greater Natural Buttes area, the Mesaverde is composed of thinner Blackhawk and Castlegate (the Star Point has pinched out) and the Sego and Neslen Formations (equivalent to the middle and upper [Bluecastle Sandstone Member] Castlegate), and the Farrer and Tuscher Formations (equivalent to the lower Price River, the upper section also having pinched out) (figure 2.13).

Star Point Sandstone: The Star Point Sandstone (Campanian) consists of 20 to 300 feet (6–90 m) of light brown to brown, fine- to medium-grained, platy, quartzose sandstone, and some shale partings and interbeds of shale and shaly siltstone (Weiss and others, 1990; Hintze and Kowallis, 2009). Depending on the facies, it displays graded bedding, laminated bedding, cross-stratification, burrowing, and flute casts or sole marks. The Star Point forms prominent cliffs in the westernmost Book Cliffs and eastern Wasatch Plateau but thins and pinches out east and southeast of Price, Utah (Newman and Chan, 1991); it is not recognized in the subsurface of the central and eastern Uinta Basin.

The Star Point Sandstone was deposited in deltaic to beach/nearshore marine environments (Weiss and others, 1990; Newman and Chan, 1991). Facies include prodelta, lower and upper delta-front to shoreface, and distributary mouth bar and channel.

Blackhawk Formation: The Blackhawk Formation (Campanian) is the major coal-producing unit in Utah. It ranges in thickness from 660 to 1500 feet (200–460 m) (Hintze and Kowallis, 2009). The Blackhawk is dominantly light-brown, locally light-gray and brownish-gray, thin- to thick-bedded, fine- to medium-grained quartzose sandstone, with interbeds of shaly siltstone, shale, carbonaceous shale, and coal (figure 2.16A) (Weiss and others, 1990). Sandstone beds contain a wide variety of sedimentary structures, including burrowing or intense bioturbation, ripples, channel scours, soft-sediment deformation, cross-stratification and planar beds, hummocky beds, and rooted zones. The Blackhawk is composed of as many as six members, in ascending order: Spring Canyon, Aberdeen, Kenilworth, Sunnyside, Grassy, and Desert (Young, 1955); only the Desert Member is present in the eastern Books Cliffs (figure 2.16B). These members form steep slopes and cliffs (i.e., the Book Cliffs).

The Blackhawk Formation was deposited in a lower coastal plain where wave-dominated deltaic processes formed beach environments. Peat swamps that developed landward and along barrier islands/strandlines provided the organic-rich environments that formed the coal-bearing strata. Facies include prodelta (which grades laterally eastward into the Mancos Shale), shoreface, distributary mouth bar and channel, lagoon, bay, swamp and peat bog, levee, crevasse splay/overbank, and coastal plain. The silt-rich lower shoreface and heavily bioturbated middle shoreface facies represent lower energy deposition; hummocky bedding in sandstone indicates short-lived, higher energy storm events. The "clean" cross-stratified upper shoreface and planar-bedded foreshore (beach) represent high-energy surf and swash zones; the tidal range was microtidal (Thomas A. Ryer, The ARIES Group, Inc., verbal communi-

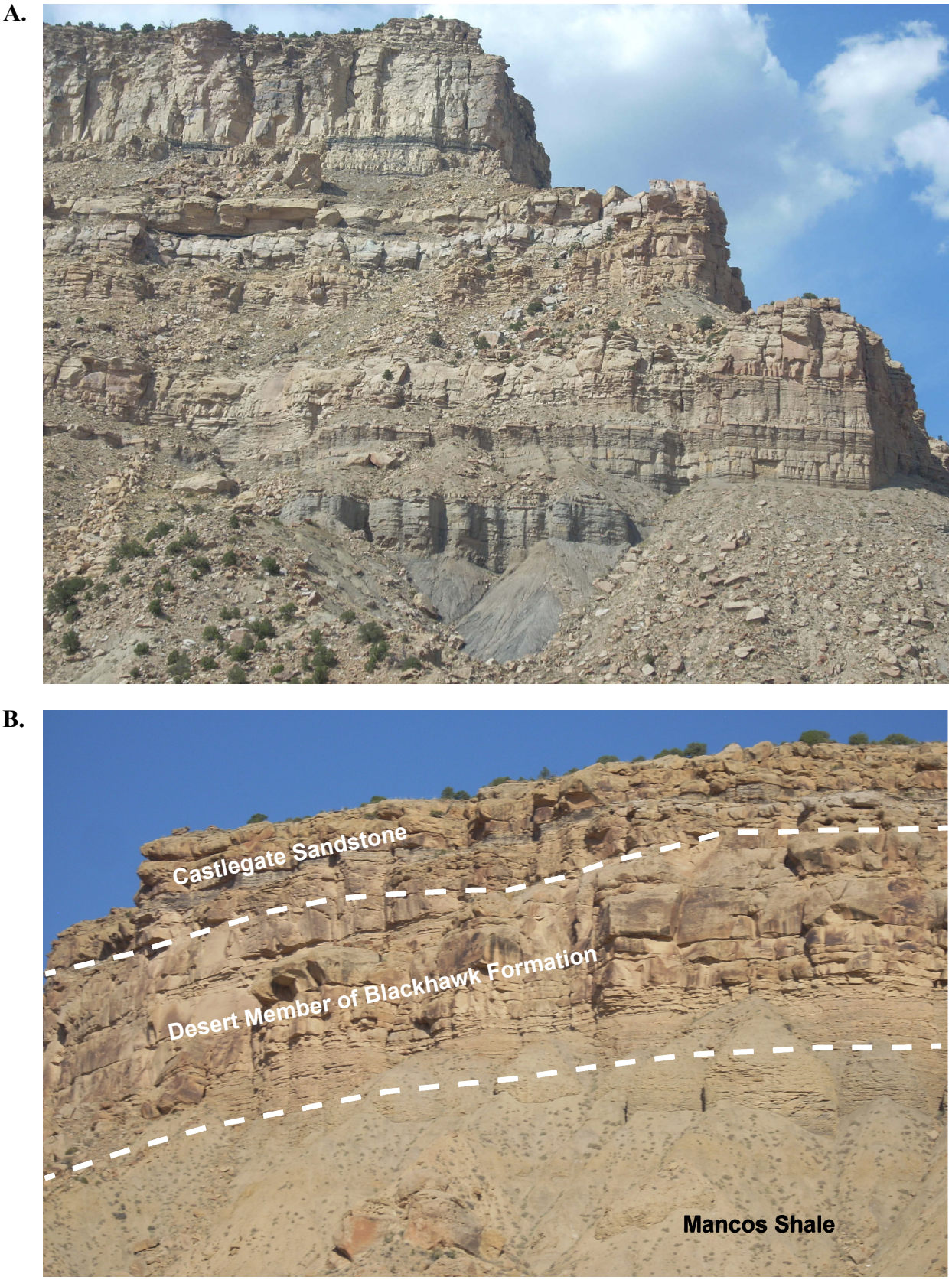

Figure 2.16. *Blackhawk Formation outcrops in the Book Cliffs.* ***A.*** *Typical section of the Blackhawk Formation showing shoreface sandstone beds and coal; between Price and Green River, Utah, along U.S. Highway 6, view to the east.* ***B.*** *The Desert Member of the Blackhawk Formation overlying the Mancos Shale and underlying the Castlegate Sandstone in the eastern Book Cliffs near the mouth of Thompson Canyon, Utah; view to the north. Note that all lower members of the Blackhawk are missing here, as well as any coal beds, having pinched out west of this location. The Castlegate consists of shoreface, fluvial, and estuarine facies. Photographs by Rebekah Stimpson, UGS.*

cation, 1994). The tops of foreshore sandstone beds are often a distinct white color and rooted where overlain by organic-rich coastal plain facies, often with tannic acids, which could bleach the underlying sandstone (Paul B. Anderson, consulting geologist, written communication, 2016).

Castlegate Sandstone: The Castlegate Sandstone (Campanian) consists of 0 to 780 feet (0–240 m) of light gray to dark gray, platy, very fine to coarse-grained quartzose sandstone (figures 2.16B and 2.17), with some conglomerate beds (Weiss and others, 1990; Hintze and Kowallis, 2009). In the eastern Book Cliffs, the Castlegate thins and becomes interbedded with minor siltstone, carbonaceous to non-carbonaceous shale, and lenses of sandy and silty marl (figure 2.16B) (Gualtieri, 1988). Bedding is laminated, thin, to medium and often lenticular, containing cross-stratification, cross-laminations, hummocky beds, and ripple marks. In the central part of the Book Cliffs, the upper section of the Castlegate is called the Bluecastle Sandstone Member (figure 2.13). However, to the east, what remains of the lower Castlegate is overlain by the Buck Tongue of the Mancos Shale and the Bluecastle Sandstone Member is equivalent to the Neslen Formation (figure 2.13) or lower Farrer Formation (Fouch and others, 1983; Franczyk and others, 1990a; Cole and others, 2008; White and others, 2008). The Castlegate forms vertical cliffs and steep slopes. The contact with the underlying Desert Member of the Blackhawk Formation is a major flooding surface (transgressive surface of erosion) where Castlegate marine shoreface sandstone and shale overlie coal beds (Cole and others, 2008).

The Castlegate Sandstone in the western Book Cliffs represents a classic example of a sand-rich braided stream environment resulting from the continuing erosion of the Sevier orogenic belt to the west (figures 2.17 and 2.18A) (Blakey and Ranney, 2008). In the eastern Book Cliffs, the Castlegate transitions into coastal plain/meanderbelt and deltaic/marginal marine environments (figures 2.16B and 2.18A) (Fouch and others, 1992a; Cole and others, 2008). These environments include transitional shoreface, tidally influenced fluvial channel, and estuarine facies (Cole and others, 2008).

Sego Sandstone: The Sego Sandstone (Campanian), which overlies the Buck Tongue, consists of 50 to 200 feet (15–60 m) of very light gray to light brown fine-grained sandstone

Figure 2.17. *Castlegate Sandstone outcrop showing classic sand-rich braided stream facies, Price River Canyon, western Book Cliffs; view to the north. Photograph by Rebekah Stimpson, UGS.*

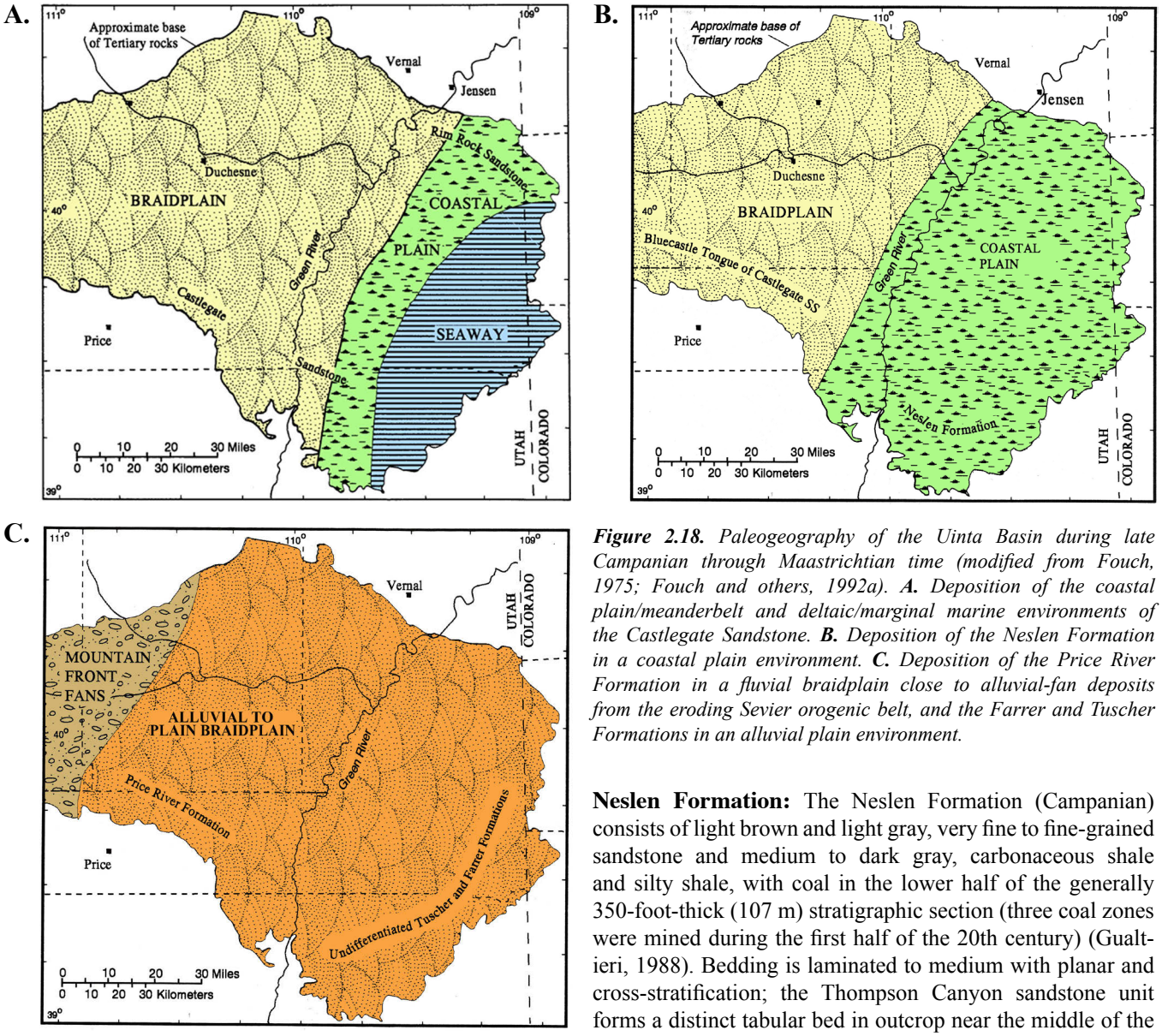

Figure 2.18. *Paleogeography of the Uinta Basin during late Campanian through Maastrichtian time (modified from Fouch, 1975; Fouch and others, 1992a).* ***A.*** *Deposition of the coastal plain/meanderbelt and deltaic/marginal marine environments of the Castlegate Sandstone.* ***B.*** *Deposition of the Neslen Formation in a coastal plain environment.* ***C.*** *Deposition of the Price River Formation in a fluvial braidplain close to alluvial-fan deposits from the eroding Sevier orogenic belt, and the Farrer and Tuscher Formations in an alluvial plain environment.*

with subordinate beds of sandy to silty shale that display a stacked series of coarsening- and thickening-upward intervals (figure 2.19) (Cole and others, 2008; Hintze and Kowallis, 2009). Laminated to medium beds are horizontal, cross-laminated, and cross-stratified (trough and sigmoidal), and contain a variety of sedimentary structures including ripples, mud drapes, scours, and burrows (Cole and others, 2008). The contact with the underlying Buck Tongue of the Mancos Shale is gradational (Gualtieri, 1988). The Sego forms cliffs and steep slopes (figures 2.19 and 2.20).

The Sego Sandstone was the last major marine complex in the Late Cretaceous, and represents a wide variety of depositional facies. These include shallow marine, wave-dominated shelf, tidal bar and creek, estuarine distributary channel and fill, fluvial channel, and oyster bioherm (Wood and Dutton, 1999; Cole and others, 2008).

Neslen Formation: The Neslen Formation (Campanian) consists of light brown and light gray, very fine to fine-grained sandstone and medium to dark gray, carbonaceous shale and silty shale, with coal in the lower half of the generally 350-foot-thick (107 m) stratigraphic section (three coal zones were mined during the first half of the 20th century) (Gualtieri, 1988). Bedding is laminated to medium with planar and cross-stratification; the Thompson Canyon sandstone unit forms a distinct tabular bed in outcrop near the middle of the Neslen. The Neslen generally coarsens upward with increasing channel-form sandstone toward the top of the formation (Cole and others, 2008). The Neslen forms ledges and steep slopes (figure 2.20). The contact with the underlying Sego Sandstone is sharp.

The Neslen Formation was deposited in a variety of depositional facies within a lower coastal plain environment (figure 2.18B). These facies include estuarine, swamp and marsh, meandering channels, and splays (Franczyk and others, 1990a; Cole and others, 2008; White and others, 2008). Sand bodies were deposited by straight (anastomosed) to moderately or highly sinuous rivers and distributary channels in wave-dominated deltas (White and others, 2008).

Farrer Formation: The Farrer Formation (Campanian) consists of gray to brown, fine- to upper-medium-grained sandstone and greenish-gray silty shale with subordinate amounts of carbonaceous shale in the lower section (Gualtieri, 1988).

Figure 2.19. *Outcrop of coarsening-upward lower Sego Sandstone in gradational contact with the Buck Tongue of the Mancos Shale, eastern Book Cliffs (Sego Canyon); view to the north. Photograph by Rebekah Stimpson, UGS.*

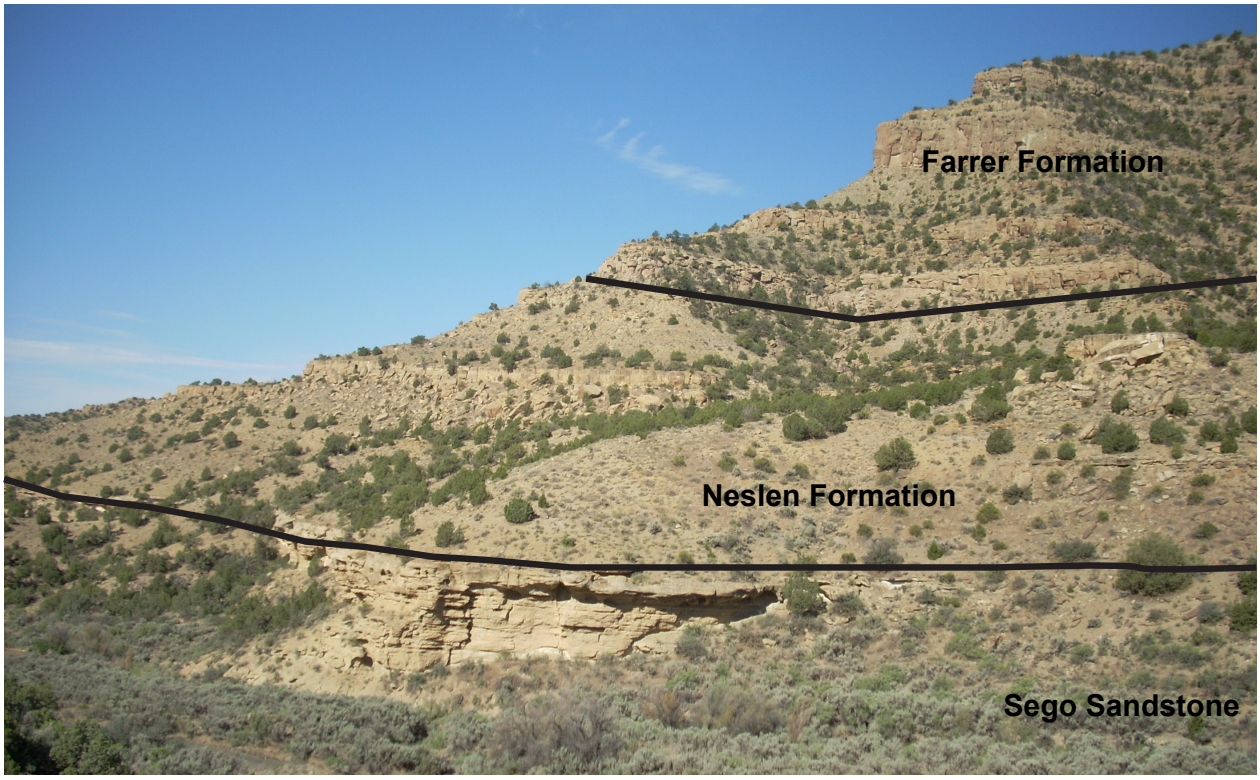

Figure 2.20. *Stratigraphic section in Sego Canyon, eastern Book Cliffs, showing, in ascending order, Sego Sandstone, Neslen Formation, and Farrer Formation; view to the west. Photograph by Rebekah Stimpson, UGS.*

Bedding is thin to thick, and sandstone beds are commonly well sorted, cross-stratified, ripple laminated, or contorted (Cole and others, 2008). The 430- to 1200-foot-thick (130–370 m) Farrer Formation is sand rich in comparison to the underlying Neslen Formation (figure 2.20) and the contact between them is gradational (Cole and others, 2008; Hintze and Kowallis, 2009). The Farrer forms small cliffs, ledges, and steep slopes.

The Farrer Formation was deposited in an upper coastal plain to alluvial plain environment, but farther landward of the seaway compared to the underlying Neslen Formation (figure 2.18C) and thus lacks swamp and marsh facies. The Farrer facies include east- and northeast-flowing, meandering, low- to moderate-sinuosity fluvial channels and braided streams, represented by single and multistoried sandstone bodies and associated floodplain deposits with splay sands (Cole and others, 2008; White and others, 2008).

Price River Formation: The Price River Formation (Campanian and Maastrichtian) consists of a sequence of alternating beds, up to 3000 feet (900 m) thick (Hintze and Kowallis, 2009), composed of light gray to gray, and grayish-brown to dark gray, poorly to moderately sorted, fine- to medium-grained sandstone, siltstone, and mudstone. The formation coarsens to the west with some beds of conglomerate and conglomeratic sandstone, and fines to the east with increased amounts of carbonaceous shale beds (Anderson, 1983; Weiss and others, 1990). The formation is thin bedded to massive, commonly thick bedded, and contains horizontal and cross-stratification, ripple marks, and disseminated carbonaceous material (Anderson, 1983). Sandstone beds in the lower section fine upward, are lenticular, and grade into one another (Anderson, 1983). The Price River forms steep, step-like slopes and ledges generally leading to an uppermost cliff (figure 2.21). Fouch and others (1983) and Hintze and Kowallis (2009) place a relatively minor unconformity at the top of the Price River Formation separating it from the overlying Maastrichtian-Paleocene North Horn Formation (figure 2.13).

The Price River Formation represents northeast-flowing, meandering fluvial deposition over a fluvial braidplain (Lawton, 1986; Hettinger and Kirschbaum, 2002) (figure 2.18C). Conglomerates were deposited closer (westward) to the eroding Sevier orogenic belt, at the edge of prograding alluvial fans.

Tuscher Formation: The Tuscher Formation (Maastrichtian) consists of brown and gray, well-sorted, fine- to medium-grained sandstone and greenish-gray silty shale with subordinate conglomerate in the uppermost section (Gualtieri, 1988). The 430- to 650-foot-thick (130–200 m) Tuscher has a significantly higher sand content compared to the underlying Farrer Formation; however, in outcrop the contact between the two is often difficult to distinguish (Cole and others, 2008; Hintze and Kowallis, 2009). The Tuscher section is characterized by a series of amalgamated, multi-storied sandstone bodies separated by thin mudrock beds that form vertical cliffs and small slopes (figure 2.22). These sandstone bodies are typically thick bedded and diplay low-angle inclined and cross-stratification, ripple laminations, contorted bedding, and scours and channel fills (Cole and others, 2008). The top of the Tuscher is marked by a major unconformity (figure 2.13).

The Tuscher Formation was deposited on an upper coastal plain to alluvial braidplain (figure 2.18C). The Tuscher facies are similar to those of the underlying Farrer Formation but are more sand rich. The amalgamated sandstone bodies represent northeast- to southeast-flowing, high-energy to low-sinuosity braided fluvial systems (Cole and others, 2008; White and others, 2008).

TERTIARY ROCKS

A major regional unconformity exists between the Mesaverde Group and the overlying Tertiary rocks (and the latest Late Cretaceous rocks where they are present [i.e., North Horn Formation]) in eastern Utah (figure 2.13). A transition from the Sevier orogeny to the Laramide orogeny occurred during the Late Cretaceous and early Tertiary, which resulted in the rise of the Uinta Mountains, the Uncompahgre uplift, and the San Rafael Swell, and the coeval subsidence of the Uinta Basin in eastern Utah. In addition, during the earliest Paleocene a depositional trough extended from the western Uinta Basin to the southwest along the margin of the Sevier orogenic belt and was the site of clastic deposition. These deposits lie unconformably above Cretaceous strata tilted during the last phase of the Sevier orogeny (Hintze and Kowallis, 2009). During much of late Paleocene and Eocene time, the Uinta Basin and much of central and southern Utah was dominated by freshwater lakes and associated deltas, with periods of alluvial clastic deposition as the lakes eventually disappeared. The combined thickness of the alluvial and lacustrine Tertiary rocks in the Uinta Basin ranges from 5000 feet (1500 m) to as great as 10,000 feet (3000 m) in the deepest part the asymmetric basin (Hintze and Kowallis, 2009).

The tight, lenticular sandstone beds within the Paleocene-Eocene Wasatch Formation are gas producers in the eastern Uinta Basin; however, where naturally fractured and overpressured in the deep center of the basin, they also produce oil. Fluvial-deltaic sandstone in the Eocene Green River Formation interfingering with carbonate and muddy lacustrine rocks is the major producer of oil in the Uinta Basin. The organic-rich shale and marlstone within the Green River provide the source for these oil accumulations in the Uinta Basin.

North Horn Formation

The North Horn Formation includes the uppermost Maastrichtian but is mainly lower Paleocene. It consists of 0 to 2500 feet (0–760 m) of tan, fine- to medium-grained, upward-fining

Figure 2.21. *Representative outcrop of fluvial siltstone and sandstone in the Upper Cretaceous Price River Formation along the Green River, Desolation Canyon; view to the east. From Morgan (2003a); photograph by Logan MacMillan, Consulting Geologist.*

Figure 2.22. *Representative outcrop of stacked amalgamated sandstone bodies of the Tuscher Formation, eastern Book Cliffs (Sego Canyon); view to the northwest. Photograph by Rebekah Stimpson, UGS.*

sandstone and reddish-brown and grayish-brown mudstone, with interbedded calcareous siltstone, limestone conglomerate, freshwater clay-rich limestone (marlstone), and some carbonaceous shale and minor coal (Anderson, 1983; Weiss and others, 1990; Hintze and Kowallis, 2009). Bed thickness is thin to medium, and sandstone beds are lenticular, conglomeratic at the base, and laterally discontinuous; some units contain minor amounts of plant detritus and oncolites. The North Horn is divided into three intervals: lower and upper variegated intervals separated by a sandy coal-bearing middle section (Lawton, 1986; Lawton and others, 1993). The North Horn forms steep slopes and ledges (figure 2.23) and thins abruptly eastward; it is not present in the eastern half of the Uinta Basin. In the west part of the basin, the North Horn intertongues with the Flagstaff Limestone to such an extent that the two formations are often mapped as an undivided unit (Witkind, 1988; Weiss and others, 1990).

The Cretaceous-Tertiary boundary (K-T boundary) lies within the middle section of the North Horn Formation. Latest Cretaceous dinosaur bones are found in the lower North Horn and Paleocene mammals have been discovered in the upper section (Spieker, 1946; Anderson, 1983). However, an iridium-rich clay layer to identify the exact stratigraphic location of the K-T boundary has yet to be discovered (Myung-Suk and Cross, 1997; Difley and Ekdale, 2002). A distinctive, white (bleached) kaolinite-rich sandstone can be traced throughout much of the formation; Weiss and others (1990) have suggested this bed as the possible boundary.

The North Horn Formation was deposited in a widespread terrestrial, high-energy environment, represented by fluvial, lacustrine, and floodplain facies (Lawton, 1986; Lawton and others, 1993). Sediments accumulated in the depositional trough that extended from the western Uinta Basin to the southwest along the margin of the Sevier orogenic belt (Hintze and Kowallis, 2009). The North Horn is the basal basin-filling deposit in the Laramide-age Uinta Basin (Fouch, 1976); however, older foreland basin sedimentation took place during the Late Cretaceous prior to the development of the basin.

Flagstaff Limestone

The Flagstaff Limestone (upper Paleocene) consists of 0 to 2000 feet (0–600 m) of dark gray to gray, dense limestone interbedded with tan to brown, fine- to medium-grained sandstone, marlstone, and variegated mudstone (figure 2.24) (Hintze and Kowallis, 2009). Limestone units are thin to thick bedded and locally very fossiliferous, containing freshwater gastropods, pelecypods, and ostracods (Anderson, 1983; Weiss and others, 1990). Locally, limestone beds are irregularly layered and contain many "bird's eye" algal nodules (Hintze and Kowallis, 2009). The Flagstaff is best expressed in outcrop as a prominent dip slope capping the western Book Cliffs that dips towards the north into the Uinta Basin. The formation is not present in the eastern Uinta Basin. Its contact with the overlying Colton Formation is marked at the base of the Roan Cliffs.

The Flagstaff Limestone was deposited in a large freshwater lake (Lake Flagstaff) that extended from the central part of the Uinta Basin through central and southwestern Utah. These lacustrine strata were deposited in the same elongated, northeast-southwest trending depositional trough as the North Horn Formation (Hintze and Kowallis, 2009) and included alluvial, marginal lacustrine, and open lacustrine facies. Lenticular sandstone bodies in the Flagstaff represent fluvial deposits associated with the margins of the lake system. Clastic deposits gradually displaced Lake Flagstaff northward until all that remained was a crescent-shaped lake, partially within the Uinta Basin (figure 2.25A) (Fouch, 1975).

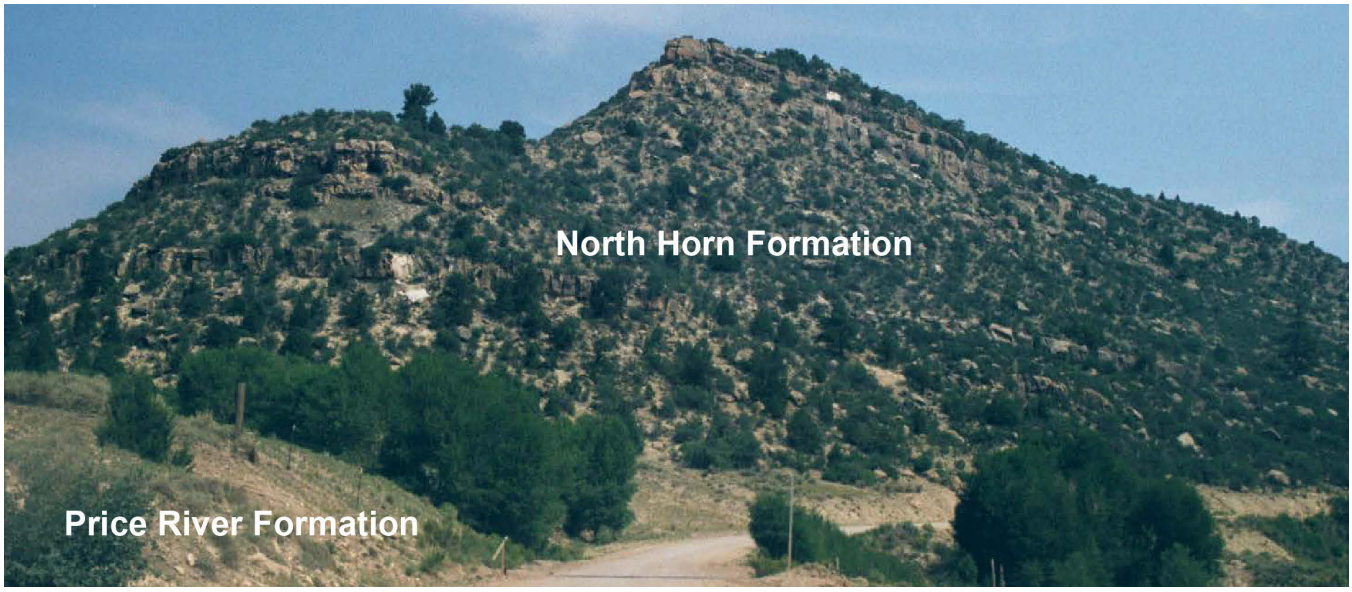

Figure 2.23. *Representative outcrop of fluvial siltstone and sandstone in the uppermost Cretaceous–lower Paleocene North Horn Formation, Soldier Canyon, Book Cliffs; view to the east. From Morgan (2003a); photograph by Craig Morgan, UGS.*

Figure 2.24. *Representative outcrop of the Paleocene Flagstaff Limestone, Price River Canyon, Book Cliffs; view to the south. Photograph by Craig Morgan, UGS.*

Colton Formation

The Colton Formation in the west, and Wasatch Formation in the east part of the Uinta Basin, are stratigraphically equivalent units (Paleocene and Eocene) (figure 2.13). The Colton consists of variegated mudstone and shaly siltstone interbedded with yellowish- to grayish-orange and grayish-brown, fine- to medium-grained quartzose sandstone with conglomerate at the base; it also contains some sparse limestone beds (figure 2.26) (Anderson, 1983; Weiss and others, 1990). Bedding is typically thin and lenticular in sandstone bodies, representing point bars and overbank sheet deposits, which are cross-stratified to massive and in places bioturbated by non-marine organisms (Anderson, 1983; Smith, 1984). Channel deposits (that may be multistoried) are sometimes exhumed with outcrops topographically above the surrounding mudstone. The mudstone beds commonly contain root structures and mudcracks. The Colton forms the western part of the Roan Cliffs along the southern margin of the Uinta Basin, characterized by reddish, steep, ledgey slopes and cliffs.

As the Uinta Mountains continued to rise during the late Paleocene and early Eocene, the alluvial Colton and Wasatch Formations began to fill the adjacent, subsiding Uinta Basin, reaching a thickness of up to 3200 feet (980 m) (Hintze and Kowallis, 2009). The Colton is a transition from alluvial plain to fluvial-deltaic to marginal lacustrine deposits (Smith, 1984; Fouch and others, 1992a). The alluvial plain consists of alluvium, alluvial and fluvial channels, overbank and floodplain deposits, and local lakes that are farther removed from the margin of the main lake (Fouch and others, 1992a). These transitional sediments are referred to as the Colton fan-delta, which was associated with both freshwater Lake Flagstaff and the later Eocene-age Lake Uinta (figure 1.3) that occupied the Uinta Basin (Weiss and others, 1990). The large, arcuate delta built into the lakes from the south-southwest, intertonguing with the lake sediments (figure 2.25B). Detrital zircon analysis suggests that the source of the Colton sediments was from the Mojave region of southern California (Dickinson and others, 2012).

Wasatch Formation

The Colton and Wasatch Formations are often undivided in the Uinta Basin, but in the central and eastern parts of the basin the Wasatch is distinguishable where it consists of red, yellow, and light gray friable sandstone, siltstone, mudstone, conglomerate, and minor interfingering limestone of the Flagstaff Limestone (figure 2.27) (Sprinkel, 2009). Sandstone is moderately

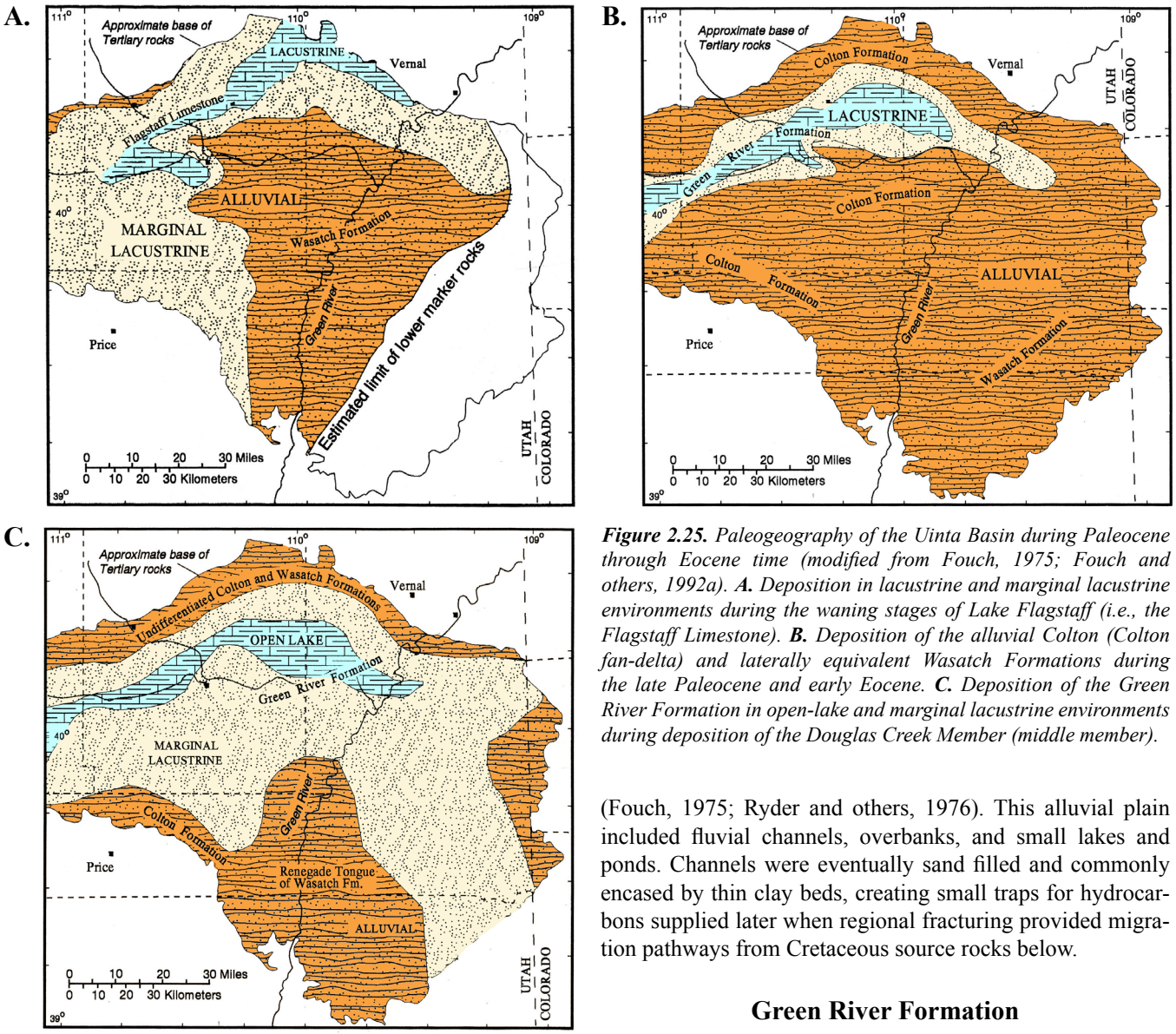

Figure 2.25. *Paleogeography of the Uinta Basin during Paleocene through Eocene time (modified from Fouch, 1975; Fouch and others, 1992a).* ***A.*** *Deposition in lacustrine and marginal lacustrine environments during the waning stages of Lake Flagstaff (i.e., the Flagstaff Limestone).* ***B.*** *Deposition of the alluvial Colton (Colton fan-delta) and laterally equivalent Wasatch Formations during the late Paleocene and early Eocene.* ***C.*** *Deposition of the Green River Formation in open-lake and marginal lacustrine environments during deposition of the Douglas Creek Member (middle member).*

well sorted and fine to medium grained. Closely spaced, low-permeability, lenticular-bedded sandstone bodies represent the principal Tertiary-age, gas-producing reservoirs in the eastern Uinta Basin, and range in thickness from 5 to 50 feet (1.5–15 m). They contain ripple laminae, small to medium cross-strata, and horizontal beds (Cole and others, 2008). Conglomerate beds are thin and contain chert and quartzite pebbles (Sprinkel, 2007). A few thin ostracodal limestone (grainstone) beds are also present within the Wasatch. In the eastern Uinta Basin, the major hiatus between the Wasatch and the underlying Upper Cretaceous Tuscher Formation (described above) is marked at the base of a conglomeratic section or lowest red or gray shale interval (Gualtieri, 1988). The Wasatch forms steep slopes, ledges, and small cliffs. It thins to the east where it onlaps the Douglas Creek arch along the Utah-Colorado border.

The Wasatch Formation was deposited predominantly in a non-lacustrine alluvial plain environment, significantly beyond the margins of Lakes Flagstaff and Uinta (figure 2.25B) (Fouch, 1975; Ryder and others, 1976). This alluvial plain included fluvial channels, overbanks, and small lakes and ponds. Channels were eventually sand filled and commonly encased by thin clay beds, creating small traps for hydrocarbons supplied later when regional fracturing provided migration pathways from Cretaceous source rocks below.

Green River Formation

The lacustrine Eocene Green River Formation is the primary oil-producing unit in the Uinta Basin (figure 1.1). It contains the oil source beds, seals, a variety of reservoir facies, and stratigraphic traps for major accumulations of oil (figure 1.4). Deep oil traps are overpressured and naturally fractured, whereas shallower traps are at normal pressure and require major hydraulic fracturing techniques, waterflooding programs, and/or horizontal drilling. The oils produced are high in paraffin (black or yellow wax) and require special heated wellsite and transportation infrastructure.

The Green River Formation consists of as much as 6000 feet (1800 m) of sedimentary strata (Hintze and Kowallis, 2009; Sprinkel, 2009). The stratigraphy is complex, and for decades many different unit names and marker beds have appeared in the literature or been used by industry (see Fouch, 1975, 1976; Ryder and others, 1976; Fouch and others, 1992a; Morgan and others, 2003, and the references pertaining to Green River nomenclature therein). Describing and

Figure 2.26. *Paleocene-Eocene Colton Formation forming the western part of the Roan Cliffs, Whitmore Park area near the head of Soldier Canyon; view to the north. Photograph by Craig Morgan, UGS.*

Figure 2.27. *Paleocene-Eocene Wasatch Formation, Hells Hole area, southeastern Uinta Basin; view to the south. From Cole and others, 2008; photograph by Rex Cole, Mesa State College.*

explaining in detail Green River stratigraphy is beyond the scope of this discussion, but we do provide a general summation in figure 2.28. The signature of each marker bed on wireline well logs is used to identify and correlate units in the subsurface throughout much of the basin. Briefly, the Wasatch Formation grades upward into and intertongues with the Green River Formation in the Uinta Basin, forming the Green River–Wasatch Formation transition unit (Sprinkel, 2009). In general, the lower member of the Green River, which is not everywhere present, consists of the basal Uteland Butte limestone and overlying carbonate marker unit (sometimes referred to as the black shale facies) (figure 2.28). The lower and middle members are separated by the carbonate marker bed and interfinger in the subsurface. The middle member is called the Douglas Creek Member in most maps and publications, and contains what is referred to as the "delta facies" and "green shale facies" (figure 2.28). The middle and upper members of the Green River are separated by the C marker bed. The upper member, named the Parachute Creek Member, contains the famous Mahogany oil-shale bed (zone) above the "transitional facies" (figure 2.28). The Parachute Creek intertongues with the overlying Uinta Formation.

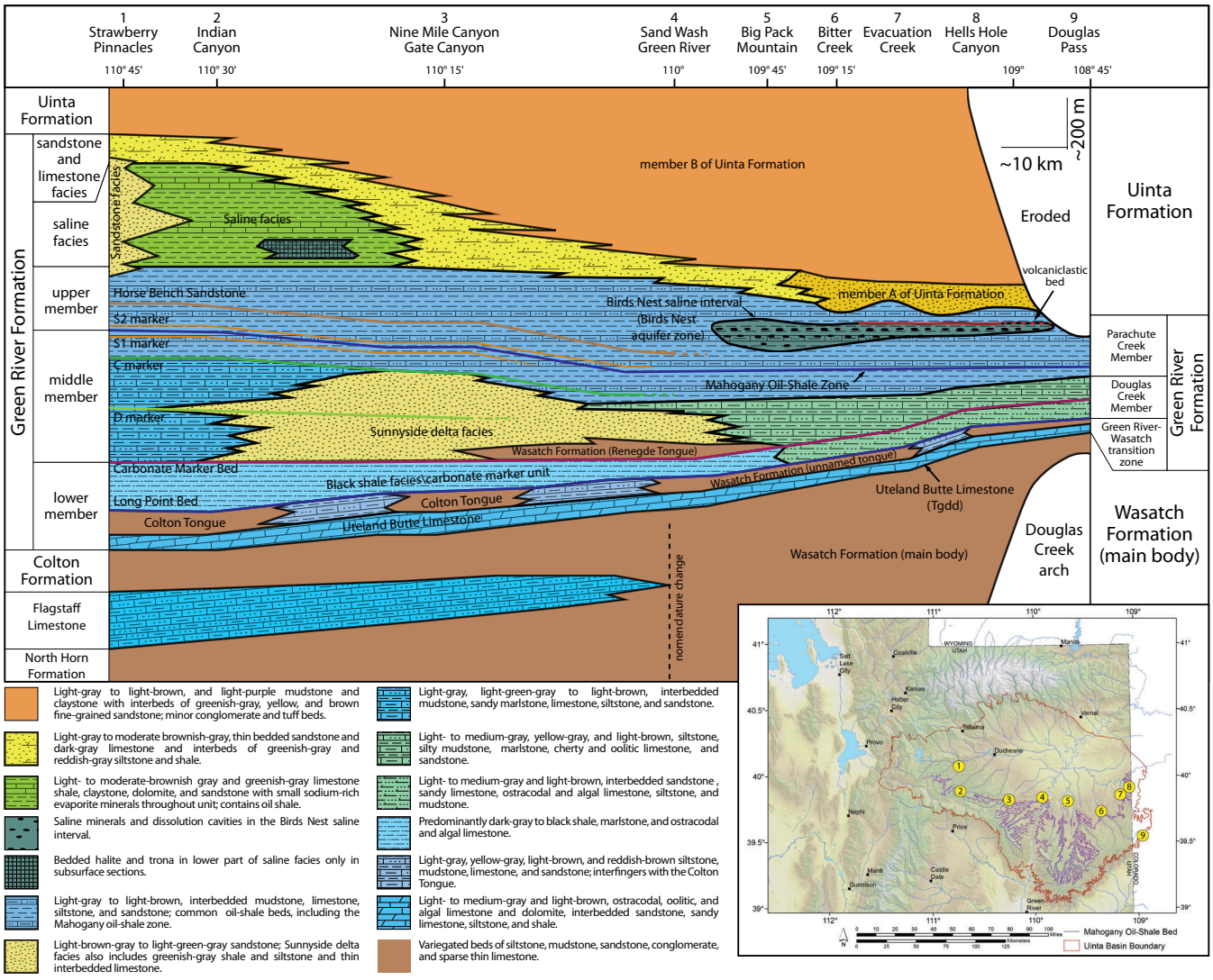

Figure 2.28. *General stratigraphy and major marker beds of the Green River Formation in the Uinta Basin. After Sprinkel (in preparation), modified from Töro and Pratt (2015) using Cashion (1967), Johnson and others (1988, 2010), Fouch and others (1994), Morgan and others (2003), Smith and others (2008), Tänavsuu-Milkevicience and Sarg (2012), and Vanden Berg and others (2013).*

In the lower member, the basal Uteland Butte limestone ranges in thickness from less than 60 feet (20 m) to more than 200 feet (60 m) and consists of limestone, dolomite, organic-rich calcareous mudstone, siltstone, and rare sandstone (figures 2.29A). Recent tight-oil horizontal drilling and exploration activities in the Uinta Basin target relatively thin, porous carbonate beds of the Uteland Butte, particularly in an area referred to as the "Central Basin Region" between Altamont-Bluebell field to the north and Monument Butte field to the south (figure 1.1). The Uteland Butte has historically been a secondary oil objective of wells tapping shallower, overlying Green River reservoirs and deeper, fluvial-lacustrine Colton Formation sandstone units in the western Uinta Basin. Dolomite, the horizontal drilling target, commonly has more than 20% porosity, but is so finely crystalline that the permeability is very low. The Uteland Butte is separated from the upper section of the lower Green River by a tongue of the Colton Formation. The section above the Colton tongue consists of light brown to light gray, fissile shale and limestone or marlstone. Limestone beds are lensoid and contain ostracods and algal laminae (Weiss and others, 1990). The lower Green River member forms steep slopes, ledges, and small cliffs.

The Douglas Creek Member (or middle member) consists of light- to medium-gray, light- to medium-brown, yellow, and light-gray siltstone, sandstone, shale, chert, and limestone (Gualtieri, 1988; Weiss and others, 1990; Sprinkel, 2009). Thick sections of sandstone dominate in the south-central part of the Uinta Basin, as seen in Ninemile Canyon (figure 2.29B), and represent the main producing reservoirs in the Monument Butte field trend in the subsurface to the north (figure 1.1). The Douglas Creek is dominated by shallowing-upward sequences of mudstones, siltstones, and sandstones, often gradually transitioning to well-developed microbial carbonate at the uppermost part of the intervals. The carbonates are commonly topped by erosional flooding surfaces. Sandstone is generally fine grained, moderately to well sorted, thin to thick bedded, discontinuous, and lenticular, mainly in

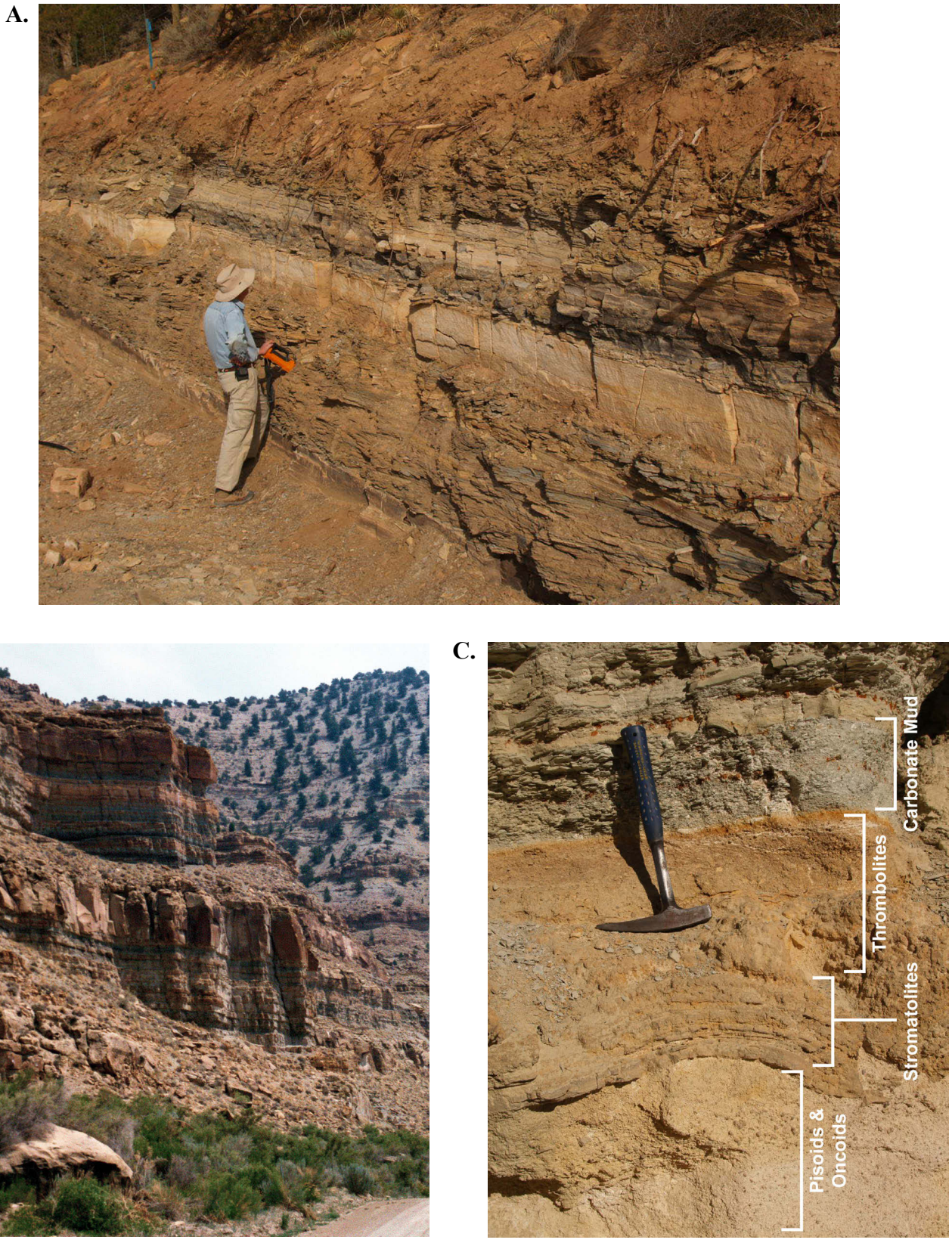

Figure 2.29. *Representative outcrops of the Eocene Green River Formation.* ***A.*** *Fresh road-cut exposure of Uteland Butte limestone consisting of interbedded dolomite and mudstone/limestone, Ninemile Canyon, southern Uinta Basin; view to the north.* ***B.*** *Depositional sequence of carbonate, green shale, and fluvial-deltaic sandstone cycles, Douglas Creek Member, Ninemile Canyon; view to the north.* ***C.*** *A typical microbialite interval and associated facies, Hells Hole area, eastern Uinta Basin. The light tan interval near the base is composed of pisoids and oncoids (as a grainstone/rudstone). The tan beds beneath the hammer are stromatolitic, whereas a thrombolite dominates the area to the right of the hammer.*

D.

E.

Figure 2.29. *Continued.* ***D.*** *Mahogany oil shale zone, Parachute Creek Member, Evacuation Creek area, eastern Uinta Basin; view to the west.* ***E.*** *The "Birds Nest" aquifer zone with dissolved nahcolite cavities in the upper Parachute Creek Member, representing the hypersaline conditions during the waning stage of Lake Uinta, Evacuation Creek, eastern Uinta Basin; view to the north. Photographs A, C, D, and E by Michael Vanden Berg, UGS; photograph B by Craig Morgan, UGS.*

channel bodies, and contains cross-stratified to planar beds, ripple marks, and scours. Limestone contains boundstone, rudstone, grainstone, packstone, wackestone, and mudstone carbonate fabrics. Constituent carbonate grains include ooids, pisoids, peloids, oncoids, coated grains, and skeletal material, especially ostracods and/or storm-generated carbonate rip-up clasts. Microbial carbonates include both stromatolites and thrombolites (clotted) that developed on a grainstone substrate (figure 2.29C) (Chidsey and others, 2015). The middle member also contains some thin, bluish-gray (weathered) to dark brown oil shale. The Douglas Creek forms large vertical cliffs, ledges, and steep slopes.

The Parachute Creek Member (or upper member) consists of moderately resistant, light- to medium-gray, light- to medium-brown, and yellow shale, marlstone and limestone, siltstone, and sandstone (Gualtieri, 1988; Weiss and others, 1990; Sprinkel, 2009). The lower Parachute Creek records fully carbonate-dominated shallowing-upward sequences, with carbonate mudstones transitioning to dolomitic microbial carbonates, again topped by an erosional flooding surface (Chidsey and others, 2015). Carbonates are similar to those in the underlying Douglas Creek Member dominated by oolites and microbialites. Both marlstone and shale can be dark brown and organic rich, including several oil shale beds, the most significant being the Mahogany oil-shale zone (figure 2.29D). Sandstone is very fine to medium grained and thin to thick bedded, containing cross-laminations and ripple marks (Gualtieri, 1988). The Parachute Creek also contains dated tuff beds and pods of the evaporite mineral nahcolite that, in some places, have been leached, leaving dissolution cavities (Sprinkel, 2009); i.e., the "Birds Nest" aquifer (figure 2.29E) discussed in later chapters. The Parachute Creek forms steep slopes, cliffs, and ledges.

The Green River Formation was deposited in marginal lacustrine and lacustrine environments, associated with an areally extensive, shallow, saline to freshwater lake (Lake Uinta) in the subsiding Uinta Basin (figures 1.3 and 2.30). The Green River contains three major depositional facies associated with Lake Uinta sedimentation: alluvial, marginal lacustrine, and open lacustrine (figure 2.25C) (Fouch, 1975). The Uteland Butte limestone records the first major transgression of Eocene Lake Uinta after the deposition of the alluvial Colton Formation, and thus it is relatively widespread in the basin. The marginal lacustrine facies, where most of the hydrocarbon production is found, consists of fluvial-deltaic, interdeltaic, and carbonate flat deposits (figures 2.29C and 2.30), including microbialites. The position of these deposits changed as the lake shoreline shifted rapidly in response to sediment input and lake-level fluctuations (figure 2.30). The Uinta Mountains were the source for the sediments in the northern part of Lake Uinta, while sediments in the southern part of the lake were sourced from the much larger (but lower relief) Four Corners area (Blakey and Ranney, 2008). The open-lacustrine facies is represented by nearshore and deeper water offshore muds, including the Mahogany oil-shale zone, which represents Lake Uinta's highest water level. Lake Uinta existed for about 13 million years and at its maximum extended into northwestern Colorado (Weiss and others, 1990). As climate changed during the late middle to early late Eocene, Lake Uinta began to shrink and created hypersaline conditions, similar to the modern Great Salt Lake in northern Utah, which are expressed by the evaporite minerals found in the upper Parachute Creek Member (figure 2.29E).

Uinta Formation

The Eocene Uinta Formation is exposed extensively throughout the central and northern Uinta Basin (figure 2.1, plate 1). The Uinta ranges in thickness from 0 to 5000 feet (0–1500 m) (Hintze and Kowallis, 2009) and, in places, is divided into lower, middle, and upper members (members A, B, and C of Sprinkel [2007, 2009]). Member A consists of yellowish-gray and yellowish-brown, very fine to fine-grained sandstone and siltstone, with minor conglomerate, shale, marlstone, and tuffaceous interbeds. It forms resistant ledges and cliffs. Member B consists of light gray, light greenish-gray, light-brown, and light-purple mudstone and claystone, with interbeds of greenish-gray, yellow, and brown fine-grained sandstone, and minor conglomerate and tuffaceous beds. It forms slopes and thin ledges. Member B contains gilsonite veins, which are mined in the eastern Uinta Basin (Boden and Tripp, 2012). Member C consists of soft, light gray, greenish-gray, white, grayish-purple, red, and pale-yellow shale, mudstone, claystone, and minor sandstone with local tuffaceous interbeds. It forms classic badland topography (figure 2.31).

The Uinta Formation represents sediments sourced from the east and northeast that filled the Uinta Basin as Lake Uinta waned and withdrew to the west (Weiss and others, 1990). The Uinta was deposited primarily in fluvial environments, but it also contains some marginal lacustrine deposits near the base.

Duchesne River Formation

The Duchesne River Formation is widely exposed throughout the northern Uinta Basin (figure 2.1, plate 1) and is characterized by its dominant red color (figure 2.32). The basal part of the Duchesne River commonly intertongues with the underlying Uinta; however, it lies unconformably on beds of the Green River Formation in certain areas. The Duchesne River ranges in thickness from 0 to 3000 feet (0–900 m) (Hintze and Kowallis, 2009) and has four members, in ascending order: Brennan Basin, Dry Gulch Creek, Lapoint, and Starr Flat. Lower members of the Duchesne River are Eocene in age and the upper members are Eocene to Oligocene (Sprinkel, 2007). The basal Eocene Brennan Basin Member consists of light- to medium-red, light reddish-brown, and yellowish-gray, fine- to medium-grained lithic sandstone and siltstone, with minor amounts of mudstone and conglomerate; it also contains well-developed pa-

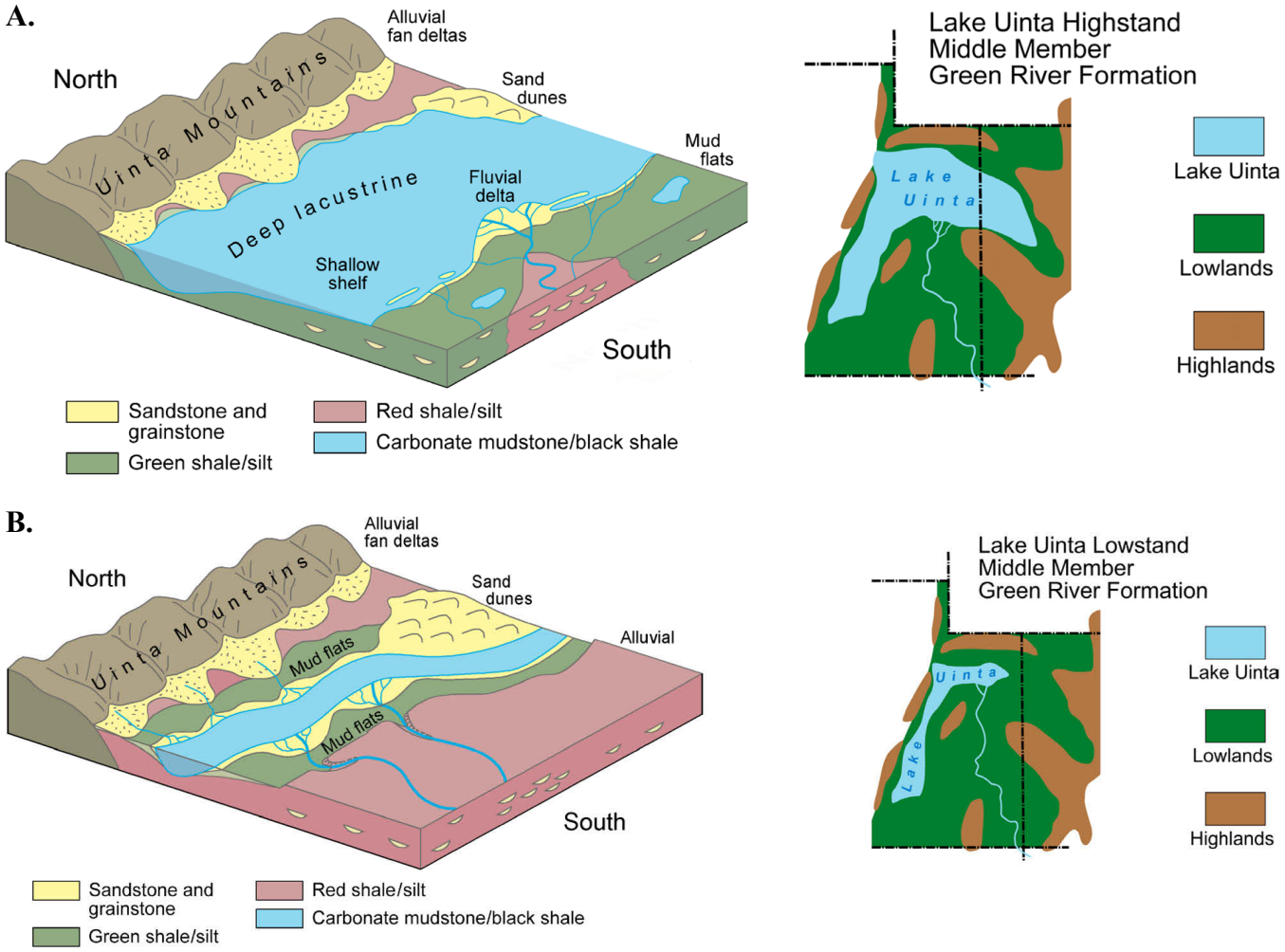

Figure 2.30. *Generalized depositional setting for Lake Uinta:* ***A.*** *high lake levels, and* ***B.*** *low lake levels. From Morgan and others (2003).*

leosols. The overlying Eocene Dry Gulch Creek Member consists of medium reddish-brown and purplish-gray, fine-grained sandstone, siltstone, mudstone, and conglomerate. The Eocene-Oligocene Lapoint Member consists of light reddish-brown and yellowish-gray, fine-grained sandstone, siltstone, and mudstone, with abundant light-greenish-gray bentonite beds. The Oligocene-aged Starr Flat Member consists of reddish-brown, reddish-purple, yellowish-gray, and greenish-gray, fine- to coarse-grained sandstone, siltstone, mudstone, and conglomerate. It is dominated by thick-bedded sandstone that coarsens upward. The Starr Flat is correlative to, and may be part of, the Bishop Conglomerate due to its similar stratigraphic relation and age (Sprinkel, 2007). Overall the Duchesne River is very thin to medium bedded, containing lenticular, channel-form sand bodies. The Duchesne River forms ledges, small cliffs, and slopes that produce badland topography in some areas.

The Duchesne River Formation was deposited mainly in a fluvial environment as the Uinta Basin continued to fill with sediment during the late Eocene and Oligocene. It contains a diverse assemblage of late Eocene-age vertebrate fossils in the lower members.

QUATERNARY DEPOSITS

Quaternary deposits are widespread in the Uinta Basin (figure 2.1, plate 1) and make up the shallow groundwater aquifers. The beginning of the Quaternary in the Colorado Plateau was characterized by the development of stream and river drainages across the lower elevations of the landscape and glaciers at higher elevations. Preserved deposits are mostly unconsolidated and vary in thickness depending on their depositional environment. The most common Quaternary materials are alluvial and alluvial-fluvial deposits, but colluvial, glacial, eolian, landslide, and debris-flow deposits occur as well and are mixed with alluvial-fluvial deposits in places (Sprinkel, 2006, 2007, 2008, 2014).

Glaciation was extensive in the Uinta Mountains during the Pleistocene. Large amounts of glacial till and outwash from melting glaciers were deposited on the southern flanks of the Uinta Mountains and the northern boundary of the Uinta Basin (Munroe and Laabs, 2009) (plate 1). Till deposits generally consist of unconsolidated, poorly sorted, angular to rounded boulders, cobbles, and pebbles of mostly red sandstone

Figure 2.31. *Badland topography formed in member C, including reddish outcrop in the distance, of the Eocene Uinta Formation about 30 miles (48 km) southeast of Vernal, Utah, Coyote Basin area along State Route 45; view to the east. Photograph by Doug Sprinkel, UGS.*

Figure 2.32. *Representative outcrop of the Eocene Duchesne River Formation along a meander of the Green River near Horseshoe Bend about 12 miles (19 km) south of Vernal, Utah; view to the east. The Duchesne River Formation was deposited by a fluvial system, possibly similar to the modern Green River, providing an example of ancient and modern fluvial environments. Photograph by Doug Sprinkel, UGS.*

and quartzite sourced from the Precambrian Uinta Mountain Group. Outwash deposits generally consist of unconsolidated, well-rounded boulders to pebbles and sand composed of mostly red sandstone and quartzite also sourced from the Uinta Mountain Group (Sprinkel, 2006, 2007, 2014; Munroe and Laabs, 2009).

Pleistocene and Holocene alluvial-fan deposits occur adjacent to uplands where there is periodic heavy rainfall, and they generally consist of unconsolidated, poorly sorted boulder, gravel, sand, and silt material. Pleistocene alluvial-fluvial and Holocene fluvial terrace deposits occur along major drainages and generally consist of unconsolidated to locally cemented silt, sand, gravel, cobbles, and boulders. Holocene fluvial stream-channel and floodplain sediments consist of unconsolidated, moderately sorted silt, sand, gravel, and cobbles deposited along major and minor drainages. Extensive sand dunes produced by wind action are present in wide, flat valley areas. Landslide and slump deposits occur in formations prone to slope failure. Debris-flow deposits occur in major drainages and consist of unconsolidated and poorly sorted heterogeneous mixtures of boulders, cobbles, gravel, sand, silt, and mud. Clasts in these Quaternary deposits are mainly composed of sandstones, quartzites, and limestones derived from local bedrock or the Uinta Mountains (Sprinkel, 2006, 2007, 2008, 2014).

CHAPTER 3:
STRUCTURAL SETTING

by

Thomas C. Chidsey, Jr., Stephanie M. Carney, and Taylor Boden

CONTENTS

INTRODUCTION 49
TECTONIC HISTORY 49
GENERAL BASIN STRUCTURE AND FOLDING 50
FAULTING 51
Uinta Basin–Mountain Boundary Fault 52
Duchesne Fault and Fracture Zone 52
JOINTING 53
FRACTURES 54
GILSONITE VEINS 57

FIGURES

Figure 3.1. Major structural features, surface faults, and fracture zones in and around the Uinta Basin 50
Figure 3.2. Structure contour map on the top of the Douglas Creek Member, Green River Formation, Red Wash field 51
Figure 3.3. North-south seismic profile showing Uinta Basin–Mountain boundary fault zone 52
Figure 3.4. North-south structural cross section from Red Wash field, Uinta Basin through the Uinta Basin–Mountain boundary fault zone 53
Figure 3.5. Duchesne fault and fracture zone 54
Figure 3.6. Jointing in the Eocene Uinta Formation 55
Figure 3.7. Examples of natural fracturing in cores from Natural Buttes field 56
Figure 3.8. Southeast-trending Cowboy gilsonite vein 57

CHAPTER 3:
STRUCTURAL SETTING

INTRODUCTION

The rocks in the Uinta Basin have been faulted, jointed, fractured, folded, and uplifted. The resultant structural features have had a significant impact on the generation and trapping of hydrocarbons in the basin as well as potential for produced-water disposal. Two major tectonic events helped shape the Uinta Basin and create the structures within it: the Late Cretaceous to early Tertiary Laramide orogeny and Tertiary-Quaternary uplift of the Colorado Plateau. Some structures in the Uinta Basin also reflect overprinting of regional Miocene extension.

Oil and gas migration along faults and fractures in Cretaceous and Tertiary strata in the eastern Uinta Basin has been proposed by Rice and others (1992). Migration along fracture networks within the Green River Formation in the central part of the basin has been noted by several workers, including Chidsey and Laine (1992) and Groeger and Bruhn (2001). These faults and fractures could also influence vertical movement of groundwater throughout the basin and within the Mesaverde, Wasatch, and Green River reservoirs.

TECTONIC HISTORY

The Colorado Plateau is relatively undeformed in comparison to the central Utah thrust belt to the west. Late Cretaceous thrust faulting of the Sevier orogenic belt, specifically the Charleston-Nebo thrust, extended to the westernmost edge of the Uinta Basin (Hintze, 1980). Synorogenic nonmarine deposition near the Uinta Basin suggests that a transition from "thin skinned" Sevier thrust deformation to Laramide basement-cored uplift occurred during the late Campanian (Lawton, 1985, 1986).

Structural basins (e.g., the Uinta and Kaiparowits in Utah) and broad, large-scale, elongate anticlinal uplifts, like the San Rafael Swell, are developed throughout the Colorado Plateau. These basins and uplifts formed in response to Laramide orogenic compressional forces between latest Cretaceous time (about 70 million Ma) and the Eocene (about 40 Ma) (Hintze and Kowallis, 2009). Stratigraphic evidence (Molenaar and Cobban, 1991) suggests that Laramide uplift began possibly in the Turonian (94–89 Ma) and ended by the close of the early Eocene (48.6 Ma).

Regional extension beginning during the Miocene (about 17 Ma) (Hintze and Kowallis, 2009) produced major north-south trending, high-angle normal faults. These faults often bound plateaus and valleys, and have lengths over 100 miles (160 km) in Utah and northern Arizona. Smaller faults also dissect high plateaus, such as the Wasatch Plateau to the southwest of the Uinta Basin. These faults extend into the western part of the basin (figure 3.1, plate 1).

The compression associated with the Laramide orogeny also caused the Colorado Plateau and most of the western U.S. to rise. Some workers believe that as the hot, young, Farallon oceanic plate slid beneath the continental plate (underplating), the crust was forced to rise in compensation (Burchfiel and others, 1992; Anderson and others, 2010). Most of the uplift occurred in the early Tertiary, but some uplift continued throughout the remainder of the Cenozoic to the present, in part, as a result of isostatic rebound from erosion and removal of thousands of feet of sedimentary strata (Hunt, 1956; Lucchitta, 1979; Graf and others, 1987; Young and Spamer, 2001; Pederson and others, 2002). By middle Tertiary time, parts of the Colorado Plateau stood as a broad high plain (Anderson and others, 2010). Of particular note in northeastern Utah was a period of crustal stability that occurred during the Oligocene about 30 Ma and replaced Uinta Basin subsidence and Uinta Mountain uplift (Hansen, 1986). The result was the development of an extensive pediment around the flanks of the Uinta Mountains. This pediment is called the Gilbert Peak erosion surface; it is capped by the Oligocene-age Bishop Conglomerate where present (Hintze and Kowallis, 2009; Sprinkel, 2010).

The uplifting of the Colorado Plateau turned the region from one of deposition to one of massive erosion by running water, mass wasting, and wind. Burial history models for the area south of the Uinta Basin near Green River, Utah, estimate the removal of 8000 vertical feet (2400 m) of section, equating to a long-term average vertical erosion rate of 0.2 feet (6.1 cm) per thousand years (Nuccio and Condon, 1996; Nuccio and Roberts, 2003). Other estimates of the stream incision rates on the Colorado Plateau range from 0.6 feet (0.2 m) per thousand years over the last one million years (Willis and Biek, 2001; Pederson and others, 2002) up to 1.3 to 1.6 feet (0.4–0.5 m) per thousand years over the last several hundred thousand years (Davis and others, 2001; Hanks and others, 2001; Marchetti and Cerling, 2001).

Most of the eroded material from the Colorado Plateau has been carried to the sea by the Colorado River system. During the early Tertiary, the regional drainages in the Colorado Plateau flowed north from central Arizona toward the Uinta Basin and other lacustrine basins (Young, 1987; Dickinson and others, 1989; Potochnik and Faulds, 1998; Young and Spamer, 2001; Blakey and Ranney, 2008). About 5.5 Ma, southwest-flowing drainages in southern Nevada, which had been lowered by structural collapse of the Basin and Range Province

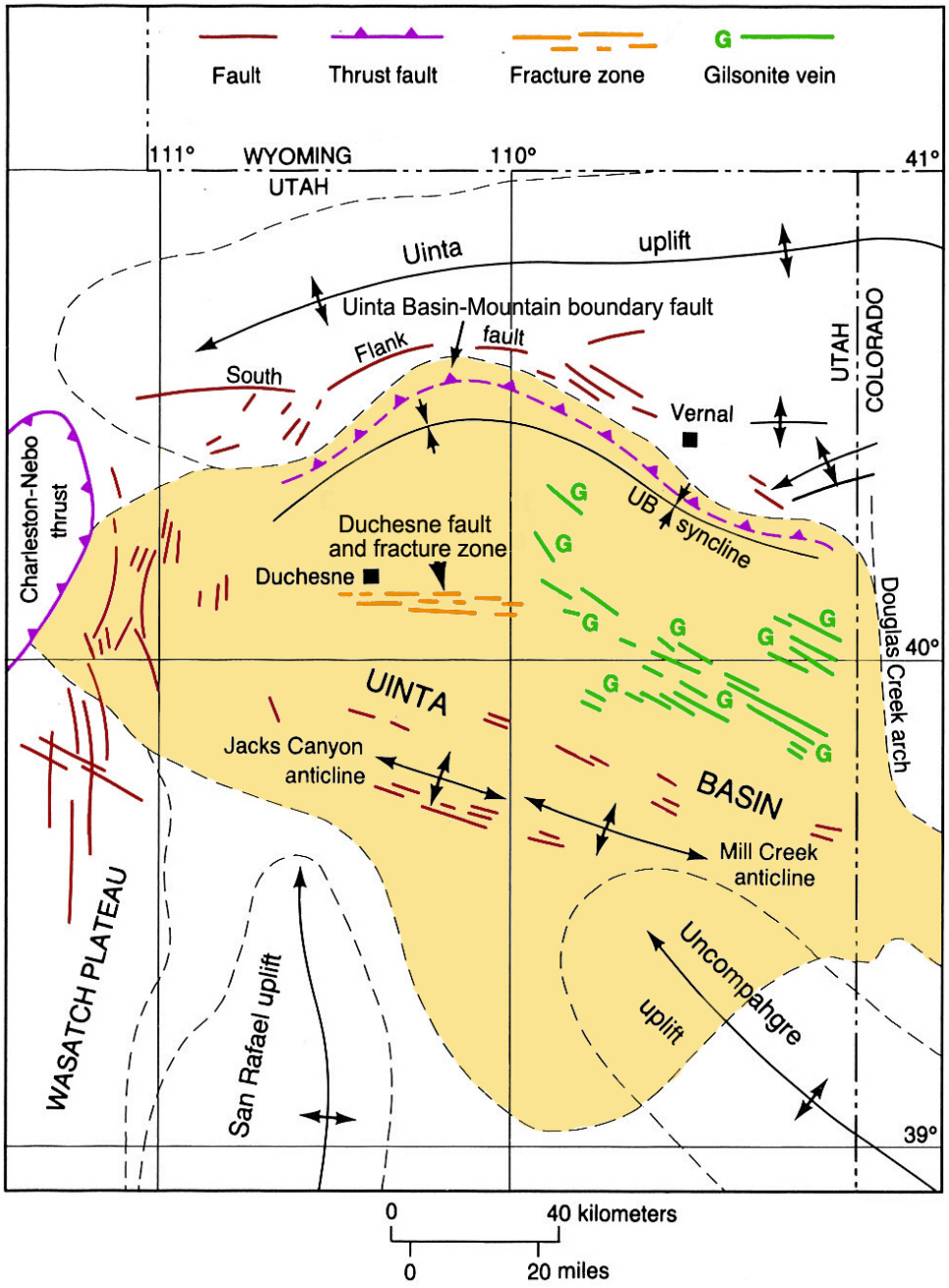

Figure 3.1. *Major structural features, surface faults, and fracture zones in and around the Uinta Basin. Uinta Basin–Mountain boundary fault after Osmond (1986); other faults and gilsonite veins from Hintze (1997) and Hintze and others (2000).*

between 10 and 15 Ma, succeeded in cutting headward into the higher Colorado Plateau to the east (Lucchitta, 1989; Potochnik and Faulds, 1998; Young and Spamer, 2001, and papers therein; Biek and others, 2010). Eventually, headward erosion managed to capture and integrate the drainages of the Colorado Plateau (including those within the Uinta Basin), reversing flow directions. As a result, the modern Colorado River system was formed. Due to the great topographic relief between the southern Nevada area and the higher Colorado Plateau, the Colorado River, Green River, and their tributaries had tremendous erosional energy and rapidly cut the Grand Canyon over a few million years (Lucchitta, 1989; Potochnik and Faulds, 1998; Young and Spamer, 2001, and papers therein; Cook and others, 2009). The new drainage system quickly eroded the soft Mesozoic strata of the Colorado Plateau creating wide valleys, narrow canyons, and entrenched meanders (Cook and others, 2009)—many of which are found in the Uinta Basin.

GENERAL BASIN STRUCTURE AND FOLDING

The Uinta Basin is a classic example of a large Laramide basin on the Colorado Plateau. The basin is asymmetrical to the north, paralleling the east-west trending Uinta Mountains (figures 2.1

and 3.1). The north flank dips 10° to 35° into the basin and is bounded by a large, north-dipping, basement-involved reverse fault—the Uinta Basin-Mountain boundary fault (UBMBF) (Campbell, 1975; Stone, 1993; Bryant, 2010). The southern flank of the Uinta Basin gently dips between 4° and 6° to the north. The syncline axis of the Uinta Basin is located near the north margin of the basin. It is related to and closely parallels the UBMBF and Uinta Mountains (Rowley and others, 1985; Bryant, 2010). The UBMBF controlled the development and downwarping of the basin in the north, whereas the southern part of the basin was influenced by the uplift of adjacent Laramide structures and remained elevated (Bryant, 2010).

Subtle structural noses are common in Tertiary rocks throughout the Uinta Basin and are typically the sites of oil and gas accumulations such as Bluebell (Lucas and Drexler, 1975) and Red Wash (figure 3.2) (Schuh, 1993) fields. The structures possibly developed as adjustments to basement faulting. Large structural features only occur along the flanks of the basin. The Jacks Canyon anticline is located along the southwestern margin (figure 3.1) and includes Nine Mile Canyon, Peters Point, and Stone Canyon fields (figure 1.1), which developed on subsidiary structures to the fold.

FAULTING

High-angle normal faults are common in the south-central and westernmost Uinta Basin (figures 2.1 and 3.1) (Weiss and others, 1990; Sprinkel, 2009, 2014). These faults are linear to slightly sinuous, ranging in length from several hundreds of feet to miles, have displacements less than 100 feet (30 m), and are often paired to form grabens. The orientation of the south-central set is northwest-southeast, reflecting the northernmost extension of the ancestral Uncompahgre uplift to the south. They probably developed during the Paleozoic along the north and northeast flanks of the Uncompahgre uplift (Stone, 1977) and were reactivated during the Laramide orogeny in the Late Cretaceous/early Tertiary (Fouch and others, 1992a, 1992b). The western fault set generally strikes north-south and likely represents the eastern continuation of Miocene regional extension.

Two structural components are unique to the Uinta Basin in comparison to other structural basins in Utah: the UBMBF and the Duchesne fault and fracture zone (DFZ) (figure 3.1, plate 1). These are described in detail in the following sections.

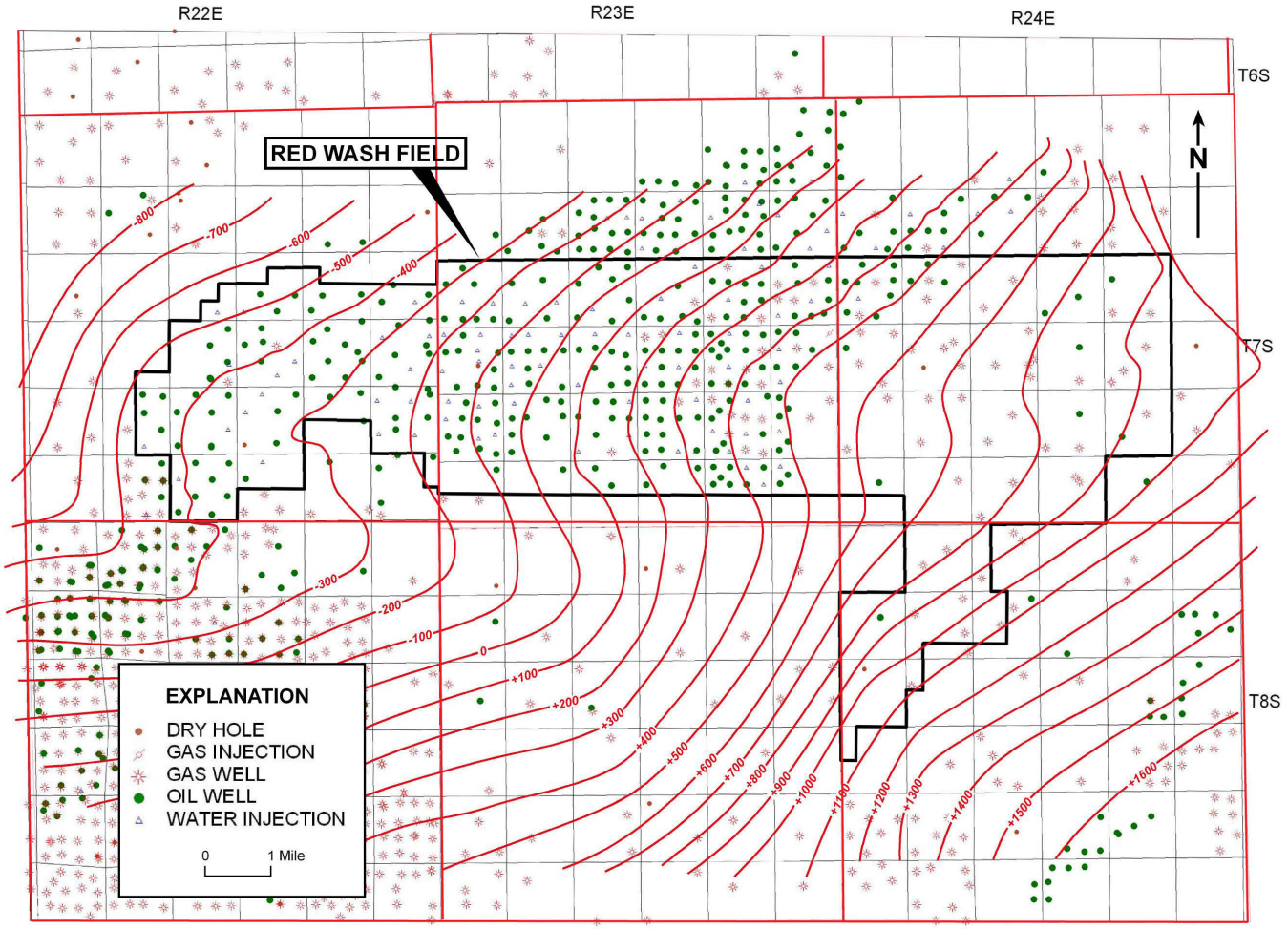

Figure 3.2. *Structure contour map on the top of the Douglas Creek Member of the Green River Formation, Red Wash field. Contour interval is 100 feet; datum = mean sea level. From Schuh (1993).*

Uinta Basin–Mountain Boundary Fault

The UBMBF, as previously discussed, is a major basement-involved reverse fault along the northern border of the Uinta Basin. Movement along the UBMBF began during Laramide time and is partly responsible for uplift of the Uinta Mountains as well as contributing to the development of the Uinta Basin (Bryant, 2010; Sprinkel, 2014). Several fault segments offsetting members of the Eocene/Oligocene Duchesne River Formation are exposed along the length of the UBMBF (Sprinkel, 2007, 2014). A series of normal fault scarps cut gravels (glacial outwash) of pre-Blacks Fork age (middle to early[?] Pleistocene) along the northwest margin of the Uinta Basin, and generally align with exposed faults that may be surface traces of the UBMBF zone where extension and relaxation has occurred. Displacement of Pleistocene deposits along the UBMBF system shows that segments of the fault have been active in the Quaternary and may continue to the present (Sprinkel, 2014). To the east, Mesozoic and middle Eocene rocks are juxtaposed across the UBMBF zone (Sprinkel, 2006, 2007).

Although the UBMBF generally does not reach the surface along much of its length, it is identifiable on seismic profiles and from well data. Figure 3.3 is a north-south seismic profile from the northern Uinta Basin through Ashley Valley field (locations shown on figures 1.1 and 2.1). This high-quality, time-migrated profile was acquired in 1985 using an airgun source (Stone, 1993). It has a horizontal exaggeration of 1.3:1 at 2.0 seconds two-way time (TWT), and a record length of 5 seconds TWT (Stone, 1993). The UBMBF is prominently displayed dipping north and appears to become relatively low-angle at depth. Strong reflectors on the profile delineate the Tertiary, Paleozoic-Mesozoic, and Precambrian Uinta Mountain Group and Red Creek Quartzite sections.

Figure 3.4 is a cross section partly parallel to the southern portion of the seismic profile from Red Wash field in the Uinta Basin through Ashley Valley field, constructed using surface geologic maps, subsurface data from oil and gas exploratory wells, and the seismic interpretation shown on figure 3.3 supplemented with other geophysical information (Stone, 1993). The UBMBF dies out and is covered by the Green River and younger formations along most of its length. At depth, the UBMBF places the Precambrian through Jurassic section in contact with source rocks within the Upper Cretaceous Mancos Shale. The oil produced from the Pennsylvanian Weber Sandstone at Ashley Valley field is a mixture from source rocks in the Mancos Shale and Permian Phosphoria Formation, based on analysis of saturated biomarkers, carbon isotopes, gas chromatography, and other geochemical techniques (Stone, 1986; Sprinkel and others, 1997; Lillis and others, 2003).

Duchesne Fault and Fracture Zone

The DFZ is a prominent east-west trending series of normal faults and associated intense fracturing (figures 3.1 and 3.5) that creates a discontinuous graben cutting beds of the Uinta Formation at the surface in the north-central part of the Uinta Basin, parallel to the Monument Butte–Brundage Canyon field trend just to the south (figure 3.1, plate 1) (Sprinkel, 2014). The faults may be related to deep-seated fractures in basement rocks. The DFZ is thought to have formed during the Laramide orogeny prior to 30 to 35 Ma (Groeger and Bruhn, 2001). A subtle anticline follows the length of the DFZ; other minor folds are also present (Groeger and Bruhn, 2001; Smith, 2004). The faults in the DFZ can be mapped east to west for over 40 miles (60 km) along a belt about 3 miles (5 km) wide (Ray and others, 1956). The stratigraphic displacements on these relatively high-angle faults range from a few inches to

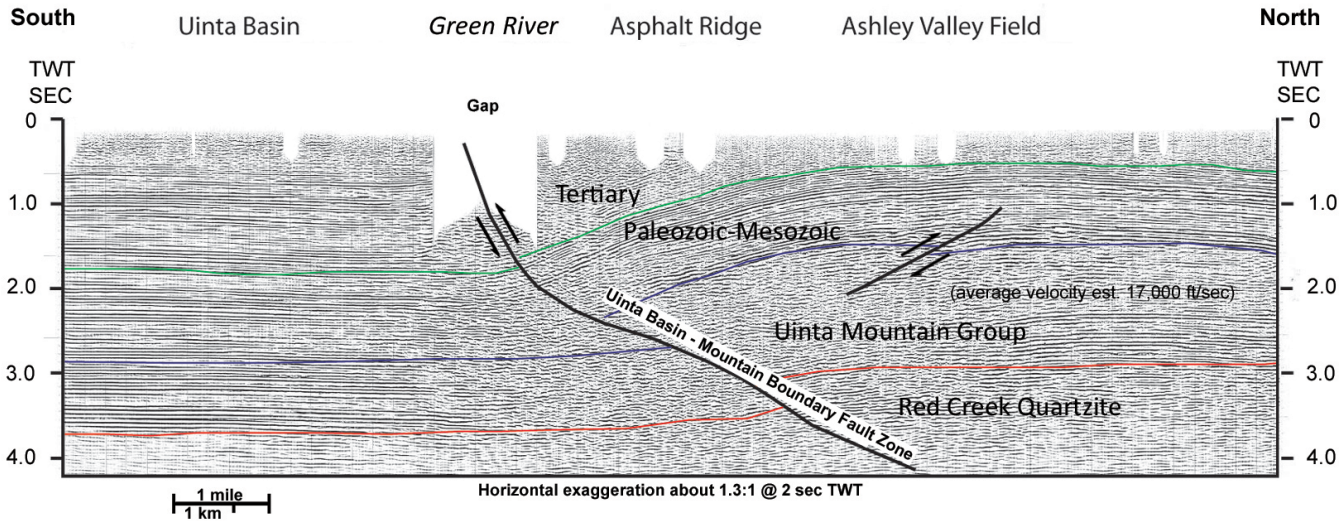

Figure 3.3. *North-south interpreted seismic profile showing prominently the Uinta Basin–Mountain boundary fault zone and the Ashley Valley field structure. Strong reflectors identify the Tertiary and Paleozoic-Mesozoic sections, and the Uinta Mountain Group and Red Creek Quartzite (the latter two of Precambrian age). Line of profile shown on figure 2.1. Seismic profile courtesy of Halliburton Geophysical Services, Inc. Modified from Stone (1993).*

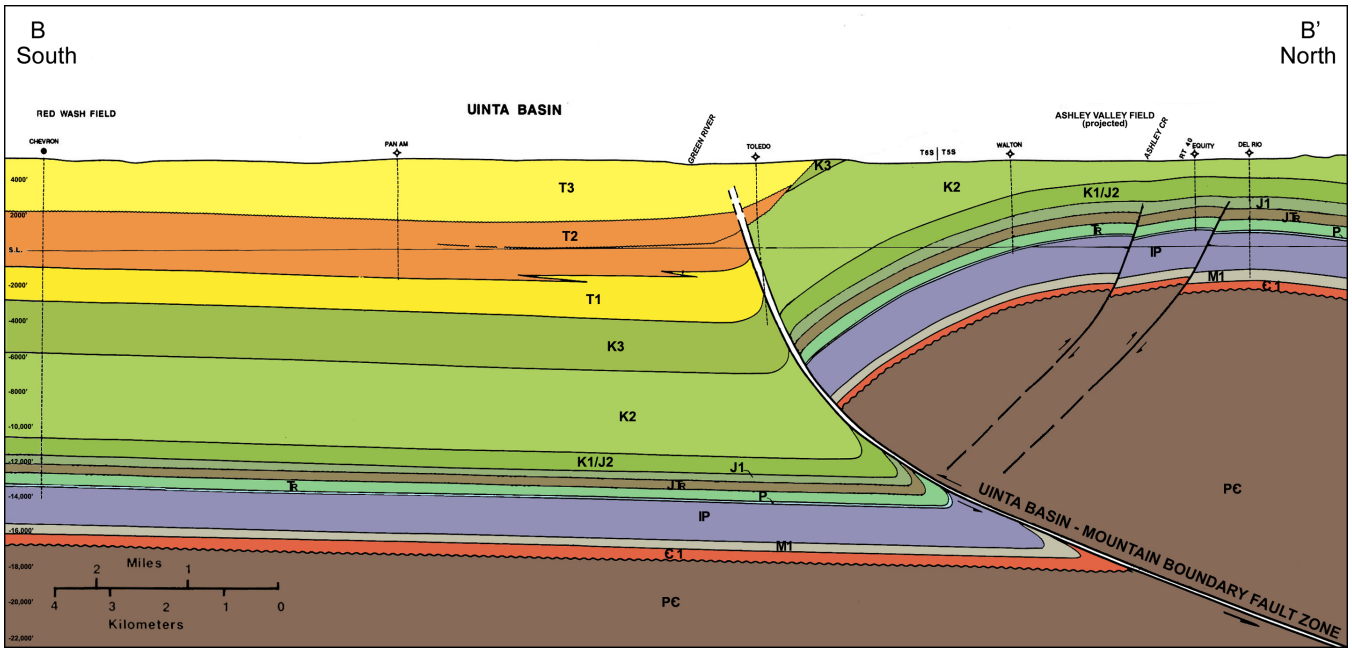

Figure 3.4. *North-south structural cross section from Red Wash field in the Uinta Basin through the Uinta Basin–Mountain boundary fault zone and the Ashley Valley field area showing the features identified on the seismic profile (figure 3.3). Line of section shown on figure 2.1. See figure 2.1 for explanation of stratigraphic abbreviations. Modified from Stone (1993).*

100 feet (30 m), with no observable horizontal component (figure 3.5) (Bereskin and others, 1993; Smith, 2004). In the western DFZ, a shallow basal detachment on a south-dipping fault produces a half-graben (Groeger and Bruhn, 2001). The northwest-trending belt of gilsonite veins (discussed later) intersects the eastern end of the DFZ. The DFZ likely predates the formation of the gilsonite veins based on spatial relationships (TerraTek, Inc., 1998).

Fracturing in the DFZ was induced by high fluid pressures applied to low-permeability rocks on local subtle folds (Smith, 2004). The deep part of the Uinta Basin to the north of the DFZ (Altamont-Bluebell field trend, figure 1.1) is characterized by overpressuring in the Green River and Wasatch/Colton reservoirs. The intense fracturing within the DFZ is postulated to have resulted from repeated cycles of (1) fluid pressure buildup, (2) fracturing, (3) fluid flow through the DFZ, (4) calcite precipitation by calcite-saturated fluids, and (5) sealing of fracture permeability (Smith, 2004). Fluid pressures were not as high to the south of the DFZ, and thus, the intensity of the fractures was significantly less.

JOINTING

Joints are prominent features in the strata of the Uinta Basin. Sandstone beds in the Uinta Basin are quartz rich and brittle, and when folded or bent produce large sets of joints, chiefly in sandstones of the Green River, Uinta, and Duchesne River Formations. These joints developed in response to the subtle folding in the Uinta Basin, regional uplift of the Colorado Plateau, and the removal of several thousand feet of overlying rock by erosion. Joints are closely spaced in many areas of the Uinta Basin, but spacing varies with bedding thickness, lithology, and structural setting (i.e., folding, regional dip, proximity to faults, etc.). Three types of joints are common: (1) near-vertical, (2) inclined, and (3) surficial (figure 3.6). These joints are best displayed close to cliff faces where slope retreat is actively taking place. They are spaced from 5 to 100s of feet (1.5–30+ m) apart, and are as much as several miles in length. Surficial joints are near-parallel to cliff faces and form from the expansion of the sandstone after rapid unloading of overlying strata. In cross section, surficial joints are closely spaced near the cliff face, from inches to a few feet apart, but disappear at depth.

Five major regional joint sets in the eastern Uinta Basin were identified by Verbeek and Grout (1993) where tight-sand gas reservoirs produce at Natural Buttes and other smaller fields (figure 1.1). The sets and their strike ranges, starting with the oldest, are: F1 – N. 15–30° W., F2 – N. 55–85° W., F3 – N. 60–80° E., F4 – N. 15–40° E., and F5 – N. 65–85° W. Joint sets F2 and F4 are very abundant, F3 is moderate, and F1 and F5 are sparse (Verbeek and Grout, 1993). Joint sets F1 through F3 formed between 43 and 10 Ma whereas sets F4 and F5 are dated beginning at 10 Ma during regional uplift (Verbeek and Grout, 1993).

Cleating in coal beds within the Ferron Sandstone and Blackhawk Formation is well developed and provides permeability for potential or producing CBM reservoirs in the Uinta Basin—e.g., Castlegate field (figure 1.1) which has produced over 13 BCF of CBM from the Blackhawk (Utah Division of Oil, Gas and Mining, 2016c). Cleats were affected by regional tectonic

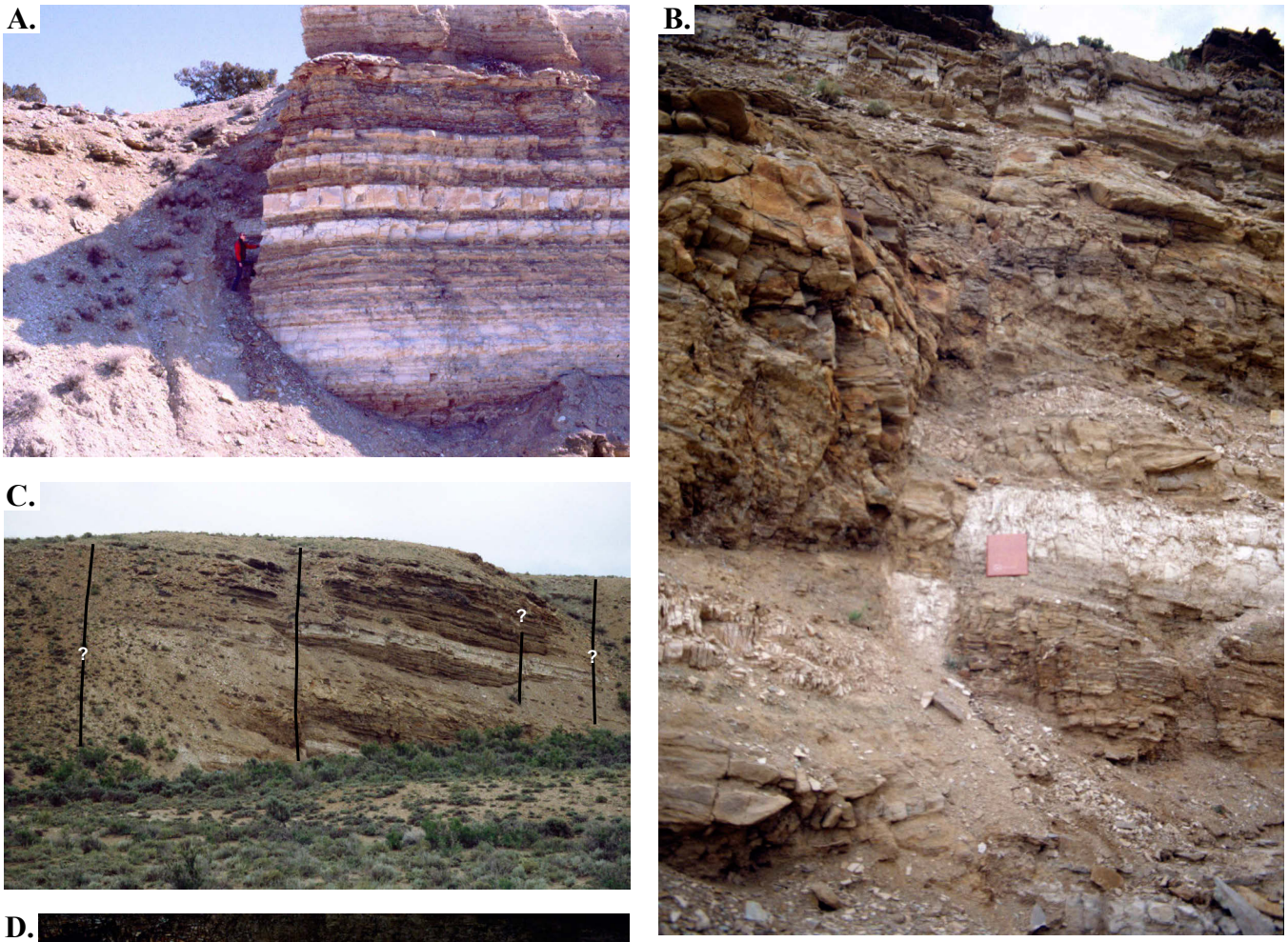

Figure 3.5. *Duchesne fault and fracture zone in the Eocene Uinta Formation, Duchesne field area (see figure 1.1).* ***A.*** *High-angle normal fault with over 50 feet (15 m) of displacement. Geologist for scale.* ***B.*** *Minor displacement on a fault dipping 78° north.* ***C.*** *Multiple faults creating south dip in the bedding.* ***D.*** *Small fault and associated closely spaced vertical fractures. Photographs by Craig Morgan, UGS.*

events resulting in regular spacing and orientations that persist over large areas (Hucka, 1991). Face cleats along the western Book Cliffs are oriented west-northwest with a secondary northeast trend (Hucka, 1991; Montgomery and others, 2004).

FRACTURES

Fractures in the Uinta Basin are closely associated with jointing and fault zones, such as the DFZ and other major faults. Fracturing in the Uinta Basin plays a major role in creating effective porosity and permeability resulting in reservoir quality capable of hydrocarbon production (figure 3.7). Understanding the characteristics and orientation of these naturally occurring fractures is also critical for planning horizontal wells and hydraulic fracturing of tight-sand and potential shale-gas reservoirs in the basin.

Regional fracture systems (tens of miles long) in the Uinta Basin are near-parallel to and possibly genetically related to major structural features bordering the basin (Stearns and Friedman, 1972). These features include the Uinta Mountains, Douglas Creek arch, San Rafael uplift, Wasatch Plateau, the buried Uncompahgre uplift, and the Charleston-Nebo thrust (figure 3.1, plate 1).

Fractures in the Uinta Basin began to develop during burial of the Wasatch and Green River Formations (Narr and Currie, 1982). Hydrocarbon generation, with resultant overpressuring, may have caused fractures to form in the deeper parts of the basin (Sweeny and others, 1987). Fractures also developed as the

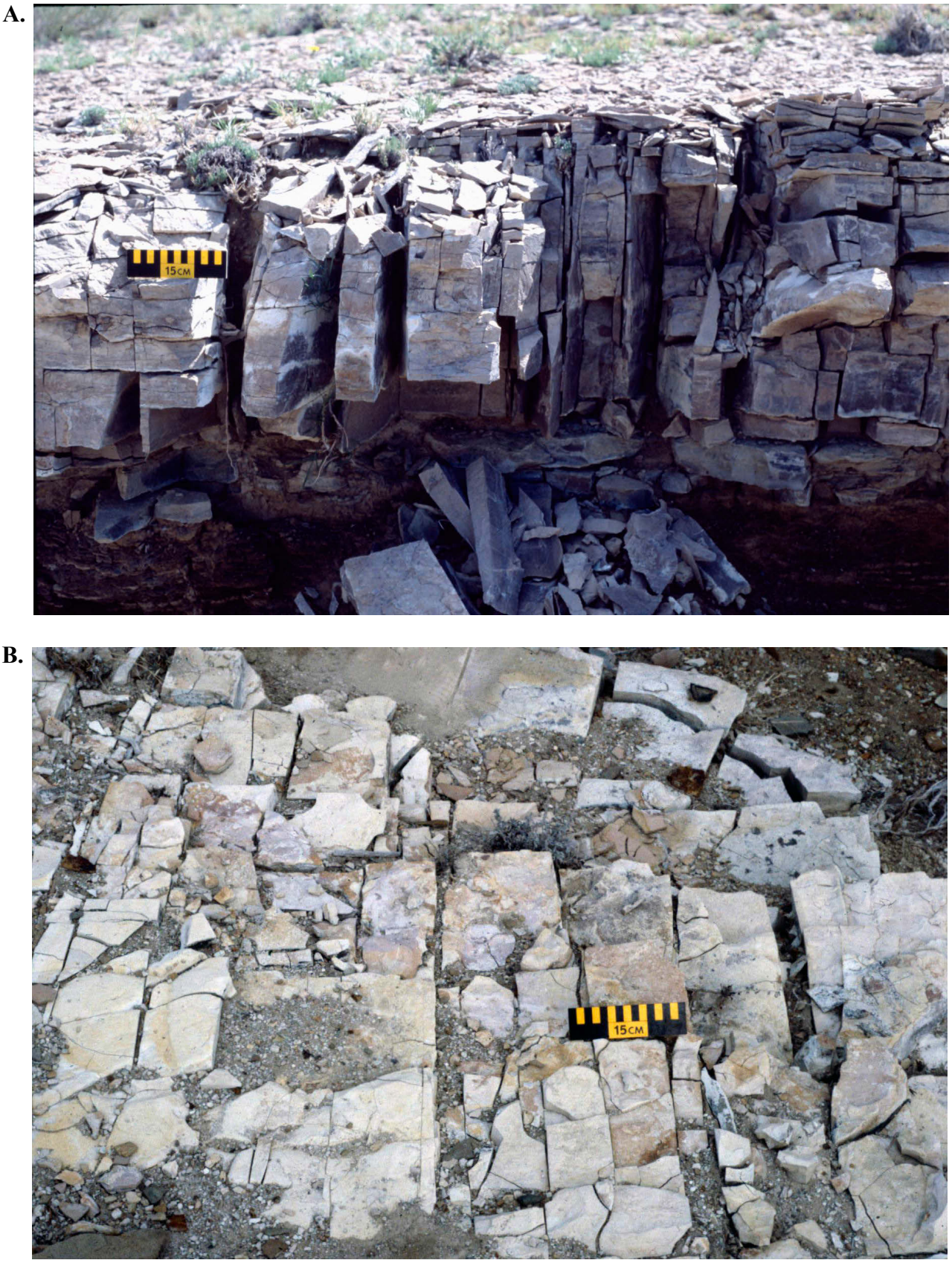

Figure 3.6. *Jointing in the Eocene Uinta Formation.* ***A.*** *Closely spaced, vertical jointing in fine-grained sandstone along the Duchesne fault and fracture zone, Duchesne field area. Joint sets shown here generally strike N. 62° E., N. 84° E., and N. 72° E. (from Chidsey and Laine, 1992).* ***B.*** *Orthogonal joint sets in fine-grained sandstone, Sowers Canyon field area. See figure 1.1 for field locations.*

Figure 3.7. *Examples of natural fracturing in cores from the NBU No. 253 well, Natural Buttes field.* ***A.*** *Open, vertical fracture in sandstone from the Castlegate Sandstone; no discernable mineralization (10,590 feet [3228 m]).* ***B.*** *Open fracture in homogenous, fine-grained sandstone from the Sego Sandstone; sandstone has 2.06% porosity (10,532 feet [3210 m]).*

Figure 3.8. *Abandoned mine workings along the southeast-trending Cowboy gilsonite vein, Uinta Formation, Uintah County. Mining occurred during the first half of the 20th century.*

result of tectonic stress in the region. Subsequent uplift of the Tertiary section expanded these existing fracture networks and possibly created additional fracture systems. Narr and Currie (1982) studied the origin of fracturing in Altamont field (figure 1.1) and suggested fractures in the basin are commonly open as a result of unloading by erosion of the overburden.

The distribution and abundance of natural fractures in the subsurface are strongly controlled by lithology and bedding characteristics (figure 3.6). They are found in most brittle units such as sandstone (figure 3.7) and carbonate beds. However, fractures also are present in shale and mudstone beds that contain significant amounts quartz silt and sand. Lucas and Drexler (1975) concluded that dense carbonate mudstone is fractured the most, followed by sandstone and then shale.

Locally, the abundance, and most importantly the orientations, of fractures are controlled by folds. In Bluebell, Peters Point, and Natural Buttes fields (figure 1.1), fractures are concentrated along subtle surface or subsurface anticlines and structural noses (Clem, 1985) and are generally parallel to the axis of these structures. Lucas and Drexler (1975) showed by determining the direction of reservoir drainage and pressure changes between wells, that the direction of connected fractures trend east-west in the shallow part of Bluebell field (parallel to the structural nose).

GILSONITE VEINS

Gilsonite veins are an unusual but significant component of the structural geology in the eastern Uinta Basin (figures 2.1 and 3.1). Gilsonite is a naturally occurring, solid, black, lightweight asphaltite (solid hydrocarbon) sourced from the Mahogany oil-shale zone of the Green River Formation (Tripp, 2004; Boden and Tripp, 2012). Gilsonite is used in a wide variety of products: printers ink, pavement sealant, adhesives, and drilling mud to name a few. It has been mined in the Uinta Basin since 1868 as open cuts (figure 3.8) and later underground (Tripp, 2004).

Deep burial and overpressuring of the Mahogany oil-shale zone generated hydrocarbons and expelled large quantities of

thermal water that hydrofractured the overlying rocks. Later, viscous petroleum was expelled and intruded into the existing fractures, enlarging and forcing them open, and subsequently solidifying into gilsonite (Tripp, 2004; Boden and Tripp, 2012).

Gilsonite veins in the eastern Uinta Basin are commonly several miles long (the longest vein system extends 24 miles [39 km]) and hosted in the Wasatch, Green River, Uinta, and Duchesne Formations (Boden and Tripp, 2012). Nearly 60 veins and vein systems totaling over 120 linear miles (190 km) in outcrop have been mapped by Boden and Tripp (2012). These veins vary in width from fractions of an inch to almost 18 feet (6 m), averaging 3 to 6 feet (1–2 m) (Tripp, 2004). They are vertical and continue into the subsurface for hundreds to as much as 2000 feet (600 m) or more, with only small variations in vein width (Tripp, 2004). The 60-mile by 30-mile (80 x 50 km) belt of gilsonite veins trends west-northwest, suggesting a genetic structural relationship to the basement-involved Uncompahgre uplift (Narr and Currie, 1982).

CHAPTER 4:

UINTA BASIN RESERVOIRS/AQUIFERS: TRIASSIC-JURASSIC GLEN CANYON GROUP THROUGH THE CRETACEOUS CEDAR MOUNTAIN AND DAKOTA FORMATIONS

---

by

Craig D. Morgan and Stefan M. Kirby

CONTENTS

INTRODUCTION 63
METHODS 63
TRIASSIC-JURASSIC GLEN CANYON GROUP AND NUGGET SANDSTONE 64
Thickness 64
Depth 65
Lithology 65
Reservoir Properties 66
Water Quality 69
Water Production, Use, and Disposal 76
Hydrocarbon Production 80
JURASSIC ENTRADA SANDSTONE 80
Thickness 80
Depth 82
Lithology 82
Reservoir Properties 82
Water Quality 86
Water Production, Use, and Disposal 88
Hydrocarbon Production 88
CRETACEOUS CEDAR MOUNTAIN AND DAKOTA FORMATIONS 88
Thickness 94
Depth 94
Lithology 94
Reservoir Properties 94
Water Quality 109
Water Production, Use, and Disposal 111
Hydrocarbon Production 111
SUMMARY 113

FIGURES

Figure 4.1. Early Jurassic Wingate Sandstone paleogeography 64
Figure 4.2. Early Jurassic Kayenta Formation paleogeography 64
Figure 4.3. Early Jurassic Navajo and Nugget Sandstone paleogeography 65
Figure 4.4. Outcrop of the Glen Canyon Group 65
Figure 4.5. Navajo facies and bedform types 66
Figure 4.6. Heterogeneity within dune sets 66
Figure 4.7. Structure on top of the Navajo/Nugget Sandstone, Uinta Basin 67
Figure 4.8. Thickness from the top of the Navajo/Nugget Sandstone to the top of the Chinle Formation 68
Figure 4.9. Frequency distribution of the gross thickness of the Glen Canyon Group/Nugget Sandstone 69
Figure 4.10. Drill depth to top of Navajo/Nugget Sandstone 70
Figure 4.11. Frequency distribution of the drill depth to top of Glen Canyon Group/Nugget Sandstone 71
Figure 4.12. Outcrop of Navajo Sandstone with large dune sets 71
Figure 4.13. Thickness of sandstone in the Glen Canyon Group/Nugget reservoir with ≥ 6% effective porosity 72
Figure 4.14. Thickness of sandstone in the Glen Canyon Group/Nugget reservoir with ≥ 12% effective porosity 73
Figure 4.15. Frequency distribution graphs of thickness of sandstone in Glen Canyon Group/Nugget Sandstone reservoir 74
Figure 4.16. Ratio of PHIE ≥ 6% and PHIE ≥ 12% to reservoir thickness versus drill depth, Glen Canyon Group/Nugget Sandstone 75
Figure 4.17. Porosity-permeability plot separated into facies, Nugget Sandstone, Anschutz Ranch East Field 76
Figure 4.18. Thickness of stratigraphic interval between the base of the moderately saline water and the top of the Navajo/Nugget Sandstone 77
Figure 4.19. Total dissolved solids versus depth, Glen Canyon Group/Nugget Sandstone 78
Figure 4.20. Produced water chemistry, Glen Canyon Group/Nugget Sandstone 78

Figure 4.21. Total water produced from the Glen Canyon Group/Nugget reservoir. 79
Figure 4.22. Frequency distribution of total water per well produced from Glen Canyon Group/Nugget reservoir 80
Figure 4.23. Water produced from Glen Canyon Group/Nugget reservoir, December 2014 81
Figure 4.24. Frequency distribution of total gas produced per barrel of water per well from the Glen Canyon Group/ Nugget reservoir 82
Figure 4.25. Total gas produced per well from the GCG/N reservoir through December 2014..... 83
Figure 4.26. Gas produced from the Glen Canyon Group/Nugget reservoir through December 2014 84
Figure 4.27. Frequency distribution of total gas produced per well from Glen Canyon Group/Nugget reservoir through December 2014 85
Figure 4.28. Frequency distribution of gas produced per well from Glen Canyon Group/Nugget reservoir, December 2014..... 85
Figure 4.29. Paleogeographic interpretation of the Entrada Sandstone..... 86
Figure 4.30. Outcrop of Entrada Sandstone dune facies..... 87
Figure 4.31. Depositional model with eolian dunes encroaching on a tidal flat, Namibia Desert..... 88
Figure 4.32. Structure on top of the Entrada Sandstone, Uinta Basin 89
Figure 4.33. Gross thickness, Entrada Sandstone 90
Figure 4.34. Net sandstone, Entrada Sandstone..... 91
Figure 4.35. Frequency distribution of the gross thickness, Entrada Sandstone 92
Figure 4.36. Frequency distribution of the net sandstone thickness, Entrada Sandstone 92
Figure 4.37. Drill depth to the top of Entrada Sandstone 93
Figure 4.38. Frequency distribution of the drill depth to top of Entrada Sandstone..... 94
Figure 4.39. Thickness of sandstone in Entrada Sandstone with 6% or more porosity..... 95
Figure 4.40. Thickness of sandstone in Entrada Sandstone with 12% or more porosity..... 96
Figure 4.41. Frequency distribution graphs of the thickness of sandstone, Entrada Sandstone 97
Figure 4.42. Ratio of PHIE ≥ 6% and PHIE ≥ 12% net sandstone thickness versus drill depth, Entrada Sandstone 98
Figure 4.43. Thickness of the stratigraphic interval between base of moderately saline water and top of Entrada Sandstone..... 99
Figure 4.44. Total dissolved solids versus depth, Entrada Sandstone..... 100
Figure 4.45. Produced water chemistry, Entrada Sandstone..... 100
Figure 4.46. Total barrels of water produced from the Entrada Sandstone 101
Figure 4.47. Frequency distribution of total water per well produced from Entrada Sandstone..... 102
Figure 4.48. Frequency distribution of total gas produced per barrel of water from Entrada Sandstone..... 102
Figure 4.49. Gas produced from the Entrada Sandstone, December 2014 103
Figure 4.50. Total gas produced per well from the Entrada Sandstone through December 2014 104
Figure 4.51. Frequency distribution of total gas produced per well from Entrada Sandstone through December 2014..... 105
Figure 4.52. Frequency distribution of gas produced per well from Entrada Sandstone, December 2014 105
Figure 4.53. Early Cretaceous paleogeography for Cedar Mountain and Dakota Formations..... 106
Figure 4.54. Structure on top of the Dakota Formation, Uinta Basin..... 107
Figure 4.55. Gross thickness of the Cedar Mountain and Dakota reservoir 108
Figure 4.56. Frequency distribution of the gross thickness of Cedar Mountain and Dakota reservoir 109
Figure 4.57. Net sandstone, Cedar Mountain and Dakota reservoir..... 110
Figure 4.58. Frequency distribution of the net sandstone thickness, Cedar Mountain and Dakota reservoir 111
Figure 4.59. Drill depth to the top of Dakota Formation..... 112
Figure 4.60. Frequency distribution of the drill depth to the top of the Dakota Formation 113
Figure 4.61. Thickness of sandstone with porosity ≥ 6%, Cedar Mountain and Dakota reservoir 114
Figure 4.62. Thickness of sandstone with porosity ≥ 12%, Cedar Mountain and Dakota reservoir 115
Figure 4.63. Frequency distribution of thickness of sandstone with ≥ 6% and ≥ 12% porosity, Cedar Mountain and Dakota reservoir..... 116
Figure 4.64. Ratio of thickness of sandstone with ≥ 6% and ≥ 12% porosity/net sandstone versus depth 117
Figure 4.65. Percent porosity versus permeability, Cedar Mountain and Dakota reservoir 118
Figure 4.66. Thickness of stratigraphic interval between the base of the moderately saline water and the top of the Dakota Formation..... 119
Figure 4.67. Total dissolved solids versus depth, Cedar Mountain and Dakota..... 120
Figure 4.68. Produced water chemistry, Cedar Mountain and Dakota reservoir..... 120
Figure 4.69. Total water produced from the Cedar Mountain and Dakota reservoir through December 2014 121
Figure 4.70. Water produced from the Cedar Mountain and Dakota reservoir, December 2014 122
Figure 4.71. Frequency distribution of the total water produced from the Cedar Mountain and Dakota reservoir 123
Figure 4.72. Frequency distribution of the gas per barrel of water produced per well, Cedar Mountain and Dakota 123
Figure 4.73. Total gas produced from the Cedar Mountain and Dakota reservoir through December 2014..... 124

Figure 4.74. Frequency distribution of total gas produced from the Cedar Mountain and Dakota reservoir through December 2014 125
Figure 4.75. Frequency distribution of gas produced from the Cedar Mountain and Dakota reservoir, December 2014 125
Figure 4.76. Gas production from the Cedar Mountain and Dakota, December 2014 126

CHAPTER 4:
UINTA BASIN RESERVOIRS/AQUIFERS: TRIASSIC-JURASSIC GLEN CANYON GROUP THROUGH THE CRETACEOUS CEDAR MOUNTAIN AND DAKOTA FORMATIONS

INTRODUCTION

The Upper Triassic–Jurassic Glen Canyon Group, Jurassic Entrada Sandstone, and Cretaceous Cedar Mountain and Dakota Formations represent both aquifers for produced-water storage and reservoirs for hydrocarbon production in the Uinta Basin (figure 1.5). These rocks were deposited in a wide variety of environments, primarily eolian, alluvial floodplain, fluvial, and marine, each with varying lithologies and petrophysical (porosity and permeability) properties. In the asymmetrical Uinta Basin, the Upper Triassic and Lower Cretaceous sections reach depths of more than 20,000 feet (6100 m).

The following sections describe the (1) thickness, (2) depth, (3) lithology, (4) porosity and permeability, (5) general water quality, (6) water production, use, and disposal, and (7) hydrocarbon production of these important, but deep formations in the Uinta Basin. These characteristics and companion maps provide the basic information required to assess or model those formations that may best serve as produced-water-storage aquifers.

METHODS

We began this study by using well databases, along with structure and thickness maps, that were developed for each reservoir (Glen Canyon Group/Nugget, Entrada, and Dakota/Cedar Mountain Formations; figure 1.5) as part of a previous study by the UGS for the Rocky Mountain Carbon Capture and Storage (RMCCS) project (McPherson and Matthews, 2014). The RMCCS required that all data be gridded at 1 square kilometer (km^2) and then upscaled to 10 km^2 for the National Carbon Sequestration Database and Geographic Information System (NATCARB) database, U.S. Department of Energy, National Energy Technology Laboratory. For the RMCCS study we mapped the Glen Canyon/Nugget and Entrada as a single reservoir. For this project, we mapped the Glen Canyon/Nugget and Entrada data as separate reservoirs and expanded and improved on the RMCCS research by correlating additional wells and calculating the thickness (feet of porosity) for each reservoir to provide a more accurate interpretation of the storage capacity of the aquifers. We compiled drill depth and thickness data for each reservoir for mapping from numerous well databases such as the Utah Division of Oil, Gas and Mining (DOGM) database, published geologic reports, internal UGS databases, and well correlations. We digitized many of the well logs into LAS format for easier correlation; other well logs were correlated using TIFF images downloaded from the DOGM website (http://oilgas.ogm.utah.gov). To ensure accuracy we quality checked formation boundaries in the databases by correlating logs and making new corrections as needed.

Roberts (2003) published a very detailed and accurate Dakota structure map of the Uinta Basin which was constructed by using Dakota well tops and projecting to the Dakota from the hundreds of shallower wells in the deeper part of the basin. We took the digital structural contour data from Roberts (2003) and converted the lines to points every 2000 meters (6505 ft). These point data were added to our Dakota well database giving us a detailed data set throughout the basin, even in areas where there were no Dakota penetrations. We used the well database to grid (1 km^2) the Dakota structure in the Uinta Basin creating an updated structure map. Computer generated structure contour maps of the Entrada and Navajo can be very inaccurate because of the lack of data in most of the basin. To create accurate maps of these aquifers we plotted the structural elevations of wells that penetrated the Entrada and Navajo/Nugget on base maps and drew structure contour maps by hand using the well data and following similar structural strike and dip of the detailed Dakota structure map. We digitized the contours drawn by hand converting them to point data which were added to the respective well databases. We used the expanded well databases to grid the structure of the tops of the Entrada and Navajo/Nugget.

Computer generated maps can produce some poor-quality interpretations in much of the basin where there are no control points. Therefore, we prepared thickness maps of the Glen Canyon Group/Nugget, Entrada, and Dakota reservoirs by hand contouring values from the respective well databases plotted on a base map. We digitized the contour lines and converted the lines to point data, and then added the point data to the respective well databases giving us an extensive basin-wide dataset. We used the expanded well databases to generate structure and thickness maps for each of the reservoirs in ArcMap® based on 1 km^2 grid cells. We used a digital elevation model (DEM) and gridded the DEM data using the same grid pattern as our structure and thickness grids (size and location) for each reservoir. We then subtracted the structural elevation grids for each reservoir from the DEM grid to produce overburden, or drill depth, grids.

For the RMCCS project, we assigned a single average porosity value to each reservoir evaluated, based on a review of geophysical well logs and published reports for the respective reservoir. This average porosity does not capture geographic and depth variations. For this project, we reviewed porosity logs (density or sonic) for each reservoir, recording the depth to the top of the reservoir and feet of porosity at 6% or more and 12% or more for each reservoir and then generated graphs for feet of porosity versus depth for 6% or more and 12% or more porosity for each reservoir. We used these data to develop predictive equations for feet of porosity at varying depths for each of the reservoirs. We used the equations to calculate the grid data of feet of porosity for each reservoir for each 1 square kilometer cell giving us a more accurate distribution of porosity.

We obtained hydrocarbon and produced water data from the DOGM website (Utah Division of Oil, Gas and Mining, 2016d) and used the data to construct cumulative and monthly production bubble maps for each reservoir.

TRIASSIC-JURASSIC GLEN CANYON GROUP AND NUGGET SANDSTONE

The Glen Canyon Group (Wingate Sandstone, Kayenta Formation, and Navajo Sandstone) and equivalent Nugget Sandstone (GCN/N) were deposited as large erg systems throughout parts of Utah, Arizona, Wyoming, and Colorado (figures 4.1 through 4.3) during the Late Triassic and Early Jurassic. The Navajo is the thickest and highest quality reservoir in the Glen Canyon Group. Figure 4.4 shows an outcrop of the Glen Canyon Group (figure 2.4 shows just the Navajo Sandstone in outcrop) and figure 4.5 shows facies and bedforms found within an eolian dune reservoir. The bedforms result in complex heterogeneity (porosity and permeability) within the reservoir (figure 4.6). Structure on top of the GCG/N reservoir shows an asymmetrical Uinta Basin with the reservoir more than 20,000 feet (6100 m) below mean sea level in the northern portion of the basin (figure 4.7).

Thickness

The GCG/N reservoir appears to be more than 1700 feet (500 m) thick in the northern part of the mapped area, but this may not be the true thickness due to steep dips and/or reverse faulting along the southern flank of the Uinta Mountains. Most wells to the west and southwest penetrated a maximum thickness of 800 to 1200 feet (250–350 m), thinning to less than 400 feet (120 m) to the east (figure 4.8). Most of the GCG/N is sandstone, therefore a net sandstone map was not prepared.

The gross thickness of the GCG/N reservoir in 375 wells studied ranges from 178 to 1725 feet (54–526 m) with an average of 882 feet (269 m) and a median of 869 feet (265 m) (figure 4.9). The Glen Canyon Group is more than 800 feet (250 m) thick throughout much of the study area, and the Navajo ac-

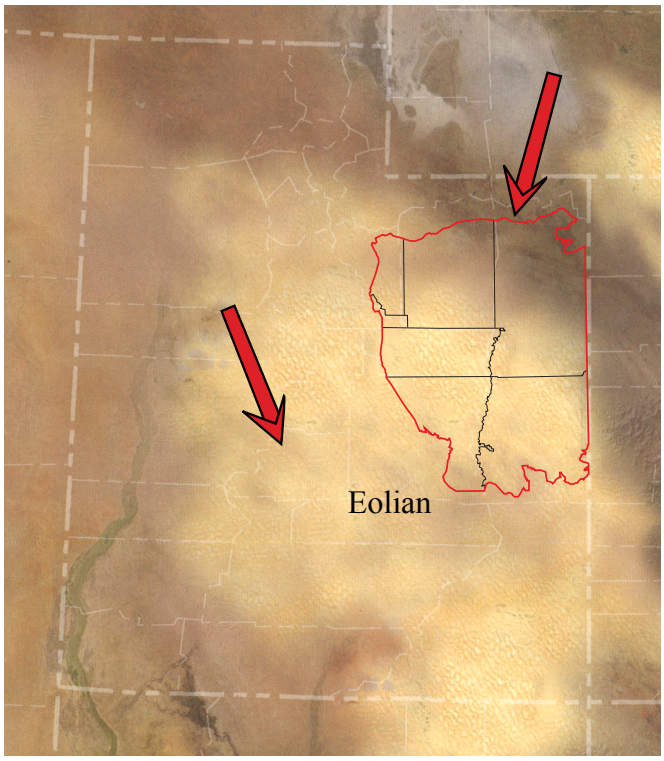

Figure 4.1. *Early Jurassic Wingate Sandstone paleogeography, dominated by dune deposits. Red arrows indicate prevailing wind directions, study area outlined in red. Modified from Blakey and Ranney (2008).*

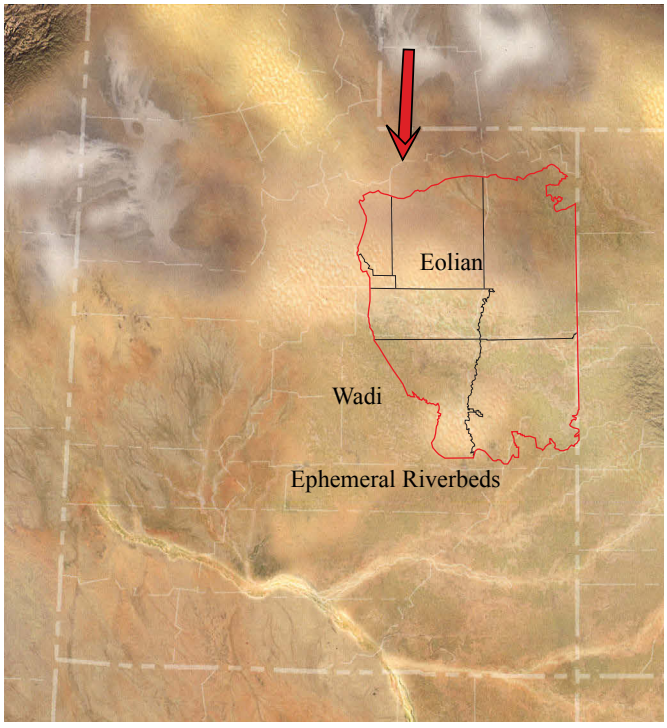

Figure 4.2. *Early Jurassic Kayenta Formation paleogeography. Sand-rich braided streams flowed west across a broad floodplain from the Ancestral Rockies. Red arrow indicates prevailing wind direction, study area outlined in red. Modified from Blakey and Ranney (2008).*

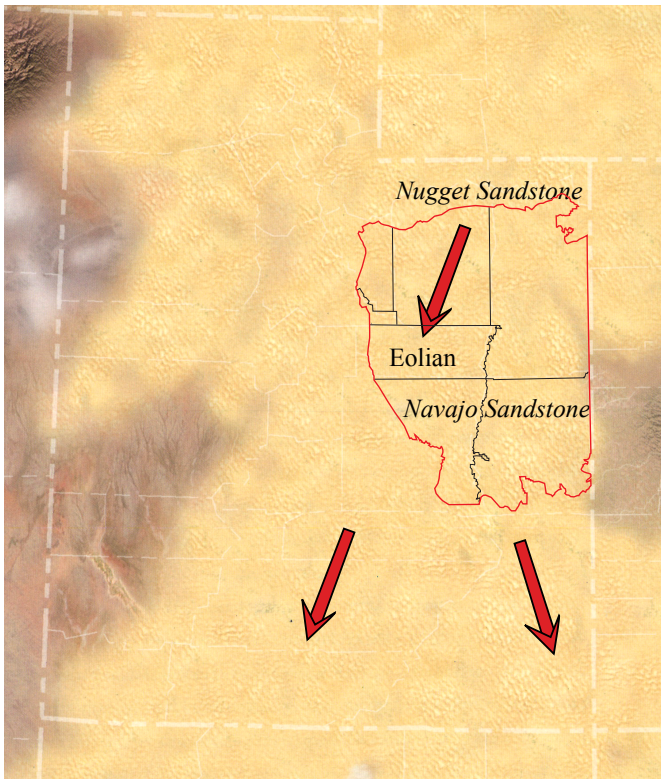

Figure 4.3. *Early Jurassic Navajo and Nugget Sandstone paleogeography. Most of the Colorado Plateau and all of the Uinta Basin were covered by extensive dune deposits. Red arrows indicate prevailing wind directions, study area outlined in red. Modified from Blakey and Ranney (2008).*

counts for a significant portion of that thickness. The Navajo is thin to completely absent over parts of the Uncompahgre uplift; however, this is not fully represented in the thickness map (figure 4.8).

Depth

Depth to the GCG/N in the deepest part of the basin, where no well has penetrated the reservoir, is projected to be more than 20,000 feet (6100 m) (figure 4.10). Drill depths in the wells studied range from 30 to 16,960 feet (9–5169 m), with an average depth of 3198 feet (975 m) and median of 2397 feet (731 m) (figure 4.11).

Lithology

The Navajo and Nugget Sandstone represent a coastal to inland dune field (Hintze and Kowallis, 2009). The dunes may have been the largest recorded in Earth's history (Kocurek and Dott, 1983) (figure 4.12). Dune deposits of the Navajo and Nugget are generally composed of well-sorted, fine- to medium-grained sandstone, and rare well-cemented interdunal deposits. The Wingate Sandstone is typically composed of smaller dunes and dune sets than those in the Navajo and Nugget. Numerous interdune deposits of reworked sand during relative rises in the water table resulted in a higher concentration of clay minerals in the Wingate. The Kayenta Formation is a series of channels deposited in a sand-rich braided stream or wadi environment separating the Wingate Sandstone from the Navajo Sandstone.

Figure 4.4. *Outcrop of the Glen Canyon Group, in ascending order: Wingate, Kayenta, and Navajo Formations along the Buckhorn Wash road, northern San Rafael Swell. The contact between the Kayenta and overlying Navajo Sandstone is gradational.*

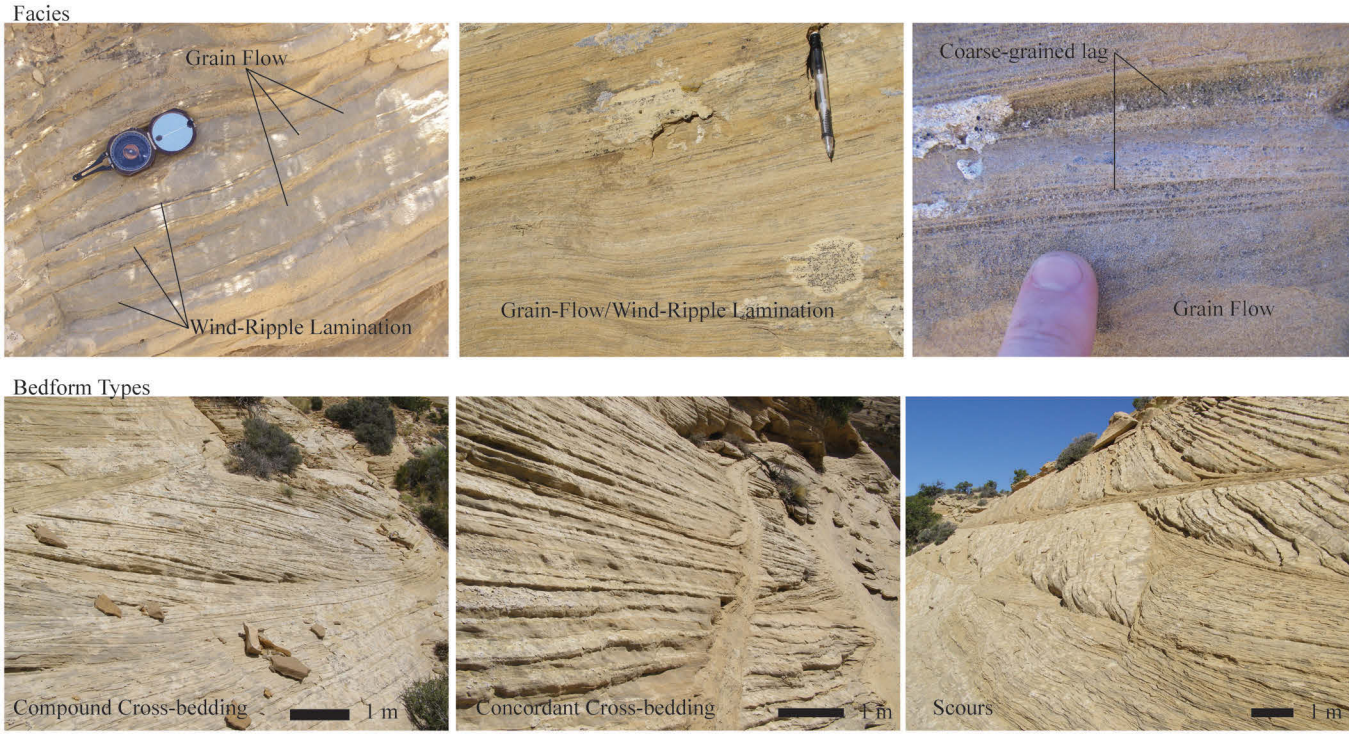

Figure 4.5. *Navajo facies and bedform types showing some of the depositional details that can affect fluid flow in an eolian dune reservoir. From Allen and others (2013).*

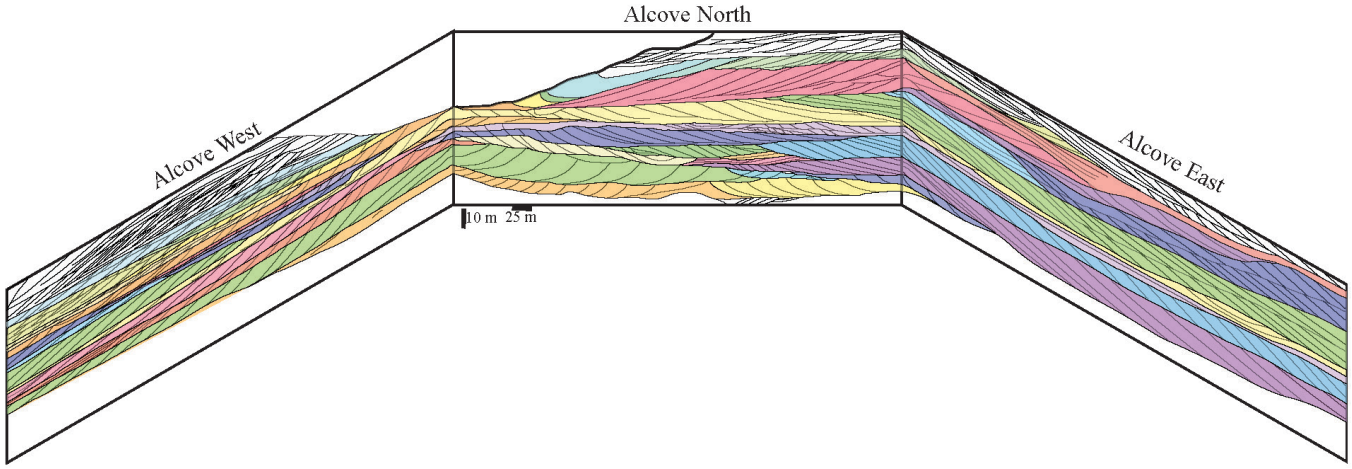

Figure 4.6. *Heterogeneity within dune sets. Three-dimensional model of a part of the Navajo Sandstone along the west flank of the San Rafael Swell. Colors represent individual dune sets through time. Bounding surfaces of the dune sets can impede fluid flow vertically and laterally. From Allen and others (2013).*

Reservoir Properties

The extensive winnowing of fines by wind resulted in clean, well-sorted sandstone with high porosity and permeability in the eolian facies of the Navajo and Nugget Sandstones. In the deeper parts of the basin, compaction and secondary diagenesis has greatly reduced the reservoir quality (figures 4.13 and 4.14). Although the Navajo and Nugget appear to be a thick, homogenous reservoir, the dune surfaces, dune set boundaries, and low-permeability interdunal deposits can affect fluid flow (figure 4.6). The Kayenta Formation is dominantly channel deposits with higher clay content than the overlying and underlying eolian deposits. Some individual channel deposits have moderate porosity and permeability but they are laterally discontinuous. The Wingate Sandstone is considered a tight sandstone reservoir with much lower porosity and permeability than the Navajo and Nugget having high concentrations of clay minerals.

Based on porosity determined from density and sonic well logs, sandstone thickness with 6% or more effective porosity (PHIE ≥ 6%) ranges from 14 to 1280 feet (4–390 m), with an average of 675 feet (206 m) and median of 761 feet (232 m). Sandstone with PHIE ≥ 12% ranges from 0 to 1138 feet

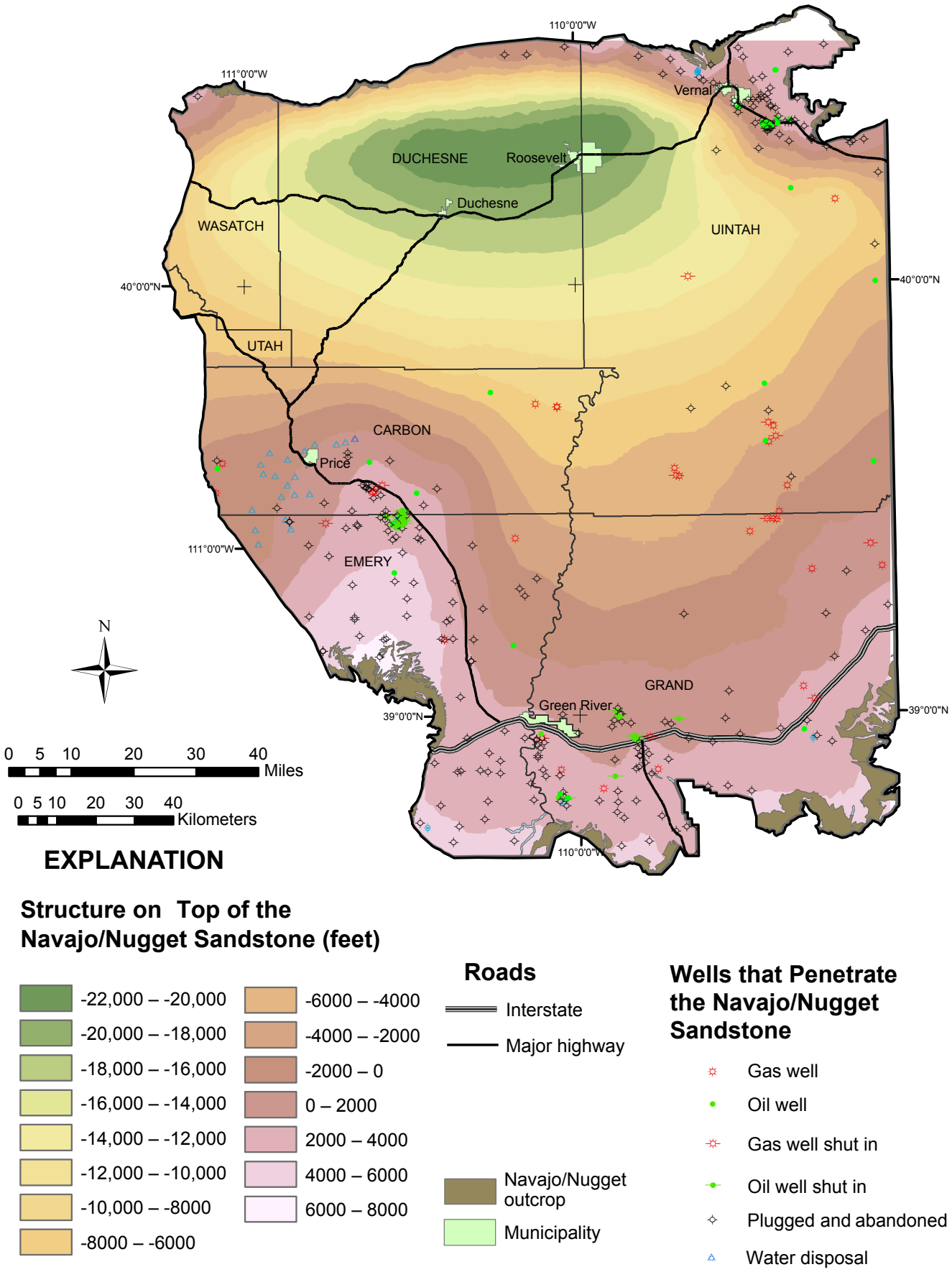

Figure 4.7. *Structure on top of the Navajo/Nugget Sandstone, Uinta Basin study area. Datum: mean sea level.*

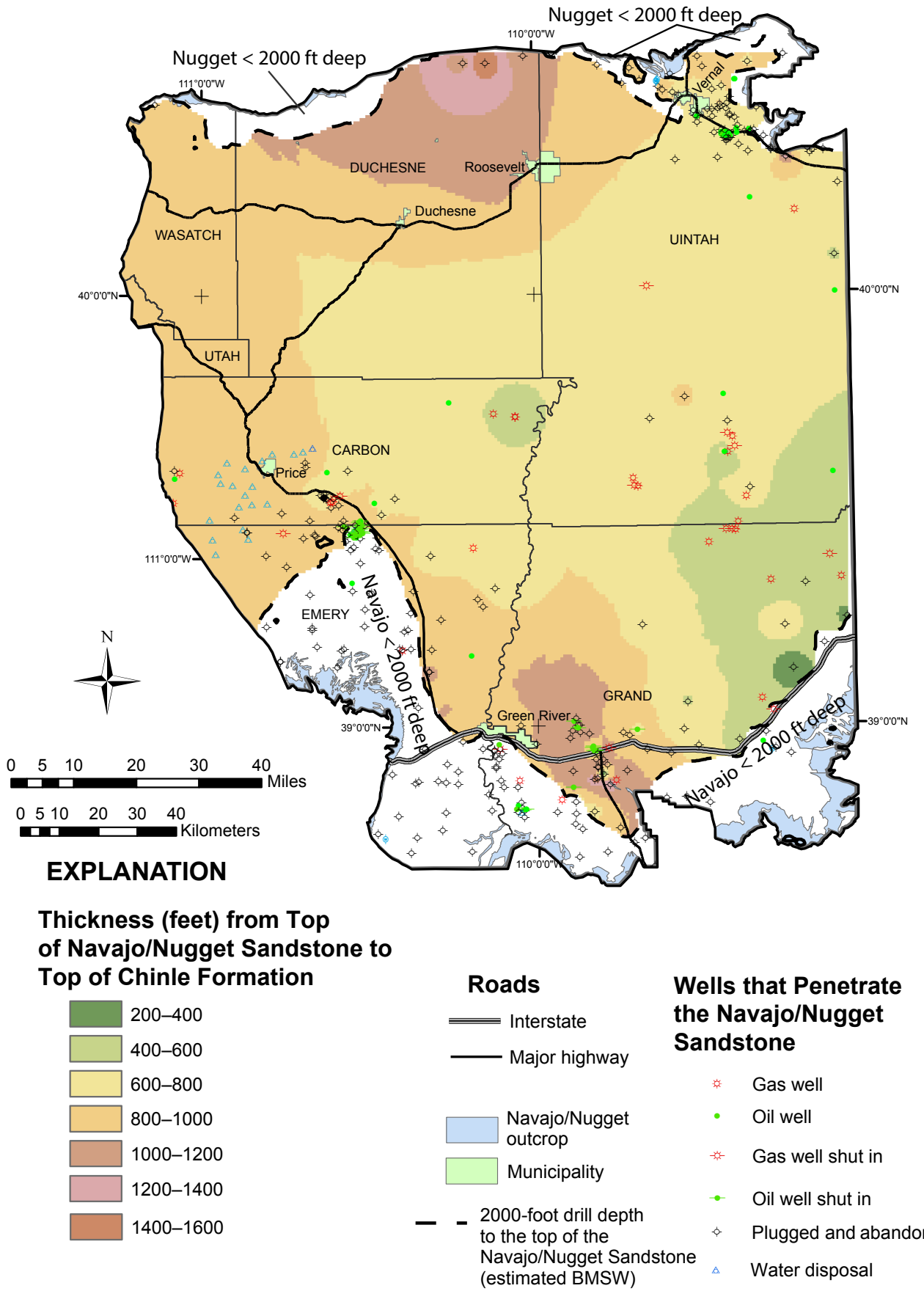

Figure 4.8. *Thickness from the top of the Navajo/Nugget Sandstone to the top of the Chinle Formation for areas greater than 2000 feet (600 m) deep. The 2000-foot drill depth is used as an estimated depth to the base of the moderately saline water (BMSW).*

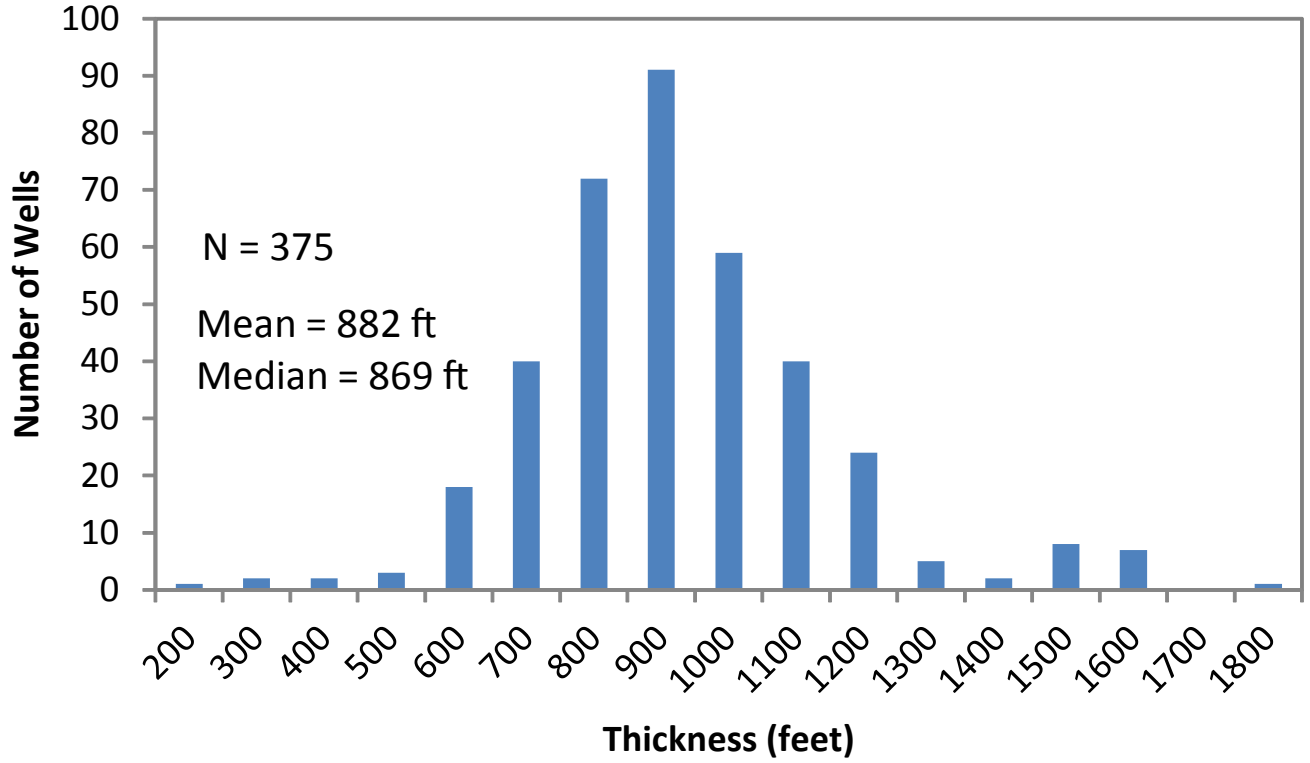

Figure 4.9. *Frequency distribution of the gross thickness of the GCG/N reservoir in the geophysical well logs studied.*

(0–347 m), with an average of 417 feet (127 m) and median of 350 feet (107 m) (figure 4.15). Figure 4.16 shows the ratio of PHIE ≥ 6% and PHIE ≥ 12% to gross reservoir thickness plotted against drill depth. Down to a depth of 5000 feet (1500 m) values range from 0.0 to 1.0, but many are in the 0.8 to 1.0 range. Below 5000 feet (1500 m) the ratio begins to decrease rapidly. The feet of sandstone with PHIE ≥ 6% and PHIE ≥ 12% in the GCG/N reservoir decreases rapidly with depth of burial (figures 4.16). However, since there are few penetrations of the GCG/N reservoir in the deeper parts of the basin, some areas of high porosity and permeability could exist at depth.

Very few GCG/N cores have been taken in the Uinta Basin. As a result, little is known about the spatial distribution or the porosity-to-permeability relationship of the reservoir. Numerous Nugget Sandstone cores have been obtained from the Utah thrust belt northwest of the Uinta Basin. Keele and Evans (2008) studied the Nugget Sandstone cores from Anschutz Ranch East field in Summit County, Utah, and developed a porosity-to-permeability plot based on facies (figure 4.17). Although the Nugget in the Utah thrust belt has undergone a much different structural and fluid-flow history than in the Uinta Basin, the thrust belt data were used as a proxy until more porosity and permeability data are gathered from the GCG/N reservoir in the Uinta Basin.

Water Quality

The northern portion of the Freethey and Stolp (2010) Glen Canyon aquifer study area in east-central Utah overlaps part of our study area. They describe groundwater flow and solute transport between the San Rafael Swell and San Rafael Desert recharge areas and the San Rafael and Green River discharge areas. The area north of Price (in the Uinta Basin) has little or negligible groundwater flow. Additional recharge areas exist along the southern boundary of the study area and along the northern mountain front boundary. There are no significant known discharge areas within the basin.

Anderson and others (2012) mapped the base of the moderately saline water (BMSW) (defined as 10,000 milligrams/liter [mg/L] total dissolved solids [TDS]) in the Uinta Basin. The drill depth to the BMSW was subtracted from the drill depth to the top of the Navajo/Nugget Sandstone to generate a map of the thickness of strata between the BMSW and GCG/N reservoir (figure 4.18). Throughout most of the basin, the GCG/N reservoir is thousands of feet below the BMSW except in Ashley Valley field (figure 1.1), where the water in the GCG/N is less than 10,000 mg/L TDS (GCG/N above the BMSW). Freethey and Stolp (2010) found that "dissolved-solids concentrations in the Glen Canyon aquifer in the area south of Price, Utah, increases from about 3000 milligrams/liter (mg/L) to greater than 10,000 mg/L in a horizontal distance of less than 5 miles (8 km) as depth of burial increases by about 1500 feet (460 m)." Anderson and others' (2012) mapping did not extend far enough south to capture the 10,000 TDS line in the GCG/N, but the 2000-foot (600 m) drill depth is used as an approximation of the BMSW in these areas based on Freethey and Stolp (2010) (figure 4.18).

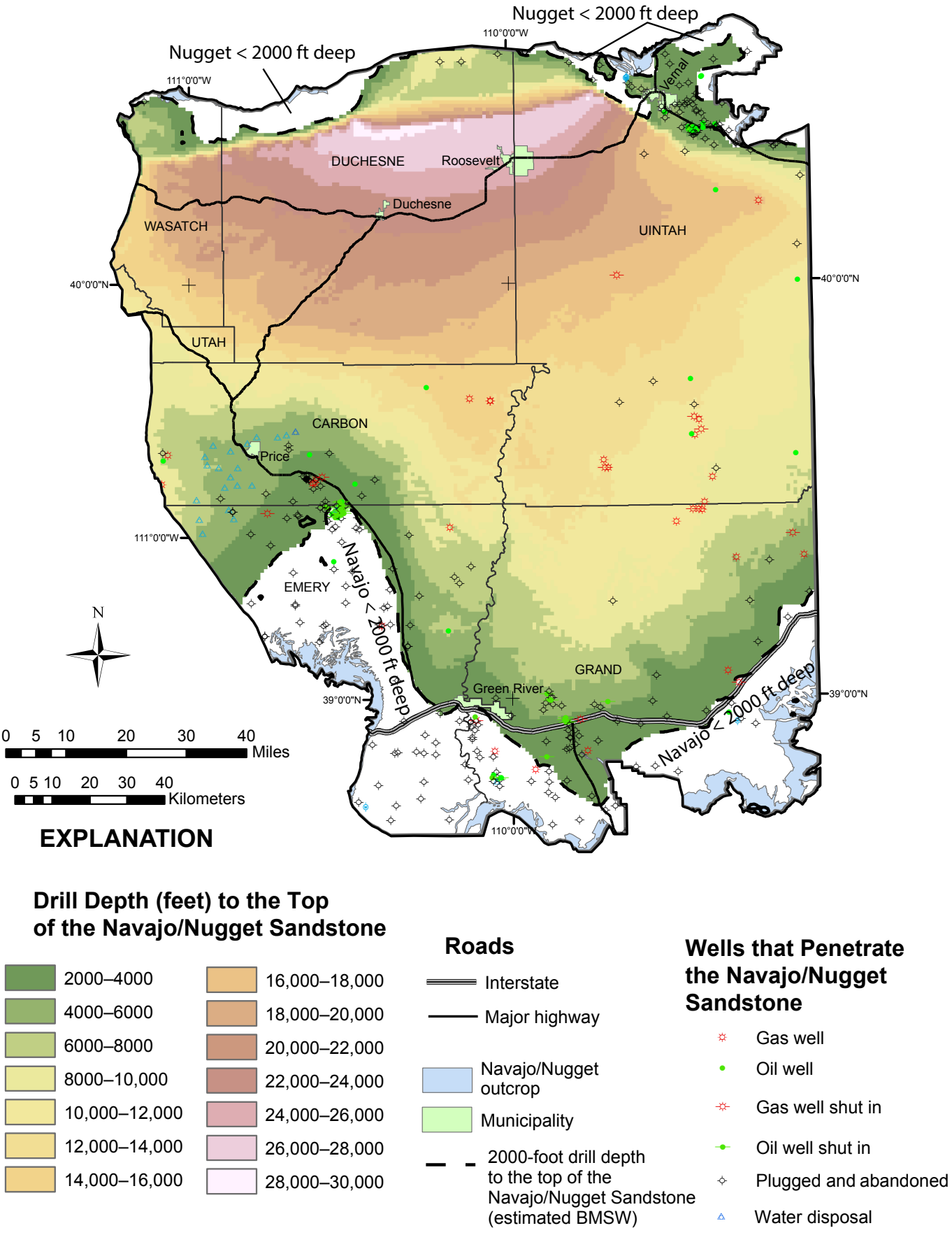

Figure 4.10. *Drill depth greater than 2000 feet (600 m) to the top of the Navajo/Nugget Sandstone. The 2000-foot drill depth is used as an estimated depth to the base of the moderately saline water (BMSW).*

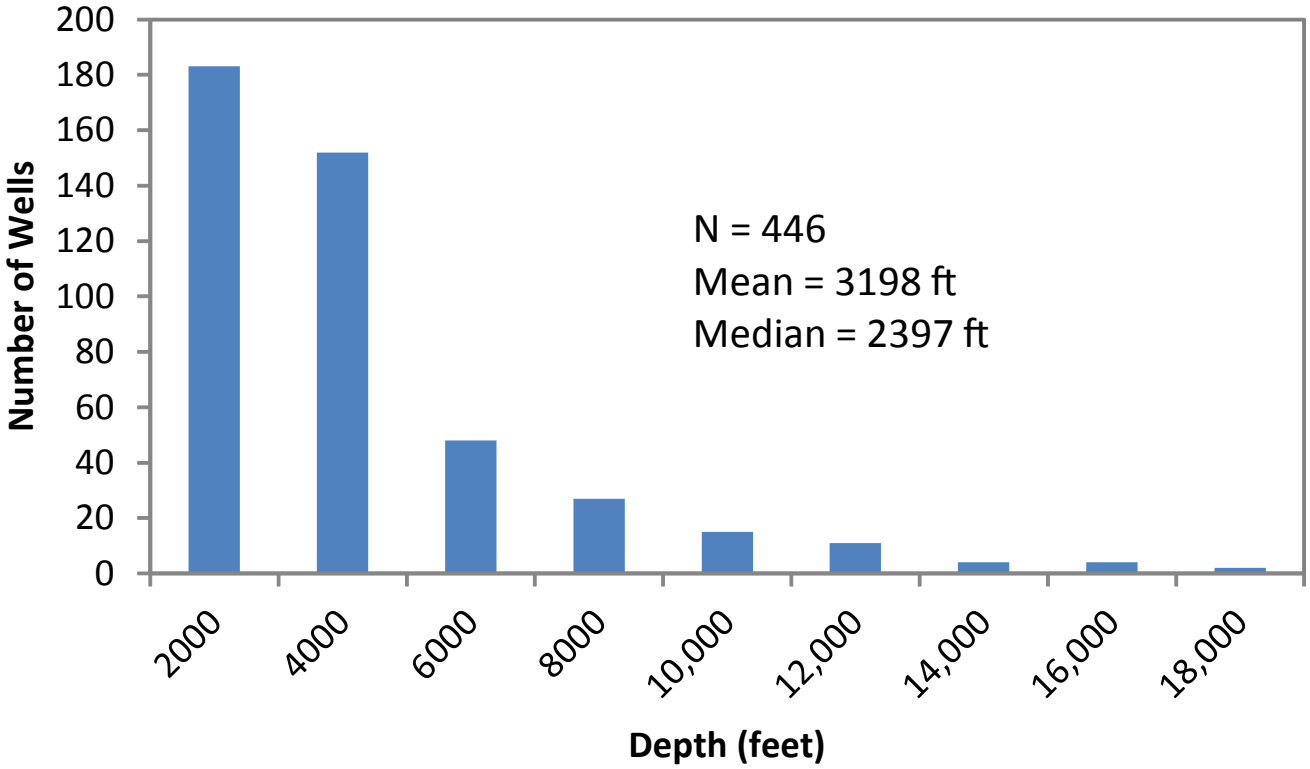

Figure 4.11. *Frequency distribution of the drill depth to the top of the GCG/N reservoir in the geophysical well logs studied.*

Figure 4.12. *Outcrop of the Navajo Sandstone with large dune sets capped by tightly cemented, low-porosity, interdunal deposit. Bounding surfaces of dune sets and interdunal deposits contribute to reservoir heterogeneity. Located in Harris Wash in Grand Staircase–Escalante National Monument, southeast of the town of Escalante in south-central Utah.*

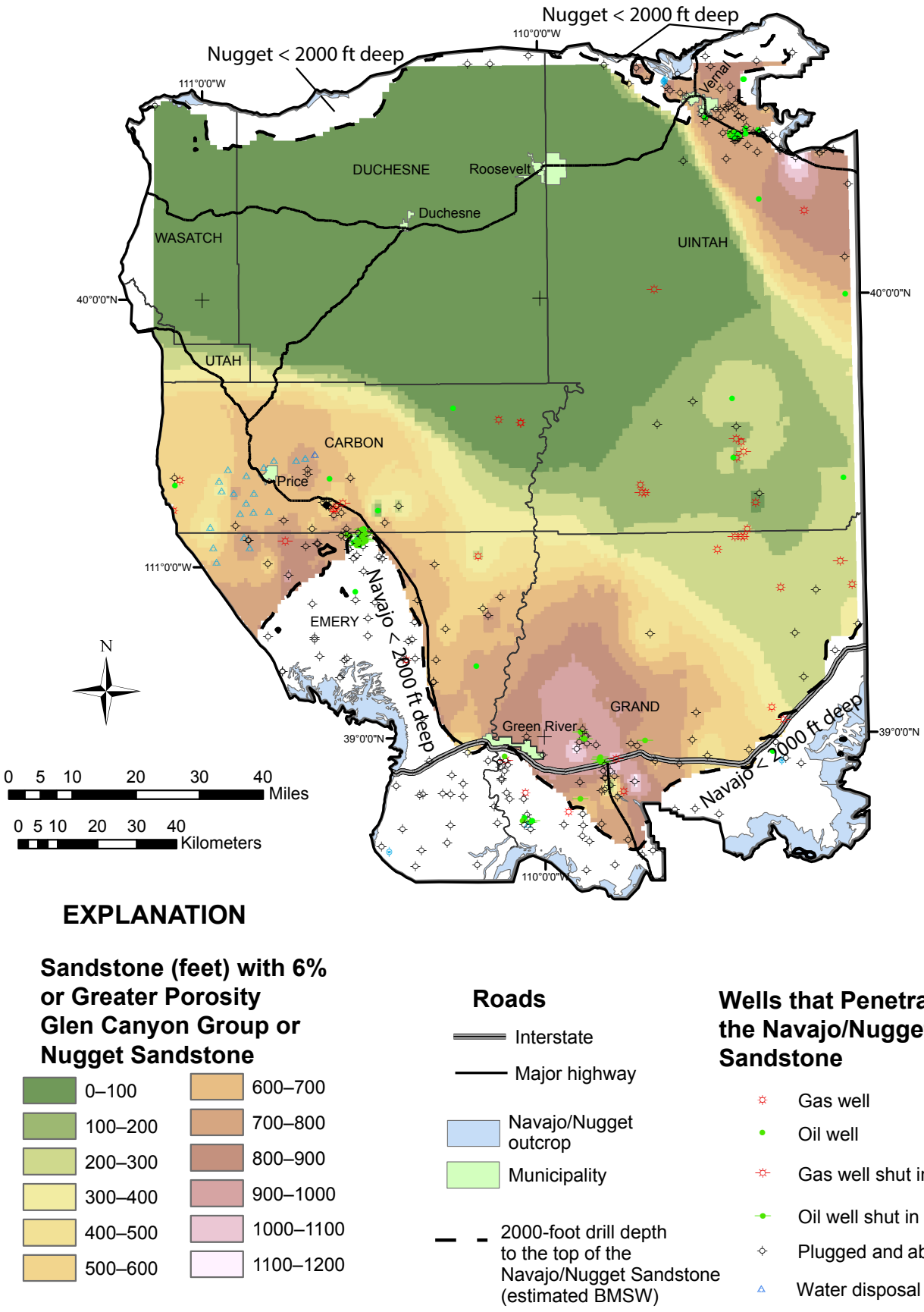

Figure 4.13. *Thickness of sandstone in the GCG/N reservoir with ≥ 6% effective porosity. Porosity determined from density or sonic well logs for areas primarily deeper than 2000 feet (600 m). The 2000-foot drill depth is used as an estimated depth to the base of the moderately saline water (BMSW).*

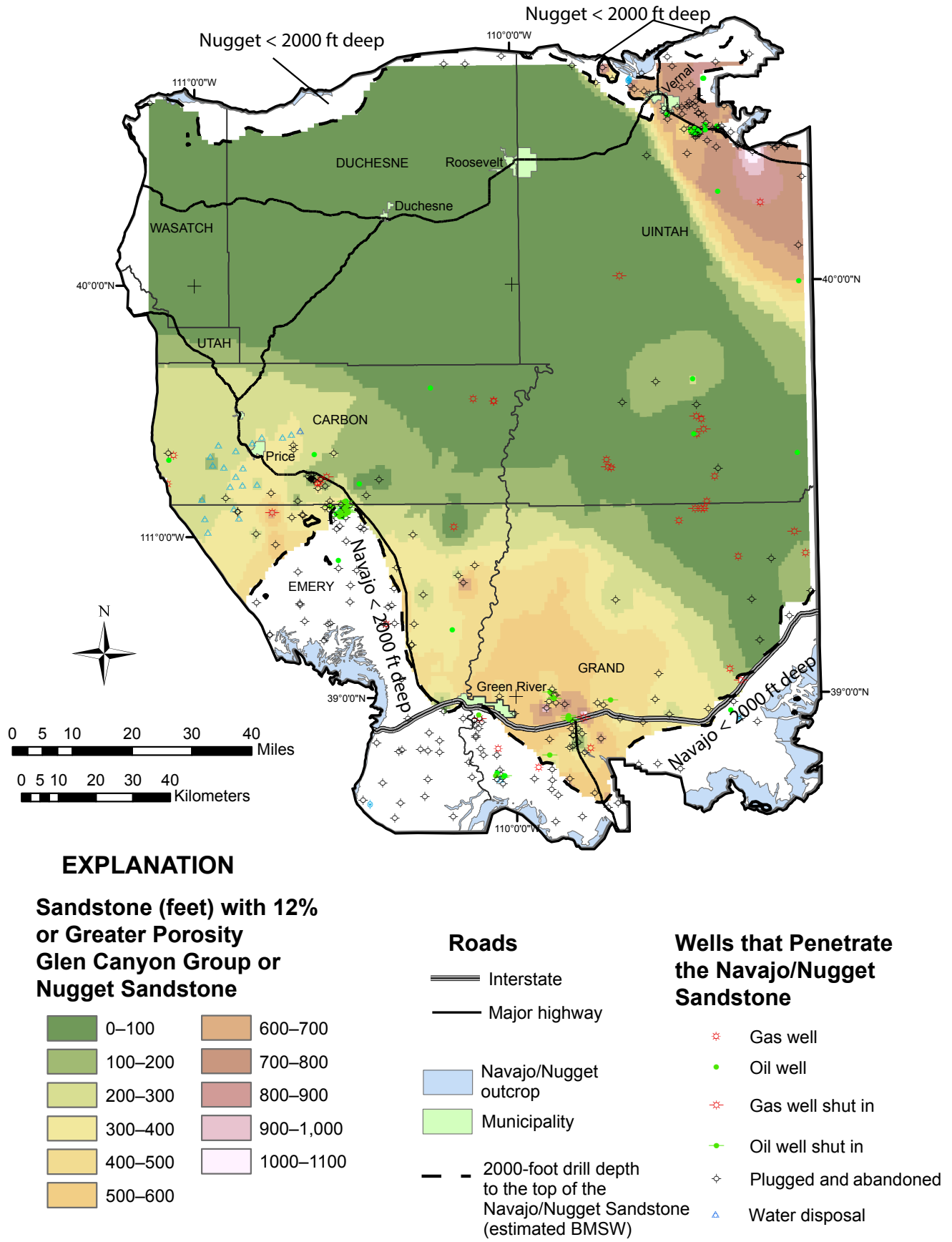

Figure 4.14. *Thickness of sandstone in the GCG/N reservoir with ≥ 12% effective porosity for areas deeper than 2000 feet (600 m). Porosity determined from density or sonic well logs. The 2000-foot drill depth is used as an estimated depth to the base of the moderately saline water (BMSW).*

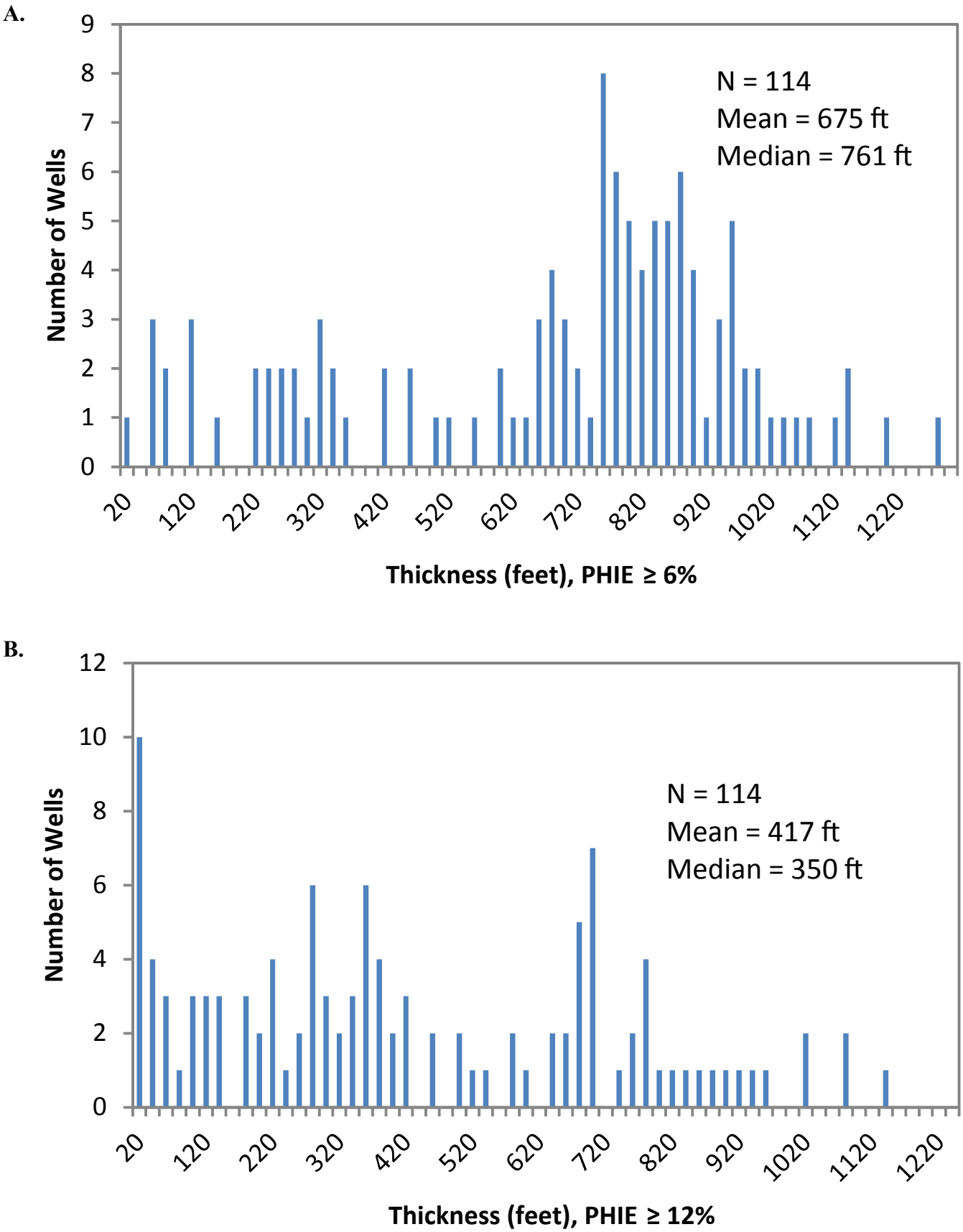

Figure 4.15. *Frequency distribution graphs of the thickness of sandstone with* ***A.*** *PHIE ≥ 6% and* ***B.*** *PHIE ≥ 12% in the GCG/N reservoir.*

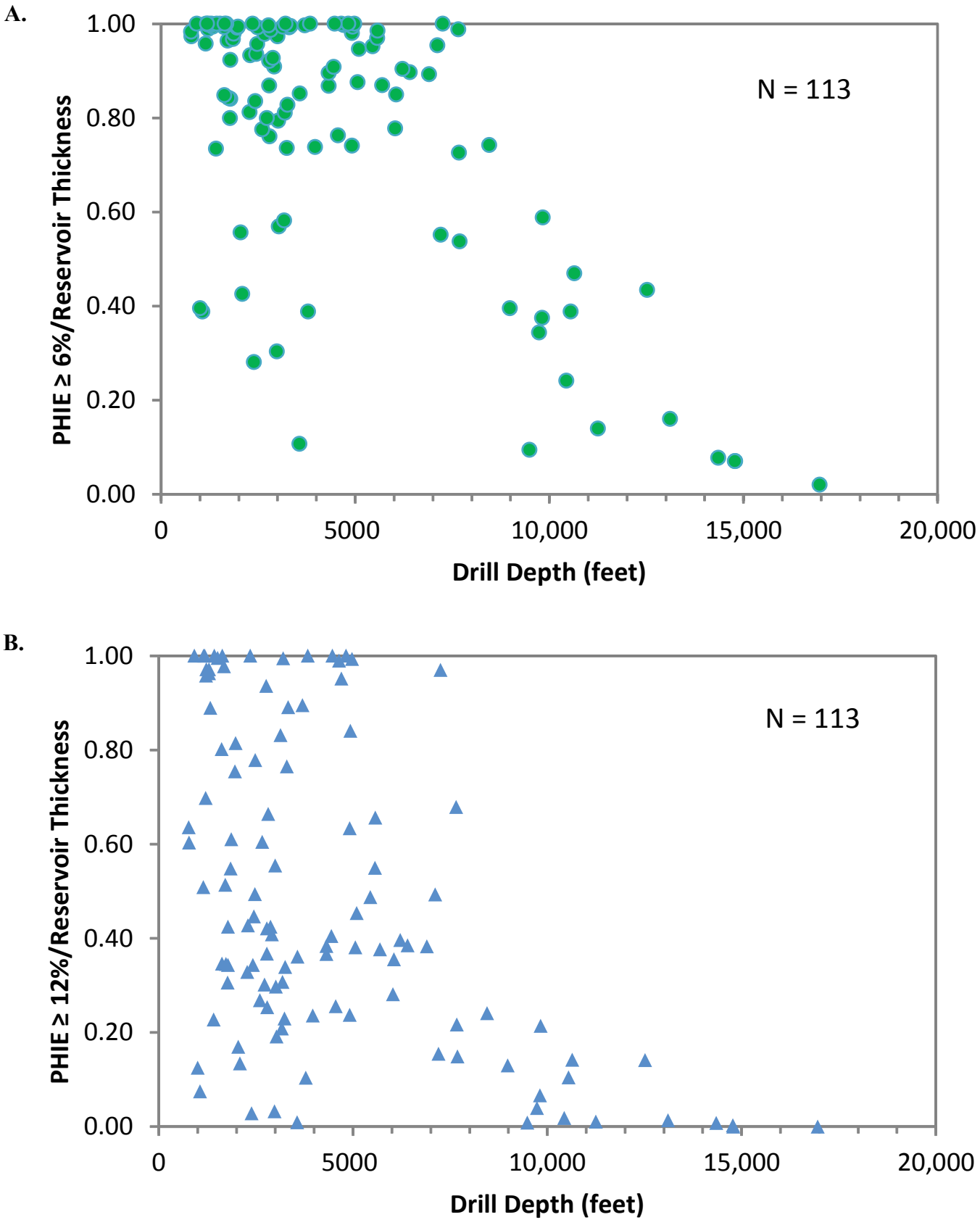

Figure 4.16. A. *Ratio of PHIE ≥ 6% to reservoir thickness versus drill depth, and* ***B.*** *ratio of PHIE ≥ 12% to reservoir thickness versus drill depth in the GCG/N reservoir. Porosity calculated from density and sonic logs.*

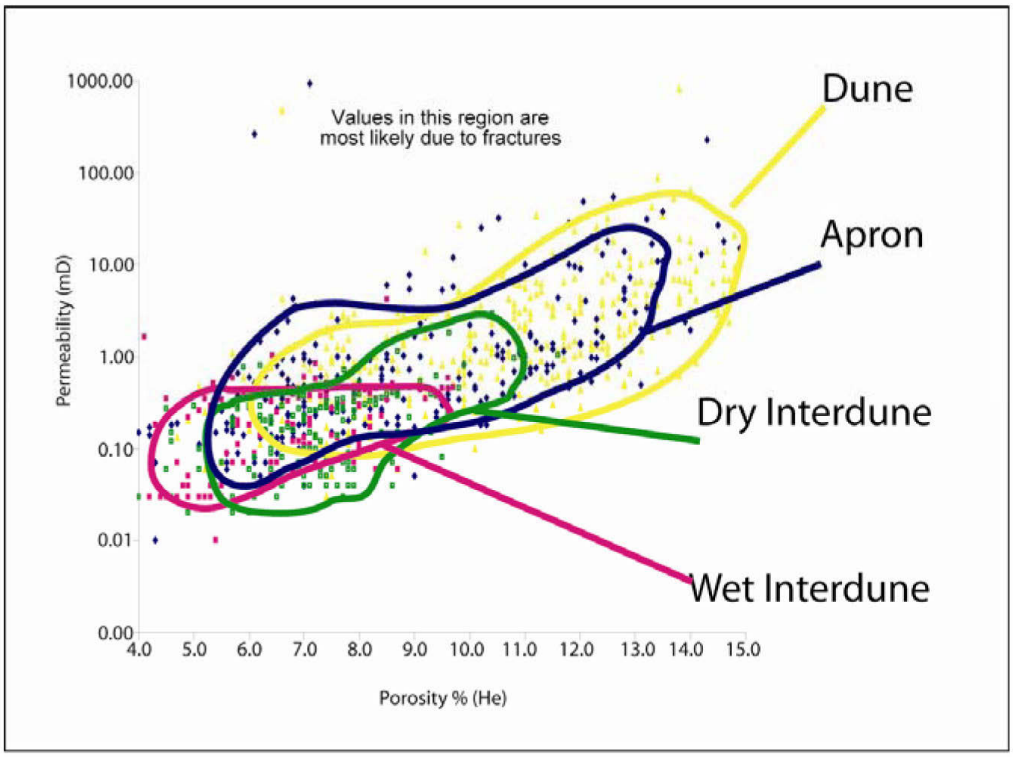

Figure 4.17. *Porosity-permeability plot for the Nugget Sandstone in the Utah thrust belt, separated into facies. The dune facies has the highest reservoir potential. Core data from the Anschutz Ranch East field, Summit County, Utah. From Keele and Evans (2008).*

Freethey and Cordy (1991) reported that Mesozoic aquifers in the upper Colorado River basin generally have sodium chloride water in the deep basins with TDS in excess of 35,000 mg/L, and shallower calcium bicarbonate water with TDS less than 2000 mg/L. Both waters have minor concentrations of iron and manganese. The hydraulic conductivity of the GCG/N aquifer is 0.1 to 10.0 feet per day (Freethey and Cordy, 1991).

Water quality data for GCG/N from oil and gas wells in the Uinta Basin are very sparse; we only found 16 samples we believe are reliable. The data show increasing TDS with depth (figure 4.19). The trend line indicates water is below 10,000 mg/L TDS to a depth greater than 6000 feet (2000 m), much deeper than expected from the work of Anderson and others (2012) and Freethey and Stolp (2010). The trend line is not considered reliable due to the few data points and the commingling of production water from other formations. The water types are sodium chloride from one deep well and a mix of all water types, except potassium chloride, from shallow depths (figure 4.20).

Water Production, Use, and Disposal

Hydrocarbon and associated water production from the GCG/N reservoir come from fields on the Uncompahgre uplift and Tavaputs Plateau (in the south-central Uinta Basin) with some water production from west of the town of Green River (Utah Division of Oil, Gas and Mining, 2016d). Through December 2014, 15 wells produced a total of 292,418 barrels of water (BW), but nearly half of that volume came from one well (figure 4.21). The average total production per well is 19,495 BW with a median of 4615 BW (figure 4.22). During December 2014, five wells produced 276 BW with more than half coming from one well (Utah Division of Oil, Gas and Mining, 2016d). Four of the wells currently producing water are on the Tavaputs Plateau; the other well is in the southeast Uinta Basin along the Uncompahgre uplift (figure 4.23). Water production per well during the month of December 2014 ranged from 0 to 140 BW.

The ratios of produced gas per barrel of water (GWR) per well range from 1 to 276 thousand cubic feet of gas (MCFG)/BW/well (figure 4.24). The average is 127 MCFG/BW with a median of 71 MCFG/BW.

The Navajo reservoir is used for produced-water disposal in the coal-bed methane fields in central Utah but is currently not used for disposal in the Uinta Basin. Freethey and Stolp (2010) developed a numerical simulation model to study the results of injecting into the Navajo. The model involved injecting 25,000 acre-feet (30 hm^3) over a 36-year period. Simulated water levels in the injection areas increased by 50 feet (15 m) and dissolved-solids concentrations increased by 100 mg/L or more. The modeled increases fit into the currently available aquifer storage. Similar results can be expected if the GCG/N reservoir is used for water disposal in the Uinta Basin. Produced water from the Navajo is probably disposed of in one or more of the four water disposal wells in the Tavaputs Plateau area in zones above the Navajo.

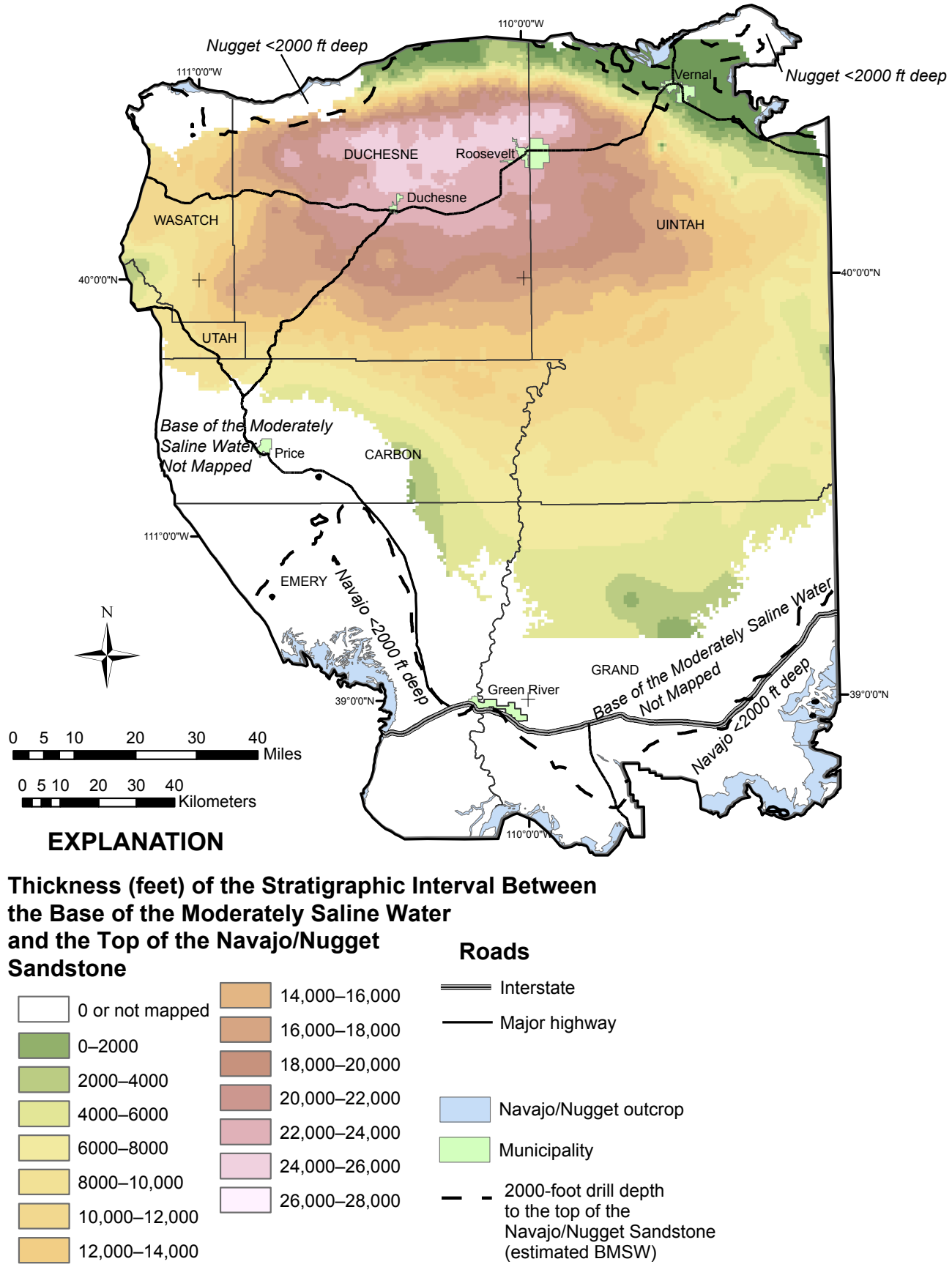

Figure 4.18. *Thickness of the stratigraphic interval between the base of the moderately saline water (BMSW) and the top of the Navajo/Nugget Sandstone. The Nugget is above the BMSW in Ashley Valley (see figure 1.1 for field location). The map was created using ArcScene® by subtracting the drill-depth map (figure 4.10) from the BMSW drill-depth map of Anderson and others (2012).*

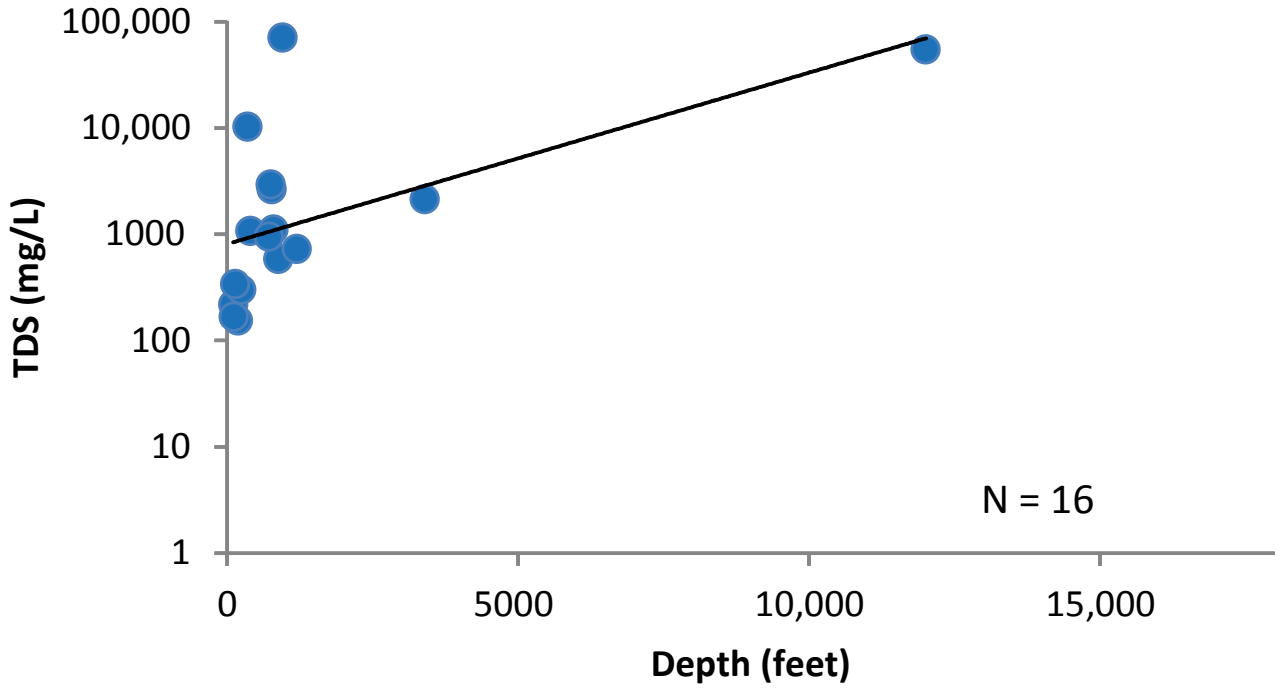

Figure 4.19. *Total dissolved solids versus depth for GCG/N water from oil and gas wells in the Uinta Basin. The exponential trend line indicates less than 10,000 mg/L TDS to a depth greater then 6000 feet (2000 m). However, the limited number of samples from deep wells (one) is insufficient to be statistically significant for such a large area.*

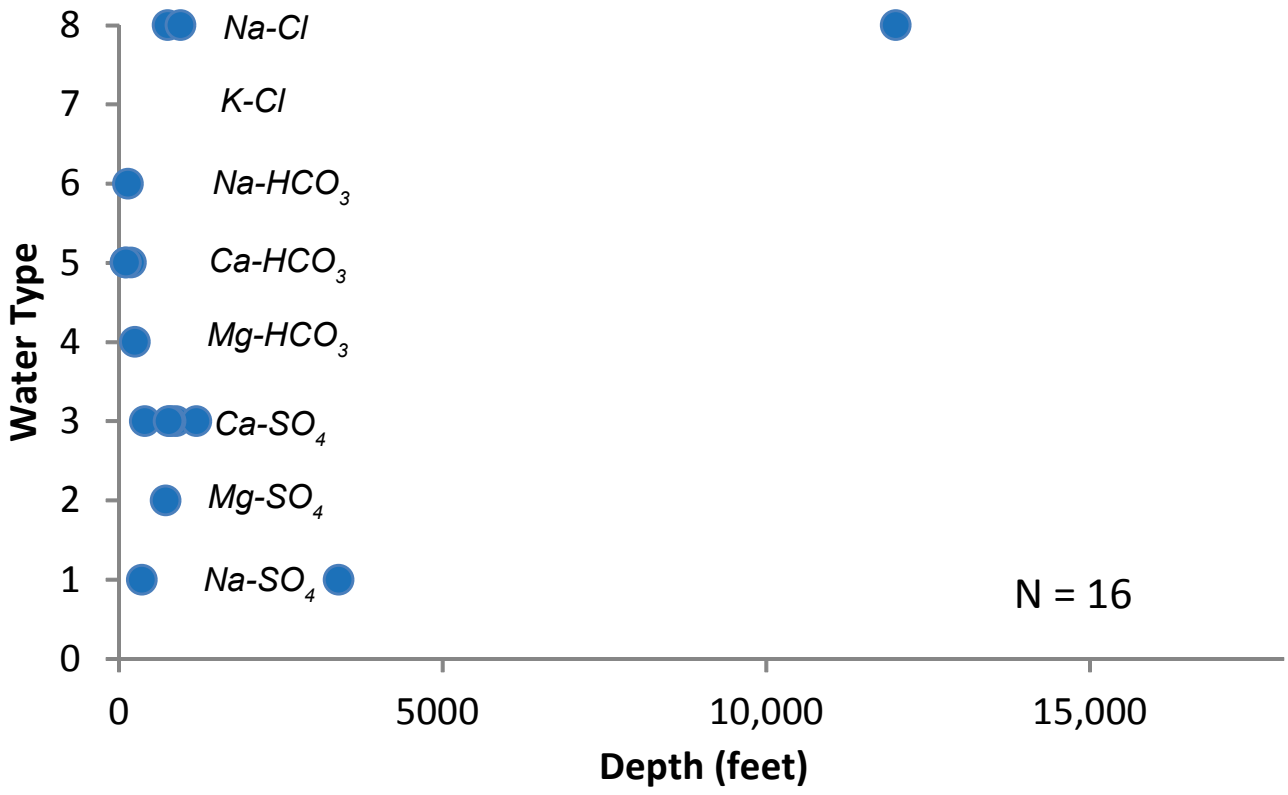

Figure 4.20. *Water produced from the GCG/N is sodium chloride (Na-Cl) from one deep well (> 5000 feet [1500 m]) and a mix of all the water types, except potassium chloride, at shallower depths. The number of samples from deep wells (one) is not statistically significant for such a large area.*

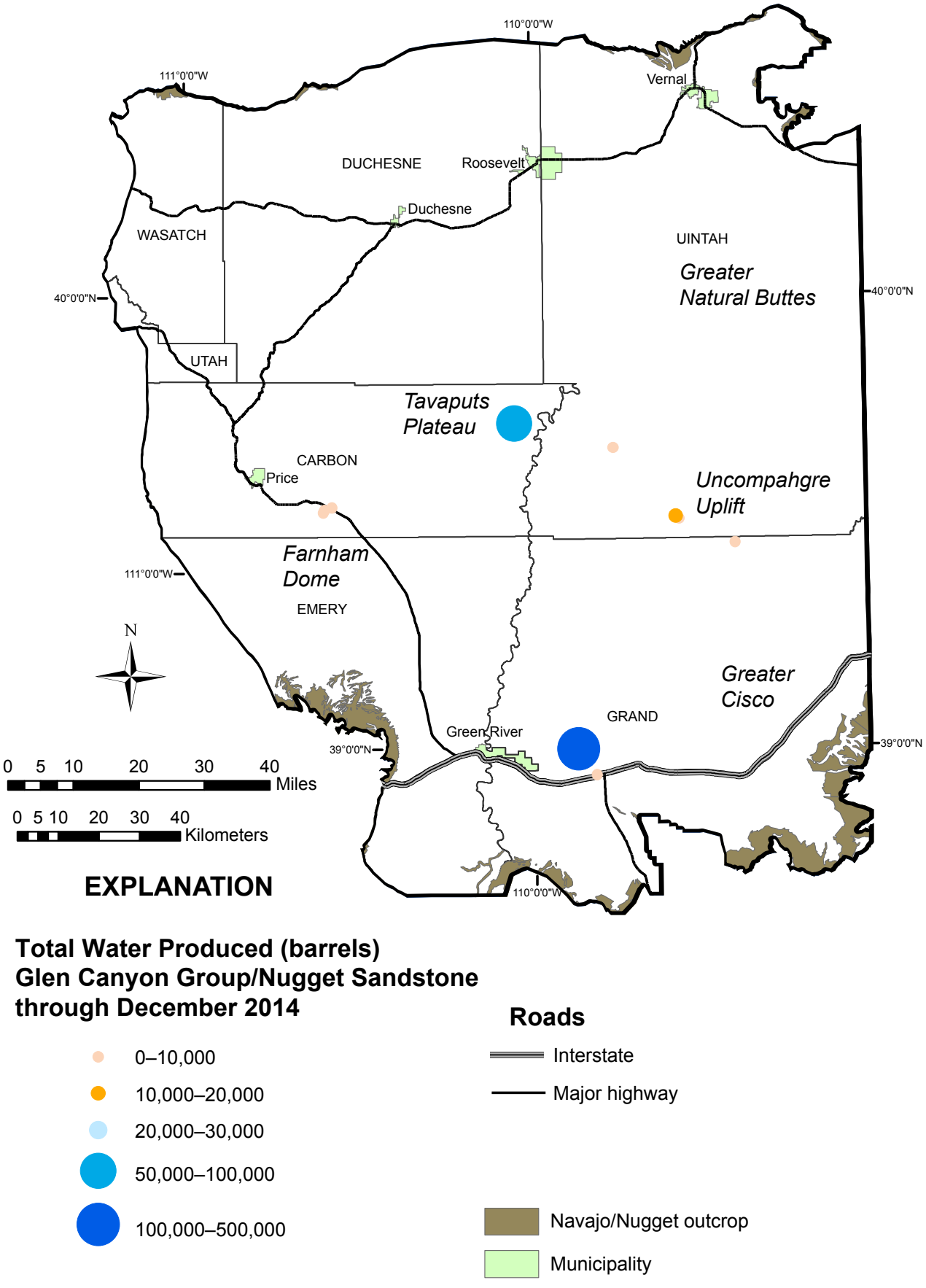

Figure 4.21. *Total water produced from the GCG/N reservoir.*

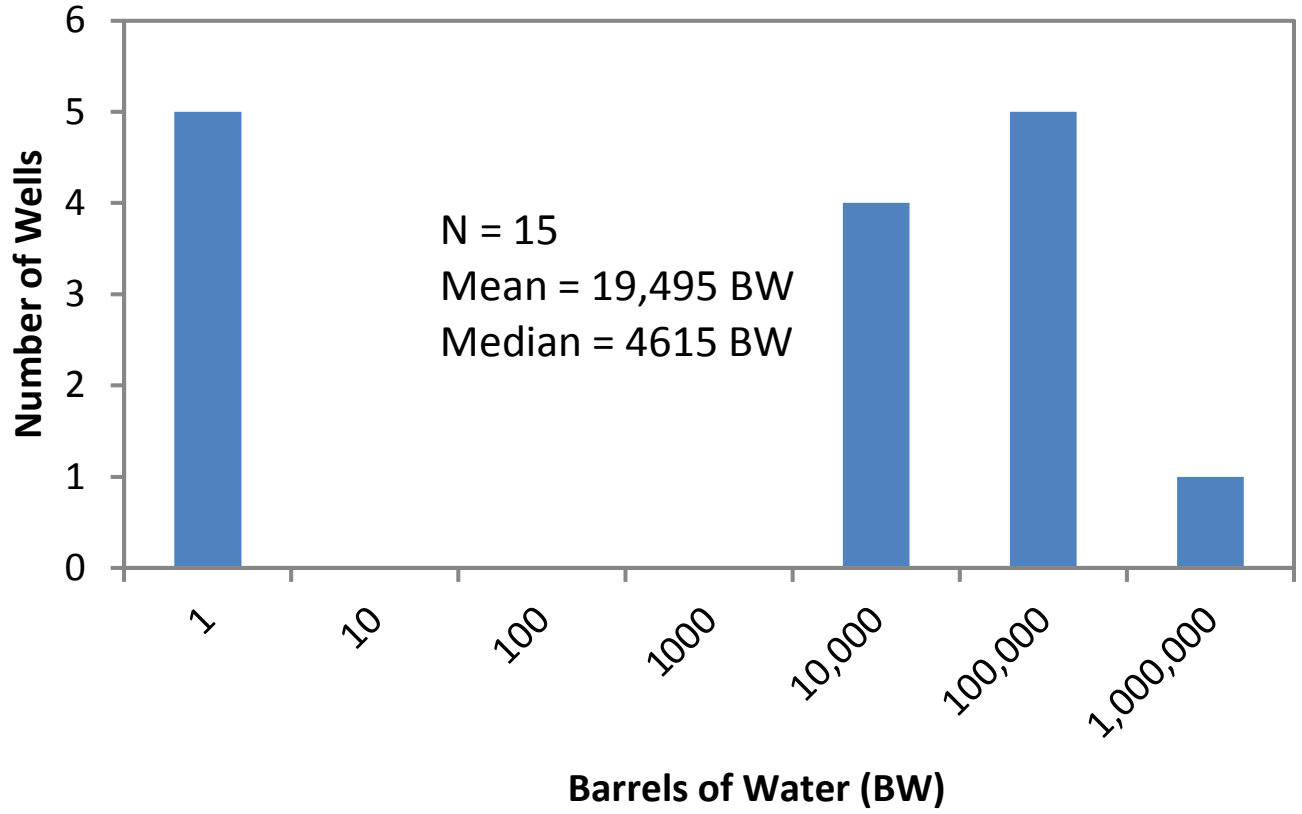

Figure 4.22. *Frequency distribution of total water per well produced from the GCG/N reservoir. Total water produced through December 2014 is 292,418 BW, with nearly half coming from one well. Water volumes range from 0 to 140,079 BW/well. Data from Utah Division of Oil, Gas and Mining (2016d).*

Hydrocarbon Production

Methane production from the GCG/N reservoir occurs along the Uncompahgre uplift and Tavaputs Plateau with minor oil and associated gas production west of the Greater Cisco area (figure 4.25). Most of the methane production is from the Navajo Sandstone with minor amounts from the Wingate Sandstone. Carbon dioxide (CO_2) is produced from the Navajo at Farnham Dome field near Wellington, Utah (figure 4.25). Total methane produced through December 2014 from 15 wells is more than 27 billion cubic feet (BCF), coming mostly from the Tavaputs Plateau (figure 4.25). Methane production from the GCG/N reservoir during December 2015 was primarily from the Tavaputs Plateau with lesser amounts from the Uncompahgre uplift and Green River Town areas (figure 4.26) (Utah Division of Oil, Gas and Mining, 2016d). Total production ranges from 0 (oil with no associated gas) to 8,012,292 MCFG/well, with an average of 1,819,612 MCFG/well and a median of 556,422 MCFG/well (figure 4.27). Methane produced during December 2014 from eight wells was 105,024 MCFG with an average of 13,128 MCFG/well and median of 7768 MCFG/well (figure 4.28).

JURASSIC ENTRADA SANDSTONE

The Jurassic Entrada Sandstone is a coastal eolian and tidal-flat–alluvial-plain deposit (figure 4.29) underlain by the marine Jurassic Carmel Formation and overlain by the J-3 unconformity, which defines the base of the marginal-marine Curtis Formation (Pipiringos and O'Sullivan, 1978). The Entrada consists of two primary facies: (1) eolian dune deposits in eastern Utah and (2) mudstone-rich, red-bed facies in central Utah. Figure 4.30 shows examples of the dune facies near Moab and mudstone-rich facies in the San Rafael Swell. Figure 4.31 is a modern analog in the Namibia Desert of the depositional interpretation of the Entrada. Structure on top of the Entrada shows an asymmetrical Uinta Basin with the Entrada more than 20,000 feet (6100 m) below mean sea level in the northern part of the basin (figure 4.32).

Thickness

The Entrada Sandstone is more than 500 feet (150 m) thick in the western Uinta Basin, but net sandstone (gamma ray ≤ 60 API) dramatically thins from east to west (figures 4.33 and 4.34). The Entrada is composed of stacked dune deposits in eastern Utah that typically are well-sorted sandstones with good porosity and permeability. The Entrada in central and western Utah has been described as sand flats or mud-rich red-bed facies. Deposits in the red-bed facies have been interpreted as marine tidal flat, sabkha, and supratidal (Smith, 1976; Marino, 1992; Marino and Morris, 1996; Hicks and others, 2010). Jennings (2014) described the Entrada in the west-central part of the state as dominantly alluvial floodplain

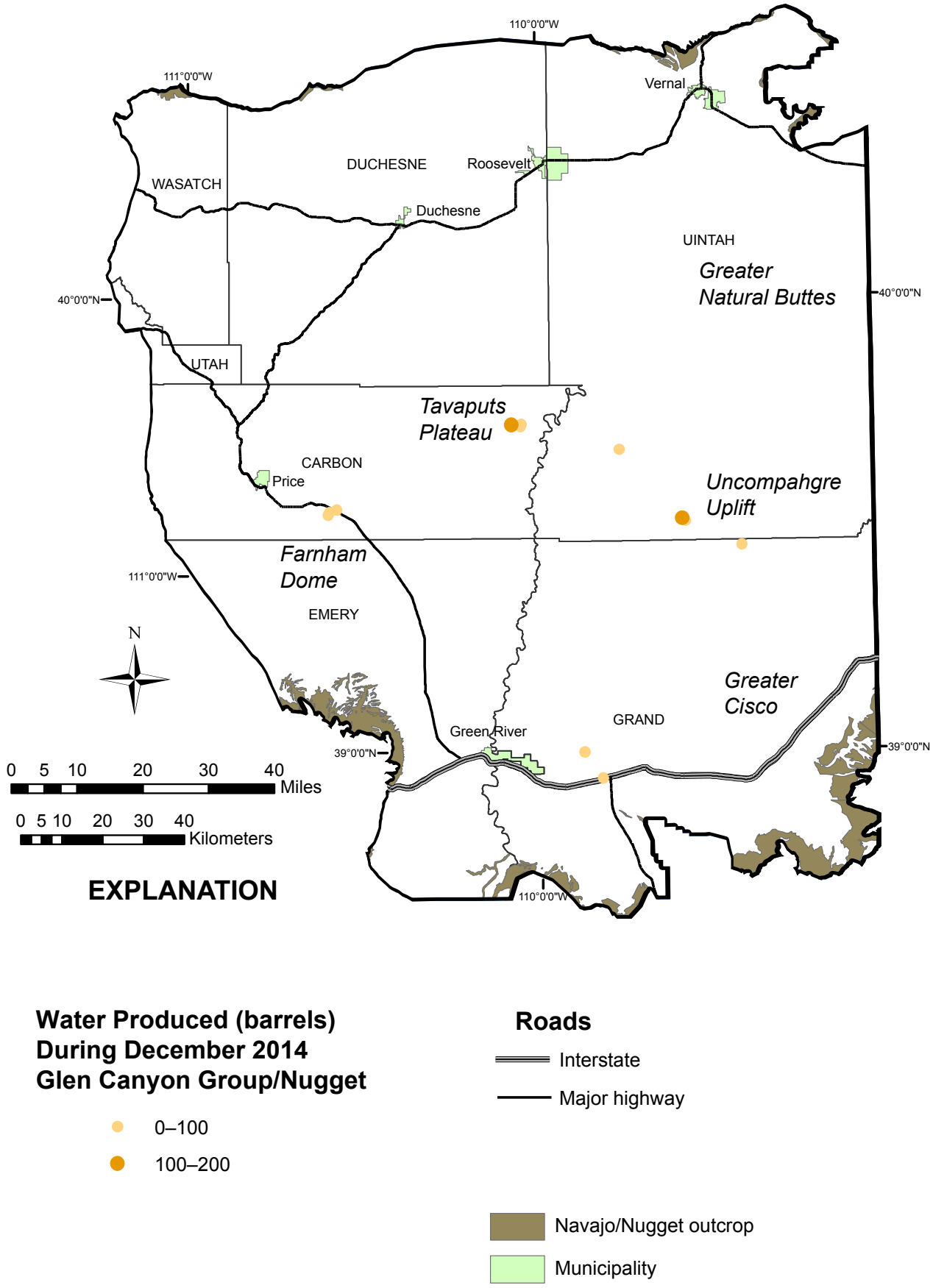

Figure 4.23. *Water produced from the GCG/N reservoir during the month of December 2014. Data from Utah Division of Oil, Gas and Mining (2016d).*

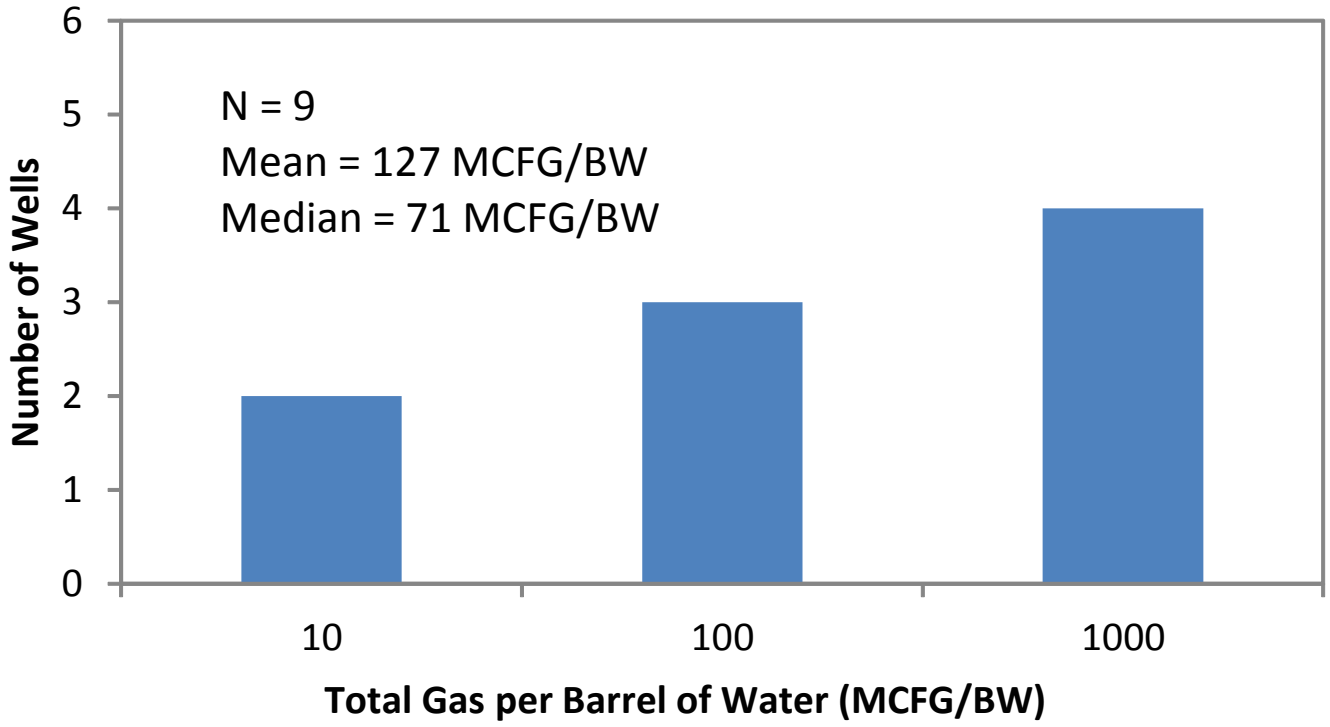

Figure 4.24. *Frequency distribution of total gas produced per barrel of water per well from the GCG/N reservoir. The range is from 1 to 276 MCFG/BW. Five wells not included in this data set produce gas and no water. Data from Utah Division of Oil, Gas and Mining (2016d).*

channels sourced from the Elko fold belt to the west. The red-bed facies has some thin (10 feet [3 m]), laterally limited eolian sandstone beds with good reservoir properties.

The gross thickness of the Entrada Sandstone in 329 wells studied ranges from 26 to 1210 feet (8–369 m), with an average of 340 feet (103 m) and median of 273 feet (83 m) (figure 4.35). The net sandstone shows rapid thinning from east (eolian facies) to west (red-bed facies) (figure 4.34). The net sandstone thickness ranges from 6 to 670 feet (2–204 m), with an average of 210 feet (64 m) and median of 194 feet (59 m) (figure 4.36).

Depth

Drill depth to the Entrada Sandstone in the deepest part of the Uinta Basin, where no well has penetrated the reservoir, is projected to be more than 28,000 feet (8500 m) (figure 4.37). Drill depths in the wells studied range from 19 to 16,550 feet (6–5044 m), with an average of 3974 feet (1211 m) and median of 2684 feet (818 m) (figure 4.38).

Lithology

The eolian facies of the Entrada Sandstone consists of fine-grained feldspathic arenite with alternating clay-rich and less clay-rich laminae (Morris and others, 2005). The eolian facies consists of high-angle, trough cross-stratified sandstone with horizontally bedded, locally algal-laminated interdunal sandstone, siltstone, and shale. The red-bed facies typically consist of red silty shale and interbedded red channel sandstone beds and thin overbank deposits. In most areas the red-bed facies contains abundant clay.

Reservoir Properties

Porosity and permeability are well developed in the eolian facies of the Entrada Sandstone. Density or sonic logs were used to determine the feet of sandstone with 6% or more porosity (PHIE ≥ 6%) and 12% or more porosity (PHIE ≥ 12%) in 120 wells. Maps of PHIE ≥ 6% and PHIE ≥ 12% follow the paleogeographic trend of the eolian facies but with porosity decreasing in the deeper basin (figures 4.39 and 4.40). Porosity in the red-bed facies is generally developed in thin, isolated sandstone beds. PHIE ≥ 6% has a range of 0 to 640 feet (0–195 m), with an average of 114 feet (35 m) and median of 72 feet (22 m) (figure 4.41). PHIE ≥ 12% has a range of 0 to 558 feet (0–170 m), with an average of 66 feet (20 m) and median of 17 feet (5 m) (figure 4.41). The ratio of PHIE ≥ 6% and PHIE ≥ 12% to net sandstone thickness was plotted against drill depth (figure 4.42). Down to a depth of 5000 feet (1500 m), values range from 0.0 to 1.0, with many in the 0.8 to 1.0 range. Below 5000 feet (1500 m) the ratio begins to decrease rapidly. Throughout much of the basin, the Entrada is projected to have less than 20 feet (6 m) of porous sandstone (figures 4.39 and 4.40). There are few penetrations of the Entrada in the deeper part of the basin, and undrilled areas of high porosity and permeability could exist at depth.

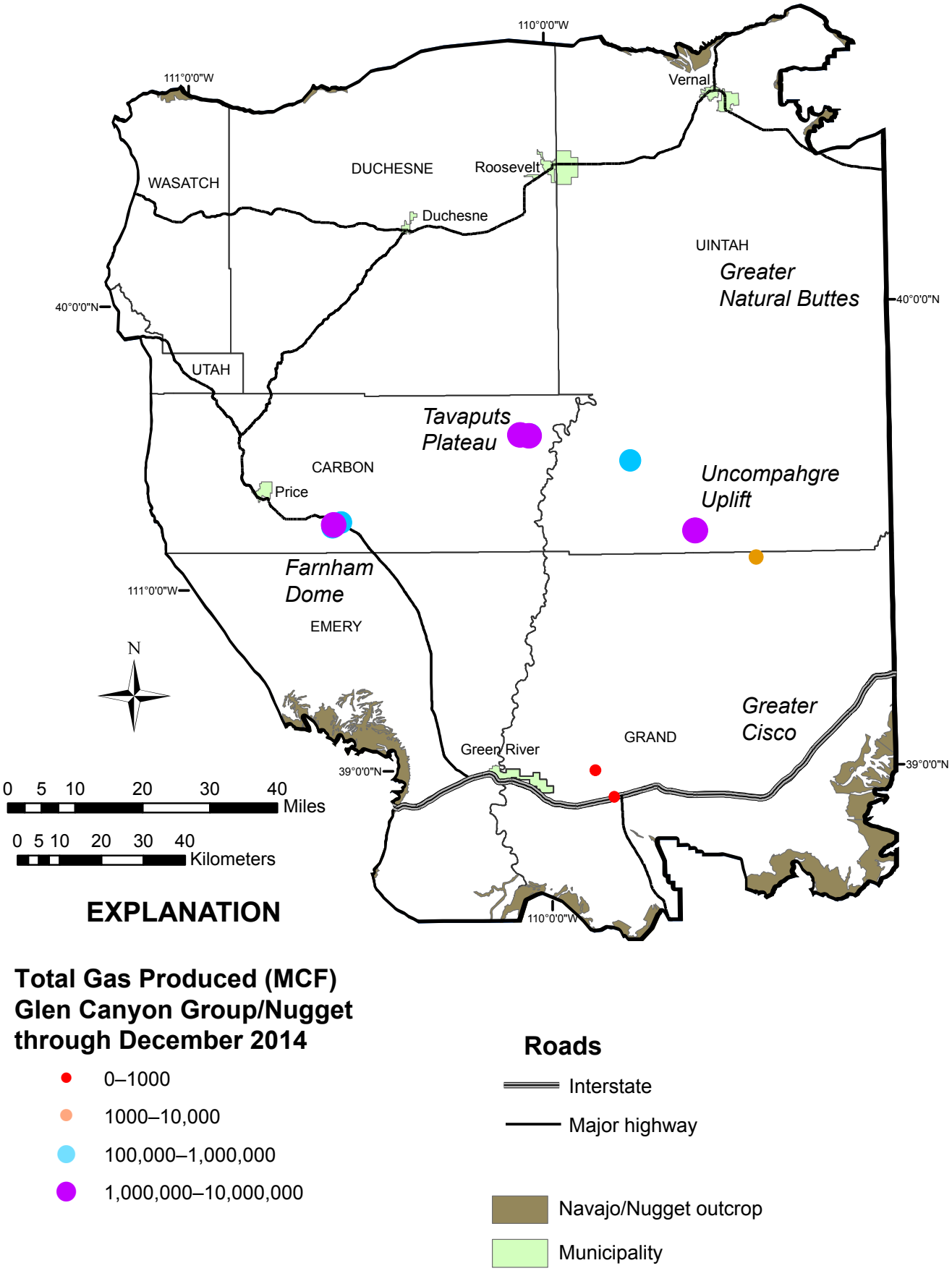

Figure 4.25. *Total gas produced per well from the GCG/N reservoir through December 2014. Data from Utah Division of Oil, Gas and Mining (2016d).*

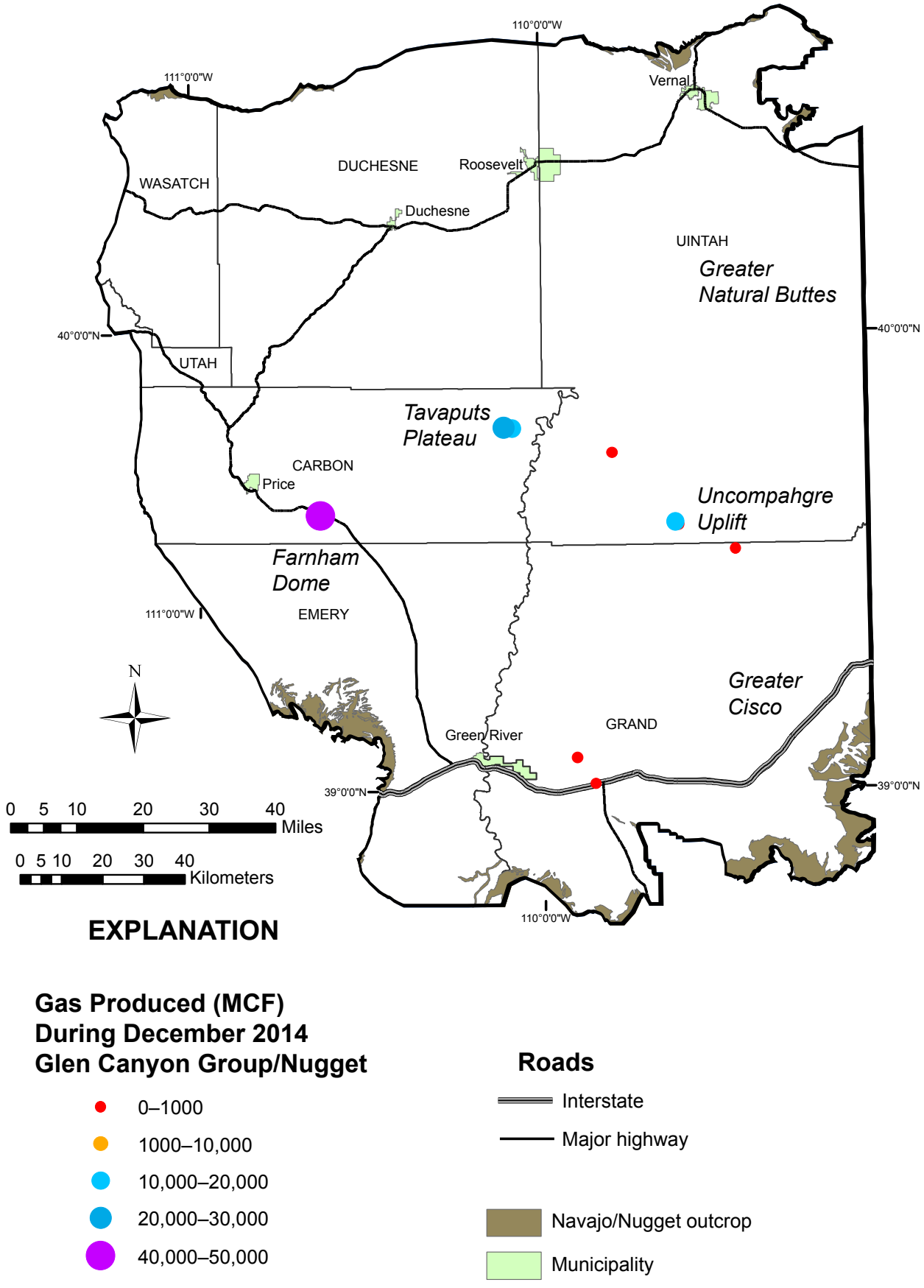

Figure 4.26. *Gas produced from the GCG/N reservoir during the month of December 2014. Data from Utah Division of Oil, Gas and Mining (2016d).*

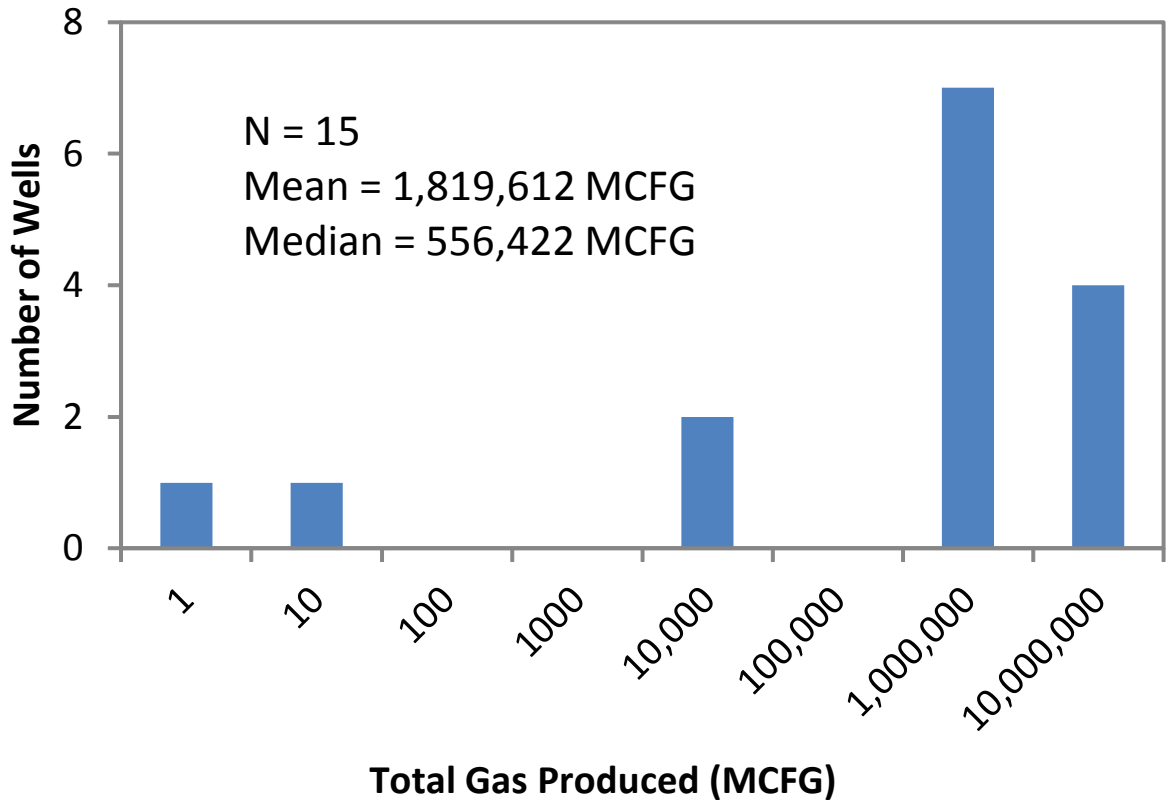

Figure 4.27. *Frequency distribution of total gas produced per well from the GCG/N reservoir through December 2014. Gas volumes range from 0 to 8,012,292 MCFG/well. Data from Utah Division of Oil, Gas and Mining (2016d).*

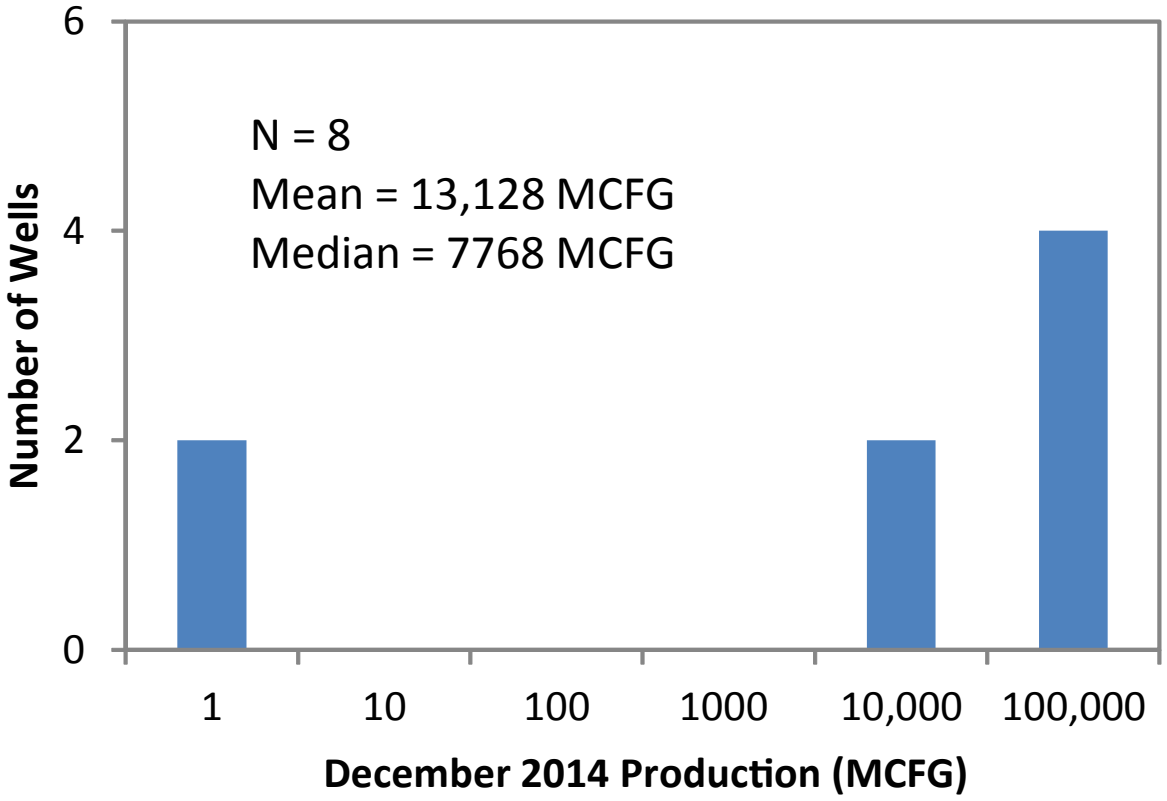

Figure 4.28. *Frequency distribution of gas produced per well from the GCG/N reservoir during December 2014. Production ranges from 1 to 48,628 MCFG/well. Data from Utah Division of Oil, Gas and Mining (2016d).*

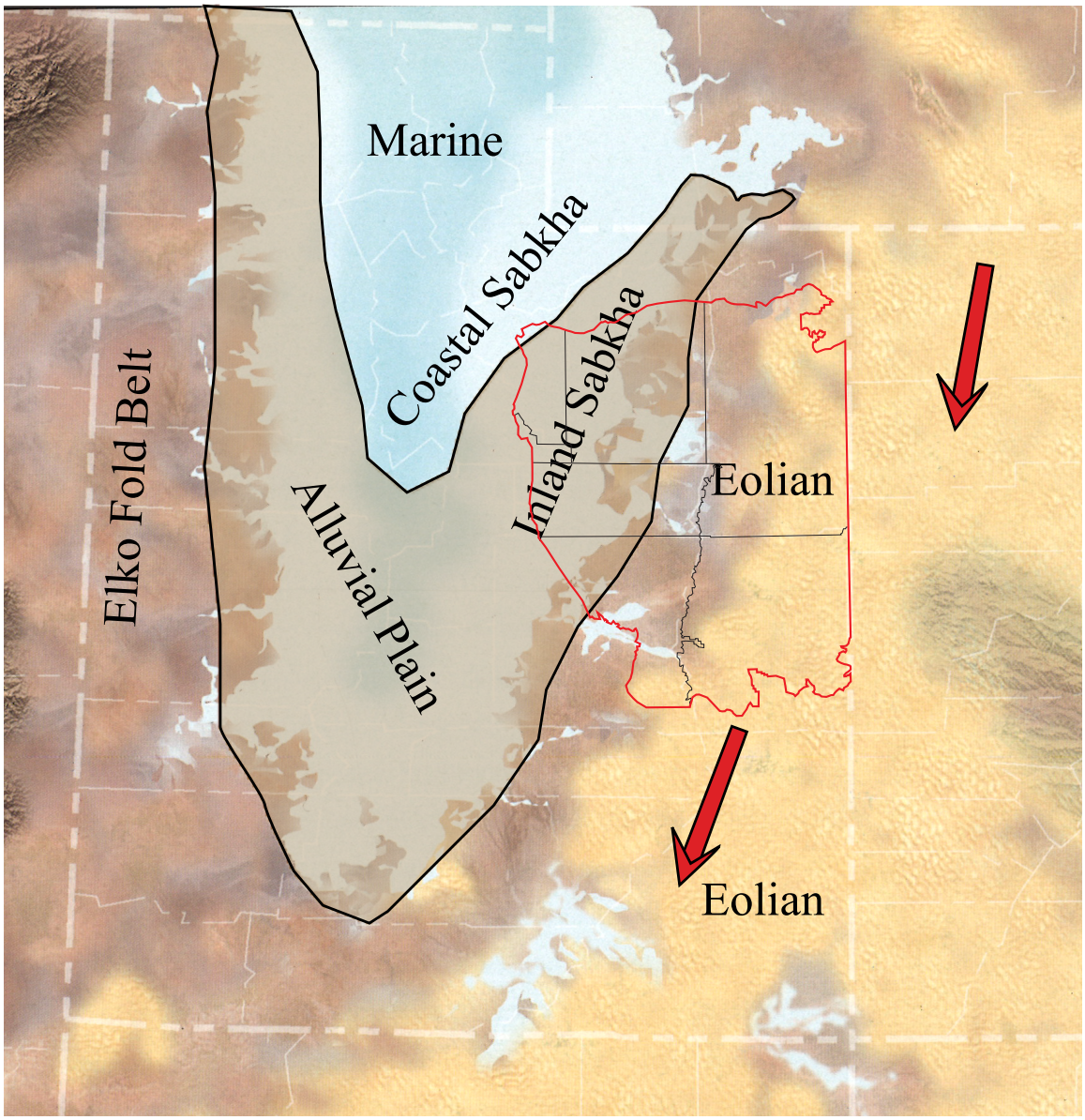

Figure 4.29. *Paleogeographic interpretation of Entrada Sandstone time. Riggs and Blakey (1993) and Peterson (1994) referred to the Entrada deposits in central Utah as sand flats, also commonly referred to as red-bed or mud-rich facies. Jennings (2014) described the Entrada in central Utah as dominantly alluvial-plain deposits sourced from the Elko fold belt to the west. Red arrows indicate wind direction during the Early and Middle Jurassic, study area outlined in red. Modified from Blakey and Ranney (2008).*

Very few Entrada Sandstone cores have been taken in the Uinta Basin. As a result, little is known about the spatial distribution or the porosity-to-permeability relationship of the Entrada. Dyer and Donoho (2008) indicate that in the Flat Rock field along the Uncompahgre uplift that overlaps the southeastern Uinta Basin, the Entrada reservoir has an average porosity of 13% and a maximum of 36%, and an average permeability of 5 millidarcies (mD) and maximum of 36 mD, at an average depth of 11,500 feet (3500 m).

Water Quality

The overlap of the northern part of Freethey and Stolp's (2010) east-central Utah Glen Canyon aquifer study area with our study area, as previously described in the GCG/N section is also pertinent to the Entrada Sandstone. As was done with the GCG/N, the structure on top of the Entrada was subtracted from the BMSW of Anderson and others (2012) to generate a map of the thickness between the BMSW and Entrada reservoir (figure 4.43). Throughout most of the basin, like the GCG/N, the Entrada reservoir is also thousands of feet below the BMSW except in Ashley Valley field (figure 1.1) where the water in the Entrada is less than 10,000 mg/L TDS (Entrada above the BMSW). Anderson and others' (2012) mapping did not extend far enough south to capture the 10,000 mg/L TDS line in the Entrada, but the 2000-foot (600 m) drill depth is used as an approximation of the BMSW in these areas based on the work of Freethey and Stolp (2010) (figure 4.43).

A.

B.

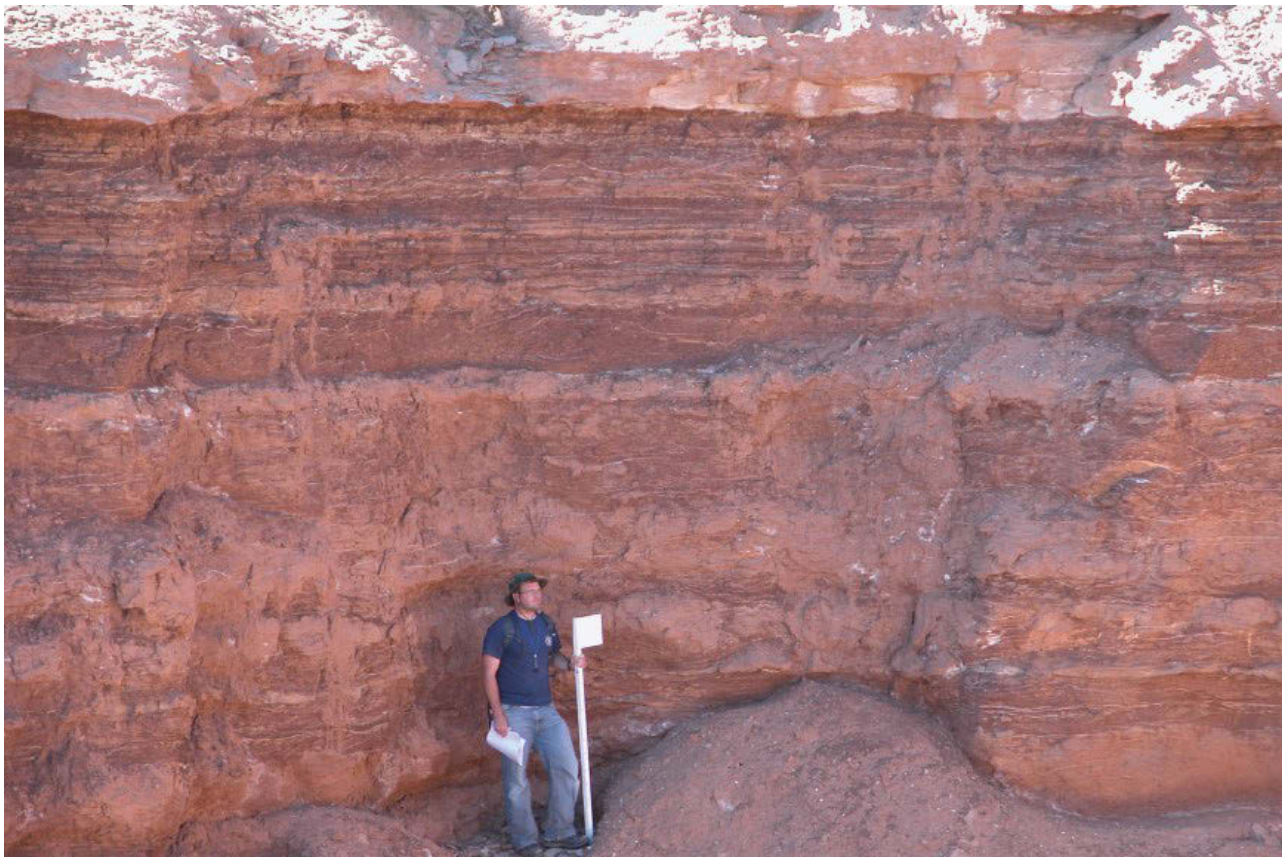

Figure 4.30. *Entrada Sandstone:* ***A.*** *dune facies in Arches National Park near Moab and* ***B.*** *mud-rich facies in the San Rafael Swell. Photograph B from Morris and Hicks (2011).*

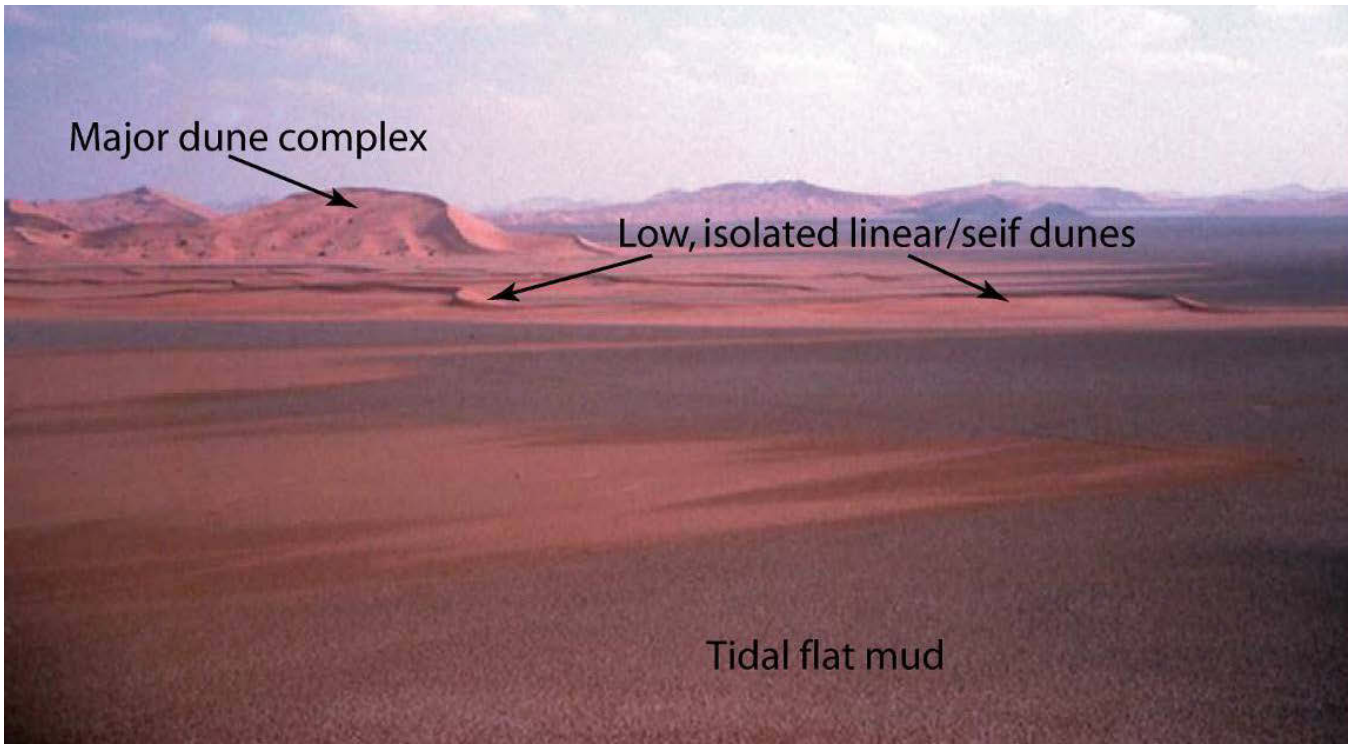

Figure 4.31. *Working depositional model (Morris and others, 2005) of the Entrada Sandstone with eolian dunes encroaching on a tidal flat, Namibia Desert.*

Water quality data for the Entrada from oil and gas wells in the Uinta Basin are very sparse; we only found 10 samples we believe are reliable. The data show increasing TDS with depth (figure 4.44). The trend line indicates water is below 10,000 TDS to nearly 7000 feet (2000 m), much deeper than expected from the work of Anderson and others (2012) and Freethey and Stolp (2010). The trend line is not considered reliable due to the few data points and the commingling of production water from other formations. The water types are dominantly sodium chloride in deep wells and a mixture of calcium bicarbonate, magnesium bicarbonate, and magnesium sulfate from shallow depths (figure 4.45), generally agreeing with Freethey and Cordy (1991). The hydraulic conductivity of the Entrada aquifer is 0.1 to 10.0 feet per day (Freethey and Cordy, 1991).

Water Production, Use, and Disposal

Nearly all of the hydrocarbon and associated water production from Entrada reservoirs has come from fields along the Uncompahgre uplift (figure 4.46). During December 2014, 23 wells produced 2670 BW from the Entrada; water volumes per well for the month ranged from 0 to 399 BW (Utah Division of Oil, Gas and Mining, 2016d). Total water produced from the Entrada through December 2014 is 448,348 BW. Total volume per well from 37 wells ranges from 0 to 62,286 BW/well with an average of 12,118 BW/well and median of 9249 BW/well (figure 4.47). The GWR has a range from 7 to 134,536 MCFG/BW (figure 4.48), excluding three wells that produced more than 9 BCFG and no water. The average GWR per well is 5670 MCFG/BW and the median is 200 MCFG/BW.

Hydrocarbon Production

Gas production from the Entrada reservoirs occurs along the Uncompahgre uplift (figures 4.49 and 4.50) in structural and fault traps. Total gas produced through December 2014 from 36 wells completed in the Entrada is 126 BCF (Utah Division of Oil, Gas and Mining, 2016d). Total gas volumes per well, range from 14,878 to 12,276,656 MCF, with an average of 3,509,967 MCFG and a median of 1,931,987 MCFG (figure 4.51). During the month of December 2014, 23 wells produced 406,387 MCFG from the Entrada (figure 4.52).

CRETACEOUS CEDAR MOUNTAIN AND DAKOTA FORMATIONS

The Cretaceous Cedar Mountain and Dakota (CMKD) Formations (figure 1.5) were mapped as one reservoir unit. Almost all production is commingled and the boundary between the two formations can be very difficult to identify in many geophysical well logs. The Jurassic Morrison Formation was originally included in this group, but the gas and water production is not regionally significant. Also, most wells drilled to test the Cretaceous through Morrison interval only partially penetrate the Morrison. The CMKD consists of southwest- to northeast-trending fluvial channels, associated overbank deposits, and marginal marine deposits in the upper Dakota (figure 4.53). Structure on top of the Dakota shows an asymmetrical Uinta Basin with the Dakota more than 20,000 feet

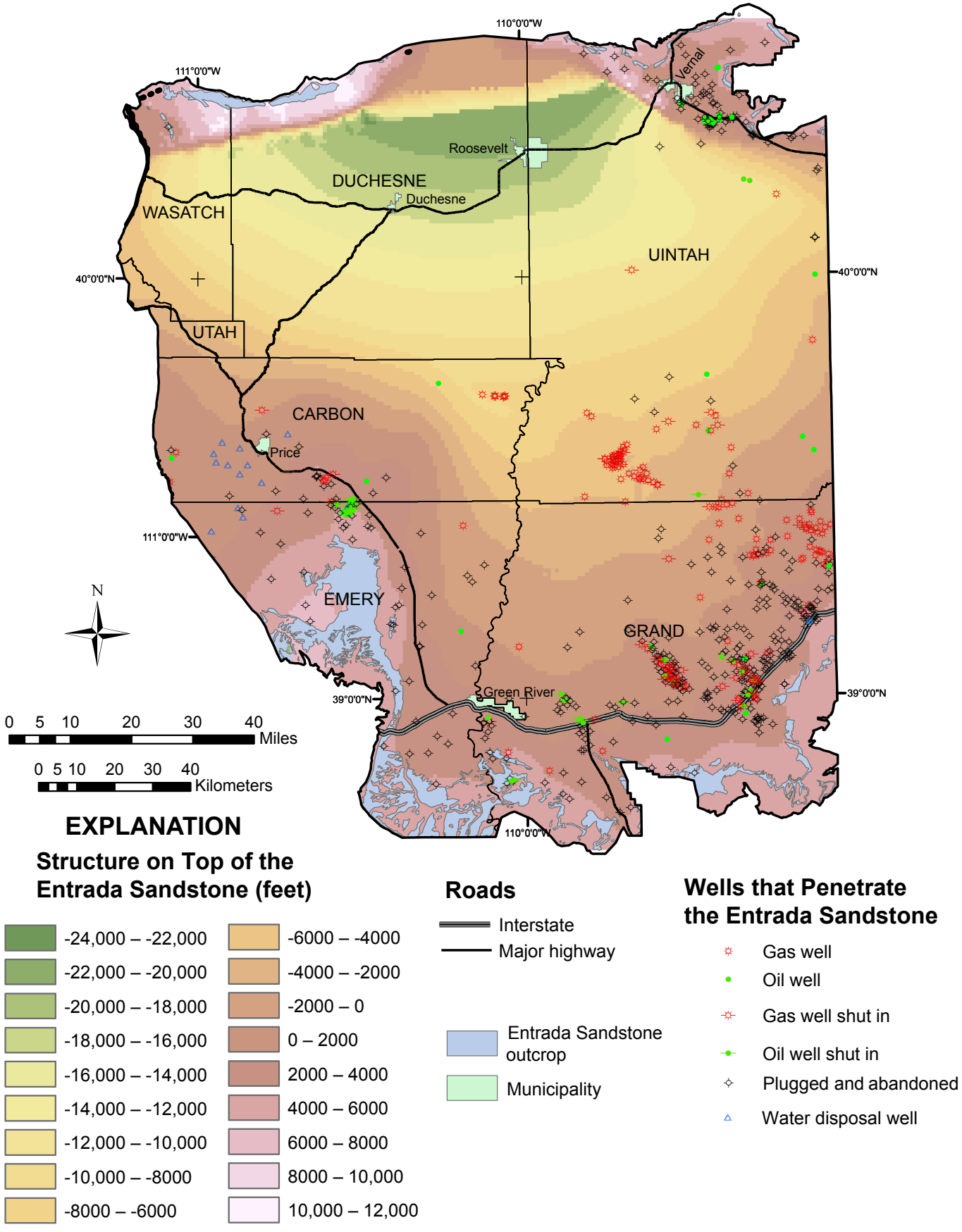

Figure 4.32. *Structure on top of the Entrada Sandstone, Uinta Basin study area. Datum: mean sea level.*

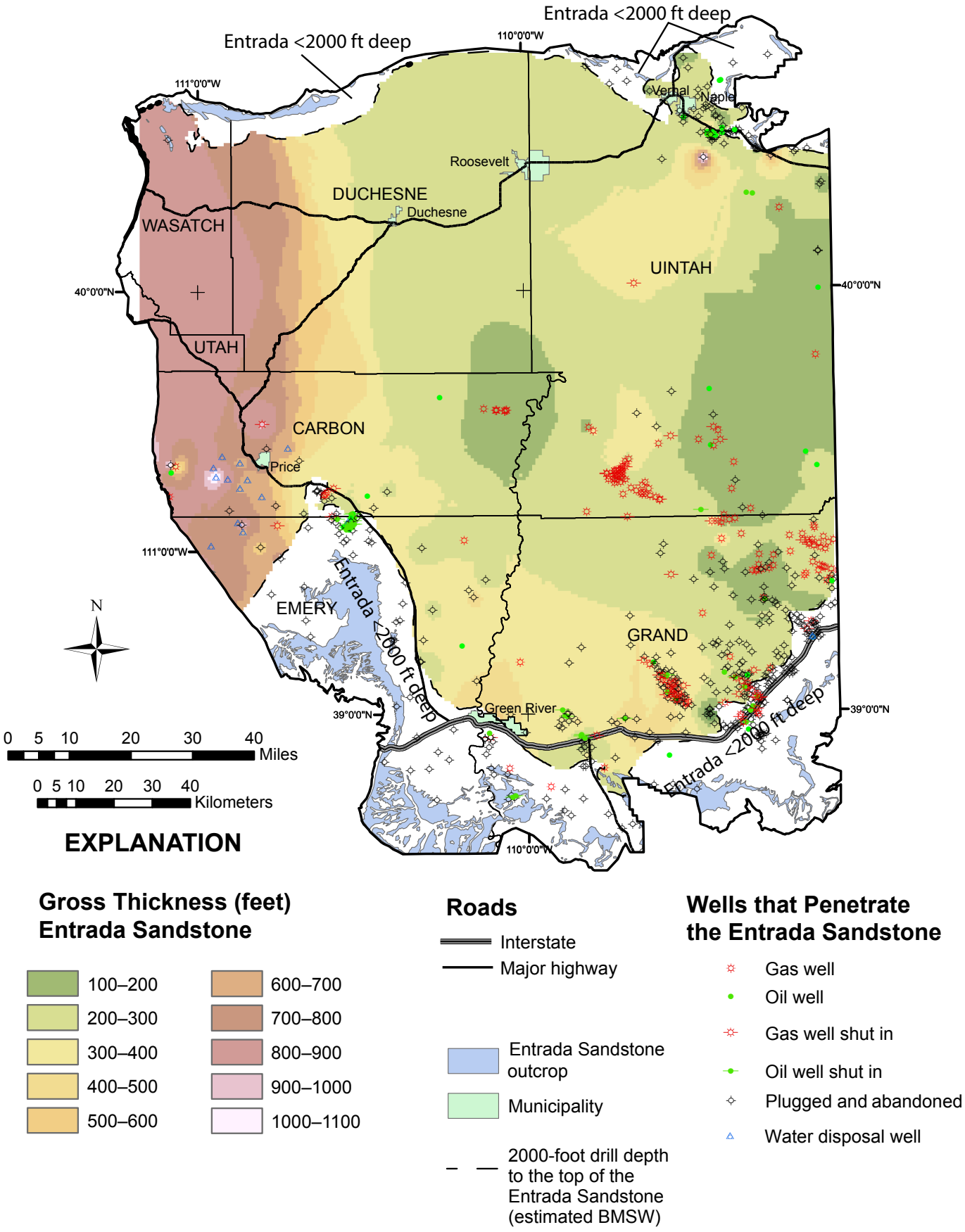

Figure 4.33. *Gross thickness of the Entrada Sandstone for areas greater than 2000 feet (600 m) deep. The 2000-foot drill depth is used as an estimated depth to the base of the moderately saline water (BMSW).*

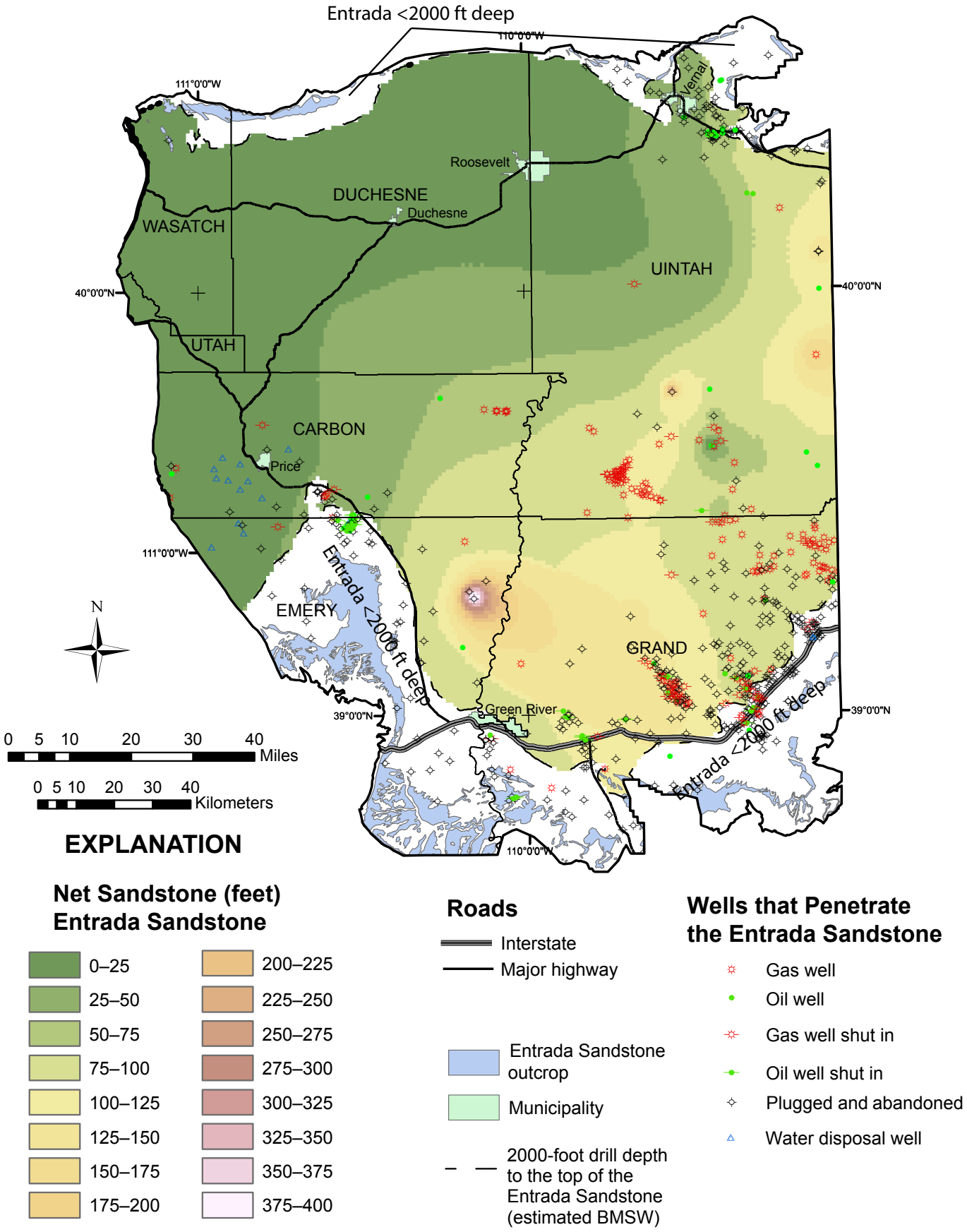

Figure 4.34. *Net sandstone thickness map (gamma ray ≤ 60 API) in the Entrada Sandstone for areas greater than 2000 feet (600 m) deep. The 2000-foot drill depth is used as an estimated depth to the base of the moderately saline water (BMSW).*

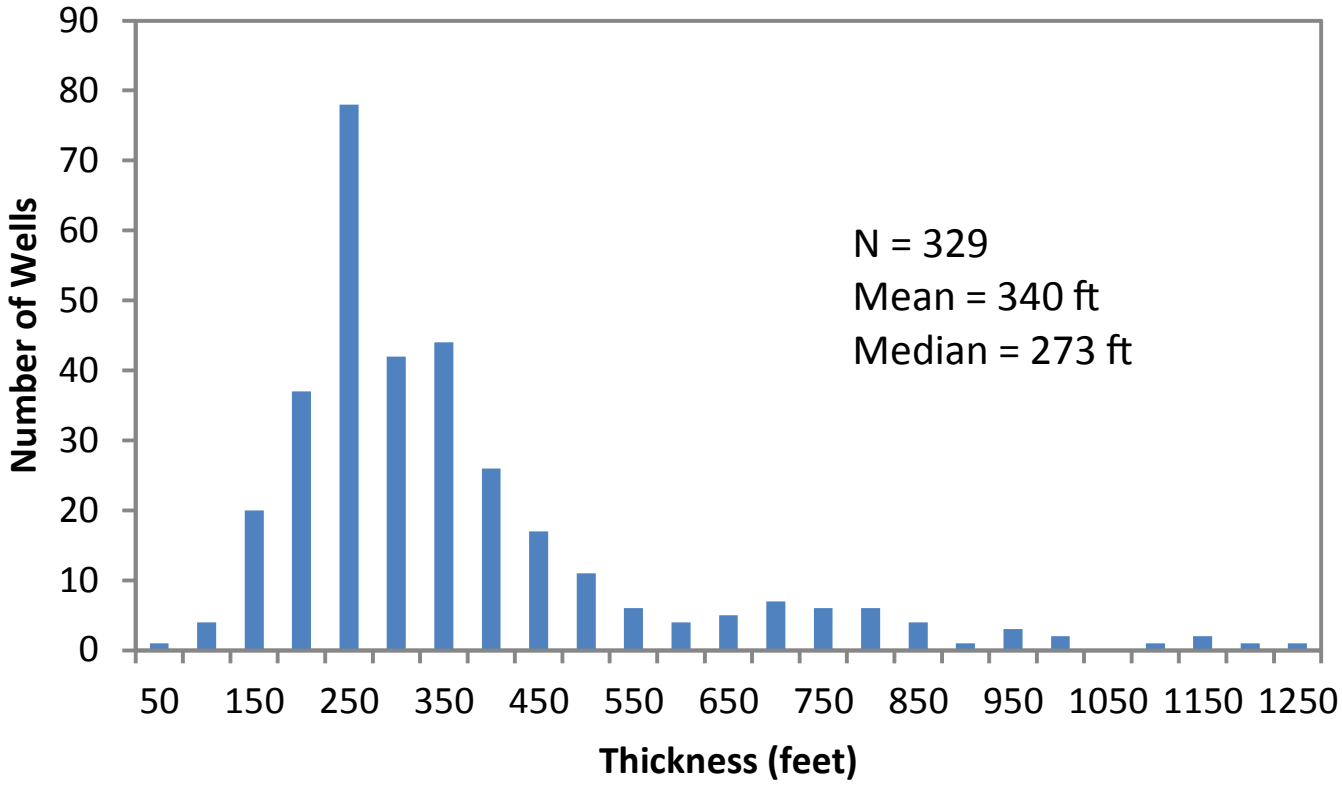

Figure 4.35. *Frequency distribution of the gross thickness of the Entrada Sandstone in the geophysical well logs studied.*

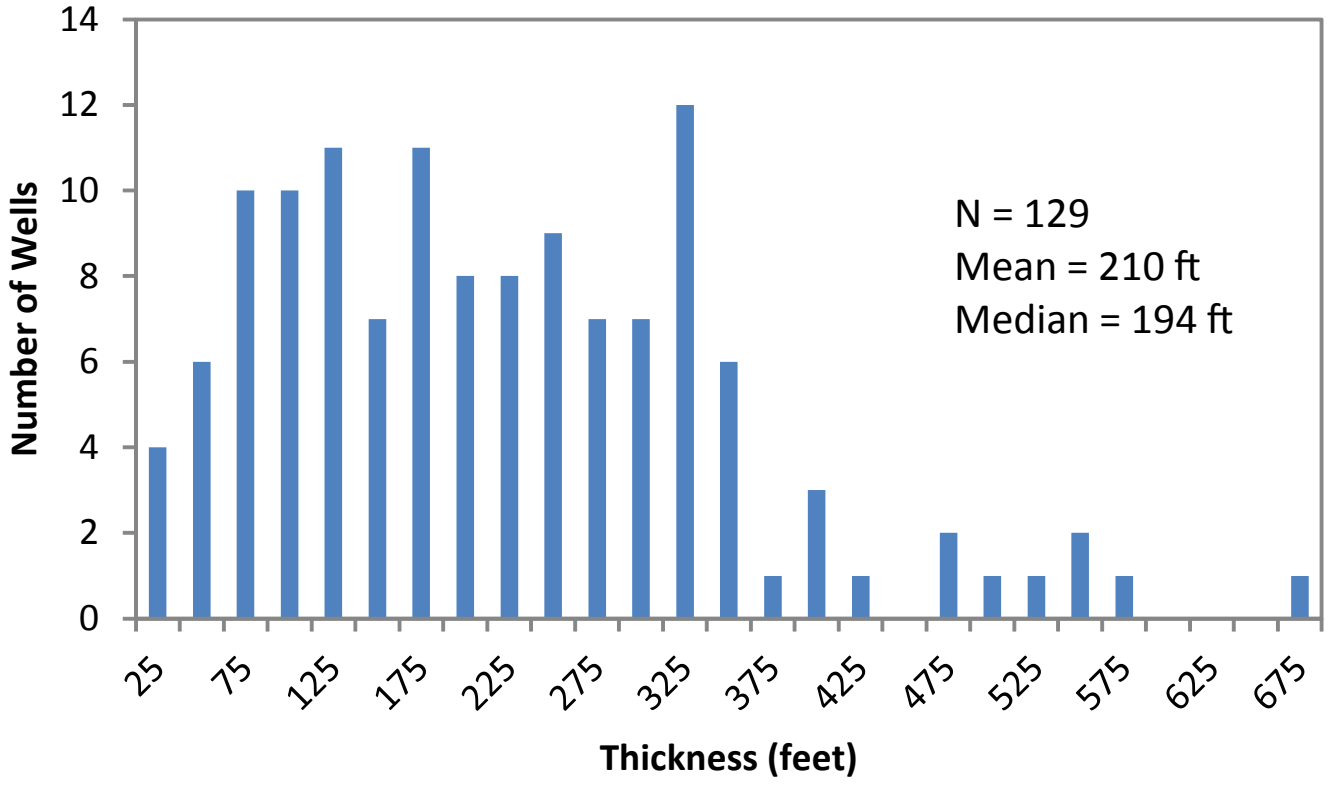

Figure 4.36. *Frequency distribution of the net sandstone thickness (≤ 60 API gamma ray) in the Entrada Sandstone in the geophysical well logs studied.*

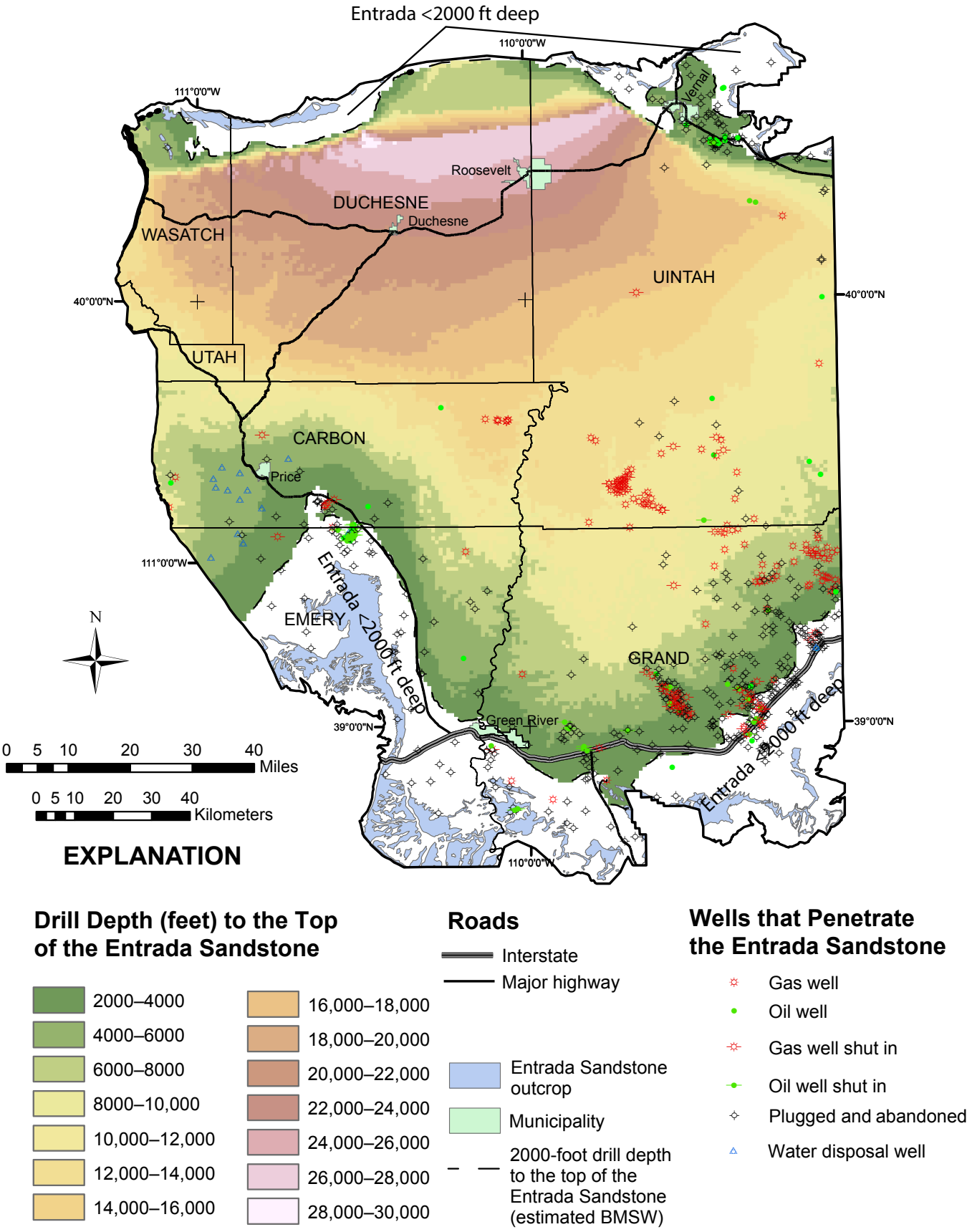

Figure 4.37. *Drill depth to the top of the Entrada Sandstone for areas greater than 2000 feet (600 m) deep. The 2000-foot drill depth is used as an estimated depth to the base of the moderately saline water (BMSW).*

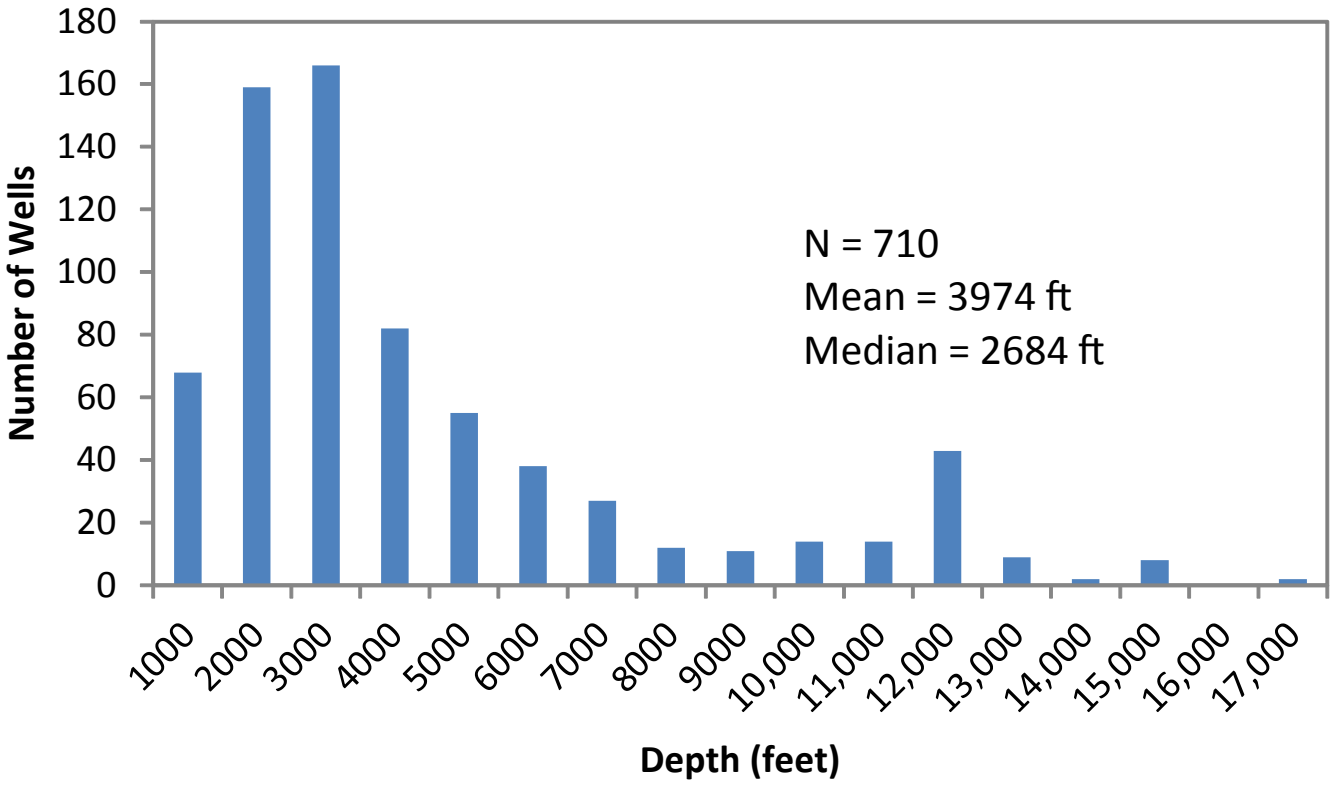

Figure 4.38. *Frequency distribution of the drill depth in feet to the top of the Entrada Sandstone in the geophysical well logs studied.*

(6000 m) below mean sea level in the northern part of the basin (figure 4.54). Significant recent UGS-funded studies of the CMKD Formations include those of McPherson and others (2006) and Currie and others (2007, 2011).

Thickness

The CMKD reservoir generally thins regionally from the southwest to northeast reflecting the proximal to distal setting relative to the Sevier orogenic belt (figure 4.55). The general paleocurrent direction illustrated in figure 4.53 follows the same regional southwest to northeast trend. Gross thickness of the CMKD reservoir ranges from 15 to 1048 feet (5–319 m), with an average of 220 feet (67 m) and a median of 203 feet (62 m) (figure 4.56). The net sandstone thickness (gamma ray ≤ 60 API) shows a southwest to northeast trend with some northwest to southeast trends in the northeast part of the Uinta Basin, possibly reflecting the influence of littoral marine sandstone deposits of the advancing Cretaceous sea (Currie and others, 2011) (figure 4.57). Net sandstone thickness of the CMKD reservoir ranges from 0 to 218 feet (0–66 m) with an average of 61 feet (19 m) and a median of 56 feet (17 m) (figure 4.58).

Depth

Drill depth to the CMKD reservoir in the deepest part of the basin, where no well has penetrated the Dakota, is projected to be more than 26,000 feet (7900 m) (figure 4.59). Drill depths in the wells studied range from 21 to 18,902 feet (6–5761 m) with an average depth of 4038 feet (1230 m) and median of 2683 feet (818 m) (figure 4.60).

Lithology

The CMKD Formations are fluvial channel, overbank deposits, and some littoral marine deposits, with carbonaceous shale and coal in the upper Dakota Sandstone. The primary reservoir lithologies are conglomerate and coarse- to fine-grained sandstone. Most of the conglomerate and coarse-grained sandstone is in the Cedar Mountain and lower Dakota. Young (1973) described the Cedar Mountain as generally conglomerate to coarse-grained sandstone with carbonate cement. Cedar Mountain sandstones are commonly cemented with calcite and rarely silica. The Dakota typically has conglomeratic sandstone at the base; a middle unit consisting of carbonaceous shale, coal, sandstone, and siltstone; and an upper unit of massive, medium-grained sandstone (Young, 1973). The Dakota sandstones are commonly cemented by silica, kaolinite, smectite, hematite, and rarely calcite (McPherson and others, 2006; Currie and others, 2007, 2011).

Reservoir Properties

Porosity and permeability within channel sandstones can be highly variable and difficult to predict. Density or sonic logs were used to determine the feet of sandstone with 6% or more porosity (PHIE ≥ 6%) and 12% or more porosity (PHIE ≥

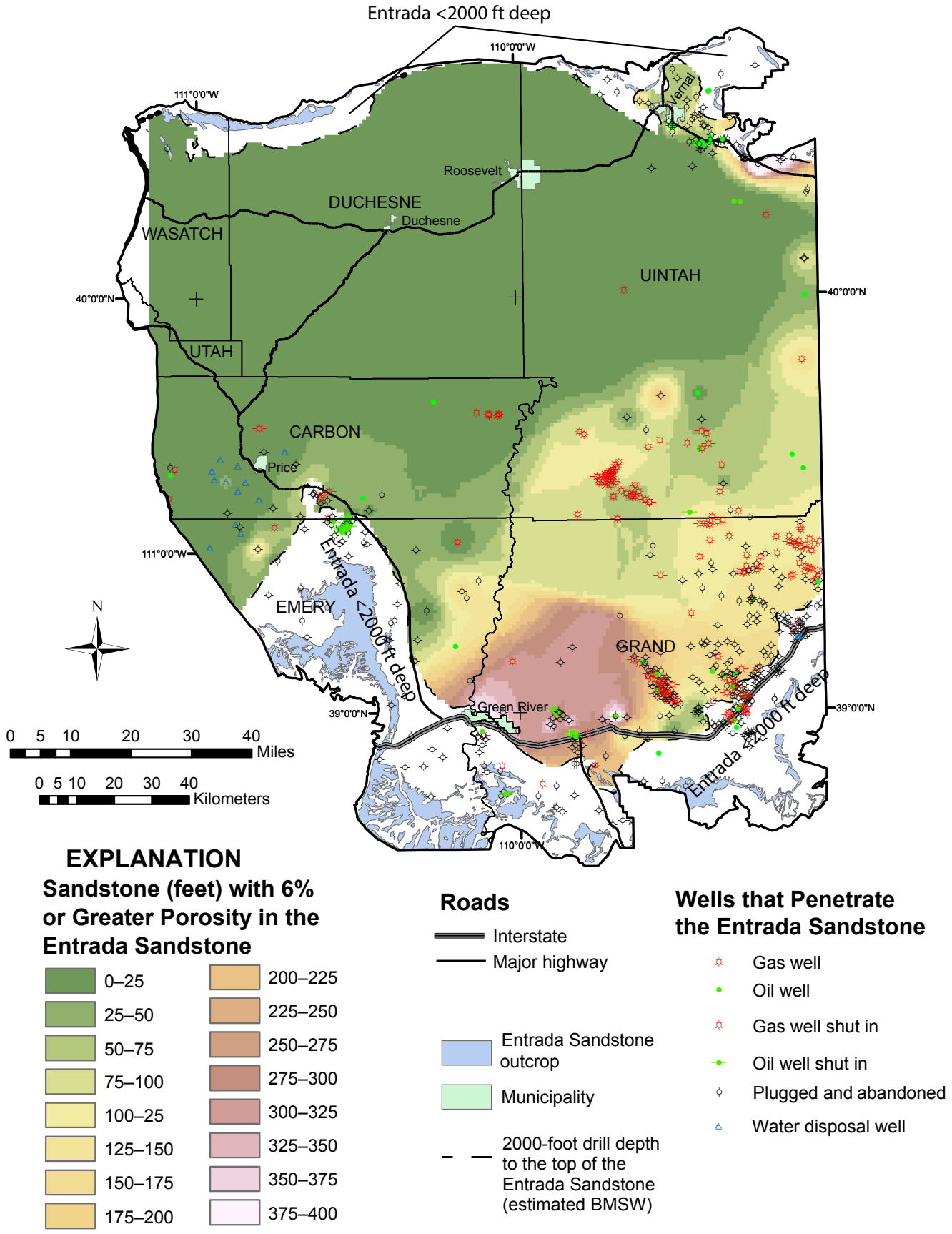

Figure 4.39. *Thickness of sandstone in the Entrada Sandstone with 6% or more porosity for areas greater than 2000 feet (600 m) deep. Porosity determined from density and sonic well logs. The 2000-foot drill depth is used as an estimated depth to the base of the moderately saline water (BMSW).*

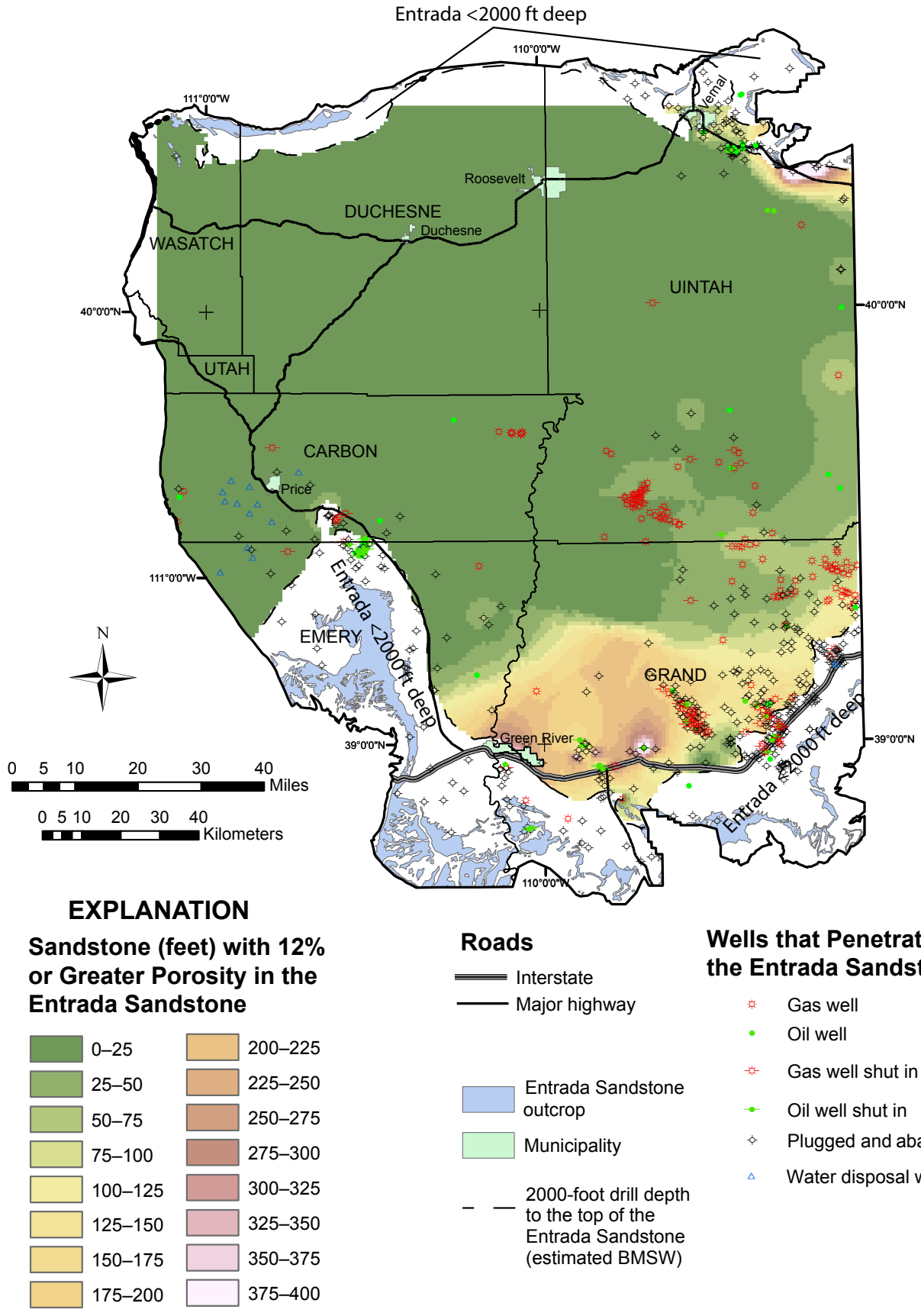

Figure 4.40. *Thickness of sandstone in the Entrada Sandstone with 12% or more porosity for areas greater than 2000 feet (600 m) deep. Porosity determined from density and sonic well logs. The 2000-foot drill depth is used as an estimated depth to the base of the moderately saline water (BMSW).*

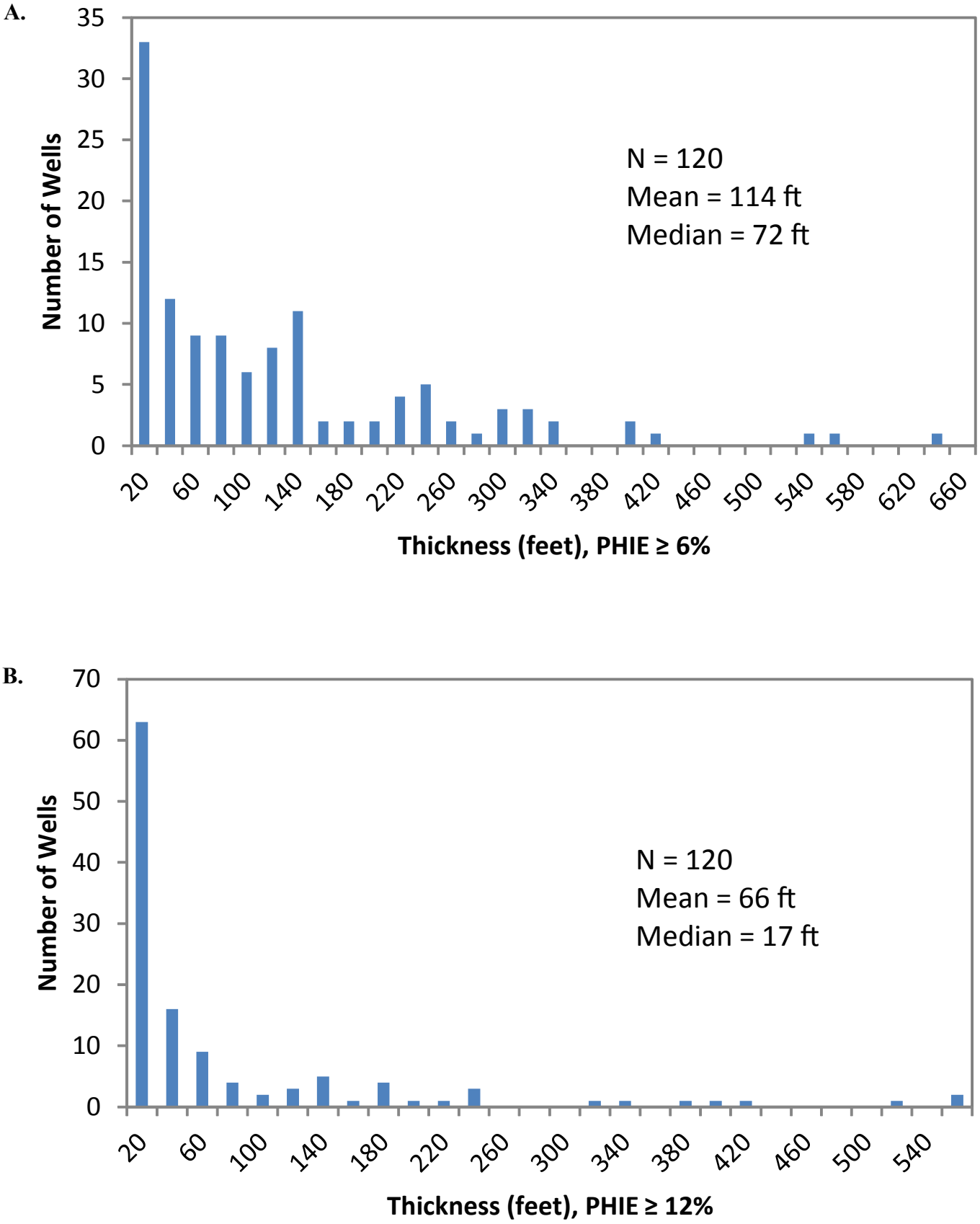

Figure 4.41. *Frequency distribution graphs of the thickness of sandstone with* ***A.*** *≥ 6% porosity (PHIE ≥ 6%) and* ***B.*** *≥ 12% porosity (PHIE ≥ 12%) in the Entrada Sandstone.*

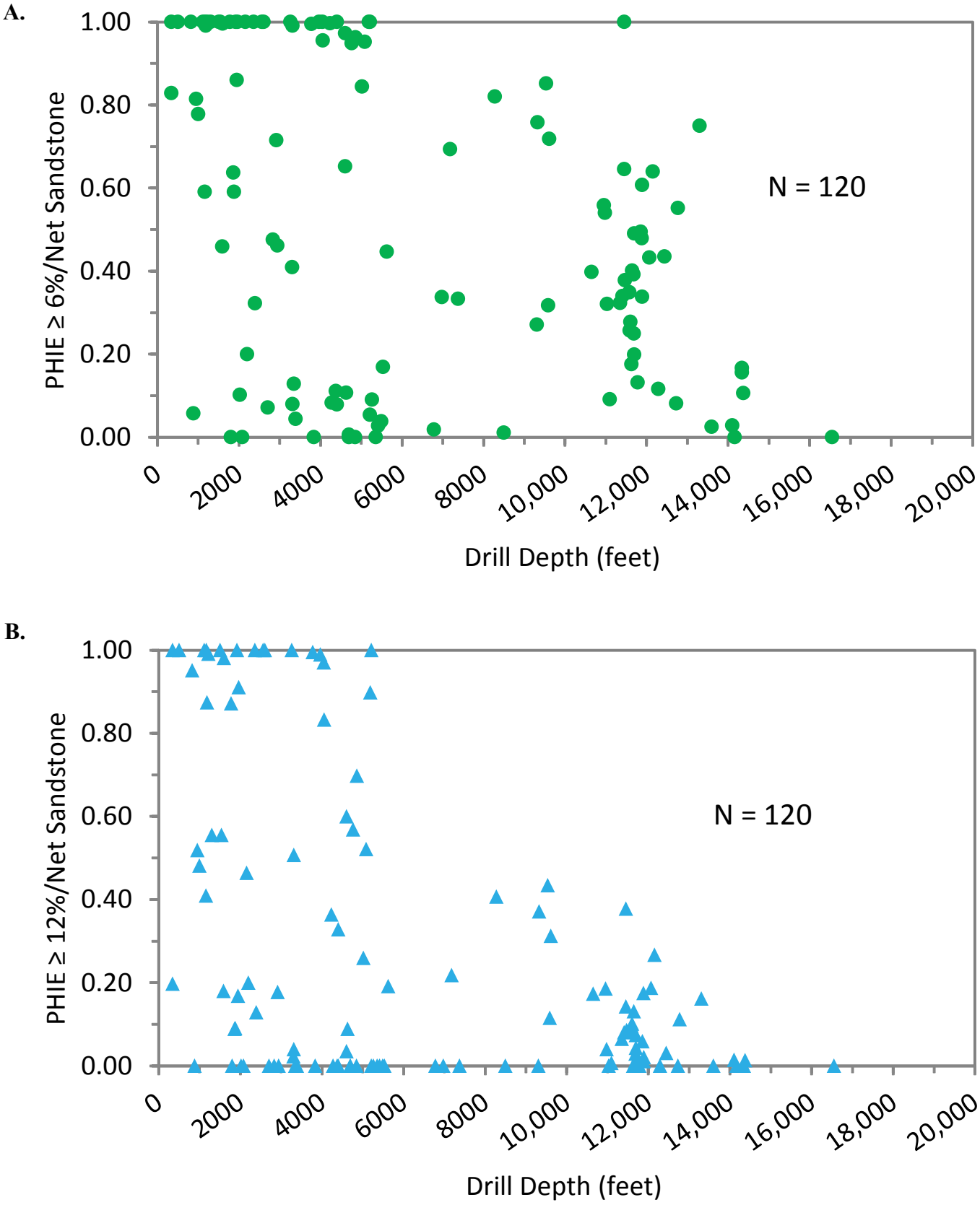

Figure 4.42. A. *Ratio of PHIE ≥ 6% to net sandstone thickness versus drill depth, and* ***B.*** *ratio of PHIE ≥ 12% to net sandstone thickness versus drill depth in the Entrada Sandstone. Porosity calculated from density or sonic logs.*

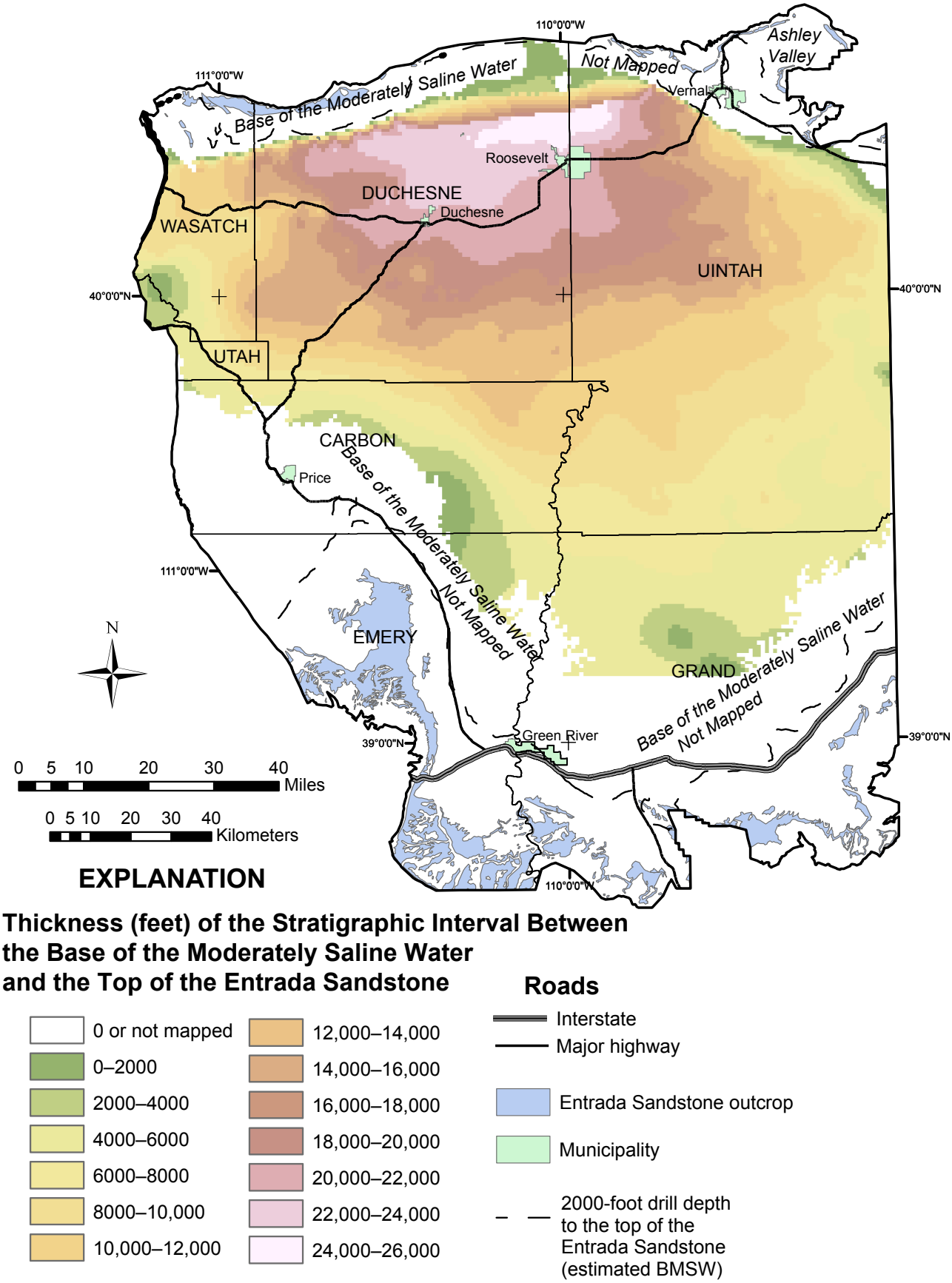

Figure 4.43. *Thickness of the stratigraphic interval between the base of the moderately saline water (BMSW) and the top of the Entrada Sandstone. The Entrada is above the BMSW in Ashley Valley (see figure 1.1 for field location). The map was created using ArcScene® by subtracting the drill-depth map (figure 4.37) from the BMSW drill-depth map of Anderson and others (2012).*

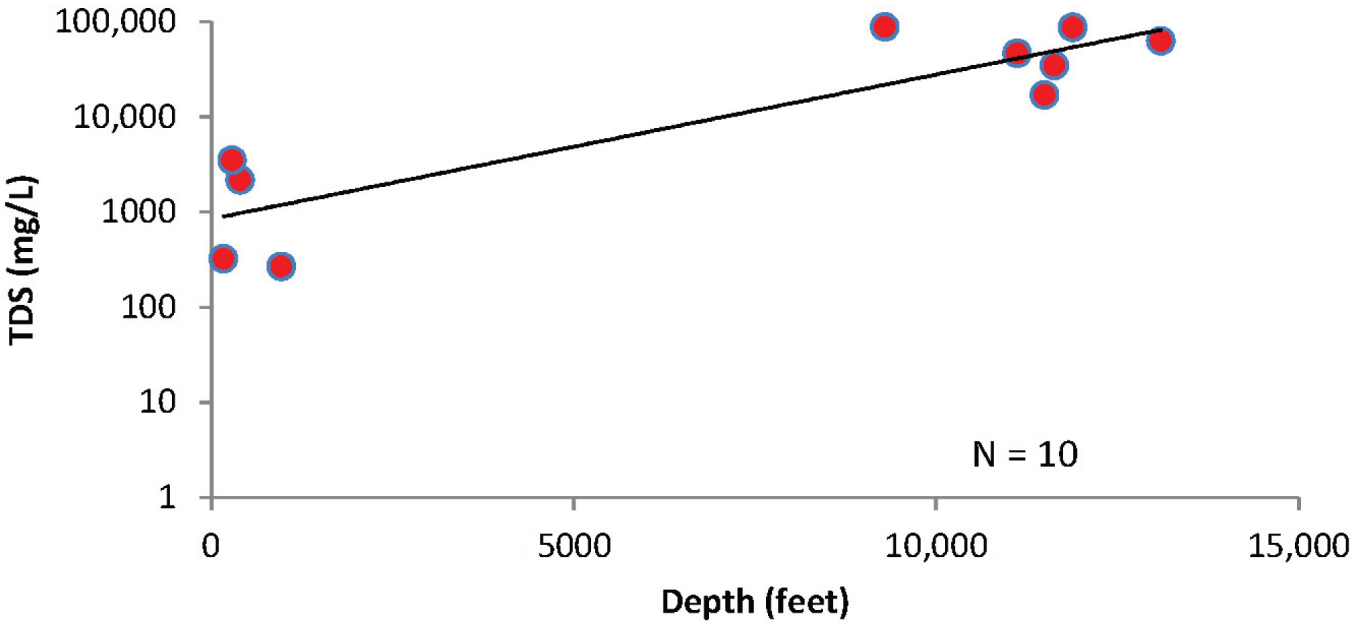

Figure 4.44. *Total dissolved solids versus depth for Entrada water from oil and gas wells in the Uinta Basin. The exponential trend line indicates less than 10,000 mg/L TDS to a depth of 7000 feet (2000 m). However, the limited number of samples (10) is insufficient to be statistically significant for such a large area.*

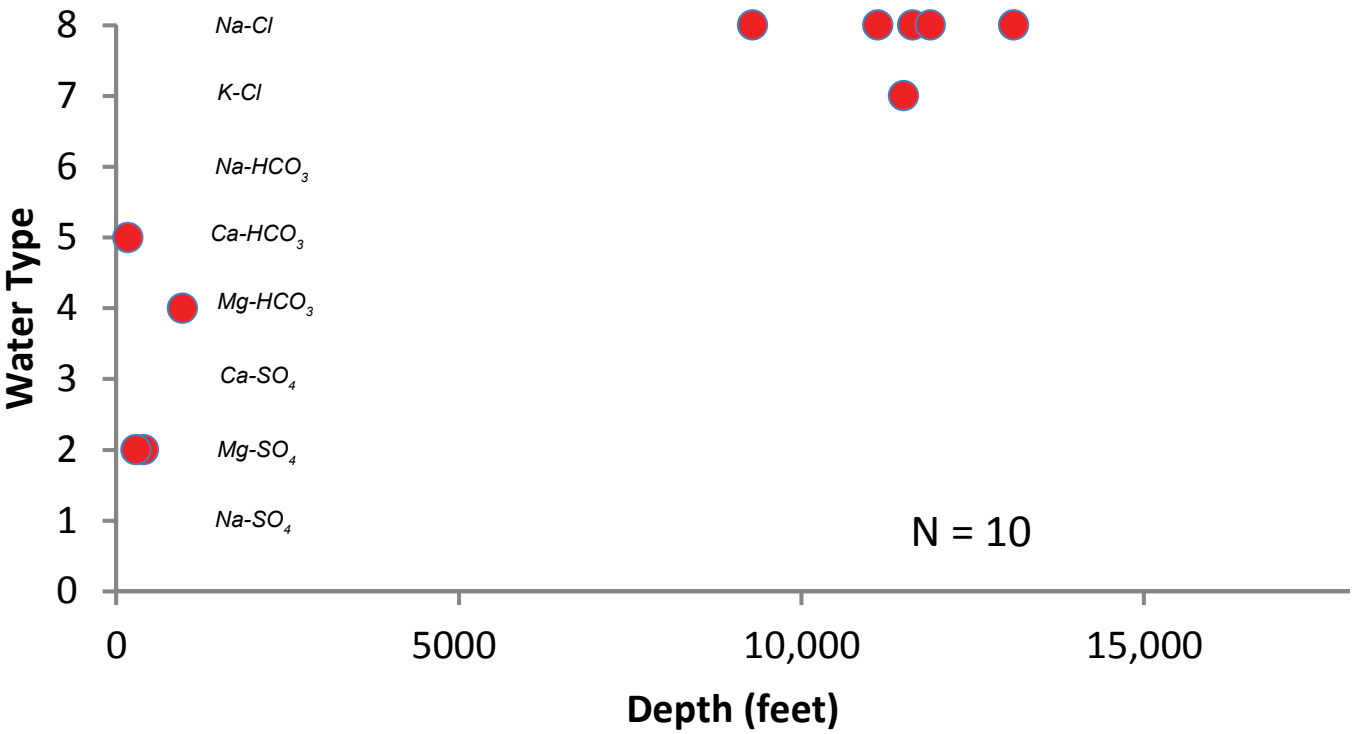

Figure 4.45. *Water produced from the Entrada is mostly sodium chloride (Na-Cl) at depths greater than 7000 feet (2000 m), and a mix of calcium bicarbonate (Ca-HCO_3), magnesium bicarbonate (Mg-HCO_3), and magnesium sulfate (Mg-SO_4) at shallower depths. The number of samples (10) is not statistically significant for such a large area.*

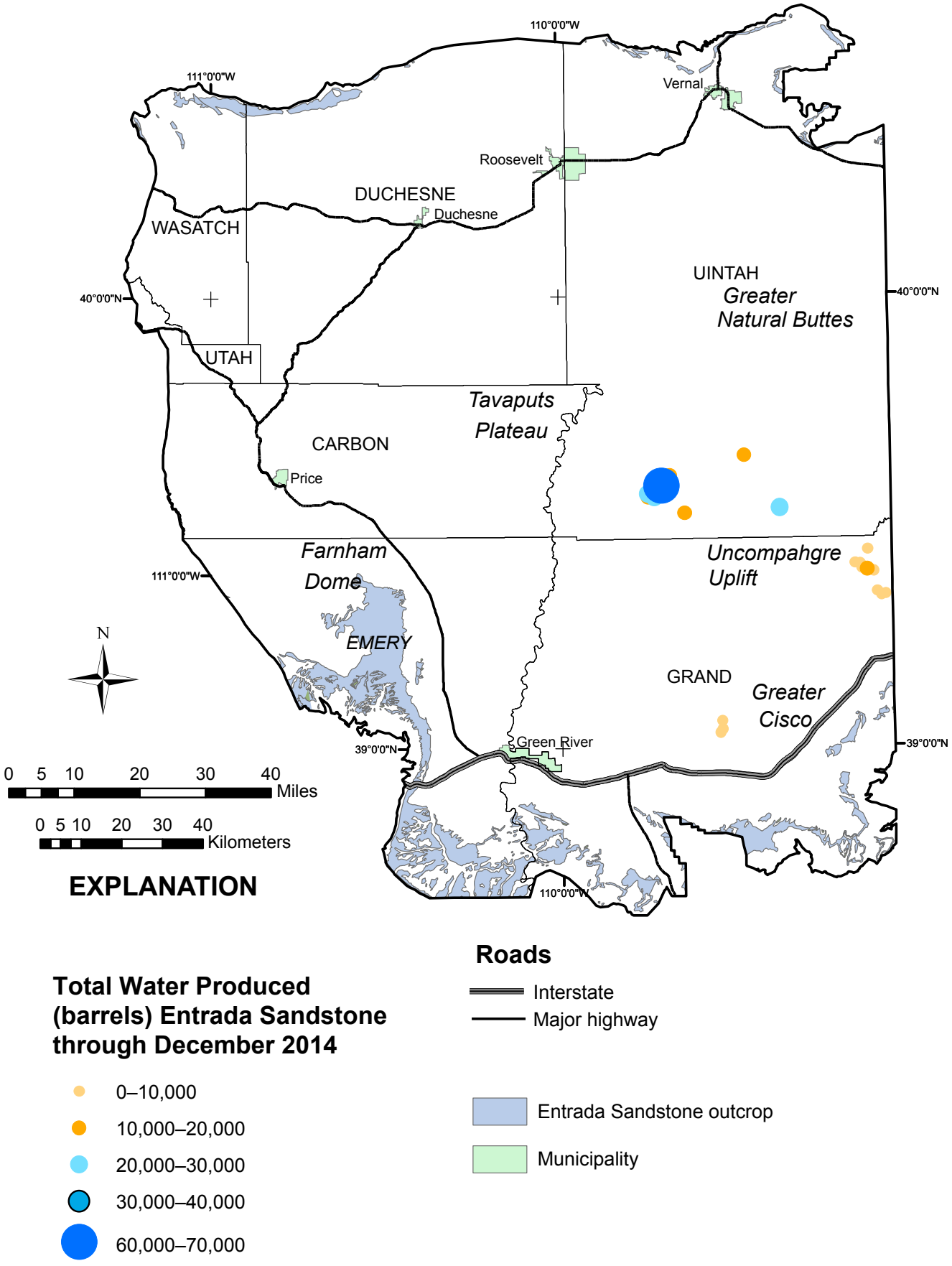

Figure 4.46. *Total barrels of water produced from the Entrada Sandstone. Data from Utah Division of Oil, Gas and Mining (2016d).*

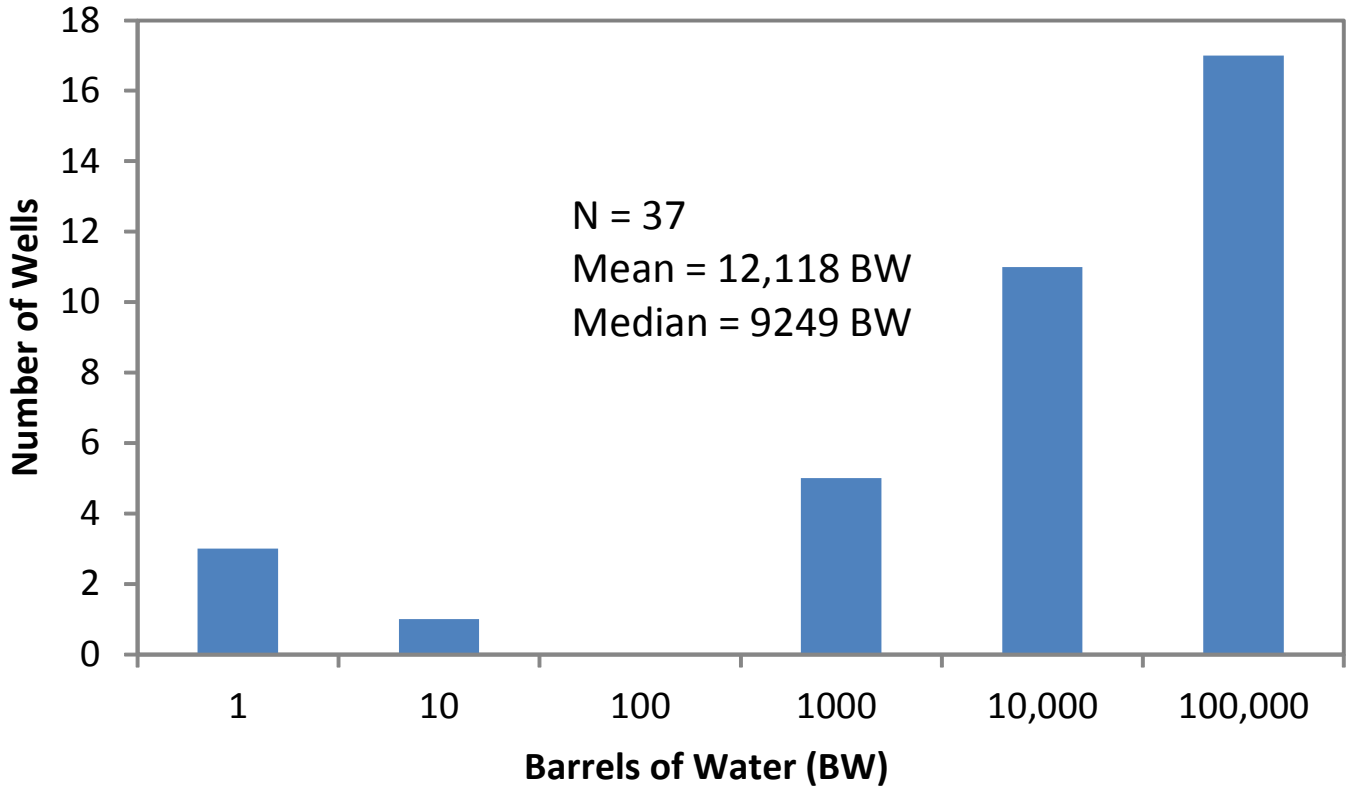

Figure 4.47. *Frequency distribution of total water per well produced from the Entrada Sandstone. Water volumes range from 0 to 62,286 BW/well. Data from Utah Division of Oil, Gas and Mining (2016d).*

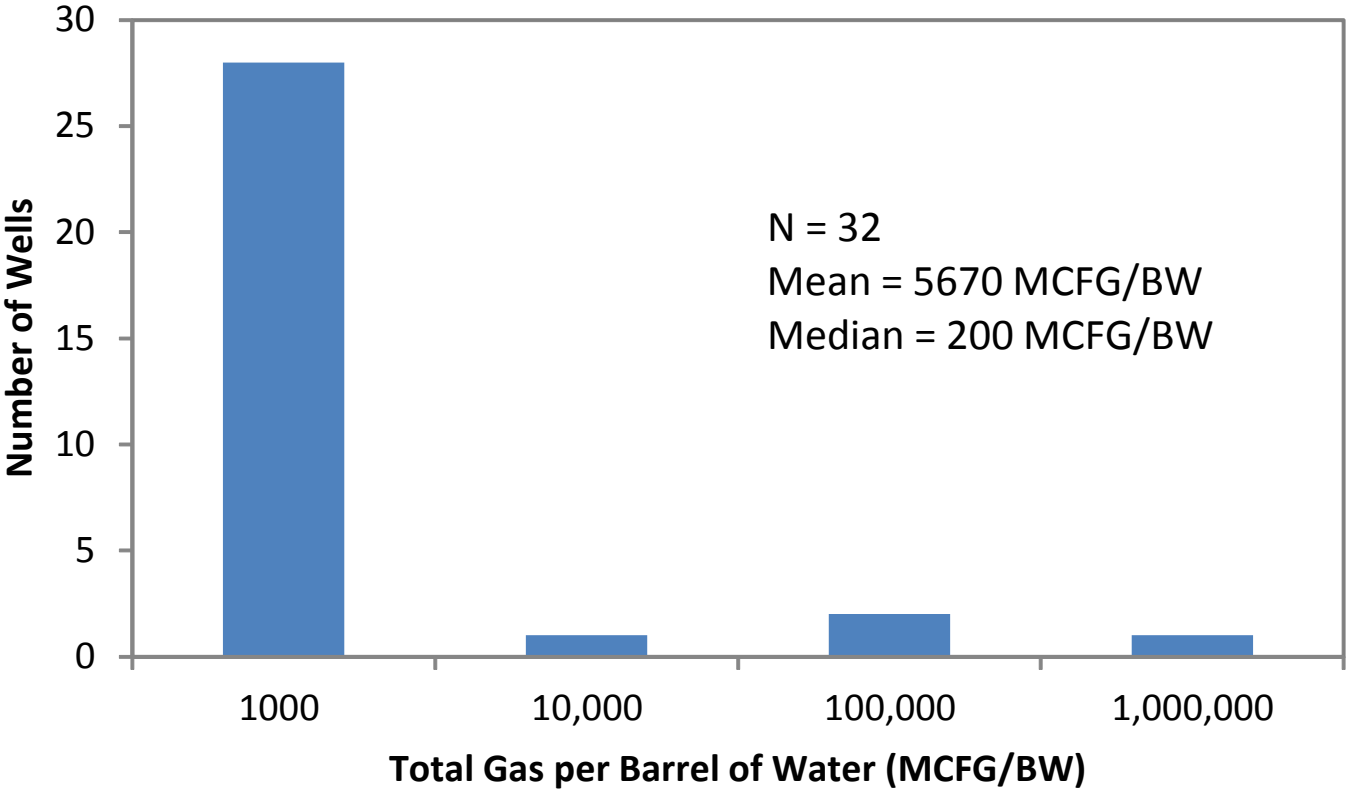

Figure 4.48. *Frequency distribution of total gas produced per barrel of water (BW). The range is from 7 to 134,536 MCFG/BW. Three wells not included in this data produced more than 9 BCF of gas and no water. Data from Utah Division of Oil, Gas and Mining (2016d).*

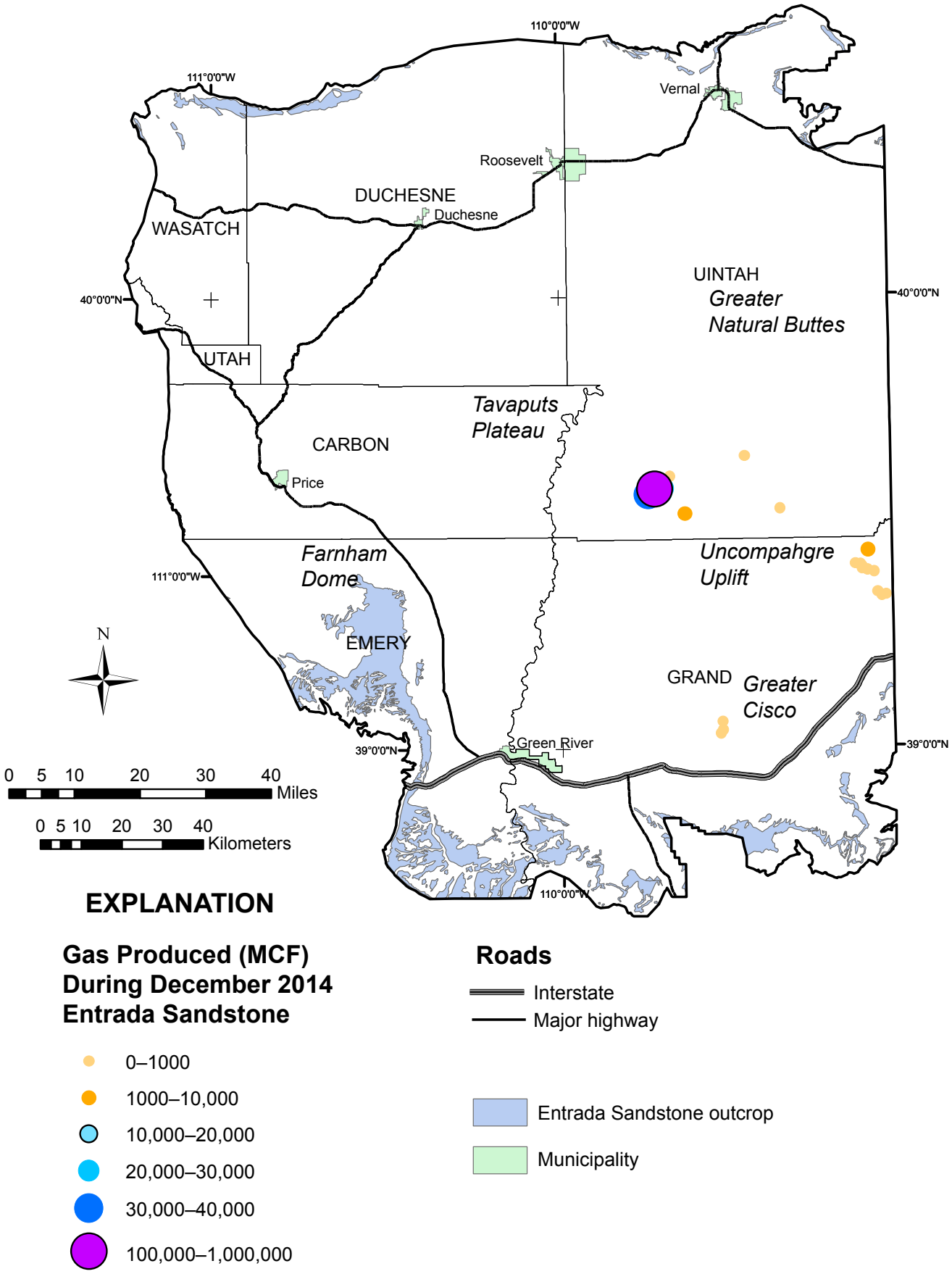

Figure 4.49. *Gas produced from the Entrada Sandstone during the month of December 2014. Data from Utah Division of Oil, Gas and Mining (2016d).*

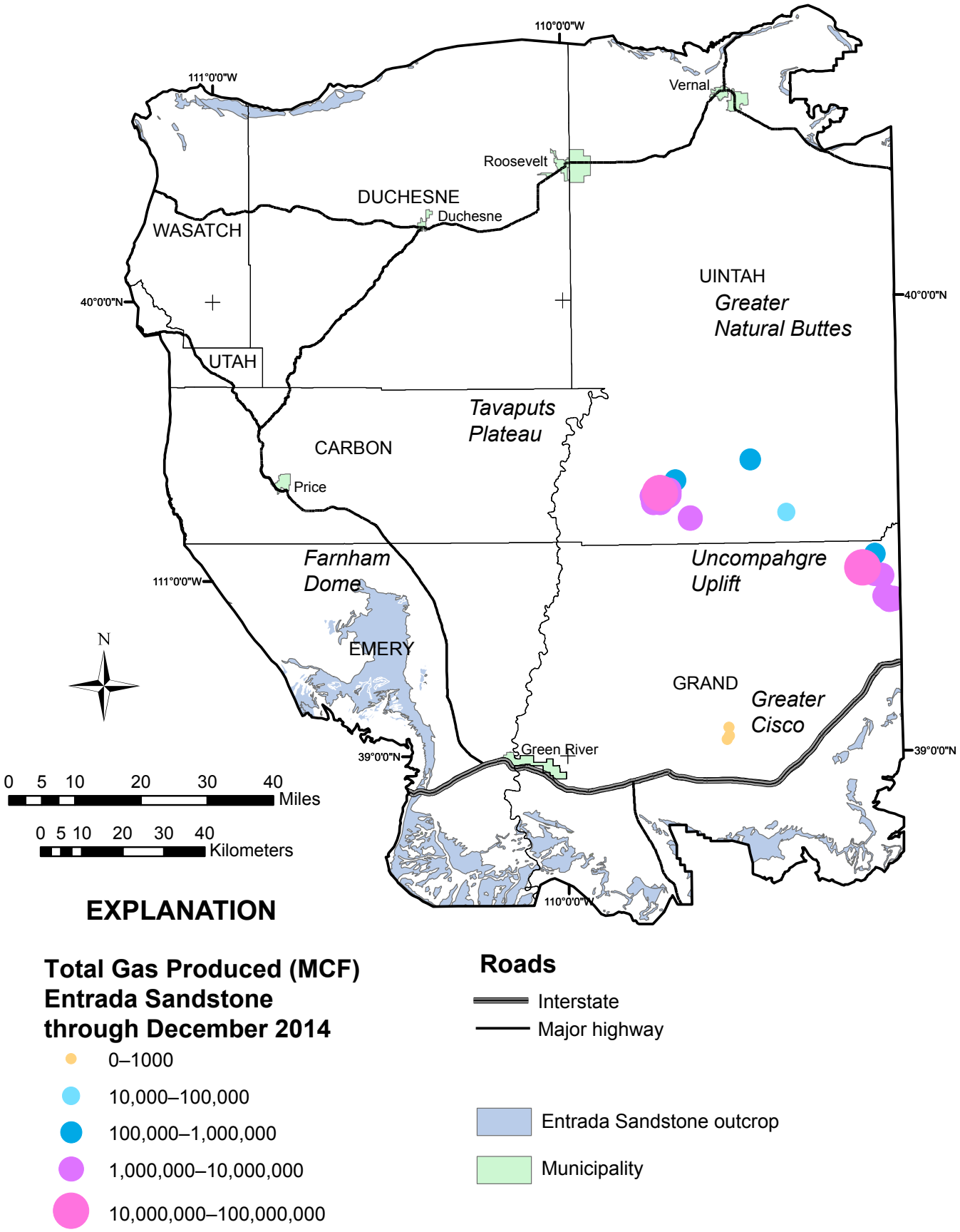

Figure 4.50. *Total gas produced per well from the Entrada Sandstone through December 2014. Data from Utah Division of Oil, Gas and Mining (2016d).*

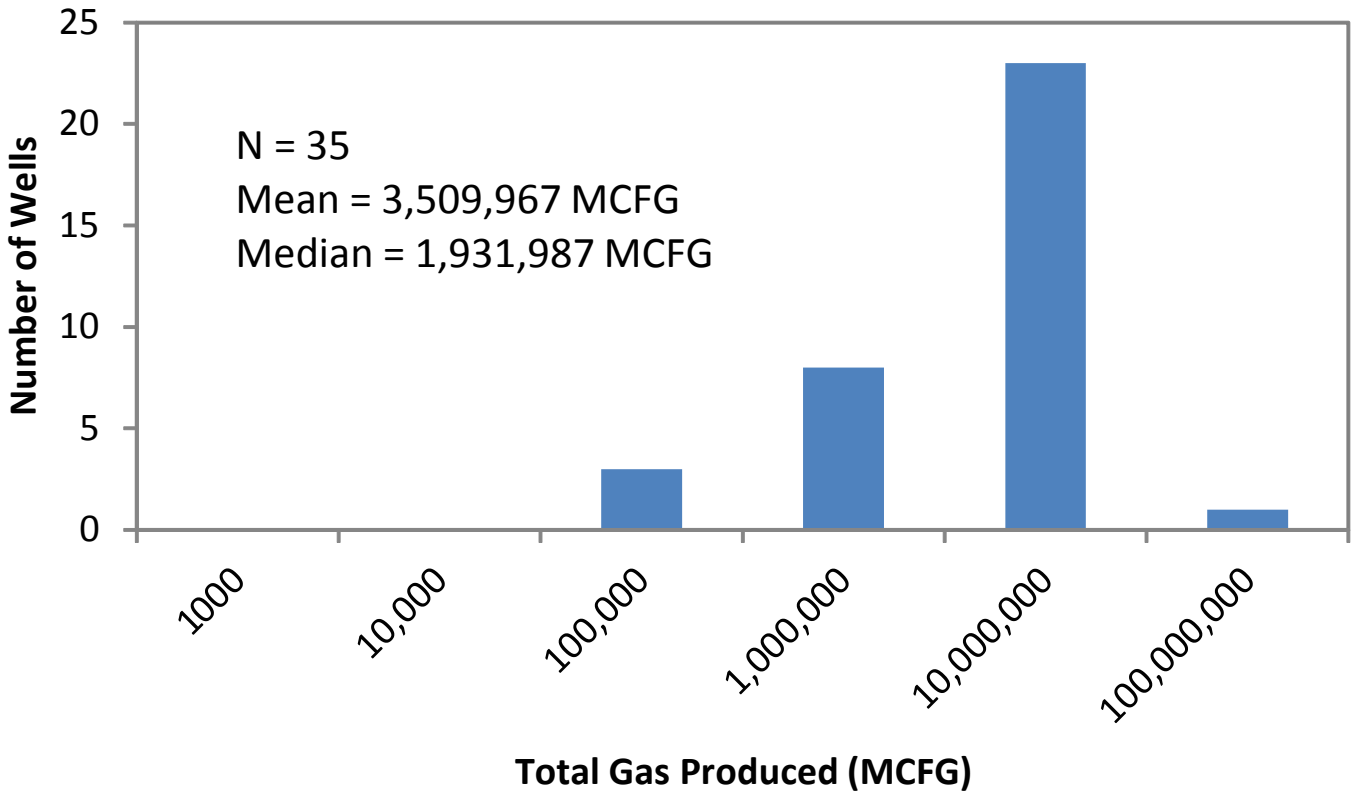

Figure 4.51. *Frequency distribution of total gas produced per well from the Entrada Sandstone through December 2014. Gas volumes range from 14,878 to 12,276,656 MCFG/well. Data from Utah Division of Oil, Gas and Mining (2016d).*

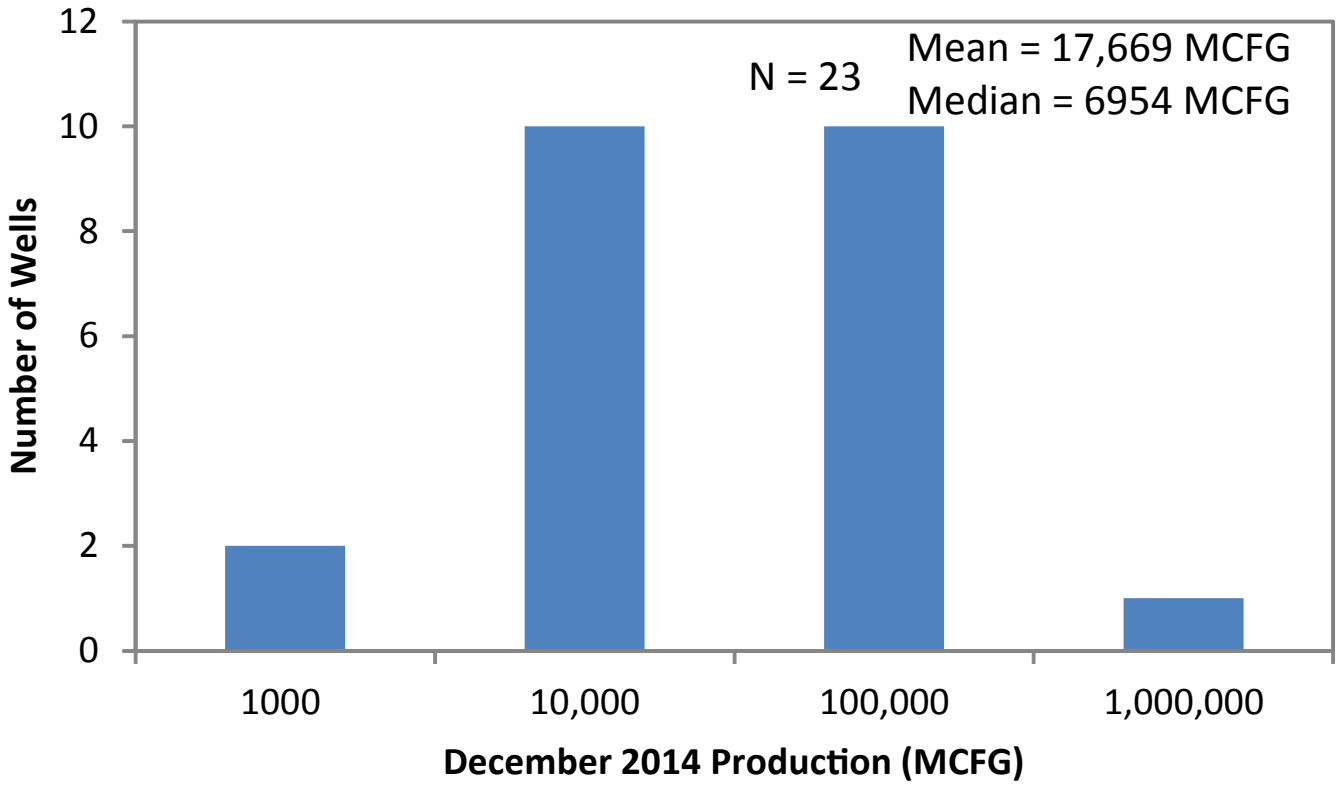

Figure 4.52. *Frequency distribution of gas produced per well from the Entrada Sandstone during December 2014. Production ranges from 118 to 181,310 MCFG/well. Data from Utah Division of Oil, Gas and Mining (2016d).*

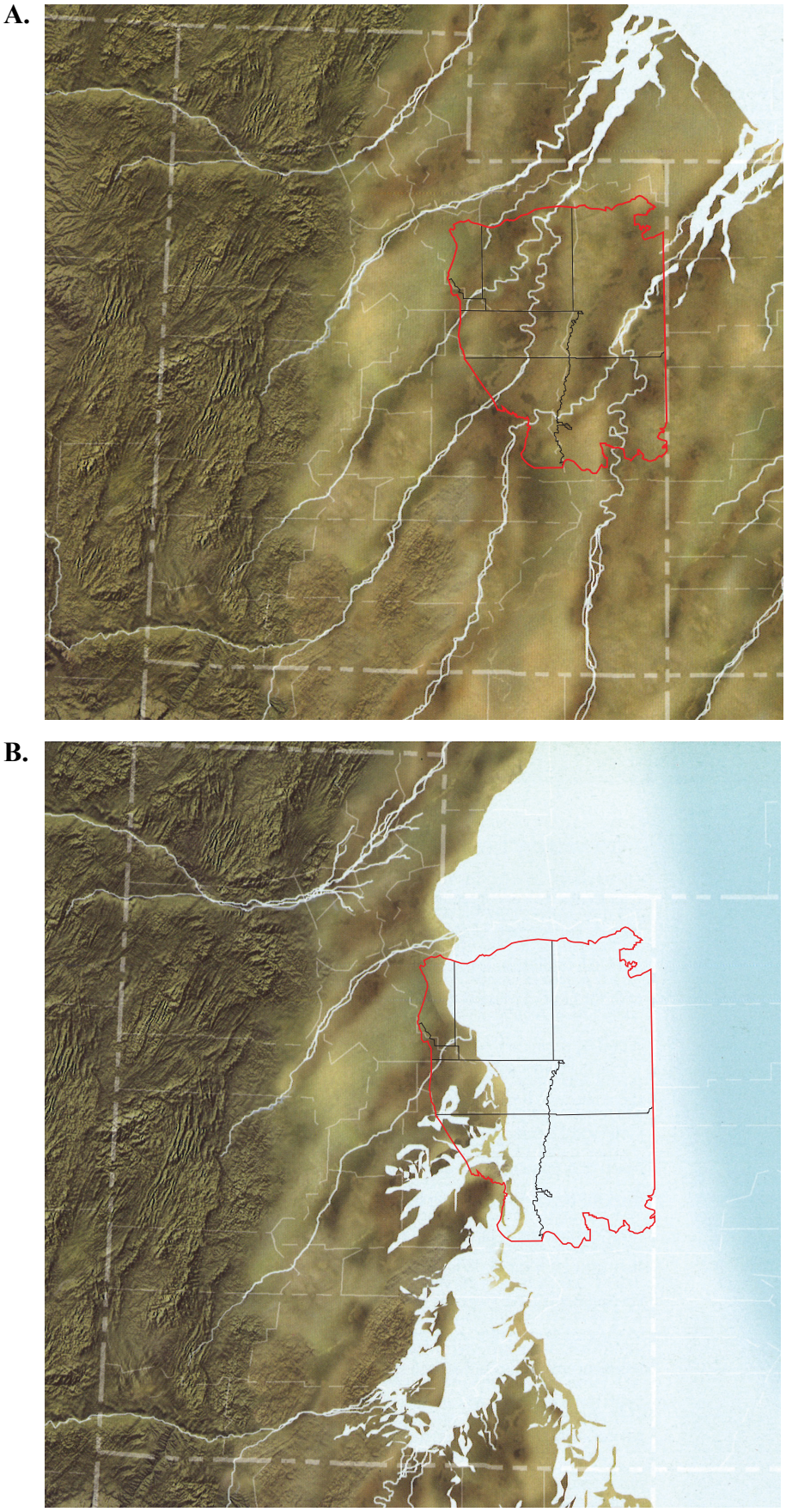

Figure 4.53. *Early Cretaceous paleogeography with study area outlined in red.* ***A.*** *Cedar Mountain Formation, Early Cretaceous (125 Ma).* ***B.*** *Dakota Formation, Early Cretaceous (105 Ma). From Blakey and Ranney (2008).*

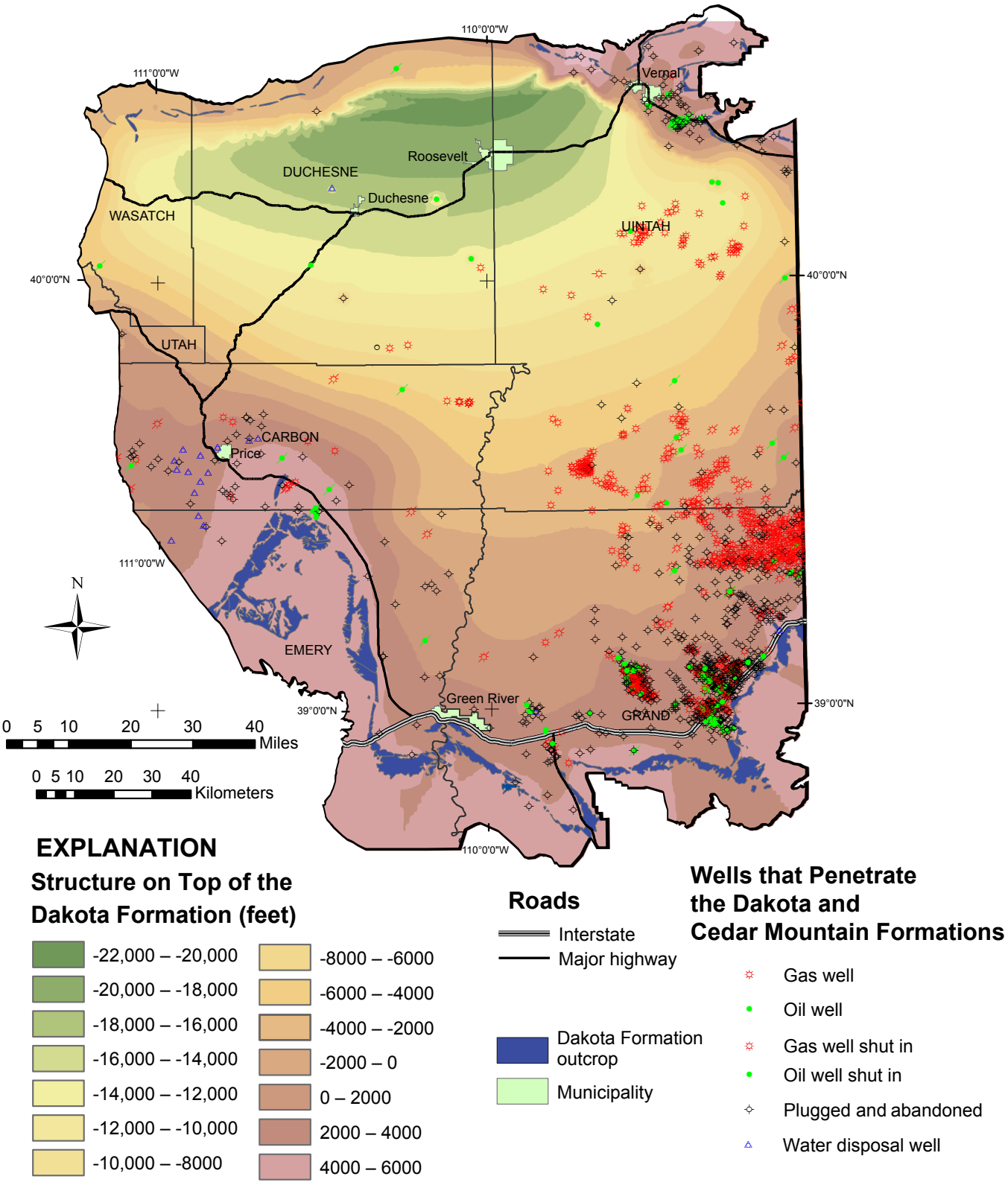

Figure 4.54. *Structure on top of the Dakota Formation, Uinta Basin study area. Datum: mean sea level.*

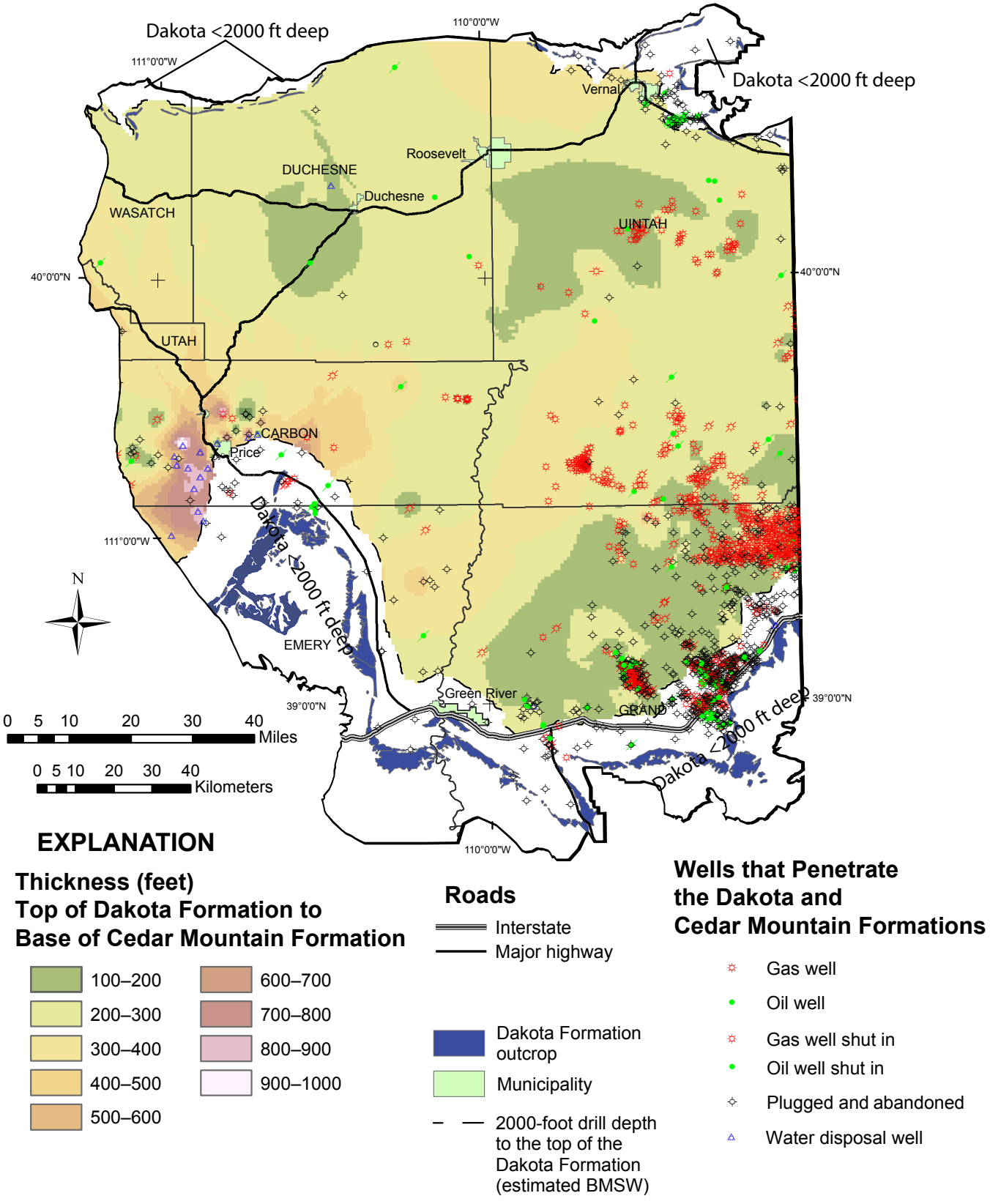

Figure 4.55. *Gross thickness of the CMKD reservoir for areas greater than 2000 feet (600 m) deep. The 2000-foot drill depth is used as an estimated depth to the base of the moderately saline water (BMSW).*

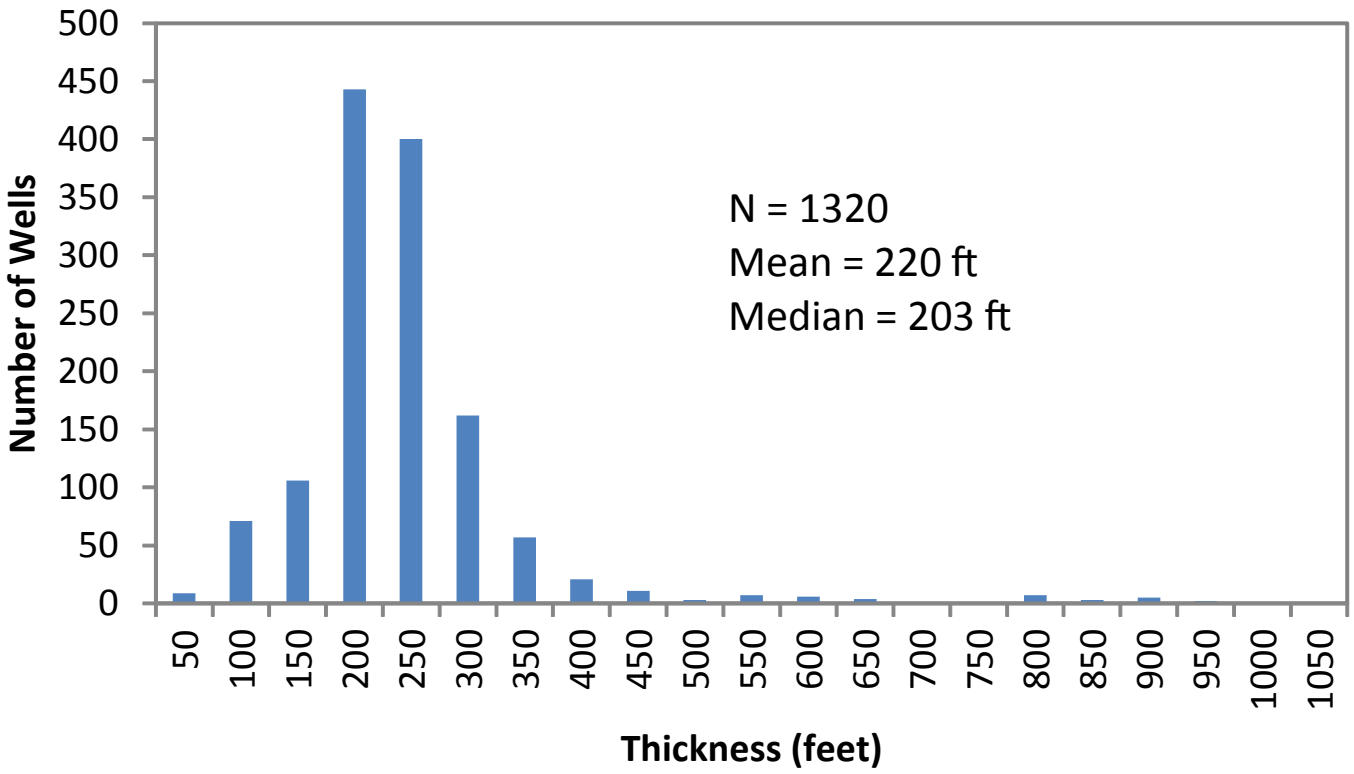

Figure 4.56. *Frequency distribution of the gross thickness of CMKD reservoir in the geophysical well logs studied.*

12%) in 428 wells. A map of PHIE ≥ 6% (figure 4.61) shows similar trends as the net sandstone thickness map (figure 4.57), indicating PHIE ≥ 6% is directly related to sandstone thickness. A porous sand trend is parallel to, but slightly southeast of the net sandstone thickness trend, and the thickness of porous sand with at least 6% porosity is generally less than half of the total sandstone thickness. The map of PHIE ≥ 12% (figure 4.62) shows a similar pattern but with greatly reduced thickness, with most of the basin being less than 20 feet (6 m). PHIE ≥ 6% ranges from 0 to 152 feet (0–46 m), with an average of 50 feet (15 m) and a median of 46 feet (14 m). PHIE ≥ 12% ranges from 0 to 144 feet (0–44 m), with an average of 30 feet (14 m) and a median of 26 feet (8 m) (figure 4.63). The ratio of PHIE ≥ 6% and PHIE ≥ 12% to net sandstone thickness was plotted against drill depth (figure 4.64). Many wells have a PHIE ≥ 6%/net sandstone ratio of 0.8 to 1.0 down to a depth of 10,000 feet (3050 m). Below 10,000 feet (3050 m) the ratio of PHIE ≥ 6%/net sandstone decreases but has a random distribution. Many of the wells have a PHIE ≥ 12%/net sandstone ratio of 0.7 to 1.0 down to a depth of 9000 feet (2750 m) but with a range of 0.0 to 1.0. Below 9000 feet (2750 m) the ratio of PHIE ≥ 12%/net sandstone decreases rapidly. Both ratios (6% and 12%/net sandstone) show a significant drop in porous reservoir with increasing depth.

Permeability is highly variable in the heterolithic channel deposits of the CMKD reservoir. Permeability varies spatially with depth, and within individual channel deposits. Currie and others (2011) used core data to plot porosity versus permeability based on grain size (figure 4.65). Permeability varied from 0.01 mD (lower limit of the core measurement) to 100 mD. A best-fit logarithmic relationship is shown, but the permeability varies by several orders of magnitude at almost every value of porosity.

Water Quality

The CMKD Formations crop out along the southern and northern margins of the Uinta Basin. The southern margin receives 6 to 10 inches (15–25 cm) of annual rainfall (Freethey and Cordy, 1991). The structural configuration creates geometry similar to a bowl with no known groundwater discharge. Deep burial suggests little or no recharge into the basin, resulting in a bowl filled with dense brine (Freethey and Stolp, 2010). As with the GCG/N and the Entrada Sandstone, the structure on top of the Dakota Formation was subtracted from the BMSW of Anderson and others (2012) to generate a map of the difference between the BMSW and CMKD reservoir (figure 4.66). Again, throughout most of the basin, the CMKD reservoir is thousands of feet below the BMSW except in Ashley Valley field where the water in the CMKD reservoir is less than 10,000 mg/L TDS (CMKD above the BMSW). As with the GCG/N and Entrada, Anderson and others' (2012) mapping did not extend far enough south to capture the 10,000 mg/L TDS line in the CMKD, so the 2000-foot (600 m) drill depth is used as an approximation of the BMSW in these areas based on the work of Freethey and Stolp (2010) (figure 4.66).

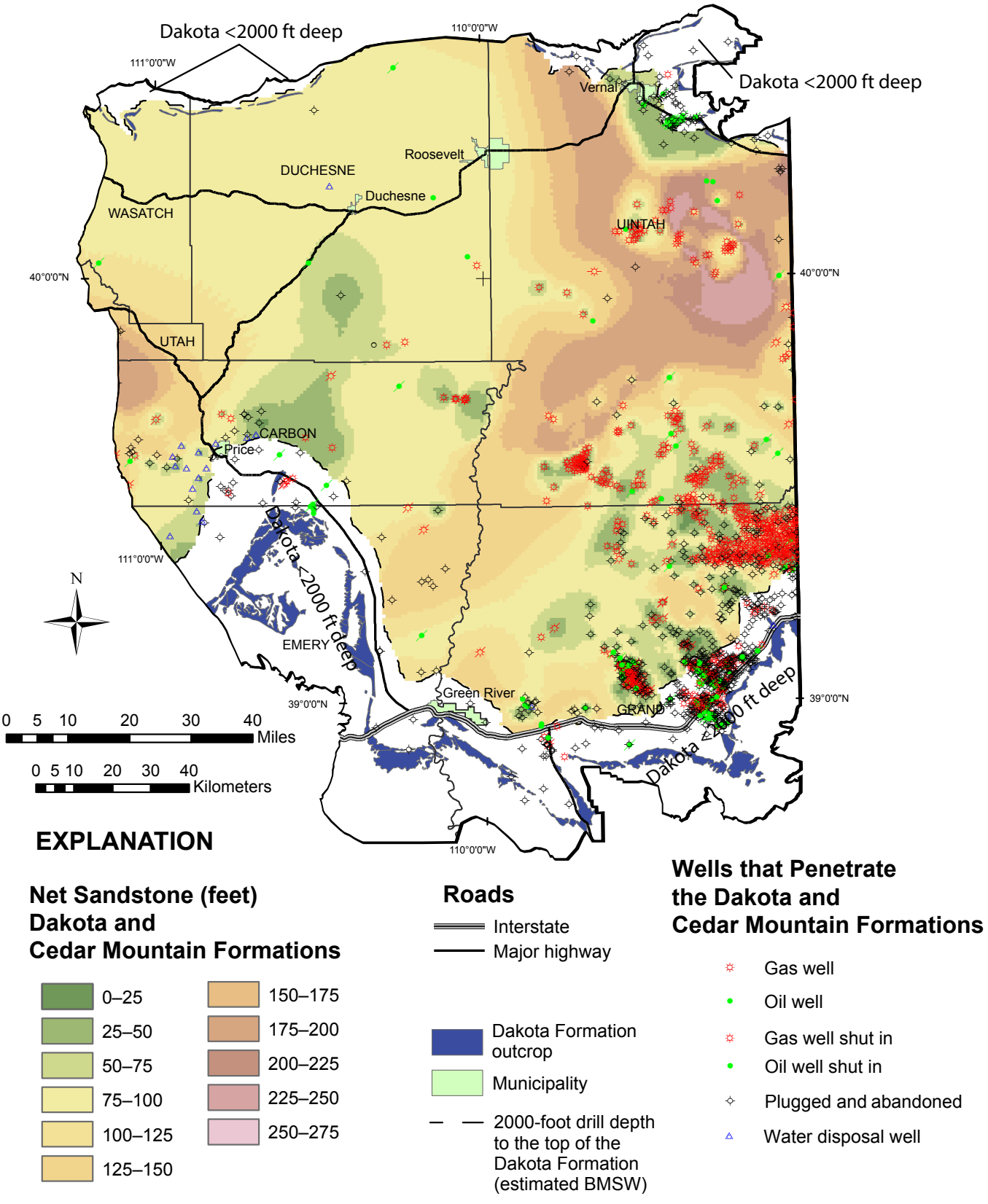

Figure 4.57. *Net sandstone thickness map (gamma ray ≤ 60 API) of the CMKD reservoir for areas greater than 2000 feet (600 m) deep. The 2000-foot drill depth is used as an estimated depth to the base of the moderately saline water (BMSW).*

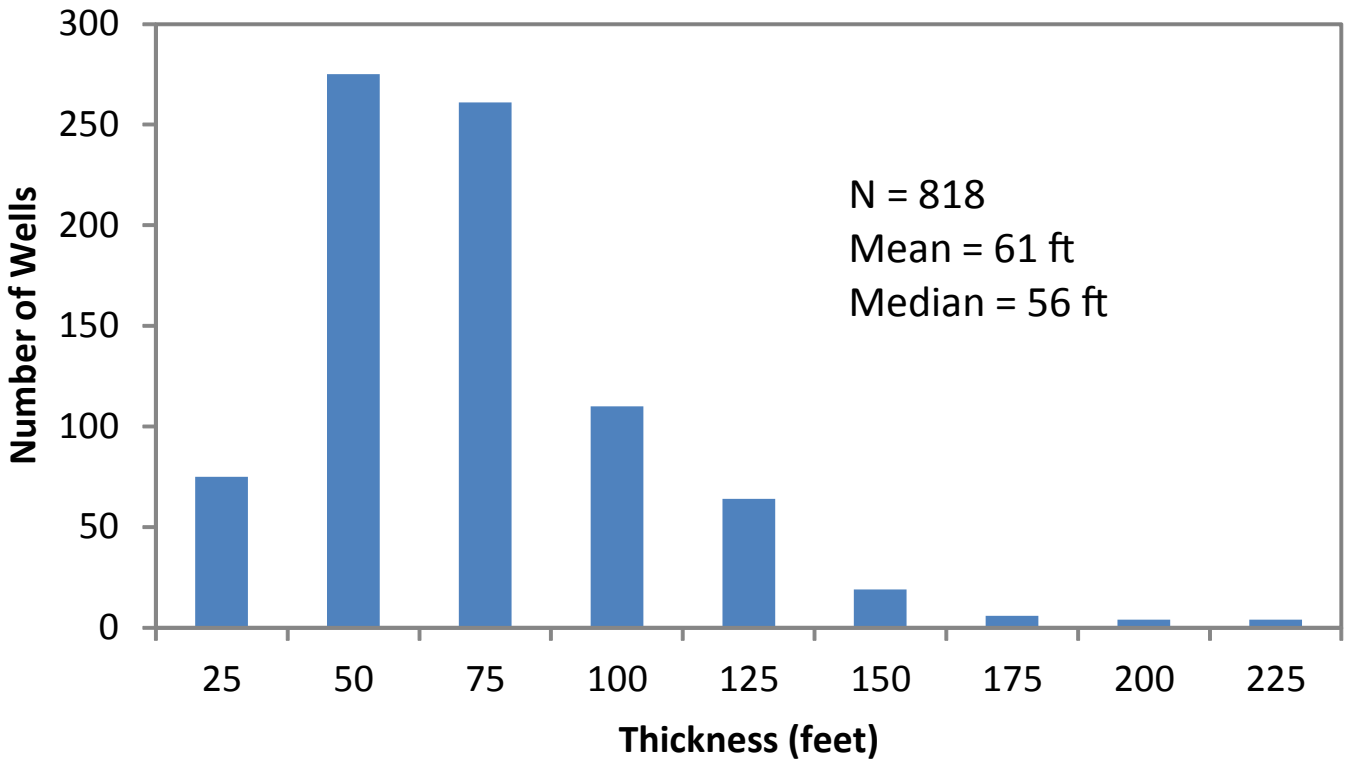

Figure 4.58. *Frequency distribution of the net sandstone thickness (≤60 API gamma ray) in the CMKD reservoir in the geophysical well logs studied.*

Water quality data for CMKD from oil and gas wells in the Uinta Basin are also very sparse; only eight reliable samples were found. As expected, the data show increasing TDS with depth (figure 4.67). As in the deeper section, the trend line indicates water is below 10,000 mg/L TDS to a depth greater than 10,000 feet (3000 m), again much deeper than expected from the work of Anderson and others (2012) and Freethey and Stolp (2010). Therefore, as was the case in the GCG/N and Entrada, the trend line is not considered reliable due to the few data points and the commingling of production water from other formations. The water types are dominantly sodium chloride in deep wells and sodium bicarbonate (one sample) from shallow depth (figure 4.68), in general agreement with Freethey and Cordy (1991). The hydraulic conductivity of the Dakota aquifer is 0.001 to 1.0 feet per day (Freethey and Cordy, 1991).

Water Production, Use, and Disposal

Historically, most of the production from the CMKD reservoir came from fields in the southern part of the basin along the Uncompahgre uplift and Greater Cisco field (figure 1.1). Recently, several wells have been drilled to the CMKD in the Greater Natural Buttes (GNB) field area. The GNB wells are typically completed with commingled production from the CMKD, Mancos, Mesaverde, and occasionally Wasatch reservoirs (figure 1.5). Production from individual reservoirs is not reported in these wells, so the volume of water and hydrocarbons produced from the CMKD alone cannot be determined. The production shown in this report as CMKD is often commingled production. The largest volume of CMKD produced water comes from the GNB area (figure 4.69), but much of this water is probably coming from the Mancos and Mesaverde. Water production for the month of December 2014 shows a pattern similar to the total production (figure 4.70). The frequency distribution of cumulative produced water (figure 4.71) ranges from 0 to 4,784,213 BW/well, with an average of 121,730 BW/well and a median of 2908 BW/well. The frequency distribution of produced gas per barrel of water produced (GWR) (figure 4.72) has a range of 0.2 to 710,662.0 MCFG/BW, with an average of 4692 MCFG/BW and a median of 79 MCFG/BW from 351 wells. Eighty-one CMKD gas wells have no associated water production.

Hydrocarbon Production

Channel and some marginal-marine deposits in the CMKD provide stratigraphic traps for hydrocarbons in the Uinta Basin. Methane is produced throughout the basin from the CMKD reservoir. Production can be spotty and volumes highly variable due to the heterogeneity and resulting compartmentalization of the channel deposits. Large volumes of gas have been produced from both the northern Greater Natural Buttes field and Uncompahgre areas (figure 4.73). Production from the Natural Buttes field is generally from newer wells that may eventually exceed production from wells in

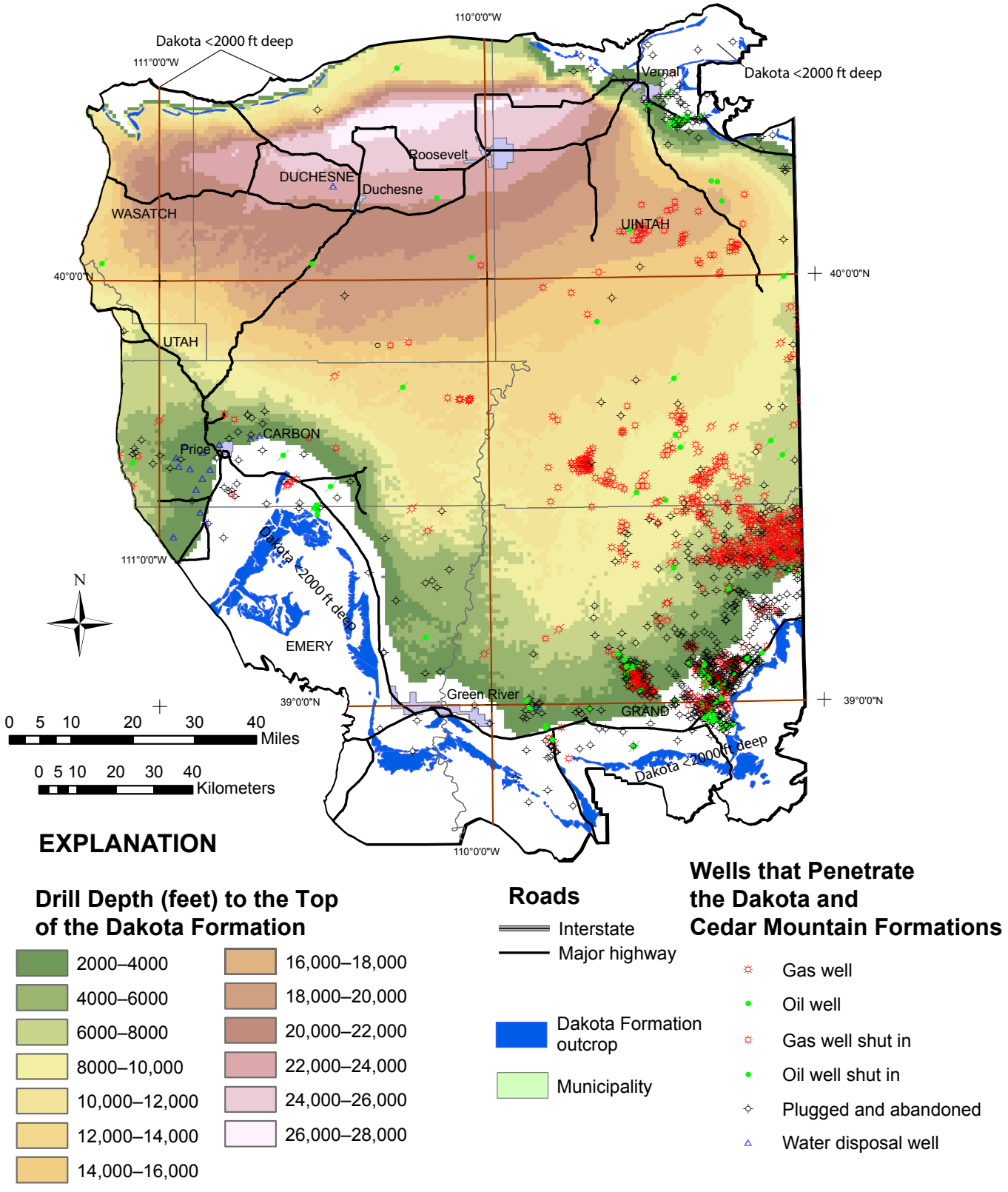

Figure 4.59. *Drill depth to the top of the Dakota Formation for areas greater than 2000 feet (600 m) deep. The 2000-foot drill depth is used as an estimated depth to the base of the moderately saline water (BMSW).*

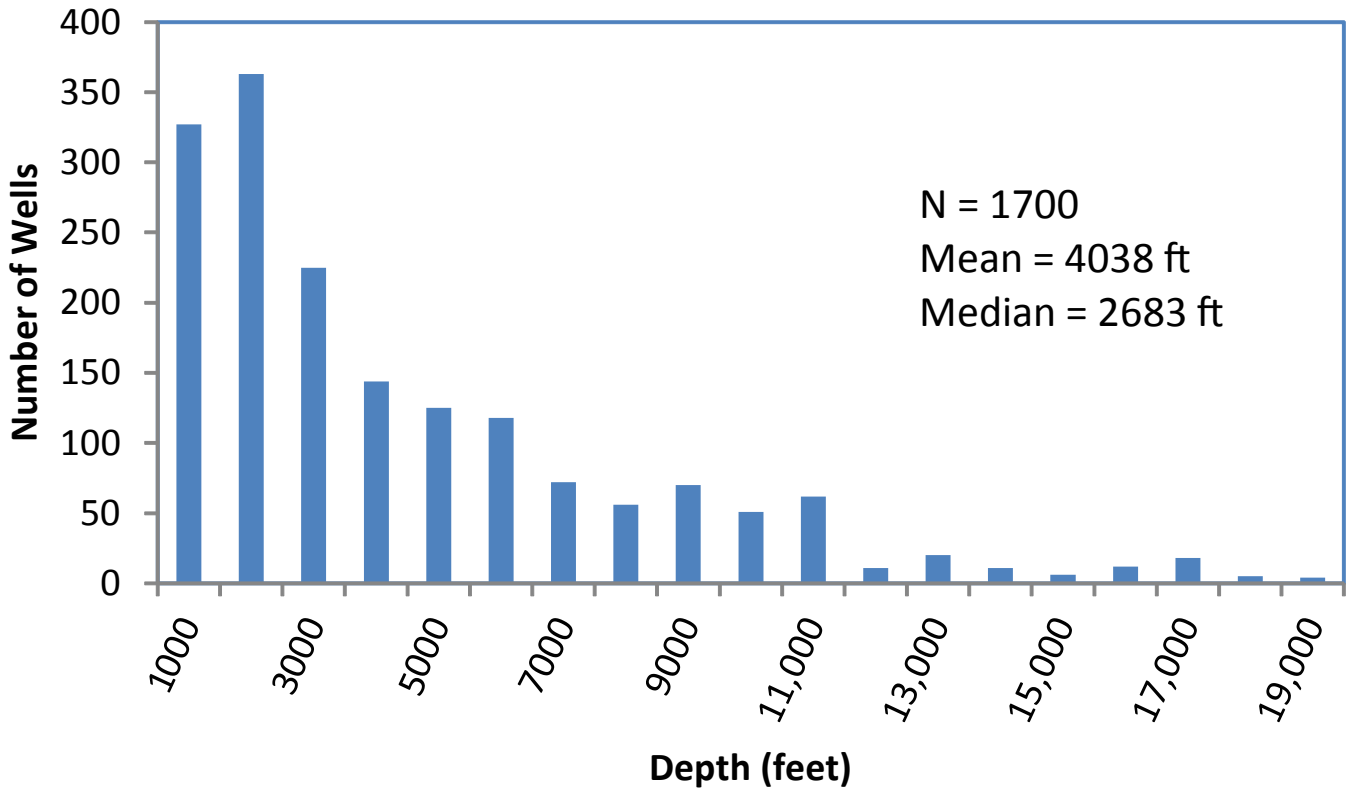

Figure 4.60. *Frequency distribution of the drill depth to the top of the Dakota Formation.*

the rest of the basin. However, production from the field is commingled and the CMKD contribution is unknown. The total gas production from the CMKD (including commingled production) ranges from 143 to 12,123,393 MCFG/well, averaging 737,753 MCFG/well and with a median of 422,803 MCFG/well (figure 4.74). Gas production for the month of December 2014 ranges from 0 to 59,485 MCFG/well, averaging 3383 MCFG/well with a median of 957 MCFG/well (figure 4.75) from 432 wells, of which 77 wells had no production. December production shows larger volumes of gas per well are being produced from the Greater Natural Buttes field area (figure 4.76).

SUMMARY

The Triassic-Jurassic GCG/N is more than 800 feet (250 m) thick throughout much of the Uinta Basin; the Lower Jurassic eolian Navajo Sandstone is the thickest and highest quality reservoir/aquifer in the GCG/N. Drill depth to the GCG/N in the deepest part of the basin is projected to be more than 28,000 feet (8500 m). The lithology of dune deposits of the Navajo (and equivalent section of the Nugget Sandstone) is generally composed of well-sorted fine- to medium-grained sandstone. Sandstone with 6% or more log porosity ranges in thickness from 14 to 1280 feet (4–390 m) and averages 675 feet. Throughout most of the basin, the GCG/N reservoir is thousands of feet below the BMSW. TDS increases with depth and the water types are sodium chloride from one deep well and a mix of all water types, except potassium chloride, from shallow depths. Hydrocarbon and associated water production, mainly from the Navajo Sandstone, comes from fields on the Uncompahgre uplift and Tavaputs Plateau; CO_2 is produced from the Navajo at Farnham Dome field. The Navajo reservoir is used for produced-water disposal in the coal-bed methane fields in central Utah, just south of the Uinta Basin proper, but is currently not used for disposal in the Uinta Basin.

The Jurassic Entrada Sandstone ranges in thickness from 26 to 1210 feet (8–369 m) and thins from east to west. Drill depths to the Entrada in the wells studied are as much as 16,550 feet (5044 m). The lithology of coastal eolian facies consists of fine-grained feldspathic sandstone, whereas the tidal-flat–alluvial-plain red-bed facies is composed of red silty shale and interbedded red channel sandstone. The Jurassic Entrada Sandstone is projected to have less than 20 feet of porous sandstone throughout much of the basin, with the best porosity and permeability in the eolian facies; however, the usable porosity begins to decrease rapidly below 5000 feet (1500 m) drill depth. The Entrada reservoir is also thousands of feet below the BMSW, and as expected, TDS increases with depth. The water types are dominantly sodium chloride in deep wells and a mixture of calcium bicarbonate, magnesium bicarbonate, and magnesium sulfate from shallow depths. Hydrocarbon and associated water pro-

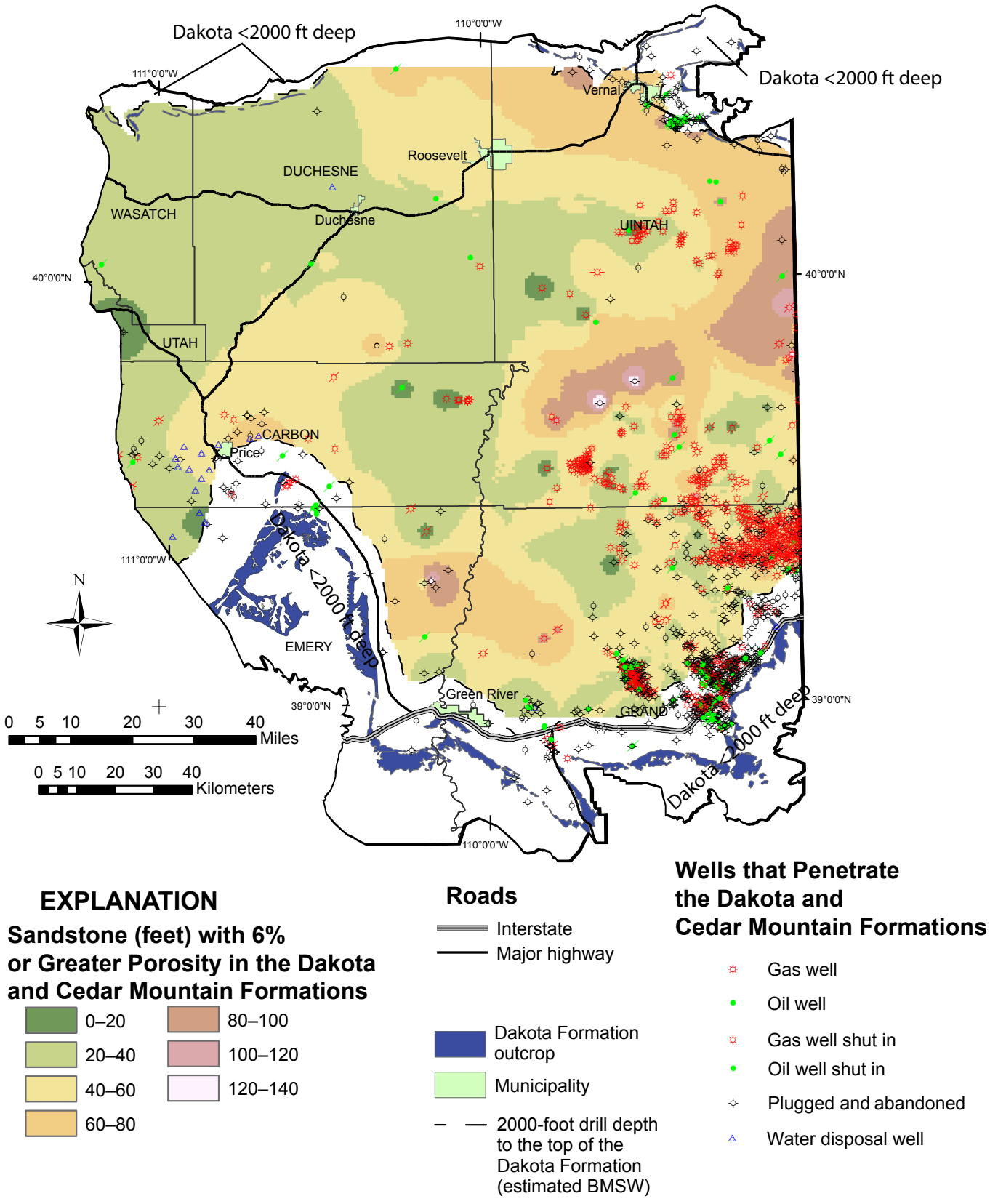

Figure 4.61. *Thickness of sandstone with porosity ≥ 6% in the CMKD reservoir for areas greater than 2000 feet (600 m) deep. Porosity derived from density or sonic well logs. The 2000-foot drill depth is used as an estimated depth to the base of the moderately saline water (BMSW).*

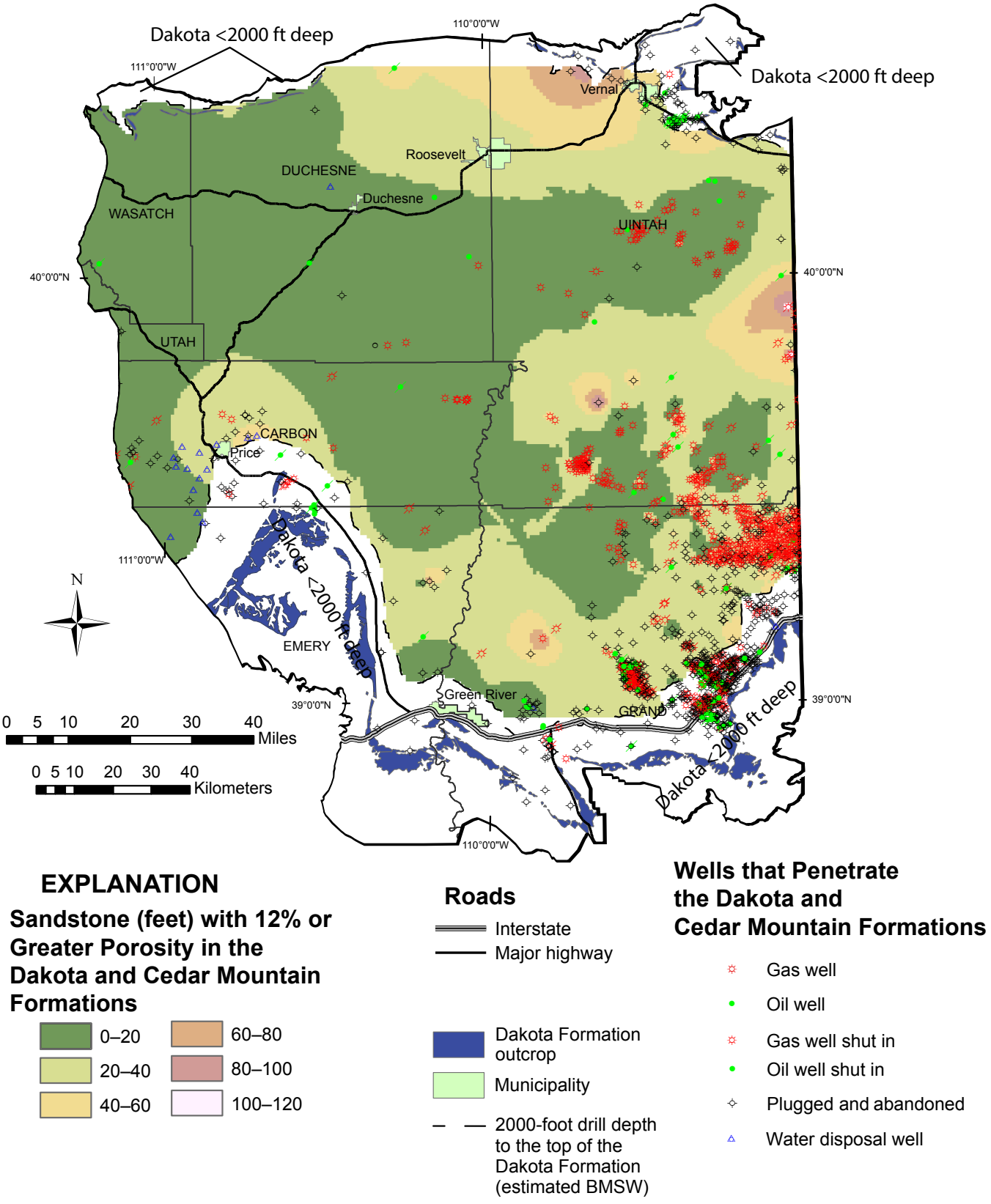

Figure 4.62. *Thickness of sandstone with porosity ≥ 12% in the CMKD reservoir for areas greater than 2000 feet (600 m) deep. Porosity derived from density or sonic well logs. The 2000-foot drill depth is used as an estimated depth to the base of the moderately saline water (BMSW).*

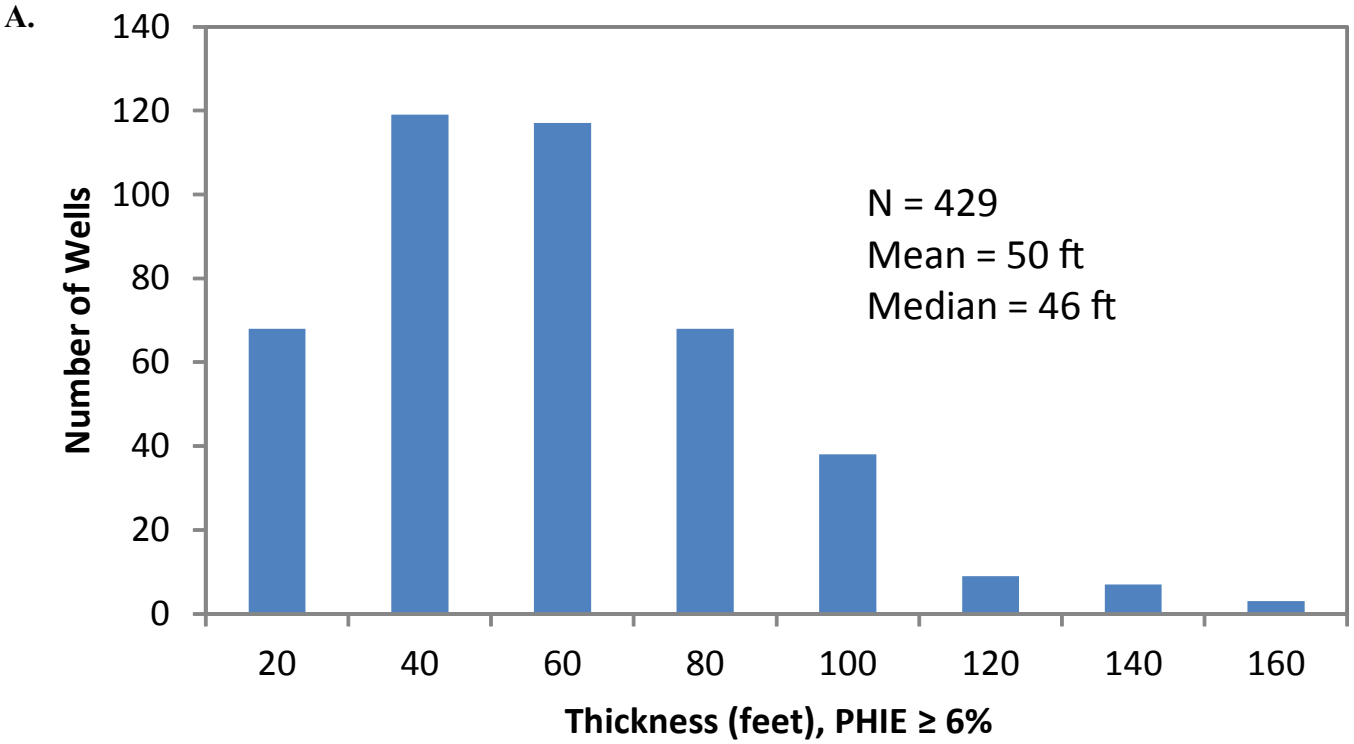

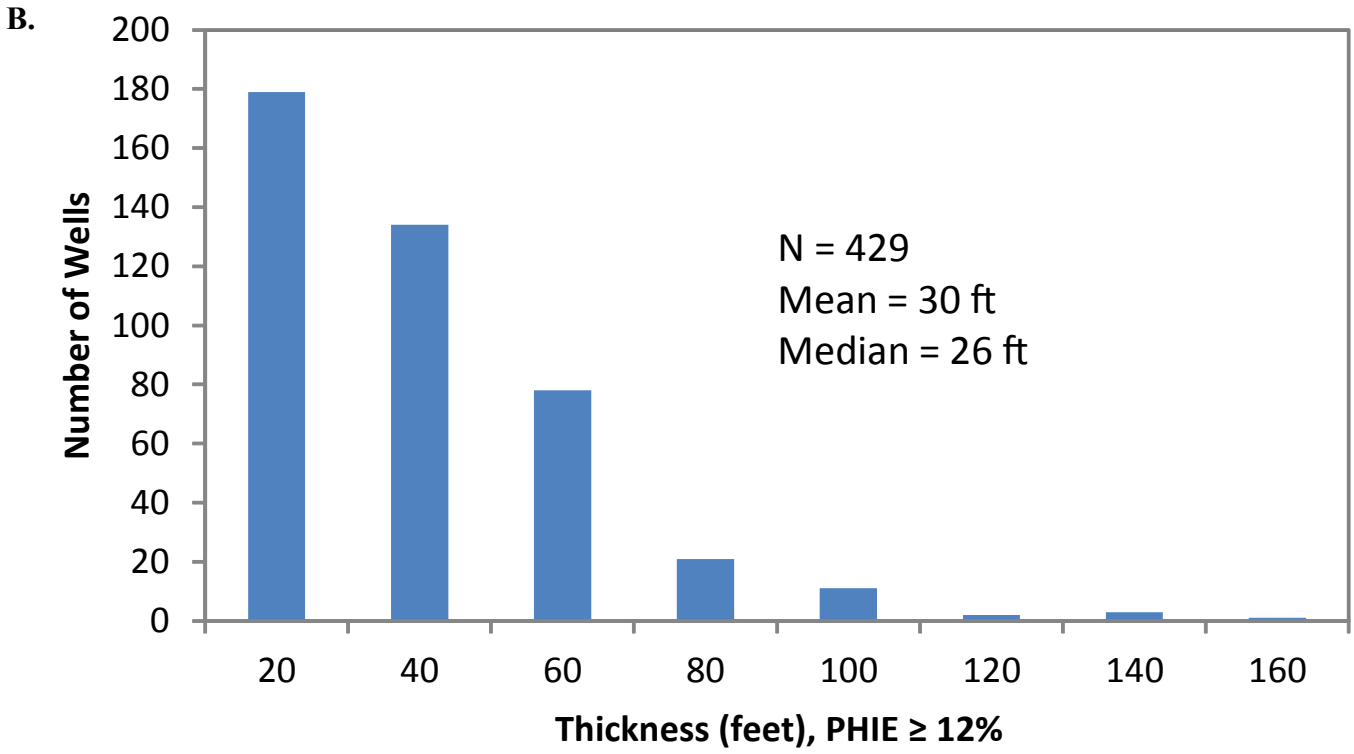

Figure 4.63. *Frequency distribution graphs of the thickness of sandstone with* ***A.*** *≥ 6% porosity and* ***B.*** *≥ 12% porosity in the CMKD reservoir.*

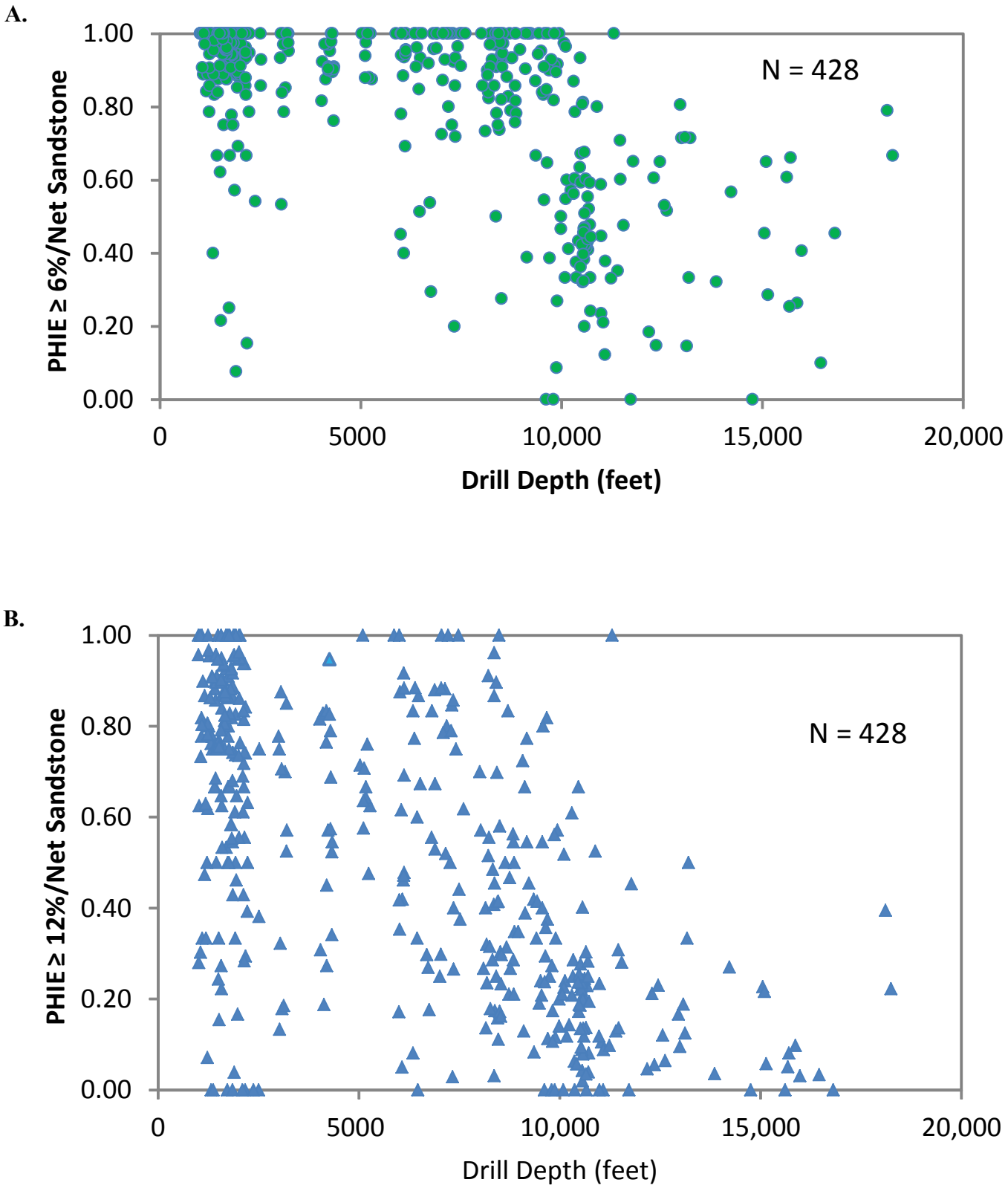

Figure 4.64. A. *Ratio of PHIE ≥ 6% to net sandstone thickness versus drill depth, and* ***B.*** *ratio PHIE ≥ 12% to net sandstone thickness versus drill depth in the CMKD reservoir. Porosity calculated from density or sonic logs.*

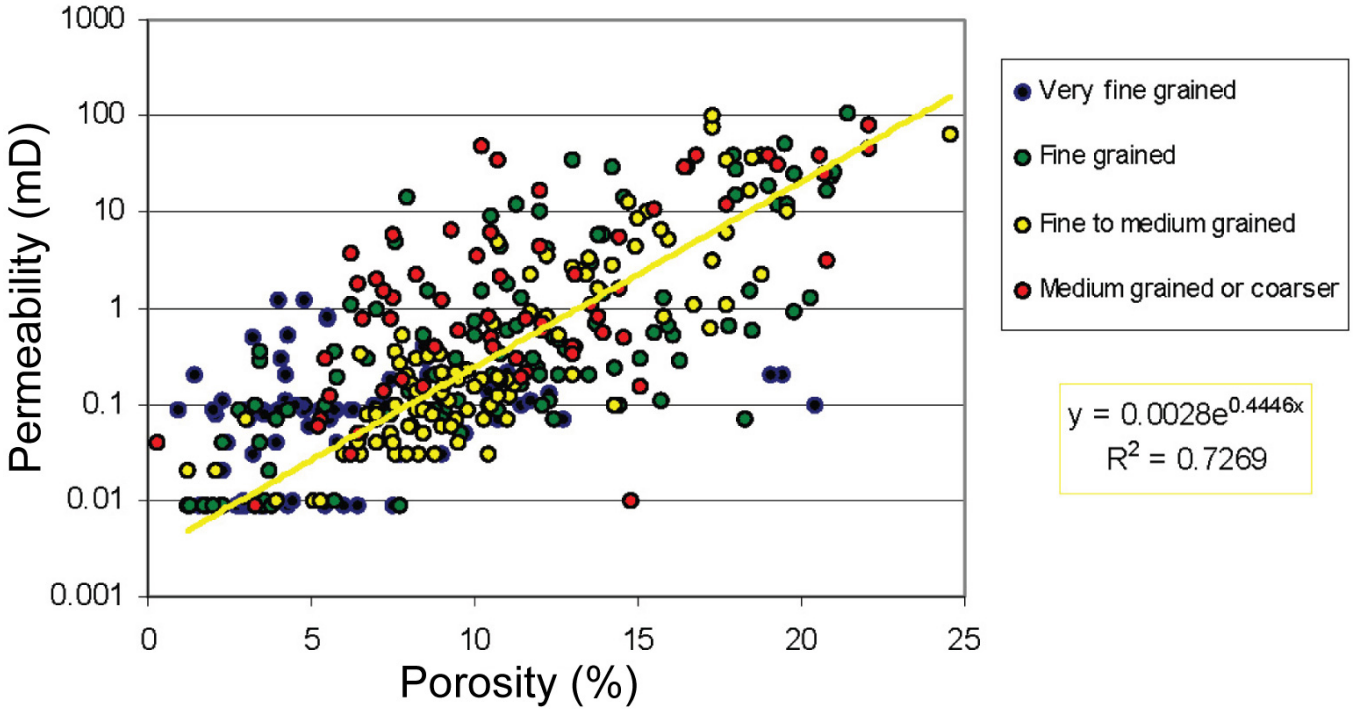

Figure 4.65. *Plot of percent porosity versus permeability for 364 CMKD core data points. Values are color coded by grain size. From Currie and others (2011).*

duction from Entrada reservoirs comes from fields along the Uncompahgre uplift. The Entrada is not used for produced-water disposal in the Uinta Basin.

The Cretaceous CMKD is mainly fluvial deposits that thicken regionally from less than 25 feet (7.6 m) in the southwest to over 250 feet (75 m) in the northeast part of the Uinta Basin. Drill depths to the CMKD reservoirs in the wells studied range from 21 to 18,902 feet (6–5761 m). The primary reservoir lithologies are conglomerate and coarse- to fine-grained sandstone. Porosity and permeability within the ancient channels are highly variable; however, a porous sand trend is parallel to, but slightly southeast of, a net sandstone thickness trend. The thickness of porous sand with at least 6% porosity is generally less than half of the total sandstone thickness. Again, throughout most of the basin, the CMKD reservoir is thousands of feet below the BMSW, and the water types are dominantly sodium chloride in deep wells and sodium bicarbonate from shallow depths. Hydrocarbon and associated water production from the CMKD reservoir comes from stratigraphic traps created by small, lenticular channel deposits. CMKD fields are located in the southern part of the basin along the Uncompahgre uplift and the Greater Natural Buttes field area where production is commingled with that of the Mancos, Mesaverde, and Wasatch reservoirs.

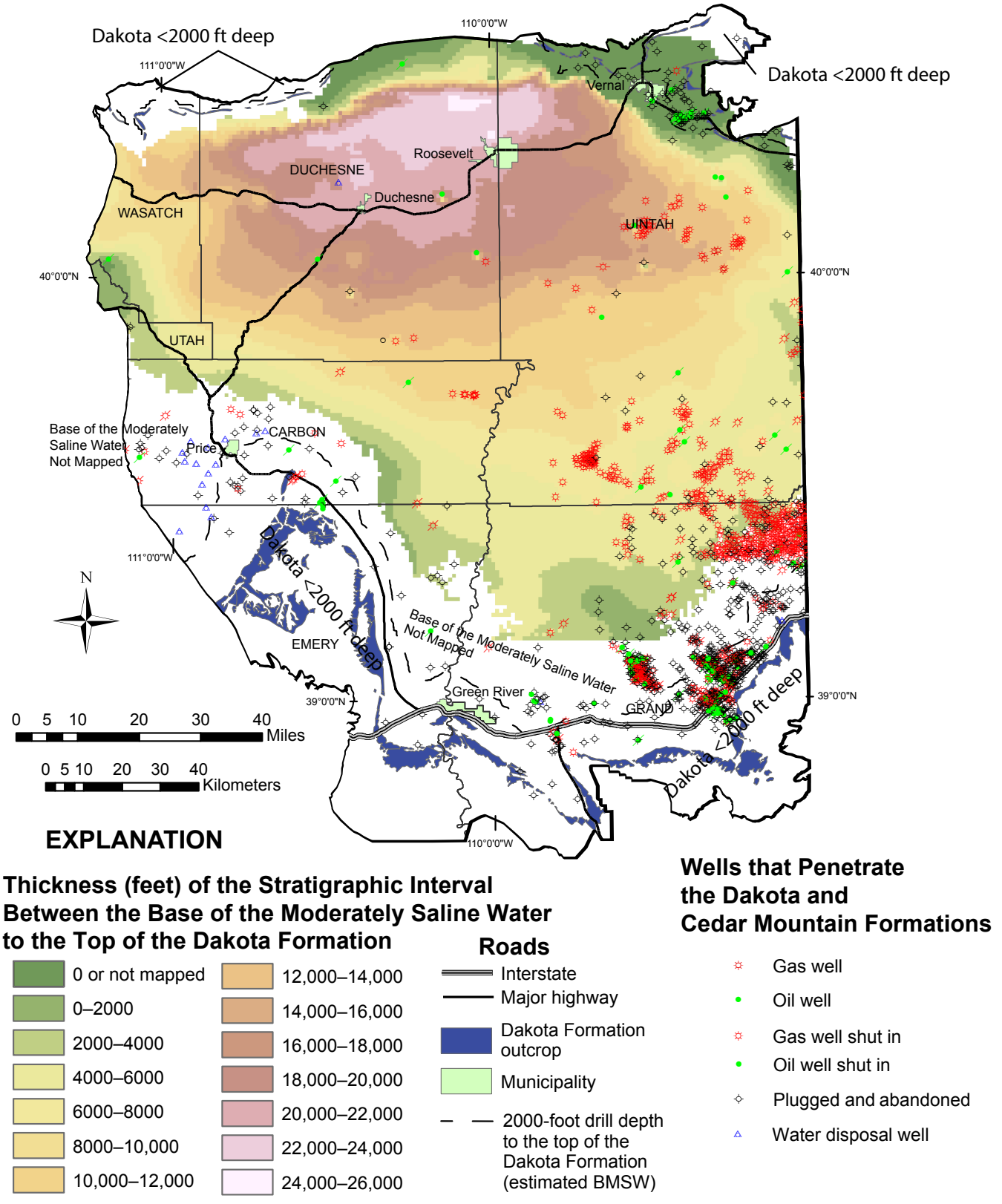

Figure 4.66. *Thickness of the stratigraphic interval between the base of the moderately saline water (BMSW) and the top of the Dakota Formation. The Dakota is above the BMSW in Ashley Valley field (see figure 1.1 for field location). The map was created using ArcScene® by subtracting the drill-depth map (figure 4.59) from the BMSW drill-depth map of Anderson and others (2012).*

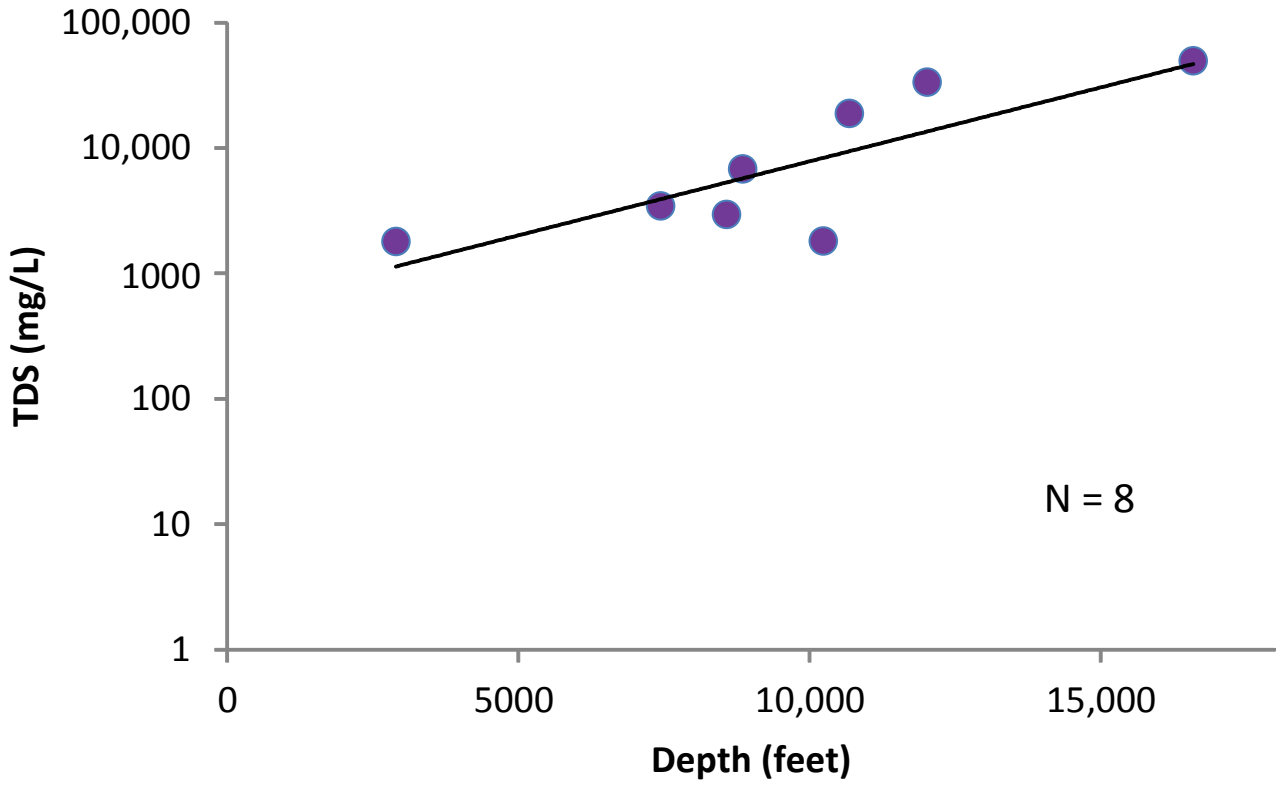

Figure 4.67. *Total dissolved solids versus depth for CMKD water from oil and gas wells in the Uinta Basin. The exponential trend line indicates less than 10,000 mg/L TDS to a depth of 10,000 feet (3000 m). However, the limited number of samples (eight) is insufficient to be statistically significant for such a large area.*

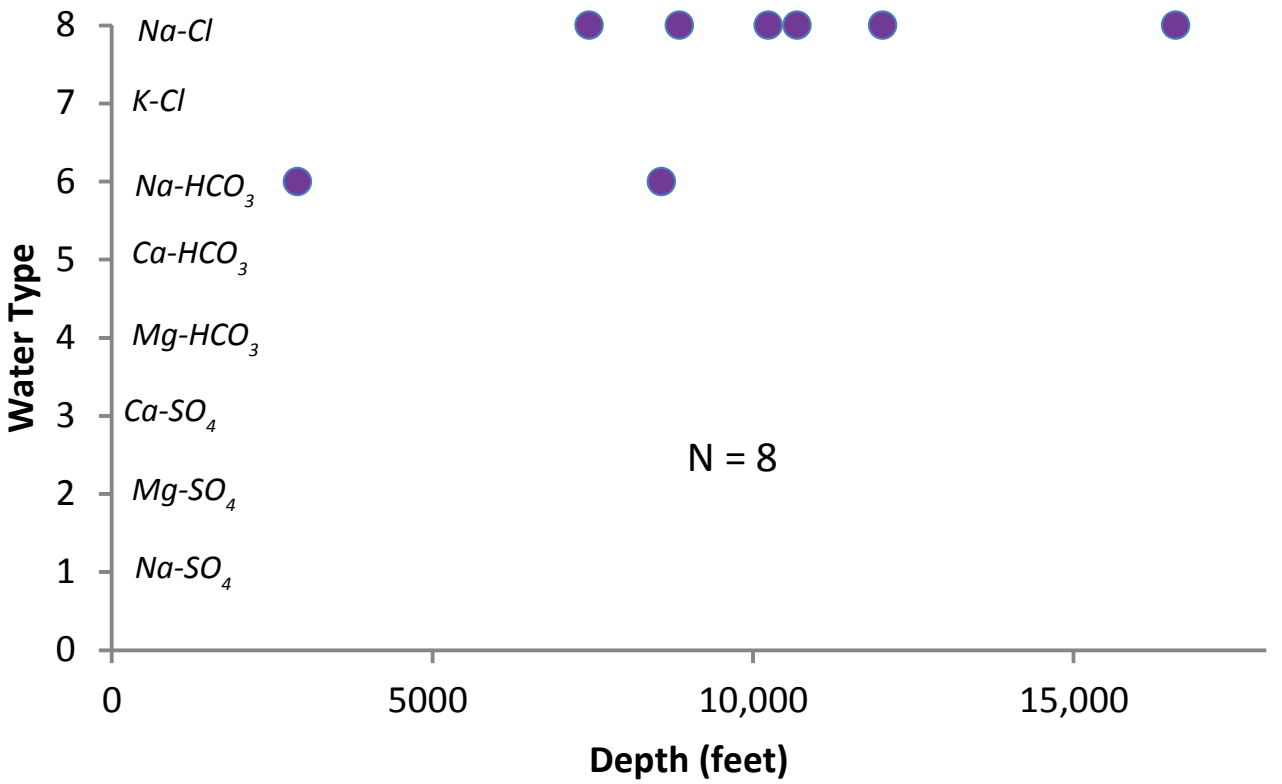

Figure 4.68. *Water produced from the CMKD is mostly sodium chloride (Na-Cl) at depths greater than 5000 feet (1500 m) and sodium bicarbonate (Na-HCO_3) at shallower depth (one sample). The number of samples (eight) is not statistically significant for such a large area.*

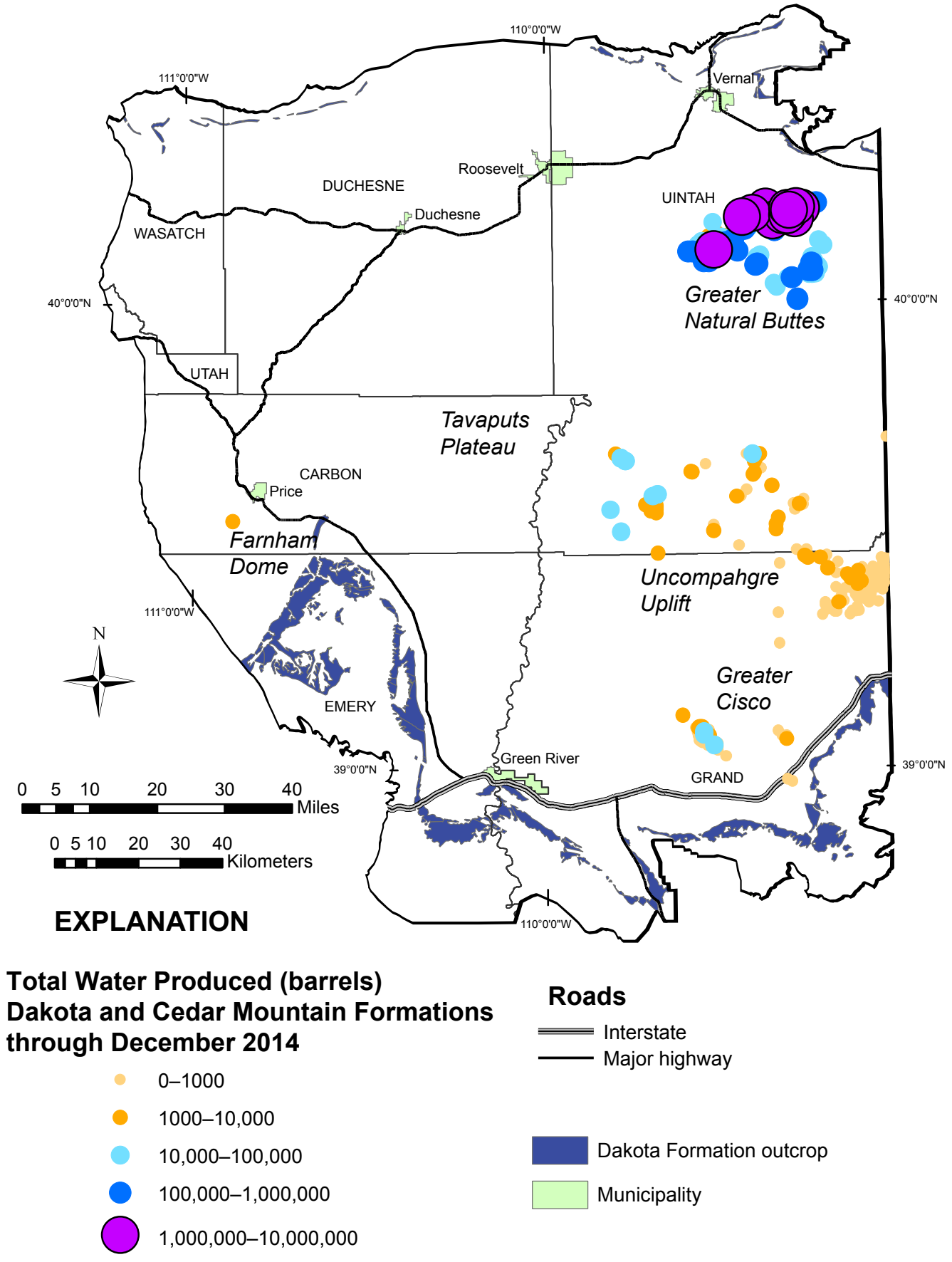

Figure 4.69. *Total water produced from the CMKD reservoir through December 2014. Many wells are completed in more than just the CMKD. As a result, much of the water may be coming from other reservoirs. Data from Utah Division of Oil, Gas and Mining (2016d).*

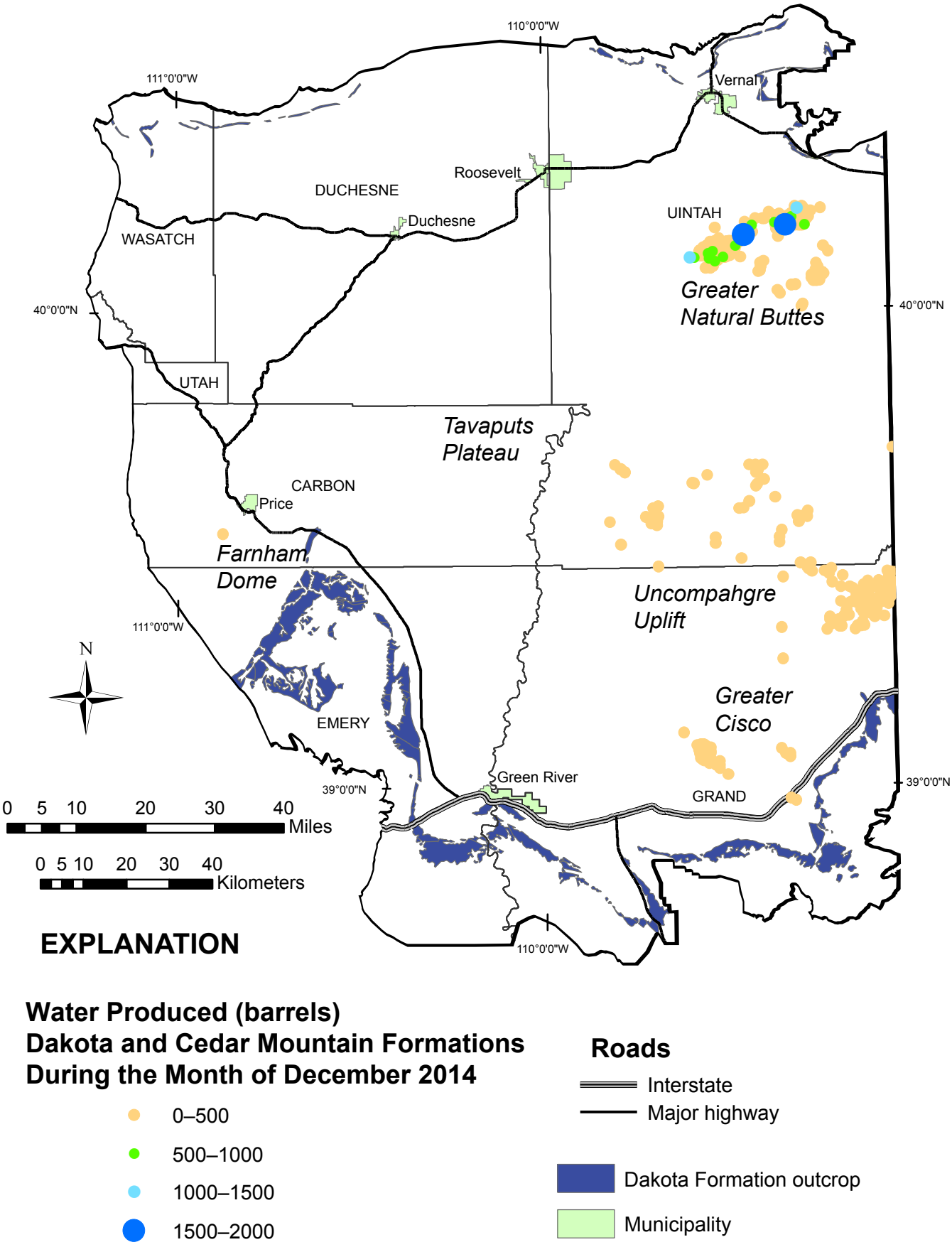

Figure 4.70. *Water produced from the CMKD reservoir during December 2014. Many wells are commingled with other reservoirs and the majority of the produced water may not be from the CMKD. Data from Utah Division of Oil, Gas and Mining (2016d).*

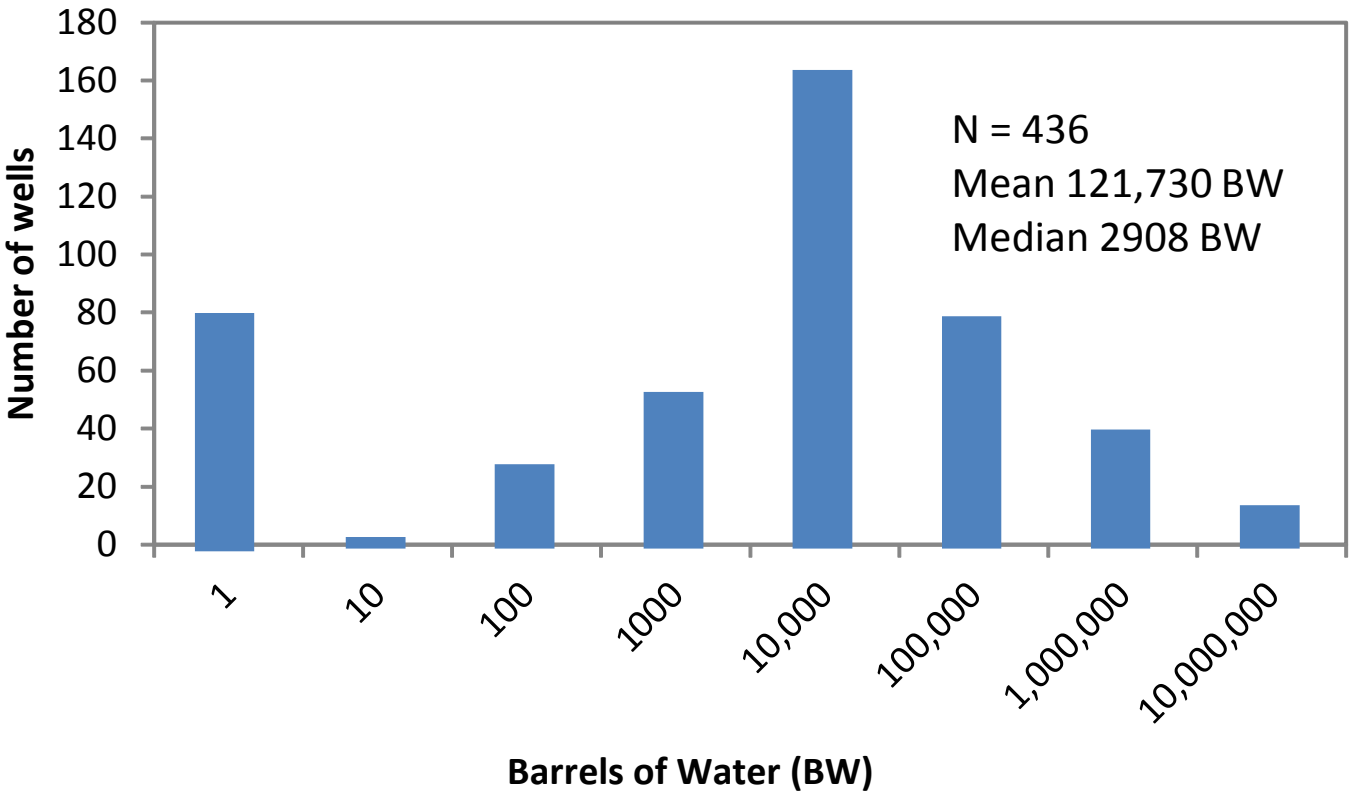

Figure 4.71. *Frequency distribution of the total water produced from the CMKD reservoir. Water volumes range from 0 to 4,784,213 BW. Many of the wells producing from the CMKD reservoir are commingled with shallower reservoirs such as the Mancos, Mesaverde, and Wasatch. Production volumes cannot be separated from the numerous commingled reservoirs. Data from Utah Division of Oil, Gas and Mining (2016d).*

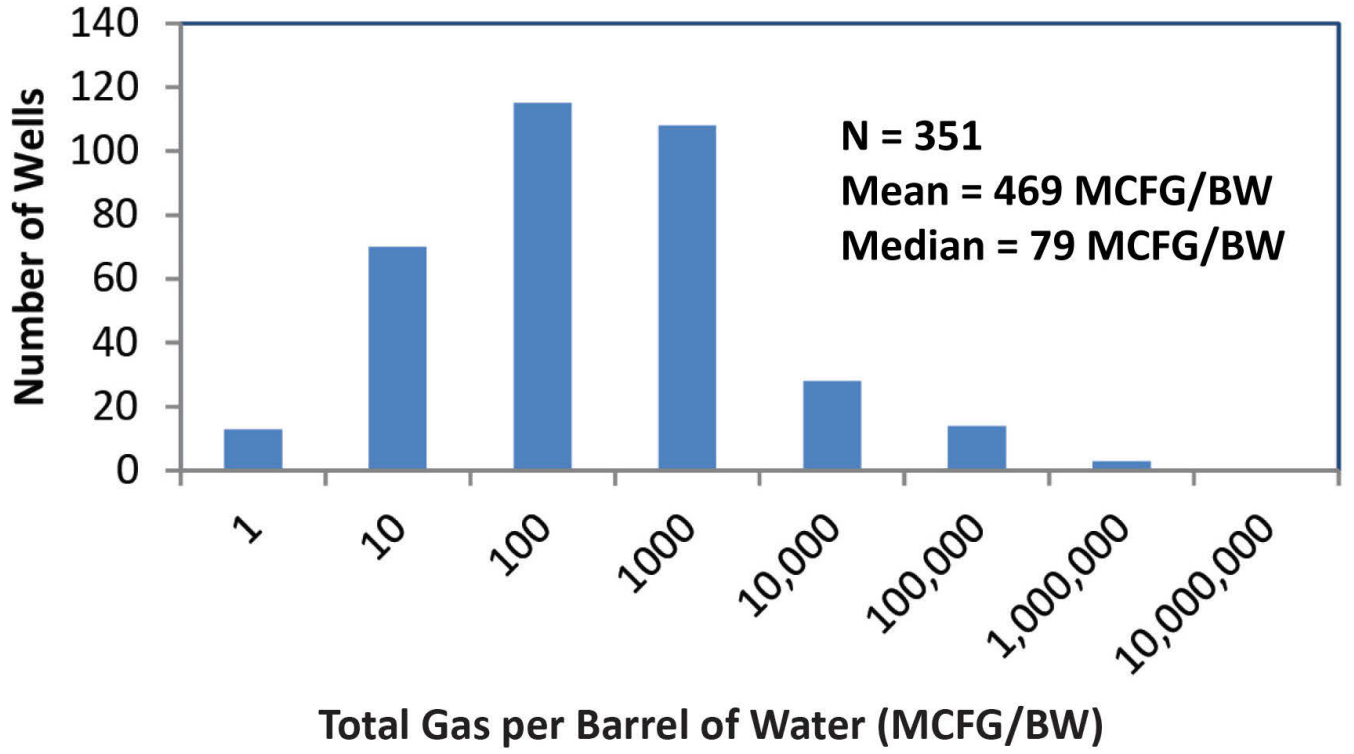

Figure 4.72. *Frequency distribution of the gas per barrel of water produced per well (GWR). The range is from 0 to 710,622 MCFG/BW. Data from Utah Division of Oil, Gas and Mining (2016d).*

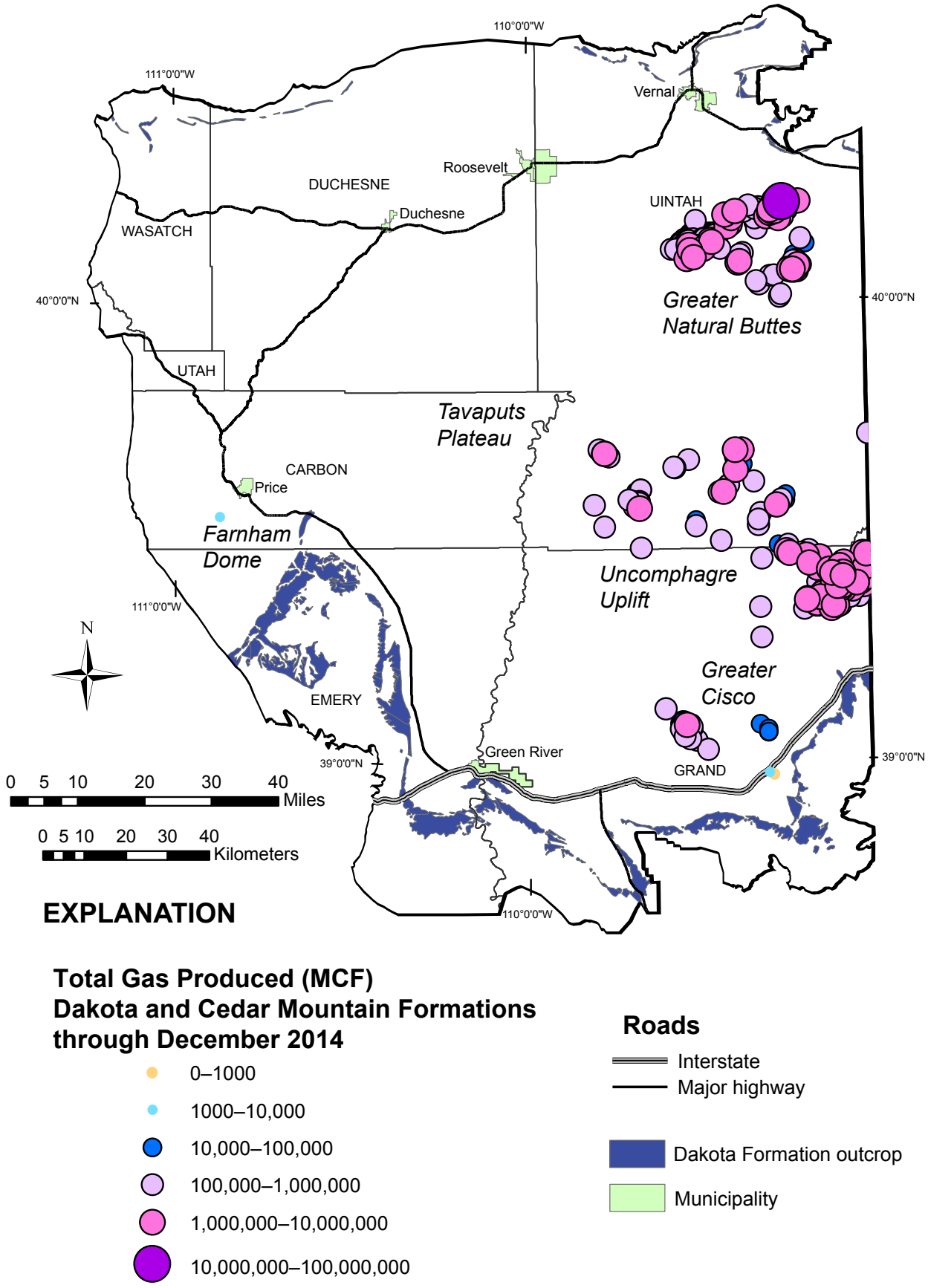

Figure 4.73. *Total gas (MCFG) produced from the CMKD through the month of December 2014. Many of the wells producing from the CMKD reservoir are commingled with shallower reservoirs such as the Mancos, Mesaverde, and Wasatch. Wells in the north are generally recently drilled and commingled with Mancos and Mesaverde. Data from Utah Division of Oil, Gas and Mining (2016d).*

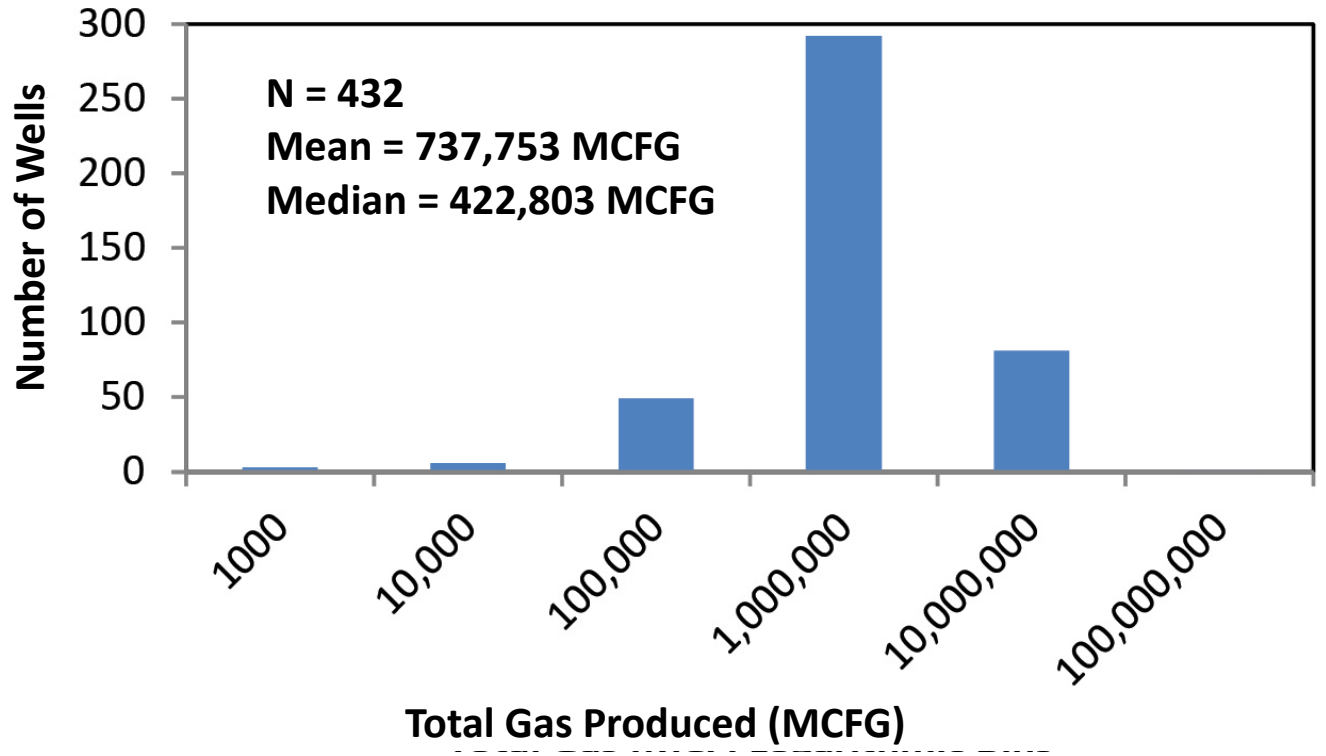

Figure 4.74. *Frequency distribution of total gas produced per well from the CMKD reservoir through December 2014. Production ranges from 143 to 12,123,393 MCFG/well. Many of the wells producing from the CMKD reservoir are commingled with shallower reservoirs such as the Mancos, Mesaverde, and Wasatch. Data from Utah Division of Oil, Gas and Mining (2016d).*

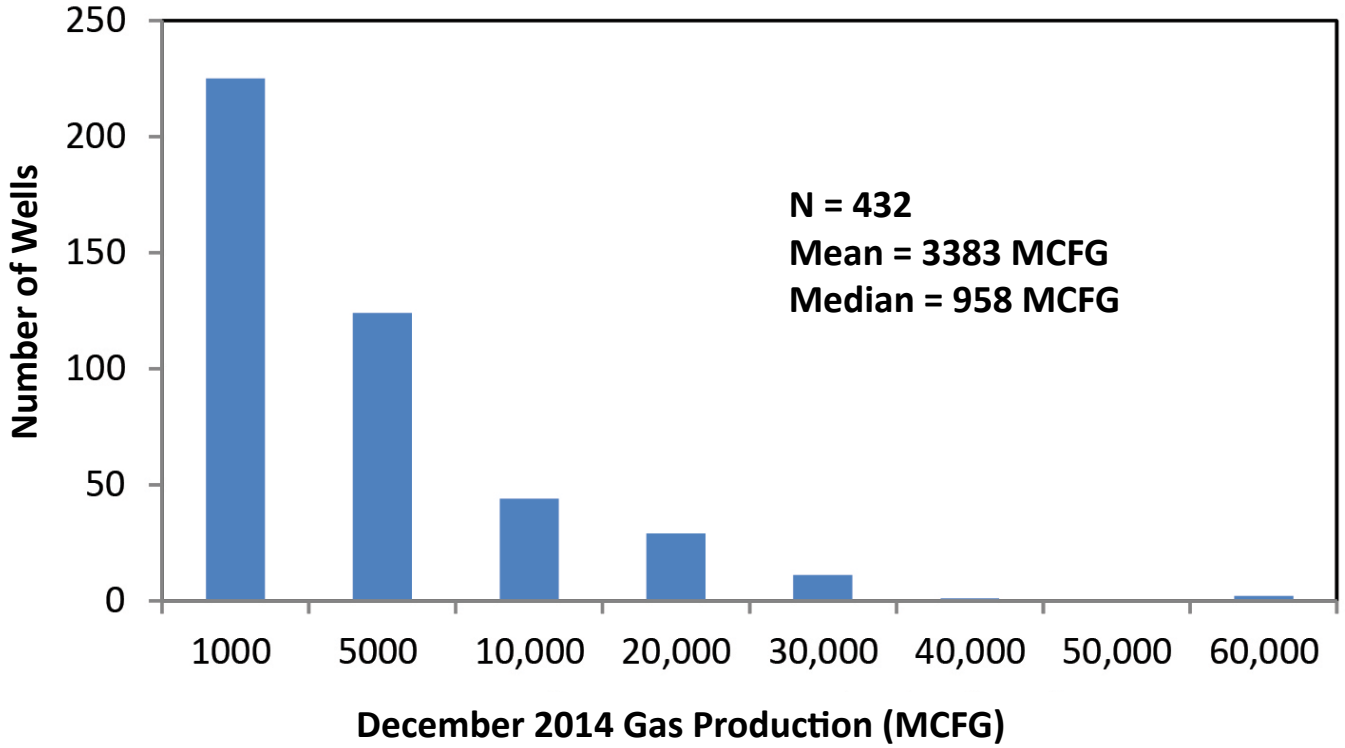

Figure 4.75. *Frequency distribution of gas produced per well from the CMKD reservoir during December 2014. Production ranges from 0 to 59,485 MCFG/well. Many of the wells producing from the CMKD reservoir are commingled with shallower reservoirs such as the Mancos, Mesaverde, and Wasatch. Data from Utah Division of Oil, Gas and Mining (2016d).*

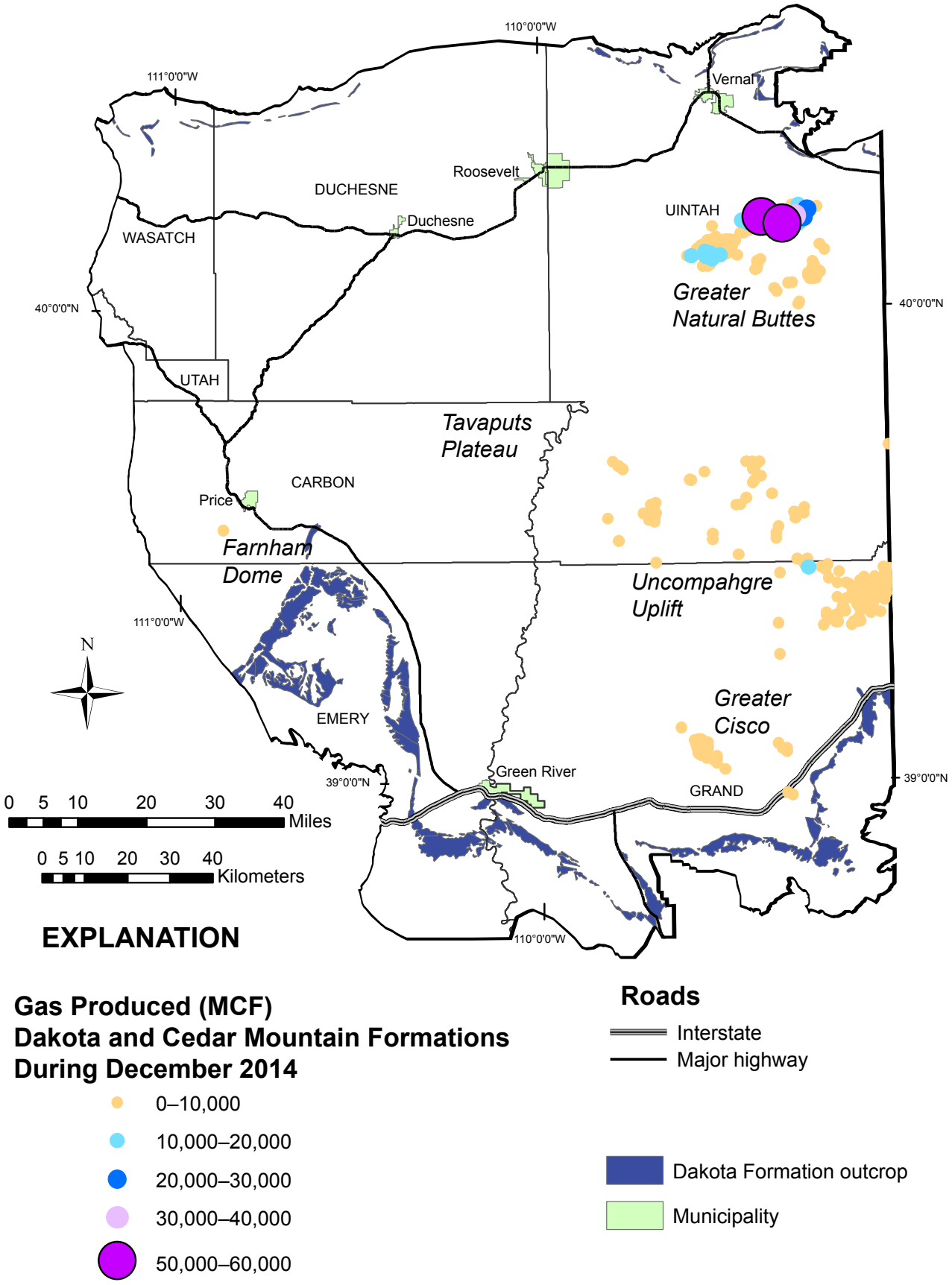

Figure 4.76. *Gas production (MCFG) from the CMKD during the month of December 2014. Many of the wells producing from the CMKD reservoir are commingled with shallower reservoirs such as the Mancos, Mesaverde, and Wasatch. Wells in the north are generally younger and commingled with the Mancos and Mesaverde. Data from Utah Division of Oil, Gas and Mining (2016d).*

CHAPTER 5:
UINTA BASIN RESERVOIRS/AQUIFERS: UPPER CRETACEOUS MANCOS SHALE

by

Robert Ressetar

CONTENTS

INTRODUCTION 129
METHODS 129
UPPER CRETACEOUS MANCOS SHALE 129
Thickness 129
Depth 130
Lithology 130
Reservoir Properties 131
Water Quality 131
Water Production, Use, and Disposal 131
Hydrocarbon Production 134
SUMMARY 136

FIGURES

Figure 5.1. Oil and gas fields in the Uinta Basin with known or potential reservoirs in the Mancos Shale 130
Figure 5.2. Stratigraphic relations of the Mancos Shale, its subunits, and adjacent formations in the Uinta Basin 131
Figure 5.3. Thickness of the Mancos Shale in the Uinta Basin 132
Figure 5.4. Structure at base of the Mancos Shale in the Uinta Basin 132
Figure 5.5. Structure on top of the Mancos B Member in the Uinta Basin 133
Figure 5.6. Average porosities in cores, lower Blue Gate Member, Mancos Shale 133
Figure 5.7. Average permeabilities in cores, lower Blue Gate Member, Mancos Shale 134
Figure 5.8. Stiff diagrams of water samples from the Mancos Shale and adjacent units 136

TABLES

Table 5.1. Water-chemistry data from wells that sampled the Mancos Shale 135
Table 5.2. Water, oil, and natural gas production from the Mancos Shale and adjacent units, 1984–2015 137
Table 5.3. Produced-water disposal wells that inject into the Mancos Shale 137
Table 5.4. Utah gas fields with reservoirs in the Mancos Shale 138

CHAPTER 5:
UINTA BASIN RESERVOIRS/AQUIFERS: UPPER CRETACEOUS MANCOS SHALE

INTRODUCTION

With an average thickness of at least 4000 feet (1200 m), the Upper Cretaceous Mancos Shale is among the thickest sedimentary formations in the Uinta Basin, exceeded only by parts of the Eocene Green River Formation (see Hintze and Kowallis, 2009, p. 202–203). The Mancos also has wide lateral extent, occurring from Arizona and New Mexico northward to Wyoming. Thickness and extent, however, do not imply that the geology of the Mancos is thoroughly understood: although many studies include the Mancos, most focus either on a small part of it or treat it generally in the context of regional investigations. Notable examples of studies of subunits of the Mancos include work on its lower portion by Molenaar and Cobban (1991) and Anderson and Harris (2006), and on its upper portion by Cole and others (1997), Hettinger and Kirschbaum (2003), Gardner and others (2004), and Hampson (2010). These studies provide reasonably detailed correlations of the more heterogeneous parts of the Mancos, where it interfingers with relatively coarse-grained clastic sediments. However, the 2000 to 3000 feet (600–900 m) of the middle Mancos has usually been treated as an undifferentiated marine mudstone (e.g., Johnson, 2003, plate 1).

METHODS

Recently, the Research Partnership to Secure Energy for America (RPSEA) funded the UGS and the University of Utah (UU) to study the hydrocarbon potential of the Mancos in the Uinta Basin and, in part, attempt to fill in some gaps in understanding Mancos geology (Ressetar and Birgenheier, 2015). The results from that project are incorporated into this chapter. The project used digital well logs from approximately 300 oil and gas exploration wells as the principal data source. Correlations using the well logs resulted in the thickness and structural maps presented below, and calculations from the logs provide estimates of water saturation in the Mancos Shale. In addition, the project analyzed Mancos cores from five wells, one from the southwestern Uinta Basin near Price, one from Main Canyon field in the southeastern basin, and three from Natural Buttes and Red Wash fields in the northeastern basin (figure 5.1 and appendix A). Core analysis included sedimentological description, geochemical and mineralogical analyses, and a variety of geomechanical tests.

UPPER CRETACEOUS MANCOS SHALE

The Mancos Shale is a widespread, thick, Upper Cretaceous marine accumulation of largely siliciclastic sediments that were deposited in the Western Interior Seaway of North America. The Mancos consists, for the most part, of sediments that were eroded from the Sevier orogenic belt and transported eastward into a foreland basin. Thus, the Mancos grades westward into more proximal, coarser grained terrigenous sediments, and into more distal, more carbonate-rich equivalents to the east. The carbonate-rich units include, notably, the Niobrara Member (or Formation), which is a significant hydrocarbon producer in Colorado and Kansas.

The Mancos Shale consists of several lower rank stratigraphic units (figure 5.2). In the Uinta Basin of Utah these are, in approximately ascending stratigraphic order, the Tununk Member (figure 2.14), Coon Spring Sandstone Bed ("Dakota Silt"), Juana Lopez Member, Ferron Sandstone Member (figure 2.15), lower part of the Blue Gate Member, Emery Sandstone Member, Mancos B Member, and upper part of the Blue Gate Member. In the western Uinta Basin, the Mancos B and upper Blue Gate Members grade into shallow-marine to terrigenous deposits of the Star Point and Blackhawk Formations. The top of the Mancos B approximately correlates with the top of the Kenilworth Member of the Blackhawk (figure 5.2; Hettinger and Kirschbaum, 2003). The Blackhawk deltaic and shoreface sands prograded over the Mancos and cap the upper Blue Gate. Since several of these lesser units have limited geographic range, a vertical section or a wellbore at any given location is unlikely to encounter all of them.

The U.S. Geological Survey (2009) includes the groundwater-bearing rocks of the Uinta Basin within the Colorado Plateaus aquifers, which largely underlie the Colorado Plateaus Physiographic Province. The Mancos confining unit, which includes most of the Mancos Shale stratigraphic unit, and the Chinle-Moenkopi are the thickest confining units in the Colorado Plateaus aquifers. The Mancos confining unit separates the underlying Dakota–Glen Canyon from the overlying Mesaverde aquifers. Some of the sandier members of the Mancos, particularly the Frontier and Ferron Sandstones (figures 2.12 and 2.15), are locally water producers, but generally the Mancos is a barrier to groundwater flow (U.S. Geological Survey, 2009).

Thickness

The maximum thickness of the Mancos Shale is about 5500 feet (1700 m) in the western Uinta Basin, and it uniformly

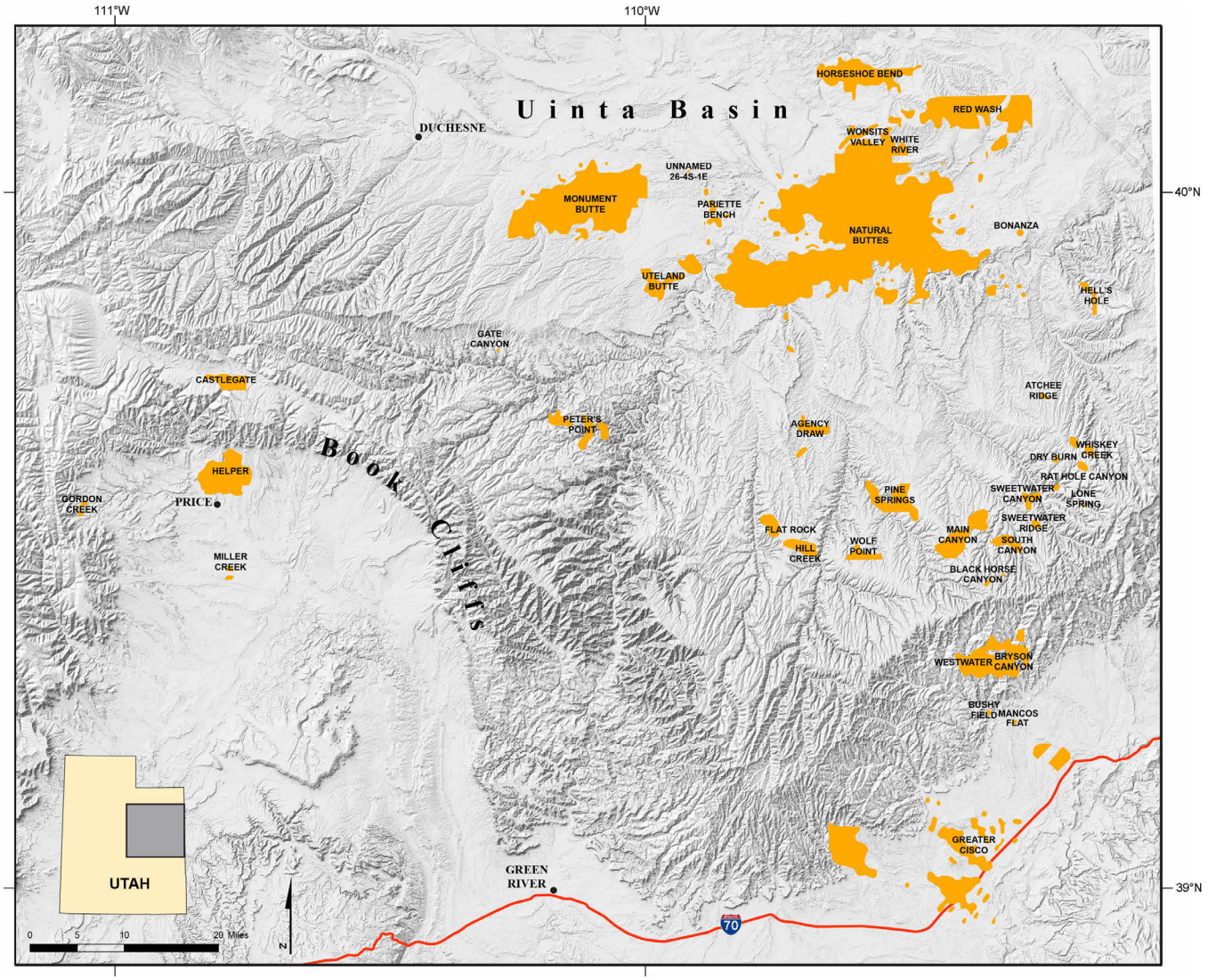

Figure 5.1. *Oil and gas fields in the Uinta Basin identified by the Utah Division of Oil, Gas and Mining with known or potential reservoirs in the Mancos Shale.*

decreases in thickness to about 3400 feet (1040 m) to the southeast (figure 5.3). Note that due to the interfingering relationship between the Mancos Shale and Star Point or Blackhawk Formations, the top of the Mancos is rather arbitrarily defined. The top of the Mancos is time transgressive, becoming younger to the east. For this report the top of the Mancos is placed where normalized gamma-ray logs show a relatively uniform downward pattern of readings greater than 70 API units.

Depth

Structure maps were made for two stratigraphic surfaces: the tops of the Dakota Formation (base of the Mancos Shale) and the Mancos B Member (figures 5.4 and 5.5, respectively). The maps show essentially the same trends of decreasing elevation from the southern margin of the Uinta Basin northward to the deepest part of the basin in northwestern Uintah County. Two northwest-trending structural highs are evident north of the Uintah-Grand County line. Also, a minor northeast-trending high is near the Carbon-Emery County line in the area where the Mancos crops out. This feature is probably related to Farnham dome, a subsidiary structure of the San Rafael Swell, a Laramide uplift that mostly developed from the Late Cretaceous to early Tertiary.

Lithology

In general, the Mancos Shale consists of marine mudstone that grades into significant amounts of shallow-marine to deltaic sandstones in the Ferron and Emery Sandstone Members. In core, the lower Blue Gate Member consists primarily of siltstone with minor amounts of very fine grained sandstone (Horton, 2012). The rocks show a variety of sedimentary structures ranging from planar lamination to ripple cross-lamination and hummocky cross-stratification. In places they contain abundant trace fossils and shell debris; plant debris is comparatively rare. X-ray fluorescence analysis of the cores

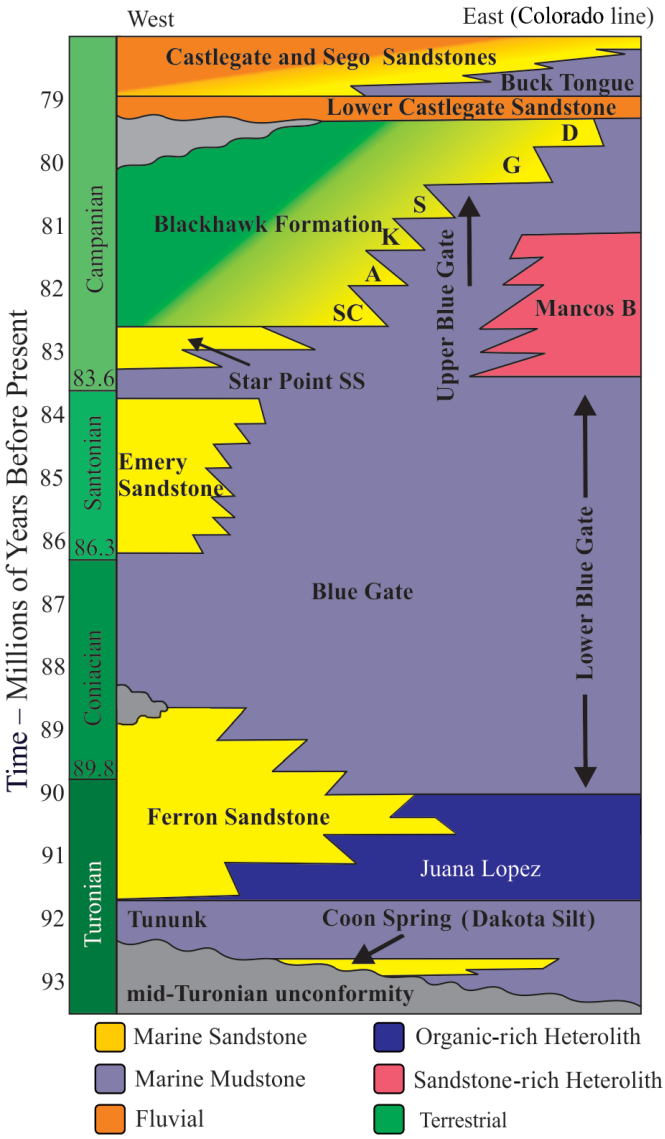

Figure 5.2. *Stratigraphic relations of the Mancos Shale, its subunits, and adjacent formations in the Uinta Basin. Members of the Blackhawk Formation are abbreviated: SC – Spring Canyon, A – Aberdeen, K – Kenilworth, S – Sunnyside, G – Grassy, D – Desert. After Birgenheier and others (2015).*

shows that the lower Blue Gate consists of 40% each clay and non-clay silicate grains, and 20% carbonate grains.

Apart from the western Uinta Basin where the Mancos transitions into nearshore facies, the Mancos contains three relatively coarse-grained units: the Coon Spring Sandstone Bed and the Juana Lopez and Mancos B Members. These consist of heterolithic siltstone- and sandstone-rich bodies that represent gravity-flow deposits (Hampson, 2010) and distal, coarsening-upward equivalents of progradational shoreface sandstone. The sandstone content of the Mancos Shale, based on gamma-ray logs of less than 60 API units, shows that sandstone constitutes less than 1% of the formation except where the Tununk and Blue Gate Members interfinger with the Ferron and Emery Sandstone Members.

Reservoir Properties

Appendix A presents porosity and permeability measurements of the lower Blue Gate Member obtained as part of the UGS-UU project on the five cored wells. The measurements on the Glen Bench and Red Wash wells were contributed by QEP Resources, and the RGU and Main Canyon measurements were made by a commercial laboratory. Average porosities range rather narrowly from 3.5% to 8.7%, and do not appear to vary with depth or geographic location in the Uinta Basin (figure 5.6). Permeabilities vary more widely, but are persistently low: the average permeabilities of the cores range from 0.03 to 164 nanodarcies (nD) (figure 5.7). These variations are at least partly related to burial depth. The samples with the highest permeabilities, from RGU and Main Canyon, are from depths of less than 1000 feet (300 m) and about 7000 feet (2100 m), respectively, whereas the Glen Bench and Red Wash samples are from depths of 9600 to 15,000 feet (2900–4600 m).

Water Quality

Of the more than 3000 groundwater analyses from the Uinta Basin in the UGS files, only five have data that include groundwater from the Mancos Shale. Even these five wells did not sample the Mancos exclusively, but commingled samples from underlying (Dakota) and overlying (Mesaverde and Wasatch) units (table 5.1). Nonetheless, similarities among the five sample groups are consistent enough to provide a general picture of Mancos groundwater quality in the Uinta Basin. The water is mostly briny or saline and has TDS concentrations ranging from 22,000 to 67,000 mg/L. Stiff diagrams (figure 5.8) show the water is predominately a sodium-chloride type with relatively less of the main ionic species.

Stoddard and McLennan (2015) applied standard log analyses to 25 wells in the UGS-UU project and calculated water saturations ranging from 35% to 95%. In general, water saturation increases with depth, and laterally to the north. For a large part of the Mancos Shale—the lower Blue Gate and Mancos B Members—water saturation in the 8000- to 12,000-foot (2400–3700 m) depth range was approximately 80% to 90%. However, at shallower depths for all units of the Mancos the water saturation is typically 35% to 60%. The high-water saturation at depth, combined with the low permeability, likely rules out the deeper parts of the Mancos as a potential target for produced-water disposal.

Water Production, Use, and Disposal

A moderate amount of water has been produced from oil and gas operations in the Mancos Shale. Between 1984 and 2015, a total of more than 422 MMBW was withdrawn from the Mancos (table 5.2). However, sorting this production total by time intervals and by producing unit within the Mancos suggests that the figure is not representative of the Mancos

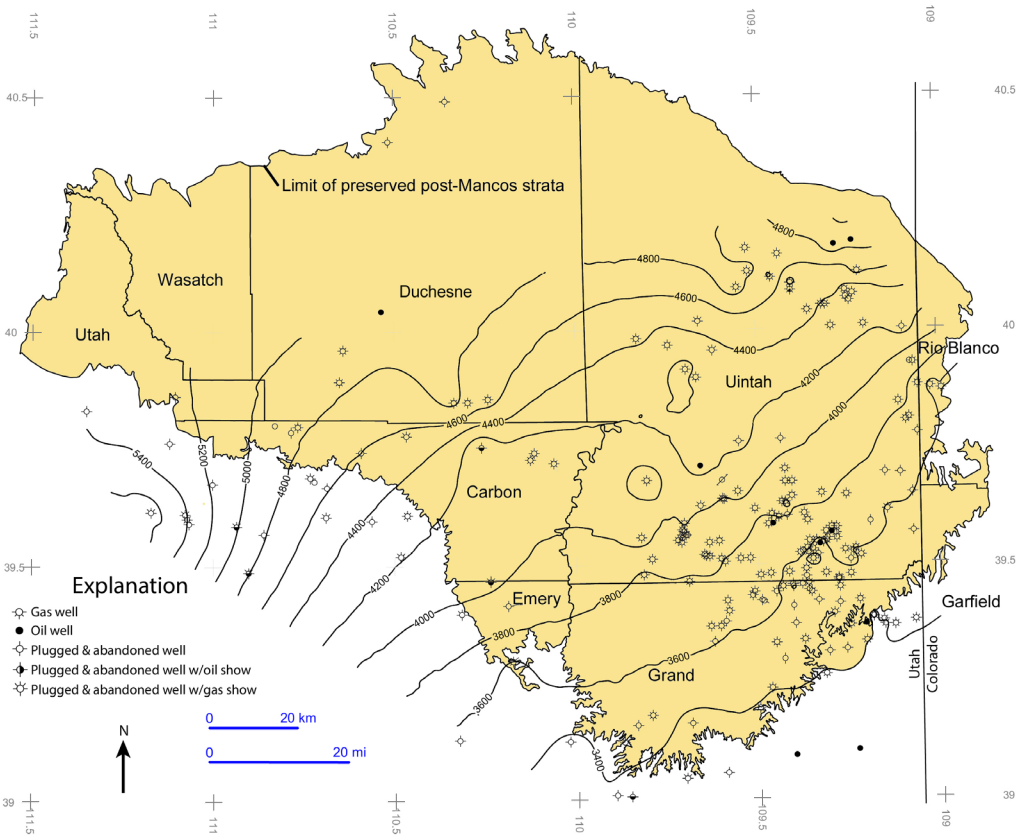

Figure 5.3. Isopach map of the Mancos Shale in the Uinta Basin. Contour interval equals 200 feet. After Ressetar and others (2015).

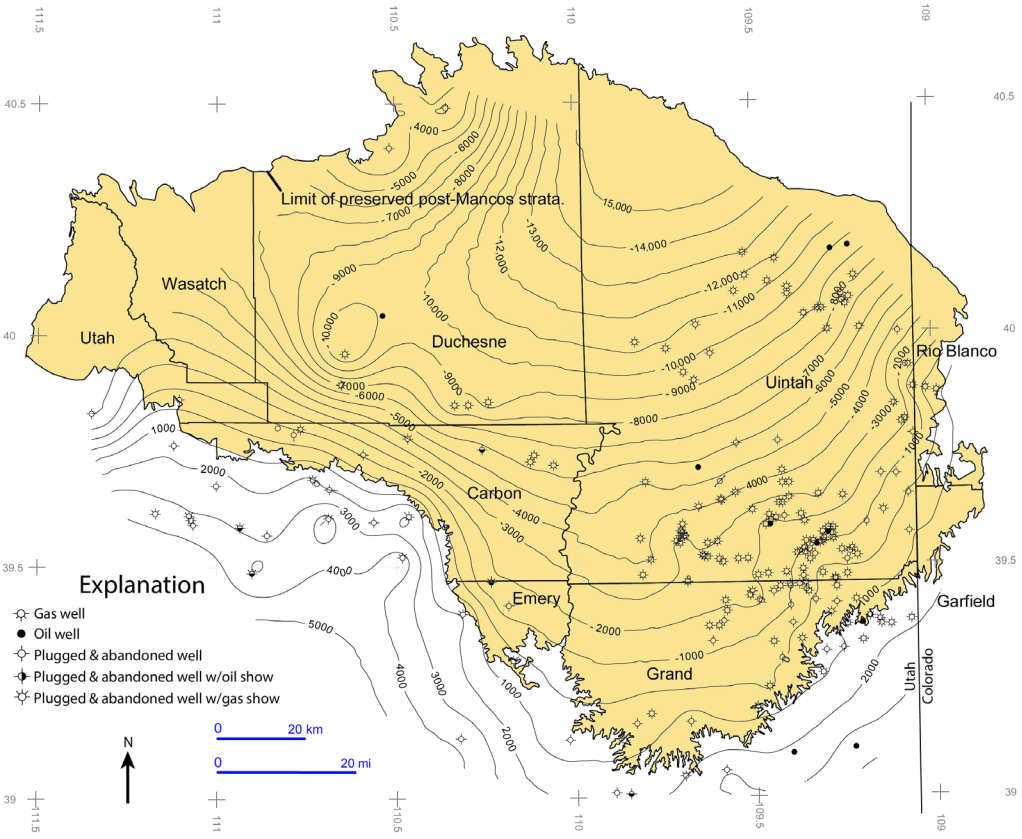

Figure 5.4. *Structural map of the base of the Mancos Shale (top of the Dakota Formation) in the Uinta Basin. Elevations in feet relative to mean sea level, contour interval equals 1000 feet. After Ressetar and others (2015).*

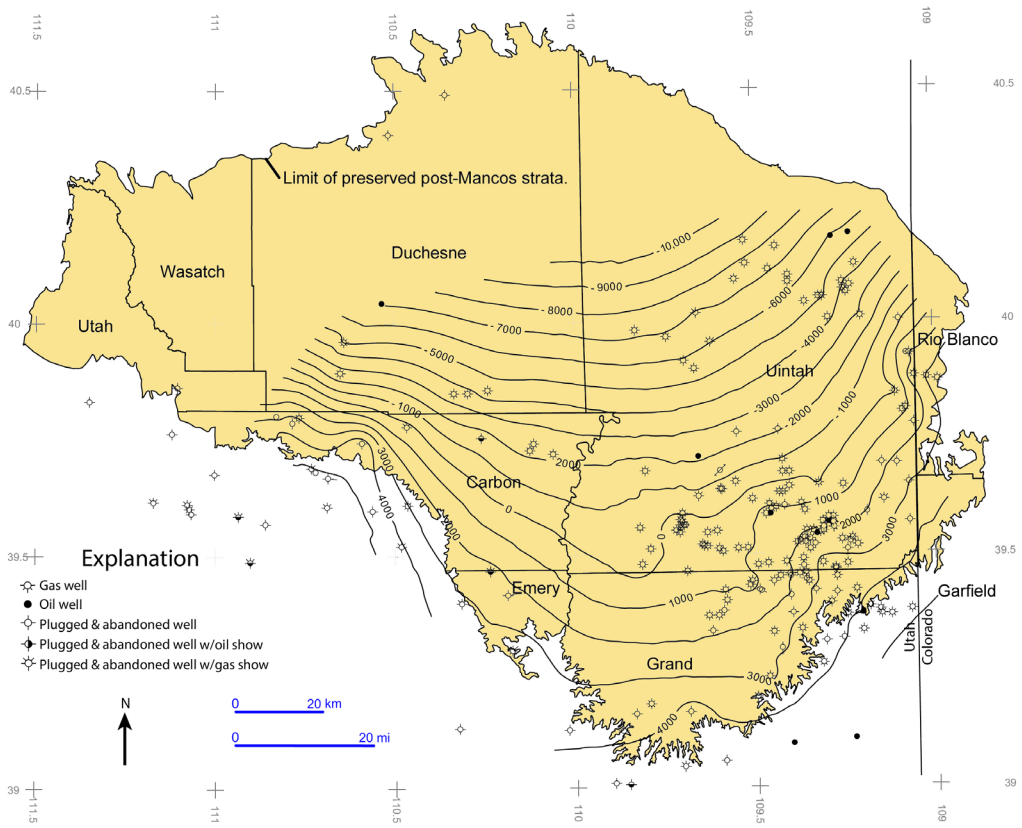

Figure 5.5. *Structural map of the top of the Mancos B Member in the Uinta Basin. Elevations in feet relative to mean sea level, contour interval equals 1000 feet. After Ressetar and others (2015).*

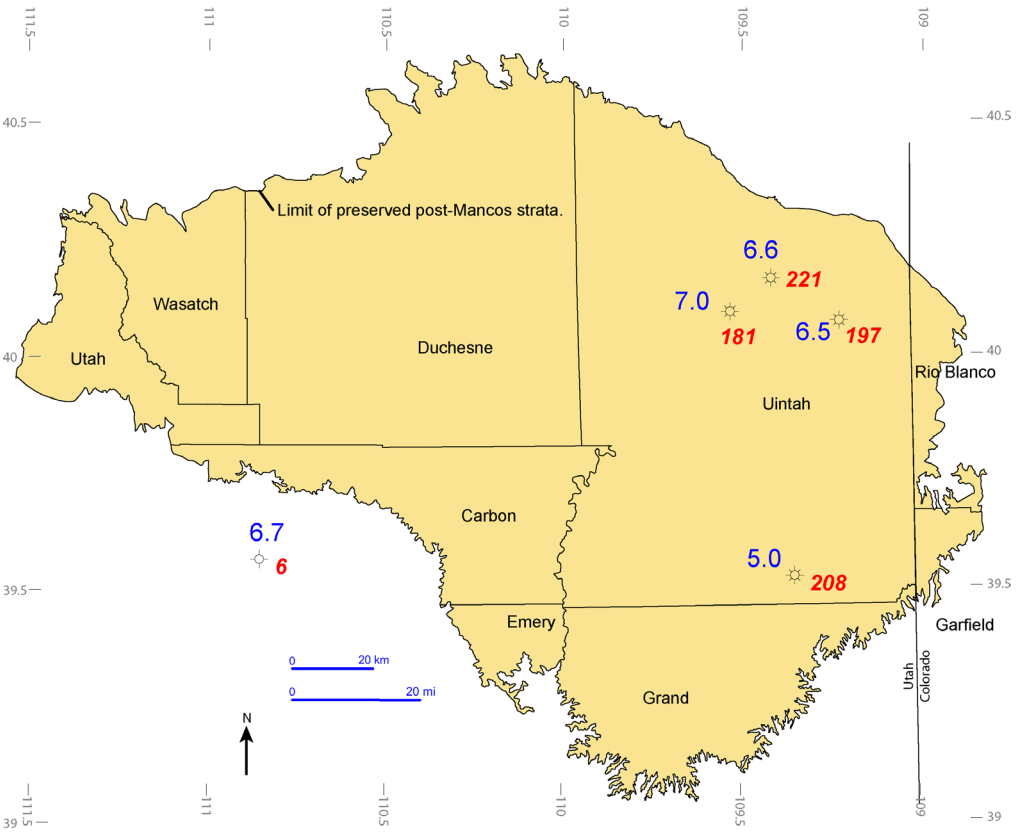

Figure 5.6. *Average porosities (%, blue numbers) in cores from the lower Blue Gate Member of the Mancos Shale. Well numbers (WSNs, red numbers) are assigned by the log analysis software and are linked to well information in appendix A.*

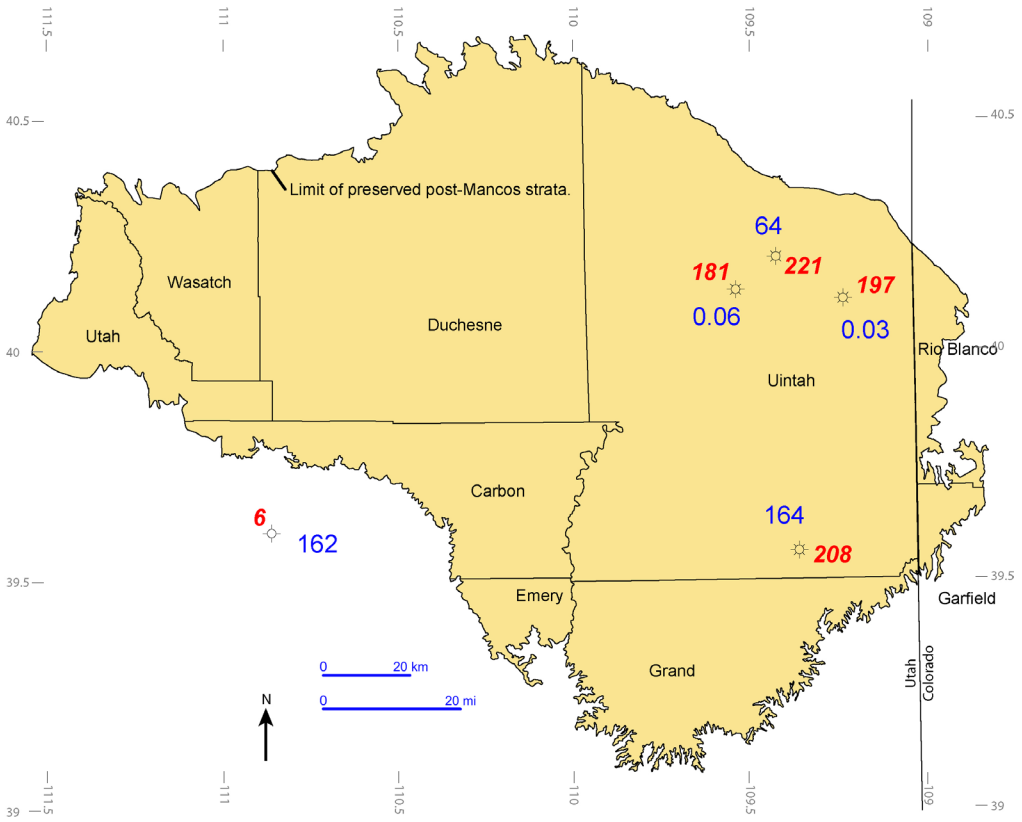

Figure 5.7. *Average permeabilities (nanodarcies, blue numbers) in cores from the lower Blue Gate Member of the Mancos Shale. Well numbers (WSNs, red numbers) are assigned by the log analysis software and are linked to well information in appendix A.*

through the greater part of the Uinta Basin. More than 99% of Mancos water production was from the Ferron Sandstone Member (table 5.2). Between 1984–1991 and 1992–2009, the annual rate of water production from the Ferron increased from 5.7 million barrels (bbls) to 14.5 million bbls. Natural gas production from the Ferron increased by a comparable amount during this period, representing development of the CBM play along the southwest margin of the Uinta Basin.

The Utah Division of Oil, Gas and Mining website lists 89 produced-water disposal wells in the Uinta Basin (broadly defined) as of the end of 2013. Nineteen of the wells, all located in the southwestern corner of the basin, inject water into the Mancos Shale (table 5.3). The Ferron Sandstone Member is the only unit in the Mancos currently used for water disposal, and all but two of the wells are likely disposing water produced by CBM extraction from the Ferron. Apparently, no produced-water disposal into the Mancos is occurring in the main part of the Uinta Basin.

Hydrocarbon Production

Oil production from the Mancos Shale began in 1902, and many shallow wells produced modest amounts of oil and gas from the eastern Uinta Basin (Curtice, 2015). Hydraulic stimulation of deep levels of the Mancos began in 1999 with the Ouray No. 34-79 well (section 34, T. 8 S., R. 21 E., SLB&M, Uintah County, API No. 43-047-33291). This well has been a successful producer but, as is typical, the contribution from the Mancos is commingled with units from the Dakota Formation to the Mesaverde Group. Table 5.2 shows the results of a search of the DOGM production records from the Mancos. As discussed above in the section on water production, hydrocarbon production is dominated by natural gas from the Ferron Sandstone Member since the 1990s. Excluding the Ferron CBM, hydrocarbon production from the Mancos is modest compared to other units in the Uinta Basin. It continues to be a secondary drilling target for shale gas.

The Uinta Basin contains 36 oil and gas fields, mainly in the southeastern part of the basin, identified by DOGM as hosting Mancos production or potential reservoirs (figure 5.1, table 5.4). However, a number of these fields are inactive, and in most of the active fields, Mancos production is commingled with production from lower reservoirs, commonly in the Dakota Formation, or overlying Cretaceous and Tertiary reservoirs, making it difficult to assess Mancos productivity. Only Atchee Ridge and Black Horse Canyon fields are considered to produce exclusively from the Mancos.

As part of the UGS-UU project, Curtice (2015) reviewed production records from 1209 wells drilled since 1998 that had at least one stimulation record in the Mancos Shale. Screening to eliminate those wells that commingled Mancos production left only 26 wells that could be described as “Mancos only.”

Table 5.1. *Water-chemistry data from five wells that sampled intervals including the Mancos Shale.*

API No.	Well Name	UTM Northing	UTM Easting	Depth Top Mesaverde Group (ft)	Depth Top Mancos Shale (ft)	Depth Base Mancos Shale (ft)	Depth Top Sample Interval (ft)	Depth Base Sample Interval (ft)	Date	Total Depth (ft)	Depth BHT (ft)	BHT[2] (°F)	Corrected BHT (°F)	Sample Temp (°F)
43-047-34753	Glen Bench 5M-9-8-22	4444327	631797	8970	~11,700	NR[1]	10,628	13,034	7/18/2005	13,039	–	–	–	–
43-047-36260	Glen Bench 16D-28-8-21	4438654	623438	8765	11,508	16,282	10,454	16,412	5/25/2006	16,490	16,440	305.0	323.0	258.4
43-047-37295	Mustang 1320-11H	4395773	616643	4647	7347	NR[1]	6278	8120	7/25/2007	8376	8366	161.0	170.2	145.5
43-047-37298	Mustang 1320-24E	4392436	617061	–	7366	NR[1]	6796	7780	7/25/2007	8208	8195	159.0	168.0	146.9
43-047-37350	Red Wash 6D-5-9-24	4436686	650013	5678	8341	11,475	4581	12,806	7/19/2007	13,000	12,999	256.0	270.3	187.8

API No.	Well Name	pH	TDS[3] (mg/L)	Water Type	HCO_3 (meq/L)	Ca (meq/L)	Mg (meq/L)	Na (meq/L)	K (meq/L)	Cl (meq/L)	SO_4 (meq/L)	Geologic Units
43-047-34753	Glen Bench 5M-9-8-22	7.7	27,493.6	–	5.2	6.9	6.7	59.0	316.2	363.6	9.7	Mesaverde-Mancos
43-047-36260	Glen Bench 16D-28-8-21	6.6	21,900.0	saline	8.36	38.92	6.17	305.14	12.79	354.69	–	Mesaverde-Mancos-Dakota
43-047-37295	Mustang 1320-11H	7.4	66,928.0	brine	12.14	98.23	22.21	1031.04	6.25	1086.99	35.57	Mesaverde-Mancos
43-047-37298	Mustang 1320-24E	7.3	45,546.0	brine	20.90	55.92	16.22	691.30	23.86	698.96	47.46	Mesaverde-Mancos
43-047-37350	Red Wash 6D-5-9-24	8.5	36,990.0	–	1.09	6.15	2.74	221.69	315.44	541.32	4.04	Wasatch-Mesaverde-Mancos-Dakota

[1] NR = not reached

[2] BHT = bottom hole temperature

[3] TDS = total dissolved solids

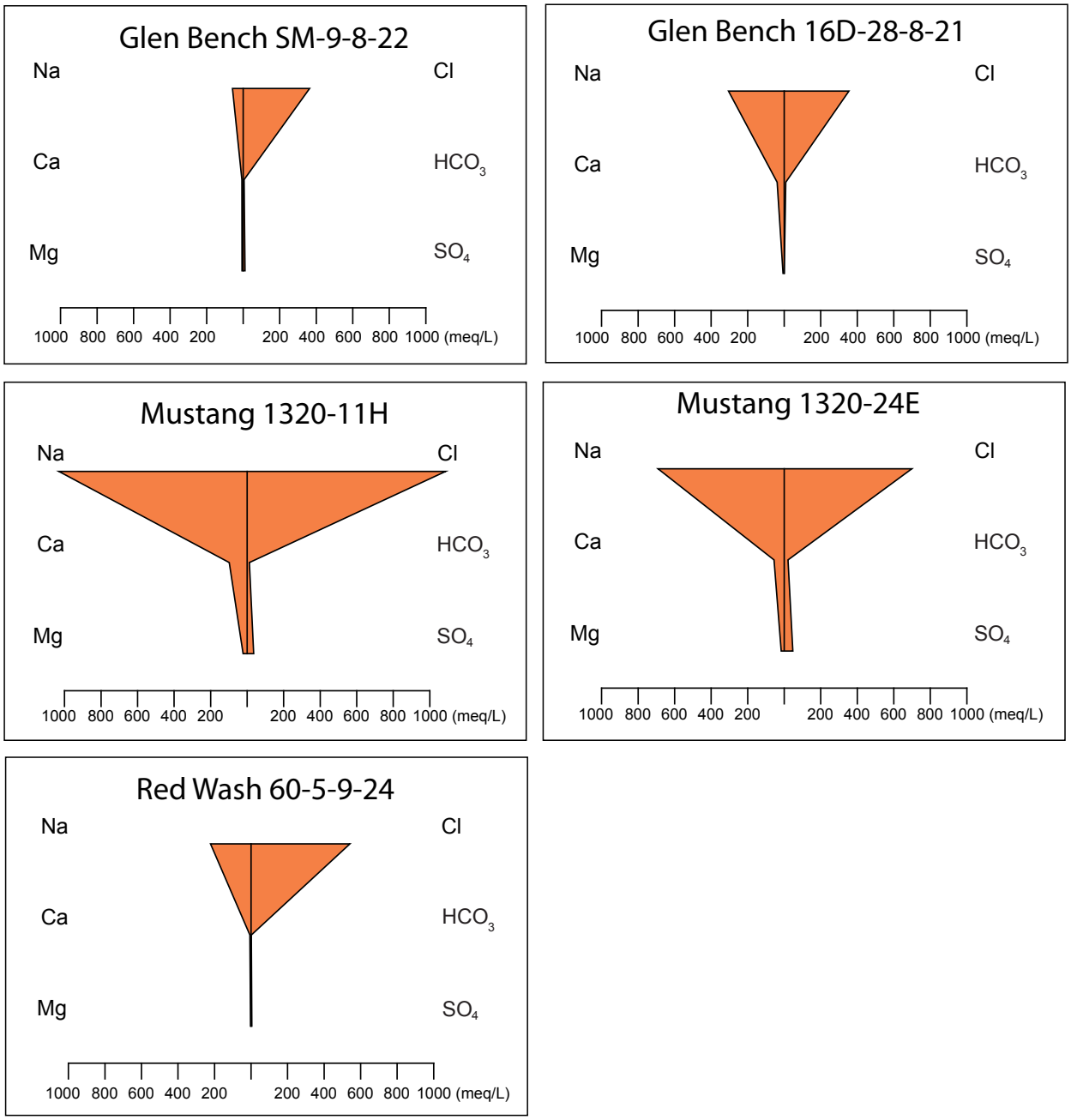

Figure 5.8. *Stiff diagrams of water samples from the Mancos Shale and adjacent units. See table 5.1 for well and chemical data.*

The only horizontal well completed in the Mancos is XTO's HCU No. 1-30F well (section 30, T. 10 S., R. 20 E., SLB&M, Uintah County, API 43-047-40396), drilled in 2010. Although this was the best performer of the "Mancos only" wells, it was not a commercial success.

Recently, Rose Petroleum reported producible oil and gas shows out of the Mancos Shale and visible oil in core from a single science well (State No. 1-34, section 34, T. 21 S., R. 23 E., SLB&M, Grand County, API 43-019-50067, currently shut-in) in the southeastern Uinta Basin, in the Greater Cisco field area, where the lower Blue Gate Member crops out (Rose Petroleum, 2015).

SUMMARY

The Upper Cretaceous Mancos Shale is a widespread, thick, marine accumulation of largely siliciclastic sediments that were eroded from the Sevier orogenic belt and transported eastward into a foreland basin in the Western Interior Seaway. The Mancos is one of the thickest (at least 4000 feet [1200 m]) confining units in the Colorado Plateaus aquifer, separating the Dakota–Glen Canyon and Mesaverde aquifers. It consists of marine mudstone that grades into shallow-marine to deltaic sandstones. The sandstone content of the Mancos constitutes less than 1% of the formation except where the Tununk and Blue Gate Members interfinger with

Table 5.2. *Water, oil, and natural gas production from the Mancos Shale and adjacent units, 1984–2015. Data source: Utah Division of Oil, Gas and Mining production records.*

Producing Formation/Member	Total Oil (Barrels)	Total Gas (MCF*)	Total Water (Barrels)	Average Gas-to-Oil Ratio	Average Oil-to-Water Ratio	Average Gas-to-Water Ratio
2009–2015						
Mancos Shale	43,224	5,165,470	785,220	92,379	0.20	19,033.40
Mancos B	12,862	664,704	5422	24,592	0.84	20,897.35
Ferron Sandstone Member	180	356,669,568	113,973,277	781	0.00	87,376.04
Frontier Sandstone	3368	5,128,480	13,126	443,231	0.24	466,289.96
Tununk Member	1518	2503	14,725	9	0.00	0.94
Tununk-Dakota	0	0	0	0	0.00	0.00
Production totals	61,152	367,630,725	114,791,770	–	–	–
1992–2009						
Mancos Shale	62,059	3,299,530	301,029	128,072.35	0.59	59,043.64
Mancos B	15,091	868,318	17,746	163,517.27	1.07	88,389.93
Ferron Sandstone Member	4162	835,804,971	261,062,072	1,307,742.70	0.00	63,058.43
Frontier Sandstone	14,819	12,668,028	43,385	1,413,230.20	1.30	1,198,778.24
Tununk Member	159	123	0	549.32	–	–
Tununk-Dakota	0	0	0	–	–	–
Production totals	96,290	852,640,970	261,424,232	–	–	–
1984–1991						
Mancos Shale	79,603	148,272	69	0.01	0.00	0.01
Mancos B	41	160,616	0	0.37	0.00	0.00
Ferron Sandstone Member	14,152	98,904,325	45,473,151	19.65	0.01	27.02
Frontier Sandstone	74,286	25,336,697	875,851	414.61	0.84	505.18
Tununk Member	313	425	0	0.27	0.00	0.00
Tununk-Dakota	0	0	0	0.00	0.00	0.00
Production totals	168,395	124,550,335	46,349,071	–	–	–
Combined production totals	**325,837**	**1,344,822,030**	**422,565,073**	–	–	–

*MCF= thousand cubic feet

Table 5.3. *Produced-water disposal wells that inject into the Mancos Shale.*

Field	Type	County	Disposal Unit	Number of Wells
Clear Creek	Gas	Carbon/Emery	Ferron Sandstone	1
Drunkards Wash	Coalbed methane	Carbon/Emery	Ferron Sandstone	11
Helper	Coalbed methane	Carbon	Ferron Sandstone	6
Wildcat	Gas	Unknown	Ferron Sandstone	1

Table 5.4. *Utah gas fields with reservoirs identified in the Mancos Shale. Gas production data from Utah Division of Oil, Gas and Mining (2016c).*

Field Number	Field Name	Status	County	Discovery Date	Producing Stratigraphic Unit			Cumulative Natural Gas Production (MCF*)	Discovery Well API Number
540	Agency Draw	Active	Uintah	1962	Wasatch	Mesaverde	Mancos	1,055,281	43-047-11120
543	Atchee Ridge	Active	Uintah	1996	Mancos B	–	–	144,547	43-047-32660
550	Black Horse Canyon	Active	Uintah	1979	Mancos	–	–	3,745,140	43-047-30765
555	Bonanza	Active	Uintah	1963	Wasatch	Mancos	–	787,288	43-047-15674
185	Bryson Canyon	Active	Grand	1928	Mancos B	Dakota	–	27,092,451	43-019-11306
167	Bushy	Active	Grand	1977	Mancos	Dakota	–	3507	43-019-30361
13	Castlegate	Active	Carbon	1998	Blackhawk	Mancos	–	13,413,584	43-007-30119
580	Dry Burn	Inactive	Uintah	1978	Mancos	–	–	0	43-047-30331
600	Flat Rock	Active	Uintah	1963	Wasatch	Mancos	–	129,156,856	43-047-10577
792	Gate Canyon	Active	Duchesne	2006	Mesaverde	Mancos	–	2,931,442	43-013-32391
20	Gordon Creek	Active	Carbon	1948	Ferron	Mancos	–	6,561,579	43-007-16107
205	Greater Cisco	Active	Grand	1925	Mancos	Dakota	Cedar Mountain	28,166,320	43-019-11513
616	Hells Hole	Active	Uintah	1989	Mancos B	Dakota	Morrison	1,922,665	43-047-31802
18	Helper	Active	Carbon	1993	Ferron	Mancos	–	209,266,618	43-007-30189
617	Hill Creek	Active	Uintah	1984	Wasatch	Mesaverde	Mancos	27,442,613	43-047-31026
620	Horseshoe Bend	Active	Uintah	1984	Green River	Mesaverde	Mancos	29,314,812	43-047-15803
626	Lone Spring	Inactive	Uintah	1996	Mancos B	–	–	0	43-047-32705
625	Main Canyon	Active	Uintah	1979	Mancos	Dakota	–	6,268,700	43-047-30394
222	Mancos Flat	Inactive	Grand	1981	Mancos	–	–	0	43-019-30789
30	Miller Creek	Inactive	Carbon	1969	Ferron	Tununk	Dakota	0	43-007-30006
105	Monument Butte	Active	Duchesne	1964	Green River	Mesaverde	Mancos	140,221,004	43-013-30561
630	Natural Buttes	Active	Uintah	1972	Mesaverde	Wasatch	Mancos	3,524,490,273	43-047-10095
640	Pariette Bench	Active	Uintah	1962	Green River	Mesaverde	Mancos	54,130,213	43-047-10873
40	Peters Point	Active	Carbon	1953	Green River	Wasatch	Mancos	181,416,062	43-007-10216
645	Pine Springs	Active	Uintah	1979	Mancos B	Dakota	–	5,317,727	43-047-15923
660	Rat Hole Canyon	Inactive	Uintah	1977	Mancos	–	–	0	43-047-30325
665	Red Wash	Active	Uintah	1951	Green River	Mesaverde	Mancos	415,946,337	43-047-15135
636	South Canyon	Inactive	Uintah	1981	Mancos B	–	–	0	43-047-31104
685	Sweetwater Canyon	Inactive	Uintah	1978	Mancos	–	–	57	43-047-30332
686	Sweetwater Ridge	Inactive	Uintah	1996	Mancos B	–	–	0	43-047-32593
695	Uteland Butte	Active	Uintah	1962	Wasatch	Mesaverde	Mancos	10,880,866	43-047-15642
265	Westwater	Active	Grand	1957	Mancos B	Dakota	–	39,561,837	43-019-10780
717	Whiskey Creek	Inactive	Uintah	1996	Mancos B	–	–	0	43-047-32602
705	White River	Active	Uintah	1961	Green River	Mancos B	–	15,439,979	43-047-15080
707	Wolf Point	Active	Uintah	1984	Mancos	Dakota	Morrison	1,524,211	43-047-30622
710	Wonsits Valley	Active	Uintah	1959	Green River	Mesaverde	Mancos	137,611,054	43-047-16509

*MCF = thousand cubic feet

the Ferron and Emery Sandstone Members. Structure maps show decreasing elevation from the southern margin of the Uinta Basin northward to the deepest part of the basin in northwestern Uintah County. Porosities range from 3.5% to 8.7%, whereas permeabilities vary more widely, but are persistently low (0.03 to 164 nD). Although data are very sparse, groundwater in the Mancos appears to be saline to briny, dominated by sodium and chloride.

The only produced-water disposal into the Mancos Shale seems to be local injection of water from CBM operations in the Ferron Sandstone Member on the southwestern margin of the Uinta Basin. Many shallow wells have produced modest amounts of oil and gas from the Mancos in the eastern Uinta Basin; however, this production is usually commingled with production from other reservoirs. The Mancos continues to be a secondary drilling target for shale gas. A moderate amount of water has been produced from the Mancos in comparison to the major reservoirs in the basin such as the Upper Cretaceous Mesaverde Group and Tertiary Wasatch and Green River Formations discussed in subsequent chapters. With very low permeability the Mancos is likely a poor candidate for produced-water disposal in most of the Uinta Basin.

CHAPTER 6:
UINTA BASIN RESERVOIRS/AQUIFERS: UPPER CRETACEOUS MESAVERDE GROUP AND UPPER PALEOCENE TO LOWER EOCENE WASATCH/COLTON FORMATION

by

Peter J Nielsen and Rebekah W. Stimpson

CONTENTS

INTRODUCTION 145
METHODS 145
UPPER CRETACEOUS MESAVERDE GROUP 151
Thickness 151
Depth 151
Lithology 151
Reservoir Properties 157
Water Quality 166
Water Production, Use, and Disposal 167
Hydrocarbon Production 167
UPPER PALEOCENE TO LOWER EOCENE WASATCH/COLTON FORMATION 168
Thickness 170
Depth 174
Lithology 175
Reservoir Properties 176
Water Quality 179
Water Production, Use, and Disposal 181
Hydrocarbon Production 184
SUMMARY 184

FIGURES

Figure 6.1. Paleogeography during Late Cretaceous through early Eocene 146
Figure 6.2. Index map of geology and chemistry data sources from the Wasatch/Colton Formation and Mesaverde Group 147
Figure 6.3. Gamma-ray trend across the Uinta Basin based on normalizing GR curves 148
Figure 6.4. Thickness of the entire Mesaverde Group 152
Figure 6.5. Structure of the top of the Mesaverde Group 153
Figure 6.6. Mesaverde Group, Book Cliffs 154
Figure 6.7. Representative outcrops of Blackhawk, Castlegate, and Price River Formations 154
Figure 6.8. Schematic block diagram of a braided-stream environment of the Castlegate Sandstone 155
Figure 6.9. Thickness of the lower Castlegate Sandstone 156
Figure 6.10. Castlegate Sandstone overlying the Desert Member of the Blackhawk Formation and the Mancos Shale 157
Figure 6.11. Thickness of the Bluecastle Sandstone Member of the Castlegate Sandstone 158
Figure 6.12. Typical outcrops of the Farrer and Tuscher Formations 159
Figure 6.13. Outcrops of the Mesaverde Group in Sego Canyon 160
Figure 6.14. Thickness of the Buck Tongue of the Mancos Shale 161
Figure 6.15. Combined thickness of the middle Castlegate, Sego, and Neslen Formations 162
Figure 6.16. Combined thickness of the Price River, Tuscher, and Farrer Formations 163
Figure 6.17. Outcrops of Buck Tongue of the Mancos Shale, Sego Sandstone, and coal-bearing Neslen Formation 164
Figure 6.18. Net to gross ratio of sands within the Mesaverde Group 165
Figure 6.19. Calculated TDS concentration with depth in the Mesaverde Group 168
Figure 6.20. TDS map of the Mesaverde Group 169
Figure 6.21. Stiff diagrams from water samples sourced from the Mesaverde Group 170
Figure 6.22. Calcium/sodium ratio map for Mesaverde Group water 171
Figure 6.23. Cumulative water production from Mesaverde Group and/or the Wasatch/Colton Formation gas reservoirs 172
Figure 6.24. Locations and volumes for water-disposal wells into Mesaverde Group and Wasatch/Colton Formation 173
Figure 6.25. Cumulative natural gas production from Mesaverde Group and/or Wasatch/Colton Formation reservoirs 174
Figure 6.26. Cumulative crude oil production from Mesaverde Group and/or Wasatch/Colton Formation reservoirs 175
Figure 6.27. Thickness of the Wasatch/Colton Formation 177
Figure 6.28. Structure of the top of the Wasatch/Colton combined formations 178
Figure 6.29. Representative outcrops of the Wasatch/Colton Formation 179
Figure 6.30. Net to gross ratio of sands within the Wasatch/Colton Formation. 180
Figure 6.31. Calculated TDS concentration with depth in the Wasatch/Colton Formation 181

Figure 6.32. TDS of the Wasatch/Colton Formation 182
Figure 6.33. Calcium/sodium ratio for the Wasatch/Colton Formation water 183
Figure 6.34. Well log for NBU No. 921-21L well, Natural Buttes field 185

TABLES

Table 6.1. Reservoir properties of the Wasatch/Colton Formation and Mesaverde Group 164
Table 6.2. Porosity values from sonic logs within the Mesaverde Group 166
Table 6.3. Porosity and permeability from the NBU No. 253 core, Natural Buttes field 166
Table 6.4. Porosity and permeability from the NBU No. 921-21L core, Natural Buttes field 167
Table 6.5. Water classification based on TDS 170
Table 6.6. Cumulative production from the Wasatch/Colton Formation and the Mesaverde Group 172
Table 6.7. Total oil, gas, and produced water between January 2009 and March 2015 for producing zones in the Wasatch/Colton Formation and Mesaverde Group 176
Table 6.8. Porosity values from sonic logs within the Wasatch/Colton Formation 180
Table 6.9. Calculated volume of water storage per radial foot in three Tuscher Formation channel sandstones, NBU No. 921-12L gas well, Natural Buttes field 186

CHAPTER 6:
UINTA BASIN RESERVOIRS/AQUIFERS: UPPER CRETACEOUS MESAVERDE GROUP AND UPPER PALEOCENE TO LOWER EOCENE WASATCH/COLTON FORMATION

INTRODUCTION

This chapter focuses on the Upper Cretaceous Mesaverde Group and the upper Paleocene to lower Eocene Wasatch/Colton Formation deposited within the Uinta Basin in fluvial, coastal-plain, swamp, delta, and marine environments (figure 6.1). Both the Mesaverde Group and the Wasatch/Colton Formation are reservoirs for oil and gas, but predominantly natural gas trapped in tight-gas sandstones (Nelson and Hoffman, 2009), which are compartmentalized fluvial channels with low permeability.

Significant saline water is often associated with the hydrocarbon production from these formations, requiring a produced-water disposal solution—the primary overall objective of this study. The produced water is typically very poor quality and unfit for beneficial use (unless treated). The current optimal strategy for dealing with produced water is to reinject it into underground reservoirs. This chapter provides an analysis of the current water quality, as well as potential disposal reservoirs, of the Mesaverde Group and the Wasatch/Colton Formation, in addition to the general stratigraphy, thickness, depth, reservoir properties, porosity and permeability, and hydrocarbon production.

METHODS

Because of the importance of the Mesaverde Group and Wasatch/Colton Formation in oil and gas production in the Uinta Basin, a higher level of scrutiny than other units in this study is justified to better understand geologic characteristics of these reservoirs across the basin. Understanding the fluid flow in, and geochemistry of, the strata and their petrophysical and petrographic properties in detail, allows modeling to predict (1) rock-water interactions, (2) water chemistry and content in the reservoirs, and (3) where produced water can be safely and inexpensively injected.

Data for this project came from subsurface well data and outcrops (figure 6.2). There are approximately 22,000 wells within the Uinta Basin that can be used for subsurface analysis. We selected 59 wells from Anderson's (2005) study of hydrocarbon potential of the Mesaverde Group in the southeastern Uinta Basin. The database from that study consisted of tops for the Wasatch/Colton and Mesaverde Group formations. We also used raster gamma logs and a few formation resistivity logs from 55 wells to identify the formation tops. For our more regional study, we expanded our search to find additional wells that penetrated the Wasatch/Colton Formation and Mesaverde Group, as well as those that had a full suite of raster log images or digital log files. Many wells penetrated to depths below the lower Castlegate Sandstone and into the Blackhawk Formation and Mancos Shale, but logging was often incomplete or the images were poor quality. Nonetheless, we identified an additional 55 wells that were distributed throughout the Uinta Basin study area and had usable and legible well logs through the formations of interest (appendix B). We have assembled data and logs from 114 wells for this study.

Gamma-ray (GR) logs were available for nearly all the wells selected for this study. Most wells had a series of sonic and resistivity logs and approximately one-third had density and porosity logs. We digitized approximately 50 GR, sonic (DT), spontaneous potential (SP), and resistivity (RES) logs for use in this study.

Formation tops and lithology can be identified from the general curve trends; however, calculating rock properties from the GR and SP curves requires the curves to be normalized. Errors are often introduced into GR and SP curves because of scale problems, different hardware configurations between companies, and different calibrations between downhole runs with different logging tools. Several studies indicate that over 90% of GR and SP logs require some sort of normalization while DT and RES logs only require occasional normalization (Shier, 2004; Robert Cluff, Discovery Group, written communication, 2014). The GR curves should be normalized to calculate accurate shale volume (V_{sh}) and net-to-gross ratios (NGR) for the different formations.

We prepared several west-to-east and north-to-south GR and SP well-log cross sections through the Uinta Basin to evaluate curve anomalies between wells in the same formations. The sections consisted of 25 to 30 closely spaced wells showing unprocessed GR or SP curves. The large number of distributed well logs allows identification of anomalous curves, shifted curves, and other scale problems (Robert Cluff, Discovery Group, written communication, 2014). The most frequent observed problem with the GR curves is different instrument response between various logging companies. Unprocessed GR

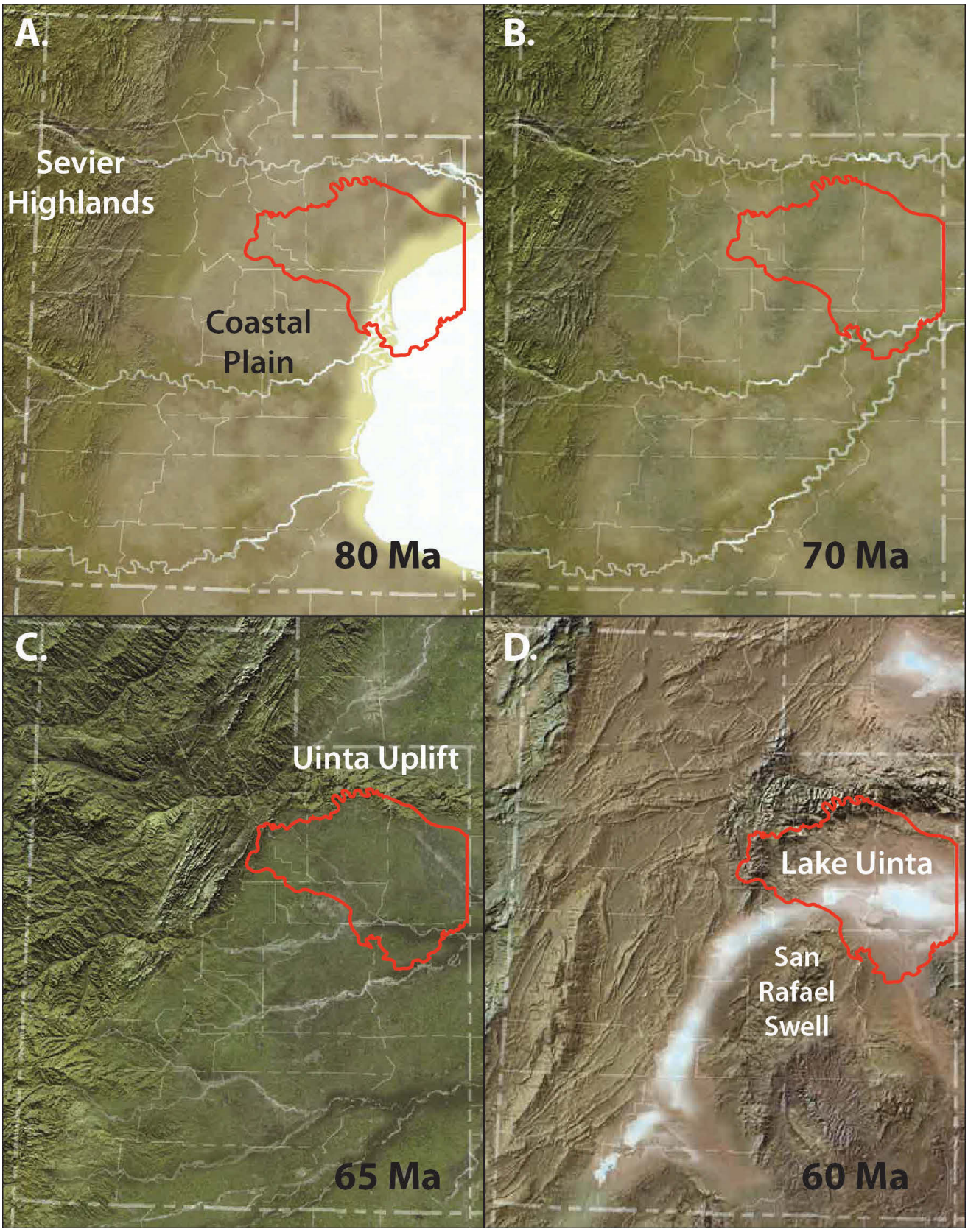

Figure 6.1. *Paleogeographic maps show the Sevier highlands west of the Uinta Basin area (shown in red), and Laramide uplifts including the Uinta Mountains and San Rafael Swell. The final eastward regression of the Mancos Sea (part of the Cretaceous Western Interior Seaway) is shown in A and B. Rivers flowed across the coastal and alluvial plain from the Sevier highlands, north from the distant Mojave region, and south from the Uinta uplift during deposition of the formations discussed in this chapter (C and D). Figures modified from Blakey and Ranney (2008).*

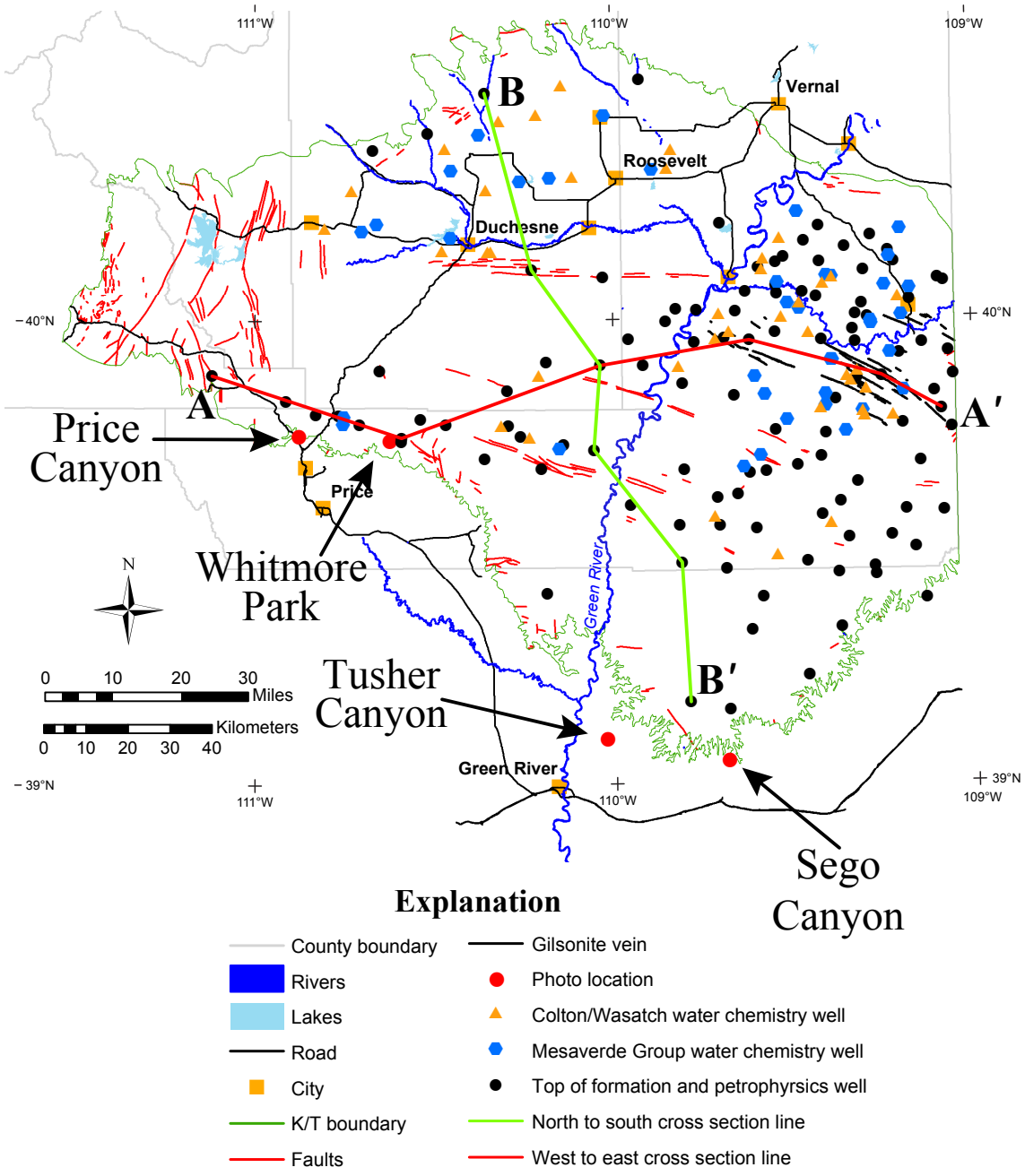

Figure 6.2. *Index map of the study area, indicating the different types of data for geology, water chemistry, and cross-section construction (plates 2 and 3).*

curves generally have similar formation responses and trends, meaning that one can pick formation tops and general lithology. However, if one compares similar shale or sandstone intervals logged with different equipment, one can see the equipment response or scale is different. The combination of downhole logging sensors and surface processing equipment is generally considered unique to that combination of equipment. Normalizing should remove instrument response peculiarities and enhance the formation response. Normalizing GR curves involves determining what a clean sand and shale response should be for a particular area or zone and then normalizing all GR curves in that defined area to that calibrated gamma ray number (GAPI) response range.

We calculated the mean GR and standard deviation for the Wasatch/Colton Formation and Mesaverde Group for each of the 50 selected wells. We also prepared a trend surface using the mean GR for the Mesaverde and Wasatch/Colton (figure 6.3). The shale content of both units increases from west to east matching the observed stratigraphy. A standard normalization of the GR curves would shift the data so that those on the western side of the basin would become siltier than they should be, and GR curves on the eastern part would become sandier. We divided the study area into three areas reflecting the eastward-increasing shale trend, and identified a type well in each area that represents each area's regional curve response (Shier, 2004). The three north-south demarcated zones

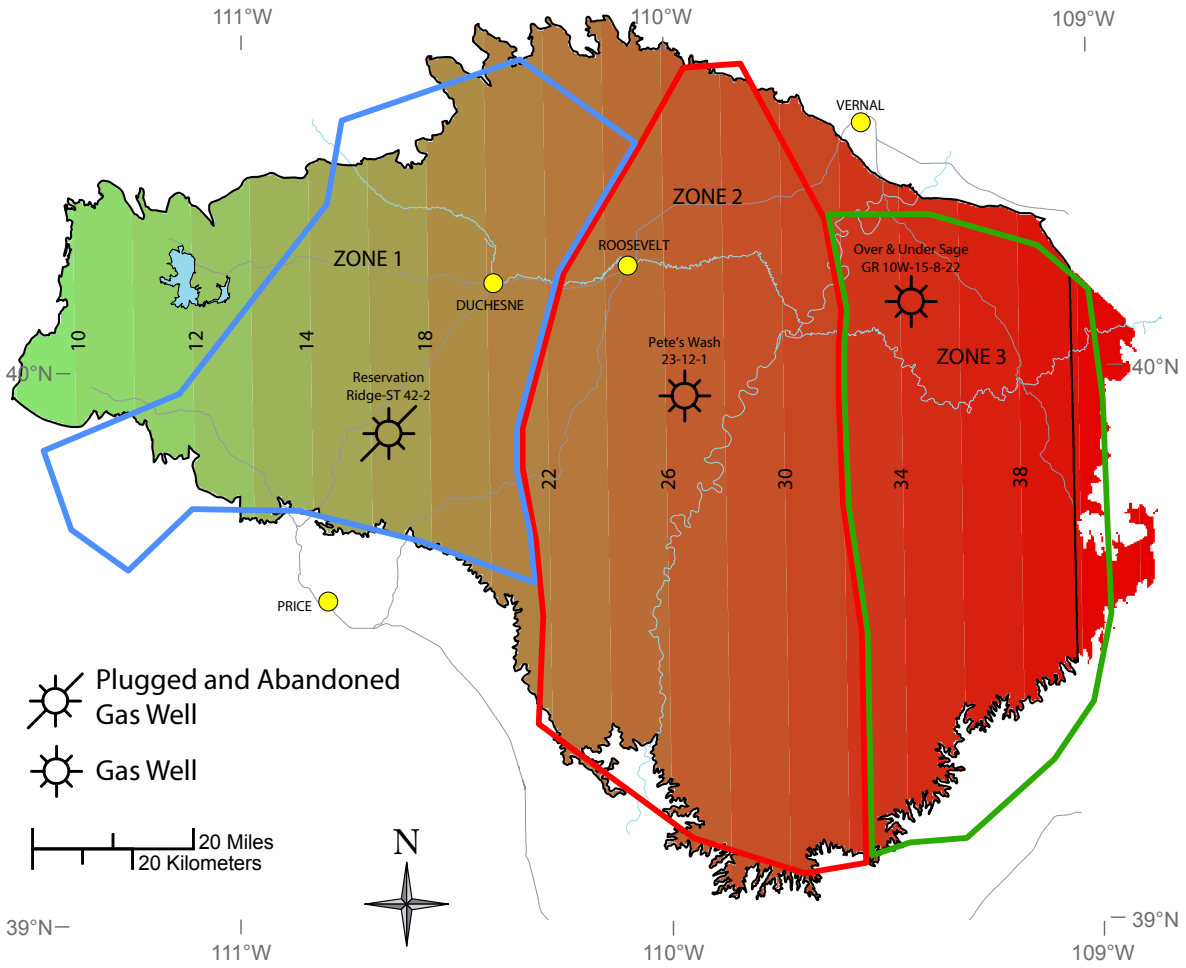

Figure 6.3. *Trend surface of mean GR across the Uinta Basin based on normalized GR from 116 well curves in this study. Three type wells have been identified representing the regional change in mean GR from west to east. Each type well and its associated zone will be the regional representation for normalizing well logs in that zone.*

dividing the basin are as follows: Zone 1 is the western third of the basin, Zone 2 is the central third, and Zone 3 is the eastern third. The method selected for GR logs in the study was to normalize high and low GR curve responses to the high and low regional type well curve GR responses. The type wells selected were Reservation Ridge State No. 42-2 (section 2, T. 11 S., R. 11 E., SLB&M, Duchesne County, API No. 43-013-33758) for Zone 1, Pete's Wash No. 23-12-1 (section 12, T. 10 S., R. 17 E., SLB&M, Uintah County, API No. 43-047-34286) for Zone 2, and Over-Under Sage GR No. 10W-15-8-22 (section 15, T. 8 S., R. 22 E., SLB&M, Uintah County, API No. 43-047-34719) for Zone 3. Each type well log penetrates both the Wasatch/Colton and the Mesaverde. The GR curves for the type wells were normalized using representative shale (highest) and sand (lowest) parts of the curve and the 10th and 90th percentile values from the curve. This essentially stretches the curves to match the expected response that a shale horizon and a sand body should have in each zone. After the GR curves were normalized for the type wells, the high and low GR parts of the curve were selected and used for the regional high and low for the remaining wells in each individual zone. GR histograms were generated and the GR high and low picks were made for each well. Each well within a zone was normalized to the zone type well with the regional patterns (Robert Cluff, Discovery Group, written communication, 2014). Below is the standard, regional equation for normalization used to prepare a normalized GR curve for each well (Shier, 2004):

$$V_{norm} = R_{min} + \frac{(R_{max} - R_{min})\,(V_{log} - W_{min})}{(W_{max} - W_{min})} \qquad (6.1)$$

where:

V_{norm} = new normalized curve value,

R_{min} = regional curve minimum (lowest picked value from type well),

R_{max} = regional curve maximum (highest picked value from type well),

V_{log} = curve value,

W_{min} = well curve minimum (lowest picked value from well), and

W_{max} = well curve maximum (highest picked value from well).

SP curves typically show good negative or positive trends but require scale shifts to be removed from the curve. The raster well logs were reviewed for each well and any shifts in the curve were noted. Individual sections of each curve were shifted by depth. SP curve histograms were prepared and the shale baseline and static spontaneous potential (SSP) were selected for each well. The shale baseline is observed in shaly zones in the wells and the value selected for the water resistivity (R_w) calculation (Rider and Kennedy, 2011). The expected SP response would be a more negative SP with increasing depth, indicating that the salinity of the deeper formation water is greater than the drilling mud. A positive SP trend in the curve indicates that the formation water has a lower salinity than the drilling mud. A review of SP curves throughout the basin showed SP curves in the middle of the basin generally show a negative shift, and SP curves around the margins have zones of positive SP shift suggesting zones of less saline water. Several positive SP shifts were identified and associated with sandy intervals, possibly indicating lower salinity or the presence of hydrocarbons. These lower salinity zones were distributed throughout the Mesaverde Group interval and may be related to recharge areas or conduits.

Shale volume curves were calculated using both the normalized GR curves and the corrected SP curves. V_{sh} indicates how the formation responds to electrical current and will impact the water saturation and bound volume of water calculations. Clay minerals in rocks lower the matrix resistivity because they conduct electrical current between their layers (Tiab and Donaldson, 2011). V_{sh} from GR curves are calculated using the GR index and the Larionov nonlinear equation for rocks older than Tertiary (Asquith and Krygowski, 2004). The GR index equation is:

$$I_{gr} = \frac{(GR_{log} - GR_{min})}{(GR_{max} - GR_{min})} \quad (6.2)$$

The nonlinear Larionov equation is:

$$V_{sh} = 0.33 * (2^{2*I_{gr}} - 1) \quad (6.3)$$

where:

I_{gr} = gamma ray index,
GR_{log} = formation gamma-ray reading,
GR_{min} = minimum gamma ray or clean sand gamma ray,
GR_{max} = maximum gamma ray or clean sand gamma ray, and
V_{sh} = volume of shale in formation as a fraction.

V_{sh} curves calculated from the SP tend to be more optimistic or show lower shale volumes than those calculated using GR curves because the SP relationship is a linear equation and clay minerals in shale can lower the formation resistivity, thereby shifting the shale baseline more negative. The equation for V_{sh} from the SP curve is:

$$V_{sh} = 1 - \frac{PSP}{SSP} \quad (6.4)$$

where:

V_{sh} = volume of shale in formation as a fraction,
PSP = pseudo-static spontaneous potential or the SP reading in a shaly zone, and
SSP = static spontaneous potential or maximum value in a clean sand zone.

The calculation of water saturation (S_w) and the bulk volume of water (BVW) for a formation requires knowing the resistivity of formation water and the porosity. Two methods were used to calculate the formation water resistivity: (1) calculation of TDS, NaCl equivalent concentration, and water salinity using several water analyses from the Wasatch/Colton interval and the Mesaverde Group; and (2) calculation of R_w from SP readings using resistivity of the borehole mud cake and formation temperatures.

The cations, anions, and TDS values are presented in appendix C. There is some uncertainty regarding the exact depth of the samples collected, and some of the samples represent mixed water from several perforated intervals. We reviewed the water chemistry database extensively and believe that we have used the best and most representative samples for the various formations. Three equations were used to estimate water resistivity using laboratory analyses and essentially convert measured components into NaCl equivalent solutions. The three equations and multipliers, found in Schlumberger (2009) and Tiab and Donaldson (2011), are:

$$C_{sp} = \Sigma_{i=1}^{n} M_i * C_{sii} \quad (6.5)$$

$$R_w 75 = \frac{1}{2.74 * 10^{-4 * Csp^{0.9555}}} + 0.0123 \quad (6.6)$$

and the Arps equation (Djebbar and Donaldson, 2012):

$$R_w FT = R_w 75 * \frac{75 + 6.77}{FT + 6.77} \quad (6.7)$$

where:

M_i = weighting multiplier for each component at a concentration range,
C_{sii} = concentration of each ion in parts per million (ppm) or mg/L,
n = number of ions,
C_{sp} = equivalent NaCl concentration,

R_w75 = resistivity of equivalent NaCl concentration at 75°F,

R_wFT = resistivity at formation temperature, and

FT = formation temperature (°F).

The second method for calculating formation water resistivity (R_w) uses the SP curve values (Asquith and Krygowski, 2004), the formation temperature estimated using a temperature gradient equation and the bottom-hole temperature (BHT), and the resistivity of the mud filtrate (R_{mf}) at the formation temperature calculated using the Arps equation shown above (equation 6.7). Formation temperature for each well is calculated using either a basin-wide temperature gradient or by using the annual mean surface temperature for the area and the BHT. An R_{mf} curve is then calculated using the Arps equation and the estimated formation temperature. An equivalent formation water resistivity (R_{we}) curve is calculated using:

$$R_{we} = R_{mf}FT * 10^{\left(\frac{\mathrm{SP}}{61 + 0.133 * \mathrm{BHT}}\right)} \qquad (6.8)$$

and an R_w curve or value by:

$$R_w = \frac{R_{we} = 0.131 * 10^{\left(\frac{1}{\log\left(\frac{\mathrm{BHT}}{19.9}\right)}\right)^{-2}}}{-0.5 * R_{we} + 10^{\frac{0.0426}{\log\left(\frac{BHT}{50.8}\right)}}} \qquad (6.9)$$

where:

R_{we} = equivalent water resistivity at formation temperature,

$R_{mf}FT$ = resistivity of mud filtrate at formation temperature,

SP = SP curve readings,

BHT = bottom-hole temperature in °F, and

R_w = resistivity of formation water at depth.

Most wells in the project had a Delta T (DT) curve, a sonic porosity (PHIS) curve, or both. Wells with PHIS curves only were back-calculated to DT using DT_{ma} and DT_{fl} values from the well logs. DT is calculated by a derivation of the Wyllie equation (Wyllie and others, 1958).

$$PHIS\,(DT_{fl} - DT_{ma}) + DT_{ma} = DT \qquad (6.10)$$

where:

$PHIS$ = sonic porosity readings or curve values,

DT_{fl} = interval transit time of the fluid in the formation in µS/ft,

DT_{ma} = interval transit time of the formation matrix in µS/ft, and

DT = combined interval transit time of the formation in µS/ft.

PHIS is calculated from the acoustic velocity curve using standard rock matrix and fluid values specified by the geologist at the well site. We reviewed the well logs and found that most of the PHIS values had DT_{ma} values of 51.3 µS/ft, a typical sandstone matrix. However, several wells had limestone PHIS values using a limestone matrix value of 47.6 µS/ft. Fluid values were all for fresh water or 189 µS/ft. To standardize the PHIS curves, we calculated a DT curve using Equation 6.10. After DT was calculated, sonic porosity – sandstone (SPHIS) curves were generated with the 51.3 µS/ft sandstone matrix and 189 µS/ft freshwater values using the standard Wyllie equation. SPHIS should indicate corrected sandstone porosities. Several wells, particularly in the eastern part of the basin, had neutron and density porosity logs. A review of several of them showed gas crossover, particularly in the Sego and Castlegate Sandstones. A sonic porosity curve adjusted for gas (SPHIS_GAS) was prepared for each well (Hilchie, 1978). In sandstone units without a neutron porosity crossover, the SPHIS_GAS porosity will be too low. The two curves, SPHIS and SPHIS_GAS, should bracket the formation porosities.

After calculating water resistivity using lab samples and SP curves, formation water saturation (S_w) was estimated using the standard Archie equation (Archie, 1942; Asquith and Krygowski, 2004).

$$S_w = \left(\frac{a * R_w}{R_t * SPHIS^m}\right)^{\frac{1}{n}} \qquad (6.11)$$

where:

S_w = formation water saturation as a fraction,

R_w = formation water resistivity,

R_t = formation resistivity or deep resistivity (RESD),

$SPHIS$ = sonic porosity for sandstone,

a = tortuosity factor or 0.81 for consolidated sands,

m = cementation exponent or 2.0 for consolidated sands, and

n = saturation exponent or 2.0 for consolidated sands.

Formation water saturation was calculated using the water resistivity from lab analyses and from the Archie equation, and there is good agreement between the results. We therefore concluded the R_w and S_w values calculated from SP curves are representative of the formations and give a good distribution of R_w and S_w for the study area.

Finally, the bulk volume of water (BVW) is calculated by the following equation (Asquith and Krygowski, 2004):

$$BVW = SPHIS * S_w \quad (6.12)$$

where:

BVW = bulk volume of water or water available to flow,
$SPHIS$ = sonic porosity for sandstone, and
S_w = formation water saturation.

The BVW indicates how much water is available to flow to the well. As the BVW approaches zero, the number approaches the irreducible water saturation number that is essentially water bound to the pore surface or clay particles.

The NGR for each formation has been calculated using the normalized GR and calculated PHIS curves. A ≥60 GAPI cutoff was applied to the normalized GR curve. The PHIS curve was used to limit the sandstone summation to a minimum porosity of 6%. All porosities are in fractional volume.

Water samples sourced from well files curated at the DOGM and company donations were compiled in a comprehensive water chemistry database by the UGS (appendix D). The structure and isopach maps of the Mesaverde Group were created in IHS Petra™ using formation tops data for the 114 wells recorded in appendix C. Sonic logs were used to calculate average formation porosity and bulk density logs were used for average formation density.

UPPER CRETACEOUS MESAVERDE GROUP

The Upper Cretaceous Mesaverde Group in the Uinta Basin comprises the sedimentary units overlying the Mancos Shale and underlying the Upper Cretaceous to Paleogene North Horn, Colton and Wasatch Formations (figures 1.5 and 2.13). Deposition occurred as the Cretaceous Western Interior Seaway regressed to the east and rivers and streams flowed eastward from the Sevier highlands in western Utah to the sea (figure 6.1). In the western landward half of the Uinta Basin, the Mesaverde Group, from oldest to youngest, is composed of the Blackhawk Formation, Castlegate Sandstone (lower, middle, and Bluecastle Sandstone members), and Price River Formation, whereas in the eastern seaward half of the Uinta Basin, the group comprises the lower Castlegate, Buck Tongue of the Mancos Shale, Sego, Neslen, Farrer, and Tuscher Formations (figure 2.13; plate 2). The group thins to the north and south from the basin middle (figure 6.4; plate 3). Depositional environments for these formations include fluvial, coastal plain, swamp, shoreface/delta, and marine (prodelta to offshore). Lithologies consist of shale to siltstone to sandstone with varying amounts of organic material (mainly plants) to coal. Several of these formations contain thick sandstone packages that provide reservoirs for hydrocarbons and water.

Thickness

Thickness of the Mesaverde Group ranges from less than 500 to ~3500 feet (150–1070 m) (figure 6.4). At the group's exposure along the Book Cliffs, the strata range from approximately 160 to 2290 feet (50–700 m) thick based on geologic mapping (Gualtieri, 1988; Weiss and others, 1990), and our data (figure 6.4) show a range of less than 500 feet (150 m) to over 2000 (600 m) feet along the southern margin of the Uinta Basin. Overall, the group is thickest in an east-west trending band along the middle of the Uinta Basin and thins toward the northern and southern margins and toward the Douglas Creek arch (Johnson and Roberts, 2003).

Depth

The Laramide-aged Uinta Basin is bounded by the San Rafael Swell and Uncompahgre uplift to the south and the Uinta Mountains along the north (Potter and others, 1991). Stratigraphic units dip gently north along the Book Cliffs in the south and outcrops along the northern margin of the basin dip steeply south (figure 6.5) (Morgan and others, 2002). Outcrops along the Book Cliffs provide a view of the intertonguing and lateral transitions of the vertical succession of sedimentary units that extend throughout the basin (figure 6.6). The deepest encounter with the Mesaverde Group is greater than 19,000 feet (5800 m) (Johnson and Roberts, 2003).

Lithology

The Blackhawk Formation is composed of interbedded sandstone, siltstone, shale, and coal (figure 6.7A). The lower part of the formation has been interpreted as a wave-dominated delta deposit, in some places reaching thicknesses of more than 1000 feet (300 m) (Franczyk and others, 1990a; Dubiel, 2000; Howell and Flint, 2005). Coal within the Blackhawk formed in widespread marshes and swamps overlying shoreface sands along the western margin of the Western Interior Seaway (Maberry, 1971; Franczyk and others, 1990a). The lower Blackhawk hosts thick and laterally continuous coal beds, whereas upper Blackhawk coals are thin and discontinuous (Dubiel and others, 2000). Sedimentation transitioned laterally (from west to east) and vertically (top to bottom) from meandering stream and overbank deposits, to peat deposits, to delta-front deposits that prograded into the sea (Maberry, 1971; Howell and Flint, 2005).

The Castlegate Sandstone braid-plain deposits overlie the meandering-stream and coastal-plain deposits of the Blackhawk Formation in the west (figure 6.7A and 6.7B) or, in the eastern Uinta Basin, the marine Mancos Shale (Howell and Flint, 2005). The lower member is composed of a thick stack of cliff-forming sandstone beds that were deposited in an east to southeast-flowing, braided, sand-rich stream environment (figures 6.7B and 6.8) and ranges in thickness from ~10 to 800 feet (3–240 m) but averages ~300 feet (90 m)

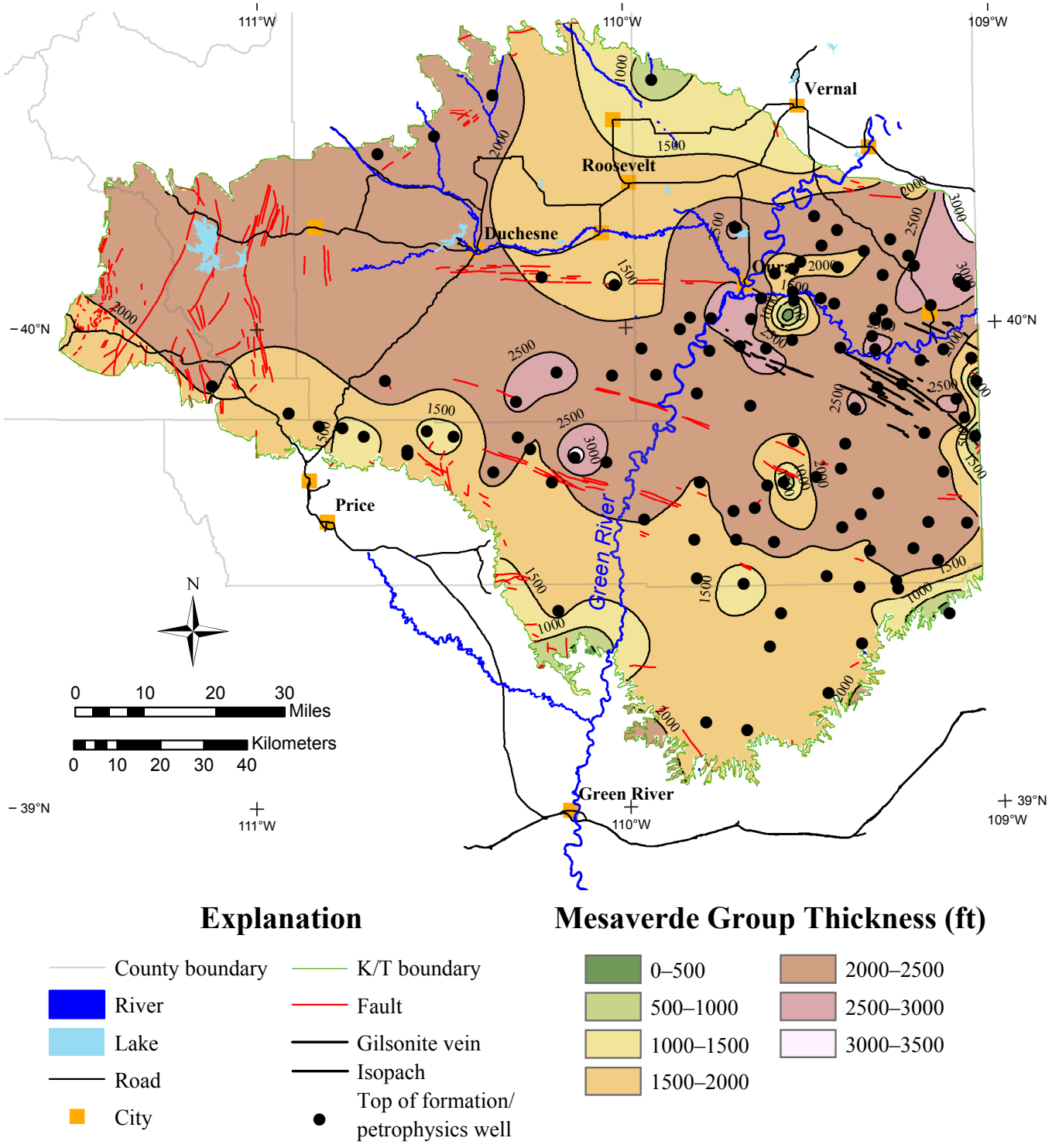

Figure 6.4. *Thickness of the entire Mesaverde Group. The contour range is 0 to 3500 feet, and the contour interval is 500 feet. Tops data are from Anderson (2005), Hettinger and Kirschbaum (2002), and well logs selected as part of this study.*

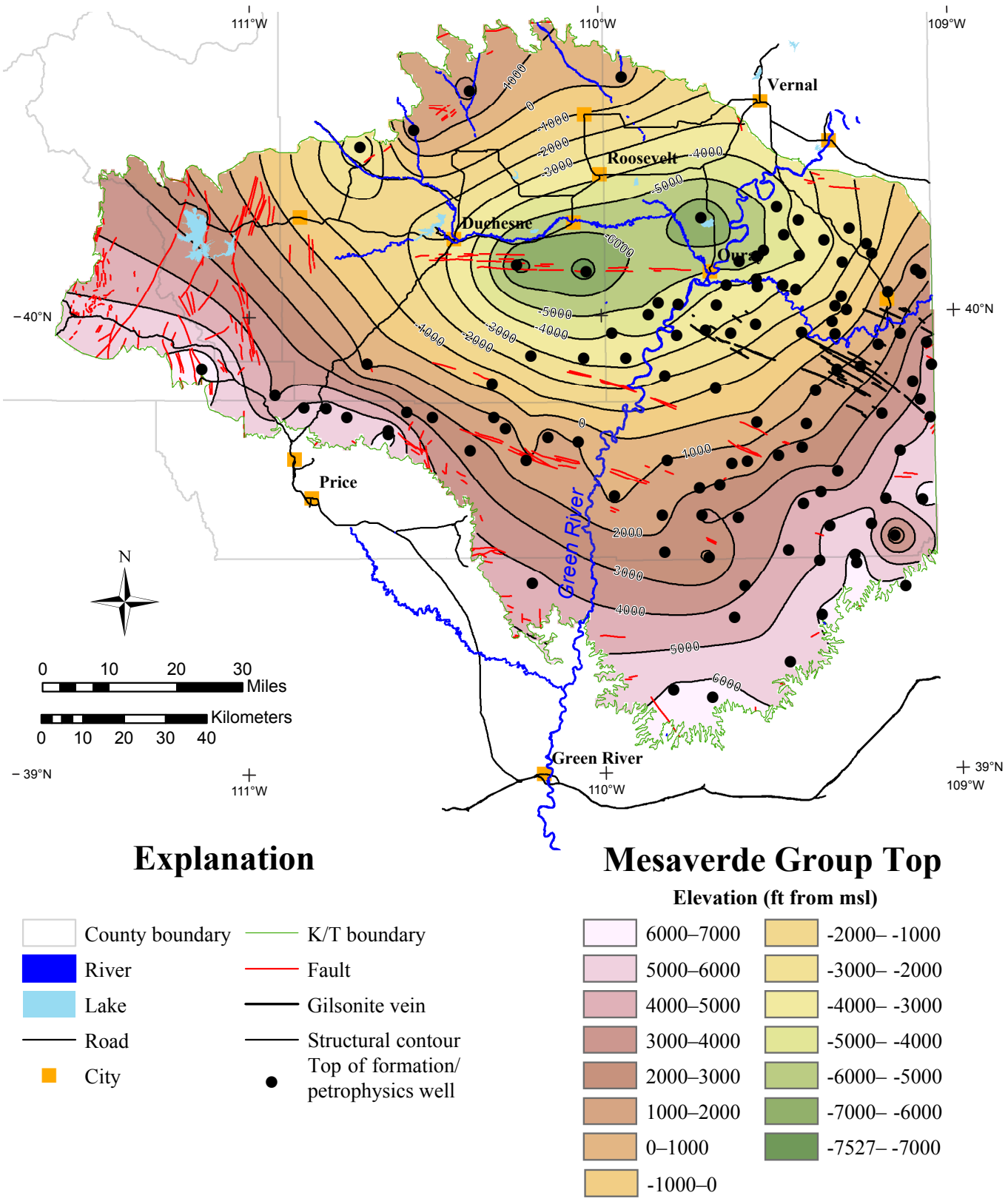

Figure 6.5. *Structure of the top of the Mesaverde Group. The contour range is -7000 to 8500 feet, and the contour interval is 1000 feet. The Mesaverde is exposed along the southern boundary of the Uinta Basin in the Book Cliffs and dips gently to the north. Mesaverde Group rocks are also exposed on the north and northeast parts of the basin. Tops data are from Hettinger and Kirschbaum (2002), Anderson (2005), and well logs selected as part of this study.*

Figure 6.6. *Classic Mesaverde Group along the Book Cliffs northwest of Green River. Photo shows the lateral transition and intertonguing of the lower Mesaverde Group and the Mancos Shale.*

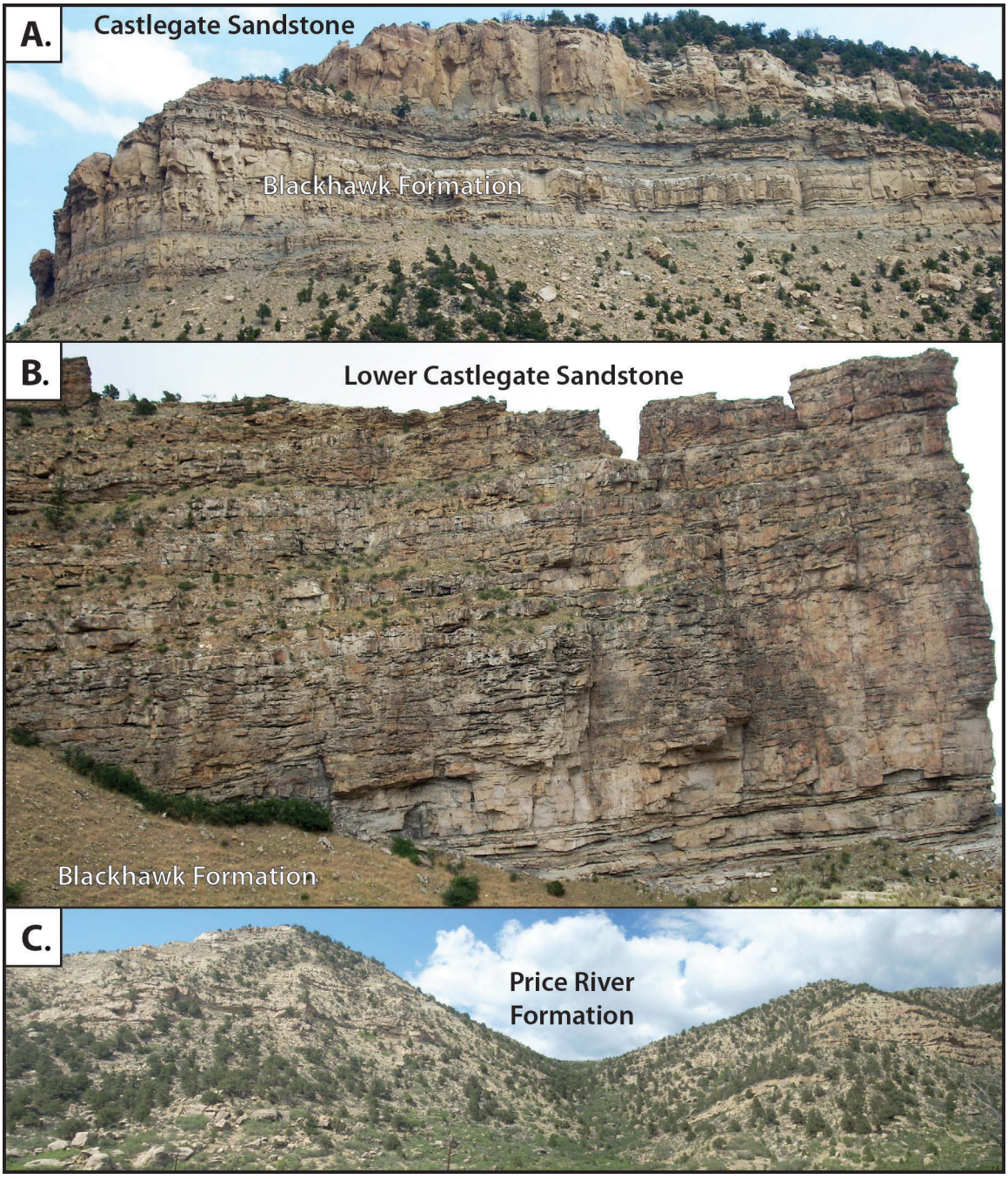

Figure 6.7. *Representative Mesaverde Group outcrops of the Blackhawk, Castlegate, and Price River Formations in the western half of the Uinta Basin.* ***A.*** *The Blackhawk Formation underlies the Castlegate Sandstone and is composed of interbedded sandstone, siltstone, shale, and coal.* ***B.*** *The Castlegate Sandstone is composed of massive sandstones deposited in a braided-stream environment.* ***C.*** *The Price River Formation overlies the Castlegate Sandstone and is composed of poorly sorted siltstone and ledge-forming sandstone beds deposited in a fluvial environment.*

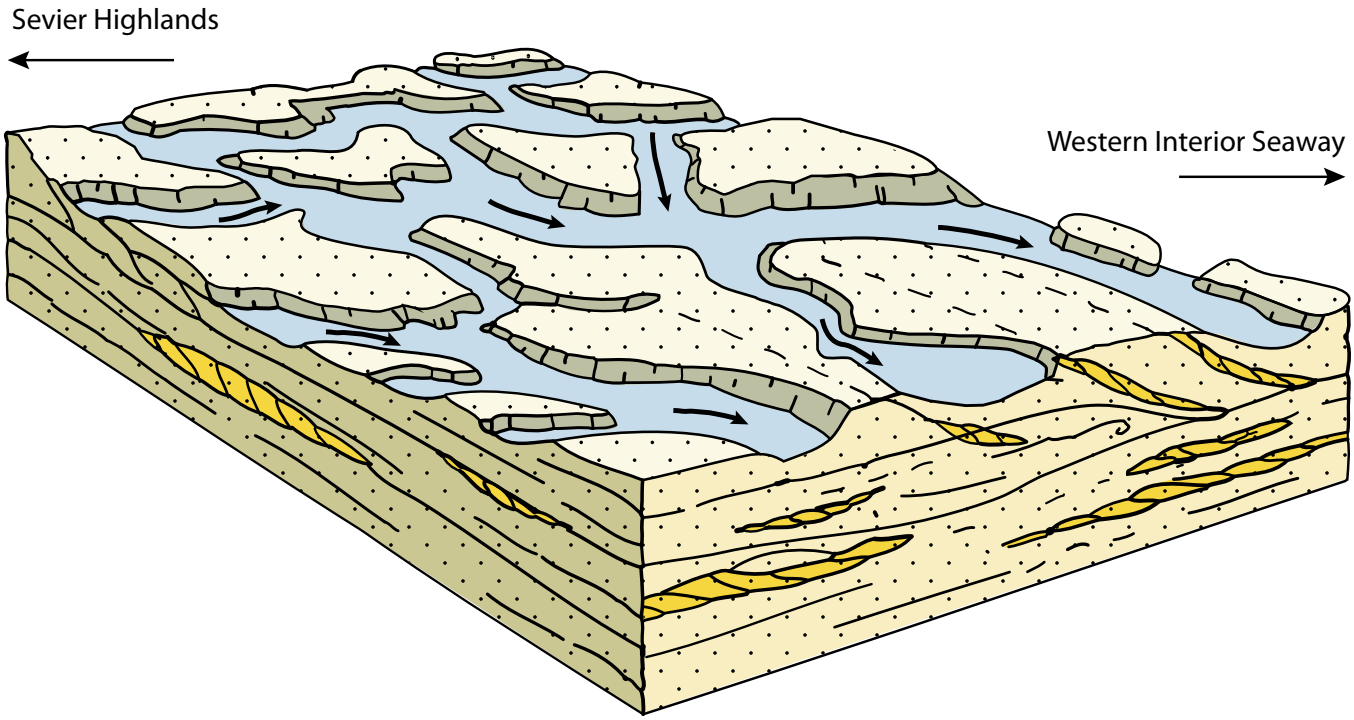

Figure 6.8. *Castlegate Sandstone was deposited in a braided-stream environment as sediments were eroded from the Sevier highlands in western Utah and transported eastward to the Cretaceous Western Interior Seaway (schematic block diagram modified from Howell and Flint, 2005).*

thick (figure 6.9; plate 2). The upper member contains interbedded mudstone and sandstone from a meandering stream system (Lawton, 1983; Hettinger and Kirschbaum, 2002). The upper unit is thickest (up to 500 feet [150 m]) in the west and thins to about 10 feet (3 m) in the east near the border between Utah and Colorado (figure 6.10). Coarse-grained sandstone zones are interpreted to be linked to thrusting during the Sevier orogeny (Chan and Pfaff, 1991).

The Bluecastle Sandstone Member (uppermost member) of the Castlegate Sandstone was deposited in an evolving meandering-stream environment within an alluvial plain and contains stacked, fine- to coarse-grained sandstone channels with trough cross-stratification (Franczyk and others, 1990b). Paleocurrent data exhibit northeast and southeast flow from the Sevier highlands to the eastern sea (Franczyk and others, 1990a). The unit preserves the last major sediment body from thrusting associated with the Sevier orogeny (Franczyk and others, 1990a) and pinches out eastward above the Neslen Formation (figure 6.11; plate 2) (Hettinger and Kirschbaum, 2002).

The Price River Formation consists of approximately 600 to 1600 (180–490 m) feet of poorly sorted siltstone and ledge-forming sandstone beds deposited within an eastward-flowing meandering fluvial system (figure 6.7C) (Lawton, 1983; Hettinger and Kirschbaum, 2002). The formation changes laterally into the Tuscher and Farrer Formations in the eastern part of the Uinta Basin (figure 6.12; plate 2). Sandstones in the upper Price River are thicker and more laterally continuous than those in the lower section (Lawton, 1983). The Price River and the Farrer contain numerous thin, isolated, heterolithic sandstone bodies from meandering and tidally influenced fluvial channels, which provide small hydrocarbon reservoirs, though the sand bodies become thicker and more interconnected up-section in the Tuscher (figure 6.12) (Aschoff, 2010).

The Buck Tongue of the Mancos Shale underlies the Sego Sandstone in the eastern half of the Uinta Basin (figure 6.13A and B) and consists of interbedded, gray sandstone, siltstone, and mudstone. The Buck Tongue includes deposits that record a marine transgression westward, then regressive deposits that prograde and thicken to the east and gradually transition upward into the Sego Sandstone (Franczyk and others, 1990a; Anderson, 2005). The unit is thickest in the easternmost part of the study area and pinches out slightly west of the present-day Green River (figure 6.14).

The Sego Sandstone is composed of stacked, cross-stratified sandstone packages with parallel laminations in its uppermost package, and has a sharp, conformable contact with the overlying Neslen Formation (figure 6.13A and 2.13B) (Franczyk and others, 1990a). The Buck Tongue of the Mancos Shale and the Sego Sandstone record the final transgression and regression of the Cretaceous Western Interior Seaway in the Uinta Basin and eastern Utah (Franczyk and others, 1990a). Sandstone thickness is on average ~180 feet (55 m) (Hettinger and Kirschbaum, 2002). The Upper Castlegate sandstone is a western equivalent of the Sego Sandstone and Neslen Formation of the eastern Uinta Basin (figure 6.15).

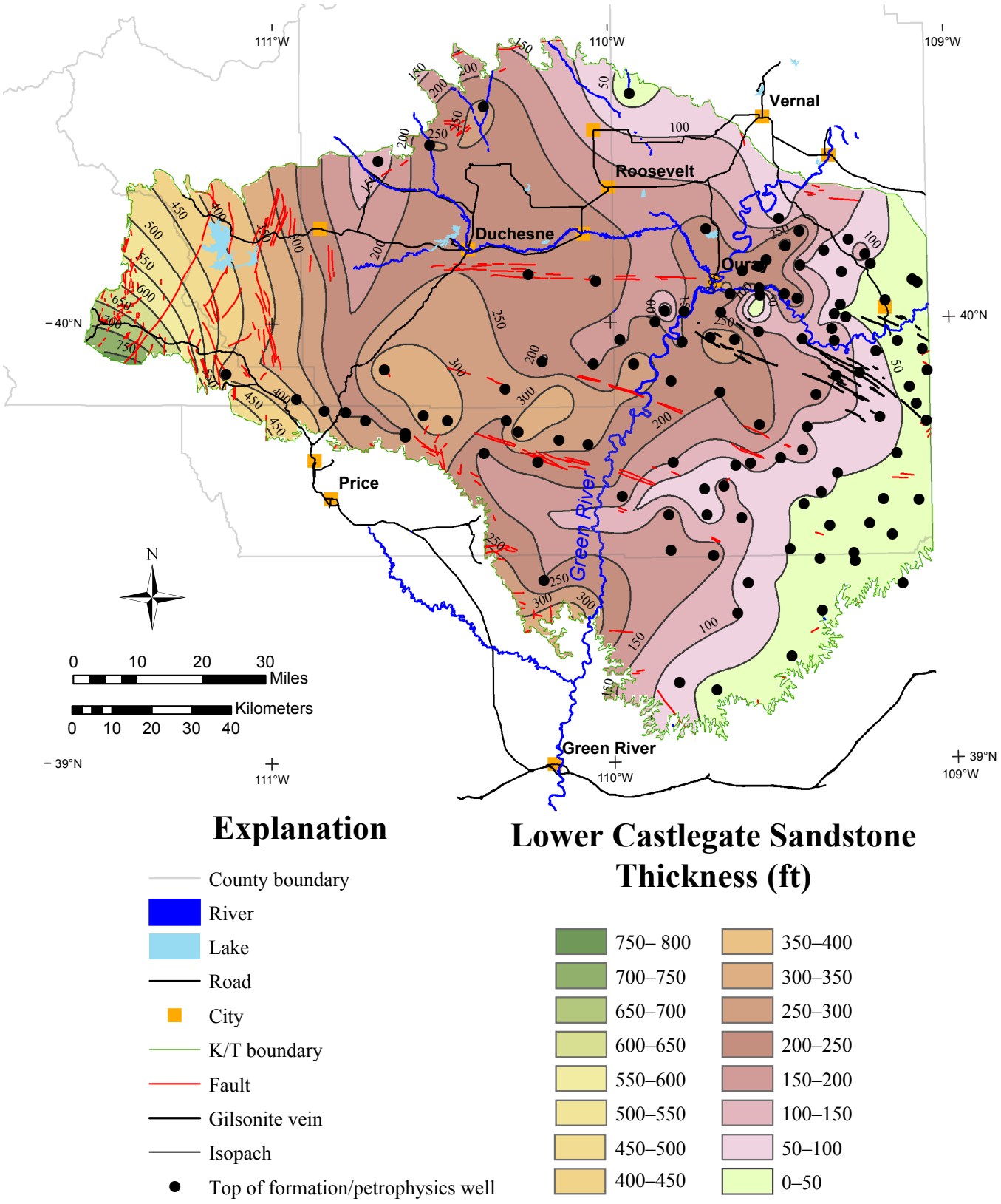

Figure 6.9. *Thickness of the lower Castlegate Sandstone. The contour range is 0 to 800 feet, and the contour interval is 50 feet. Tops data are from Hettinger and Kirschbaum (2002), Anderson (2005), and picks from well logs as part of this study.*

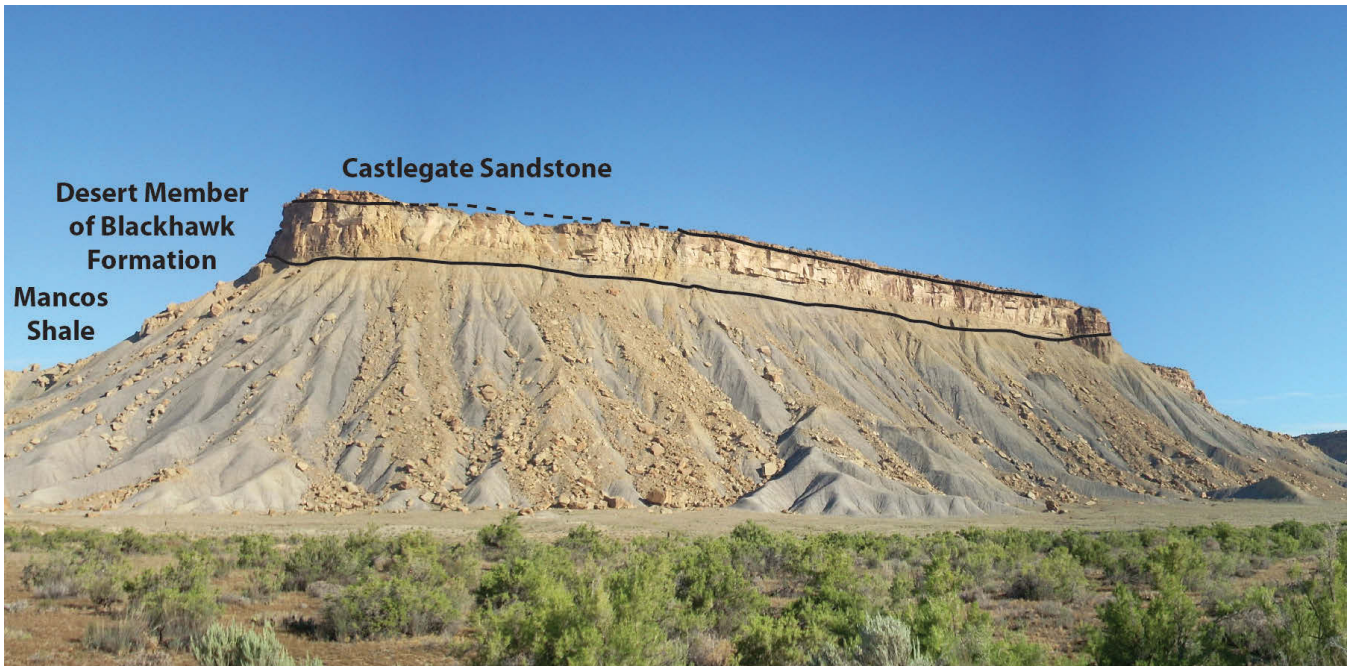

Figure 6.10. *Castlegate Sandstone overlying the Desert Member of the Blackhawk Formation and the Mancos Shale at the mouth of Thompson Canyon, east of Green River. Note that the Castlegate has thinned considerably eastward in comparison to the thick section to the west shown on figure 6.7B.*

Deposited by eastward-flowing rivers in a coastal plain (figure 6.1B) behind the shorelines of the Sego Sandstone, the Neslen Formation contains carbonaceous mudstone, coal, and channelized sandstone beds that increase in abundance toward the top of the unit (figure 6.13) (Franczyk and others, 1990a; Cole and others, 2008). The Neslen is the eastern lateral equivalent of the upper Castlegate Sandstone of the western Uinta Basin (see figure 2.13; also see Hettinger and Kirschbaum, 2002; Johnson and Roberts, 2003; White and others, 2008). Franczyk and others (1990a) reported total thickness of these units ranges from 175 to 670 feet (50–204 m), and Anderson (2005) reported the average thickness is ~250 feet (76 m) (figure 6.15). In outcrop, the Thompson Canyon sandstone, approximately in the middle of the Neslen Formation, forms a continuous sandstone ledge up to 15 feet (4.5 m) thick (figure 6.13A) (Fisher, 1936). The coal beds are discontinuous and range from 1 to 7 feet (0.3–2.1 m) thick (figure 6.13C) (Franczyk and others, 1990a; Hettinger and Kirschbaum, 2002).

Like the equivalent Price River Formation, the Farrer Formation was deposited by an east- and northeast-flowing, straight to sinuous river system that crossed a coastal plain (figure 6.1B) (Cole and others, 2008). The sandstone bodies preserve anastomosing channels, and, as the sandstones become thicker up section, the Farrer Formation transitions into the Tuscher Formation (figure 6.12) (Keighin and Fouch, 1981). The sandstone is very fine to medium-grained with interbedded mudstone resultant from floodplain deposits (Hettinger and Kirschbaum, 2002). The Farrer contains significantly more sandstone and less carbonaceous material than the underlying Neslen (Franczyk and others, 1990a). The maximum thickness of the Farrer Formation is 950 feet (290 m) in Tusher Canyon and it thins westward (the Price River, Farrer, and Tuscher Formations are combined on figure 6.16) (Lawton, 1983).

The eastern Uinta Basin's Tuscher Formation is correlative to the west with the upper Price River Formation (Lawton, 1983). The Tuscher is approximately 250 feet (76 m) thick, comprising multi-story, thick sandstone bodies overlying the Farrer Formation, and was also deposited within a northeast-flowing fluvial environment (figures 6.1B and 6.12B) (Lawton, 1983; Hettinger and Kirschbaum, 2002; Cole and others, 2008). Excellent outcrops of the Neslen, Farrer, and Tuscher Formations can be found in Sego and Tusher Canyons along the southeastern Book Cliffs in Grand County (figures 6.12A and 6.17). Contacts between the Neslen, Farrer, and Tuscher are gradational, but the Tuscher can be identified from the Farrer Formation by the presence of lighter-colored and more massive sandstones (Franczyk and others, 1990a, 1990b; Anderson, 2005). The Farrer and Tuscher Formations migrated with the coastal plain during the final eastward progradation and filling of the foredeep as the Western Interior Seaway regressed to the east (Keighin and Fouch, 1981).

Reservoir Properties

We compared the net sand having ≥ 6% porosity to the gross thickness of sand in some individual formations as well as for the full Mesaverde Group (table 6.1). A discussion of the reservoir properties for the Mesaverde Group follows.

Appendix E shows the NGR and average porosity (PHIA) calculations for the combined Mesaverde Group. The NGR

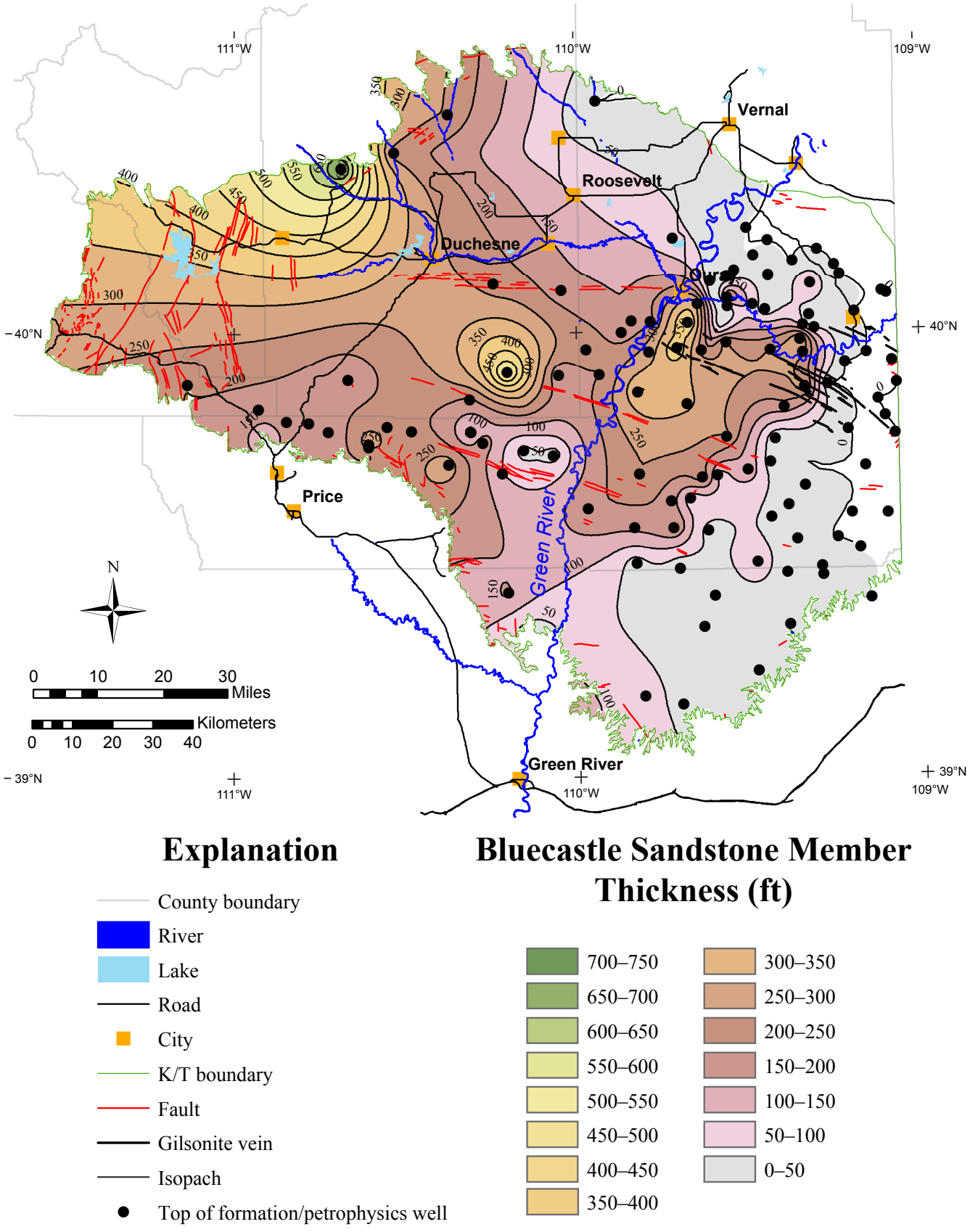

Figure 6.11. *Thickness of the Bluecastle Sandstone Member of the Castlegate Sandstone. The contour range is 0 to 750 feet, and the contour interval is 50 feet. The coarse-grained, pebbly unit is thickest in the northwestern region of the Uinta Basin and pinches out into the Neslen Formation in Sego Canyon to the southeast (Hettinger and Kirschbaum, 2002). Tops data are from Hettinger and Kirschbaum (2002), Anderson (2005), and from well logs used as part of this study.*

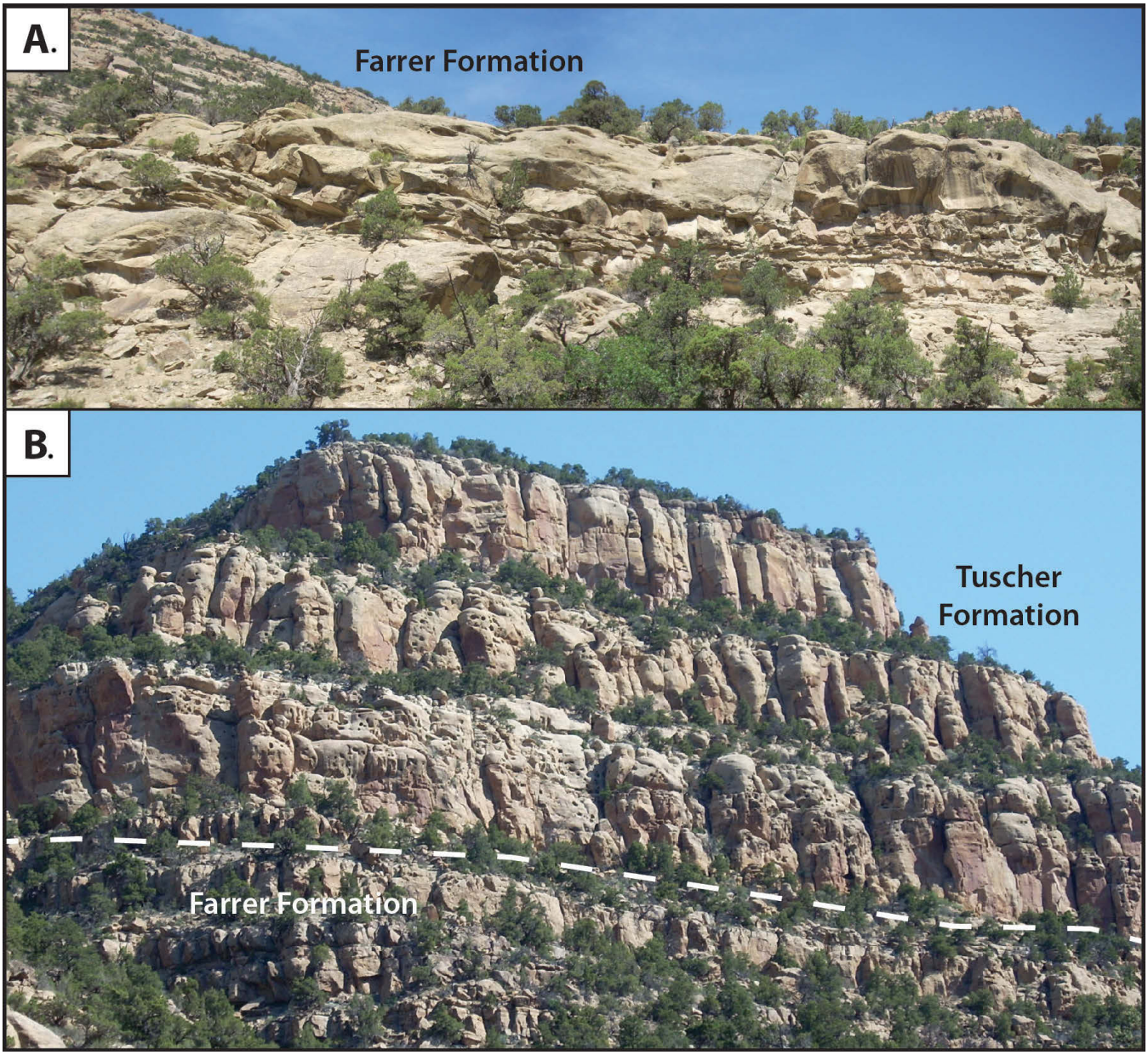

Figure 6.12. *Typical outcrops of the* ***A.*** *Farrer Formation and* ***B.*** *the overlying Tuscher Formation in Sego Canyon. The Farrer and Tuscher Formations are the eastern lateral equivalents of the Price River Formation.*

calculation used a minimum 6% PHIS and a maximum 60 GAPI GR cutoff to arrive at the net sand thickness. The average PHIA, at baseline 6% porosity, of all wells is 21% (table 6.1), and the values range from 13% to a high of 35% (appendix E), which is lower than the Wasatch/Colton interval (discussed later). NGR is generally higher in the Mesaverde (0.76) than the Wasatch/Colton Formation (0.67) (table 6.1), reflecting an overall higher-porosity sand component in the Mesaverde (figure 6.18). There are very thick sequences of Mesaverde sandstone with porosity ≥ 6%. We suggest the sandy formations in the upper part of the Mesaverde could make favorable injection units, particularly around the margins of the basin where water saturation in the upper Mesaverde sandstones may be lower, thus allowing higher water disposal volumes.

The Price River Formation is the youngest formation in the western Mesaverde Group, and it is chronostratigraphically equivalent to the Tuscher and Farrer Formations on the eastern side of the basin. NGR, gross sand, and PHIA averages for wells that penetrate the Price River Formation are recorded in appendix E. The average NGR is 0.68, gross sand is 435 feet (133 m), and the PHIA is 15% (table 6.1). However, the Price River has much thinner stacked sequences of sandstone. Well logs through the interval show interbedded sandstone and silty or shaly sandstone. Two wells, Yellowstone River Tribal No. 1 (section 17, T. 1 N., R. 4 W., UBL&M, Duchesne County, API No. 43-013-30047) and Skyline Govt. No. 1 (section 10, T. 11 S., R. 7 E., SLB&M, Utah County, API No. 43-049-30003), have gross sand thicknesses of 1652 and 1115 feet (9503 and 340 m), respectively, reflecting an area of the basin

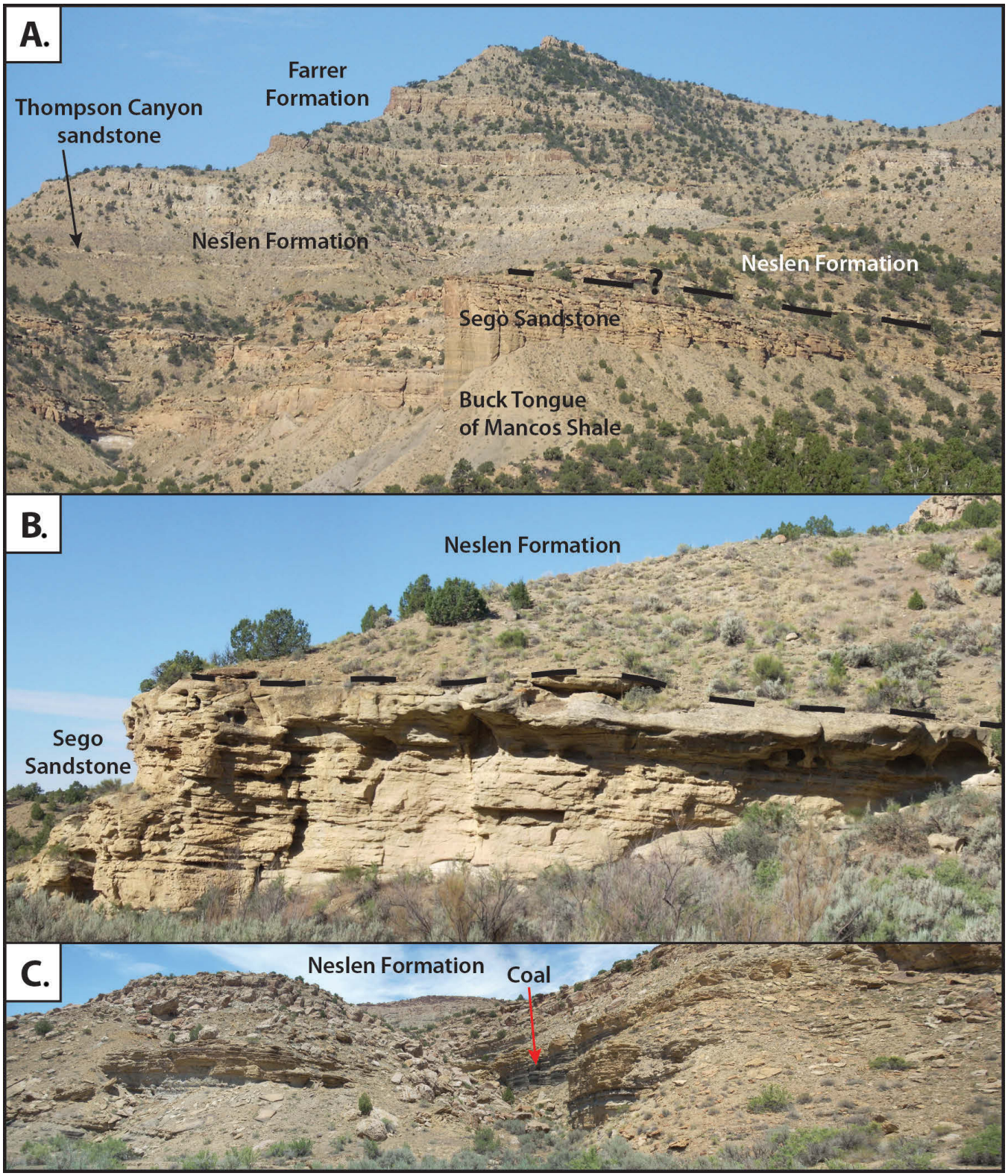

Figure 6.13. *Excellent outcrops of the Mesaverde Group in Sego Canyon.* ***A.*** *The Buck Tongue of the Mancos Shale underlies the Sego Sandstone, above which are the Neslen and Farrer Formations.* ***B.*** *The Sego Sandstone is overlain by the heterogeneous Neslen Formation.* ***C.*** *The Neslen Formation contains several coal-bearing layers deposited in a coastal plain (Franczyk and others, 1990a).*

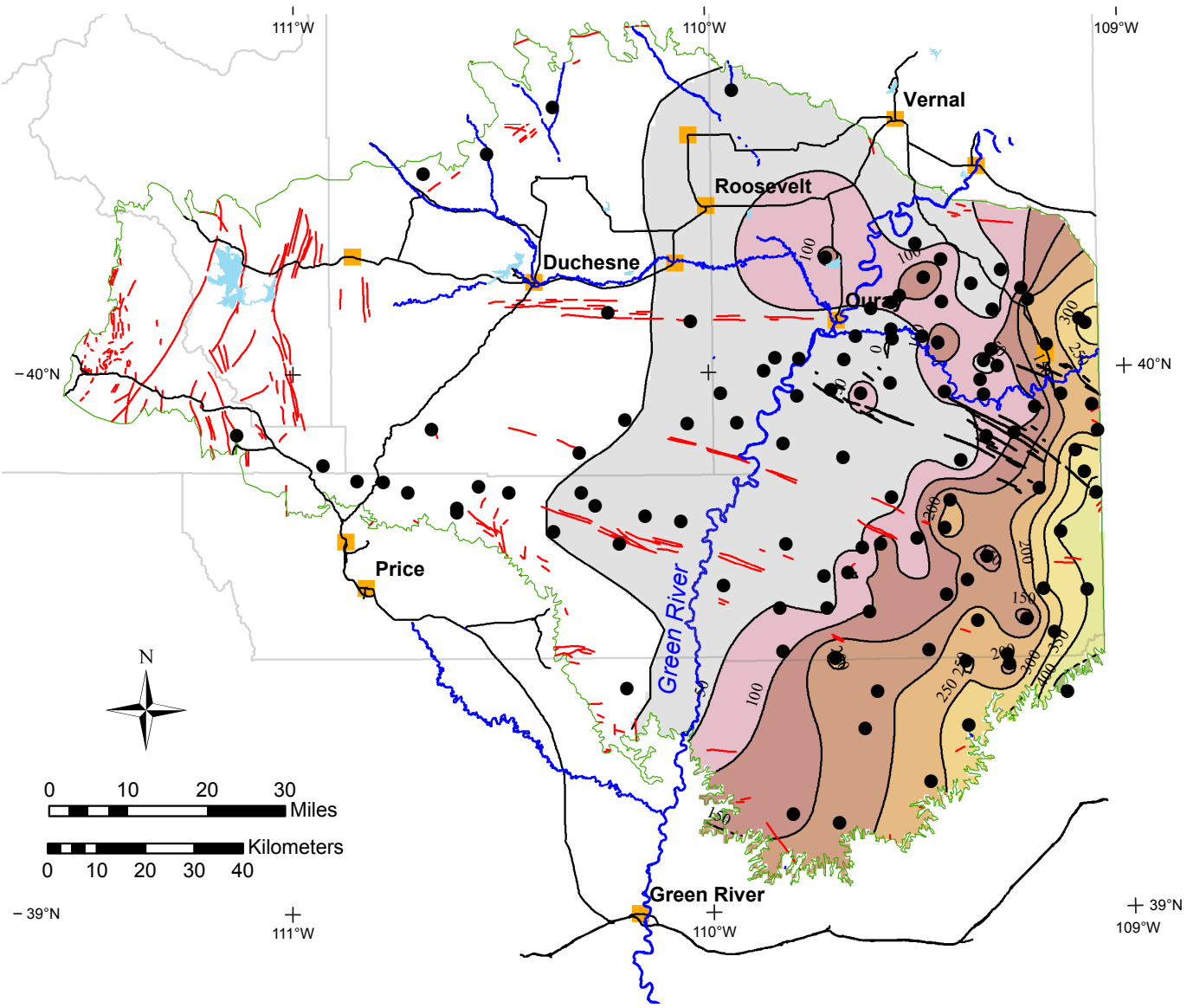

Figure 6.14. *Thickness of the Buck Tongue of the Mancos Shale. The contour range is 0 to 500 feet, and the contour interval is 50 feet. The Buck Tongue is thickest in the eastern Uinta Basin (seaward) and thins to the west (landward). Tops data are from Hettinger and Kirschbaum (2002), Anderson (2005), and from well logs as part of this study.*

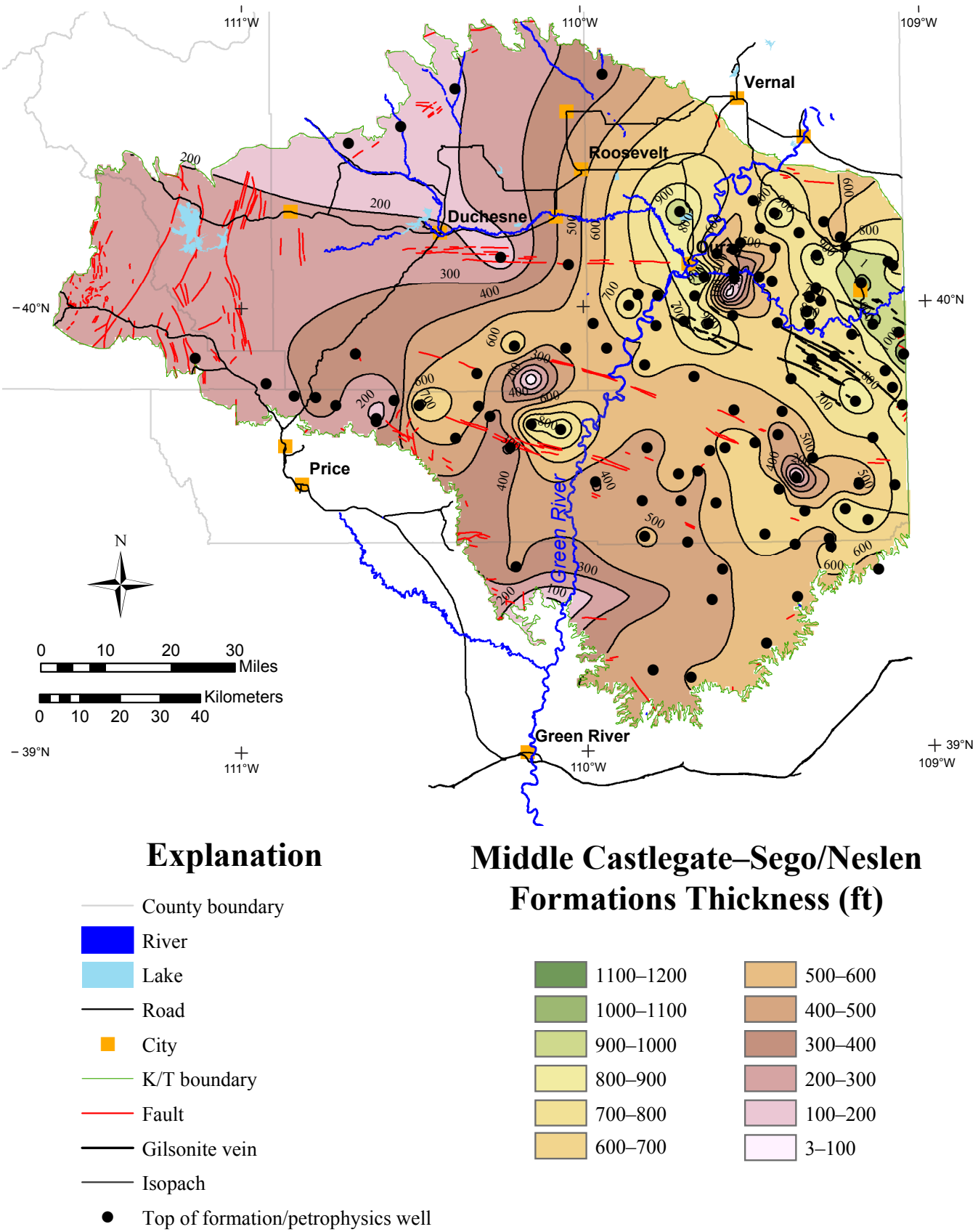

Figure 6.15. *Combined thickness of the middle Castlegate Sandstone in the west and Sego Sandstone and Neslen Formation in the east. The contour range is 100 to 1000 feet, and the contour interval is 100 feet. The middle section of the Castlegate is thinnest in the western part of the Uinta Basin and transitions to thicker sections of the Neslen Formation and Sego Sandstone in the east. Tops data are from Hettinger and Kirschbaum (2002), Anderson (2005), and well logs from additional wells as part of this study.*

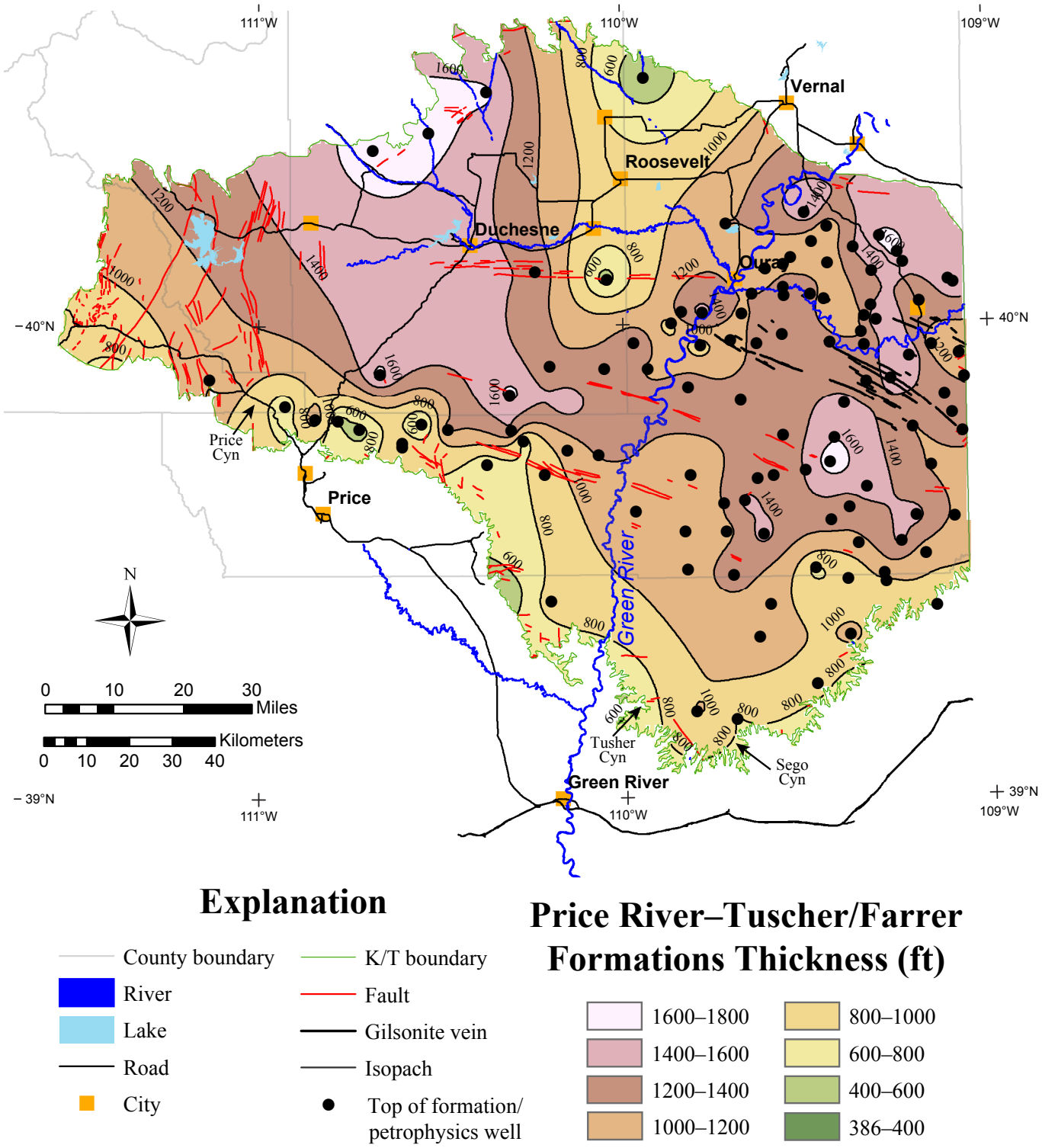

Figure 6.16. *Combined thickness of the Price River Formation in the west and the Tuscher and Farrer Formations in the east. The contour range is 386 to 1800 feet, and the contour interval is 200 feet. The Price River is thickest in the northwestern region of the Uinta Basin, thins in the middle of the basin, and splits into the thicker Tuscher and Farrer Formations in the eastern part of the basin. Tops data are from Hettinger and Kirschbaum (2002), Anderson (2005), and well logs as part of this study.*

Figure 6.17. *Buck Tongue of the Mancos Shale, overlain by the Sego Sandstone and the coal-bearing Neslen Formation, Tusher Canyon.*

Table 6.1. *Reservoir properties of the Wasatch/Colton Formation and Mesaverde Group. The Wasatch/Colton values are combined values. The Mesaverde values were calculated for the entire thickness from the top of the Price River Formation–Tuscher Formation to the base of the lower Castlegate Sandstone. The Castlegate values are inclusive of Bluecastle Sandstone Member, and middle and lower members.*

Producing Reservoirs	Average Net Sand ≥ 6% Porosity (ft)	Average Gross Sand (ft)	Average Net to Gross Sand (NGR)	Average Porosity (PHIA, %)	Average Unit Thickness (ft)	Minimum Thickness (ft)	Maximum Thickness (ft)
Wasatch/Colton	1340	2232	0.67	24	2312	330	4677
Mesaverde Group	1528	2042	0.76	21	2121	894	3089
Price River Formation	283	435	0.68	15	1255	490	1702
Tuscher Formation	116	150	0.79	16	504	193	783
Farrer Formation	167	211	0.74	15	777	255	1296
Bluecastle Sandstone Member, Castlegate Sandstone	53	108	0.58	13	193	24	725
Middle Castlegate Sandstone	85	125	0.69	14	445	145	814
Neslen Formation	87	110	0.78	15	475	169	814
Sego Sandstone	59	79	0.83	15	182	83	287
Lower Castlegate Sandstone	77	143	0.61	12	157	8	370
Castlegate Sandstone	201	342	0.64	13	727	8	2382

with a higher concentration of fluvial channels. The net sand in these two wells is higher than other wells, but NGR is generally lower because of the high gross sand thickness. Injecting high volumes of produced water into this formation would require either a long perforated interval through the extent of the formation, or many very detailed perforations targeting clean sands.

The Tuscher Formation is generally sandy, and well logs of Tuscher show several thick, blocky sandstone intervals, which likely represent thick, meandering fluvial channels. The channels are bounded vertically by silty to shaly sandstones. The blocky channels in the Tuscher do not show a fining-upward trend and the contacts appear to be sharp. The lateral continuity of the channels has not been established as part of this study. However, two nearby wells typically show similar, blocky, sandy channels in GR logs. This suggests that the channel sands may be continuous laterally over a larger area. The average PHIA in the Tuscher is 16%, and the average gross sand thickness is 150 feet (46 m) (table 6.1). The average NGR of 0.79 is slightly higher than for the Price River Formation, suggesting that a greater percentage of the gross sand has high porosity (table 6.1, appendix E). This implies that the sands are cleaner and sharply contrast with the silty and shaly sands above and below. This could make the channel sandstones in the Tuscher on the eastern side of the basin favorable injection locations for disposal of produced water.

GR curves from the Farrer Formation show several thick, interbedded sand-silt channel sandstone sequences. The Farrer has an average gross sand thickness of 211 feet (64 m), which is higher than that of the Tuscher Formation above and one-half of the gross sand thickness in the Price River Formation (table 6.1). The average NGR is 0.74, nearly matching the Tuscher NGR above (table 6.1). The Farrer has significant sandstone channels, but they are broken up by finer-grained interbeds and not as thick as

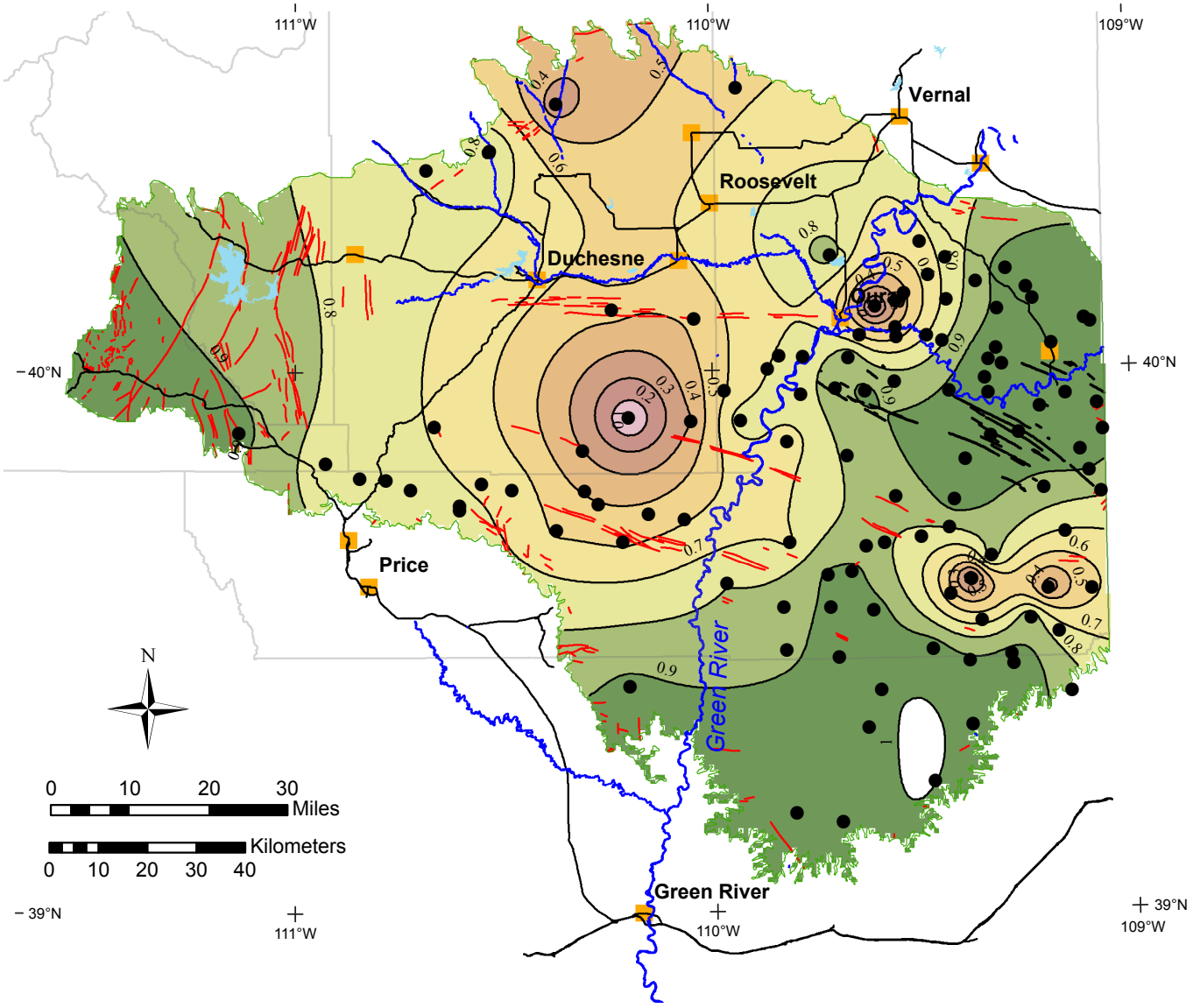

Explanation

- County boundary
- River
- Lake
- Road
- City
- K/T boundary
- Fault
- Gilsonite vein
- NGR contour
- Top of formation/ petrophysics well

Mesaverde Group Net ≥ 6% Porosity Sand to Gross Sandstone Ratio

0.9–1	0.4–0.5
0.8–0.9	0.3–0.4
0.7–0.8	0.2–0.3
0.6–0.7	0.1–0.2
0.5–0.6	0.08–0.1

Figure 6.18. *Net to gross ratio (NGR) of sands within the Mesaverde Group.*

the Tuscher channels. The Farrer could also provide some good candidate sandstones for water injection, similar to the Tuscher.

Porosity values for all sands in the Mesaverde Group are linked to the thermal maturity and depositional environments; values range from 5% to 8%, and the highest log porosity is 13% (Schmoker and others, 1992). Calculated average porosity values without porosity limits, using sonic logs, for each formation within the Mesaverde are presented in table 6.2. The data indicate that the overall average porosity for the sandstones in the Mesaverde, unadjusted for the presence of hydrocarbons, is 15%. The highest calculated porosity is within the Tuscher Formation (16.2%), followed by the Neslen and Farrer (15.6% and 15.5%, respectively). When adjusted for the presence of oil or gas, the average porosity value for the group decreases to 10% (gas) and 13% (oil). Further subdivision into units or facies would provide a more accurate representation of high- and low-porosity zones within each formation, but this level of detail was beyond the scope of this project. Tables 6.3 and 6.4 display porosity and permeability data from two cores within Greater Natural Buttes field area. As expected, permeability values from the tight sand bodies in the study interval are extremely low. One value of 162.33 mD from 10,532 feet (3210 m) in the NBU No. 253 core (section 10, T. 9 S., R. 21 E., SLB&M, Utah County, API No. 43-047-32917) is higher and reflects fracture permeability.

Water Quality

Water samples sourced from the Mesaverde Group vary considerably with regard to TDS. Mesaverde water ranges from fresh to brine, with most of the samples falling in the saline category (figures 6.19 and 6.20; table 6.5). Stiff diagrams displayed geographically in figure 6.21 show water samples near the southwestern border of the Uinta Basin are fresher than the saline samples found deeper to the east-northeast. A study from the U.S. Environmental Protection Agency (2004) suggests that recharge occurs around the basin edges and that most is sourced from the Uinta Mountains along the northern basin margin.

Appendix C contains calculated Mesaverde Group R_w, which is inversely related to TDS values. As with the Wasatch/Colton Formation, the Mesaverde has higher R_w values along the southern Book Cliffs and along the north and northeastern parts of the basin. This is expected since the flow-residence time of the water in the formation has not been sufficient to dissolve high quanities of minerals along a flow path. Higher R_w values are observed in the Mesaverde in the central part of the basin (eastern Duchesne County) and could possibly be associated with the east-west trending Duchesne fault zone (figure 2.1, plate 1) that might allow downward percolation of fresher water to the strata at that location. Higher water resistivity is also observed parallel to northwest-trending gilsonite veins (figures 2.1 and 3.1; plate 1). Fresher waters are found along the eastern edge of the Uinta Basin southeast of Bonanza, possibly resulting from freshwater recharge to exposures along the Douglas Creek arch. Groundwater leached from the overlying Flagstaff Limestone into the Mesaverde Group in the western Uinta Basin leaves a carbonate signature in the calcium/sodium (Ca/Na) ratio (figure 6.22). The lower Douglas Creek carbonate interval and Uteland Butte shale in the lower Green River Formation could also be a source of calcium; however, the Ca/Na ratios (see Wasatch/Colton water quality section on page 179) do not show high values from two wells in the same location.

Table 6.3. *Porosity and permeability from the NBU No. 253 core, Natural Buttes field.*

Depth (ft)	Permeability (mD)	Porosity (%)
10,532	162.330	2.06
10,572	0.068	5.69
10,580	0.007	5.13
10,612	0.042	5.74
10,651	0.007	3.88
10,677	0.007	5.43
10,700	0.007	5.72

Table 6.2. *Porosity values from sonic logs within the Mesaverde Group.*

Producing Reservoir	Count	PHIS[1] (average)	Gas Adjustment[2]	Oil Adjustment[2]
Mesaverde Group	33	0.146	0.102	0.131
Price River Formation	35	0.154	0.108	0.139
Tuscher Formation	26	0.162	0.113	0.146
Farrer Formation	28	0.155	0.109	0.140
Castlegate Sandstone	35	0.131	0.092	0.118
Bluecastle Sandstone Member, Castlegate Sandstone	25	0.115	0.081	0.104
Middle Castlegate Sandstone	34	0.153	0.107	0.138
Neslen Formation	25	0.156	0.109	0.140
Sego Sandstone	25	0.150	0.105	0.135
Lower Castlegate Sandstone	34	0.114	0.080	0.103

[1]PHIS (sonic porosity) is the sandstone matrix porosity and not reflective of the entire formation.
[2]Gas adjustment is 70% of the PHIS and oil adjustment is 90% of the PHIS.

Table 6.4. *Porosity and permeability from the NBU No. 921-21L core, Natural Buttes field.*

Depth (ft)	Permeability (mD)	Porosity (%)
9325.8	0.011	5.79
9326.8	0.002	4.22
9333.8	0.001	3.33
9340.8	0.001	2.53
9342.8	0.001	2.03
9348.8	0.001	2.30
9352.8	0.005	2.15
9354.8	0.002	1.62
9356.8	0.001	2.26
9358.8	0.005	5.29
9360.8	0.002	4.13
9362.8	0.014	4.07
9364.8	0.003	4.04
9366.8	0.001	0.57
9368.8	0.001	1.04
9372.8	0.003	2.84
9374.8	0.002	2.68
9376.8	0.004	2.39
9378.8	0.009	2.90
9379.8	0.002	1.94
9382.8	0.001	2.51
9384.8	0.005	3.13
9387.8	0.007	5.29
9390.8	0.002	4.37
9394.8	0.001	3.73
9396.8	0.004	5.59
9398.8	0.002	4.58
9399.8	0.002	2.25
9401.8	0.003	2.95
9403.8	0.008	5.55
9405.8	0.014	7.65
9406.8	0.020	8.64
9407.8	0.019	8.36
9409.8	0.009	6.11
9411.8	0.031	3.46
9413.8	0.001	1.85
9424.8	0.000	0.43
9427.8	0.000	2.27
9429.8	0.000	1.83

Water saturation values in the Mesaverde Group and Wasatch/Colton Formation have similar trends. S_w values are lower in the southern and southeastern area near Book Cliff outcrops. Lower S_w values possibly reflect the presence of hydrocarbons and/or the generally higher silt and shale content in the Mesaverde in the central and eastern parts of the basin. Water saturation values increase to 100% on the western and northern sides of the basin. The reason for this is unknown but may be related to coarse grain size and a higher recharge rate in those areas. BVW values are generally above 20% in the Mesaverde, meaning there is available water to flow in the pores.

The R_w values in the Mesaverde Group suggest variably salt-saturated water will be produced from its formations. Western and near-outcrop areas of the Uinta Basin could produce water in the lower saline range. Where R_w values approach 0.1 to 0.3, either saline or brine solutions could be produced with hydrocarbons. S_w and BVW values indicate the presence of hydrocarbons and water and that pore water is available to flow in the wells. Further studies should be conducted to correlate TDS and NaCl waters from laboratory analyses to formation water resistivity from logs.

Water Production, Use, and Disposal

Significant water production occurs from oil and gas fields producing from the Mesaverde Group (figure 6.23). These fields include Big Valley, Devil's Playground, Gate Canyon, Natural Buttes, Nine Mile Canyon, Pariette Bench, Peter's Point, Red Wash, and Rock House (figure 1.1) (Wood and Chidsey, 2015). Cumulative water production from all of the fields producing from the Mesaverde Group from first production through December 2014 was nearly 700 million bbls (table 6.6); note that production is commonly commingled with additional formations (Utah Division of Oil, Gas and Mining, 2015c).

Figure 6.24 shows the water-disposal well locations and water volumes for wells perforated in the Mesaverde Group. As of March 2015, there was only one Mesaverde disposal well, Jack Cyn U ST 14-32 (section 32, T. 12 S., R. 16 E., SLB&M, Carbon County, API No. 43-007-30913), originally a gas well completed in the Castlegate Sandstone, that was converted into an injection well in 2010. It has injected 710,626 BW since completion with an injection rate of approximately 431 barrels per day (BPD). The well is located in an area with an NGR between 0.61 and 0.70, suggesting good porosity sandstone, and where we map TDS of 25,000 to 30,000 mg/L.

Hydrocarbon Production

The Mesaverde Group is a primary hydrocarbon producer in the Uinta Basin, along with the Green River and Wasatch/Colton Formations. Natural gas is produced primarily from non-marine, lenticular, fluvial, tight-gas sandstone packages within the Neslen, Farrer, and Tuscher Formations in the central and eastern Uinta Basin, characteristic of basin-centered,

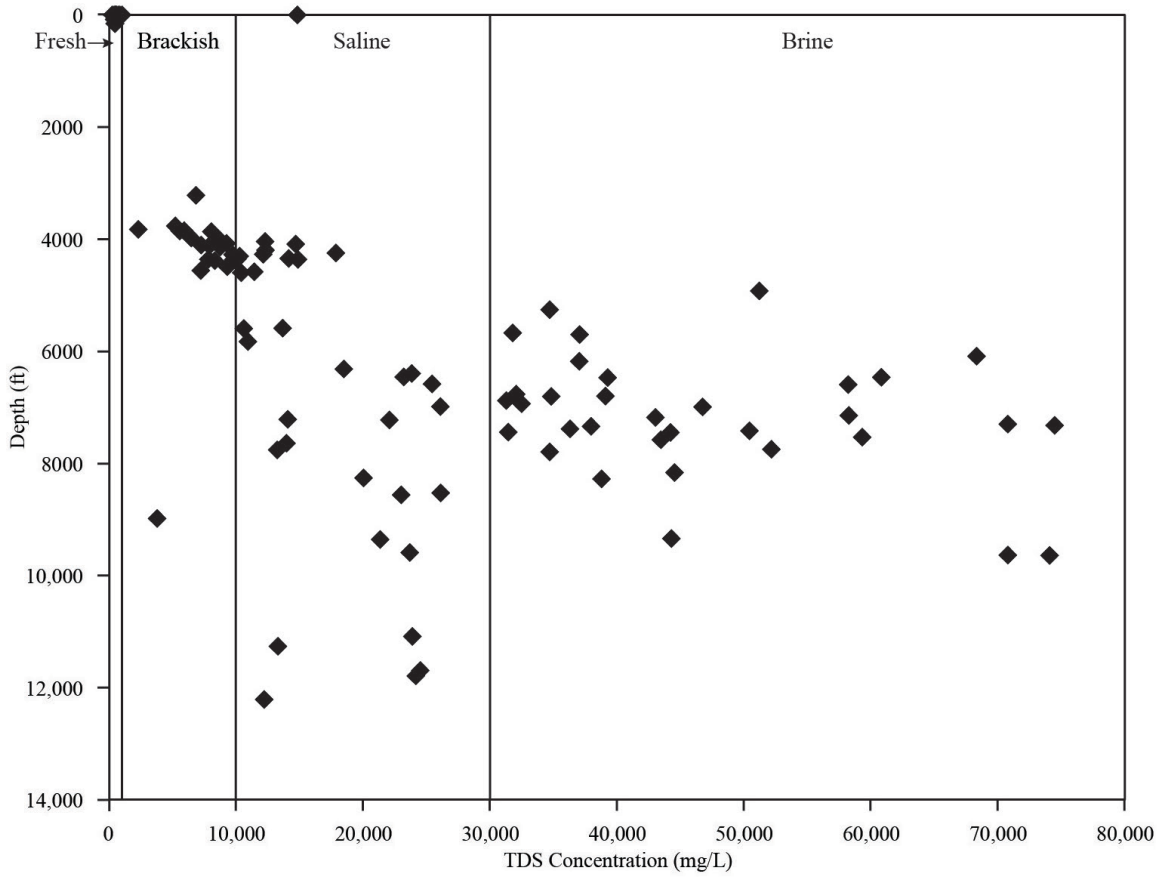

Figure 6.19. *Calculated TDS concentration with depth in the Mesaverde Group (number of samples: fresh – 13, brackish – 20, saline – 34, brine – 33).*

deep, tight-gas, pressure-drive systems rather than unconventional shale gas or coalbed methane systems (figure 6.25) (Keighin and Fouch, 1981; Anderson, 2005; Wood and Chidsey, 2015). Sandstone reservoirs in the Mesaverde are generally discontinuous, isolated, lenticular bodies of fluvial origin deposited when rivers carried sediment from the west (landward) to the eastward-regressing Cretaceous Western Interior Seaway (Johnson and Roberts, 2003). Production from the Mesaverde Group is typically commingled with the Wasatch/Colton Formation (figure 6.26). Though not as abundant as natural gas, oil produced from the Mesaverde Group is waxy and has the characteristics of oils sourced from coal or coal-rich organic matter, possibly from the lower Mesaverde coals in the Neslen Formation and Sego Sandstone (Lillis and others, 2003).

Between January 2009 and March 2015, the Mesaverde Group produced approximately 4.5 MMBO, 258.7 million cubic feet of gas (MMCFG), and 35.4 MMBW, and has a gas-oil ratio (GOR) of 57,047 and a oil-water ratio (OWR) of 0.13 (table 6.7). Commingled Mesaverde production increases to approximately 4.7 MMBO, 284 MMCFG, and 38 MMBW, and has a GOR of 60,243 and a OWR of 0.12. The GOR and OWR from table 6.7 indicate that Mesaverde production will produce more water for disposal than Wasatch/Colton production in the Uinta Basin.

UPPER PALEOCENE TO LOWER EOCENE WASATCH/COLTON FORMATION

Much of the Wasatch/Colton Formation formed when the paleo-California River transported sediment from as far south as the Mojave region in present-day California to the Uinta Basin and the deposits lapped onto the Douglas Creek arch (Dickinson and others, 2012). Previous studies (Osmond, 1964; Dickinson and others, 1986; Estes-Jackson and others, 2008) proposed the Wasatch/Colton formed as a result of erosion from nearby Laramide uplifts, or from recycled material from Laramide uplifts deposited by the California River (Wernicke, 2011). Detrital zircon ages, paleocurrents, and sandstone petrofacies indicate the southern portion, at least, had a more distant, southwestern source (Davis and others, 2010; Dickinson and others, 2012), and the northern portion of the formation may have formed from erosion of the Uinta uplift (Franczyk and others, 1990b; Jones and Plink-Björklund, 2015). The Colton Formation was previously known as the upper member of the Wasatch Formation, but later gained formation status and comprises the beds between the Flagstaff Limestone and the Green River Formation (Spieker, 1946). The Wasatch is the section of rock between the Mesaverde and the Green River where the Flagstaff Limestone is not present (figure 2.13). We aggre-

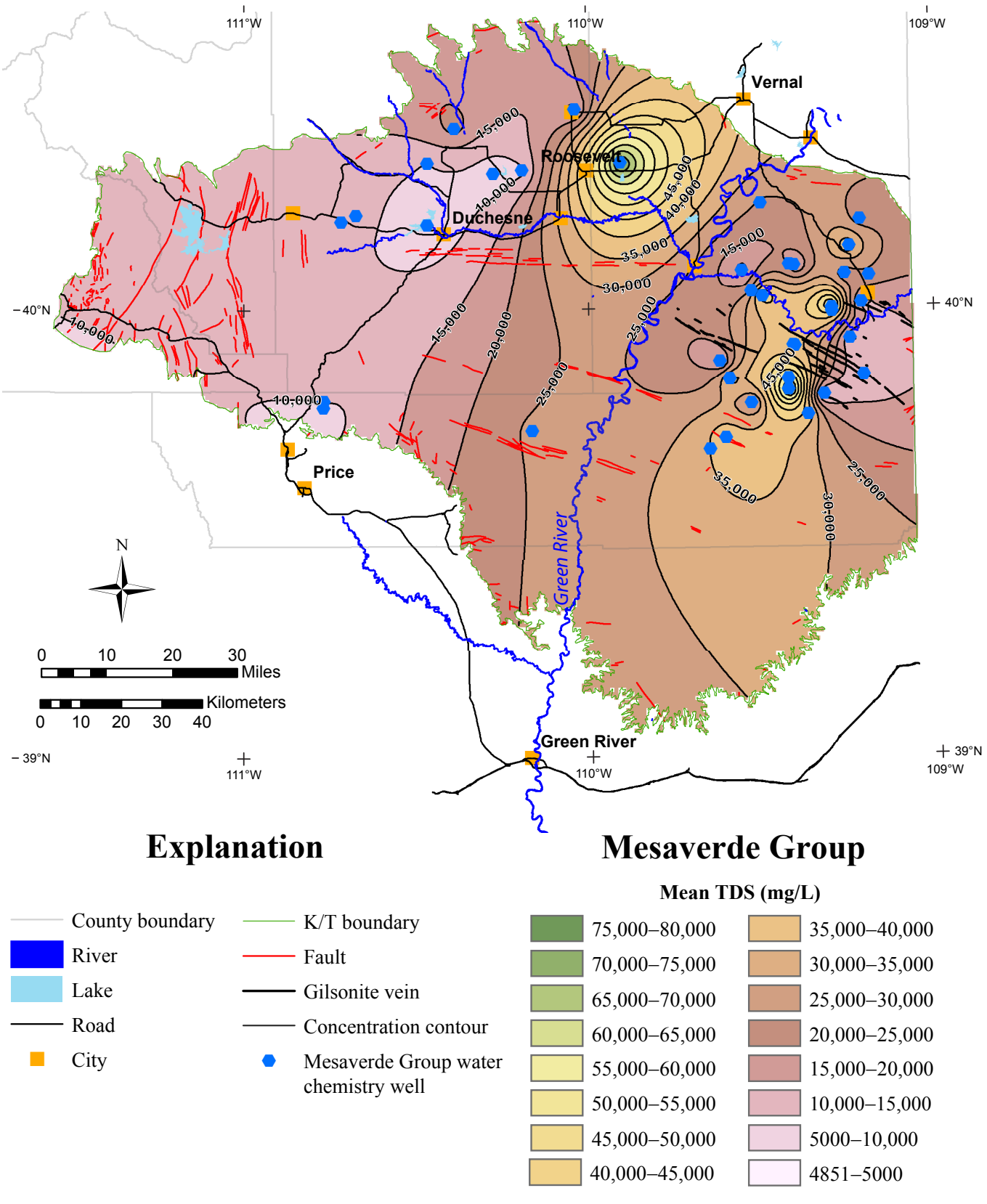

Figure 6.20. *TDS map of the Mesaverde Group. Contour intervals are 5000 mg/L. Data are from water samples from wells perforated in the Mesaverde and may not correspond to the wells used for the formation tops and thicknesses.*

Table 6.5. *Water classification based on total dissolved solids (Masters and Ela, 2007).*

Water Classification	Total Dissolved Solids (mg/L)
Fresh water	<1000
Brackish water	1000–10,000
Saline water	10,000–30,000
Brine	>30,000

gate the Colton and Wasatch Formations for this study because they are time equivalent (Sendziak, 2012), their faunas are the same, both formed in a fluvial depositional environment (figure 6.1C and 6.1D), they have similar lithologies (Spieker, 1946), and the production as reported by DOGM is not separated.

Thickness

The Wasatch/Colton Formation is exposed along the Roan Cliffs. Mapped thicknesses range from 400 to over 4000 feet

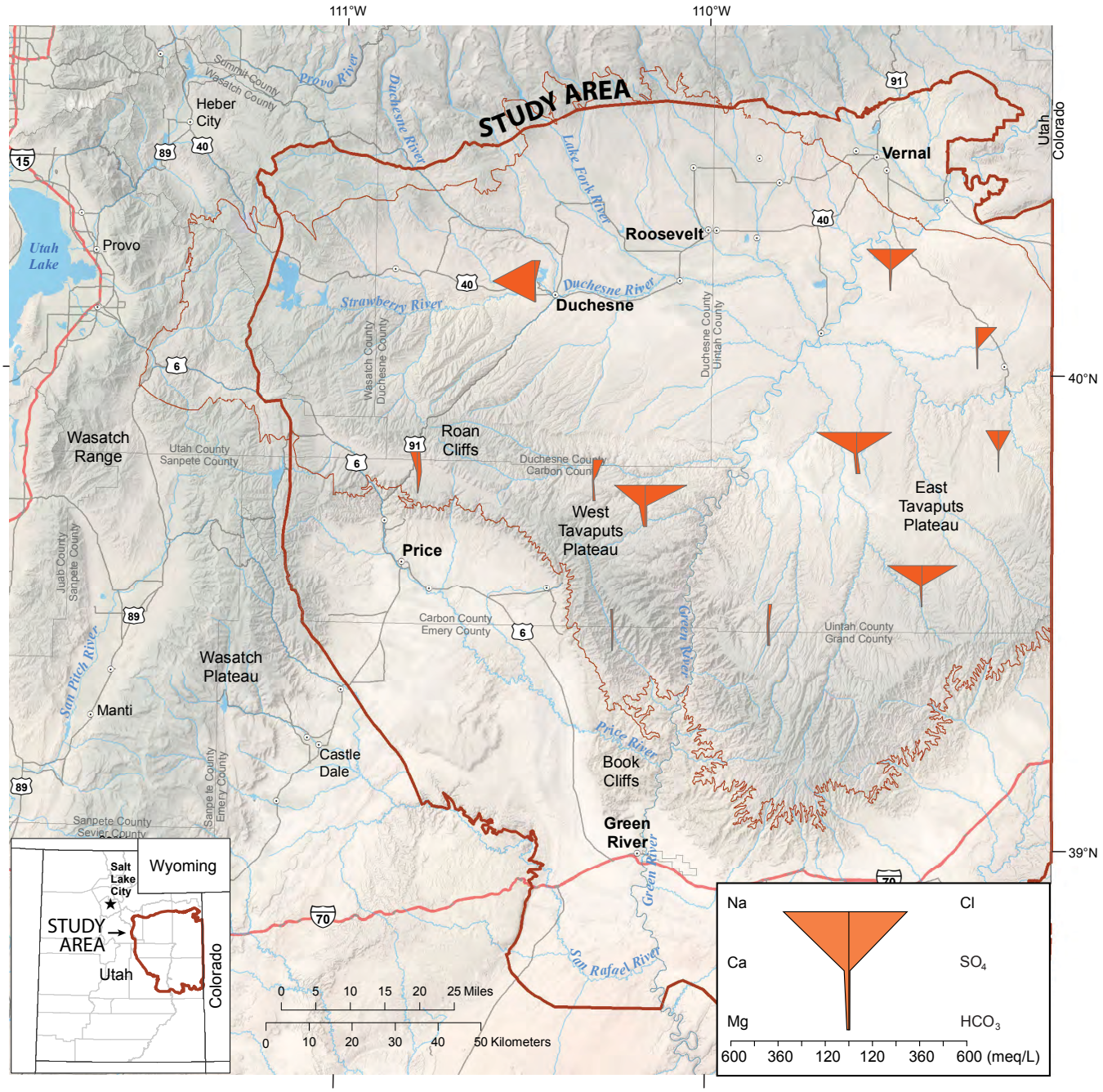

Figure 6.21. *Stiff diagrams from water samples sourced from the Mesaverde Group. Samples are freshest along the edges of the Uinta Basin and become saline in the basin interior.*

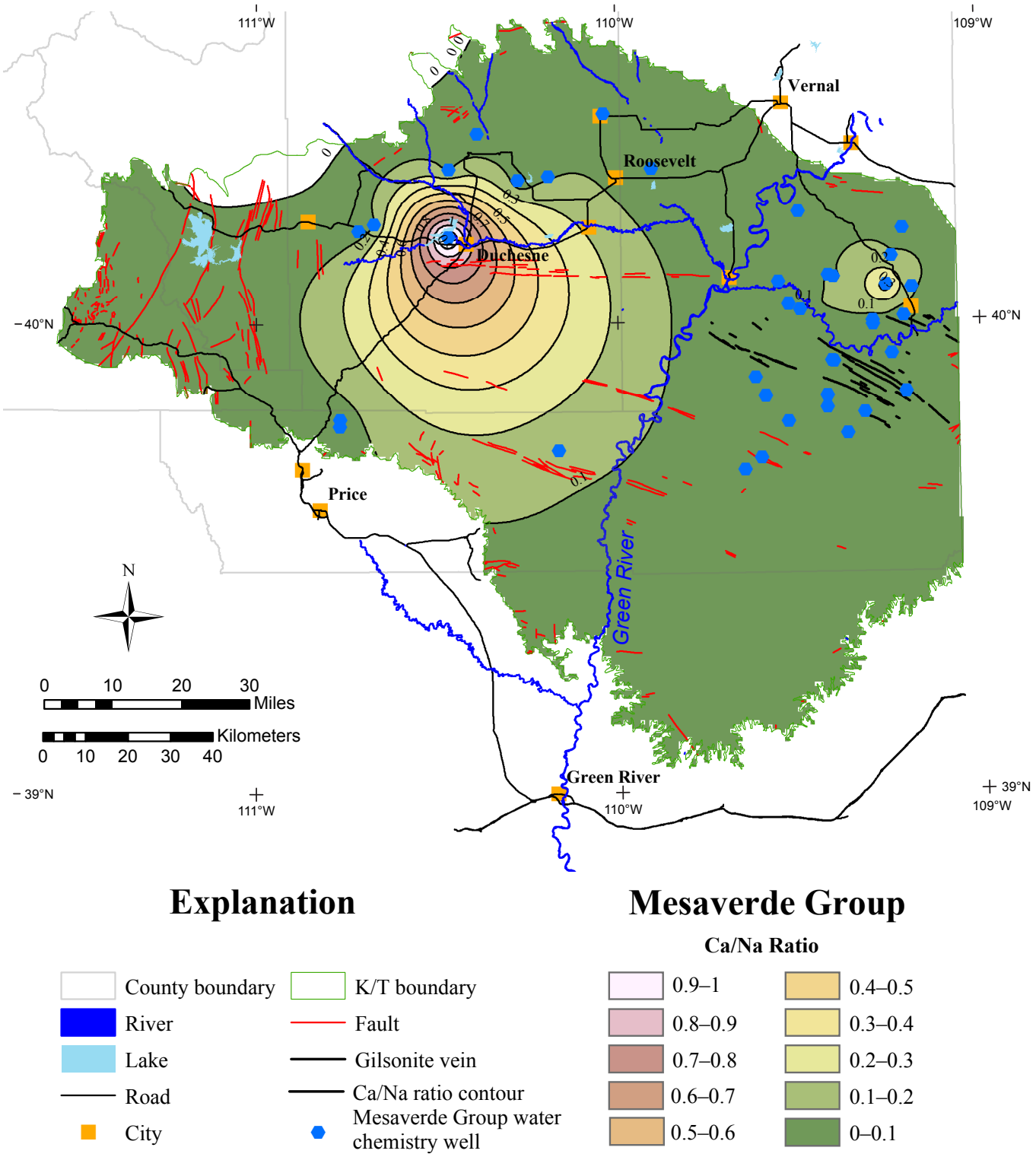

Figure 6.22. *Calcium/sodium ratio map for Mesaverde Group water. The Ca/Na ratio reveals the possible dissolution of carbonate from the Paleocene Flagstaff Limestone in the north-central part of the basin. The lower Green River carbonates are not suspected as being the source since a similar pattern is not observed in the Colton/Wasatch Ca/Na ratios (see figure 6.33).*

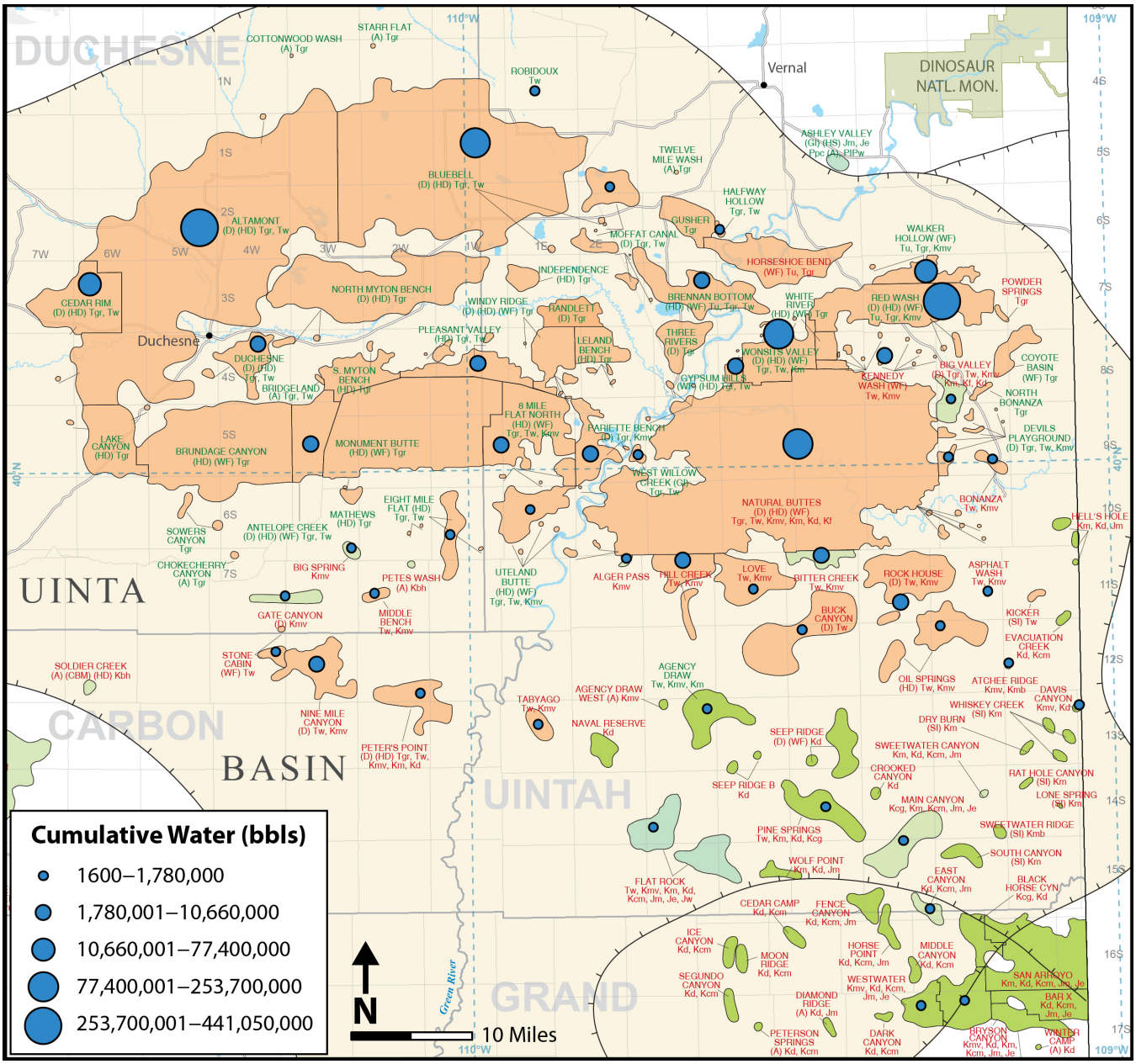

Figure 6.23. *Cumulative water production from Mesaverde Group and/or Wasatch/Colton Formation gas reservoirs in Uinta Basin fields. Production from a particular formation is not reported separately so data used on this map combine production from all producing formations in the field. Data are from the Division of Oil, Gas and Mining (2015). The field areas are color-coded by geologic age of the producing reservoirs; symbols of the producing reservoirs are listed under the field names (see figure 2.1 for age and formation names). Field designations are also listed under the field names: (A) = abandoned, (CBM) = coalbed methane, (D) = produced water disposal project, (HD) = horizontal drilling, (SI) = shut-in field, (WF) = waterflood project. Modified from Wood and Chidsey (2015).*

Table 6.6. *Cumulative production through December 2014 from the Utah Division of Oil, Gas and Mining (2015c); several fields produce from both the Wasatch/Colton Formation and the Mesaverde Group, and their water production is commingled.*

Producing Reservoir	Cumulative Oil (bbls)	Cumulative Gas (MCF)	Cumulative Water (bbls)
Wasatch	451,040,245	4,782,087,711	1,179,713,835
Mesaverde	151,041,333	4,540,565,692	668,422,168

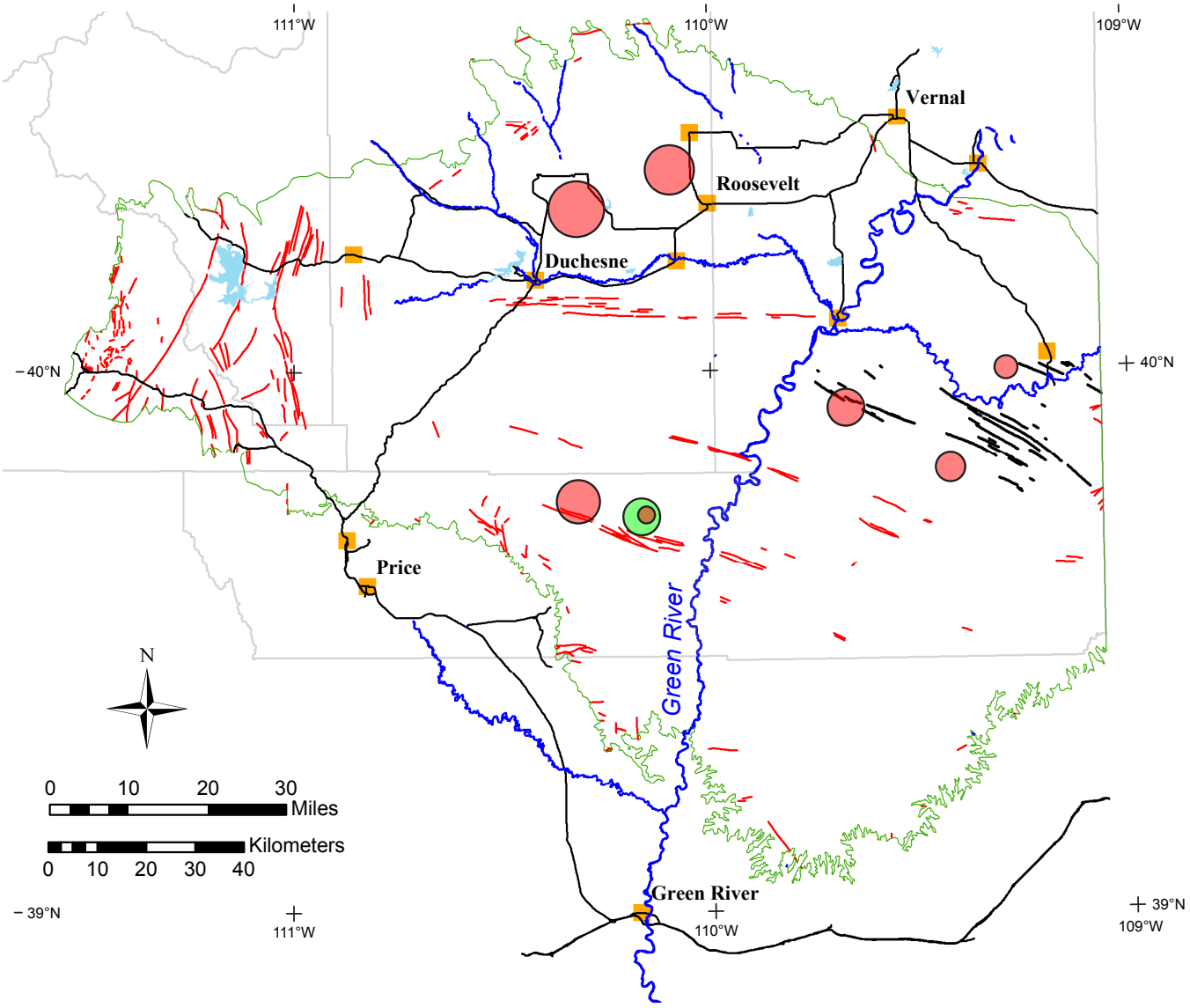

Explanation

- Wasatch/Colton disposal wells (7)
- Mesaverde Group disposal wells (1)
- County boundary
- River
- Lake
- Road
- City
- K/T boundary
- Fault
- Gilsonite vein

Barrels of Disposed Water

- 163,204
- 163,205–225,394
- 225,395–242,951
- 242,952–763,225
- 763,226–1,858,315
- 1,858,316–11,623,891
- 11,623,892–24,356,752

Figure 6.24. *Locations and total cumulative volumes for water-disposal wells into the Mesaverde Group and Wasatch/Colton Formation. Injection began in 1988 into the Wasatch/Colton and 2010 into the Mesaverde Group. Data are from the Division of Oil, Gas and Mining (2015).*

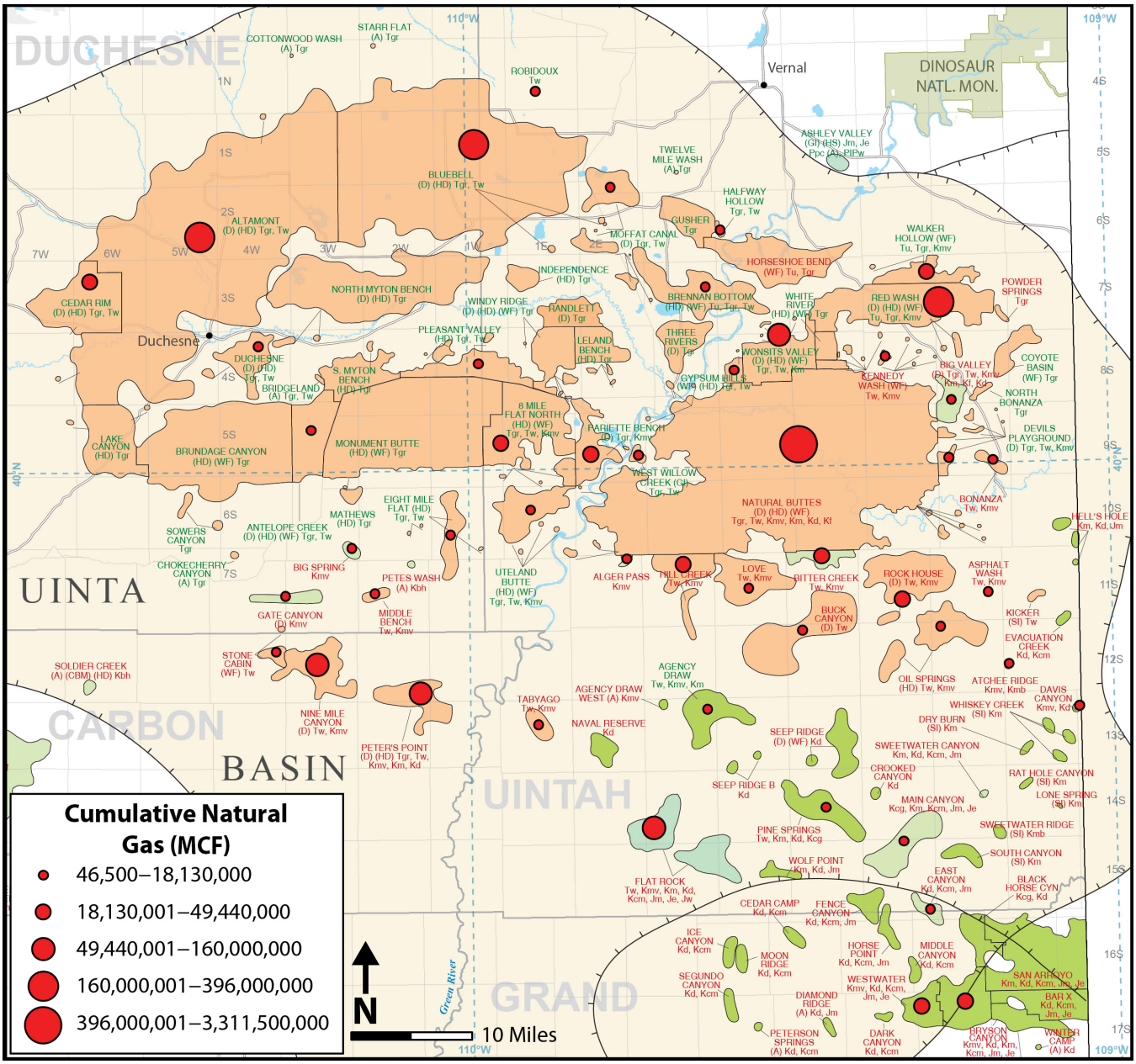

Figure 6.25. *Cumulative natural gas production (in MCF) from Mesaverde Group and/or Wasatch/Colton Formation reservoirs in Uinta Basin fields. Production from a particular formation is not reported separately so data used on this map combine production from all producing formations in the field. Names in red denote fields that produce(d) primarily nonassociated natural gas whereas those in green primarily produce(d) oil. The field areas are color-coded by geologic age of the producing reservoirs; symbols of the producing reservoirs are listed under the field names (see figure 2.1 for age and formation names). Field designations are also listed under the field names: (A) = abandoned, (CBM) = coalbed methane, (D) = produced water disposal project, (HD) = horizontal drilling, (SI) = shut-in field, (WF) = waterflood project. Modified from Wood and Chidsey (2015).*

(120–1200+ m) (figure 6.27). The unit is thickest in a northeasterly trending band starting north of Helper and extending toward Jensen in the northeastern Uinta Basin and thins away from this curved band (figure 6.27). At depth, Nelson and Hoffman (2009) reported the formation to be 3000 feet (900 m) thick in the west and 2000 feet (600 m) thick in the eastern Uinta Basin. The Wasatch/Colton depositional basin has shifted toward the south compared to the older Mesaverde Group basin (compare figure 6.4 to 6.27).

Depth

The Wasatch/Colton Formation is exposed along the southern margin of the Uinta Basin along the Roan and Book Cliffs (Witkind, 1988) and along a thin strip of the northeastern margin of the basin along Raven Ridge (Sprinkel, 2007). The Uinta Basin is an asymmetrical syncline and, as mentioned above, units within the southern and central parts of the basin dip gently northwest whereas outcrops along the northern

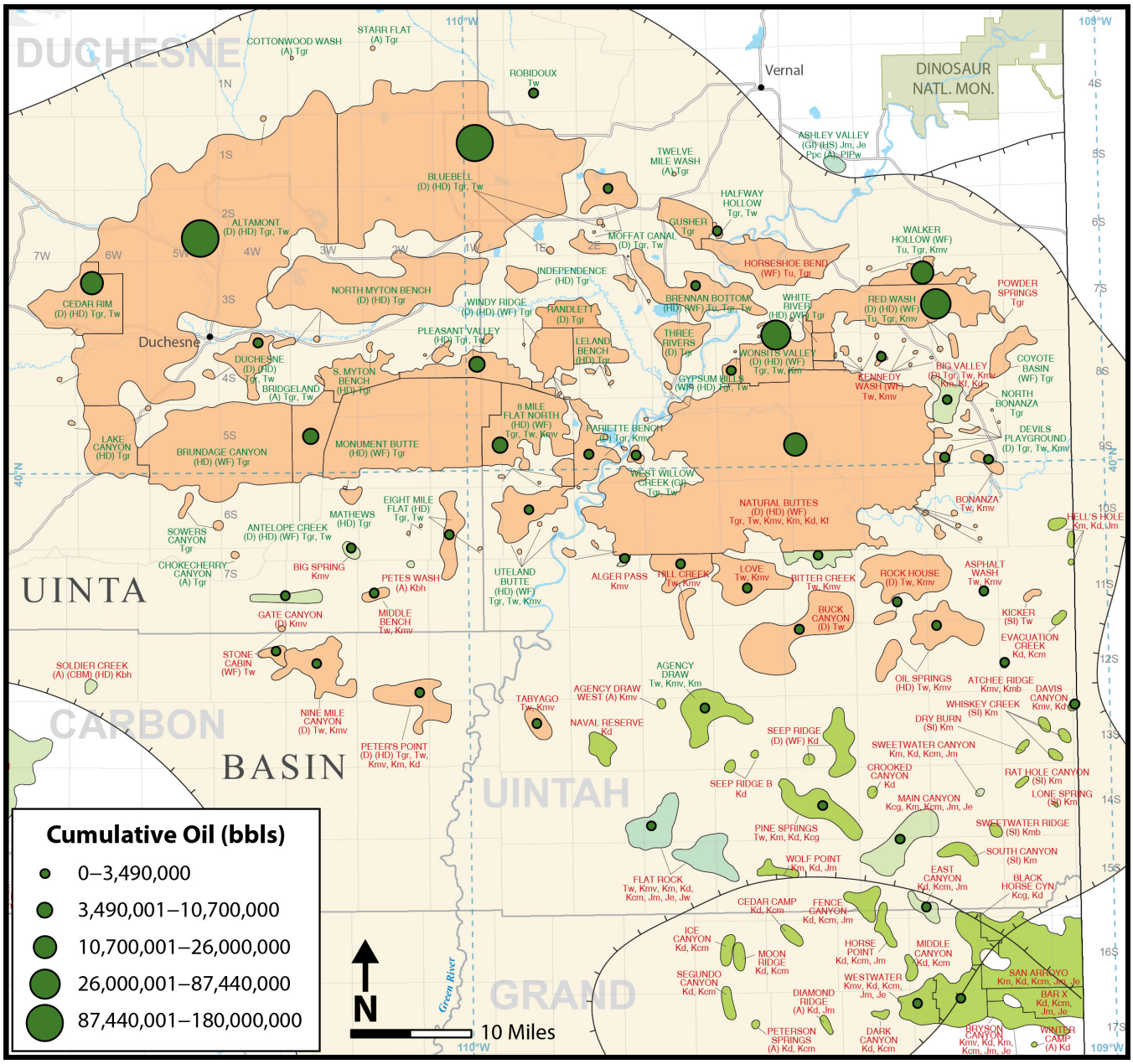

Figure 6.26. *Cumulative crude oil production (in barrels [bbls]) from Mesaverde Group and/or Wasatch/Colton Formation reservoirs in Uinta Basin fields. Production from a particular formation is not reported separately so data used in this map combine production from all producing formations in the field. Names in red denote fields that produce(d) primarily nonassociated natural gas whereas those in green primarily produce(d) oil. The field areas are color-coded by geologic age of the producing reservoirs; symbols of the producing reservoirs are listed under the field names (see figure 2.1 for age and formation names). Field designations are also listed under the field names: (A) = abandoned, (CBM) = coalbed methane, (D) = produced water disposal project, (HD) = horizontal drilling, (SI) = shut-in field, (WF) = waterflood project. Modified from Wood and Chidsey (2015).*

margin dip steeply to the south (figure 6.28) (Keighley, 2015). In the deepest area of the Uinta Basin, the Wasatch/Colton top reaches depths greater than 16,000 feet (4900 m).

Lithology

The Wasatch/Colton Formation contains discontinuous, lenticular, fluvial, red to tan channel sandstones and variegated shale floodplain sediments that were deposited adjacent to Lake Uinta (figures 1.3 and 6.29) (Bredehoeft and others, 1994; Johnson and Roberts, 2003; Estes-Jackson and others, 2008; Nelson and Hoffman, 2009). Jones and Plink-Björklund (2013) divide the Wasatch/Colton into three packages: (1) a lower package containing isolated, filled, fluvial channels up to ~30 feet (9 m) thick, interpreted to have been rapidly deposited; (2) a middle package composed of amalgamated, filled, fluvial channels up to ~100 feet (30 m) thick, deposited in a system with a high depositional rate; and (3) an upper pack-

Table 6.7. *Total oil, gas, and produced water from January 2009 through March 2015 for producing zones in the Wasatch/Colton Formation and Mesaverde Group. The formations generally show combined perforations. Wasatch/Colton and Mesaverde production is summarized at the bottom of the table. Data are from the Division of Oil, Gas and Mining (2015).*

Producing Reservoir	Total Oil (bbls)	Total Gas (MCF)	Total Produced Water (bbls)	Gas-Oil Ratio (cfg/BO)	Oil-Water Ratio (BO/BW)	Gas-Water Ratio (cfg/BW)
Mesaverde–Lower Douglas Creek Member, Green River Formation	–	220,692	95,186	–	0.00	2318
Mesaverde–Middle Douglas Creek Member, Green River Formation	–	139,642	75	–	0.00	1,861,893
Mesaverde–Mancos Shale	183,884	24,854,696	2,597,971	135,165	0.07	9567
Mesaverde	4,534,438	258,675,908	35,383,530	57,047	0.13	7311
Mesaverde–North Horn	589	392,231	6033	665,927	0.10	65,014
Mesaverde–Flagstaff	5028	7987	32,922	1589	0.15	243
Wasatch–North Horn	255	107,574	2283	421,859	0.11	47,120
Wasatch–Mesaverde	8,344,623	1,483,576,425	123,247,961	177,788	0.07	12,037
Wasatch–Middle Mesaverde	249,077	15,756,764	1,971,082	63,261	0.13	7994
Wasatch/Colton	13,336,887	156,082,095	36,037,750	11,703	0.37	4331
Wasatch	21,935,870	1,655,530,845	161,291,998	575,471	0.14	10,264
Mesaverde (comingled)	4,718,911	284,283,169	38,082,795	60,243	0.12	7465

age with isolated sandstone channels up to ~50 feet (15 m) thick, deposited at a moderate rate in a fluvial environment. The formation is thickest in the south-central Uinta Basin (figure 6.27) and thins towards the margins of the basin (Johnson, 2003). The thickest region curves from the Uinta uplift in the northwest through the center of the basin and ends near Jensen, Utah (Franczyk and others, 1990b). Sandstones in the Wasatch/Colton record the progradational deltas marking the transition from the shallow Lake Flagstaff to Lake Uinta (Morris and others, 1991). Thick channel sandstones of the Wasatch Formation interfinger with, and are equivalent to, the middle Green River Formation (Morgan, 2003a).

Reservoir Properties

We calculated several reservoir properties for the Wasatch/Colton interval (table 6.1). Two reservoir properties describe the amount of sand (gross sand) and porous sand (net sand) in a defined interval. Gross sand is the thickness of sand (in a particular well or interval) that meets a particular GAPI classification. In our study, gross sand was defined as sand intervals having normalized GR values of <60 GAPI regardless of other parameters. Net sand is further defined as having a porosity value greater than or equal to a defined value. Correctly adjusted or calculated porosity from acoustic, density, or resistivity logs is used for the porosity comparison. In our study, net sand is defined as having a GR value less than or equal to 60 GAPI and acoustic (sonic) sandstone porosity ≥ 6%.

The Colton reservoir in the western part of the Uinta Basin is a smaller percentage of the combined Wasatch/Colton reservoir area. Most of the reservoir properties come from logs through the Wasatch the east part of the basin. However, several logs, through the Colton, were used for petrographic analaysis. Appendix E lists the NGR sand parameters from GR and PHIS curves in the Wasatch/Colton Formation. The NGR was calculated using a minimum 6% porosity and a maximum 60 GAPI cutoff for the net sand portion. The Wasatch/Colton interval has great thicknesses of sandstone and the NGR is generally over 50% (figure 6.30; table 6.1). The average porosity of the Wasatch/Colton Formation for the entire Uinta Basin area is 24% (table 6.1). Sixteen out of 44 wells have PHIA values less than 20%. The generally higher NGR and PHIA in this interval suggest favorable conditions for water disposal. Since the Wasatch is an oil reservoir in the central parts of the basin, it would lend itself to waterflooding or injection for disposal.

Permeability of Wasatch Formation sandstones in the Greater Natural Buttes field area ranges from less than 0.01 mD to 0.1 mD with a median permeability of 0.095 mD (Stancel and others, 2008). Estes-Jackson and others (2008) reported Wasatch permeability values from 0.22 to 37 mD. Using PHIS values from sonic logs, the average porosity, not limited by 6% or greater porosity, in the Wasatch and Colton equals about 16% and 15%, respectively (table 6.8), but these values decrease when adjusted for the presence of hydrocarbons. Porosity values within the Wasatch/Colton Formation have a wider range and higher average compared to the Mesaverde Group.

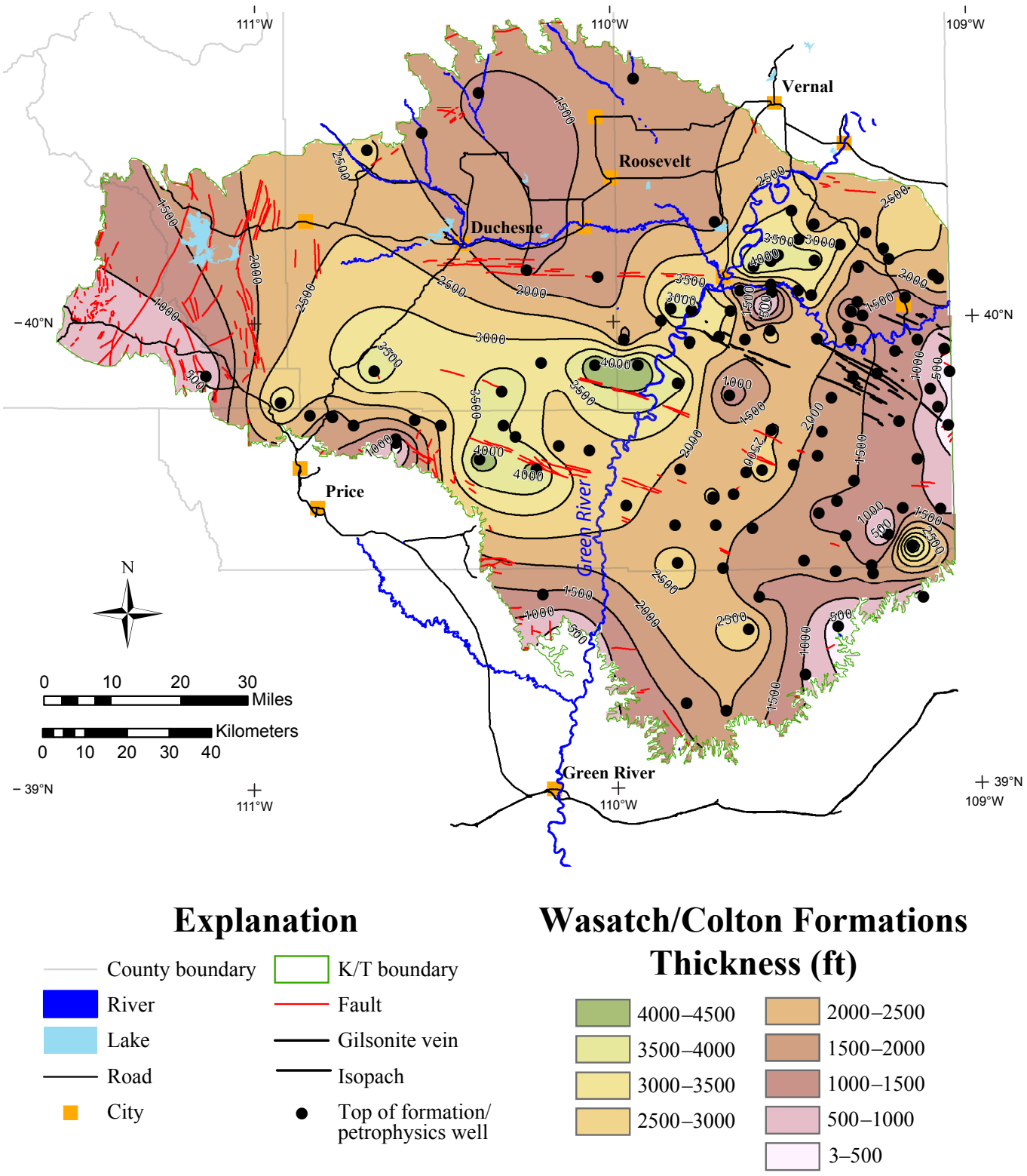

Figure 6.27. *Thickness of the Wasatch/Colton Formation. The contour range is 0 to 4500 feet, and the contour interval is 500 feet. Tops data are from Hettinger and Kirschbaum (2002), Anderson (2005), and selected well logs as part of this study.*

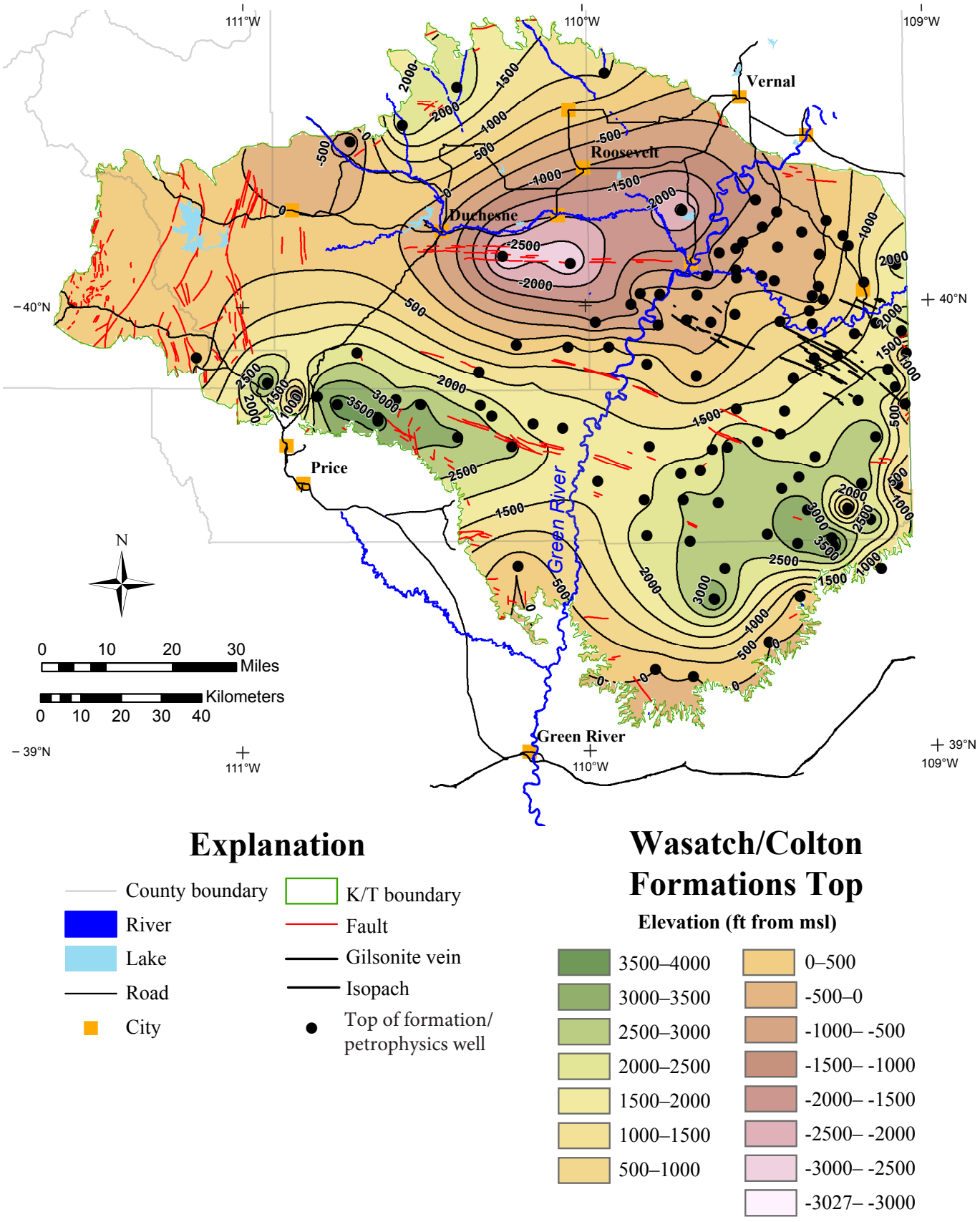

Figure 6.28. *Structure of the top of the Wasatch/Colton combined formations. Contour interval is 500 feet. Tops data are from Hettinger and Kirschbaum (2002), Anderson (2005), and selected well logs as part of this study.*

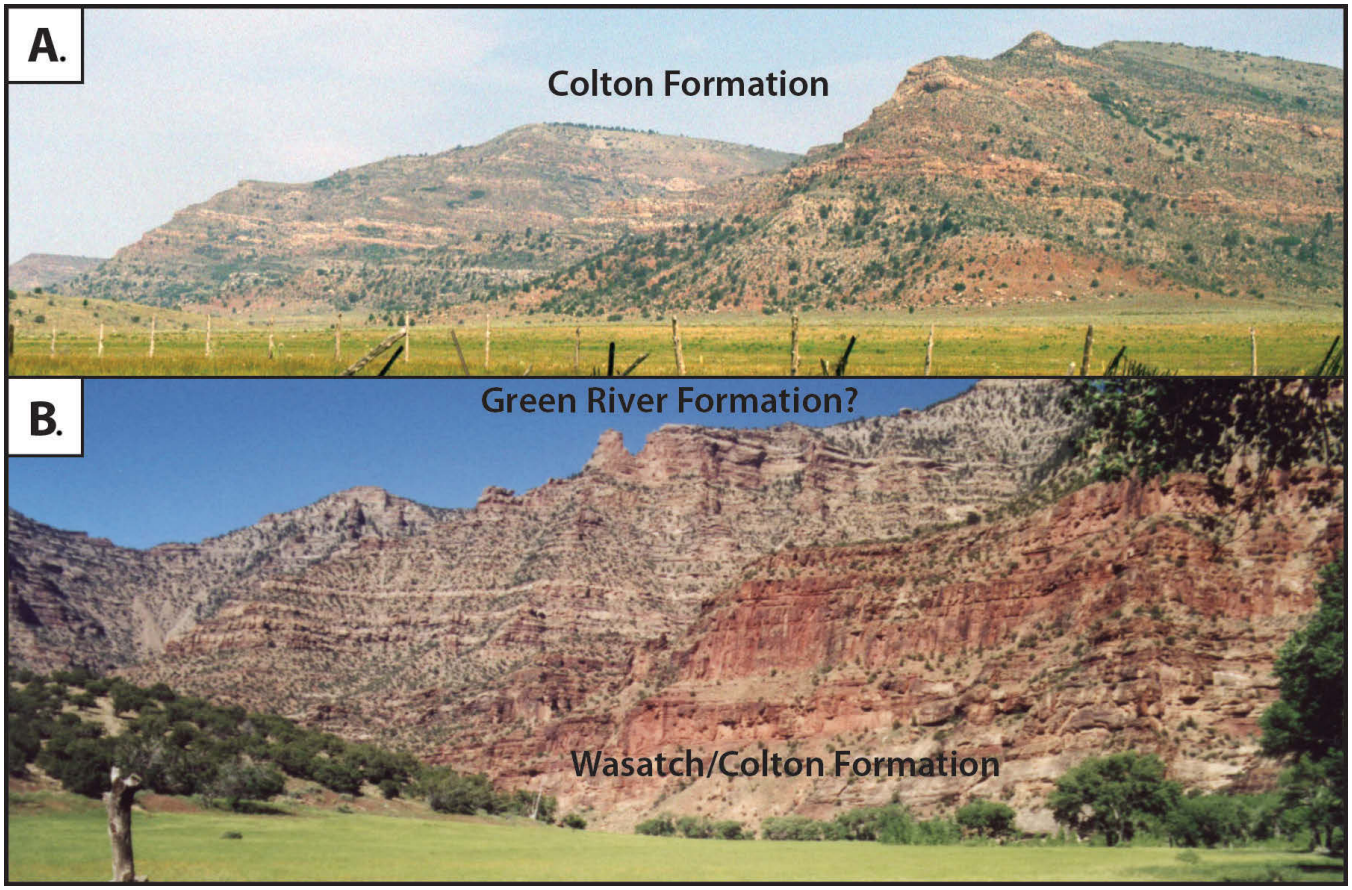

Figure 6.29. *Representative outcrops of the Wasatch/Colton Formation.* ***A.*** *Outcrop of the Colton Formation at Whitmore Park along the western Roan Cliffs. The formation in this locality is composed of red to tan silty slopes and cliff-forming channel sandstones that pinch out laterally.* ***B.*** *A closer view of the Wasatch/Colton Formation along the Green River in Desolation Canyon, southern Uinta Basin. Photos by Craig D. Morgan, UGS.*

Water Quality

Water quality data from the Wasatch/Colton Formation predominantly range from brackish to brine (table 6.5; figures 6.31 and 6.32). We attempted to determine if R_w, S_w, and BVW data could be determined from PHIS, SP, and RESD logs and if they correlate to several water samples identified from the water sample database in appendix D. Appendix E shows R_w values for the Wasatch/Colton Formation. Higher R_w values, indicating fresher water, are found around the margins of the basin, likely directly related to recharge at the southern, eastern, and northern outcrops (figure 2.1). There is also a high-R_w location at the approximate Three Rivers location north of Ouray and contiguous with the trend of the gilsonite veins (figures 2.1, 3.1, and 3.7, plate 1). The R_w values calculated from well logs generally match those values calculated from laboratory samples. We predict, however, that formation water from the Wasatch/Colton will have low resistivity values, indicating at least saline to brine water for treatment. Calcium-sodium ratios from water in the Wasatch/Colton are higher in the western Uinta Basin, possibly due to ancient recharge from the Wasatch Plateau (figure 6.33). It could also suggest local connections to the Flagstaff limestones or the lower carbonaceous section of the Green River Formation. The R_w calculated from well logs and TDS from water samples appear to correlate. Patterns from an R_w contour map from the Wasatch/Colton would be similar to the TDS map presented on figure 6.32.

Water saturation was calculated using PHIS and SP curves from several wells. The Wasatch/Colton interval generally has 20% to 40% water saturation with pockets of 60% to 100% saturation. Higher (>20%) saturations occur near regional features such as the gilsonite veins (figure 2.1, plate 1) and along northern outcrops. Southern outcrop locations have a water saturation of approximately 20%. Although S_w data are sparse in the northern part of the basin, the closest available wells with data show high water saturation, and it is very likely that water saturation approaches 100% on the northwestern side of the basin, reflecting lower hydrocarbon concentration. However, the predicted S_w and BVW values could change if more data were available in the northwestern part of the Uinta Basin. BVW values generally vary in the interval and are between 0.2% and 11%. A BVW approaching zero indicates irreducible water that is not available for flow. The existing BVW and S_w data suggest that water will flow from the formation and that the Wasatch/Colton possibly has pore space available for water disposal. As noted earlier, the

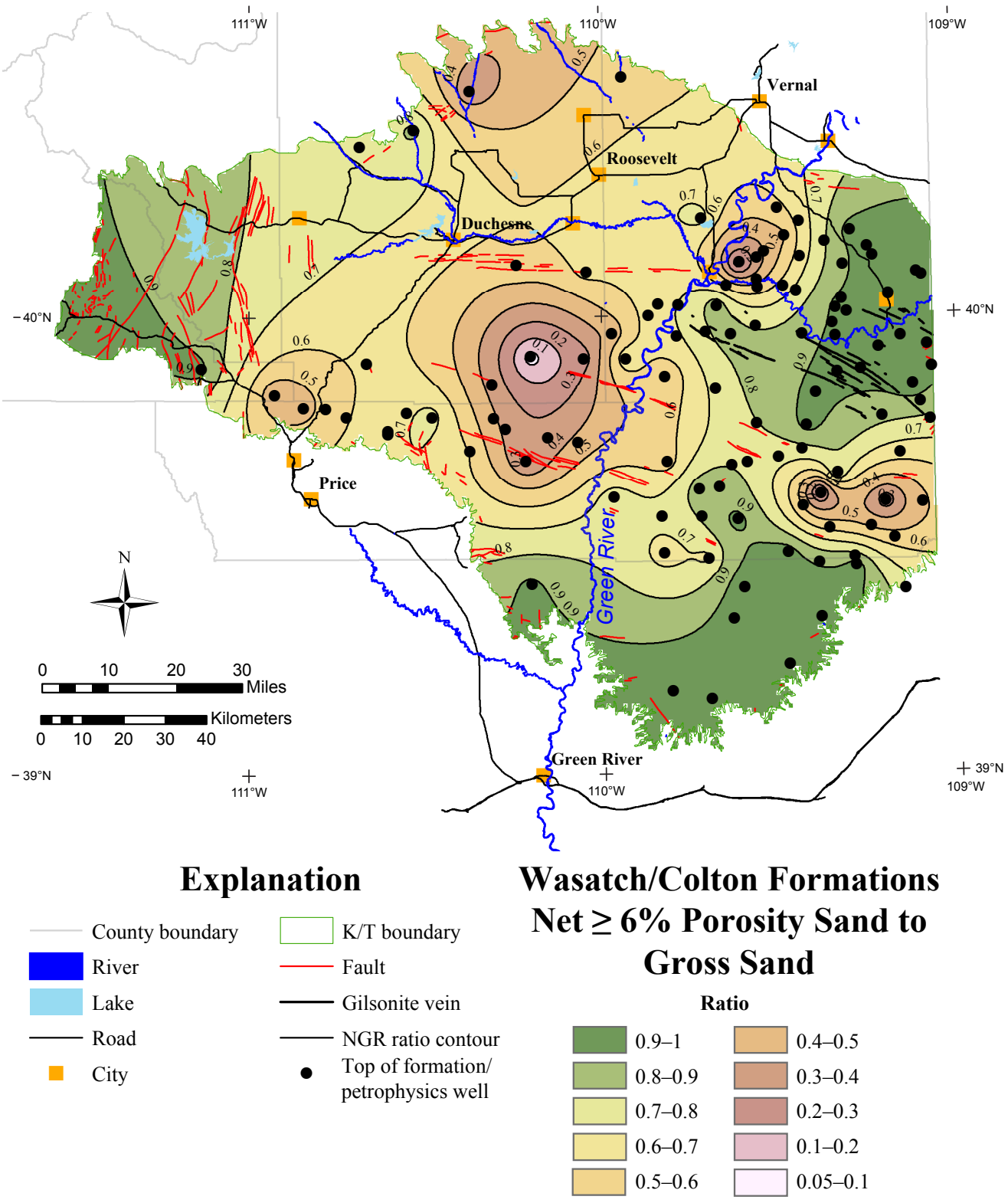

Figure 6.30. *Net to gross ratio (NGR) of sands within the Wasatch/Colton Formation.*

Table 6.8. *Porosity values from sonic logs within the Wasatch/Colton Formation.*

Formation	Count	PHIS (average)	Gas Adjustment	Oil Adjustment
Wasatch	24	0.16	0.112	0.144
Colton	32	0.15	0.105	0.135

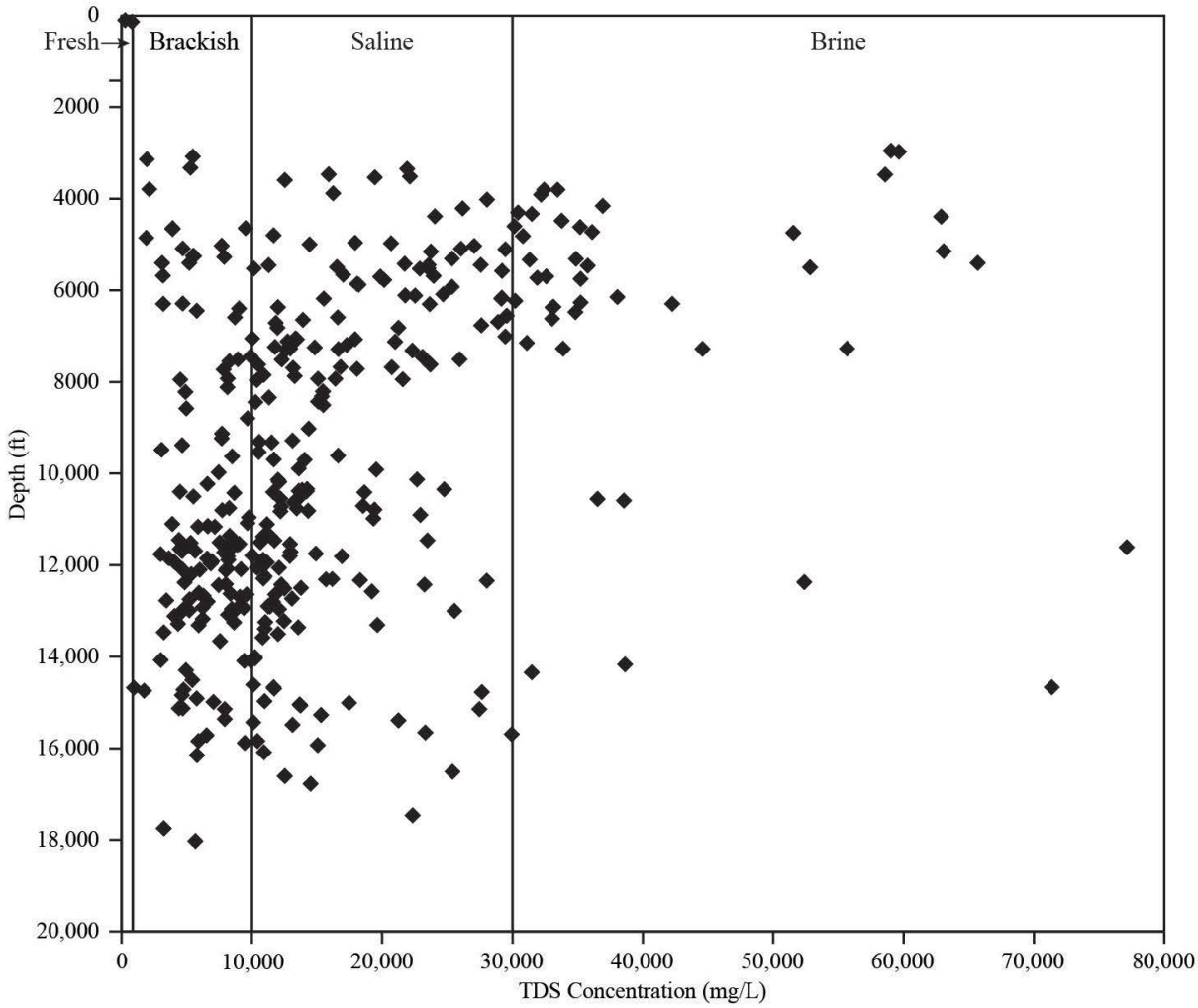

Figure 6.31. *Calculated TDS concentration with depth in the Wasatch/Colton Formation (number of samples: fresh – 5, brackish – 129, saline – 178, brine – 45).*

Wasatch/Colton strata are highly interbedded sandstone and shale, but sandstone beds should be injectable and available for waterflooding disposal purposes.

Water Production, Use, and Disposal

Significant water production occurs within oil and gas fields producing from the Wasatch/Colton Formation. These fields include Altamont, Antelope Creek, Big Valley, Bluebell, Buck Canyon, Cedar Rim, Devils Playground, Duchesne, Moffat Canal, Natural Buttes, Nine Mile Canyon, Peter's Point, Rock House, and Wonsits Valley (figures 1.1 and 6.23) (Wood and Chidsey, 2015). Cumulative water production from all fields producing from the Wasatch/Colton Formation from first production through December 2014 totals nearly 1.2 billion barrels (table 6.6); again, production is commingled with additional producing formations in each field (Utah Division of Oil, Gas and Mining, 2015c).

Figure 6.24 shows seven water disposal wells completed into either the Wasatch/Colton Formation, or a combination of North Horn and Wasatch/Colton Formations, or lower Green River and Wasatch/Colton Formations. Over 663 million barrels has been injected into the Wasatch/Colton Formation between the first completion in 1986 and March 2015. One water disposal well in Bluebell field (figure 6.23) has been injecting since 1986. Figure 6.24 shows the injection volumes in red for the Wasatch/Colton disposal wells. Two wells, Lake Fork No. 2-23B4 (section 23, T. 2 S., R. 4 W., UBL&M, Duchesne County, API No. 43-013-30038) and Central Bluebell No. 2-26A (section 26, T. 1 S., R. 2 W., UBL&M, Duchesne County, API No. 43-013-30389) are private, fee-based disposal wells and have the highest injection rates of 2483 and 1103 BPD, respectively. The water injection rates into the private wells are two to three times higher than the injection rates for other wells in the same formations. The private wells are in an area with NGR values of 0.51 to 0.60, so they should have over 50% sand with high porosity. Typically, the injection rates in the Wasatch/Colton Formation are lower than the single Mesaverde Group disposal well rate of 431 BPD. This implies an overall lower NGR exists for the disposal wells completed in the Wasatch/Colton. It may be difficult to locate and complete high-porosity zones in the Wasatch/Colton that are not already producing hydrocarbons.

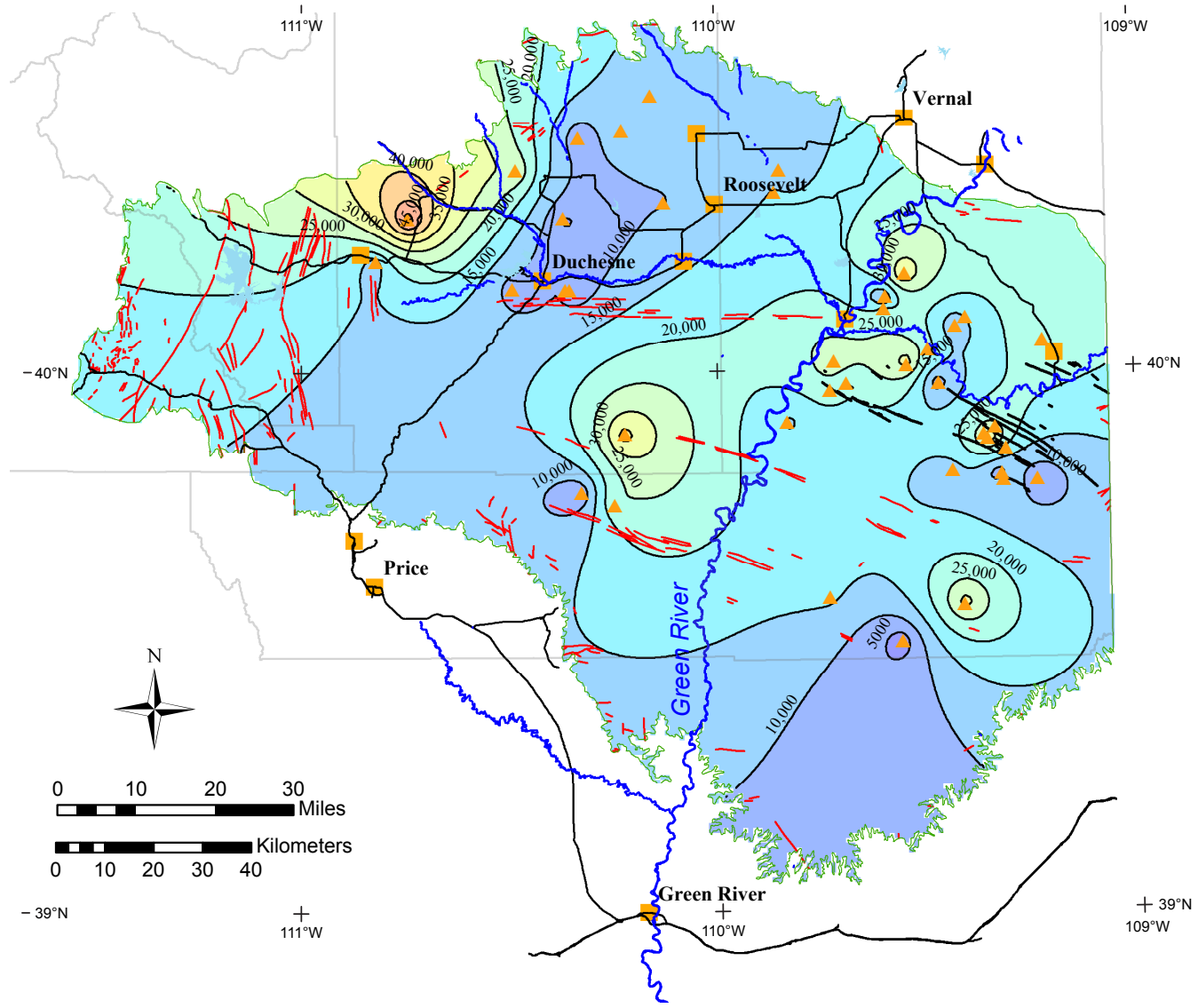

Explanation

- County boundary
- River
- Lake
- Road
- City
- K/T boundary
- Fault
- Gilsonite vein
- TDS concentration contour
- Wasatch/Colton water chemistry well

Wasatch/Colton Formations

TDS (mg/L)

- 50,000–55,000
- 45,000–50,000
- 40,000–45,000
- 35,000–40,000
- 30,000–35,000
- 25,000–30,000
- 20,000–25,000
- 15,000–20,000
- 10,000–15,000
- 5000–10,000
- 2025–5000

Figure 6.32. *TDS map of the Wasatch/Colton Formation. Contour intervals are 5000 mg/L.*

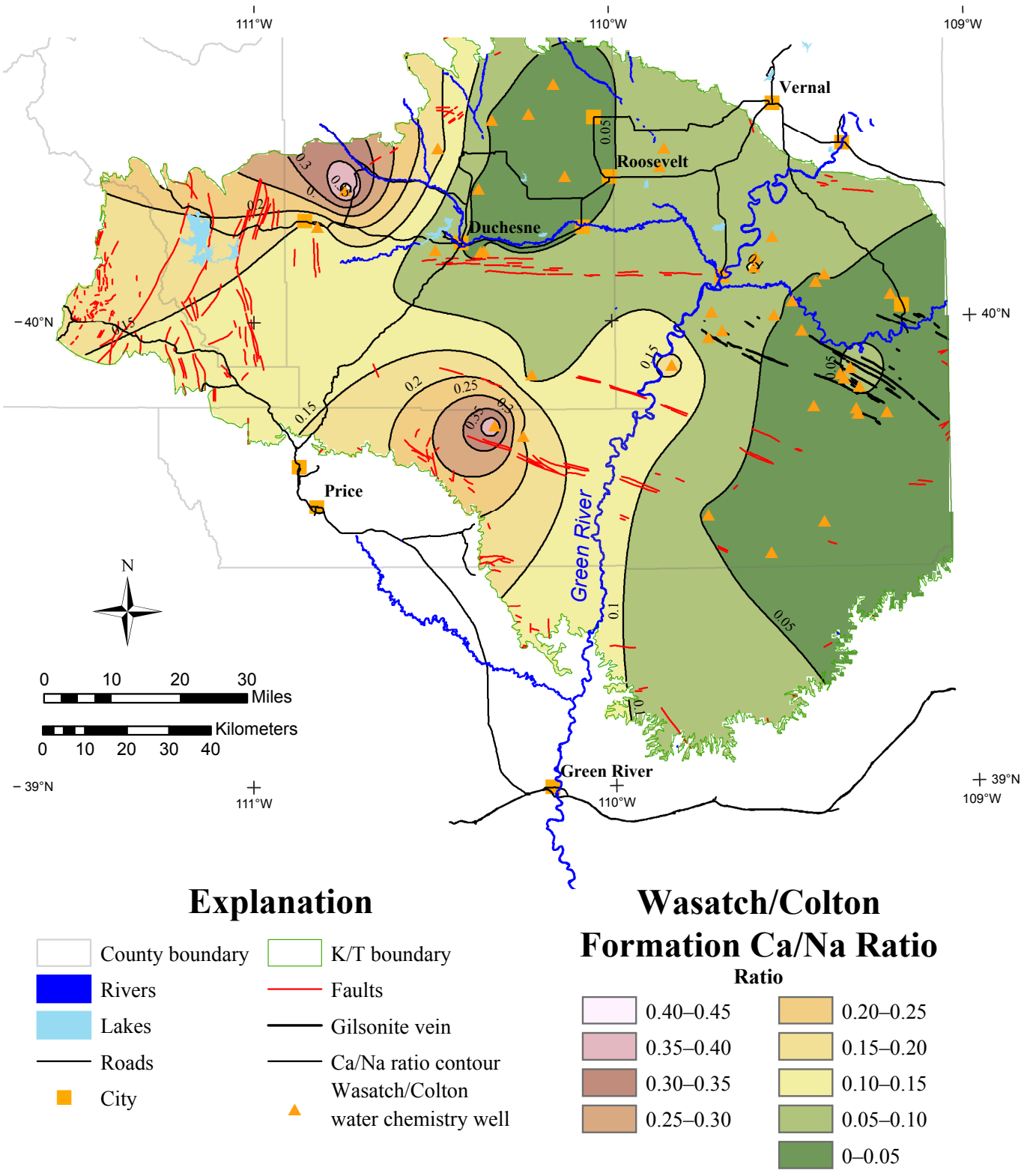

Figure 6.33. *Calcium/sodium ratio map for the Wasatch/Colton Formation water. The Ca/Na ratio values from the Wasatch/Colton are highest in the western Uinta Basin.*

Produced water from the Wasatch/Colton Formation and Mesaverde Group presents challenges for disposal. The high salt concentration precludes surface disposal into river and stream drainage systems and use for irrigation water without treatment, and it is expensive to evaporate. We believe that there are two options for disposing of produced water from the Mesaverde Group and the Wasatch/Colton Formation. One option would be to desalinate produced water to decrease the TDS to a level where the water can be used in hydraulic fracturing operations, possibly for irrigation water, or for other surface uses. The second option would be injection into sandstones of the Mesaverde Group or into the Wasatch/Colton Formation, either as disposal or waterflooding.

During our review and selection of formation tops for this project, we looked at numerous wells and found several candidate sandstones for injection throughout the Uinta Basin. For example, NBU No. 921-21L well (section 21, T. 9 S., R. 21 E., SLB&M, Uintah County, API No. 43-047-39256) in Natural Buttes field was drilled and completed in 2008, and has good logs and available core data. Figure 6.34 is the NBU No. 921-21L well log from 8200 to 8500 feet (2500–2590 m) measured depth, starting 60 feet (18 m) above the top of the Tuscher Formation and extending approximately 240 feet (73 m) below the upper contact. The zone was selected because it has three prominent, thick sandstone channels that can be traced laterally in several wells. Figure 6.34 shows the three identified sandstone channels, labeled S1, S2, and S3, with their measured depths and thickness. The GR log indicates they are essentially clean sands, and the NPHI and DPHI logs show gas crossover and an average porosity of 10% to 11%. We assume that the clean sandstones may have bed boundaries or other sedimentological structures and variations that could inhibit horizontal flow through the sandstones. Although these are gas-producing units, we calculated the radial volumetric storage potential of the three sandstones and present our results in table 6.9. The table presents 10-foot (3 m) radial increments from the 8200- to 8500-foot (2500–2590 m) interval. At radial distances of 100 and 1000 feet (30 and 305 m) from the well, we estimate storage of 42,375 BW and 4.2 MMBW, respectively, in the three sandstone channels. We did not attempt to calculate the radial flow rate using the Darcy equation as part of this study so the time involved in injecting this amount of water is unknown. There are likely hundreds of candidate sandstone channels in the Mesaverde Group formations. We believe other suitable sandstone channels exist in the Wasatch/Colton Formation interval as well; however, we think water disposal there will be less favorable since the sandstones are typically interbedded with siltstone. We believe the Mesaverde Group can provide good injection zones for water disposal in areas where they are not gas productive.

Hydrocarbon Production

Hydrocarbons produced from the Wasatch/Colton Formation are primarily found in channel sandstones and are interpreted to have been sourced from coals and carbonaceous shales in the Mesaverde Group (Lillis and others, 2003; Nelson and Hoffman, 2009). Production from the Wasatch/Colton is often commingled with the Mesaverde Group, Green River Formation, North Horn Formation, and Flagstaff Limestone. Table 6.7 shows the oil, gas, and water production from January 2009 through March 2015 from wells producing from the Wasatch and Mesaverde. Graphical cumulative gas and oil production reports are presented on figures 6.25 and 6.26.

The Wasatch/Colton Formation produces oil from over 4500 feet (1400 m) of strata, is up to 16,000 (4800 m) feet deep, and first became a target for horizontal drilling in the early 1990s (Chidsey and Laine, 1992). As shown in table 6.7, the Wasatch/Colton Formation interval produced 13.3 MMBO, 156 BCFG, and over 36 MMBW. The GOR is 11,703 whereas the OWR is 0.37. If commingled Wasatch production (Wasatch in table 6.7) is taken into account, approximately 21.9 MMBO, 1655 BCFG, and 161 MMBW have been produced with a GOR of 75,471 and an OWR of 0.14.

SUMMARY

The Cretaceous Mesaverde Group, a major producer of gas from tight-sand reservoirs, is more than 2000 feet (600 m) thick in much of the Uinta Basin; the upper formations of the Mesaverde Group may provide favorable locations for water disposal. Drilling depths for the Mesaverde Group are between 2000 feet (600 m) in the east to 12,000 feet (3700 m) in the middle of the basin. Much of the Mesaverde was deposited in a fluvial environment, and lithologies vary but are sand-dominated. Formation water types range from brackish to brine, and the freshest samples occur along the margins of the Uinta Basin. Hydrocarbons and associated water from the Mesaverde Group are predominantly produced in the eastern and southern Uinta Basin.

GR and SP curves for 115 wells were normalized and corrected to regional high and low response. Porosities from acoustic and density curves were recalculated to estimate sandstone porosity. The average sandstone porosity in the Mesaverde Group is 21%, ranging between 13% and 35%. A few permeability values were obtained from DST tests and a few core tests and range between 0.1 mD to 0.001 mD. The Mesaverde NGR is 0.76, indicating significant sand with porosity greater than 6%. The Bluecastle Tongue and lower members of the Castlegate Sandstone have the lowest NGR in the group at 0.58 and 0.61, respectively. The Sego, Farrer, and Tuscher Formations of the Mesaverde Group have the highest NGR values at 0.79, 0.74, and 0.83, respectively. However, the Sego Sandstone has the lowest average gross sand thickness at 79 feet (24 m). The Farrer and Tuscher Formations have average gross sand thicknesses of 150 and 211 feet (46 and 64 m). We believe that the Farrer and Tuscher are good candidates for disposal wells. Both formations, particularly the Tuscher Formation, have thick-blocky sandstones with good

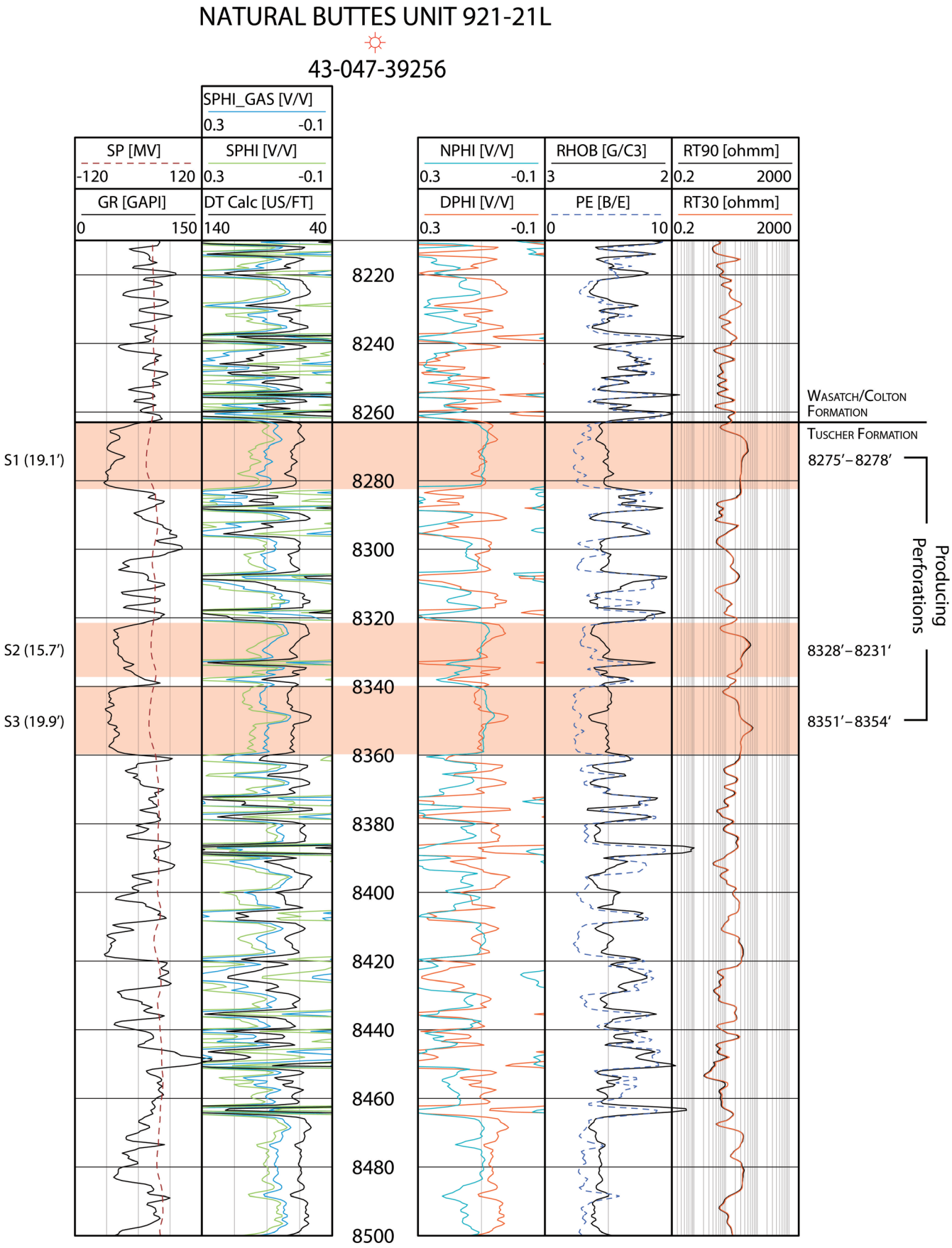

Figure 6.34. *Well log for NBU No. 921-21L, Natural Buttes field, revealing three large sandstone packages in the upper Tuscher Formation. Modeled sandstones are identified as S1, S2, and S3 on the left side of the log, and sandstone thickness is presented on the right side.*

Table 6.9. *Calculated volume of water storage per radial foot in three Tuscher Formation channel sandstones from the NBU No. 921-12L gas well, Natural Buttes field.*

		Radial Distance from Well (ft)														
		10	20	30	40	50	60	70	80	90	100	200	400	600	800	1000
Sandstone	**S1**															
Top (ft)	8263	Hydrostatic Head in Well: 3801 psi														
Bottom (ft)	8282															
Thickness (ft)	19															
Porosity (v/v)	0.11															
Volume (ft^3)		5969	23,876	53,721	95,504	149,226	214,885	292,482	382,018	483,491	596,903	2,387,610	9,550,442	21,488,493	38,201,766	59,690,259
Barrels of Water		156	624	1403	2495	3898	5613	7640	9979	12,630	15,592	62,368	249,474	561,316	997,895	1,559,211
Sandstone	**S2**															
Top (ft)	8321	Hydrostatic Head in Well: 3828 psi														
Bottom (ft)	8336															
Thickness (ft)	15															
Porosity (v/v)	0.10															
Volume (ft^3)		4712	18,850	42,412	75,398	117,810	169,646	230,907	301,593	381,704	471,239	1,884,956	7,539,822	16,964,600	30,159,289	47,123,889
Barrels of Water		112	448	1007	1790	2798	4029	5483	7162	9064	11,191	44,762	179,048	402,858	716,193	1,119,051
Sandstone	**S3**															
Top (ft)	8340	Hydrostatic Head in Well: 3836 psi														
Bottom (ft)	8359															
Thickness (ft)	19															
Porosity (v/v)	0.11															
Volume (ft^3)		5969	23,876	53,721	95,504	149,226	214,885	292,482	382,018	483,491	596,903	2,187,610	9,550,442	21,488,493	38,201,766	59,690,259
Barrels of Water		156	624	1403	2495	3898	5613	7640	9979	12,630	15,592	62,368	249,474	561,316	997,895	1,559,211
TOTALS																
Barrels of Water		424	1695	3814	6780	10,594	15,255	20,763	27,120	34,324	42,375	169,498	677,996	1,525,490	2,711,983	4,237,473
Gallons of Water (42 gal/bbl)		17,797	71,190	160,176	284,758	444,935	640,706	872,072	1,139,033	1,441,588	1,779,739	7,118,955	28,475,819	64,070,593	113,903,277	177,973,870

Note: The top, bottom, and porosity (v/v = volume/volume) of the S1, S2, and S3 sandstone channels in the Tuscher Formation were picked from the well log of the NBU No. 921-21L. The well log is shown on figure 6.34. Hydrostatic head (pounds per square inch [psi]) at the top of the zone is provided for a column of saline water. Volume (ft^3) is the pore volume at the radial distance from the well. The barrels of water are storage volumes and do not indicate radial flow from the well.

porosity. We calculated that three sandstone channels, or 53 vertical feet (16 m) of sandstone, would be able to dispose of 4.2 MMBW in a 1000-foot (305 m) radius around a well if continuous and homogeneous.

The Paleocene to Eocene Wasatch/Colton Formation is the other major producer of gas from tight-sand reservoirs in the Uinta Basin, ranges in thickness from 400 to over 4000 feet (120–1200+ m), and may provide locations suitable for wastewater disposal. Drilling depths to the Wasatch/Colton Formation range from 800 feet (240 m) in the east to 7500 feet (2300 m) in the middle of the basin. Drilling depths increase to over 11,000 feet (3400 m) in the northwestern part of the basin. Most of the water samples from the formations range from brackish to brine. Hydrocarbons and associated water from the Wasatch/Colton are produced throughout the central Uinta Basin.

The Wasatch/Colton Formation has an average sandstone porosity of 24%. However, we do not have good permeability data for the Wasatch/Colton and estimate it to be 0.1 mD, or very similar to the Mesaverde Group. The average NGR is 0.67, significantly less than typical Mesaverde Group. The Wasatch/Colton has a higher average gross sand thickness at 2232 feet but less sand with porosities ≥ 6%. The Wasatch/Colton is typically siltier and has thinner sandstone beds. We believe there are probably areas of the Wasatch/Colton where sufficient thicknesses of sand are available for water disposal. However, disposal would require long perforated zones and targeted zones.

Many water quality samples were analyzed from the Wasatch and commingled Wasatch with other units. Fresh to brackish water is typically found in the subsurface several miles from the southern outcrop locations of the Wasatch/Colton Formation. Water in the interior of the basin is saline to marginally briny. Ca/Na ratios indicate surface recharge is dissolving the Paleocene Flagstaff Limestone/Green River carbonates and flowing into the lower Wasatch Formation. Water samples are fresh from the Mesaverde Group in very close proximity to the southern Roan and Book Cliffs outcrops and along the north and northeastern outcrops. However, within a short distance into the basin, the water samples are saline to brine in almost all of the Mesaverde, with low R_w values (typically 0.1 to 0.3 ohm/m). Ca/Na values in the Mesaverde also show mixing with carbonate waters from overlying strata. This suggests likely hydrologic connections between the Wasatch and underlying formations and/or updip carbonate-bearing formations in the Uinta Basin.

One water-disposal well currently injects into the Castlegate Sandstone. The average disposal rate is 431 BPD, which is significantly lower than the regional produced-water rate. Seven disposal wells inject into the Wasatch/Colton intervals. Approximately 663 million barrels of produced water has been disposed in the interval by the seven wells. The average injection rate for these wells is similar to or lower than the Castlegate well. Two private disposal wells with rates of 2483 and 1103 BPD are exceptions. The private wells are likely injecting into much longer perforated zones or at higher pressure.

We believe there are candidate sandstones in the Wasatch/Colton for water disposal. However, they will require targeting very specific sandstones and need long perforated zones, both costly to perform. The Mesaverde Group also has candidate sandstone intervals for water disposal. The Farrer and particularly the Tuscher Formations, in the middle to eastern side of the basin, have thick, stacked sandstone channels with good porosity that can accommodate produced water.

CHAPTER 7:
UINTA BASIN RESERVOIRS/AQUIFERS: EOCENE GREEN RIVER FORMATION

by

Stephanie M. Carney and Michael D. Vanden Berg

CONTENTS

INTRODUCTION 191
METHODS 191
EOCENE GREEN RIVER FORMATION 193
Thickness 195
Depth 195
Lithology and Stratigraphy 195
Reservoir Properties 204
Water Quality 204
Water Production, Use, and Disposal 205
Hydrocarbon Production 209
SUMMARY 216

FIGURES

Figure 7.1. Location of study area, the outcrop of the top and base of the Green River Formation, and the outcrop of the Mahogany bed 192
Figure 7.2. Paleogeographic reconstruction of the Uinta Basin during the Eocene epoch 194
Figure 7.3. Thickness map of entire Green River Formation 196
Figure 7.4. Thickness of lower Green River Formation, below the Mahogany bed 196
Figure 7.5. Thickness of upper Green River Formation, above the Mahogany bed 197
Figure 7.6. Structure of the top of the Green River Formation 197
Figure 7.7. General stratigraphic columns of the Green River Formation 198
Figure 7.8. Compilation of Green River Formation stratigraphic nomenclature 198
Figure 7.9. Extent of the phase 1 hypersaline interval, upper Green River Formation 199
Figure 7.10. Utah State No. 13X-2 core description and images of phase 2 hypersaline zone 200
Figure 7.11. Extent of phase 2 hypersaline interval (Birds Nest aquifer), upper Green River Formation 201
Figure 7.12. Isopach of "large-evaporite-nodule" facies (upper and lower Birds Nest aquifers), phase 2 hypersaline zone 202
Figure 7.13. Shrine Hospital No. 1 core description and images of the phase 3 hypersaline zone 203
Figure 7.14. Extent of the phase 3 hypersaline interval, upper Green River Formation 204
Figure 7.15. Total dissolved solids concentrations, lower Green River Formation 206
Figure 7.16. Total dissolved solids concentrations, upper Green River Formation 206
Figure 7.17. Total dissolved solids concentrations, Birds Nest aquifer (phase 2 hypersaline zone) 207
Figure 7.18. Depth from the base of the moderately saline water to the top of the Green River Formation 208
Figure 7.19. Cumulative produced water, Green River Formation 209
Figure 7.20. Total cumulative water production by well, Green River Formation 210
Figure 7.21. Location of injection wells disposing produced water into the Green River Formation 211
Figure 7.22. Volume of water that has been injected into the Green River Formation from each injection well 211
Figure 7.23. Water injected into the Green River Formation via disposal wells 212
Figure 7.24. Volume of oil produced from the Green River Formation by field 213
Figure 7.25. Volume of gas produced from the Green River Formation by field 213
Figure 7.26. Cumulative oil and gas by well from the Green River Formation 214

TABLE

Table 7.1. Examples of wells with varied water sample depths, dates, and total dissolved solids concentrations 193

CHAPTER 7:
UINTA BASIN RESERVOIRS/AQUIFERS: EOCENE GREEN RIVER FORMATION

INTRODUCTION

Paleocene and Eocene sedimentary rocks make up more than half (>16,000 feet [4900 m]) of the sedimentary sequence within the Uinta Basin (Anders and others, 1992; Morgan, 2003b), and the Eocene Green River Formation (GRF) constitutes up to 7000 feet (2100 m) of that total (Hintze and Kowallis, 2009; Sprinkel, 2009). As briefly described in chapter 2, the GRF was deposited in marginal lacustrine and lacustrine environments associated with an areally extensive, shallow, saline to freshwater lake—Lake Uinta—in the subsiding Uinta Basin (figures 1.3 and 2.30). The formation is present throughout the Uinta Basin; the base is exposed in outcrop along the southern basin boundary and dips to the north-northwest where it is buried over 10,000 feet (3000 m) (figure 7.1). The GRF is an important conventional and unconventional oil and gas source for Utah; the amount of hydrocarbons produced per year solely from the formation accounts for approximately 20% of the state's total oil and 5% of the state's total gas (Utah Division of Oil, Gas and Mining, 2015).

Previous water chemistry studies show that salinity of groundwater significantly varies laterally and vertically throughout the Uinta Basin (Wanty and others, 1991; Anderson and others, 2012). This study was conducted to further define water chemistry trends specifically in the GRF. An extensive water chemistry database, part of a larger groundwater study, was created (appendix F) that contains data from all producing formations within the basin. This database was compiled from several sources: Howells and others (1987), Gwynn (1992, 1995), Zhang and others (2009), and Anderson and others (2012), as well as previously unpublished USGS data, UGS data, and several company reports. Information from this water chemistry database was used to create regional maps displaying the distribution of TDS concentrations (mg/L) in the GRF. In addition, updated structure contour and isopach maps were generated for the GRF, as well as tabulations of formation-specific hydrocarbon and water production, and water injection volumes.

METHODS

Ancient Lake Uinta started as a freshwater system (Uteland Butte member of the lower GRF), but quickly turned saline (above the Long Point bed within the Carbonate Marker Unit); however, the lake did not become hypersaline until late in its existence (upper GRF). Therefore, evaporite mineral deposition and preservation only occurred at and above the Mahogany bed, as the lake began to shrink and disappear (Vanden Berg and Birgenheier, 2017). This scenario created a natural divide between the characteristics of the groundwater within the upper GRF, above the Mahogany bed, and the characteristics of the groundwater within the lower GRF, below the Mahogany bed (figure 2.28). Subsequent analyses and interpretations will focus on these two broad intervals.

We compiled formation tops from several previous studies, the DOGM online database, company reports, and internal UGS files. This dataset includes tops for the Wasatch Formation and GRF, including the Mahogany bed. From these data, we created structure contour and various isopach maps. Maps were made using the Inverse Distance Weighting (IDW) method within ArcGIS™.

In addition, we used the compiled water chemistry database (appendix F) to create maps displaying TDS concentrations for water within the GRF. The chemistry data are assigned to either the upper or lower GRF based on the sample depth relative to the Mahogany bed. Because the upper GRF interfingers with the Uinta Formation above (figure 1.5), the boundary between the two formations is often difficult to identify. We included several samples obtained from this transition zone in the evaluation of the upper GRF. Most of these samples are from the northwest part of the basin and have high TDS values due to evaporite mineral dissolution from sediments laid down during the hypersaline last remnant of ancient Lake Uinta.

In most cases, operators obtained the water chemistry analyses from samples taken during oil and gas well drilling. A single well commonly had samples taken from multiple depths within the formation or multiple samples taken from the same depth (table 7.1). The sample interval can be less than tens of feet or up to hundreds or thousands of feet. For example, the Red Wash Unit No. 32-27AG well (section 27, T. 7 S., R. 22 E., SLBL&M, Uintah County, API No. 43-047-35670) has water chemistry data from four water samples: two samples from a depth of 5535 to 5539 feet (1687–1688 m), one sample from 5745 to 5749 feet (1751–1752 m), and a final sample from 5922 to 5928 feet (1805–1807). In contrast, the Fenceline Federal No. 3-24-8-16 well (section 24, T. 8 S., R. 16 E., SLBL&M, Duchesne County, API No. 43-013-32363) has only one water sample that represents over 1500 feet (500 m) of strata from 4736 to 6461 feet (1444–1969 m). Furthermore, some wells with several water samples taken from the same depth were sampled during different years. An example is the Natural Duck No. 1-15 well (section 15, T. 9 S., R. 20 E., SLBL&M, Uintah County, API

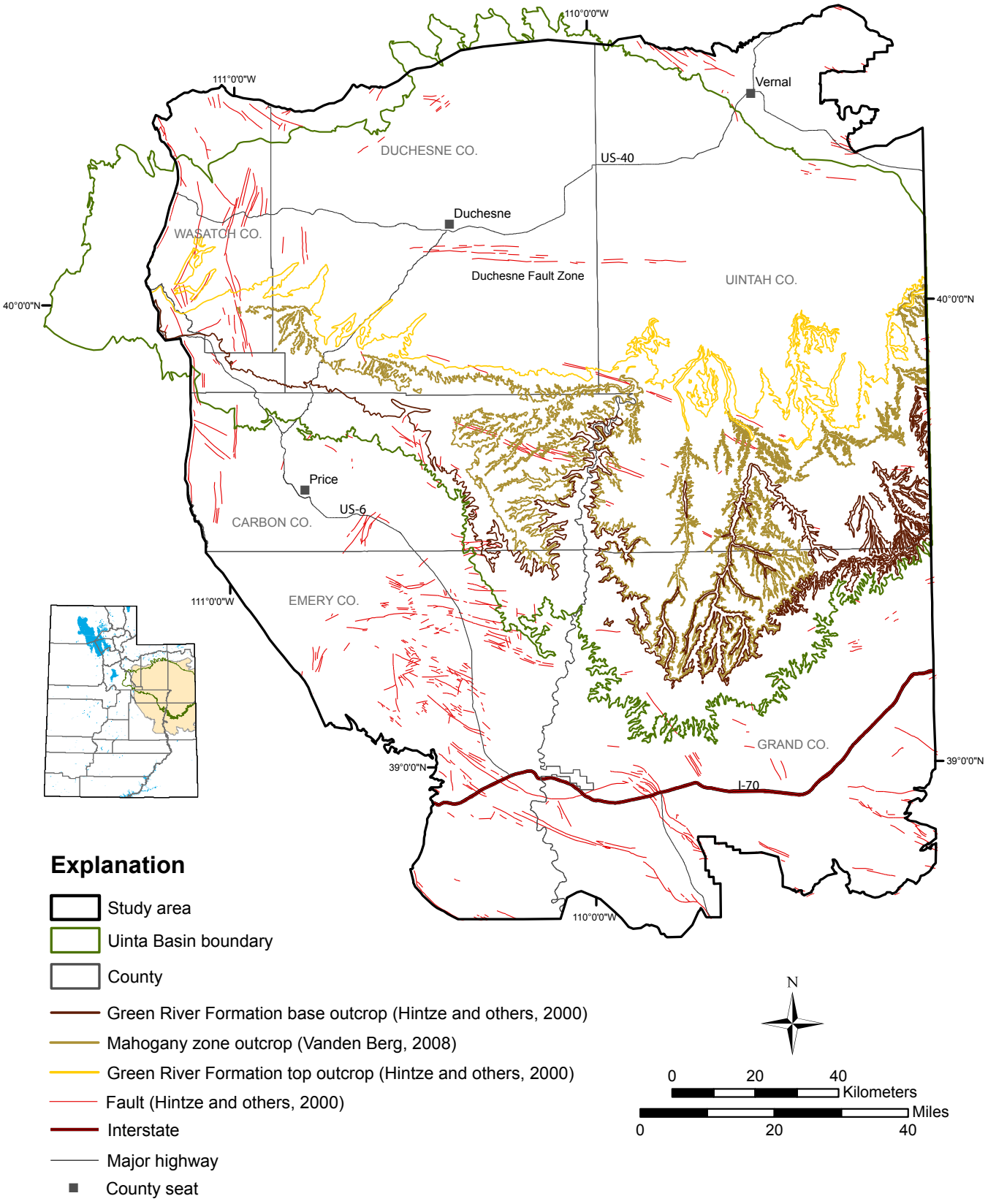

Figure 7.1. *Overview map showing location of study area, the outcrop of the top and base of the Green River Formation, and the outcrop of the Mahogany bed.*

Table 7.1. *Examples of wells with varied water sample depths, dates, and total dissolved solids (TDS) concentrations.*

Well Name	Sample Depth (ft)	Date Sampled	TDS (mg/L)	Balanced*	Upper or Lower GRF	Sample Selected
Red Wash Unit 32-27AG	5535–5539	2/7/2005	25,720	Yes	Lower	Chose sample at 5745–5749 ft depth, which had more recent sample date and TDS value closest to average value of all three 2005 samples
	5535–5539	2/9/2005	42,005	Yes	Lower	
	5745–5749	1/20/2005	29,220	Yes	Lower	
	5922–5928	12/10/2004	37,835	Yes	Lower	
Fenceline Federal 3-24-8-16	4736–6461	11/21/2006	24,478	Yes	Lower	Only sample for this well
Natural Duck 1-15	4788–4796	5/13/1987	72,962	Yes	Lower	Chose most recent sample
	4788–4796	8/18/1978	18,399	Yes	Lower	
Lake Fork 2-23B4	4204–4645	11/3/1987	65,371	Yes	Upper	Chose both samples since one represented upper GRF and one represented lower GRF
	11050–11220	6/7/1973	6693	Yes	Lower	
Red Wash Unit 41-9F	1818–1836	5/1/1956	2390	Yes	Upper	Used an average TDS value
	1818–1836	5/23/1956	2394	Yes	Upper	
Windmill	1382	7/15/2009	2394	No	Upper	Chose most recent, balanced sample
	1382	9/21/2010	2106	Yes	Upper	
Island Unit 3	3310–3337	10/21/1960	2490	No	Lower	Chose most recent, balanced sample (TDS = 31,000)
	3488–3514	Unknown	28,490	Yes	Lower	
	3488–3514	7/12/1962	31,000	Yes	Lower	
	3488–3514	7/12/1962	31,008	Yes	Lower	

*The sum of ions equals the measured TDS.

No. 43-047-30393), which had a water sample taken from 4788 to 4796 feet (1459–1462 m) in 1978 and then a second sample taken from the same interval in 1987. In some cases, wells had multiple water samples taken at different depths over different years.

Fully analyzing the extreme complexity of the groundwater in the GRF, stratigraphically and through time, was beyond the scope of this project. This study focuses on overall averages and trends. To this end, the data were culled, filtered, and averaged so that each well had one representative data point for the upper and/or lower GRF. A sample that was "balanced" (sum of ions equal to measured TDS) and had the most recent sample date was usually selected to represent the well in the final dataset. Samples that were "out of balance" were only used for areas in the basin with sparse data. For samples taken over multiple depths, the most recent sample closest to the median depth was selected.

EOCENE GREEN RIVER FORMATION

Structural asymmetry of the Uinta Basin, coupled with the surrounding Laramide highlands, created an internally drained basin and lake system—Lake Uinta, which existed throughout the Eocene epoch (figure 7.2). The GRF is a synorogenic deposit of this lake system (Keighley and Flint, 2008). The depocenter of the lake was focused in the northern part of the basin, parallel to the synclinal axis of the Uinta Basin, but the location shifted from west to east, then west again, over the lifespan of the lake. Lake Uinta was fringed by alluvial fans and delta complexes, the sediment for which was supplied from the surrounding highlands (Ryder and others, 1976). In the northwest, deposition of sediments occurred along the deep lake margin, and sandbodies are interpreted to be thin gravity-flow and shoreface deposits dominated by quartz-rich sediment (Castle, 1990; Remy, 1992; Borer, 2003). Along the northeast margin, sediments were deposited in wave-dominated lacustrine and alluvial-fan environments (Borer and McPherson, 1998). Along the south and southwest margins of the lake, fluvial and deltaic deposits dominate due to slower depositional rates and a low topographic gradient (Ryder and others, 1976). A large fluvial-deltaic complex, termed the Sunnyside delta, developed along the southern shore of Lake Uinta and extended into the center of the basin (Remy, 1992). The delta consists of fluvial-deltaic, feldspar-rich sandstone, mudstone, and carbonate, and serves as an oil and gas reservoir for many fields in the basin (Fouch, 1975). Over time, lake level fluctuated due to tectonic and climatic changes, and organic-rich lacustrine carbonate and shale were interbedded with alluvial and fluvial sandstone, creating source/reservoir packages (Keighley and others, 2002; Keighley and Flint, 2008).

Figure 7.2. *Paleogeographic reconstruction of the Uinta Basin during the Eocene epoch (from Blakey and Ranney, 2008). Green outline is approximate location of Uinta Basin.*

Thickness

An isopach map representing the entire GRF shows that the thickest section of the formation (~6900 feet [2100 m]) occurs in the western part of the Uinta Basin, and the formation thins to the east (~1700 feet [520 m]) (figure 7.3). The lake generally covered the entire basin soon after its formation, with a depocenter, and thicker strata, centered to the west-northwest during lower GRF time. Figure 7.4 displays thickness of the lower GRF (below the Mahogany bed) with strata up to 3900 feet (1200 m) thick to the west and only 1700 feet (520 m) thick in the marginal lacustrine areas to the east. Deposits in the central and western parts of the basin are also thicker due to the Sunnyside delta sands coming into the basin in this area. As the lake dried and disappeared, it shrank from east to west (Vanden Berg and Birgenheier, 2017). Therefore, the lake was much longer lived in the west and deposited a much thicker section of upper GRF. This is illustrated on figure 7.5 which shows sediments thickening from about 200 feet (60 m) in the east to 3200 feet (980 m) in the west.

Depth

A structure contour map of the GRF shows the top is at an elevation of ~2000 feet (600 m) below sea level in the north-central area of the Uinta Basin and 6700 feet (2040 m) above sea level in the south, which reflects the basin's asymmetrical shape (figure 7.6). An approximate GRF top was picked in roughly 250 wells across the basin. Due to complex interfingering with the Uinta Formation above, the top of the GRF is difficult to pick consistently using geophysical well logs.

Lithology and Stratigraphy

The GRF is a complex sedimentary deposit. In general, the lower part is characterized by fluvial-deltaic sand interbedded with lacustrine organic-rich mud and carbonate. The upper GRF is dominated by alternating organic-rich and organic-lean marlstone with distinct stages of evaporite mineral deposition (Vanden Berg, 2008; Vanden Berg and others, 2013; Vanden Berg and Birgenheier, 2017). The formation interfingers with the Wasatch/Colton Formation below and the Uinta Formation above (figure 7.7). Because of its depositional complexity, stratigraphic nomenclature for the GRF varies from west to east and has been defined and re-defined by several previous researchers such as Bradley (1931), Fouch (1975), Ryder and others (1976), Weiss and others (1990), Fouch and others (1994), Ruble (1996), and Morgan (2003b). Nomenclature is often based on facies that tend to interfinger and change laterally within the basin. Four marker beds, deposited during maximum flooding events of Lake Uinta, can be helpful for regional correlation. These beds are the Long Point bed carbonate marker, middle marker, and Mahogany bed. Figure 7.8 shows how several researchers have divided the GRF over the years (Morgan, 2003b).

Sediments in the lower GRF were deposited in marginal- to open-lacustrine environments during the early, expansive rise in lake level and subsequent fluctuations. Nearly all oil, gas, and associated water produced from the GRF is out of reservoirs in the lower part of the formation. The dominant reservoirs are fluvial and deltaic sands from the Sunnyside delta in the south (e.g., Monument Butte field), alluvial and wave-dominated shoreline sands in the northeast (e.g., Red Wash and Wonsits field), and deltaic/alluvial sands shed from the north-northwest off the Uinta Mountains (e.g., Altamont and Bluebell fields) (see figure 1.1 for field locations). These sands, as well as associated carbonate grainstone reservoirs, are typically lenticular in geometry and are interbedded with open-lacustrine limestones and shales, reducing the connectivity between individual reservoirs. This also creates a situation where groundwater chemistry can vary significantly laterally and vertically. Some carbonate deposits, such as the dolomite intervals within the basal Uteland Butte member of the lower GRF, create a more laterally consistent reservoir, but despite the high porosity (up to 30%), permeability is very low (Vanden Berg and others, 2014).

For this study, the base of the upper GRF is marked by the Mahogany bed, which is a very organic-rich (up to 40% TOC) marlstone deposited during the maximum highstand of Lake Uinta (U.S. Geological Survey, 2010b; Tänavsuu-Milkeviciene and Sarg, 2012). The Mahogany interval and younger strata in the upper GRF record three phases of hypersaline conditions and evaporite mineral deposition (Vanden Berg and others, 2013; Vanden Berg and Birgenheier, 2017). These intervals containing evaporite minerals greatly influence groundwater chemistry within.

The phase 1 hypersaline zone occurred during Lake Uinta's maximum lake transgression (Mahogany bed) and was restricted to the paleo-depocenter in the northeast part of the basin (figure 7.9). Evaporite mineral deposition covers an area of approximately 203 square miles (525 km^2) and is characterized by large nahcolite ($NaHCO_3$) nodules and minor associated small evaporite mineral crystals that formed within or near the Mahogany zone (Vanden Berg and Birgenheier, 2017). Evidence of these large nodules in core indicates that no post-deposition dissolution has taken place within the phase 1 hypersaline zone (figure 7.9), thus these evaporite minerals will have little influence on groundwater salinity.

The phase 2 hypersaline zone has previously been identified and studied as the Birds Nest aquifer interval or Birds Nest saline interval, historically by Cashion (1967) and Dyni (1996). Most recently, Vanden Berg and others (2013) completed a very extensive report on the Birds nest aquifer, which includes a detailed discussion of its origin, properties, and groundwater characteristics. The beginning of this hypersaline interval is related to a strongly regressive phase of Lake Uinta and is correlative to the Horse Bench Sandstone, which was deposited in the southwest part of the Uinta Basin (Dyni, 1996; Toms, 2014).

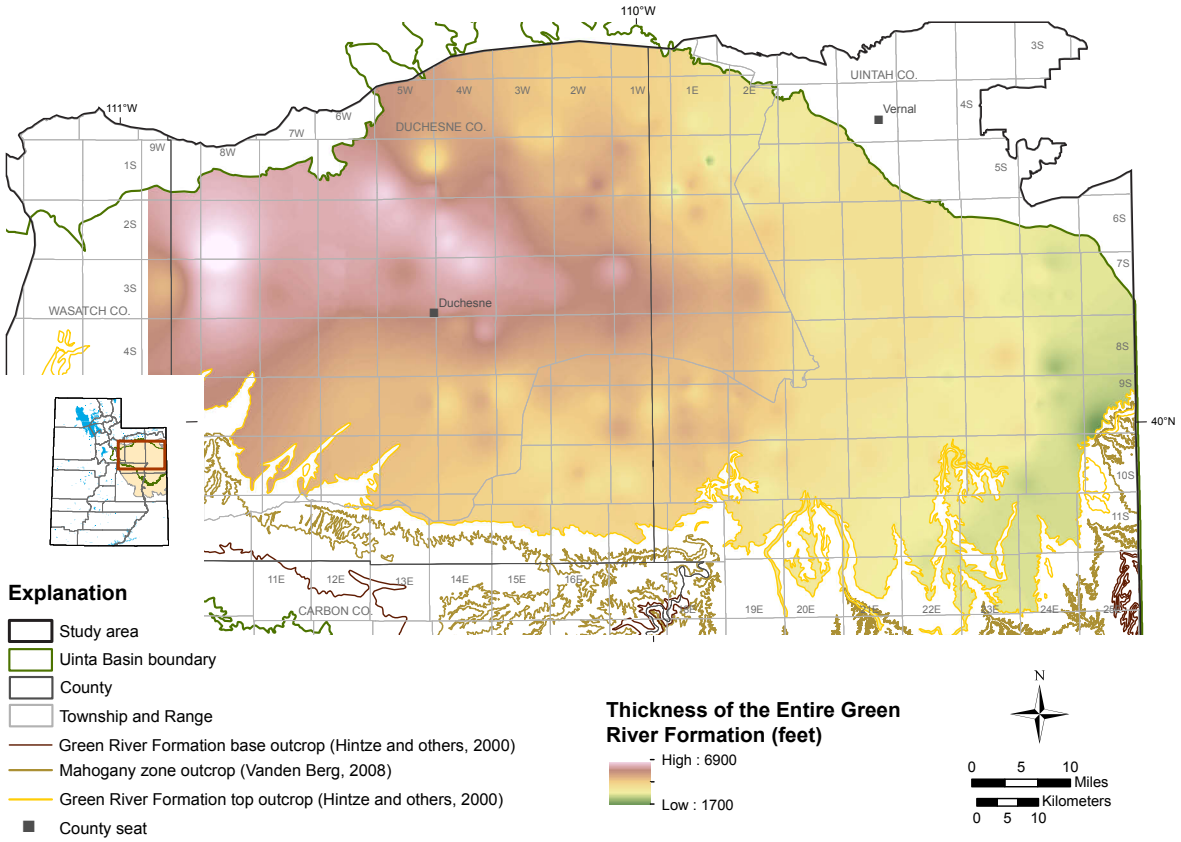

Figure 7.3. *Thickness map of entire Green River Formation.*

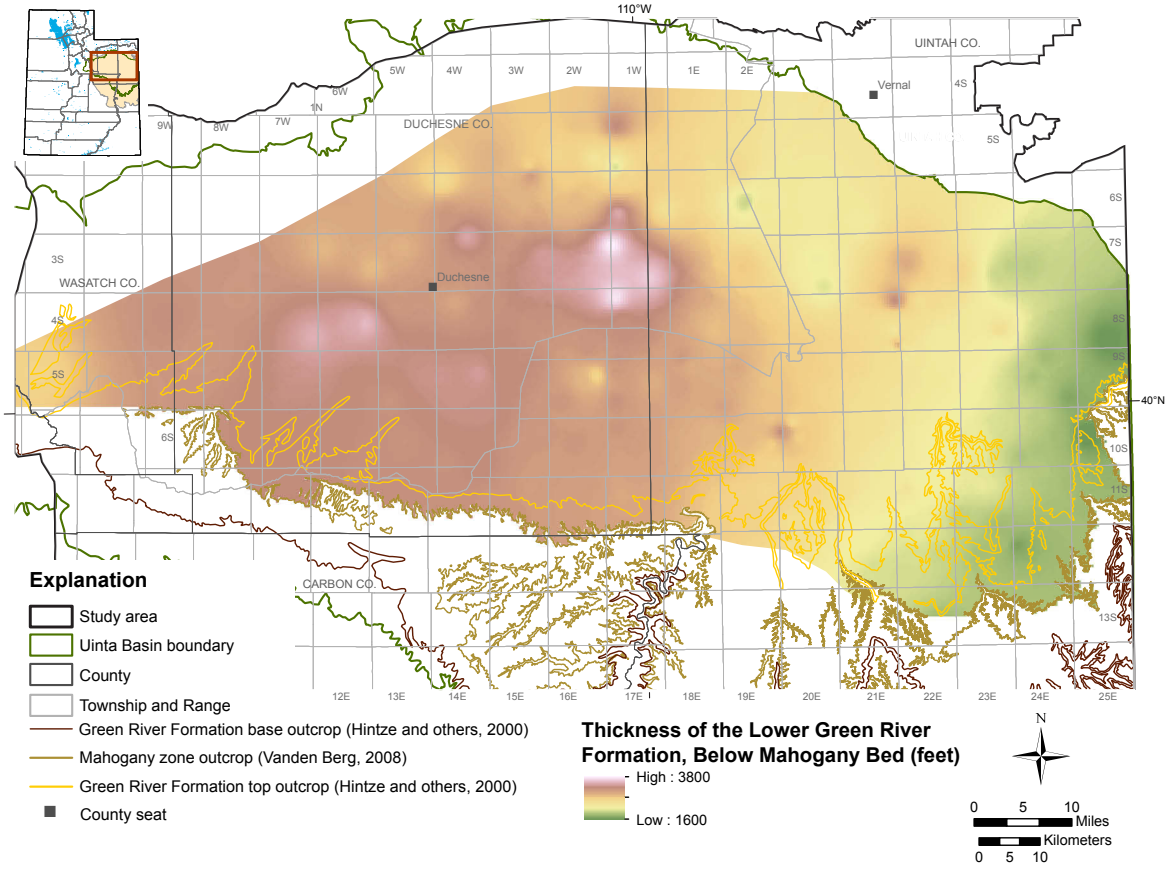

Figure 7.4. *Thickness map of lower Green River Formation, below the Mahogany bed.*

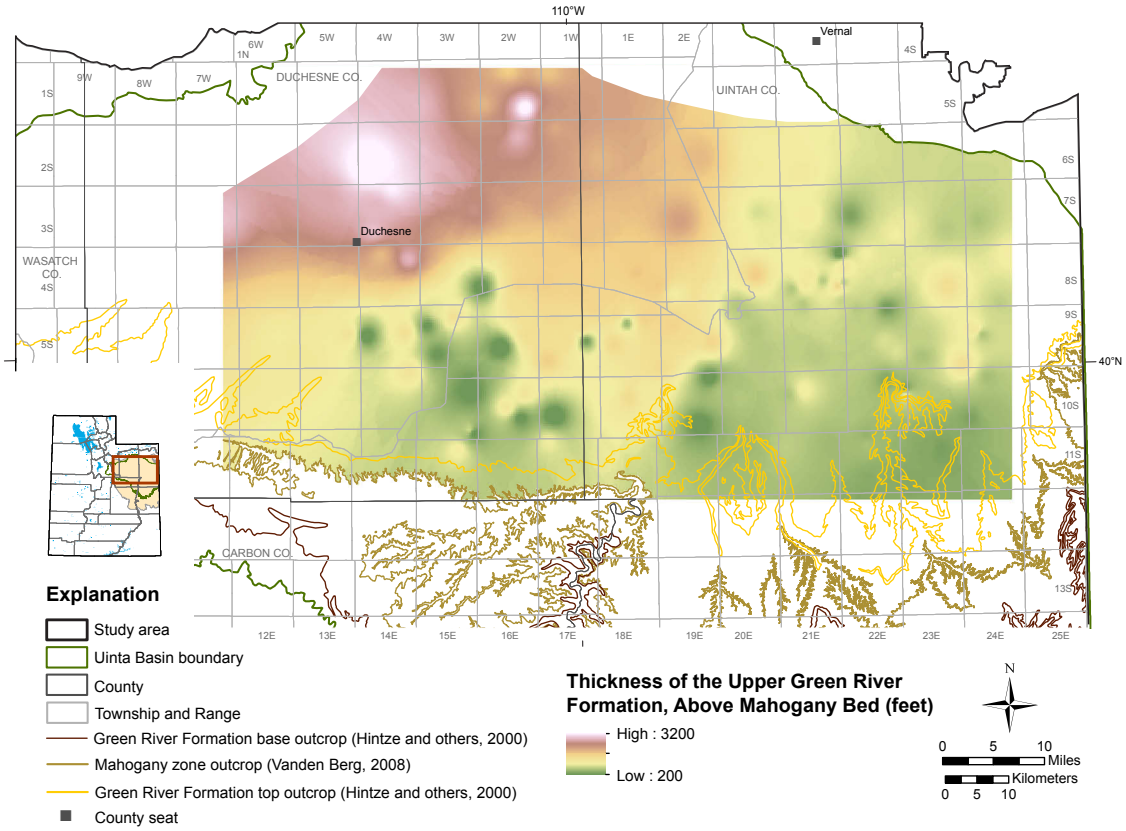

Figure 7.5. *Thickness map of upper Green River Formation, above the Mahogany bed.*

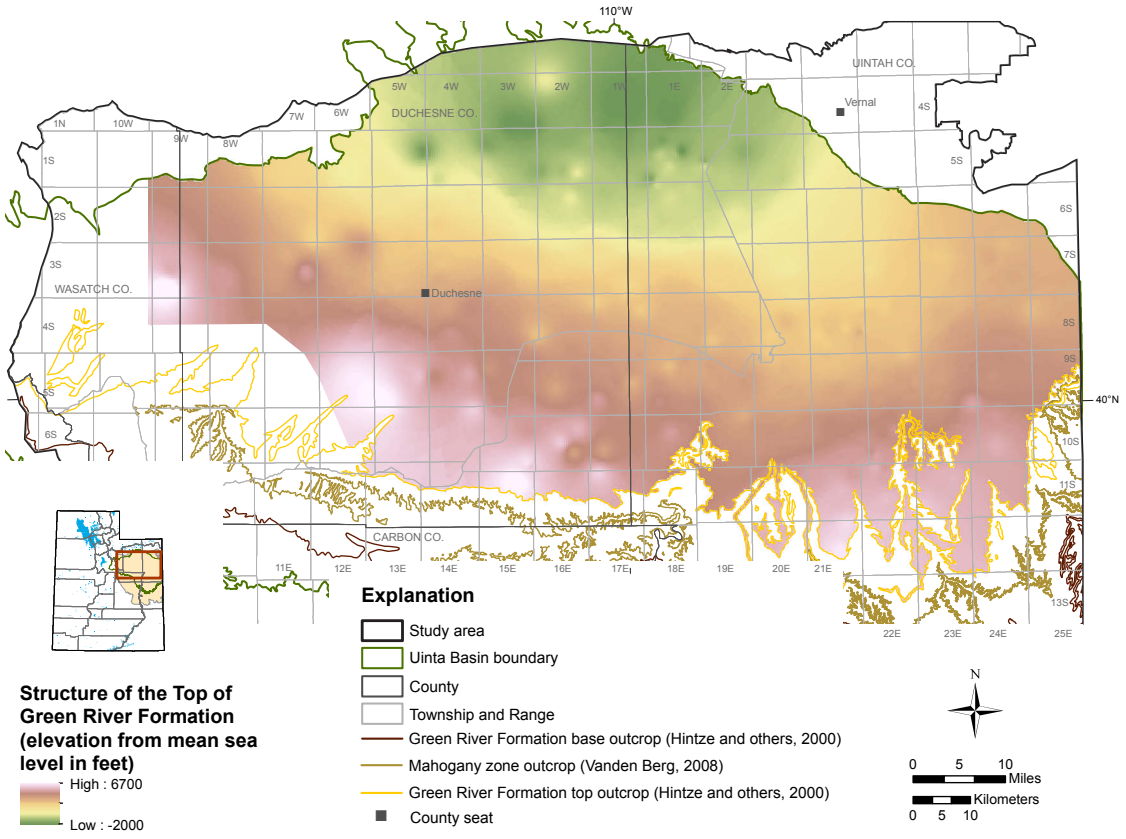

Figure 7.6. *Structure map of the top of the Green River Formation, illustrating the northerly dip of the beds.*

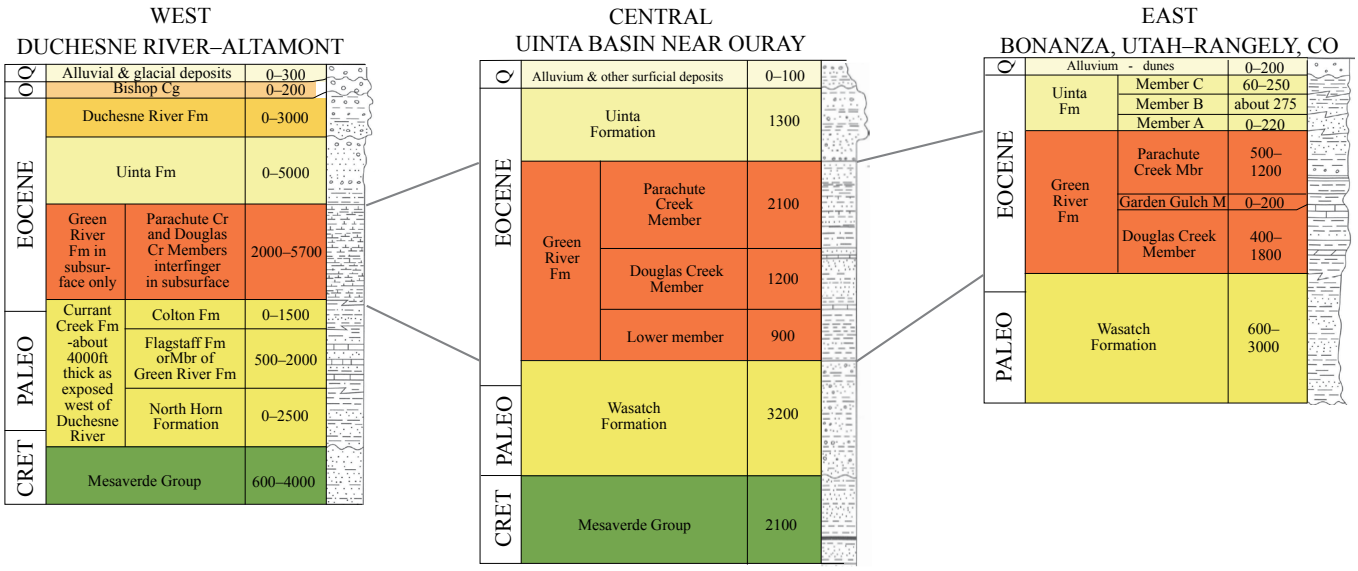

Figure 7.7. *General stratigraphic columns of the Green River Formation (from Hintze and Kowallis, 2009).*

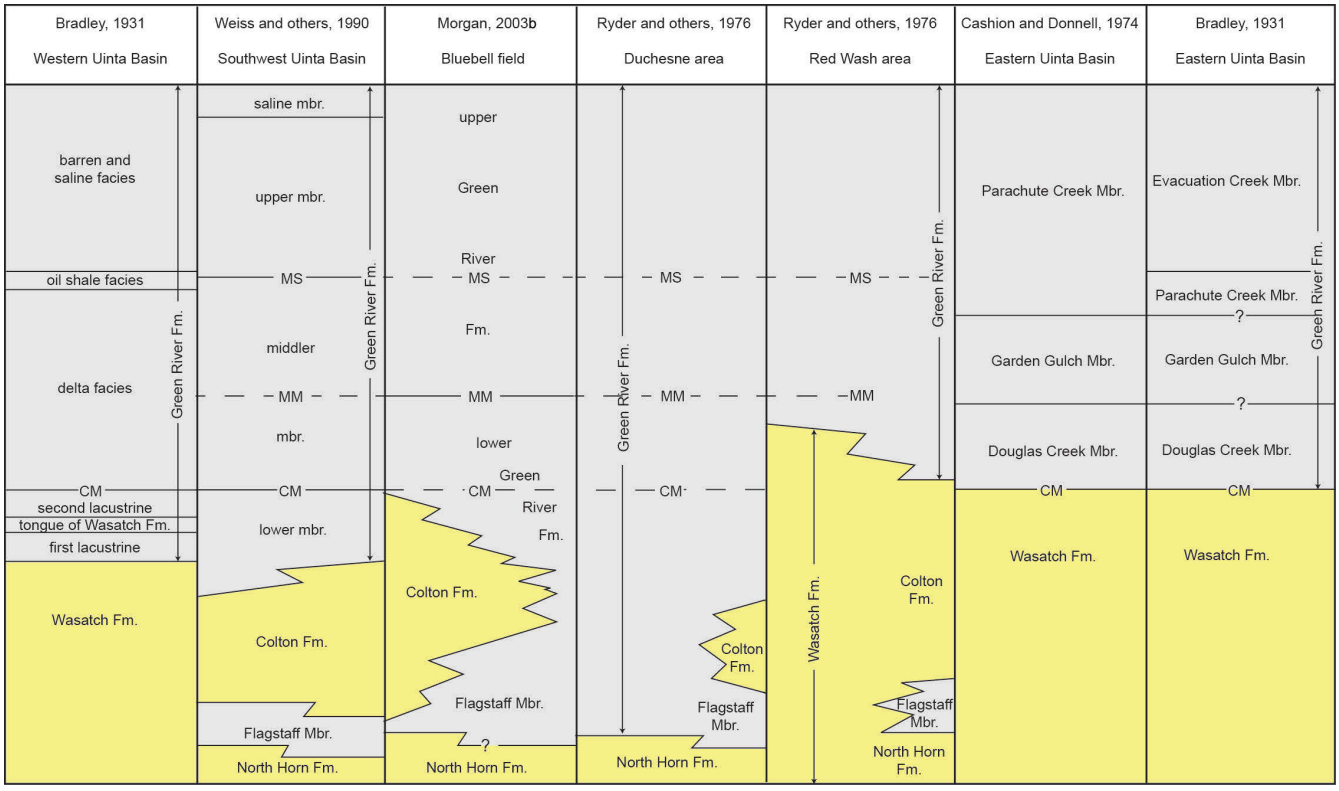

Figure 7.8. *A compilation of the various stratigraphic nomenclature used for the Green River Formation throughout the years and across the basin. CM = carbonate marker; MM = middle marker; MS = Mahogany shale (bed) (modified from Morgan, 2003b).*

The phase 2 hypersaline zone is separated into two distinct facies: the large-evaporite-nodule (LEN) facies and the small-evaporite-crystal (SEC) facies. Two distinct intervals, a lower and an upper zone, of the LEN facies occur within an overall, more regionally extensive SEC facies zone (figure 7.10). The more extensive lower LEN facies represents the first phase 2 deposition of large nahcolite nodules in the basin's paleo-depocenter (figure 7.11). This interval is overlain by a thick sequence of organic-lean marlstone (oil shale) with only minor evaporite mineral deposition—mostly small crystals and shortite ($Na_2Ca(CO_3)_2$) (SEC facies). A more areally restricted upper large nodule zone records a second period of nahcolite nodule deposition followed again by a sequence of organic-lean marlstone with only minor small evaporite crystals (figure 7.11). Similar to the phase 1 hypersaline zone, the large evaporite nodules found in phase 2 correlate well with the area in the Uinta Basin of highest oil yield within the middle R-8 oil shale interval (Bed 44 to Bed

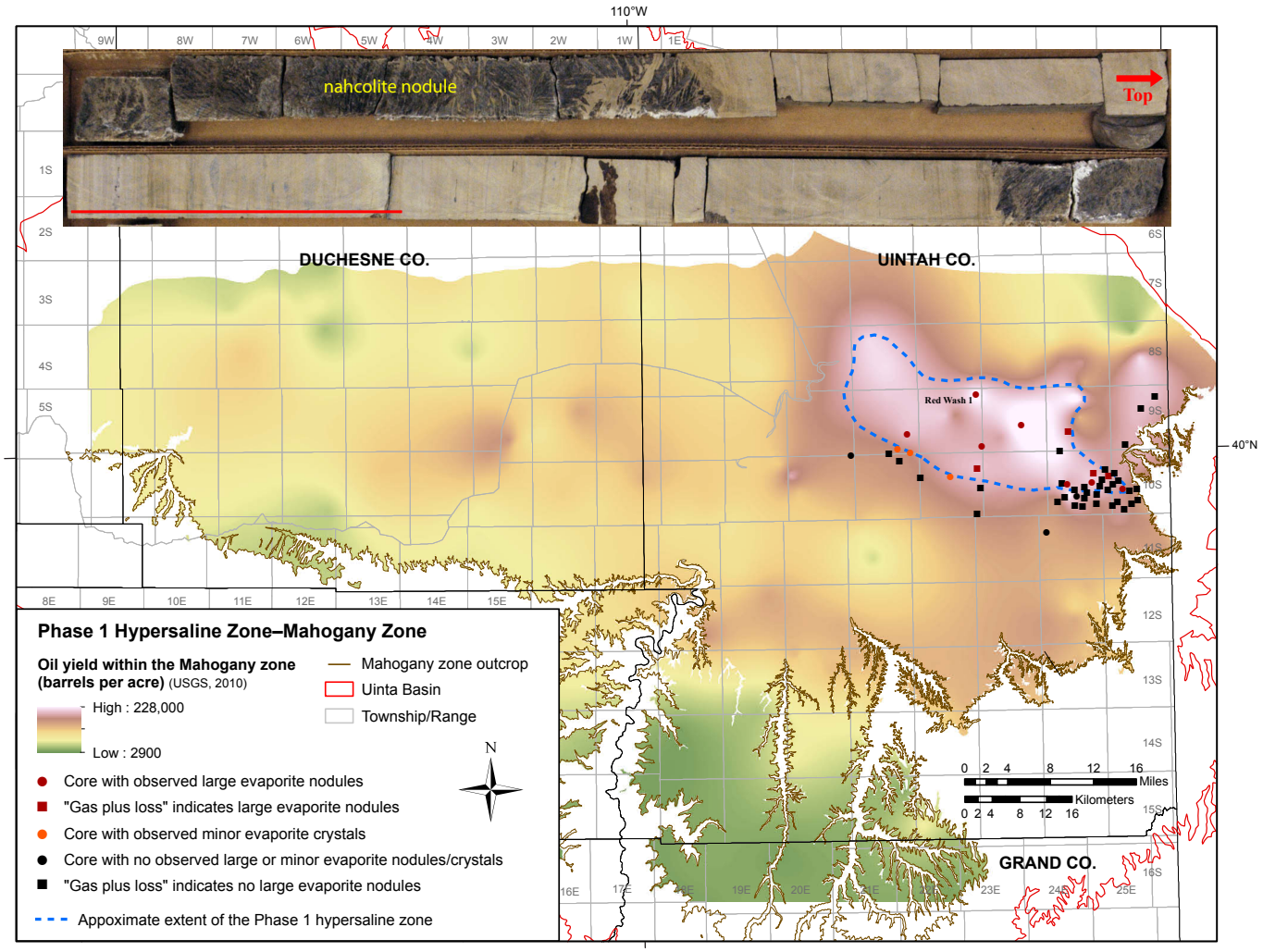

Figure 7.9. *Extent of the phase 1 hypersaline interval in the upper Green River Formation. Evaporite mineral deposition occurred within the paleo-depocenter of the lake during Mahogany zone time, as illustrated by organic-richness (oil yield) in barrels per acre (U.S. Geological Survey, 2010b). The extent was identified by examining core and "gas-plus-loss" measurements from Fischer assay analyses. During the heating of rock samples for Fischer assay analysis, nahcolite within a sample will decompose, giving off large amounts of carbon dioxide recorded as "gas plus loss." Therefore, a high weight percent of "gas plus loss" indicates the presence of significant evaporite minerals. This phenomenon is discussed in detail by the U.S. Geological Survey (2010a). The inset photo displays intact nahcolite nodules within the Red Wash No. 1 core.*

76) measured in barrels per acre (U.S. Geological Survey, 2010b) (figure 7.11). Again, this area of high organic matter accumulation is recognized as the paleo-depocenter of the basin and would be the same place large nahcolite nodules might form. Extending away from the basin's paleo-depocenter and the area with the LEN facies, the overall phase 2 hypersaline zone thins and contains only deposits of small evaporite crystals (figure 7.11). This transition is confirmed in the southern part of the basin where cores and outcrop exposures are present, and it is presumed that the same transition to small evaporite crystals exists to the north, but no cores exist to confirm this hypothesis. The 16X-23D-36 core (section 23, T. 3 S., R. 6 W., UBL&M, Duchesne County, API No. 43-013-50623), on the far western side of the basin, captured a small portion from the same stratigraphic interval that displays small evaporite crystals, confirming that the SEC facies extend nearly basin wide.

After defining the areal extent of the LEN zones, the tops database could be used to create isopach maps of the upper and lower zones. The lower LEN zone, as defined by 217 wells, covers 719 square miles (1862 km^2) and averages 84 feet (26 m) thick (figure 7.12). The lower zone has the shape of an elongated oval and is thickest in the center (between 100 and 110 feet [30–34 m] thick), and gradually thins toward the north and south (between 33 and 40 feet [10–12 m] thick). The upper LEN zone, as defined by 150 wells, covers 410 square miles (1062 km^2) and averages 79 feet (24 m) thick (figure 7.12). The interval is thickest near its center (between 100 and 110 feet [30–34 m] thick) and gradually thins toward its edges (between 33 and 40 feet [10–12 m] thick) defining the bowl-like structure of the ancient lake's depocenter.

The phase 3 hypersaline zone has been previously recognized as the "saline facies" of Bradley (1931), Dane (1954), Dyni

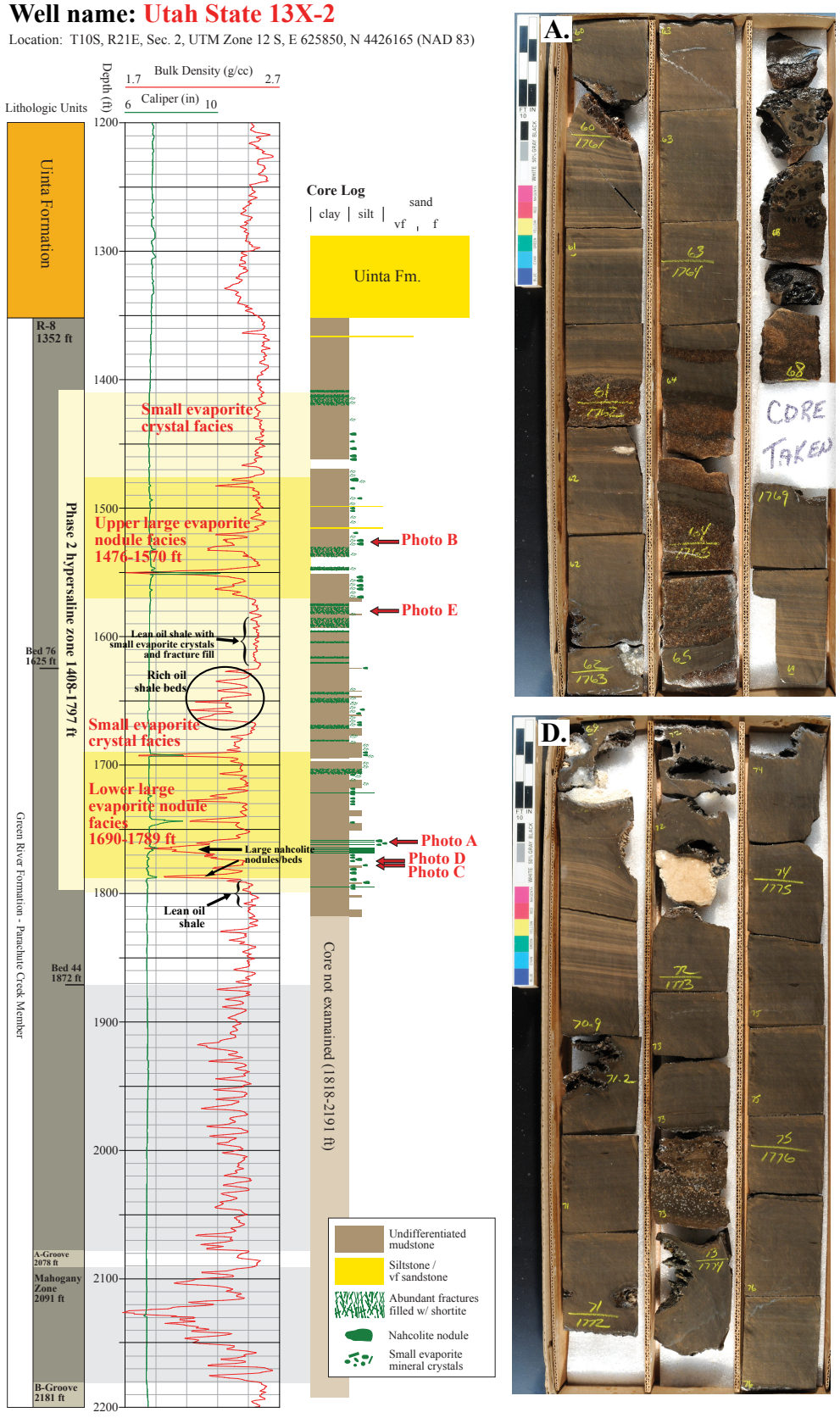

Figure 7.10. *The Utah State No. 13X-2 core represents a typical phase 2 hypersaline zone section from the basin's paleo-depocenter. The phase 2 hypersaline zone in this area is nearly 400 feet (120 m) thick and contains two intervals with large evaporite mineral nodules/beds. The upper large-evaporite-nodule zone is 94 feet (29 m) thick (1476 to 1570 feet [450–479 m]) and the lower zone is 99 feet (30 m) thick (1690 to 1789 feet [515–545 m]).* ***A.*** *Nahcolite beds, 1760 to 1769 feet (536–539 m).* ***B.*** *Dissolved nahcolite nodule, 1528 feet (466 m).* ***C.*** *Dissolved nahcolite nodule lined with pyrite, 1774 feet (541 m).* ***D.*** *Dissolved nahcolite nodules, 1769 to 1776 feet (539–541 m).* ***E.*** *Shortite fracture fill, 1580 feet (482 m).*

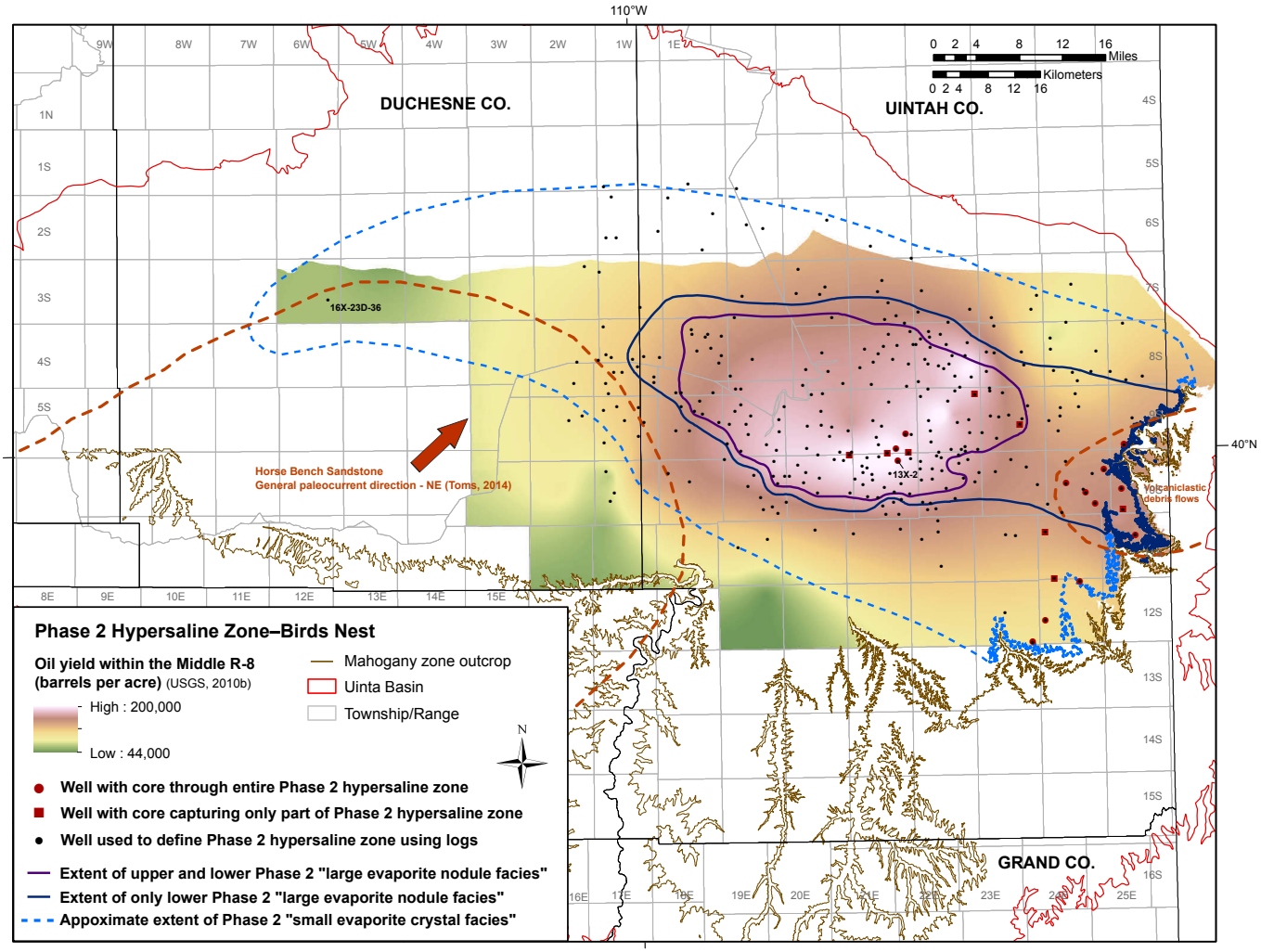

Figure 7.11. *Extent of the phase 2 hypersaline interval (Birds Nest aquifer) in the upper GRF. The most abundant evaporite mineral deposition occurred within the paleo-depocenter of the lake during middle R-8 time, as illustrated by organic-richness (oil yield) in barrels per acre (U.S. Geological Survey, 2010b). Evaporite mineral distribution was influenced by two significant siliciclastic deposits, the Horse Bench Sandstone on the west side of the basin and volcaniclastic debris flows on the east side.*

(1976), and Dyni and others (1985). This interval is well exposed in Indian Canyon on the southwestern side of the Uinta Basin and measures about 1100 feet (340 m) thick. Similar to the other hypersaline intervals, there is an area within the interpreted paleo-depocenter of the basin that contains a greater concentration of evaporite minerals. However, instead of large nodules of nahcolite, which define the former two phases, the third phase is characterized by deposition of bedded halite (first appearance in the Uinta Basin) mixed with beds/crystals of other sodium-rich minerals such as trona (Na_2CO_3•$NaHCO_3$•$2H_2O$), wegscheiderite (Na_2CO_3•$NaHCO_3$), leucosphenite ([Na_2Ca,Ba]$10B_2Ti_5Si_{19}O_{15}$), reedmergnerite ($Na_2B_2SiO_6$), searlesite ($Na_2B_2Si_4O_6$•$2H_2O$), and eitelite (Na_2CO_3•$MgCO_3$), as well as nahcolite and shortite (Milton and others, 1954a, 1954b; Dyni and others, 1985).

The Shrine Hospital No. 1 core (section 10, T. 3 S., R. 5 W., UBL&M, Duchesne County, API No. 43-013-30393) is the only core that captured the bedded evaporites found in the phase 3 hypersaline zone (figure 7.13). This core was extensively studied by Dyni and others (1985) so only a brief description is included here. Between 4165 and 4251 feet (1269–1296 m), three prominent evaporite beds occur that are 2, 6, and 12 feet (0.6, 1.8, and 3.7 m) thick and are composed of primarily halite with lesser amounts of wegscheiderite (figure 7.13). An additional six thinner beds of mixed sodium carbonate minerals (nahcolite, trona, wegscheiderite, and eitelite) range from 0.3 to 1.5 feet (0.1–0.5 m) in thickness. These evaporite mineral sequences are interbedded with brown dolomitic marlstone that contains scattered crystals and thin layers of shortite, nahcolite, northupite (Na_2CO_3•$MgCO_3$•NaCl), and eitelite (small crystal facies) (Dyni and others, 1985). In the lower part of the core is a light bluish-gray tuff bed (Fat tuff), 6.2 feet (1.9 m) thick, that can be correlated to several other cores in the area.

The bedded evaporite minerals found in the Shrine Hospital No. 1 core can be readily identified using geophysical logs, in particular the density logs and washouts in the caliper log. By analyzing logs from oil and gas wells in the surrounding area, it is possible to estimate the regional extent of the evaporite

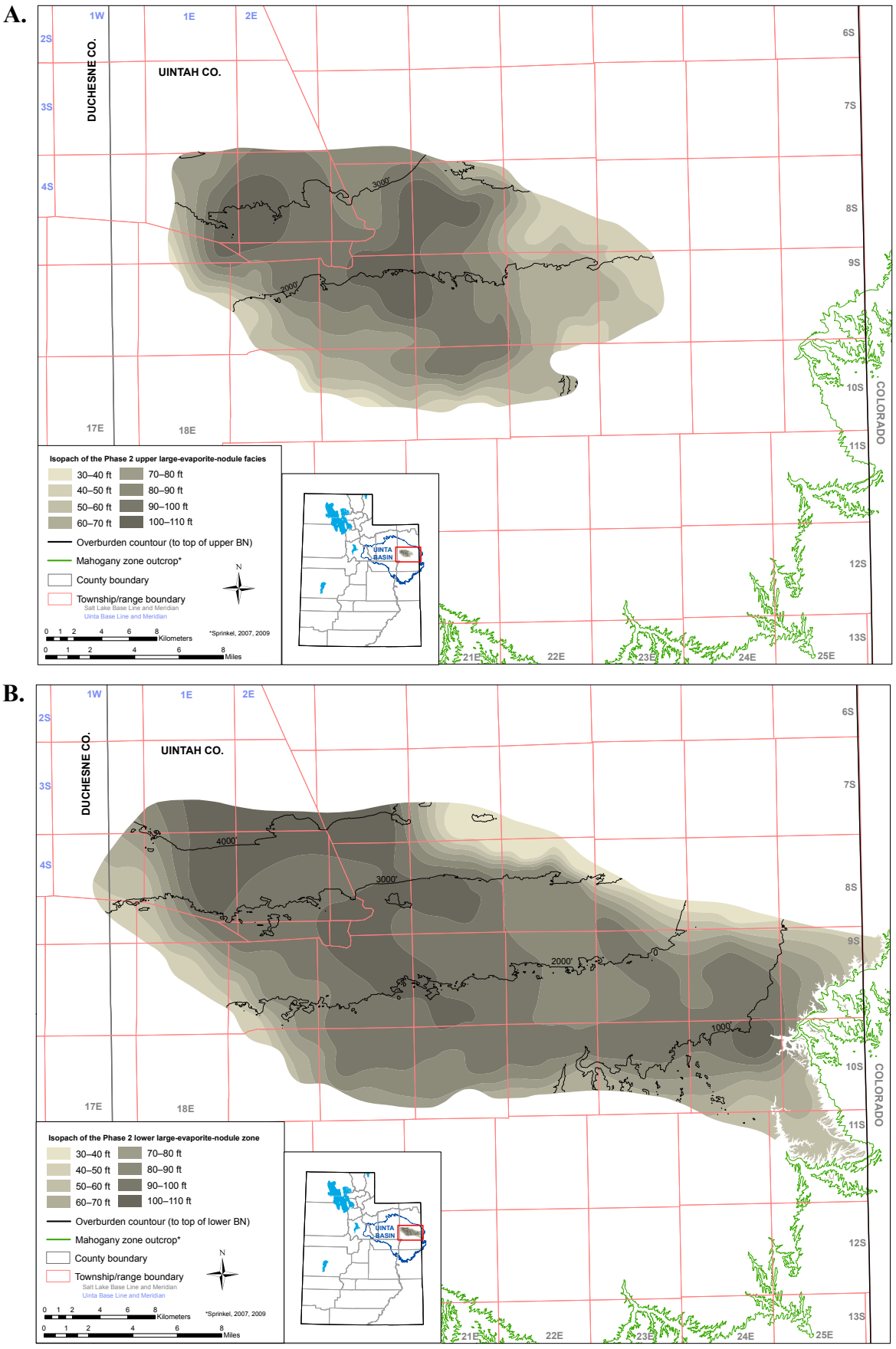

Figure 7.12. *Isopach maps, with depth contours, of the* ***A.*** *upper and* ***B.*** *lower "large-evaporite-nodule" facies (upper and lower Birds Nest aquifers) from the phase 2 hypersaline zone.*

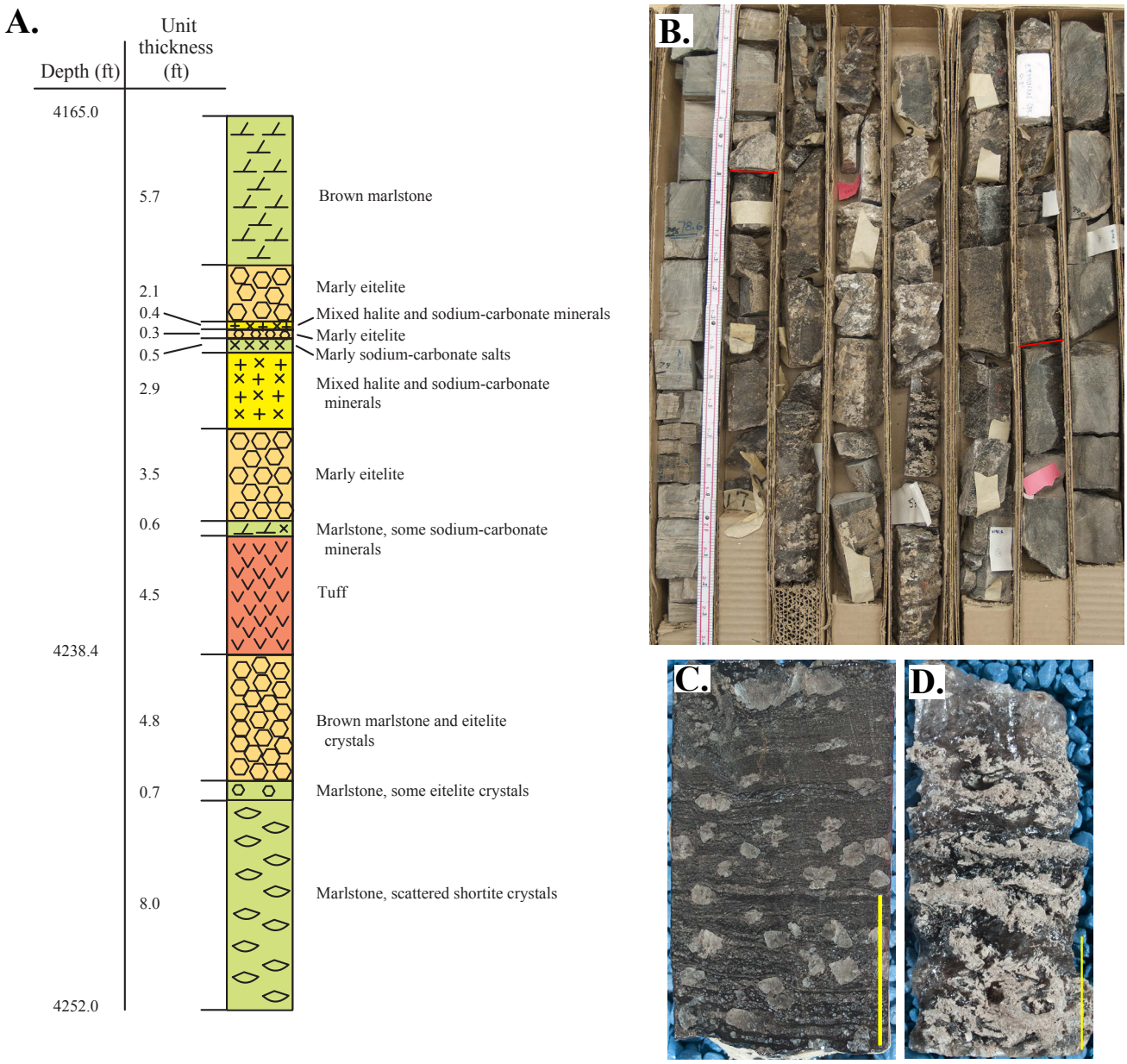

Figure 7.13. *Shrine Hospital No. 1 core representative of the phase 3 hypersaline zone section.* ***A.*** *Generalized lithologic description of the Shrine Hospital No. 1 core, showing bedded evaporite minerals from the phase 3 hypersaline zone (from Brownfield and others, 2010).* ***B.*** *Several feet of bedded halite with smaller wegscheiderite crystals and other sodium-rich evaporite minerals (between red lines) from 4180.3 to 4192.5 feet (1274.2–1277.9 m) (mineral identification from Dyni and others, 1985).* ***C.*** *Large subhedral crystals of eitelite in marlstone (oil shale), 4248.4 feet (1294.9 m) (mineral identification from Dyni and others, 1985). Yellow bar equals one-tenth foot.* ***D.*** *Bedded halite (darker gray, glassy, partially dissolved) with wegscheiderite crystals (light gray, more resistant), 4187.1 feet (1276.2 m) (mineral identification from Dyni and others, 1985). Yellow bar equals one-tenth foot.*

mineral beds. The phase 3 hypersaline zone covers an estimated area of 117 square miles (303 km^2) (figure 7.14) (Vanden Berg, in preparation), which correlates well with the area in the Uinta Basin having the thickest interval of GRF, where the lake persisted the longest.

Again, similar to phase 1 and 2, the area of bedded evaporite minerals seems to be surrounded by an area containing only smaller evaporite mineral crystals (SEC facies) with a more expansive area to the west (figure 7.14). The extent of the SEC facies is roughly defined to the south by the presence of evaporite minerals captured in several cores: Half Moon Canyon 1, Sams Canyon 1, Marine Minerals Core Hole 1, and Marine Minerals Core Hole 2, all of which can be correlated with the Fat tuff. This interval is also exposed in outcrop, but only the Indian Canyon exposures have been thoroughly studied (Dyni and others, 1985). The western extent can be approximated based on previous field-based studies that indicate small evaporite mineral crystals in the "saline facies" in outcrops 15 miles (24 km) west of Indian Canyon along the Walker Hollow road (Dane, 1954) and as far away as 40 miles (64 km) west of Indian Canyon, southwest of Strawberry Reservoir,

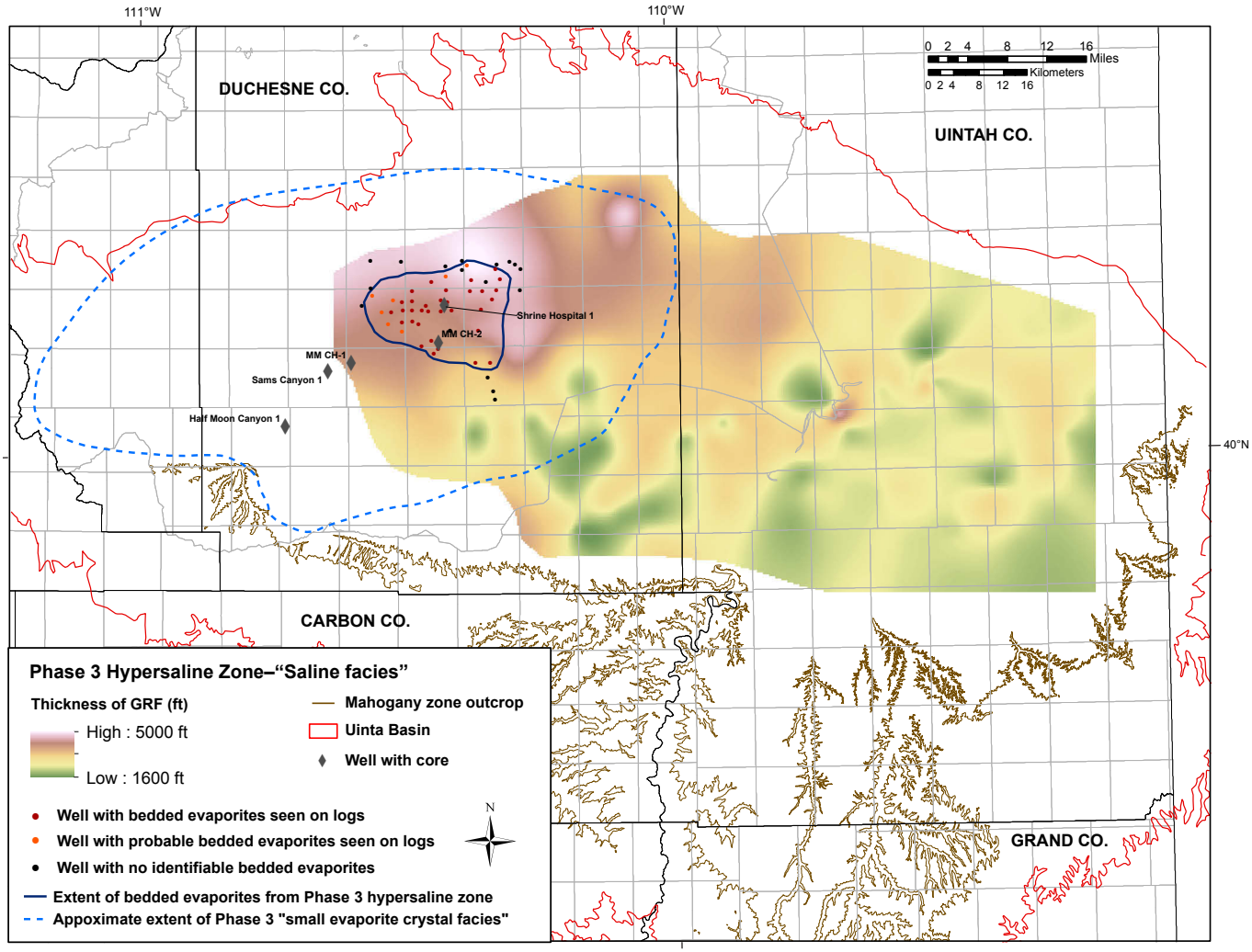

Figure 7.14. *Extent of the phase 3 hypersaline interval in the upper GRF. The area with bedded salt deposition occurs within the area of thickest sediment accumulation in the GRF, representing the paleo-depocenter of Lake Uinta during its final phase of existence.*

in sections 10 and 15, T. 5 S., R. 12 W., UBL&M, Duchesne County (Dyni and others, 1985). The northern boundary of the phase 3 SEC facies cannot be accurately defined due to a lack of core or exposures in the area, but is presumed to pinch out or interfinger with Uinta Formation sands coming off the Uinta uplift not far north of the bedded evaporite zone (figure 7.14).

Reservoir Properties

Porosity in GRF reservoirs generally ranges from 5% to 30%, but is highly variable depending on reservoir and porosity type, and location (Lucas and Drexler, 1975; Osmond, 1985; Fouch and others, 1992a, 1992b; Kelly and Castle, 1992; Vanden Berg and others, 2014; Schamel, 2015). Permeability typically ranges from 0.1 to 42 mD, and is similarly highly variable (Fouch and others, 1992a; Kelley and Castle, 1992). Reservoir porosity and permeability are greatly affected by diagenetic processes. For example, compaction (extreme in the Altamont-Bluebell field area), quartz overgrowths, extensive carbonate cementation, and authigenic clay formation (illite [Altamont-Bluebell], kaolinite [Monument Butte-Natural Buttes], chlorite, and smectite) have all reduced reservoir porosity and permeability in the GRF (Pitman and others, 1982; Colburn and others, 1985; Fouch and others, 1992b; Kelly and Castle, 1992). In contrast, secondary dissolution of both framework grains and carbonate cement has increased reservoir porosity and permeability as much as 25% in some areas (Kelly and Castle, 1992). Natural, open fractures greatly enhance permeability in reservoirs, especially in the northern part of the basin in the Cedar Rim, Altamont, and Bluebell fields (Narr and Currie, 1982; Morgan, 2003b).

Water Quality

Groundwater movement in the Uinta Basin generally follows the slope and direction of major streams and rivers (Price and Miller, 1975; Wallace, 2012a). For the southeastern part of the basin, flow direction is from the southeast to the northwest, and for the north, groundwater generally flows from northwest to southeast. Recharge to the basin mostly occurs from the Uinta Mountains to the north, with a smaller amount coming from outcrops along the southern and eastern margins of

the basin (Zhang and others, 2009). However, the complexity of the GRF reservoirs, their lenticular morphology, and their common enclosure within low-permeability facies such as lacustrine limestone and shale, create significant heterogeneity in overall groundwater characteristics.

In general, water quality in the lower GRF tends to have an overall TDS concentration greater than 10,000 mg/L (416 out of 532 wells/samples), but values range from 650 to 110,000 mg/L (figure 7.15). Areas of lowest TDS concentration are coincident with areas of recharge along outcrops near the Douglas Creek arch to the east-southeast and along the Wasatch Plateau to the west. In addition, an area to the north seems to record low-TDS water, indicating recharge from the Uinta Mountains, but data are sparse. An area of high TDS concentration occurs in a northeast-southwest-trending zone in the central part of the basin and is roughly coincident with the surface location of the Green River. Within this zone, the highest TDS values (>60,000 mg/L) occur in water located between 300 and 800 feet (90–240 m) of elevation (above mean sea level) and 1200 to 2000 feet (370–600 m) below the Mahogany bed. The dominant cations and anions are sodium (Na), chloride (Cl), and sulfate (SO_4); bicarbonate (HCO_3), calcium (Ca), and magnesium (Mg) occur in minor amounts. As stated above, the general groundwater flow directions are towards the major river systems (e.g., the Green River). This area of higher TDS could represent long-residence-time water funneling towards the Green River from outcrop areas to the east and west, picking up solutes as it travels.

TDS values for the upper GRF range from 600 mg/L up to 300,000 mg/L and are heavily influenced by the existence of evaporite minerals in certain areas of the basin (saline phases as identified above) (figure 7.16). The isolated and few nahcolite nodules found within the phase 1 hypersaline zone, located within the Mahogany zone, do not influence groundwater salinity and therefore this interval is not displayed on figure 7.16.

Groundwater related to the phase 2 hypersaline interval (Birds Nest aquifer) varies significantly from southeast to northwest. Using data compiled during this study and from Vanden Berg and others (2013), it was possible to delineate a southeast to northwest transition from low to higher TDS water within the Birds Nest aquifer (figure 7.17). Chemistry of water to the northwest of the boundary (averaging >10,000 mg/L TDS and as high as 100,000 mg/L TDS) is distinct from that in the southeast (averaging <10,000 mg/L TDS and down to near 1000 mg/L TDS). The observed variations in Birds Nest aquifer salinity are most likely due to differing amounts of evaporite mineral dissolution. Areas where Birds Nest aquifer TDS values are <10,000 mg/L are located near and immediately downdip from areas of aquifer recharge such as Evacuation Creek, the White River, and outcrops to the east and south. In these areas, continuous freshwater recharge and flushing over time have likely removed all the original natural evaporite minerals. Areas where the Birds Nest aquifer salinity is known to exceed 10,000 mg/L TDS are located away from active aquifer recharge and flushing, so the original evaporite minerals are still present and possibly undergoing active dissolution. Wells with high TDS concentrations have water chemistry with abundant sodium (Na) and bicarbonate (HCO_3), as expected from the dissolution of nahcolite (Na_2HCO_3). For example, water analysis from this interval in the Hoss No. 904-36 well (section 36, T. 8 S., R. 22 E., SLBL&M, Uintah County, API No. 43-047-50304) has 62,537 mg/L of HCO_3 and 27,800 mg/L of Na. In contrast, water from the same interval from a well farther south, the Bonanza No. 1023-14C well (section 14, T. 10 S., R. 23 E., SLBL&M, Uintah County, API No. 43-047-38299) contains only 585 mg/L of HCO_3 and 1059 mg/L of Na.

High-TDS areas in the upper GRF in the northwest and central parts of the basin are likely due to the presence of disseminated and bedded evaporite minerals of the phase 3 hypersaline zone, stratigraphically higher than the Birds Nest aquifer. Several sample sites, indicated as red triangles on figure 7.16, are from the Uinta Formation-Green River Formation transition zone. Two wells within the phase 3 bedded hypersaline zone have water chemistry strongly reflective of the mineral halite. The Altamont No. 1 salt water disposal well (section 24, T. 2 S., R. 6 W., UBL&M, Duchesne County, API No. 43-013-30372) has 120,000 mg/L of Na and 180,000 mg/L of Cl, and the Ute No. 1-14C6 well (section 14, T. 2 S., R. 6 W., ULB&M, Duchesne County, API No. 43-013-30056) has 122,443 mg/L of Na and 141,600 mg/L of Cl, but also has significant HCO_3 (12,200 mg/L), indicating the presence of nahcolite. All other wells in the phase 3 hypersaline zone have water with varying concentrations of Na, Cl, and HCO_3, as well as varying amounts of minor constituents including Mg, SO_4, and Ca. As shown on the TDS map of the upper GRF (figure 7.16), not only do the bedded salts influence groundwater chemistry, but the larger area of SEC has a significant impact on overall water quality.

Anderson and others' (2012) study of water quality in the Uinta Basin produced a map of the BMSW (TDS of 10,000 mg/L). Using the newly updated structure contour map of the GRF, we created a map to show where the top of the GRF is relative to the BMSW (figure 7.18). The map shows that the top of the GRF is as much as 6000 feet (1800 m) below the BMSW in the north, whereas the top of the formation is above the BMSW (up to 5300 feet [1600 m]) in the southern, western, and eastern parts of the basin.

Water Production, Use, and Disposal

Total cumulative water production from the GRF varies across the Uinta Basin from 15 bbls at Oil Springs field in the southeast, where the only well to produce from the GRF is now plugged and abandoned, to over 347 million bbls at Red Wash field in the northeast (figure 7.19). The cumulative total of water produced from the GRF is over 754 million bbls (MMB) from 5355 wells in 46 named fields, 3 wildcats, and 3 undesignated fields, as of December 2014 (Utah Divi-

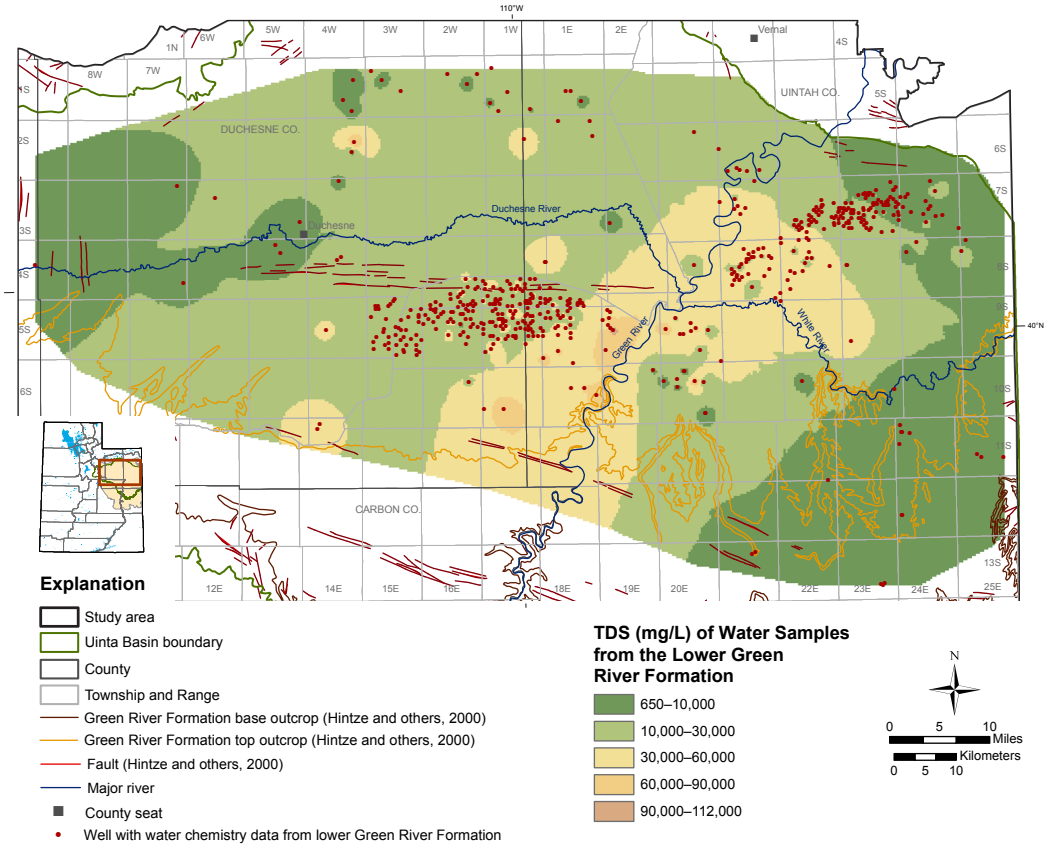

Figure 7.15. *Available total dissolved solids concentrations (mg/L) from water samples taken within the lower Green River Formation (data from Anderson and others [2012] and U.S. Geological Survey [2014]).*

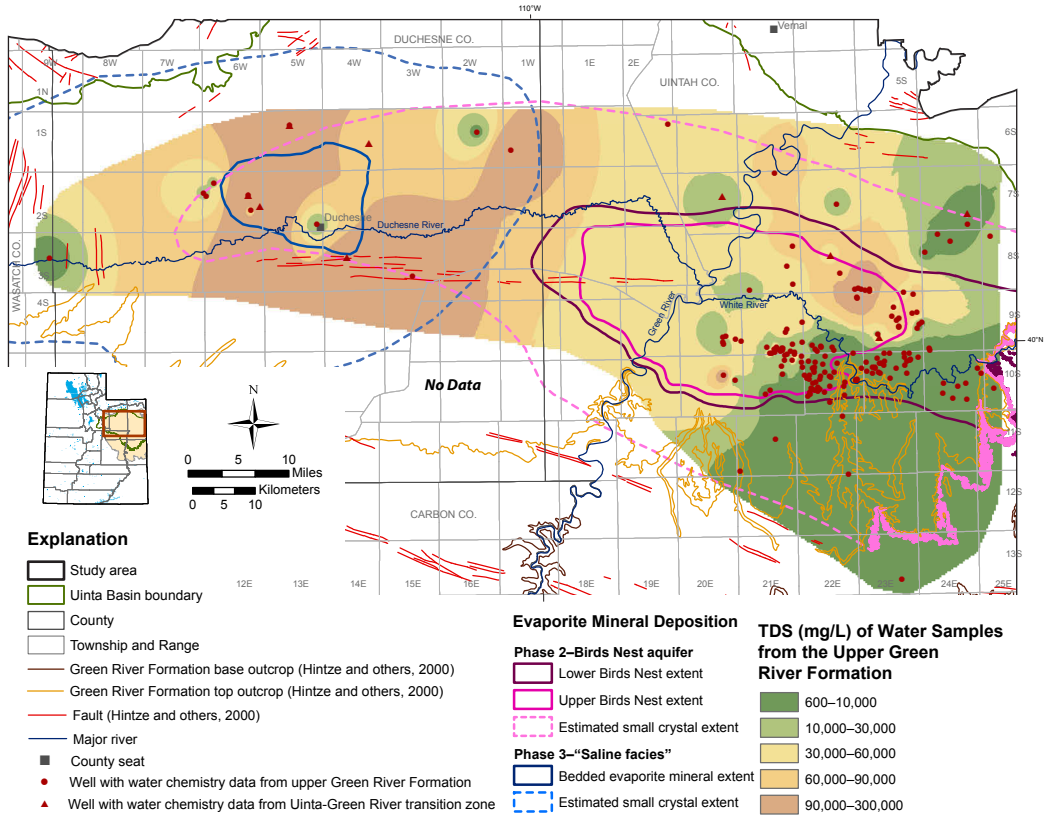

Figure 7.16. *Available total dissolved solids concentrations (mg/L) from water samples taken within the upper Green River Formation (data from Anderson and others [2012] and U.S. Geological Survey [2014]).*

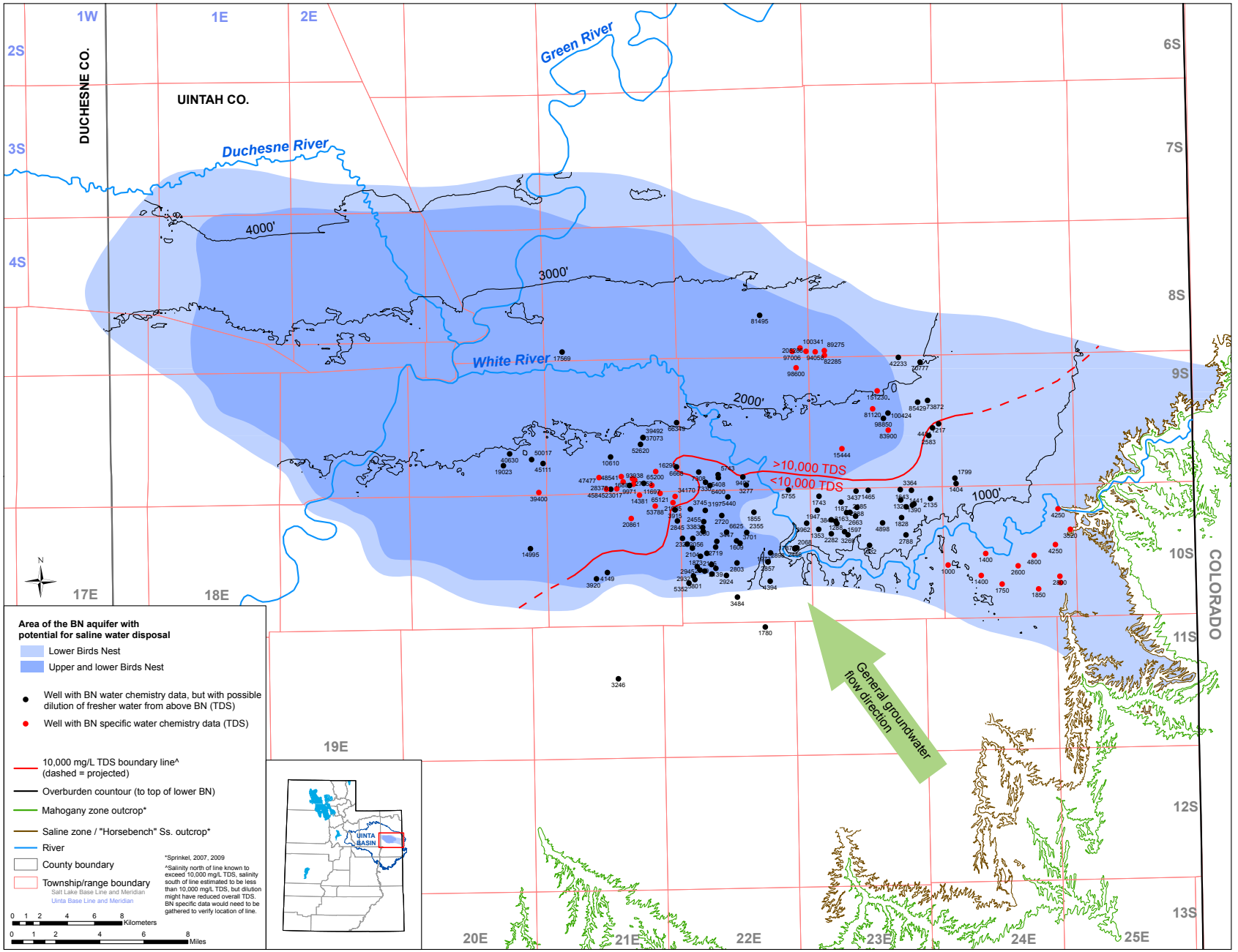

Figure 7.17. *Available total dissolved solids concentrations (mg/L) from water samples taken within the Birds Nest aquifer (phase 2 hypersaline zone) (from Vanden Berg and others, 2013).*

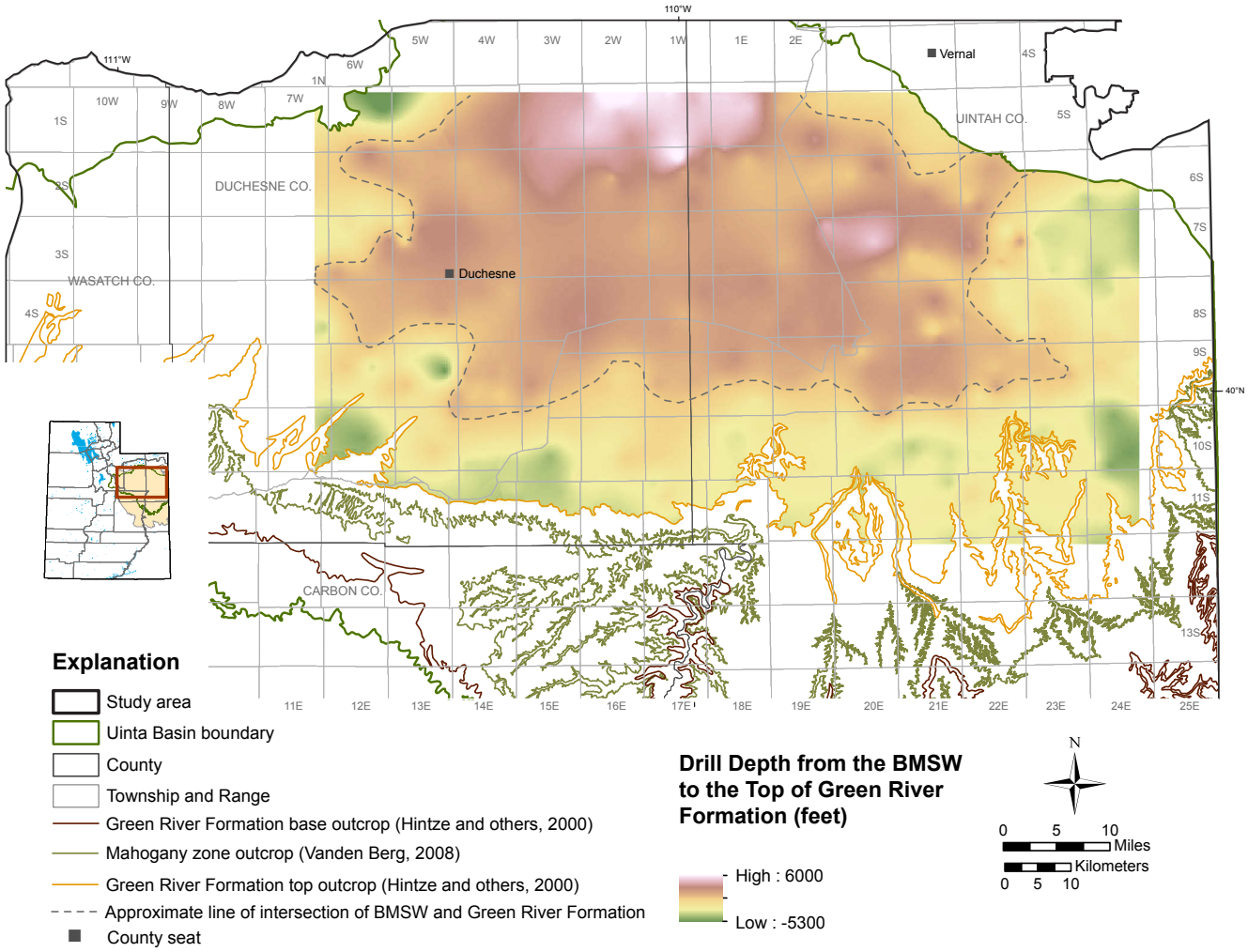

Figure 7.18. *Depth from the base of the moderately saline water (BMSW) to the top of the Green River Formation (Anderson and others, 2012).*

sion of Oil, Gas and Mining, 2015). The average cumulative water volume produced per well equals about 140,000 bbls (140 MB), but this average is skewed high due to a minority of wells with greater than 1 MMB of production. The vast majority of wells (4400 out of 5310) have cumulative production between 1000 and 100,000 BW (figure 7.20A) and more than half have a daily production between 1 and 10 bbls (figure 7.20B). A word of caution—several thousand wells in the Uinta Basin produce from both the GRF and the underlying Wasatch Formation. This production is commingled and there is no way to distinguish production between the formations. The commingled data are not included in this study.

At Monument Butte field (figure 1.1) and several other Uinta Basin fields, produced water from the GRF reservoirs is treated and used for major EOR waterflood programs. In 2012, for example, 8.2 MMBW was produced at Monument Butte and 22 MMBW was injected for waterflooding.

Elsewhere, water produced from the GRF, and other formations, is currently disposed using injection wells and evaporation ponds. There were 51 salt water disposal wells active in the GRF as of May 2015 (figures 7.21 and 7.22) (Utah Division of Oil, Gas and Mining, 2015). Twenty of these wells are in the western part of the basin and 31 are in the east, where more than half inject into the Birds Nest aquifer (denoted by star shape on figure 7.21). The total volume of water injected as of May 2015, is 356 MMB (Utah Division of Oil, Gas and Mining 2015) and most wells injected between 1 million and 10 million total bbls or 1 to 2500 BPD (figure 7.23). Of the total water volume injected, 137 MMB has been injected into the lower GRF and 219 MMB in the upper GRF, of which 121 MMB went into the Birds Nest aquifer.

The Birds Nest aquifer (phase 2 hypersaline zone) has significant potential for water disposal as discussed in detail by Vanden Berg and others (2013). In an area of known evaporite mineral dissolution, the upper Birds Nest zone has an area of ~359 square miles (930 km^2) and a mean thickness of 81.7 feet (24.9 m), which equals a total volume of 8.2 x 10^{11} cubic feet (2.3 x 10^{10} m^3). Vanden Berg and others (2013) calculated a macro pore volume (at 2.5%) of 20.4 billion cubic feet (578 million m^3) (469,157 acre-feet [579 hm^3]) for saline water storage/disposal. For the lower Birds Nest, they estimated an area of 498.6 square miles (1292 km^2), a mean thickness of 85.2 feet (26.0 m), a total volume of 1.2 x 10^{12} cubic feet (34

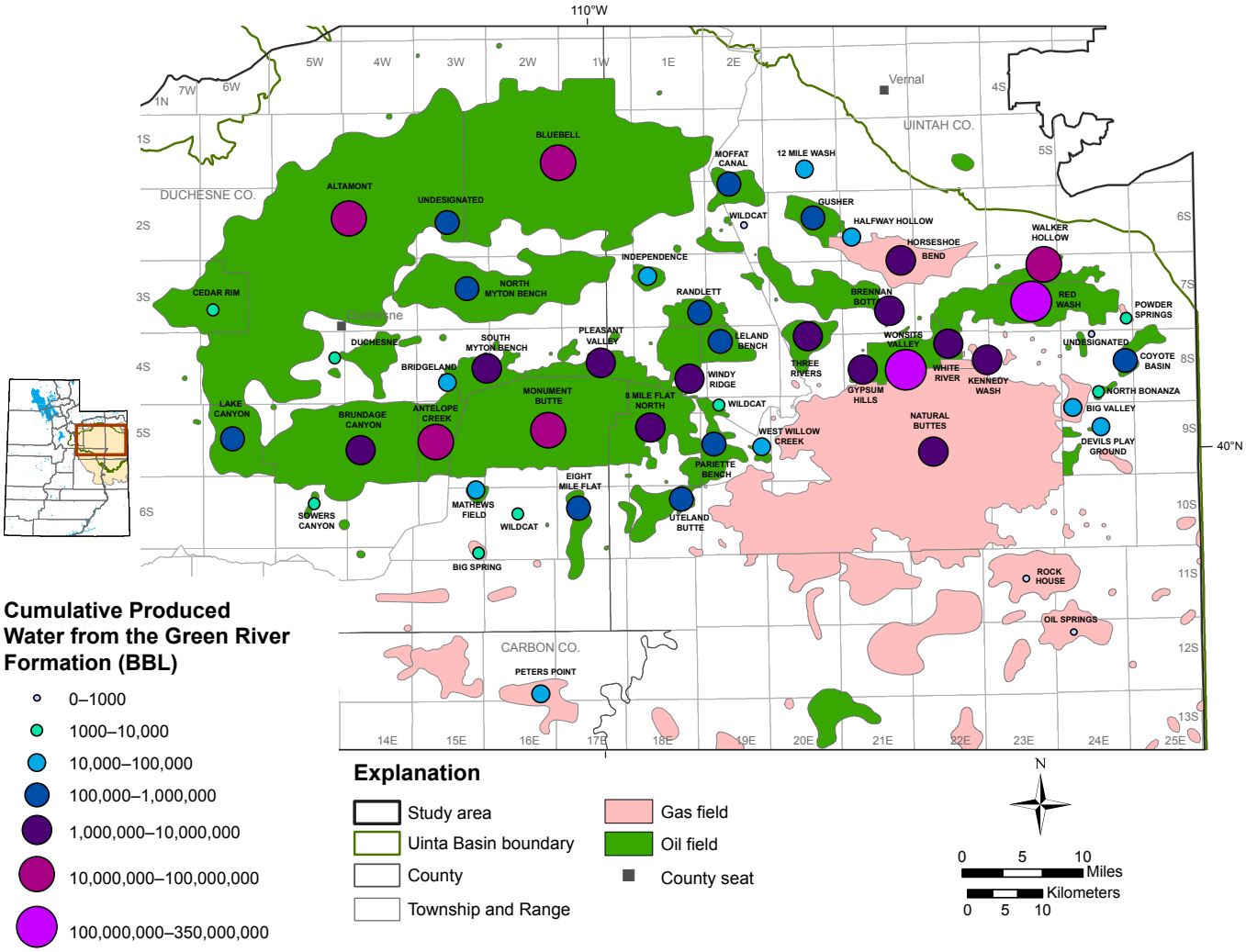

Figure 7.19. *Bubble map showing cumulative produced water (barrels) from the Green River Formation by oil or gas field (through December 2014) (Utah Division of Oil, Gas and Mining, 2015).*

x 10^{10} m^3), and a macro pore volume (at 2.5%) of 29.6 billion cubic feet (8.38 billion m^3) (679,908 acre-feet [838 hm^3]). However, several assumptions were made to derive these numbers; actual reservoir storage could vary significantly (see Vanden Berg and others [2013] for a detailed discussion of the Birds Nest aquifer and its disposal potential).

Hydrocarbon Production

Cumulative hydrocarbon production from the GRF totals over 315 MMBO and 900 BCFG, as of December 2014. The producing reservoirs are stratigraphic and fracture-enhanced structural traps composed of lenticular sandstone beds, carbonate beds, and shale (Morgan, 2003b). Production of oil and gas from the GRF is largely focused in the north-central, south-central, and northeast parts of the basin (figures 7.24 and 7.25). The fields with highest cumulative oil production are Red Wash (85 MMBO), Monument Butte (65 MMBO), and Wonsits Valley (48 MMBO), and fields with highest cumulative gas production are Red Wash (373 BCF), Monument Butte (129 BCF), and Brundage Canyon (113 BCF). Total oil production from the GRF averages about 60,000 bbls per well, with the best producer reaching 2.7 MMBO (Woodward No. 1-21A2 well, section 21, T. 1 S., R. 2 W., UBL&M, Duchesne County, API No. 43-013-30130, Bluebell field, figures 7.24 and 7.25). However, most wells have produced between 10,000 and 100,000 bbls of oil (BO) (3528 out of 5306 wells) and between 1 and 25 BO per day (4017 out of 5257 wells) (figure 7.26A and C). Total gas production from the GRF is much more variable and averages about 170 MMCF per well, with the best producer reaching a very high 45 BCF (RW No. 32-33C well, section 33, T. 7 S., R. 24 E., SLBL&M, Uintah County, API No. 43-047-15171, Red Wash field, figures 7.24 and 7.25). However, most wells have cumulatively produced between 10 MMCFG and 1 BCFG (4223 out of 5304 wells) with daily production between 10 and 50 MCF (2946 out of 5263 wells) (figure 7.26B and D). As stated above, several thousand wells in the Uinta Basin produce from both the GRF and the underlying Wasatch Formation and the commingled data are not included in this study.

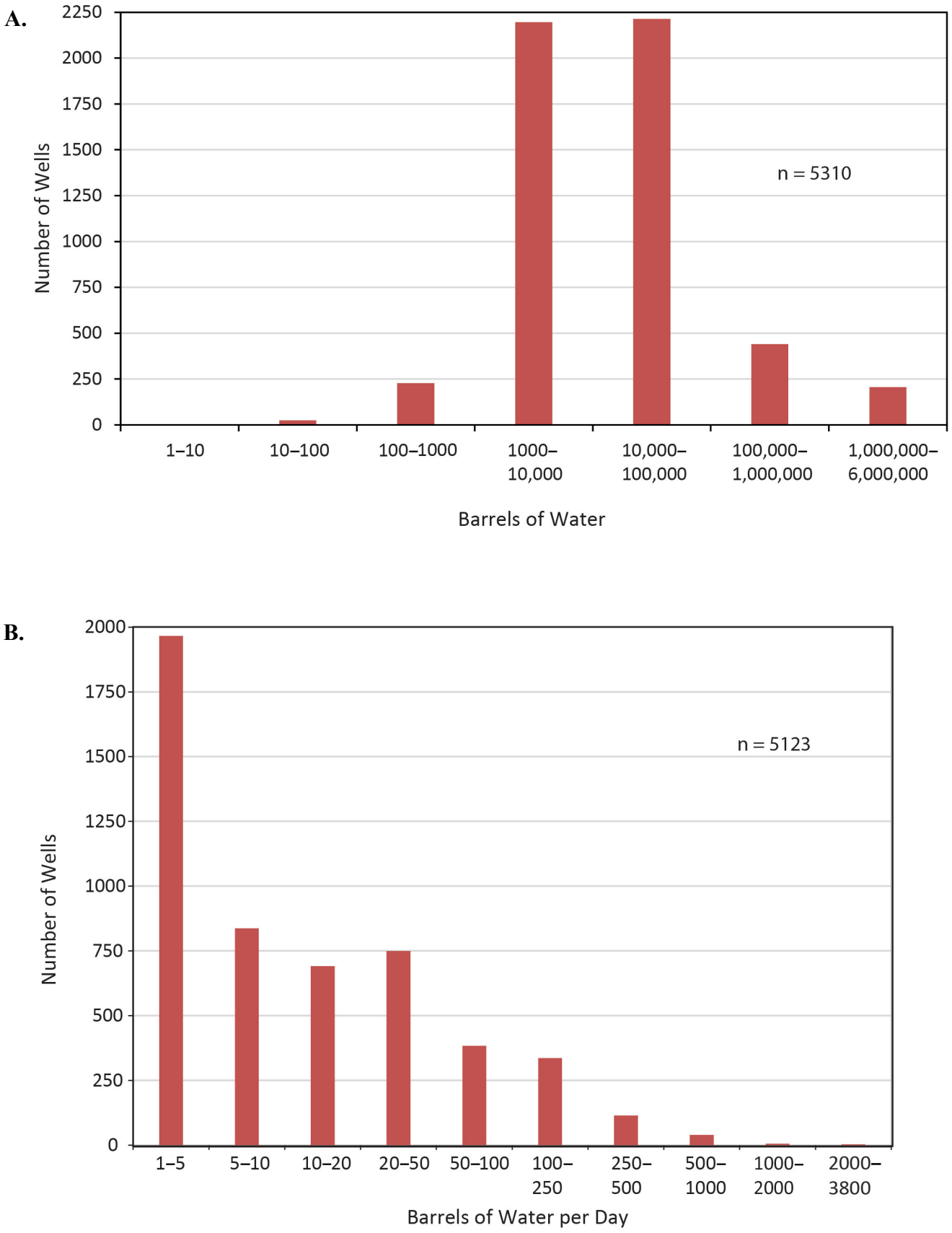

Figure 7.20. *Histogram displaying total water production (barrels) by well from the Green River Formation (through December 2014) (Utah Division of Oil, Gas and Mining, 2015).* ***A.*** *Cumulative water production.* ***B.*** *Water production per day.*

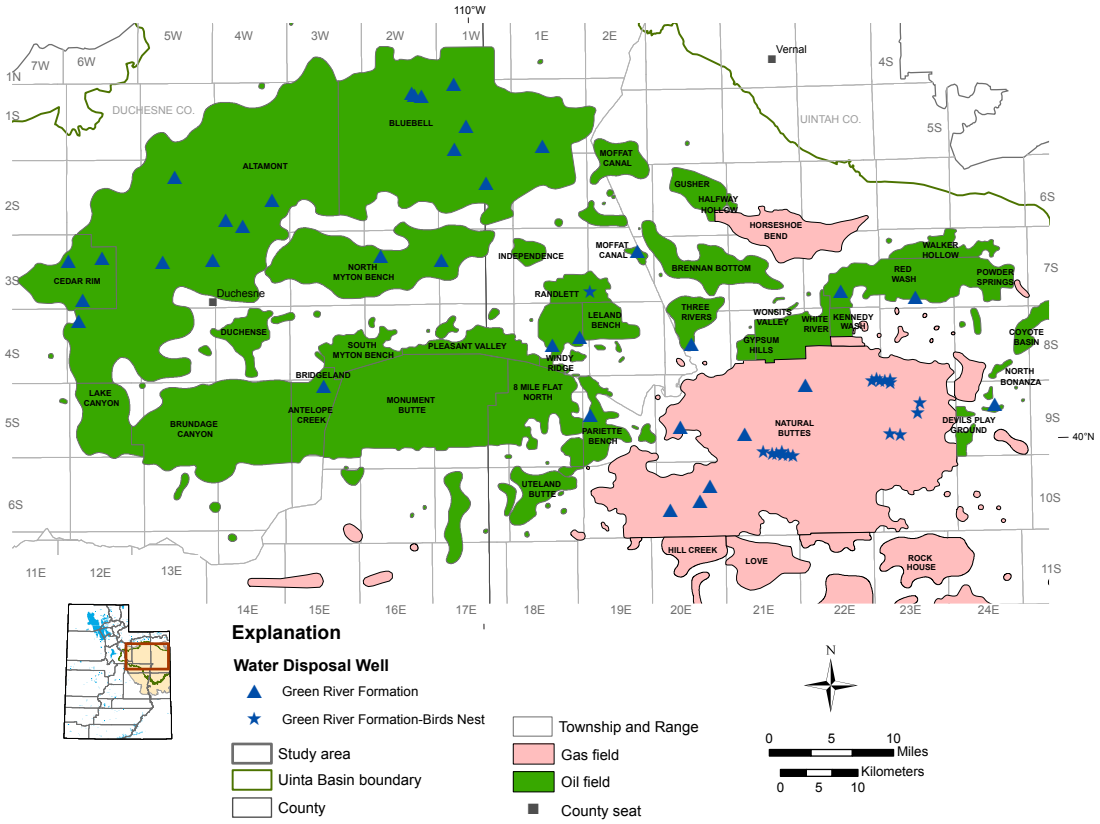

Figure 7.21. *Location of injection wells disposing produced water into the Green River Formation as of May 2015 (Utah Division of Oil, Gas and Mining, 2015).*

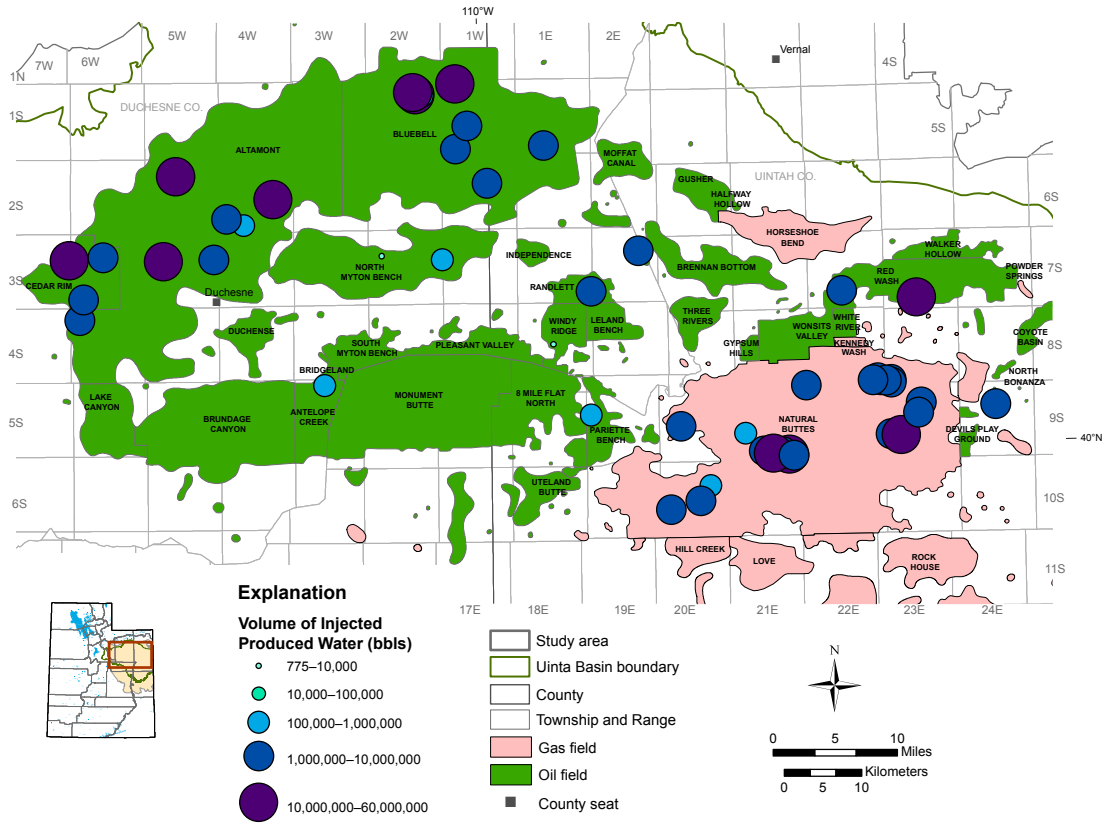

Figure 7.22. *Bubble map showing the volume of water (barrels) that has been injected into the Green River Formation from each injection well as of May 2015 (Utah Division of Oil, Gas and Mining, 2015).*

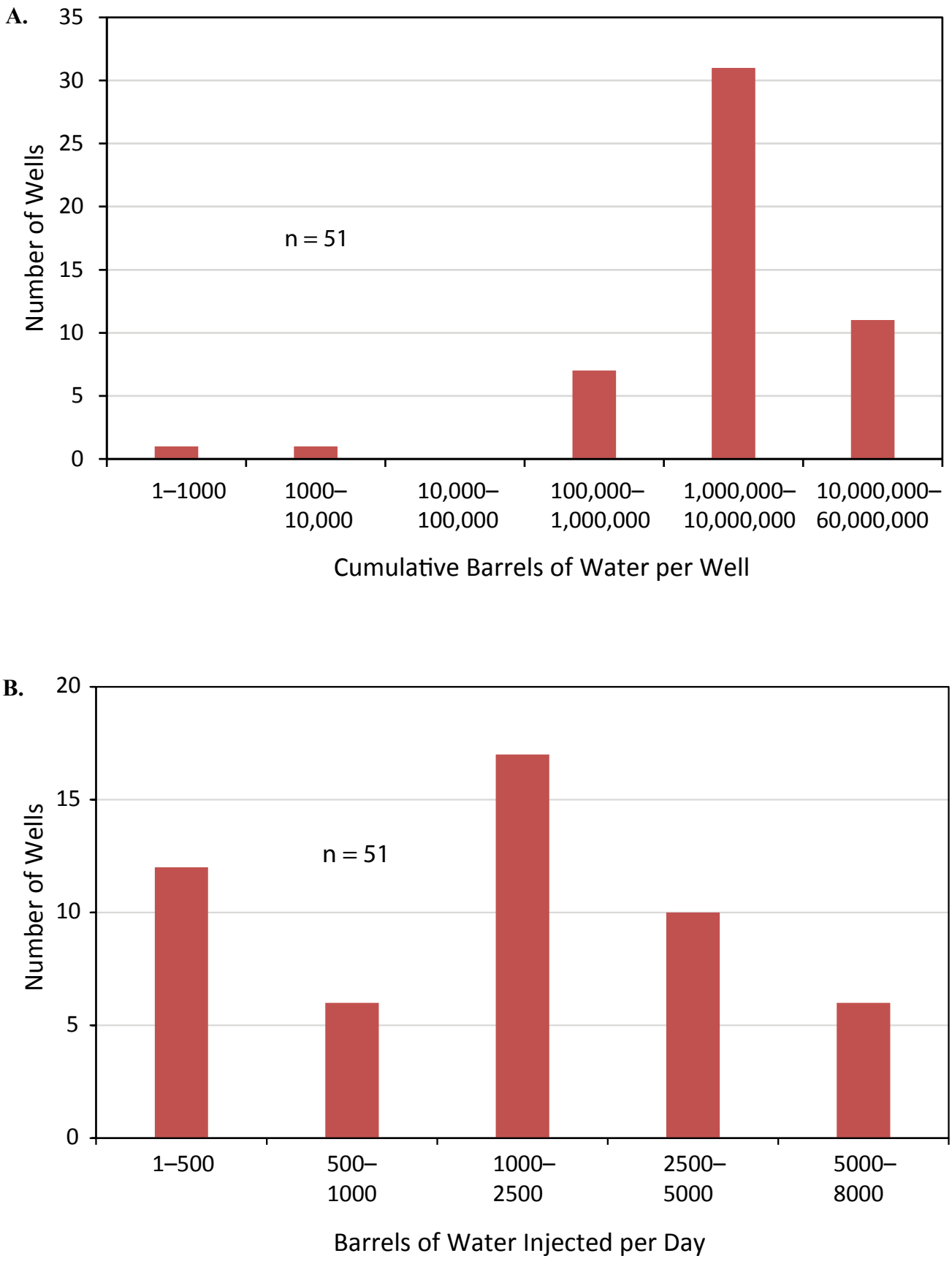

Figure 7.23. *Histograms displaying water (barrels) injected into the Green River Formation via disposal wells (through March 2015) (Utah Division of Oil, Gas and Mining, 2015).* ***A.*** *Cumulative water injection per well.* ***B.*** *Water injection per day per well.*

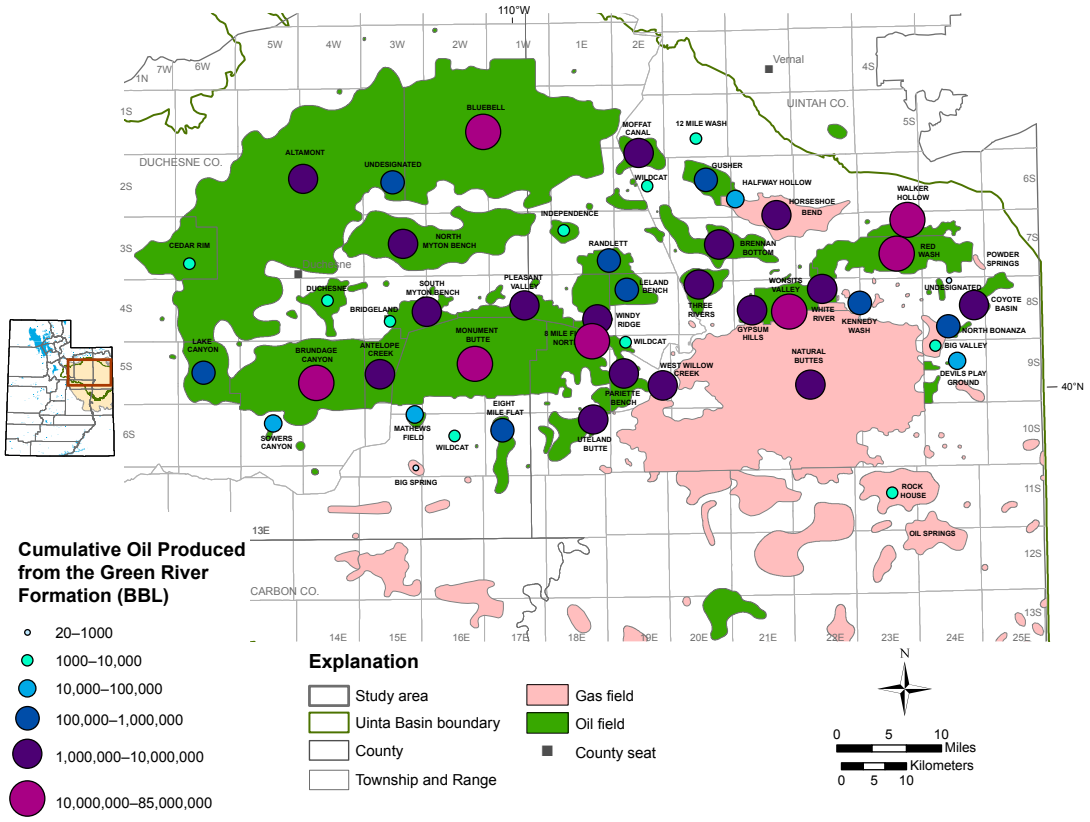

Figure 7.24. *Bubble map showing the volume of oil (barrels) produced (as of May 2015) from the Green River Formation by field (Utah Division of Oil, Gas and Mining, 2015).*

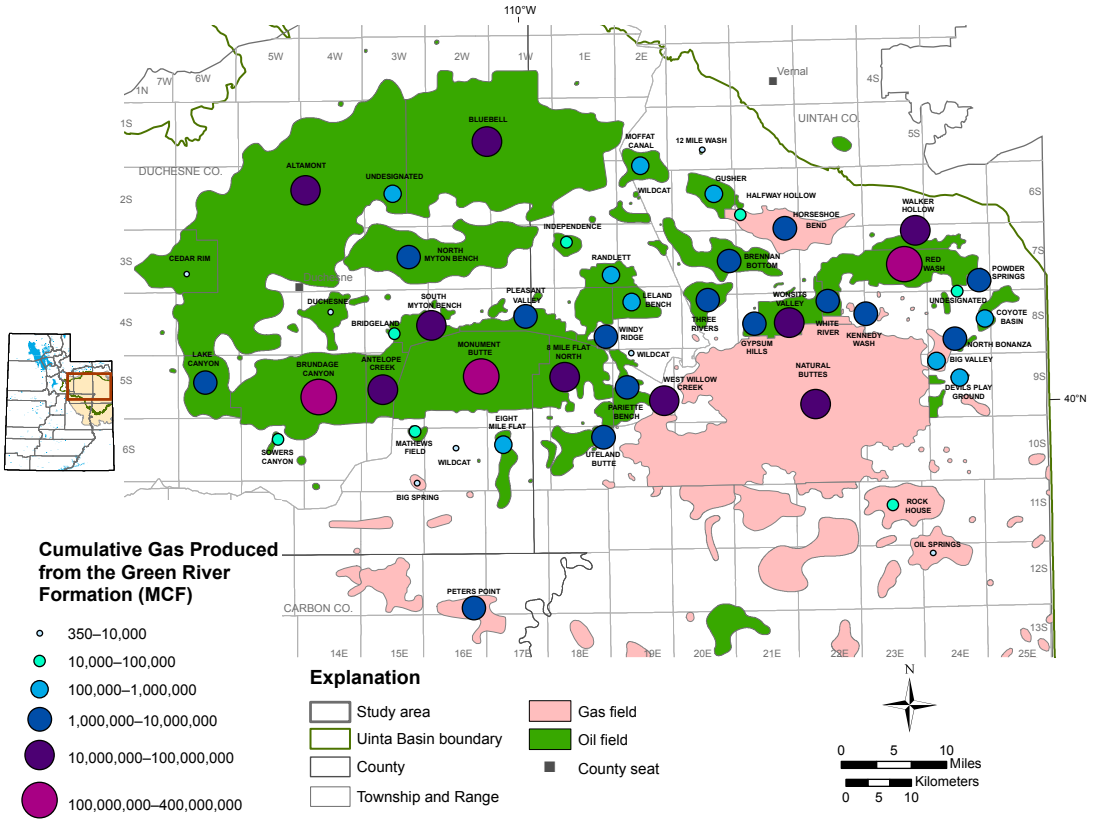

Figure 7.25. *Bubble map showing the volume of gas (MCF) produced (as of May 2015) from the Green River Formation by field (Utah Division of Oil, Gas and Mining, 2015).*

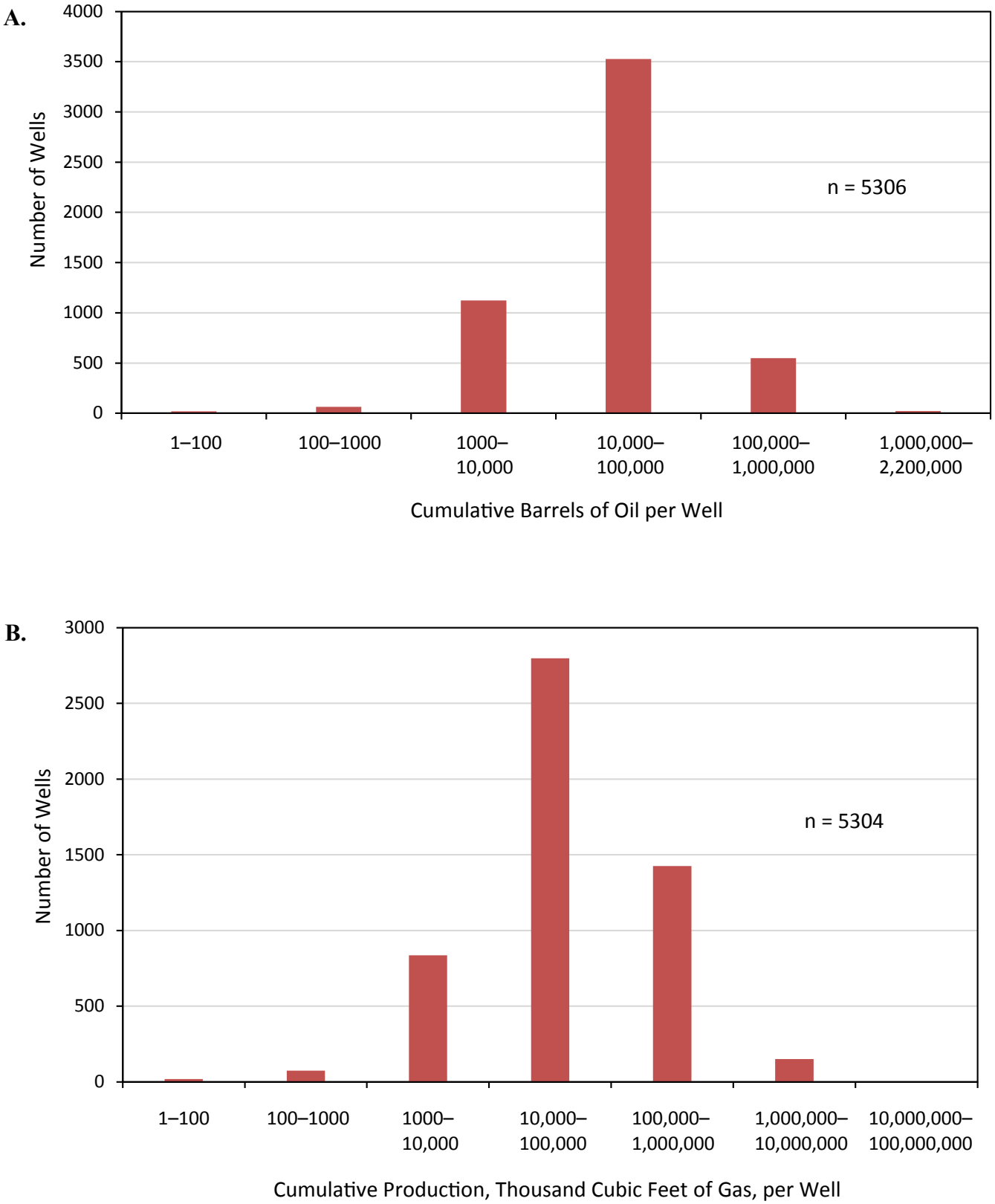

Figure 7.26. *Histograms displaying cumulative* ***A.*** *oil (barrels) and* ***B.*** *gas (MCF) and daily production of* ***C.*** *oil (barrels) and* ***D.*** *gas (MCF) by well from the Green River Formation (through December 2014) (Utah Division of Oil, Gas and Mining, 2015).*

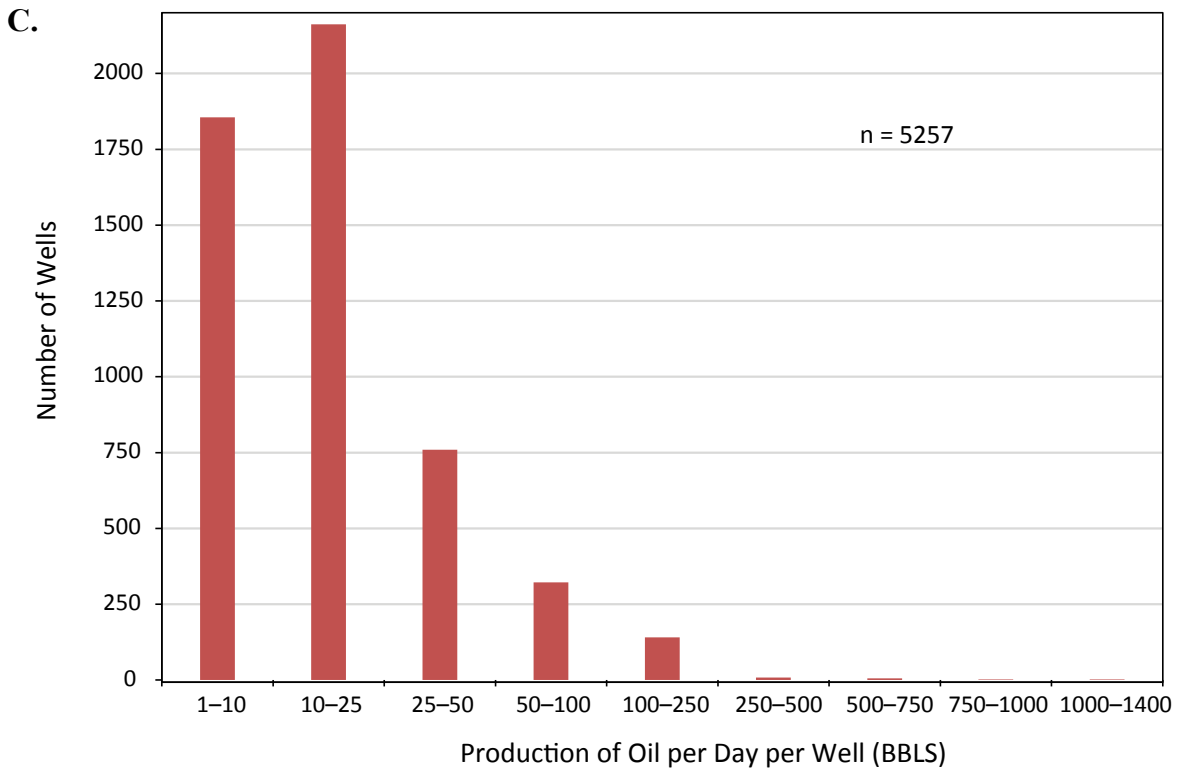

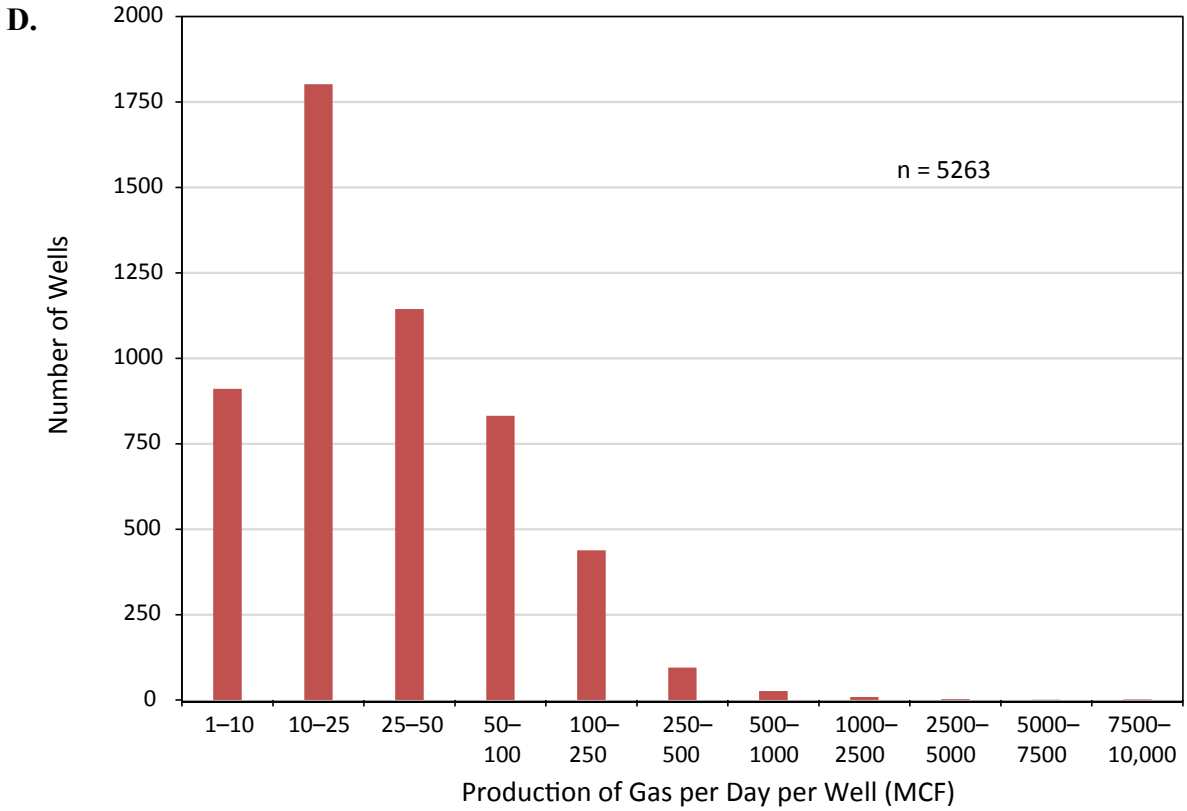

Figure 7.26 *Continued.*

SUMMARY

The GRF is a complex lacustrine sedimentary deposit that is up to 7000 feet (2100 m) thick. The lower GRF, defined as below the Mahogany bed in this study, is mostly lacustrine organic-rich mud and limestone (main source rocks) interbedded with fluvial-deltaic sand and carbonate grainstones (main reservoir rock). The upper GRF, defined as above the Mahogany bed, consists of alternating organic-rich and organic-lean marlstone with three distinct stages of evaporite mineral deposition, the second of which includes the Birds Nest aquifer. Production from the GRF has totaled 315 MMBO, 900 BCFG, and 754 MMBW as of December 2014.

Water quality in the complex lower GRF varies widely from 650 to 112,000 mg/L TDS. Groundwater movement in the Uinta Basin generally follows the slope and direction of major streams and rivers, with recharge mostly from the Wasatch Range to the west, the Douglas Creek arch and Uncompahgre uplift to the east-southeast, and the Uinta Mountains to the north. Groundwater in the lower GRF seems to travel toward the Green River in the central part of the basin and coincides with an area of higher TDS water.

Water quality in the upper GRF also varies widely from 600 to over 200,000 mg/L TDS. Groundwater in the upper GRF is highly influenced by the location of evaporite mineral deposition, which occurred in three distinct phases and locations.

The unique Birds Nest aquifer (phase 2 hypersaline zone) in the upper GRF in the eastern part of the Uinta Basin and the area located around the phase 3 hypersaline interval in the western part of the basin, as well as select areas in the lower GRF, serve as excellent produced-water disposal zones since reservoir water already exceeds 10,000 mg/L TDS. In fact, over 356 MMB of produced water has already been disposed of into GRF reservoirs.

CHAPTER 8:
SUMMARY OF THE COMPILED FLUID GEOCHEMISTRY DATABASE FOR THE UINTA BASIN

by

Stefan M. Kirby

CONTENTS

INTRODUCTION 219
BACKGROUND 219
DATA ANALYSIS 220
SUMMARY 226

FIGURES

Figure 8.1. Number of samples for each geologic unit 220
Figure 8.2. Location of select fluid geochemical samples 221
Figure 8.3. Total dissolved solids versus depth for select samples 222
Figure 8.4. Summary of sample depth by geologic unit 224
Figure 8.5. Summary of total dissolved solids by geologic unit 226
Figure 8.6. Summary of water types by geologic unit 228
Figure 8.7. Major ion chemistry versus total dissolved solids 229
Figure 8.8. Piper plot of select samples 229

TABLES

Table 8.1. Summary of depth distribution of select water chemistry samples 223
Table 8.2. Summary of total dissolved solids distribution for select water chemistry samples 225
Table 8.3. Water type distribution for select samples 227

CHAPTER 8:
SUMMARY OF THE COMPILED FLUID GEOCHEMISTRY DATABASE FOR THE UINTA BASIN

INTRODUCTION

Fluid chemistry of groundwater and produced water places basic constraints on oil and gas operations and development. In the Uinta Basin significant quantities of both produced water and groundwater are used for various phases of oil and gas development and rural agricultural and domestic water supply. The basic chemistry of these fluids controls their ultimate use and value.

The database presented in this chapter is a compilation of available major ion chemistry for both produced water and groundwater in the greater Uinta Basin area. These data include time series and other samples from a variety of geologic units and depths that provide both a record of geochemistry through time and baseline chemistry for the Uinta Basin of eastern Utah.

BACKGROUND

The compiled fluid geochemistry database covers an area that includes the Uinta Basin and adjoining areas to the south and west. Sample locations range from approximately 38°30′ to 40°30′ north latitude and from 111°30′ to 109° west longitude. The database forms the basis for water chemistry used for various sections of the larger Uinta Basin produced-water study (appendix F).

The database includes fluid geochemical analyses of groundwater from springs and wells in addition to produced water collected as part of oil and gas exploration and production. The data were taken from four primary sources: (1) the National Water Information System (NWIS) database (U.S. Geological Survey, 2014), (2) the chemistry database included in Utah Geological Survey Special Study 144 (Anderson and others, 2012), (3) samples compiled from DOGM (Utah Division of Oil, Gas and Mining, 2014), and (4) new samples collected as part of this study. The database contains 4184 samples that include a mix of unique samples for a given location and depth as well as samples that represent a time series of multiple samples from a given location and depth.

Each sample in the database includes data source, basic location information, and a unique identifier. Other data fields are populated as those data are available. General data fields include a site name, site number, altitude, depth of sample, and date of sampling. Site name includes a general name of the sample site when known. The site number field includes the API number for samples from oil and gas wells or the NWIS number for groundwater samples compiled from the USGS database (U.S. Geological Survey, 2014). The altitude is the land surface elevation in feet derived from the 5 meter (16.4 feet) digital elevation model for Utah for a given location. The depth of the sample is listed as a discrete value in feet below land surface. The source databases contain depth of sample information as either a single discrete depth or an open or screened interval. Depth was calculated as the midpoint of the open interval for samples that list screened or open interval.

Sample chemistry fields in the database include temperature, pH, conductivity, TDS, and chemical concentration values. Solute concentrations for CO_2, HCO_3, Ca, Mg, Na, K, SO_4, F, SiO_2, and NO_3 are in mg/L. The concentration of As is µg/L. The sources from which the data are compiled overlap in part and duplicate measurements indicated by identical chemistry and location information were removed.

The milliequivalent concentration of each major solute concentration in the database was calculated using standard methods with the AquaCHEM software. Milliequivalent concentrations were used to calculate charge balance of the percent difference between the sum of charge equivalents for major anions and cations. Samples were given a qualitative balance field indicating whether a sample has charge balance plus-or-minus 5%, between 5% and 10%, and greater than 10%.

Geochemical samples were subdivided based on calculated water type or hydrochemical facies. Water type was calculated for all samples using AquaCHEM geochemical software based on standard methodologies presented by Kehew (2000). Water type is listed in both long and short forms in separate database fields. The long water type lists the two or three major anions and cations for a given sample, and the short water type provides only the single anion and cation with greatest relative concentration.

Five standard scaling and corrosion indices were calculated for samples that had sufficient data using the AquaCHEM software. These indices are (1) Puckorius, (2) Larson-Skold, (3) Residual-Ca, (4) Ryznar, and (5) LSI. The Puckorius, Ryznar, Residual-Ca, and LSI scaling indices give estimates of the propensity for the formation of calcium carbonate scale based on measured water chemistry. Lower values of these scaling indices indicate a greater tendency for calcium carbonate scaling. These scaling indicators do not give absolute

scaling potential but are instead intended to show relative scaling potential based on water chemistry. The Larson-Skold index is an estimate of the corrosive potential of moderately alkaline waters (Larson and Skold, 1958). Larson-Skold values greater than 1.2 indicate a tendency towards high corrosion rates. Values less than 0.8 indicate a low tendency for corrosion and values between 1.2 and 0.8 indicate a moderate tendency for corrosion.

Samples are categorized into 12 simplified geologic units based on geologic unit information in the original data source. Compiled samples lacking geologic unit information were categorized based on depth information when possible. The simplified geologic units are Unconsolidated, Uinta–Duchesne River, upper Green River, lower Green River, Green River (undivided), North Horn, Wasatch/Colton, Mancos, Mesaverde, Dakota–Cedar Mountain, Entrada, and Glen Canyon. Geologic units other than these are categorized as "other." Samples from the Green River Formation were informally separated into upper and lower Green River based on the position of the sample either above or below the Mahogany bed. Green River samples where the Mahogany bed was not identified are listed as "Green River (undivided)." Samples collected from multiple open intervals in different geologic units or open intervals that span geologic unit boundaries are classified as "mix." More detailed geologic unit information and geologic unit name from the source database are included in the "geo notes" field of the database.

Many samples contain incomplete data and/or have a poor geochemical balance. Many other samples represent repeat sampling of discrete locations and depths. To summarize the geochemistry and facilitate analysis of fluid geochemistry by geologic unit, a subset of samples that includes the highest quality geochemical analyses and/or most recent and relevant samples was chosen from the larger database. Chosen samples are indicated by a value of 1 in the "pick" field. Chapters 4 through 7 in this report discuss the fluid geochemistry for many of the simplified geologic units in greater detail. These chapters also depict the spatial distribution of water chemistry for the various geologic units.

DATA ANALYSIS

Samples were selected from the database to analyze trends in water quality. Samples were chosen for each simplified geologic unit based on electrolytic charge balance, location, depth, date of sampling, and completeness of the data. For locations with multiple samples, the most recent sample with charge balance nearest zero was chosen. The geochemical trends of the selected samples are summarized in this section. The selected samples are subsequently referred to as the select samples.

A total of 1377 samples were chosen from the larger database to summarize trends in fluid geochemistry (figure 8.1). More

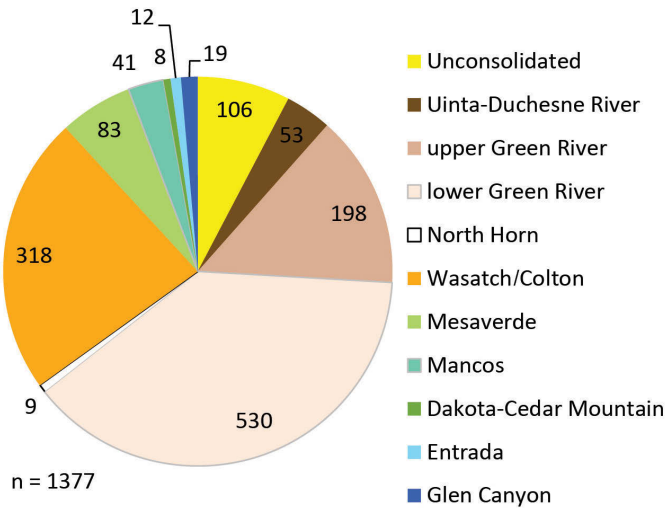

Figure 8.1. *Pie graph of the number of samples for each geologic unit.*

than half of the samples (728) are from either the upper or lower Green River Formation, and nearly a quarter (318) are from the Wasatch/Colton Formation.

A map of the select samples shows that most samples lie within the Uinta Basin and immediately to the south in eastern Utah (figure 8.2). Sample distribution by geologic unit is tightly clustered by the distribution of oil and gas wells in the Uinta Basin and water wells elsewhere. Unconsolidated samples are limited to areas of valley fill in the southeast part of the study area and along major drainages in the Uinta Basin. Samples from the Uinta–Duchesne River unit are scattered across the northwest part of the basin where these rocks are exposed (figure 2.1 and plate 1). Samples from the upper and lower Green River units are densely clustered in areas of oil and gas production within the Uinta Basin. North Horn samples are clustered primarily southwest of the Uinta Basin along the east flank of the Wasatch Plateau. Most Wasatch/Colton samples are located in the northern and eastern parts of the Uinta Basin where this unit is a significant oil and gas reservoir. Mesaverde samples are primarily found in areas where this unit produces gas in the southeast part of the basin. Most Mancos samples are located to the southeast of the Uinta Basin just east of the Wasatch Plateau. Several Mancos samples are from the eastern part of the Uinta Basin. Dakota–Cedar Mountain samples are scattered across the eastern half of the basin. Both the Entrada and Glen Canyon samples are widely scattered across the map area. Notable samples from Entrada and Glen Canyon units occur in the northeast and east parts of the Uinta Basin and south of the basin where these units are important aquifers.

The depth of select samples ranges from zero in the case of several spring samples from the Green River and Unconsolidated units to slightly more than 18,000 feet (5500 m) for samples of produced water from the Wasatch/Colton unit (figure 8.3). For select samples with known depth, data were binned by depth range to show depth trends for the geologic units

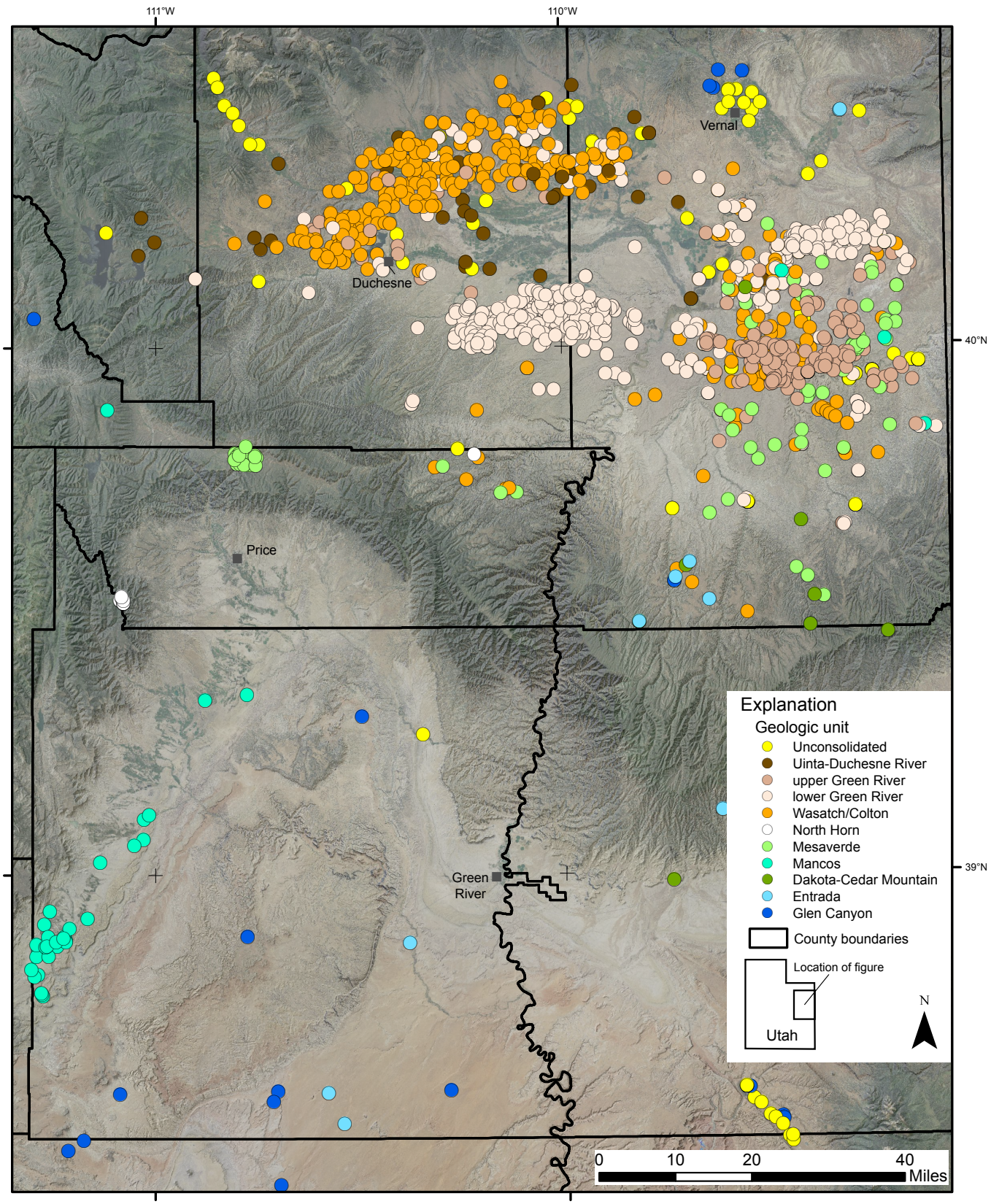

Figure 8.2. *Location of select fluid geochemical samples. Samples in this subset of the database were selected to represent geochemistry of simplified geologic units.*

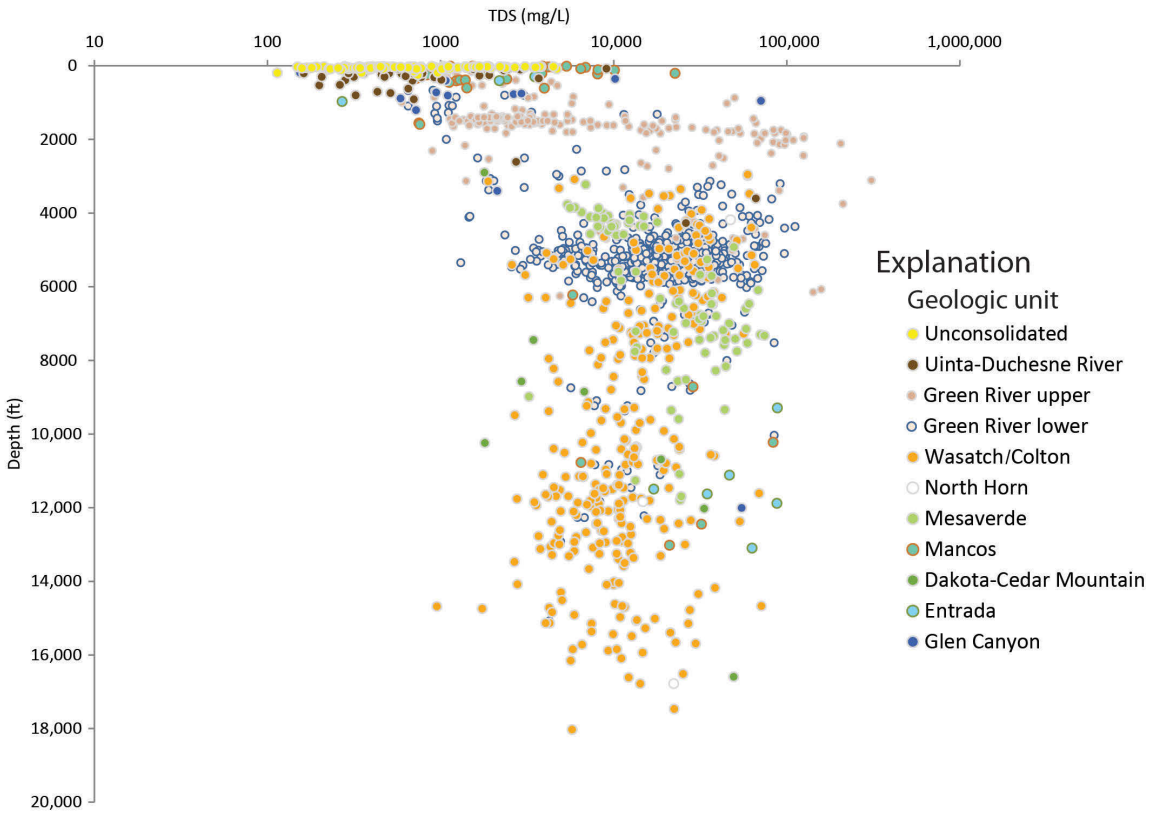

Figure 8.3. *Total dissolved solids (TDS) versus depth for select samples.*

(table 8.1, figure 8.4). The samples cluster in depth ranges depending on the geologic unit. Nearly all samples for the Unconsolidated and Uinta–Duchesne River units are from depths of 500 feet (150 m) or less and represent groundwater supply wells. Nearly all samples from the upper Green River are from depths between 1000 and 2500 feet (300 and 760 m). Samples from the lower Green River range in depth from 2500 to 15,000 feet (760–4600 m), with most samples between 5000 and 10,000 feet (1500–3000 m) in depth. Samples from the Wasatch/Colton unit cluster between 5000 and 15,000 feet (1500–4600 m) in depth. Samples from the North Horn unit range from several thousand to greater than 15,000 feet (4600) in depth. Most samples from the Mancos unit occur at depths less than 500 feet (150 m) from groundwater wells completed in the Ferron Sandstone Member of the Mancos. These Mancos wells represent shallow CBM dewatering wells located southwest of the Uinta Basin. Samples from the Mesaverde and Dakota–Cedar Mountain units come from depths between several thousand and 15,000 feet (4600 m). Nearly two-thirds of the samples from the Glen Canyon unit are from depths less than 1000 feet (300 m); a few additional samples also exist for the Glen Canyon as deep as 15,000 feet (4600 m). The greatest percentage of Entrada samples occurs between depths of 10,000 and 15,000 feet (3000 and 4600 m).

Figure 8.3 also shows TDS versus depth for select samples. TDS concentration for various geologic units increases with depth from 0 to 2000 feet (0–600 m) but is generally below 10,000 mg/L. Below 2000 feet (600 m) TDS concentrations span a large range from several thousand up to 100,000 mg/L. The select samples for the Mesaverde show a general trend of increasing TDS with increasing depth. Other units, including the upper and lower Green River and Wasatch/Colton, show little correlation between TDS and sample depth. Several deep (>9000 feet [275 m]) samples from the Entrada and Glen Canyon units have relatively high TDS values between 10,000 and 100,000 mg/L.

TDS values are binned by concentration range to explore trends in the TDS concentration for each of the simplified geologic units (table 8.2, figure 8.5). All select samples from the Unconsolidated unit have TDS values less than 10,000 mg/L, with nearly half of the samples having a concentration between 1000 and 5000 mg/L. Most samples from the Uinta–Duchesne River unit have TDS concentrations less than 10,000 mg/L and nearly 40% of these samples have TDS less 500 mg/L. The Uinta–Duchesne River unit also contains small percentages (<10%) of samples having TDS concentrations greater than 25,000 mg/L. Early Tertiary-age geologic units including the upper and lower Green River, North Horn, and Wasatch/Colton units have samples with much higher TDS values. More than 40% of the samples in the lower Green River and Wasatch/Colton units have TDS between 10,000 and 25,000 mg/L. The upper Green River unit has 50% of its samples with TDS between 1000 and 5000 mg/L. Most North Horn samples have TDS less than 500 mg/L. Samples from Cretaceous-age geologic units including the Mancos, Mesaverde, and Dakota–Cedar Mountain have TDS distributions similar to those of the

Table 8.1. *Summary of depth distribution of select water chemistry samples.*

Depth (ft)	Geologic Unit											
	Unconsolidated	**Uinta–Duchesne River**	**upper Green River**	**lower Green River**	**North Horn**	**Wasatch/ Colton**	**Mesaverde**	**Mancos**	**Dakota–Cedar Mountain**	**Entrada**	**Glen Canyon**	**All Units**
<500	84	39	9	0	0	0	0	22	0	3	7	164
500–1000	0	9	11	5	0	0	0	2	0	1	6	34
1000–2500	0	0	141	13	0	0	0	2	0	0	1	157
2500–5000	0	5	21	159	1	31	30	0	1	0	1	249
5000–10,000	0	0	8	338	0	116	48	2	3	1	0	516
10,000–15,000	0	0	0	14	1	145	4	4	3	5	1	177
>15,000	0	0	0	1	1	26	0	0	1	0	0	29
total observation	84	53	190	530	3	318	82	32	8	10	16	1326
<500	100%	74%	5%	0%	0%	0%	0%	69%	0%	30%	44%	12%
500–1000	0%	17%	6%	1%	0%	0%	0%	6%	0%	10%	38%	3%
1000–2500	0%	0%	74%	2%	0%	0%	0%	6%	0%	0%	6%	12%
2500–5000	0%	9%	11%	30%	33%	10%	37%	0%	13%	0%	6%	19%
5000–10,000	0%	0%	4%	64%	0%	36%	59%	6%	38%	10%	0%	39%
10,000–15,000	0%	0%	0%	3%	33%	46%	5%	13%	38%	50%	6%	13%
>15,000	0%	0%	0%	0%	33%	8%	0%	0%	13%	0%	0%	2%
sum	100%	100%	100%	100%	100%	100%	100%	100%	100%	100%	100%	100%

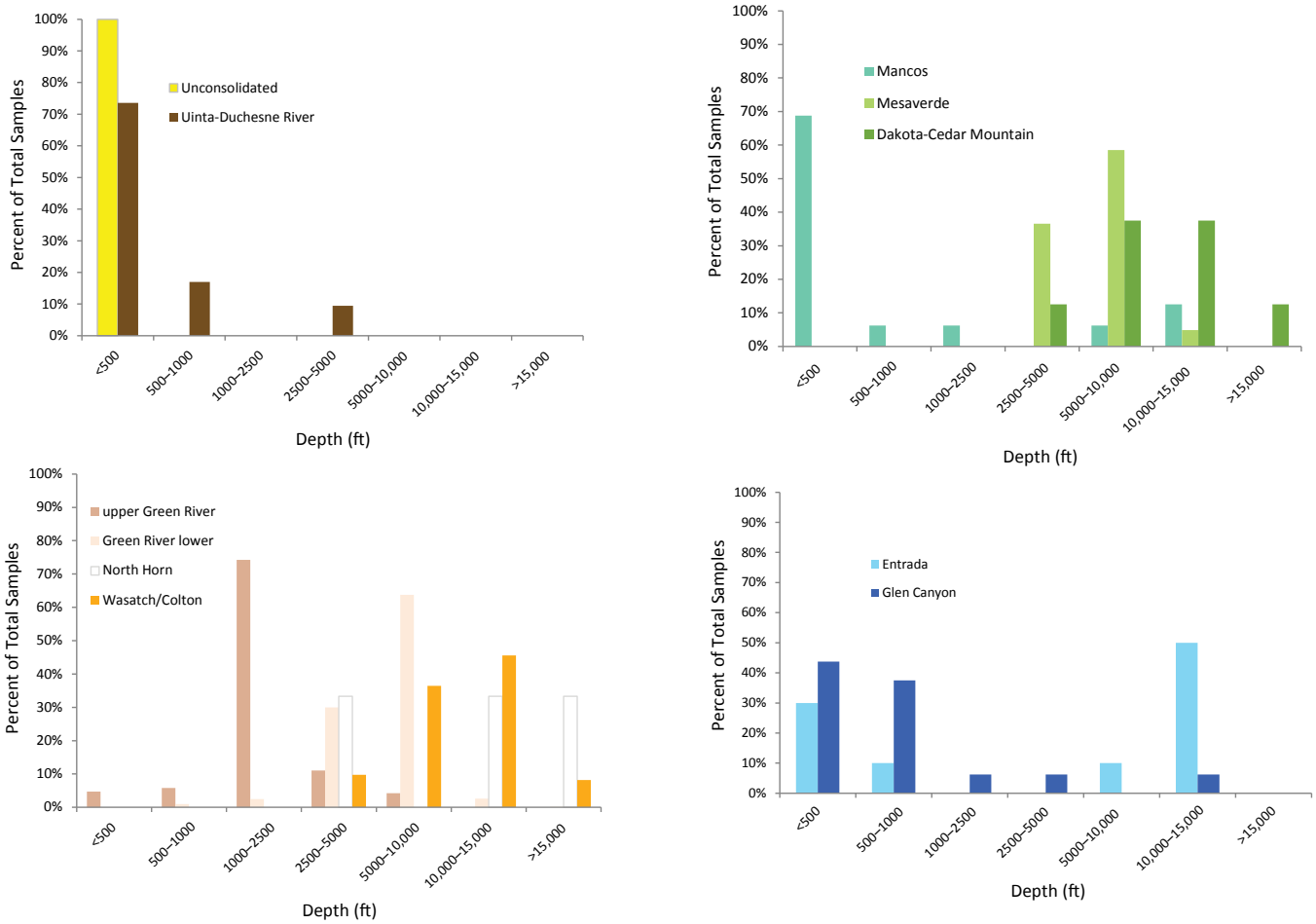

Figure 8.4. *Summary of sample depth by geologic unit. Data correlate with that in table 8.1.*

early Tertiary-age units. Nearly 50% of the samples from both the Mancos and Dakota–Cedar Mountain units have TDS concentrations between 1000 and 5000 mg/L. The Mancos unit has 20% of samples with TDS between 500 and 1000 mg/L, and the remainder of the Mancos samples have TDS greater than 5000 mg/L. More than 20% of samples from the Dakota–Cedar Mountain unit have TDS between 25,000 and 50,000 mg/L. Approximately 30% of the Mesaverde unit samples are in the 10,000 to 25,000 mg/L range. A smaller percentage of Mesaverde samples are in the 5000 to 10,000 mg/L or 25,000 to 50,000 mg/L ranges. No Mesaverde samples have TDS less than 5000 mg/L. Samples from the Glen Canyon and Entrada units have more evenly distributed TDS concentrations than the other units. The samples for the Entrada unit include TDS concentrations that range from less than 500 to more than 50,000 mg/L; most Entrada samples are in the 1000 to 5000 or the greater than 50,000 mg/L TDS concentration ranges. The majority of Glen Canyon samples have TDS concentrations less than 5000 mg/L and smaller percentages of samples in the 10,000 to 25,000 and greater than 50,000 mg/L ranges.

Major ion chemistry is both a product and driver of water-rock interaction, scaling, corrosion, and ultimately the use of a fluid. The select samples for each geologic unit were subdivided into groups based on the major ion water type (table 8.3, figure 8.6). The total number of water types represent nine major ion combinations of NaCl, $NaSO_4$, $NaHCO_3$, CaCl, $CaSO_4$, $CaHCO_3$, MgCl, $MgSO_4$, and $MgHCO_3$. Potassium water types are found in only three samples and are excluded from the water type percentages in table 8.3 and the bar graphs on figure 8.6. Major ion chemistry is variable across the geologic units, with oil- and gas-producing geologic units, such as the upper and lower Green River, Wasatch/Colton, Mesaverde, Mancos, and Dakota–Cedar Mountain, having sodium chloride- or sodium bicarbonate-dominated water types. The Unconsolidated, Uinta–Duchesne River, Entrada, and Glen Canyon units have a greater diversity of water types and include a significant fraction of calcium bicarbonate and calcium sulfate samples. Samples from the Unconsolidated and Uinta–Duchesne River units are primarily bicarbonate water types that include either sodium or calcium as the major cation. Both these units have a small fraction of samples (less than 10%) of magnesium water types. Two-thirds of the North Horn samples are calcium bicarbonate water type and the remainder is sodium chloride water type. Nearly half of the Entrada samples are sodium chloride water type. Just more than half of the Glen Canyon samples are calcium bicarbonate and calcium sulfate waters.

Table 8.2. *Summary of total dissolved solids distribution for select water chemistry samples.*

TDS (mg/L)	Geologic Unit											
	Unconsolidated	**Uinta–Duchesne River**	**upper Green River**	**lower Green River**	**North Horn**	**Wasatch/ Colton**	**Mesaverde**	**Mancos**	**Dakota–Cedar Mountain**	**Entrada**	**Glen Canyon**	**All Units**
<500	33	21	0	0	6	0	0	0	0	2	7	69
500–1000	22	16	5	7	0	1	0	8	0	0	3	62
1000–5000	50	12	98	45	0	41	1	20	4	3	6	280
5000–10,000	1	1	19	63	0	76	18	7	1	1	0	187
10,000–25,000	0	0	25	234	2	140	30	3	1	1	1	437
25,000–50,000	0	2	16	144	1	48	25	2	2	2	0	242
>50,000	0	1	34	37	0	12	9	1	0	3	2	99
total observation	106	53	197	530	9	318	83	41	8	12	19	1376
<500	31%	40%	0%	0%	67%	0%	0%	0%	0%	17%	37%	5%
500–1000	21%	30%	3%	1%	0%	0%	0%	20%	0%	0%	16%	4%
1000–5000	47%	23%	50%	8%	0%	13%	1%	49%	50%	25%	32%	20%
5000–10,000	1%	2%	10%	12%	0%	24%	22%	17%	13%	8%	0%	14%
10,000–25,000	0%	0%	13%	44%	22%	44%	36%	7%	13%	8%	5%	32%
25,000–50,000	0%	4%	8%	27%	11%	15%	30%	5%	25%	17%	0%	18%
>50,000	0%	2%	17%	7%	0%	4%	11%	2%	0%	25%	11%	7%
sum	100%	100%	100%	100%	100%	100%	100%	100%	100%	100%	100%	100%

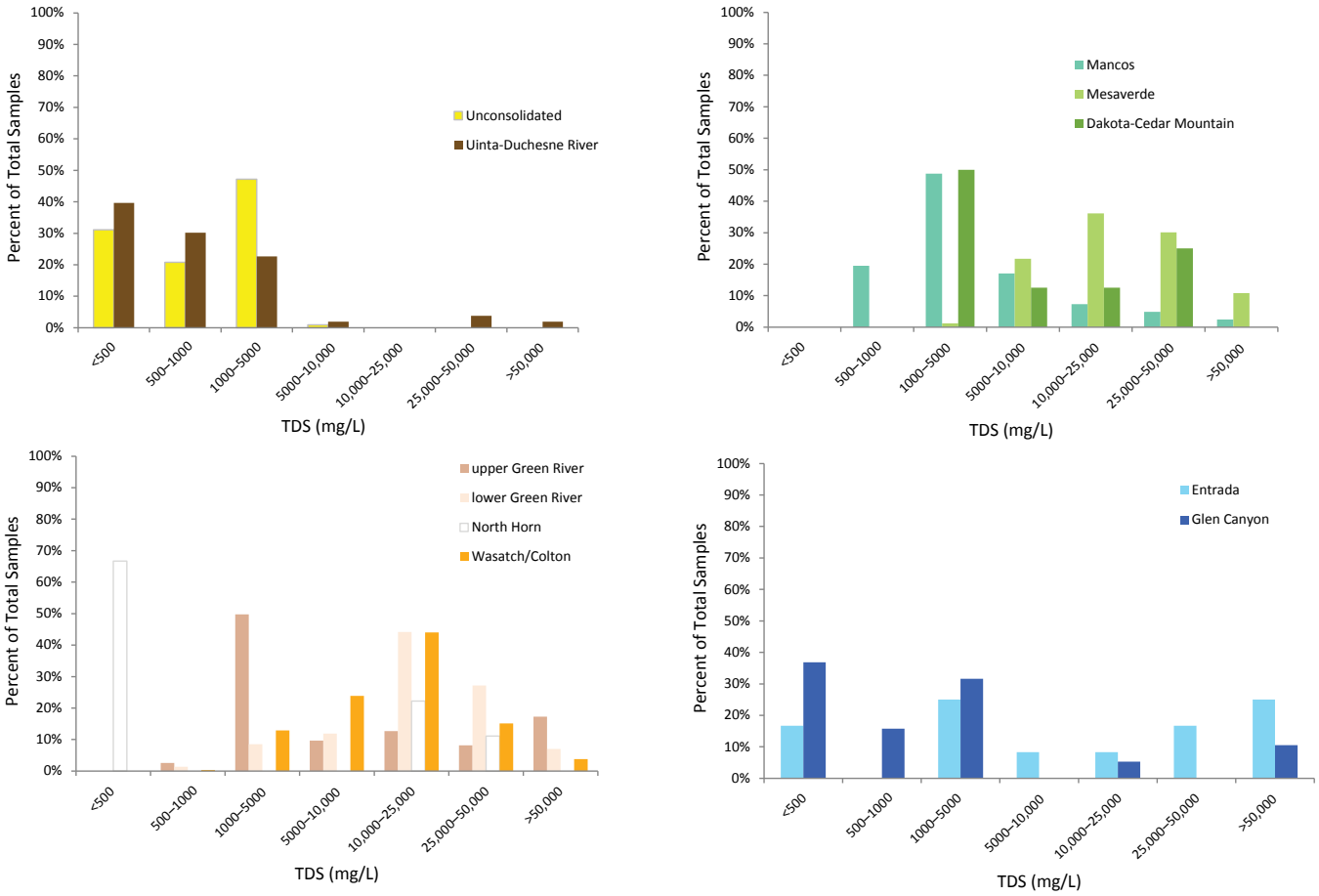

Figure 8.5. *Summary of total dissolved solids (TDS) by geologic unit. Data correlate with that in table 8.2.*

A plot of major ion chemistry versus TDS indicates the solutes that are the source of dissolved solids (figure 8.7). Samples with TDS greater than 10,000 mg/L are dominated by sodium chloride, sodium bicarbonate, and sodium sulfate water types. Samples from the lower Green River include calcium chloride and magnesium chloride water types with TDS greater than 10,000 mg/L. Most samples with TDS less than 1000 mg/L are bicarbonate water types and the samples with the lowest TDS concentrations are calcium bicarbonate type. TDS concentrations between 1000 and 10,000 mg/L mostly correspond to sodium water types.

A piper diagram of all select samples (figure 8.8) shows that water chemistry spans a wide range from waters that are dominated by calcium and bicarbonate to waters dominated by sodium and chloride. These chemical differences are most prominent between geologic units that are predominately oil and gas producers (upper and lower Green River, Wasatch/Colton, and Mesaverde) and geologic units that are predominately groundwater aquifers (Unconsolidated, Uinta–Duchesne River, and Glen Canyon). The chemistry of samples from the upper and lower Green River, Wasatch/Colton, and Mesaverde geologic units are tightly clustered due to consistently high concentrations of sodium and chloride. Variation in chemistry in these units is related to variation in sulfate concentrations. The chemistry of samples from the Unconsolidated and Uinta–Duchesne River units spans a wide range that overlaps chemistry of many of the other units.

A statistical summary of the major ion concentrations of select samples for each geologic unit is presented in appendix G. This summary includes a geometric mean, median, maximum, minimum, and standard deviation for the major ions of calcium, magnesium, sodium, potassium, bicarbonate, chloride, sulfate, and TDS.

SUMMARY

The database compiled as part of this report includes fluid chemistry for groundwater and produced water from the Uinta Basin and surrounding areas in eastern Utah. These samples come from either groundwater from springs and water wells or produced water collected as part of oil and gas exploration and production. The database contains 4184 samples and includes a mix of unique samples for a given location and depth as well as samples that represent a time series of multiple samples from a given location and depth. Each sample in the database includes data source, basic location informa-

Table 8.3. *Water type distribution for select samples.*

Water Type	Geologic Unit											
	Unconsolidated	Uinta–Duchesne River	upper Green River	lower Green River	North Horn	Wasatch/ Colton	Mesaverde	Mancos	Dakota–Cedar Mountain	Entrada	Glen Canyon	All Units
Na-Cl	0	6	77	386	3	290	61	7	6	5	3	844
Na-HCO_3	20	24	96	61	0	4	21	0	2	0	1	229
Na-SO_4	23	7	10	16	0	16	0	6	0	1	2	81
Ca-Cl	0	0	2	27	0	7	0	0	0	0	1	37
Ca-HCO_3	33	8	2	1	6	0	0	0	0	1	5	56
Ca-SO_4	16	1	0	0	0	0	0	0	0	1	5	23
Mg-Cl	1	0	0	11	0	1	0	0	0	0	0	13
Mg-HCO_3	6	6	0	0	0	0	0	0	0	1	1	14
Mg-SO_4	7	1	0	0	0	0	0	1	0	2	1	12
K-Cl	0	0	0	0	0	0	1	0	0	1	0	2
K-HCO_3	0	0	1	0	0	0	0	0	0	0	0	1
K-SO_4	0	0	0	0	0	0	0	0	0	0	0	0
total observation	106	53	187	502	9	318	82	14	8	11	19	1309
Na-Cl	0%	11%	41%	77%	33%	91%	74%	50%	75%	45%	16%	65%
Na-HCO_3	19%	45%	51%	12%	0%	1%	26%	0%	25%	0%	5%	18%
Na-SO_4	22%	13%	5%	3%	0%	5%	0%	43%	0%	9%	11%	6%
Ca-Cl	0%	0%	1%	5%	0%	2%	0%	0%	0%	0%	5%	3%
Ca-HCO_3	31%	15%	1%	0%	67%	0%	0%	0%	0%	9%	26%	4%
Ca-SO_4	15%	2%	0%	0%	0%	0%	0%	0%	0%	9%	26%	2%
Mg-Cl	1%	0%	0%	2%	0%	0%	0%	0%	0%	0%	0%	1%
Mg-HCO_3	6%	11%	0%	0%	0%	0%	0%	0%	0%	9%	5%	1%
Mg-SO_4	7%	2%	0%	0%	0%	0%	0%	7%	0%	18%	5%	1%
sum	100%	100%	100%	100%	100%	100%	100%	100%	100%	100%	100%	100%

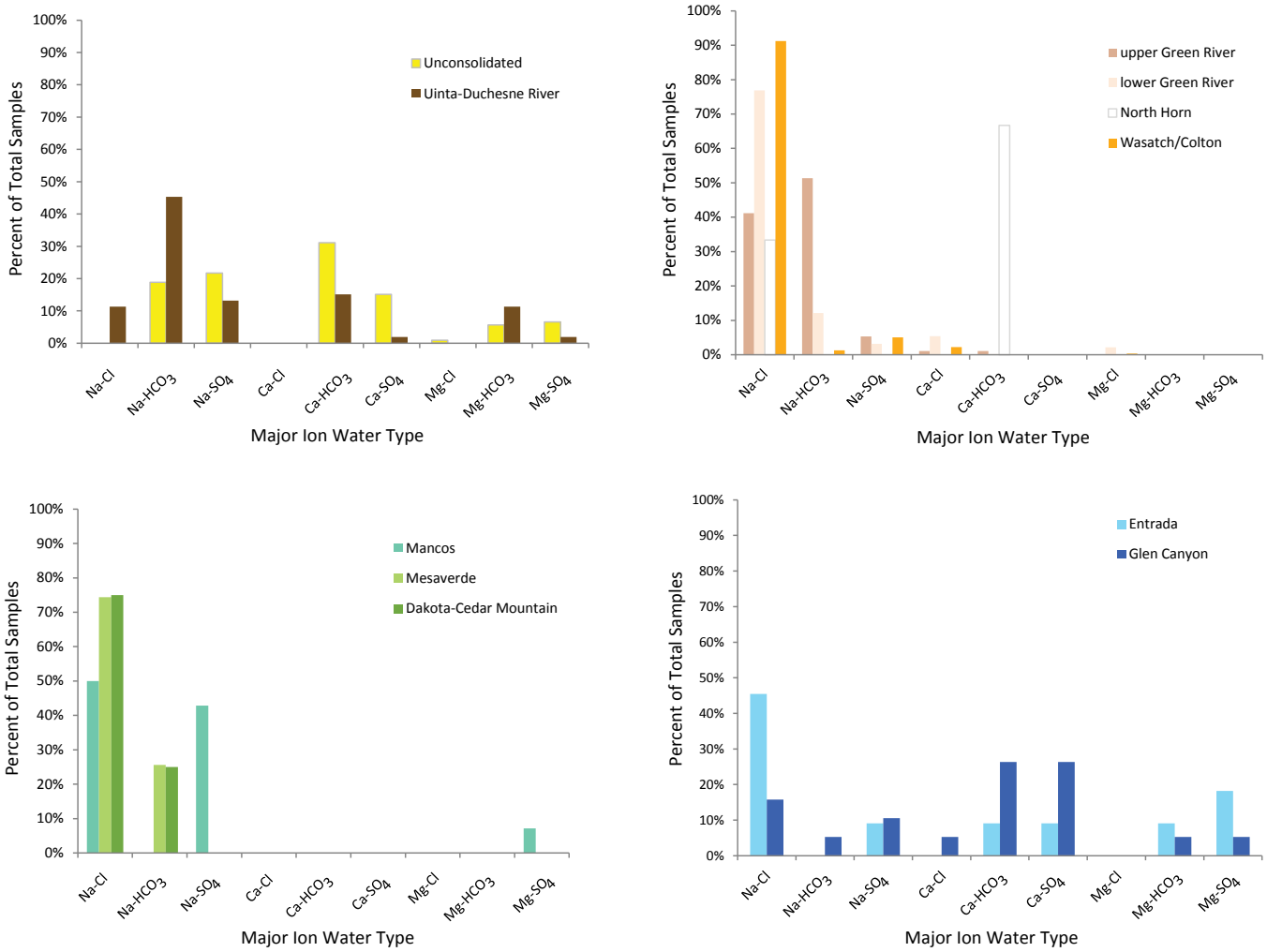

Figure 8.6. *Summary of water types by geologic unit. Data correlate with that in table 8.3.*

tion, and a unique identifier. All other data fields are populated when the data are available. Samples are categorized into 12 simplified geologic units based on geologic unit information in the original data source or depths. Sample chemistry fields in the database include temperature, pH, conductivity, TDS, and chemical concentration values. AquaCHEM software was used to calculate charge balance of the major anions and to delineate a water type for each sample. Five scaling and corrosion indices were calculated for the compiled samples with sufficient data using the AquaCHEM software. The resulting dataset was cleaned for duplicates based on samples having identical sample information.

Samples were selected from the larger database to analyze general trends in water chemistry. Samples were chosen for each simplified geologic unit based on electrolytic charge balance, location, depth, date of sampling, and completeness of the data. For locations with multiple samples, the most recent sample with charge balance nearest zero was chosen. Based on these criteria a total of 1377 samples were chosen from the database to represent chemistry trends in the various geologic units.

The spatial distribution of samples is controlled by the distribution of oil and gas wells in the Uinta Basin and water wells elsewhere. Collection depths for the select samples range from the surface to just over 18,000 feet (5500 m). Sample depth is generally less than 500 feet (150 m) for samples taken from important regional aquifers such as the Unconsolidated, Uinta–Duchesne River, and Glen Canyon geologic units, and generally between 2500 and 15,000 feet (760 and 4600 m) for the upper and lower Green River, Wasatch/Colton, Mesaverde, and Dakota–Cedar Mountain units. Both the spatial and depth distribution of select samples tend to be clustered due to the origin of samples, either from oil and gas wells or from more typical groundwater samples. This clustering may limit the validity of generalized chemical trends applied over areas or depths not represented in the database.

TDS is variable across the select database. The highest TDS concentrations tend to correlate with sodium chloride or sodium bicarbonate water types that are typical of the upper and lower Green River, Wasatch/Colton, and Mesaverde units. These samples are predominately produced water and the high

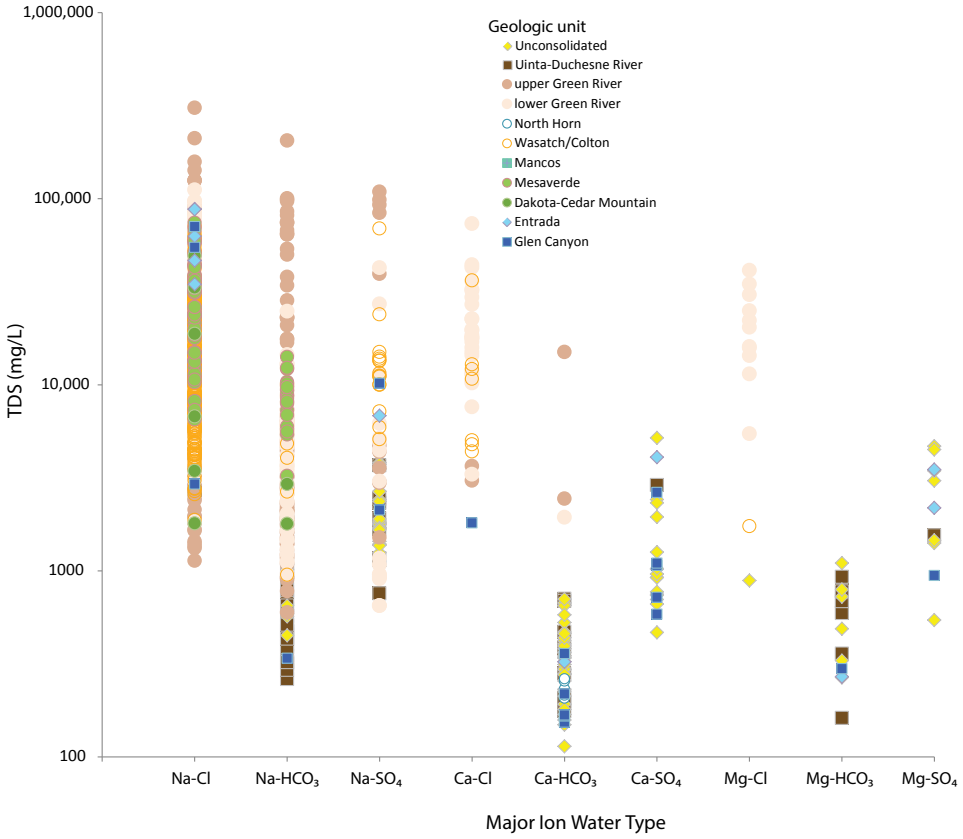

Figure 8.7. *Major ion chemistry versus total dissolved solids (TDS).*

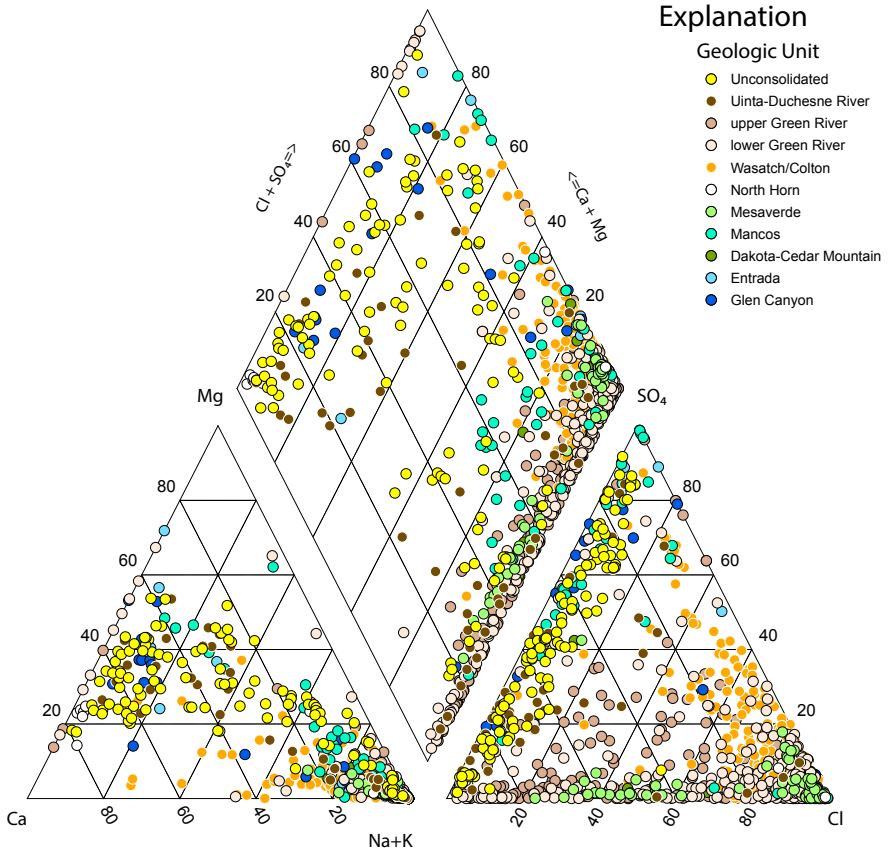

Figure 8.8. *Piper diagram of select samples.*

TDS may be the result of oil and gas generation processes, long residence time, and/or increased water-rock interaction within these units. Lower TDS concentrations and bicarbonate water types are typical of the Unconsolidated, Uinta–Duchesne River, Glen Canyon units. These chemistries likely result from a relatively active meteoric groundwater system within these units where they are near the surface. Few data exist for any of the units at significant depths (>1000 feet [300 m]) away from areas of oil and gas development.

The dataset contains many samples that represent repeat measurements of discrete locations and intervals through time. These time series samples were not analyzed in this report because of the project scope. Future work on the time series samples could yield unique perspectives on large-scale geochemical changes resulting from oil and gas development activities. The select samples in this database may also be used for important baseline chemistry over large areas of eastern Utah.

The samples in this database represent a unique regional-scale snapshot of fluid geochemistry across an active petroleum province, including both the shallow meteoric groundwater system and the deeper basin fluid system. Further study and geochemical analysis of these data could yield insight into large-scale fluid evolution in both active petroleum provinces and similar geographic settings elsewhere.

CHAPTER 9:
HANDLING AND MANAGEMENT OF WATER PRODUCED FROM OIL AND GAS RESERVOIRS IN THE UINTA BASIN

by

David E. Tabet

CONTENTS

INTRODUCTION 235
UTAH WATER QUALITY STANDARDS 235
Utah Groundwater Classification Scheme 235
Class I Groundwater 235
Class II Groundwater 236
Class III Groundwater 236
Class IV Groundwater 237
Utah Total Maximum Daily Loads 237
WATER FACILITIES 237
History of Utah Water Facility Development and Use 237
Produced Water Volume in the Uinta Basin 238
Water Disposal Wells 238
Waterflood Injection Projects 241
Water Evaporation Ponds 242
Water Used for Hydraulic Fracturing 246
UINTA BASIN PETROLEUM-RELATED WATER HANDLING PRACTICES 249
Introduction 249
Current Practices of Selected Companies 249
Anadarko Petroleum/Kerr-McKee (Natural Buttes Gas Field) 249
Drilling and completion practices 249
Produced-water management practices 250
EOG Resources (Natural Buttes Gas Field) 251
Field development activities 251
Produced-water management practices 252
XTO Energy (Natural Buttes Gas Field) 252
Field development activities 252
Produced-water management practices 252
GASCO Energy (West Tavaputs Plateau Gas Development) 253
Field development activities 253
Produced-water management practices 253
Enervest Operating, LLC (West Tavaputs Plateau Gas Development) 253
Field development activities 253
Produced-water management practices 254
Newfield Exploration (Monument Butte Oil Field) 254
Field development activities 254
Produced-water management practices 254
Opportunities for Water Reuse in Utah 255
Best Water Handling Practice Recommendations 257
SUMMARY 258

FIGURES

Figure 9.1. Cumulative number of produced-water disposal wells in the Uinta Basin, from 1968 through 2014 239
Figure 9.2. Location of 2014 water-disposal wells by field in the Uinta Basin 240
Figure 9.3. Location of enhanced-oil-recovery waterflooding projects and wells in the Uinta Basin 243
Figure 9.4. Types of water evaporation ponds in the Uinta Basin 245
Figure 9.5. Location of water evaporation ponds in the Uinta Basin 248
Figure 9.6. Annual amount of water used in fracture stimulations by county for the Uinta Basin from 2011 through 2014 248
Figure 9.7. Example of Anadarko's Completion Technology System (ACTS) at Natural Buttes field 250
Figure 9.8. Schematic diagram of the Newfield Beluga plant's Veolia water-treatment process 256

TABLES

Table 9.1. Groundwater classes and standards 236
Table 9.2. Uinta Basin active wells and annual produced-water volumes by county, 2008–2014 239
Table 9.3. Uinta Basin annual produced-water volumes per well by county, 2008–2014 239
Table 9.4. Number of active produced-water disposal wells in the Uinta Basin by county, 2008–2014 241
Table 9.5. Uinta Basin disposal well-injection volumes, 2008–2014 241
Table 9.6 Number of water-disposal wells in the Uinta Basin, 2014 242
Table 9.7. 2014 Uinta Basin enhanced oil recovery water-injection and produced-water volumes 244
Table 9.8. Uinta Basin enhanced oil recovery water injection volumes, 2008–2014 244
Table 9.9. Produced water delivered to Uinta Basin evaporation ponds, 2010–2013 246
Table 9.10. Approved commercial disposal facilities as of June 2015 247
Table 9.11. Annual number of wells with fracture stimulations in the Uinta Basin by county for the years 2011–2014 248
Table 9.12. Annual number of barrels of water used in fracture stimulations in the Uinta Basin by county for the years 2011–2014 248
Table 9.13. Annual number of barrels of water used per well in fracture stimulations in the Uinta Basin by county for the years 2011–2014 249
Table 9.14. Annual number of wells fracture stimulated, barrels of water used in stimulations, and the number of barrels used per well in Uintah County for the year 2013 249
Table 9.15. Veolia Water Technologies's reported processing performance data for waterflood applications 256
Table 9.16. Publicly operated wastewater treatment plants in Duchesne and Uintah Counties, Utah, and their average annual flow in barrels per year 257

CHAPTER 9:
HANDLING AND MANAGEMENT OF WATER PRODUCED FROM OIL AND GAS RESERVOIRS IN THE UINTA BASIN

INTRODUCTION

According to Clark and Veil (2009), produced water is the largest by-product and waste stream associated with gas and oil production in the United States. Water handling and management practices for wastewater resulting from gas and oil production in the Uinta Basin are subject to regulation by various federal and state agencies including the UDWQ within the Utah Department of Environmental Quality (UDEQ), DOGM, and the EPA, as well as by local county regulatory agencies.

Regulation of water use associated with the petroleum industry has evolved over time, and presently is designed mainly to protect underground and surface freshwater supplies and surface habitat, including fauna, flora, and the atmosphere. Water management issues related to gas and oil development in Utah primarily involve water used for drilling and completion of wells, water for flushing of certain reservoirs to enhance oil recovery, and water to suppress dust emissions from dirt roads, as well as the disposal of water produced as a by-product of gas and oil production. Some synoptic studies of produced-water management have been carried out in the past, but when local case studies are provided, they mostly tend to focus on waters associated with CBM or on the larger producing basins such as the Denver and Piceance of Colorado, the Appalachian of Pennsylvania, the Anadarko and Arkoma of Oklahoma, the Fort Worth and Permian of Texas, the Williston of North Dakota, and the Big Horn, Green River, Powder River, and Wind River of Wyoming, rather than on the waters associated with conventional oil and gas production in the Uinta Basin of Utah (IOGCC and ALL Consulting, 2006; Benko and Drewes, 2008; Guerra and others, 2011; Dahm and Chapman, 2014). The best previous synopsis of produced water and disposal in Utah was a report prepared for the Argonne National Laboratory (Clark and Veil, 2009), which gave a snapshot of conditions and practices as of 2007.

This chapter first defines the water quality standards established in Utah. It next provides an extensive updated discussion that attempts to describe and quantify the water streams involved in water management practices associated with gas- and oil-well drilling and completion, EOR waterflooding, and water disposal via deep underground injection wells for the Uinta Basin. The amount of water used for suppression of dust on dirt access roads is not reported on a regular basis to a regulatory agency and therefore is not included in this chapter.

This chapter also reviews petroleum water-management practices by specific companies, as well as trends as far back as records are readily available, but concentrates mainly on practices and quantities of water usage in the 10 years prior to 2014. For example, water used in hydraulic fracture stimulation of gas and oil wells was not required to be reported to FracFocus (2015) by the Utah DOGM until November 1, 2012, before which such reporting was simply voluntary, and so earlier records for such usage are scant and incomplete.

UTAH WATER QUALITY STANDARDS

Utah Groundwater Classification Scheme

The UDWQ has established a groundwater classification scheme in Utah with four major classes, and three subclasses under the highest class (table 9.1) (Utah Department of Environmental Quality, 2015a). Each of the groundwater classes and subclasses has different management prescriptions to protect groundwater quality. The UDWQ drinking water classes and standards are defined under Utah Administrative Code (Rule R317-6) and that can be found at https://rules.utah.gov/publicat/code/r317/r317-006.htm.

The following sections are taken from the Utah Administration Code, Rule R317-6, Groundwater Quality Protection, as in effect on January 1, 2017. Refer to the website listed above for the complete description of definitions, groundwater quality standards, etc.

Class I Groundwater

- CLASS IA groundwater is referred to as “pristine” and is classified as such by exhibiting both of the following characteristics:
  - TDS of less than 500 mg/L, and
  - no contaminant concentrations that exceed the groundwater quality standard as defined in Utah Administrative Rule 317-6-2.
- For facilities located above CLASS IA groundwater, that discharge or will probably discharge to the groundwater, and that are under the regulatory authority of the Ground Water Quality Protection Program (GWQPP), groundwater quality protection levels will be established as follows:
  - TDS may not exceed the greater of 1.25 times the background or background plus two standard deviations.

Table 9.1. *Groundwater classes and standards in Utah (Utah Division of Environmental Quality, 2015a).*

Groundwater Class	Class Name	TDS Range
Class IA	Pristine	<500 mg/L, as defined in Utah Administrative Rule 317-6-3, and no contaminant concentrations exceeding the maximum contaminant levels defined in Rule 309-103
Class IB	Irreplaceable	<2000 mg/L; any contaminants present must not exceed the groundwater quality standard or 1.1 times background concentration
Class IC	Ecologically Important	not based on TDS
Class II	Drinking Water	500 – <3000 mg/L
Class III	Limited Use	3000 – <10,000 mg/L
Class IV	Saline	≥ 10,000 mg/L

  - When a contaminant is not present in a detectable amount as a background concentration, the concentration of the pollutant may not exceed the greater of 0.1 times the groundwater quality standard as defined in Utah Administrative Rule 317-6-2, or the limit of detection.
  - When a contaminant is present in a detectable amount as a background concentration, the concentration of the pollutant may not exceed the greater of 1.25 times the background concentration, 0.25 times the groundwater quality standard, or background plus two standard deviations; however, in no case will the concentration of a pollutant be allowed to exceed the groundwater quality standards.
- CLASS IB groundwater is referred to as "irreplaceable" when it is a source of water for an existing community public drinking water system for which no reliable supply of comparable quality and quantity is available because of economic or institutional constraints.
- For facilities located above CLASS IB groundwater, that discharge or will probably discharge to the groundwater, and that are under the regulatory authority of the GWQPP, groundwater quality protection levels will be established as follows:
  - TDS may not exceed the lesser of 1.1 times the background value or 2000 mg/L.
  - When a contaminant is not present in a detectable amount as a background concentration, the concentration of the pollutant may not exceed the greater of 0.1 times the groundwater quality standard, or the limit of detection.
  - When a contaminant is present in a detectable amount as a background concentration, the concentration of the pollutant may not exceed the greater of 1.1 times the background concentration or 0.1 times the groundwater quality standard; however, in no case will the concentration of a pollutant be allowed to exceed the groundwater quality standard as defined in Utah Administrative Rule 317-6-2.
- CLASS IC groundwater is referred to as "ecologically important" when it is a source of groundwater discharge important to the continued existence of an existing wildlife habitat.
- Class IC groundwater will be protected as a source of water for potentially affected wildlife habitat. Limits on increases of TDS and organic and inorganic chemical compounds will be determined in order to meet applicable surface water standards.

Class II Groundwater

CLASS II groundwater is also referred to as "drinking water quality" and is classified as such by exhibiting both of the following characteristics:

- TDS greater than 500 mg/L and less than 3000 mg/L, and
- no contaminant concentrations that exceed ground water quality standards.

For facilities located above CLASS II groundwater, that discharge or will probably discharge to the groundwater, and that are under the regulatory authority of the GWQPP, groundwater quality protection levels will be established as follows:

- TDS may not exceed the greater of 1.25 times the background value or background plus two standard deviations.
- When a contaminant is not present in a detectable amount as a background concentration, the concentration of the pollutant may not exceed the greater of 0.25 times the groundwater quality standard, or the limit of detection.
- When a contaminant is present in a detectable amount as a background concentration, the concentration of the pollutant may not exceed the greater of 1.25 times the background concentration, 0.25 times the groundwater quality standard, or background plus two standard deviations; however, in no case will the concentration of a pollutant be allowed to exceed the groundwater quality standard.

Class III Groundwater

CLASS III groundwater is also referred to as "limited use" and is classified as such by exhibiting one or both of the following characteristics:

- TDS greater than 3000 mg/L and less than 10,000 mg/L, or
- one or more contaminants that exceed the groundwater quality standards.

For facilities located above CLASS III groundwater, that discharge or will probably discharge to the groundwater, and that are under the regulatory authority of the GWQPP, groundwater quality protection levels will be established as follows:

- TDS may not exceed the greater of 1.25 times the background value or background plus two standard deviations.
- When a contaminant is not present in a detectable amount as a background concentration, the concentration of the pollutant may not exceed the greater of 0.5 times the groundwater quality standard, or the limit of detection.
- When a contaminant is present in a detectable amount as a background concentration, the concentration of the pollutant may not exceed the greater of 1.5 times the background concentration, 0.5 times the groundwater quality standard, or background plus two standard deviations; however, in no case will the concentration of a pollutant be allowed to exceed the groundwater quality standard.

Class IV Groundwater

CLASS IV groundwater is also referred to as "saline" and is classified as such by containing greater than 10,000 mg/L of TDS. Most water produced as a by-product of oil and gas production in Utah is CLASS IV, or saline in quality, although some of Utah's produced water falls in the 3000 to 9999 mg/L TDS category, or CLASS III.

No protection levels for CLASS IV groundwater have been established to date by the Executive Secretary of the GWQPP to protect human health and the environment.

Utah Total Maximum Daily Loads

Section 303(d) of the U.S. Clean Water Act requires states to develop Total Maximum Daily Loads (TMDLs) to establish allowable loadings of pollutants, or other quantifiable factors, for water bodies in the state based on the relationships between pollutant sources and in-stream water quality conditions (U.S. Environmental Protection Agency, 2015). These load limits are designed for waters that do not meet water quality standards even after technology-based controls are used.

Several watershed areas in the Uinta Basin have been listed by the UDEQ (2015b) as impaired waters for TDS. Some bedrock formations in the basin contain soluble saline minerals, particularly the Green River, Wasatch, and Mancos Formations (figure 2.1, plate 1), with dissolved salts contributing TDS to water flowing over or through them. In addition to natural salt loading from runoff, seepage of water from irrigation canals, de-icing salts along roads, and deep percolation of irrigation waters contribute to salt loading in tributaries of the Duchesne River. Other human disturbances of salt-bearing strata, such as surface facilities for oil and gas development, can lead to increased runoff and potential salt loading.

Fortunately for Utah, a report by the U.S. Geological Survey (Vaill and Butler, 1999) on dissolved-solids trends in the Colorado River Basin waterways from 1970 through 1996 noted that there has been a historic downward trend in TDS concentrations in the Duchesne River watershed. Therefore, it appears that the land owners and surface management agencies in Utah have put in place practices that are effectively reducing dissolved-solid loads entering the Duchesne River and probably other Uinta Basin watersheds. The improvements in TDS concentration are mainly the result of better irrigation practices, but also from close monitoring and regulation of land-disturbing activities like petroleum development. A new study looking at trends since 1996 would be helpful.

WATER FACILITIES

History of Utah Water Facility Development and Use

Regulation of petroleum development operations by the State of Utah formally began in 1955 with the creation of the Oil and Gas Conservation Commission, which was charged to prevent the waste of oil and gas, encourage conservation, and protect the correlative rights of oil and gas owners. The regulations prior to 1970 mainly involved sound well drilling, construction, spacing, and abandonment to protect the petroleum resource and the surrounding environment during development. In 1968, the Utah Legislature reorganized the Division of Oil and Gas Conservation as part of the Department of Natural Resources, and in 1975 renamed it the Division of Oil, Gas and Mining (i.e., DOGM). Following the creation of the EPA in December 1970, as new federal laws were passed through the 1970s and 1980s to help mitigate the potential impacts of petroleum development activities on the local and regional air, fauna, flora, cultural, socio-economic, and water resources, DOGM periodically updated its regulations to match those required in new federal laws. For example, in 1982 DOGM received primacy from the EPA in the regulation of Class II water injection wells (see DOGM home page under "About Us" at http://oilgas.ogm.utah.gov/oilgasweb/about-us/about-us-main.xhtml).

Strategies and technologies utilized by the petroleum industry to address produced-water management generally fall into three categories: (1) minimization of produced water, (2) recycling or reuse of produced water, and (3) some form of disposal (National Petroleum Council, 2011). Also, in general as field development has increased in area and number of wells over time, operators in Utah have moved from small isolated systems, either commercially run or company-owned, to more

integrated and comprehensive, generally company-owned, water-handling and treatment facilities, as economies of scale and centralization could be realized as field size grew or field consolidation occurred through mergers or acquisitions. One major example of this type of development was the consolidation of more than 15 smaller individual EOR waterflood units into the single giant Greater Monument Butte waterflood unit in 2010 by Newfield Exploration Company.

Also, as demand for fresh water has grown with increased petroleum development, certain companies have looked (and no doubt more in the future will look) for ways to increase water reuse and reduce their demand for limited freshwater supplies. Notably, Anadarko/Kerr-McGee has developed water-handling systems to reuse water for drilling and fracture stimulation of wells and cut its freshwater usage for these development steps by close to 100%. In addition, EOG Resources plans to use wastewater from the Bonanza coal-fired power plant (about 40 miles [60 km] southeast of Vernal) of Deseret Generation and Transmission for 88% of the water needed to drill and complete the 2808 new gas wells it proposes at the Chapita Wells unit of Greater Natural Buttes field (figure1.1). Most of the larger Uinta Basin petroleum operators have installed, or are in the process of installing, centralized water collection and treatment plants to reduce or eliminate water storage at individual well sites and the need to have trucks transport the produced water from well sites to disposal or reuse sites, resulting in less dust and diesel emissions from reduced trucking and less traffic and human activity in their fields, which might disturb flora and fauna living in the area. One regulatory and operational trend in the past five years has been an effort to reduce or minimize the use of surface ponds for storage and evaporation of produced water. Both companies and regulators see pond facilities as costly and difficult to maintain over time, possessing a large disturbance footprint, and having a higher potential for leakage and emissions in a sensitive environment.

Service industries understand that water management for petroleum companies in the U.S. is a growing industry and are looking for new and more cost-effective ways to serve this greater than $6 billion industry (Bluefield Research, 2014). Several of the larger Uinta Basin operators have developed and posted company water policies on their websites and are actively looking for ways to reduce water use and wastewater production, and find ways to reuse existing water supplies, and anticipate or adapt to an ever-changing regulatory landscape. The State of Utah encourages voluntary efforts to conserve and reuse water in Utah (Utah Division of Water Resources, 2005), and although initial emphasis was placed on municipal water systems, the State will no doubt encourage and foster petroleum company efforts in this regard.

Produced Water Volume in the Uinta Basin

The amount of water produced in association with petroleum production in the four-county (Uintah, Duchesne, Carbon, and northern Grand) area comprising the Uinta Basin has increased about 35% from 2008 to 2014, with the volume rising from about 86 to 116 MMB over that time frame. The increase in produced water reflects a similar increase in petroleum development over that period as the number of active wells increased nearly 41% from 9070 in 2008 to 12,780 in 2014 (table 9.2).

All of the counties, except for Grand County, have seen the number of wells increase over the years tabulated above, and the greatest increases in new active wells and produced-water volumes have taken place in Duchesne and Uintah Counties. Since the wells in Duchesne County are mainly developed for oil production and those in Uintah County are mainly focused on gas production, the number of bbls of produced water per county in table 9.2 were divided by the number of active wells to arrive at a tabulation of BW per well for each county by year as shown in table 9.3.

Table 9.3 shows different trends over time for each of the counties involved, but cumulatively the amount of produced water per well from the four-county area has decreased for most years over the seven-year study period. Most of the cumulative decline in bbls per well can be attributed to the major decline in produced water per well coming from the CBM fields of Carbon County, and the fact that more recent wells in that county have been conventional gas wells that typically are lower volume water producers. The amount of water produced per well has generally decreased over the time frame studied for the predominantly Wasatch Formation and Mesaverde Group gas wells of Uintah County. Interestingly, in the predominantly Green River Formation oil-producing wells of Duchesne County the amount of water produced per well has been generally increasing from 2008 to 2014, so it is evident that oil and gas wells in the Uinta Basin operate differently in terms of their produced-water behavior. Grand County's Uinta Basin gas wells generally produce from older Dakota–Cedar Mountain–Morrison reservoirs and are the lowest volume water producers per well in the basin. Thus, the data above illustrate that the amount of water produced per well across the Uinta Basin is affected by the formation being produced as well as the type of product predominantly being produced, either oil or gas. Other factors, such as depth of the producing formation, well completion technology (vertical versus horizontal), and well spacing variations from field to field may also affect the amount of water produced per well, and some of this local detail is provided in discussions of the individual operators' activities below.

Water Disposal Wells

DOGM's website information on wells classified as water-disposal wells indicates that the number of disposal wells in the Uinta Basin has grown from a single well in 1961 to 92 in 2014 (figures 9.1 and 9.2). Over this period, it appears that 106 disposal wells were completed and 14 were subsequently plugged and abandoned or converted to gas wells. Whereas 91 wells are classified as water-disposal wells in the DOGM well

Table 9.2. *Uinta Basin active wells and annual produced-water volumes by county, 2008–2014 (in million barrels [MMBW]).*

	2008		2009		2010		2011		2012		2013		2014	
County	**# of Wells**	**MMBW**	**# of Wells**	**MMBW**	**# of Wells**	**MMBW**	**# of Wells**	**MMBW**	**# of Wells**	**MMBW**	**# of Wells**	**MMBW**	**# of Wells**	**MMBW**
Uintah	5612	47.91	5837	46.46	6182	51.51	6564	52.84	7055	48.61	7519	53.56	7797	61.33
Duchesne	1981	20.93	2062	21.39	2340	24.21	2611	29.74	2841	34.91	3093	39.14	3340	43.44
Carbon[1]	899	17.31	942	19.21	967	17.47	1050	16.94	1090	14.07	1084	12.37	1099	11.21
Grand[2]	578	0.05	578	0.03	567	0.03	565	0.04	572	0.03	556	0.08	544	0.24
TOTAL	9070	86.20	9419	87.09	10,056	93.22	10,790	99.56	11,558	97.62	12,252	105.14	12,780	116.22

[1]Includes some CBM wells
[2]Includes some Paradox Basin wells

Table 9.3. *Uinta Basin annual produced-water volumes per well by county, 2008–2014.*

	2008	2009	2010	2011	2012	2013	2014
County	**Bbls/well**	**Bbls/well**	**Bbls/well**	**Bbls/well**	**Bbls/well**	**Bbls/well**	**Bbls/well**
Uintah	8537	7960	8332	8050	6890	7124	7866
Duchesne	10,565	10,373	10,346	11,390	12,288	12,653	13,007
Carbon[1]	19,255	20,393	18,066	16,133	12,908	11,411	10,202
Grand[2]	87	52	53	71	52	135	447

[1]Includes CBM wells
[2]Includes some Paradox Basin wells

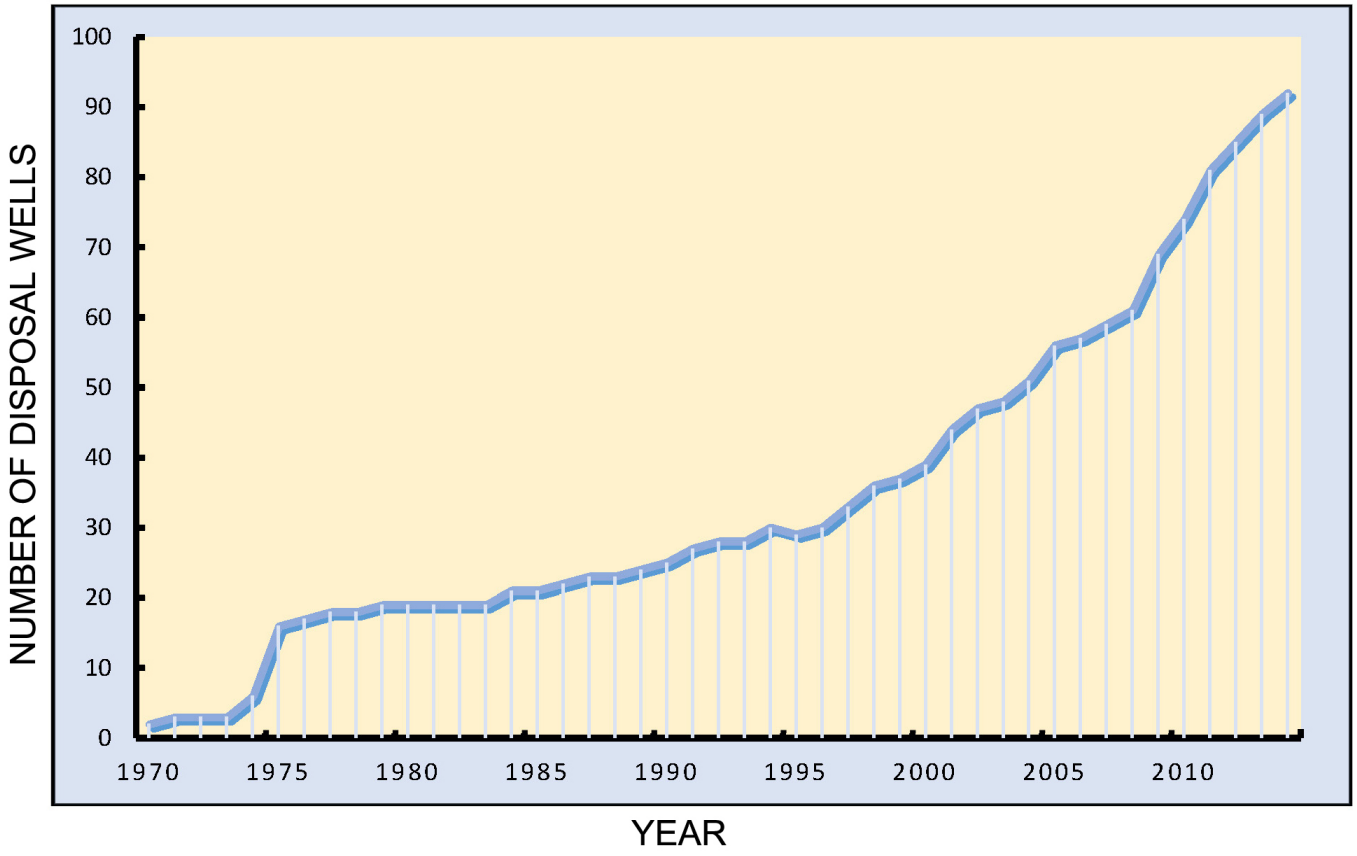

Figure 9.1. *Cumulative number of produced-water disposal wells in the Uinta Basin, from 1968 through 2014 (source: Division of Oil, Gas and Mining website).*

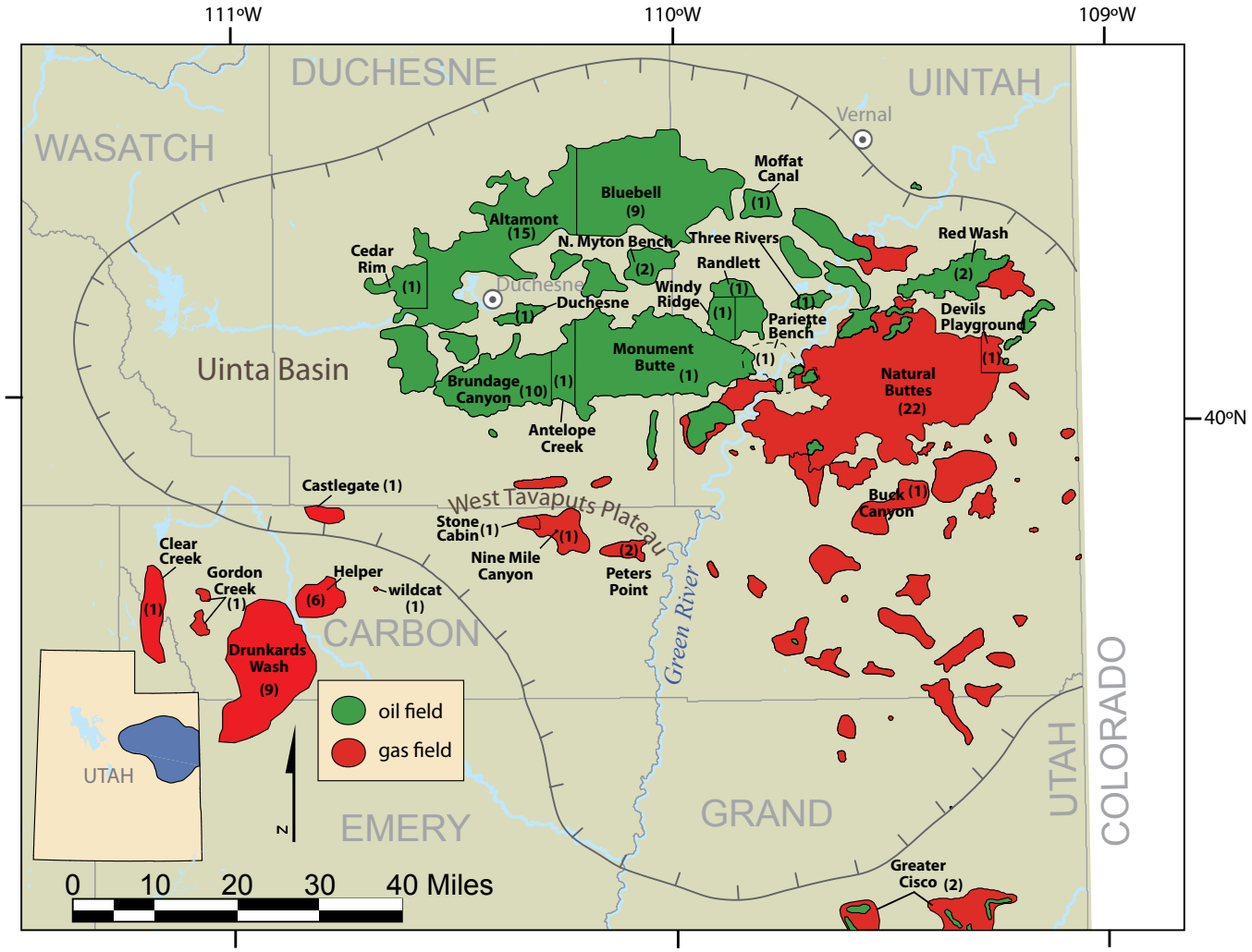

Figure 9.2. *Location of 2014 water-disposal wells by field in the Uinta Basin. Number of disposal wells shown in parentheses beneath field names.*

file records, examination of the Disposal Well Volumes part of the DOGM website found disposal volumes for 92 wells for 2014 since one well is both a gas producer and a disposal well but is classified as a gas well. The first major growth spurt was in 1975, when 10 disposal wells were completed as part of the development of the Altamont and Bluebell fields (figure 1.1). Disposal-well additions averaged about one well every five years from 1977 to 1988, then increased to an average of one new disposal well per year from 1989 to 1995. From 1996 through 2008 the average annual increase in disposal-well completions rose to about three new wells per year, when coalbed gas development in Carbon County and tight-sand gas development in Uintah County were undergoing steady development. The Uinta Basin disposal-well completion rate increased from 2009 through 2014 at an average rate of about six new disposal wells per year, although the rate has slowed somewhat in the past two years. As of the end of 2014, the 92 active produced-water disposal wells listed in the DOGM Disposal Well Volumes files for the Uinta Basin study area were distributed among the four counties as such: 21 in Carbon County, 38 in Duchesne County, 2 in Grand County, and 31 in Uintah County (table 9.4).

The volume of water disposed via injection annually in the Uinta Basin has increased with the added number of disposal wells, from 43.07 MMB in 2008 to 67.55 MMB in 2014 (table 9.5). Within the four-county Uinta Basin area all the counties, except Carbon County, have seen their annual and average per well water-disposal volumes increase over time. In the period from 2008 through 2014, the water-disposal volume has increased 174% in Duchesne County, 251% in Uintah County, and from nothing to over 330,000 BW in Grand County. Meanwhile, Carbon County has seen the annual amount of water disposed in wells decrease from 16.06 MMB in 2008 to 12.05 MMB in 2014. The average amount of water disposed per well has been similar in Carbon, Duchesne, and Uintah Counties, averaging about 0.8 MMB per well annually, while ranging on average between 0.4 and 1.4 MMB per well annually. However, in Grand County the average water disposed per well annually has been less than 0.2 MMB, ranging between 0.13 and 0.19 MMB per well per year.

Half of the produced-water disposal wells (46) are associated with gas fields, both CBM and tight-gas sand developments, whereas the remaining 46 produced-water disposal wells are

Table 9.4. *Number of active produced-water disposal wells in the Uinta Basin by county, 2008–2014.*

	2008	2009	2010	2011	2012	2013	2014
County	**# of Wells**	**# of Wells**	**# of Wells**	**# of Wells**	**# of Wells**	**# of Wells**	**# of Wells**
Uintah	15	26	29	29	16	30	31
Duchesne*	23	23	24	28	27	28	38
Carbon*	18	19	20	19	19	20	21
Grand	0	0	1	1	1	1	2
TOTAL	56	68	74	77	63	79	92

* Includes CBM disposal wells

Table 9.5. *Uinta Basin disposal well-injection volumes, 2008–2014 (in million barrels [MMBW]).*

	2008	2009	2010	2011	2012	2013	2014
County	**MMBW**	**MMBW**	**MMBW**	**MMBW**	**MMBW**	**MMBW**	**MMBW**
Uintah	10.67	12.46	20.27	23.53	22.21	23.68	26.81
Duchesne*	16.34	16.64	16.73	20.78	24.47	28.06	28.36
Carbon*	16.06	20.75	18.47	16.81	14.68	12.97	12.05
Grand	0.00	0.00	0.00	0.13	0.19	0.17	0.33
TOTAL	43.07	49.85	55.47	61.26	61.54	64.88	67.55

* Includes CBM disposal wells

associated with oil field developments in the Uinta Basin (figure 9.2), mainly in those fields not employing waterflood EOR techniques such as Altamont and Bluebell oil fields. Natural Buttes gas field has the greatest number of water-disposal wells (22) of any field in the Uinta Basin, but at least five different companies operate individual disposal wells in their portion of the field. Several fields (Buck Canyon, Duchesne, Nine Mile Canyon, and Wonsits Valley) have had disposal wells in the past or have wells that were inactive in 2014. New fields adding water-disposal wells in 2014 in the Uinta Basin included the Three Rivers and Windy Ridge oil fields. Whereas most of the Uinta Basin disposal wells are operated by producing companies for their own disposal needs, at least six disposal wells were operated in 2014 by commercial ventures that would accept water from any operator willing to pay for water disposal. Altamont, Bluebell, and Greater Cisco fields each had two commercial disposal wells operating within the field area. In 2014, the 92 water-disposal wells were distributed among 22 producing Uinta Basin fields and one wildcat area (table 9.6).

Waterflood Injection Projects

Since 2010, the Uinta Basin has had 16 active EOR waterflood injection projects in operation (figure 9.3). All of these projects inject water, produced or fresh, via wells into Green River Formation reservoirs to flush residual oil left behind after primary production toward other producing wells in the same field. The 16 active EOR waterflood injection projects in the Uinta Basin involve 1586 permitted water-injection wells. Collectively, all these EOR water-injection wells pumped 44.29 MMBW underground in 2014. Water produced with the oil from all the same fields where EOR water injection occurred totaled 24.91 MMB in 2014, and assuming all the produced water was reinjected for EOR, then the Uinta Basin operators needed to use over 19 MMB of fresh water to achieve the full water volumes used in the EOR efforts in 2014.

Most of these waterflood projects are small, and only six involve more than 10 water-injection wells (table 9.7). The Antelope Creek project of Petroglyph Operating Company; the Gypsum Hills, Red Wash, and Wonsits Valley projects of QEP Energy Company; and the Walker Hollow project of Citation Oil and Gas Corporation each operated between 11 and 109 water-injection wells at their sites in 2014. By far the largest EOR waterflood injection project in the Uinta Basin in 2014 was Newfield Production Company's Greater Monument Butte Unit (GMBU) project that involved 1347 water-injection wells and injected 35.75 MMBW by itself. Newfield created this giant waterflood injection project in 2010 by combining at least 22 smaller projects, including Ashley, Beluga, Blackjack, Canvasback, Castle Draw, East Pariette, Fenceline, Hawkeye, Humpback, Jonah, Lone Tree, Monument Butte, Monument Butte East, Monument Butte NE, Pariette, Pleasant Valley, Sand Wash, S. Monument Butte, South Wells Draw, Sundance, West Point, and West Willow Creek, into one unified project. Merging many smaller waterflood projects into one larger one can offer an operator economies of scale in terms of water handling, processing, procurement, transportation, and overall project management, leading to improved project operating costs. Newfield has plans to drill over 5700 new oil wells at the GMBU, of which perhaps half will eventually be converted to injection wells, so the amount of water injected for EOR will likely more than double as the GMBU progresses toward full-

Table 9.6 *Number of water-disposal wells in the Uinta Basin, 2014.*

Field Name (commodity – producing formation)	Disposal Wells
Altamont (oil – Green River Fm.)	15
Antelope Creek (oil – Green River Fm.)	1
Bluebell (oil – Green River Fm.)	9
Brundage Canyon (oil – Green River Fm.)	10
Castlegate (CBM – Mesaverde Gp.)	1
Cedar Rim (oil – Green River Fm.)	1
Clear Creek (gas – Ferron Ss. Mbr. of the Mancos Sh.)	1
Devils Playground (gas – Mesaverde Gp. and Wasatch Fm.)	1
Drunkards Wash (CBM – Ferron Ss. Mbr. of the Mancos Sh.)	9
Gordon Creek (gas – Ferron Ss. Mbr. of the Mancos Sh.)	1
Greater Cisco (gas – Morrison, Cedar Mountain, and Dakota Fms.)	2
Helper (CBM – Ferron Ss. Mbr. of the Mancos Sh.)	6
Moffat Canal (oil – Wasatch and Green River Fms.)	1
Natural Buttes (gas – Mesaverde Gp., Wasatch and Green River Fms.)	22
North Myton Bench (oil – Green River Fm.)	2
Pariette Bench (oil – Green River Fm.)	1
Peters Point (gas – Mesaverde Gp. and Wasatch Fm.)	2
Randlett (oil – Green River Fm.)	1
Red Wash (oil – Green River and Uinta Fms.)	2
Stone Cabin (gas – Mesaverde Gp. and Wasatch Fm.)	1
Three Rivers (oil – Green River Fm.)	1
Windy Ridge (oil – Green River Fm.)	1
wildcat gas (gas – Ferron Ss. Mbr. of the Mancos Sh.)	1
Total	**92**

field development. It remains to be seen if further waterflood project consolidation occurs in other areas of the Uinta Basin as oil development expands there as well.

According to DOGM online records (http://oilgas.ogm.utah.gov/oilgasweb/live-data-search/lds-injection/injection-proj-vol-lu.xhtml), the amount of water injected annually by all 16 of the Uinta Basin EOR waterflood injection projects has increased from 25.45 MMB in 2008 to over 44.29 MMB in 2014 (table 9.8). Over the same time period the water produced annually with the oil from the fields where these EOR projects occur has risen from 12.9 MMB in 2008 to over 24.9 MMB in 2014. The annual deficit of produced water to injected water for the combined Uinta Basin EOR waterflood projects has increased from about 12.5 MMB in 2008 to over 19.3 MMB in 2014, although the deficit temporarily dipped below the 2008 level between 2009 and 2011. Whereas the overall volume of water injected for EOR has increased over time, the increase has not been uniform across all the EOR projects. In fact, as shown in table 9.8, only the GMBU waterflood project has had significant increases in the volume of water injected annually, with the volume of water injected for EOR in 2014 more than tripling the 10.71 MMB injected in 2008. Meanwhile, the remaining 15 projects have had relatively flat to declining volumes of water injected. It is also of note that the GMBU waterflood project has steadily increased its portion of the total volume of water injected for EOR from 42% in 2008 to over 80% in 2014, at 35.75 of the 44.29 MMBW injected that year. In 2008, the GMBU project involved water-injection volumes only 33% above those at the Red Wash project, but by 2014 the Red Wash water-injection project had shrunk and the GMBU project had grown such that the water injected at GMBU was 1084% greater than at the Red Wash project.

Water Evaporation Ponds

Most of Utah's tight gas production comes from Uintah County where produced-water evaporation ponds associated with disposal facilities must have a conditional use permit (CUP) according to Uintah County rule 17.140 (2016) summarized below, and all such facilities are subject to annual reviews. All facilities must comply with State of Utah DOGM General Rules, and the CUP application must include a copy of the DOGM application and approval. A Uintah County Operations Certificate must be issued prior to an applicant receiving any production water.

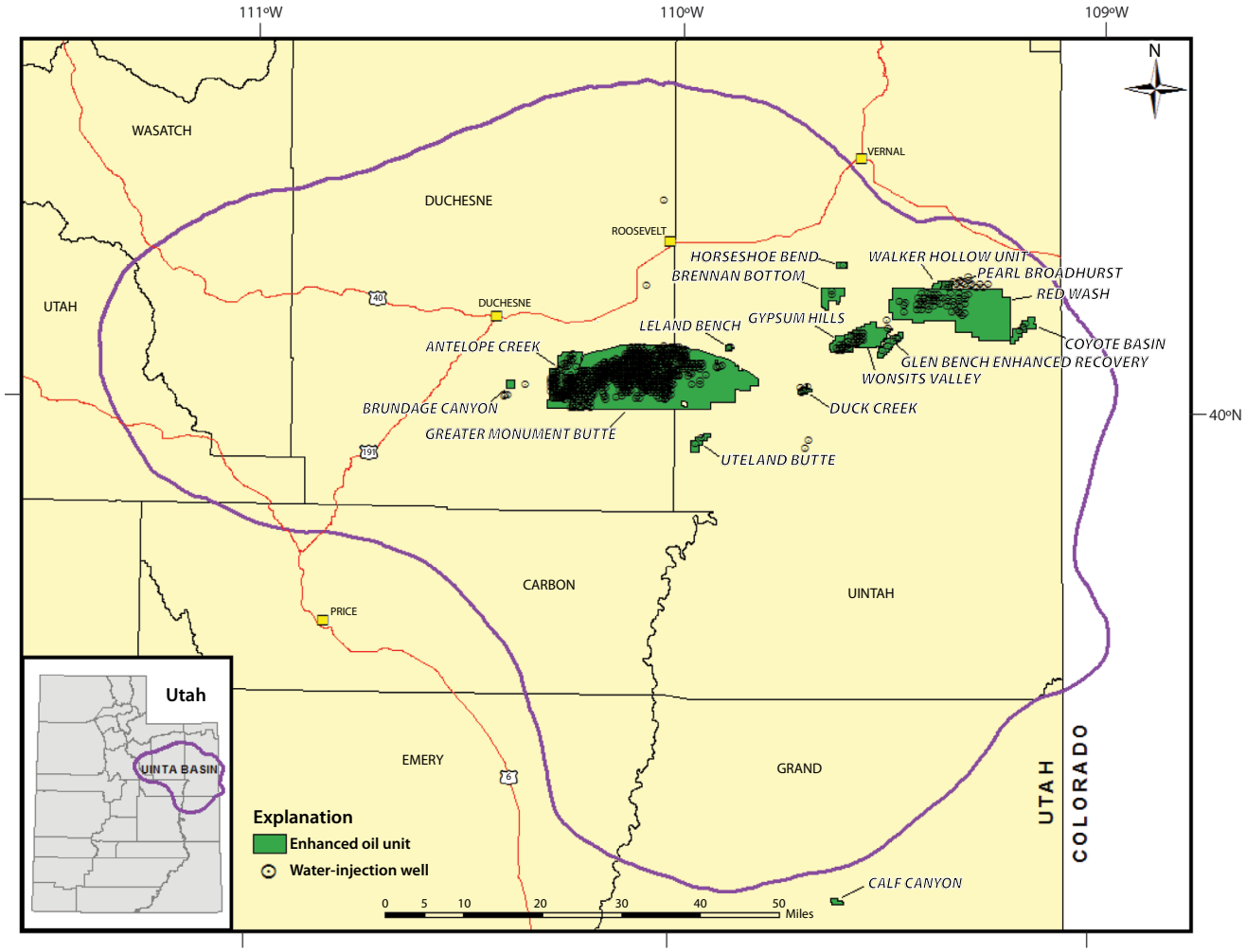

Figure 9.3. *Location of enhanced-oil-recovery waterflooding projects and wells in the Uinta Basin.*

All evaporation ponds and water treatment plants must be located a minimum of 2 miles (3.2 km) from any state or federal highway, city, town, or residential use (as determined by the Uintah County transportation system map) and from the property line of a parcel containing a primary residential use. Any site located within 5 miles (8.1 km) of a residence shall have a real-time meteorological station on the site for data collection and analysis of at least wind speed and direction.

The number of produced-water disposal ponds is limited to the amount approved on the CUP certificate. Sites cannot be enlarged, or modified, without approval from the Uintah County Planning Commission. Any leaks must be reported to Uintah County within 24 hours of an occurrence.

Signs providing emergency contact information must be provided at the receiving areas and adjacent to ponds. An operator must be on site at all times for monitoring of the site during receiving operations unless specific approval is given for the site to be unmanned. Spray evaporation systems must be operated such that all spray-borne suspended or dissolved solids remain within the perimeter of the lined pond area (figure 9.4A). Odors must be controlled to prevent nuisance complaints. A wind sensor is required on all open ponds to automatically shut down spray devices if wind speed causes any spray to leave the lined pond area. A copy of the bond with DOGM shall be provided and kept on file with Uintah County.

DOGM rules R649-9-3 and R649-9-4 cover specific requirements applicable to petroleum field waste-disposal and evaporation facilities, respectively. Siting a petroleum waste-disposal facility must conform to the following requirements:

(1) “be located on level, stable ground, and an acceptable distance from any established intermittent drainage;”

(2) “at least one mile from residences or occupied buildings not associated with the facility;” and

(3) not within aquifer recharge areas, protection zones for public drinking water sources, floodplains, drainage bottoms, areas on or near faults; not within 500 feet (152 m) of a wetland, water-course or lakebed; and not over permeable soil where groundwater is less than 50 feet (15.2 m) below the surface, or areas above a subsurface mine.

Table 9.7. *2014 Uinta Basin enhanced oil recovery water-injection and produced-water volumes (in millions of barrels).*

Project Name (oil field)	Project Number	County	# of Wells	Injected Water 2014	Produced Water 2014	Short/Excess 2014
Antelope Creek	390	Duchesne	109	1.596	1.412	-0.184
Brundage Canyon	700	Duchesne	9	0.258	1.838	1.580
Uteland Butte	338	Duchesne	2	0.004	0.100	0.096
Greater Monument Butte Unit	398	Duchesne-Uintah	1347	35.747	10.704	-25.043
Calf Canyon (Left Hand Canyon)	360	Grand	2	0.009	0.000	-0.009
Brennan Bottom	490	Uintah	2	0.030	0.223	0.193
Coyote Basin	350	Uintah	2	0.000	0.010	0.010
Duck Creek (Pariette Bench)	370	Uintah	5	0.027	0.440	0.412
Glen Bench Enh. Rec. (White River)	480	Uintah	5	0.369	0.085	-0.285
Gypsum Hills	300	Uintah	11	0.206	0.142	-0.064
Horseshoe Bend	530	Uintah	1	0.000	0.078	0.078
Leland Bench	600	Uintah	1	0.090	1.533	1.443
Red Wash	140	Uintah	52	3.019	4.533	1.514
Walker Hollow & Pearl Broadhurst	190 & 590	Uintah	16	1.669	1.719	0.050
Wonsits Valley	230	Uintah	22	1.261	2.089	0.828
TOTAL			1586	44.286	24.907	-19.379

Source: Division of Oil, Gas and Mining website
Notes:
(1) Shortages are made up with freshwater supplies.
(2) Excesses are disposed of in deep wells or evaporation ponds.
(3) 1 barrel = 42 gallons

Table 9.8. *Uinta Basin enhanced oil recovery water injection volumes, 2008–2014 (in millions of barrels).*

Enhanced-Oil Project Name	County	2008	2009	2010	2011	2012	2013	2014
Antelope Creek	Duchesne	1.88	1.71	1.48	1.20	1.25	1.40	1.60
Brundage Canyon	Duchesne	0.00	0.02	0.17	0.36	0.74	0.37	0.26
Uteland Butte	Duchesne	0.04	0.03	0.01	0.03	0.03	0.01	0.00
Greater Monument Butte	Duchesne-Uintah	10.71	11.08	15.12	16.55	22.26	29.96	35.75
Calf Canyon	Grand	0.00	0.00	0.00	0.00	0.00	0.00	0.01
Brennan Bottom	Uintah	0.09	0.08	0.06	0.07	0.04	0.04	0.03
Coyote Basin	Uintah	0.00	0.00	0.00	0.00	0.00	0.00	0.00
Duck Creek	Uintah	0.00	0.28	0.13	0.05	0.06	0.05	0.03
Glen Bench (Enhanced Recovery)	Uintah	0.44	0.42	0.42	0.47	0.43	0.38	0.37
Gypsum Hills	Uintah	0.35	0.25	0.38	0.25	0.36	0.24	0.21
Horseshoe Bend	Uintah	0.00	0.00	0.01	0.00	0.02	0.11	0.00
Leland Bench	Uintah	0.01	0.03	0.03	0.07	0.11	0.11	0.09
Pearl Broadhurst	Uintah	0.16	0.13	0.13	0.14	0.11	0.11	0.15
Red Wash	Uintah	8.05	4.87	4.33	3.94	3.39	3.00	3.02
Walker Hollow	Uintah	1.30	1.21	1.25	1.24	1.29	1.31	1.52
Wonsits Valley	Uintah	2.41	2.72	2.07	1.96	1.37	1.32	1.26
TOTAL		25.45	22.82	25.59	26.33	31.46	38.40	44.29

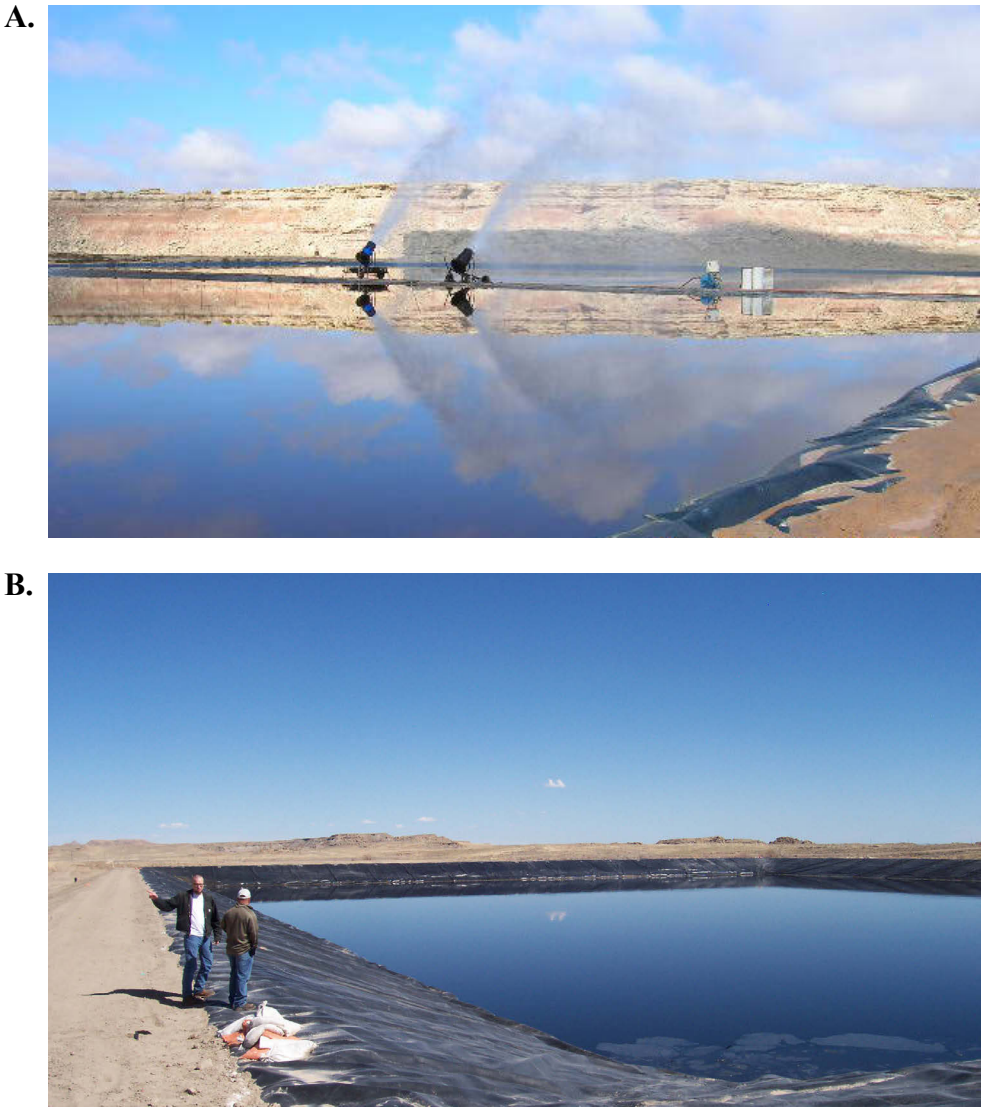

Figure 9.4. *Types of water evaporation ponds in the Uinta Basin.* ***A.*** *Spray evaporation system at Brennan Bottom disposal facility evaporation pond, Uintah County.* ***B.*** *Liner system and levee at the Sand Pass Ranch evaporation pond, Duchesne County. Photos by Brad Hill, Utah Division of Oil, Gas and Mining.*

A DOGM petroleum waste-disposal facility permittee must provide a waste-stream management plan that details the estimated quantity and quality of the liquid and solid waste materials accepted at the facility and a description of the physical and chemical processes used in the treatment of the waste streams, as well as the method and schedule of disposal of all solid and liquid waste streams produced at the facility, including how odors will be managed and kept from creating an environmental or nuisance problem. The disposal facility plan must include a contingency plan designed to minimize any hazards to fresh water, public health and safety, or the environment in the event of an unplanned fire, explosion, or accidental release of oil field wastes to the air, soil, surface or groundwater.

If a DOGM petroleum waste-disposal facility permittee plans to include evaporation ponds, in addition to meeting the siting requirements above, the evaporation ponds shall be designed for 10 acre-feet (0.012 hm^3) or less of water, and the pond capacity should be adequate to contain all produced water delivered, even in times of minimum evaporation rates. The applicant must provide an estimate of the maximum daily quantity and representative quality of the produced water to be disposed at the evaporation site, including concentrations of chlorides, sulfates, pH, TDS, and any other significant constituents required by DOGM. The evaporation ponds need to be constructed with a double liner system including a leak detection system between the primary (minimum 60-mil high-density polyethylene [HDPE] or equivalent) and secondary (minimum 40-mil HDPE or equivalent) liner systems. The pond liner material shall be impervious and resistant to weather, tears and punctures, sunlight, hydrocarbons, aqueous acids, alkalis, salt, fungi, or other substances that may be contained in the produced water. Water unloading systems associated with the ponds may also require a leak detection system. The ponds are to be constructed with 2-foot (0.6 m) free-board at all times and the grade of the pond levee is to be no steeper than 3:1 on

the inside of the levee and no steeper than 2:1 on the outside of the levee (figure 9.4B). Any hydrocarbon accumulation on a pond, other than de minimis quantities, is considered an operating violation and must be corrected within 24 hours.

The above summary provides the basic highlights of the Utah rules governing petroleum waste-disposal facilities and evaporation ponds. For the exact particulars of the DOGM rules regarding waste-disposal facilities and evaporation ponds the reader is referred to the DOGM rules webpage found at http://oilgas.ogm.utah.gov/oilgasweb/rules/rules-main.xhtml.

DOGM collects quarterly information from operators of evaporation ponds, both commercial and private, on the amount of water delivered to each pond, as well as information on whether leaks were detected or not. Commercial ponds are those that take water for disposal for a fee, and private ponds are those operated by companies for their own needs. DOGM kindly provided the UGS water delivery volume data for 2010 through 2013, and the annual results are summarized in table 9.9.

Table 9.9 shows the amount of water delivered annually to all evaporation ponds in the Uinta Basin has varied from 11.9% and 17.3 MMB per year with a four-year annual average of 13.76 MMB. The percentage of water delivered to commercial evaporation ponds varied over the four years from 60% to 73%, and averaged 67.3% of the total delivered to all ponds. The amount of produced water delivered to evaporation ponds varied from year to year and a long-term trend is difficult to discern with only four years of data. The least amount of water delivered to evaporation ponds was in 2011, and the greatest amount was in 2012.

A list of commercial disposal facilities, which commonly have evaporation ponds, is provided on the DOGM website. The 20 commercial facilities in the Uinta Basin are listed in table 9.10, and their locations are shown on figure 9.5.

Water Used for Hydraulic Fracturing

The amount of water used in hydraulic fracturing of wells in Utah is the hardest water stream to quantify because reporting of such water use was not mandatory in Utah until November 2011, when DOGM began requiring companies to report the amount of water and additives used in hydraulic fracturing well completions to the FracFocus' chemical disclosure registry website (http://fracfocus.org/). Thus, reported water volumes used in hydraulic fracturing before 2012 are incomplete because not all companies participated in the voluntary reporting effort, and FracFocus only began collecting data itself in 2011. As of mid-2015, the FracFocus website did not have its records available in a digital tabular format, only in PDF image format, which makes compilation of the hundreds of Uinta Basin fracture stimulation records cumbersome, tedious, and subject to clerical data entry errors. DOGM kindly provided the UGS with a batch download in digital format of all the wells with fracture stimulations in Uintah County during 2013 for use in our study. Data for other years and counties for this study were tallied one at a time from the PDF records available on the FracFocus website. Some wells received more than one fracture stimulation in a year and care was taken to tally such wells only once with a cumulative amount of water used in all treatments. Occasionally, duplicate records were encountered and the duplicates were removed from our final well tally and volume of water used. As of mid-2015, FracFocus had only posted records for the first half of 2014, so the information posted in the tables and chart below for 2014 only reflect one-half of a year.

Table 9.9. *Produced water delivered to Uinta Basin evaporation ponds, 2010–2013 (barrels).*

Type	2010	2011	2012	2013
Commercial	9,076,507	7,196,591	12,495,939	8,569,282
Private	4,569,698	4,704,461	4,759,001	3,678,693
TOTAL	13,646,205	11,901,052	17,254,940	12,247,975

Source: Utah Division of Oil, Gas and Mining; written communication

For the two full years (2012 and 2013) reported in table 9.11, the number of wells fracture stimulated in the Uinta Basin averaged 1010, and the two years with only partial reporting each were about half that amount. Uintah County, where most of the natural gas development is occurring, has generally had the greatest proportion of fracture stimulated wells, except for the first half of 2014 when Duchesne County took the lead. Only a small number of fracture stimulations of wells occurred in Carbon or Grand Counties in the four years tabulated.

Table 9.12 provides a tally of BW used in fracture stimulations of wells by county for the four years with data available for the Uinta Basin, and shows that the two years with full reporting averaged about 10 MMBW per year. Some of the wells tallied have had more than one fracture stimulation at a given time (multiple intervals), and some have been fracture stimulated more than once (multiple times in the same interval or subsequent stimulations of new intervals). If the second half of 2014 equals the first half of the year as reported to FracFocus, then the full year for 2014 may also entail over 10 MMBW used for fracture stimulations in the Uinta Basin. The annual water usage in fracture stimulations by county is also depicted graphically on figure 9.6.

Since the data reporting water used in fracture stimulations of oil and gas wells are not complete for all the years studied, one way to look for changes in usage from year to year is to convert the data to water used per well treated by dividing the total water used in a year by the number of wells fracture stimulated during that year. Table 9.13 shows that the BW per well used in fracture stimulations varies for each county and over time. Carbon County has the most variable water usage per well over time, ranging from none in 2014 to over 19,000 BW per well for the two wells in 2013. The amount

Table 9.10. *Utah Division of Oil, Gas and Mining approved commercial disposal facilities as of June 2015. Locations shown on figure 9.5; those in Duchesne County are relative to the Uintah Base Line & Meridian, all the others are relative to the Salt Lake Base Line & Meridian.*

Type/Operator	Section	Township	Range	County	Facility/Area
*/Brennan Bottom Disposal	19	6 South	21 East	Uintah	12 Mile Wash
- /Brennan Bottom Disposal	9	9 South	22 East	Uintah	Glen Bench
*/Dalbo, Inc.	35	5 South	20 East	Uintah	Ace Disposal
	2	6 South	20 East	Uintah	Ace Disposal
*/Dalbo, Inc.	5	9 South	22 East	Uintah	Glen Bench
- /Danish Flats Env. Services	8	20 South	24 East	Grand	Danish Flats
- /Eastern Water Solutions	12	6 South	19 East	Uintah	EWS E. Gusher
*/Integrated Water Management, LLC	30	2 South	4 West	Duchesne	IWM/N. Blue Bench
*/Iowa Tanklines, Inc.	30	4 South	2 West	Duchesne	Pleasant Valley
*/LaPoint Recycle & Storage	12	5 South	19 East	Uintah	LaPoint
- /Monarch Natural Gas, LLC	36	9 South	18 East	Uintah	Desert Spring
- /Monarch Natural Gas, LLC	29	9 South	18 East	Uintah	Eight Mile Flat
- /New Water Financial, LLC	10	19 South	25 East	Grand	Harley Dome 1
- /OWL SWD Operating, LLC	8	20 South	24 East	Grand	Danish Flats
*/R N Industries, Inc	4, 9	2 South	2 West	Duchesne	Bluebell
*/R N Industries, Inc	26, 35	8 South	21 East	Uintah	Wonsit
- /R N Industries, Inc	2	9 South	22 East	Uintah	Chapita
- /R N Industries, Inc	5	9 South	22 East	Uintah	Glen Bench
- /R N Industries, Inc	36	10 South	20 East	Uintah	Seep Ridge
- /R N Industries, Inc	25, 26, 35, 36	4 South	3 West	Duchesne	Pleasant Valley
*/Western Water Solutions (temporarily closed as of June 9, 2015)	9, 10	4 South	1 West	Duchesne	Sand Pass Ranch

- Facility is approved to accept only produced water and associated RCRA-exempt fluids.
* Facility is approved to accept produced water and associated RCRA-exempt fluids and waste material resulting from crude oil spill clean-up operations.

of water used per well for fracture stimulation for Duchesne County has been the most consistent over time, averaging about 8665 BW per well for the four years for which we have data. With only one full year and one partial year of data, and only five wells stimulated, Grand County does not have any discernable trend or consistency in terms of water usage per well. The water usage per well for fracture stimulation completions in Uintah County appears to be rising gradually over time, increasing from 7778 BW per well in 2011 to 12,760 BW per well in 2014. Many factors can contribute to changes in the amount of water used for fracture stimulating a well such as well depth, number or intervals stimulated, the thickness of the interval(s) stimulated, whether the well is vertical or horizontal, and the susceptibility of the reservoir rocks to fracturing. Also, in some instances it has been found that larger fracture stimulation treatments may be more effective than smaller treatments, which may cause water usage to increase over time.

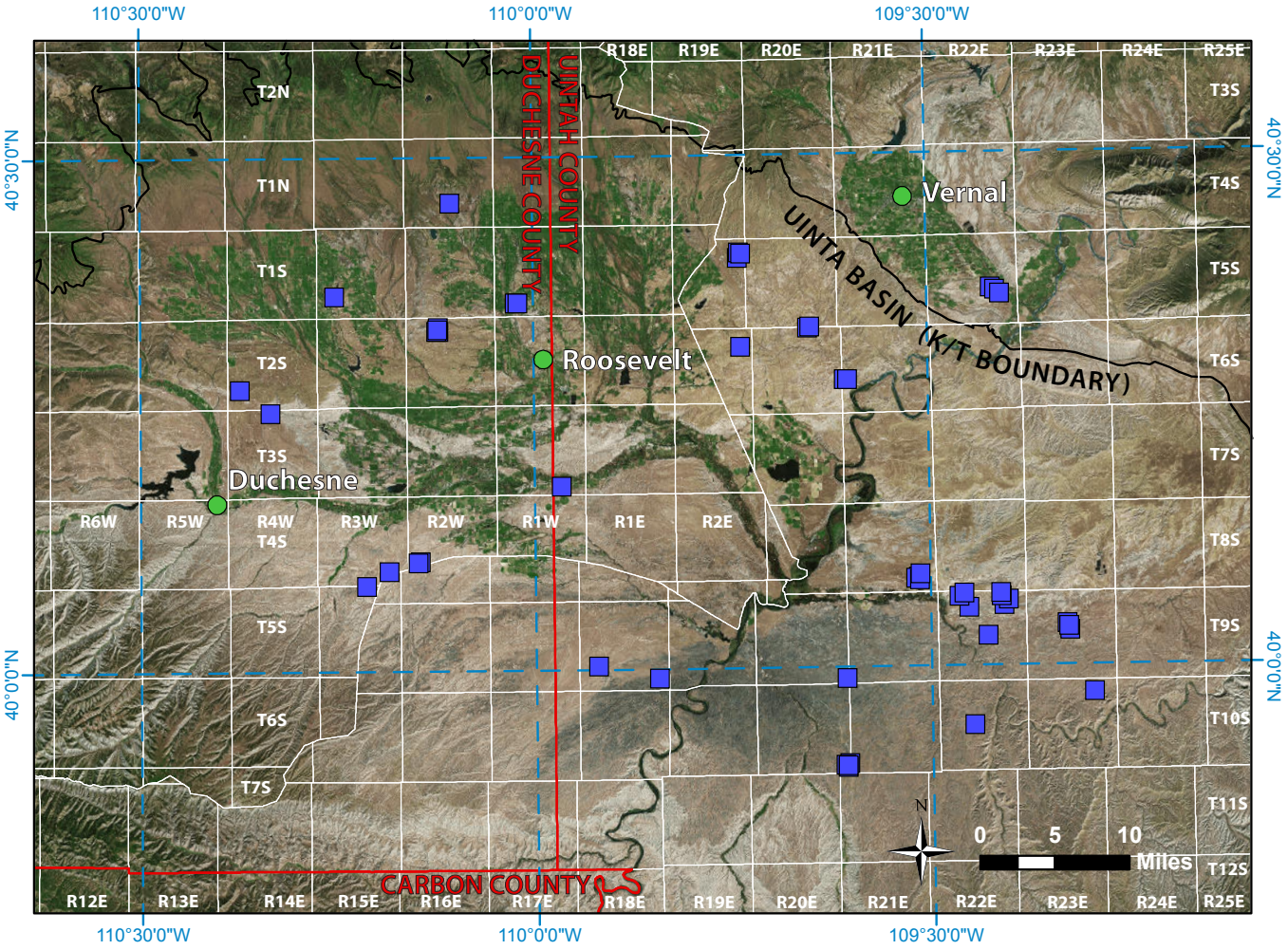

Figure 9.5. *Location of water evaporation ponds (blue squares) in the Uinta Basin. Blue squares are larger than actual ponds. Modified from Lyman and others (2013).*

Table 9.11. *Annual number of wells with fracture stimulations in the Uinta Basin by county for the years 2011–2014.*

County	2011 (part)	2012	2013	2014 (1/2)
Carbon	25	34	2	0
Duchesne	138	326	490	299
Grand	0	0	4	1
Uintah	330	576	588	228
TOTAL	493	936	1084	528

Note: 2011 is a partial year and 2014 is for the first half only.

Table 9.12. *Annual number of barrels of water used in fracture stimulations in the Uinta Basin by county for the years 2011–2014.*

County	2011 (part)	2012	2013	2014 (1/2)
Carbon	150,949	198,006	38,533	0
Duchesne	1,136,421	3,058,977	4,315,481	2,461,673
Grand	0	0	21,121	1422
Uintah	2,566,602	6,243,948	6,234,542	2,909,366
TOTAL	3,853,972	9,500,932	10,609,677	5,372,461

Note: 2011 is a partial year and 2014 is for the first half only.

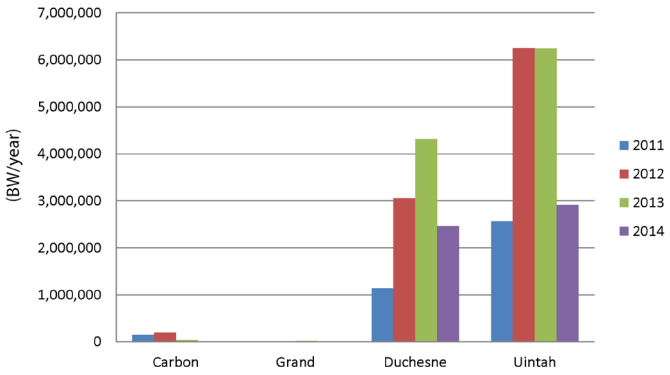

Figure 9.6. *Annual amount of water used in fracture stimulations by county for the Uinta Basin from 2011 through 2014 (note: 2011 and 2014 are only partial year tallies).*

Table 9.14 shows that during 2013, water used in fracture stimulations in Uintah County varied based on the purpose of the well completed. The wells for this county for 2013 were divided into two classes, either Wasatch-Mesaverde Formation gas (Greater Natural Buttes field) or Green River Formation oil wells. Each category cumulatively used about the same amount of water for fracture stimulations during 2013,

Table 9.13. *Annual number of barrels of water used per well in fracture stimulations in the Uinta Basin by county for the years 2011–2014.*

County	2011 (part)	2012	2013	2014 (1/2)
Carbon	6038	5824	19,267	none
Duchesne	8235	9383	8807	8233
Grand	none	none	5280	1422
Uintah	7778	10,840	10,603	12,760

Note: 2011 is a partial year and 2014 is for the first half only.

Table 9.14. *Annual number of wells fracture stimulated, barrels of water used in stimulations, and the number of barrels used per well in Uintah County for the year 2013.*

Field Name	Wells Fractured	Barrels Used	Barrels Per Well
Greater Natural Buttes (gas)	329	3,103,534	9433
various Green River oil fields	259	3,131,008	12,089
TOTAL	588	6,234,542	10,603

but since there were more gas wells than oil wells, the amount used per well was about 28% more for oil wells than gas wells. Interestingly, the amount of water used for fracture stimulations during 2013 in Duchesne County, where Green River Formation oil completions predominate, averaged 8807 BW per well compared to an average of 12,089 BW per well in Uintah County for the same year. Thus, even wells drilled for the same purpose can vary from county to county for the average amount of water used per well in fracture stimulations.

UINTA BASIN PETROLEUM-RELATED WATER HANDLING PRACTICES

Introduction

Water management/handling practices in the Uinta Basin cover a range of possibilities. Small operators are generally dependent on outside vendors to haul and dispose of produced water at commercial disposal wells or pits. Large operators commonly design and construct complex centralized water-collection, handling, and disposal facilities that allow for capture and reuse of flow-back formation fracturing fluids, centralized facilities for treatment of produced water, a series of injection wells or evaporation ponds for water disposal, and minimizing trucking needs. Water treatments may include settling tanks which skim oil off the top and settle sediments at the base, oil-water separators, hydrocyclones, flotation cells, chemical flocculation of clays, and filtration systems (walnut shell, sock, or ceramic) before final disposal. To help understand the range of operational practices used or possible, a review of the practices employed by various gas and oil operators in the Uinta Basin is provided in the following section. Other practices are employed in other states in the U.S., and no doubt some new practices that find success elsewhere may be tried in Utah in the future to see if the same successes can be replicated here.

Current Practices of Selected Companies

The following companies are all operators of large gas and oil fields with more integrated water-handling and processing facilities. The first three companies discussed operate parts of the Greater Natural Buttes field, the second group includes two gas developers in the West Tavaputs Plateau area of the Uinta Basin, and last, for comparison, is the operator of the large Greater Monument Butte field.

Anadarko Petroleum/Kerr-McKee (Natural Buttes Gas Field)

Drilling and completion practices: Anadarko Petroleum received approval for full-field development from the BLM in 2012 (U.S. Bureau of Land Management, 2012a). For well drilling, Anadarko uses only closed-loop drilling procedures to ensure that no fluids are lost from the drill site and that other emissions are best contained (Kenny Gathings, Anadarko Petroleum, verbal communication, November 2013). Air drilling is not used since dust from a site could not be completely contained. Drilling of a typical well might use between 3000 and 6000 gallons of water for a 9000- to 10,000-foot- (2700–3050 m) deep well. As of mid-2014, Anadarko had 2796 gas wells (2679 producing, 92 shut-in, and 25 temporarily abandoned), 9 water-disposal wells, and 1 water-supply well in Uintah County. Anadarko has recently employed from one to four rigs to maintain its development schedule of 200 to 400 wells per year. At the end of 2014, Anadarko had reduced the number of drill rigs operating to one. As of mid-2014, the company also had 626 approved Applications for Permit to Drill (APDs) new wells, and had three locations where approved drilling operations had commenced, but had been temporarily suspended. For full-field development, Anadarko anticipates drilling over 4700 new wells (Kenny Gathings, Drilling Manager, Anadarko Petroleum, verbal communication, November 2013). Assuming an average of 150 new wells per year, Anadarko will be adding these new wells over 31 years, until about 2045, to finish drilling 4700 new gas wells at Natural Buttes field.

For gas well completions, Anadarko typically fracture stimulates the tight-sand reservoirs to increase gas-flow connectivity between the reservoir and the wellbore. Anadarko estimates that a single fracturing job would entail about 60,000 gallons (1430 bbls) of water (Kenny Warren, Anadarko Petroleum, verbal communication, November 2013). This estimate reflects a single stage of fracture stimulation since Anadarko's reports to the FracFocus website (http://fracfocus.org/) show water volumes for an individual Natural Buttes well ranging from 200,000 to 700,000 gallons per well, no doubt because some wells had multiple perforation segments (stages)

that were individually fracture stimulated. Thus, to drill and complete a new gas well at Natural Buttes field could require from 203,000 to 706,000 gallons of water (4833–16,810 BW; 0.62–2.17 acre-feet [0.00076–0.00267 hm^3]). If we assume 150 new wells are drilled and fracture stimulated per year, then associated annual water usage for fracture stimulations could range from 30.45 to 105.9 million gallons (724,950–2,521,500 BW; 93–325.5 acre-feet [0.11–0.40 hm^3]).

Water for fracture stimulation is contained on a well site in portable tanks of 500 to 1000 gallons. To reduce freshwater consumption for fracture stimulations, Anadarko uses its Anadarko Completion Technology System (ACTS) to catch flow-back water from a series of one to six wells on a single pad in lined and netted pits. The pits allow the solid drill cuttings to settle out in the bottom and then the settled water is treated (generally with bleach) to kill bacteria and settle out iron. The treated flow-back water is transferred via aluminum pipe or truck to the next site for use in fracturing other wells. Piping by temporary surface lines is the predominant transfer method between a group of closely spaced wells to reduce truck traffic and related emissions (figure 9.7); trucking is mainly employed where the pumping distance via pipe is prohibitively expensive. With a slight loss of fluid in each well, Anadarko (2015) needed to make up less than 10% of its water required for fracture stimulation from freshwater sources and over 90% of its water used in fracture stimulations was recycled water, thereby reducing freshwater usage and trucking costs. If annual water usage for fracture stimulations is estimated at 30.45 to 105.9 million gallons (see above paragraph), then if reuse is estimated at 90%, Anadarko's ACTS program will use 27.4 to 95.3 million gallons (0.65–2.27 million bbls) of flow-back water annually and significantly reduce the use of fresh water needed for field development.

Rather than flaring gas during the flow-back phase of the well completion, Anadarko connects the well to the gas sales pipeline as soon as possible. This practice avoids product loss due to flaring and its associated air emissions.

Produced-water management practices: Anadarko has no use for the water produced from a well other than collecting the initial flow-back water portion from the fracture stimulation phase of well completion, which is reused at new wells for other fracture stimulations. Therefore, water produced with gas is considered a waste stream and Anadarko has determined that within its operating area the best and most cost-effective way to handle to wastewater is disposal in deep saline aquifers via Class II disposal wells. To handle the disposal of produced water from 2700+ existing wells and 4700+ future wells, Anadarko has designed and built an integrated field-wide water handling, treatment, and disposal system for its produced-water waste stream. In 2013, Anadarko had nine disposal wells, and eight water-treatment facilities de-

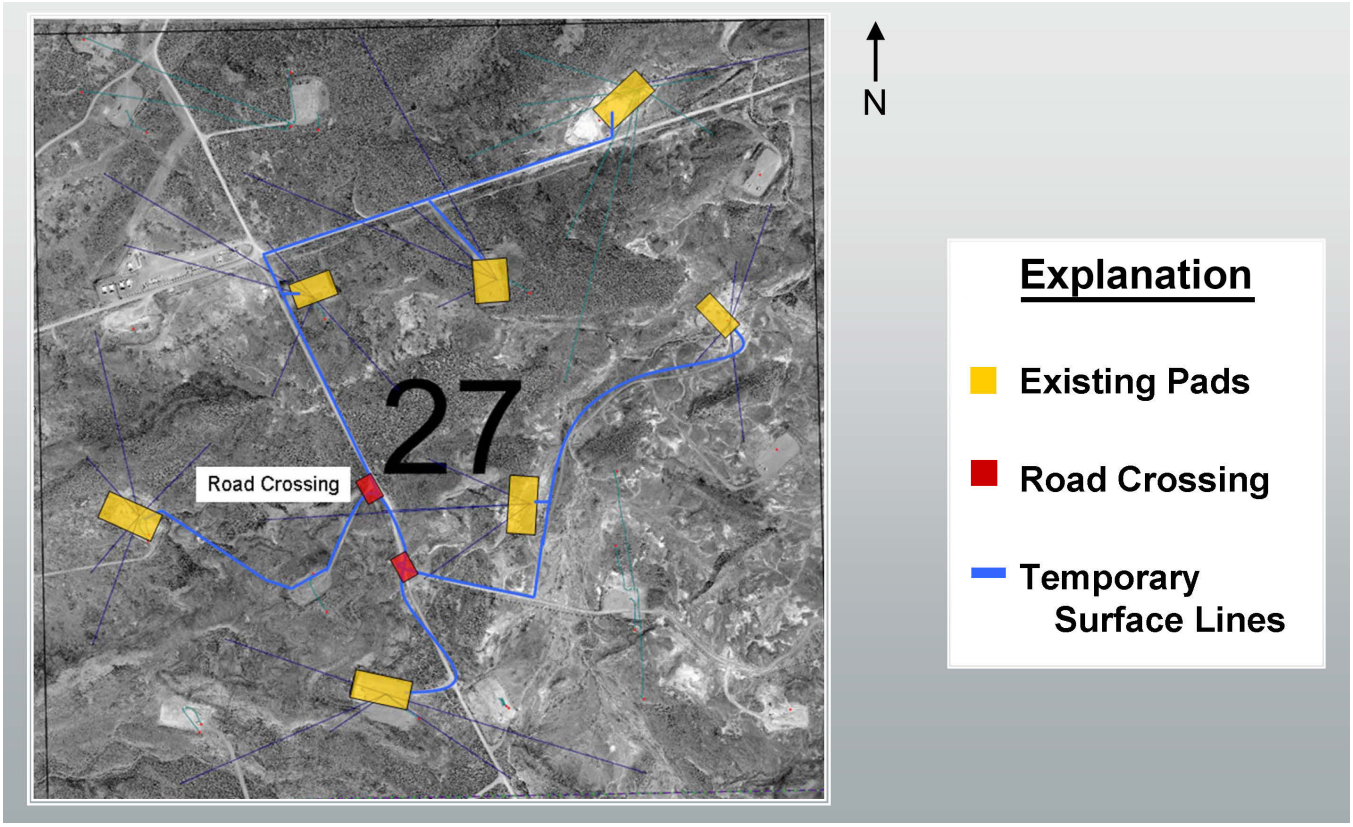

Figure 9.7. *Example of Anadarko's Completion Technology System (ACTS) at Natural Buttes field showing closely spaced drilling pads containing multiple wells and temporary surface pipeline to transport and reuse hydraulic fracturing flow-back fluids. Area shown is 1 square mile (2.6 km^2), section 27, T. 9 S., R. 21 E., Salt Lake Base Line & Meridian, Uintah County. Illustration courtesy of Anadarko Petroleum.*

signed to handle 60,000 bbls of produced water per day, but at that time was handling in the range of 30,000 to 40,000 BPD (John Kynaston and Mike Merrill, Anadarko Petroleum, verbal communications, November 2013). According to the Record of Decision (ROD) document for the Greater Natural Buttes Final Environmental Impact Statement (EIS) (U.S. Bureau of Land Management, 2012b), full gas field development will entail an average annual produced-water volume of 1385 acre-feet (1.71 hm^3) (10.75 million BW; 451.3 million gallons), of which, Anadarko estimated 75% would be disposed of by underground injection, and 25% would be disposed of by evaporation. Three of the water-treatment facility sites have pits for evaporation and overflow capacity in case a disposal/treatment plant went offline. All of the water-treatment and disposal-well facilities are interconnected by a system of pipelines that can be controlled to move water to any water-treatment site or disposal well should any one need to be taken off line for maintenance or repair. The UGS toured two of the eight water-treatment facilities, Blue Feather and Pipeline, to get an understanding of the water-treatment technologies employed in preparing the produced water for final disposal in an underground saline aquifer.

Anadarko's produced-water disposal system network represents, particularly the Blue Feather site, the newest water-treatment technology whereby even the truck unloading part of the facility offers a pretreatment separation of the water, other liquids, and solids by pumping the off-loaded water through a centrifugal spiral that separates different densities of materials to the various water-processing or product tanks on site. Liquid hydrocarbons go to the products tank, and sufficiently clean water to the bulk disposal tank, and water needing additional treatment to the settling or Induced Gas-Flotation Tanks (IGT). Water is trucked mainly from newly completed wells before they are fully connected to the water gathering system or from selected wells that periodically need to be disconnected from the water gathering system. A water-treatment plant's first set of gun barrel tanks is simple gravity settling tanks where solids sink and are collected from the bottom, condensate hydrocarbon liquids are skimmed from the top, and the leftover water needing further treatment is sent to the intermediate IGTs for additional cleaning. In the IGTs, gas is pumped into water at the bottom of the tank as small bubbles, and the water needing treatment is introduced from the top of the tank at an angle in such a way as to create a downward spiraling of the fluid. This downward spiral reacts with the gas to float oil droplets to the top of the tank in a frothing action that further cleans the water from the initial gravity settling tanks before the water is sent to the final bulk storage tanks, where the water can be pumped to one of nine injection wells for ultimate disposal. When the water is pumped from the "bulk" water-storage tanks to the disposal well it is sent through a system of 5-micron sock filters to further clean the water and help protect the disposal well and pipeline gathering system from corrosion and abrasion. The piping in the system is all stainless steel to handle the inherent high salinity and corrosive nature of the produced water (John Kynaston and Mike Merrill, Anadarko Petroleum, verbal communication, November 2013). Water can be sent from a water-treatment site to any of the nine injection wells operated by Anadarko, which meters the water sent from each treatment plant so that deliveries to each disposal well maintain a constant injection rate, or the injection rate can be adjusted to accommodate flows from one or several water-treatment facilities. The maximum injection rate for each well is capped by the results of mechanical integrity tests performed on each well before it is put into service, and routinely performed every five years to test that the well is still in good working condition.

At the second water-treatment site visited, Anadarko had a similar progressive system of treatment tanks installed with initial gravity settling tanks, followed by "bulk" water holding and treatment in liquid-hydrocarbon condensate storage tanks. An intermediate IGT was tested at this site, but either because the water offloading system did not offer water pretreatment, the delivered water was somehow different, or for some other reason, the IGT did not work properly at this site but simply made a mixed suspension of oil in the water rather than actively separating the oil as expected. This second site also included a new solid "sludge" treatment set of tanks where the solids were heated and treated before landfilling to recover residual condensate product from the solids before ultimate disposal offsite. Anadarko had learned that the landfill operator was treating the solids before disposal and recovering the oil, so Anadarko decided to recover the product for themselves before landfilling the produced solids. This second water-treatment site also included legacy evaporation/settling ponds that Anadarko had used previously for water handling and disposal. When water is pumped to the ponds it can be sent through a network of sock, walnut shell, and MyCelX coated filters to ensure that 99% of the oil is removed before the water enters the ponds. Anadarko is moving away from the use of open evaporation pits as a primary disposal method since they no longer find them an economic or environmentally acceptable water handling technique.

Expansion of the number of evaporation ponds and the use of water cannons on ponds has been discontinued because (1) the cannons floated on the ponds to spray water into the air to enhance evaporation frequently plugged and needed servicing, (2) it was difficult to keep waterfowl off the ponds, (3) filtering the water going into the ponds was costly, and (4) open ponds (rather than closed tanks) allowed for more airborne hydrocarbon emissions than Anadarko preferred. Therefore, the evaporation ponds are mainly used for backup storage when the existing storage tanks and disposal wells are unable to handle all the produced water on a daily basis.

EOG Resources (Natural Buttes Gas Field)

Field development activities: EOG Resources operates the Chapita Wells unit of Natural Buttes gas field. For development work in the past few years, where practical, EOG has been drilling up to five directional wells per drill site to reduce

overall footprint for roads, well pads, and collection lines in this unit. The number of producing gas wells EOG operated at the Chapita Wells unit was 1250 as of November 2014. In 2014, EOG also operated 10 active water-disposal wells at the Chapita Wells unit of Natural Buttes gas field, 51 shut-in gas wells, and 68 plugged and abandoned wells, for a success ratio of over 99% of the wells drilled. EOG also had permits to drill another 275 gas wells. According to DOGM production records through June 2014, EOG's gas wells averaged 70 MCFG and 13 BW per day during the first half of the year.

According to plans filed with the BLM, EOG hopes to drill as many as 2808 new gas wells on its land holdings, and drilling and completion of each well could use up to 16,850 BW for a cumulative water requirement of 47,314,800 BW over the life of the project. EOG plans to minimize fresh water usage in the drilling and completion of new wells by only using 12% from freshwater sources, and obtaining the remaining 88% from recycled water from the Bonanza power plant of Deseret Generation and Transmission. Assuming the drilling development period spans 15 years, then EOG could use 378,518 bbls of fresh water and 2,775,802 bbls of recycled power plant water annually.

Produced-water management practices: In the past EOG has used commercial produced-water disposal facilities, and it presently has regulatory approval to use commercial disposal facilities run by R N Industries in the Uinta Basin if necessary. In 2012, all of EOG's gas wells had individual water holding tanks and the produced water was trucked to disposal wells or holding ponds that EOG operated at the Chapita Wells unit. In addition to disposal of produced water in its own disposal wells, EOG had disposed produced water at the Brennan Bottom commercial site located in section 19, T. 6 S., R. 21 E., SLBL&M, Uintah County. In 2013, when EOG only completed and hydraulically fractured one well due to low gas prices, its plan for an integrated liquids-gathering system (LGS) at the Chapita Wells unit was approved by the BLM (U.S. Bureau of Land Management, 2013a). Because mineral ownership differences preclude EOG from commingling the products from the Mesaverde and Wasatch reservoirs, EOG's new, centralized LGS will only handle the products from the Mesaverde reservoirs, whereas the fluids from the wells tapping the Wasatch reservoirs will still be stored in tanks at each well site until they are trucked to a disposal or marketing site. According to the April 2013 BLM ROD for the LGS (U.S. Bureau of Land Management, 2013a), EOG's proposed project would consist of an integrated system of buried pipelines connecting and coordinating the transport of hydrocarbon and fresh and produced water among Mesaverde gas wells, up to 14 centralized gas-processing plants, existing freshwater supply ponds, existing produced-water disposal ponds, water-disposal wells, and gas and oil sales points. The LGS system is planned to be connected to only about half of the wells in the field at full development. As of early 2015 at the Chapita Wells unit, EOG's three centralized LGS facilities simply separate produced water from salable hydrocarbons, and send the produced water to any of three produced-water underground disposal facilities, or in an emergency to a pond at the Red Wash site (section 2, T. 9 S., R. 22 E., SLBL&M, Uintah County), at the White River site, or ponds at its Coyote Wash disposal-well facility (section 16, T. 9 S., R. 23 E., SLBL&M, Uintah County). The 3 existing and 11 proposed LGS and centralized gas processing facilities will reduce truck traffic and associated emissions at the Chapita Wells unit, and through centralization create economies of operating scale in water handling that may allow EOG to experiment with further treatment and possible reuse of some produced water.

According to EOG's website, the company is committed to actively managing and conserving water resources where it operates. For example, EOG continues to test water reuse technologies, take steps to minimize overall water usage in the drilling and completion of wells, properly dispose of produced water, evaluate alternative sources of water, and responsibly manage the water used, produced, and disposed of at its operations. In March 2014, EOG installed water-treatment and reuse facilities at its Eagle Ford play development operations in West Texas. Perhaps in the future when natural gas prices rise, EOG will also test water reuse technologies in the Natural Buttes field area in combination with its recently completed centralized water handling system.

XTO Energy (Natural Buttes Gas Field)

Field development activities: XTO Energy purchased its holdings in the Uinta Basin from Dominion Energy in July 2007, but development of these leases began as early as the 1950s. Through August 2014, XTO operated 571 gas and 5 oil wells in Uintah County, with the majority (500) in Natural Buttes gas field, and the remaining 76 producing wells scattered among Alger Pass (9), Fence Canyon (2), Hill Creek (51), Love (8), and Rock House (1) gas fields, and the Uteland Butte (1) and West Willow Creek (4) oil fields. In addition to these producing oil and gas wells, XTO had 42 shut-in gas wells and 1 shut-in oil well, 2 temporarily abandoned gas wells, 44 plugged and abandoned gas wells and 4 plugged and abandoned oil wells, and 4 water-disposal wells in Natural Buttes gas field. According to DOGM records through August 2014, XTO's 576 Uintah County wells averaged about 0.6 BO, 71.8 MCFG, and 3.6 BW per day through the first eight months of 2014. In August 2014, XTO had permits to drill 83 new gas wells, 55 at Natural Buttes, 21 at Hill Creek, and 7 at Love field.

Produced-water management practices: According to the BLM's environmental assessment (U.S. Bureau of Land Management, 2013b) for XTO's planned infill development at the River Bend unit of Natural Buttes gas field, produced water and condensate are separated and stored in steel tanks at each well pad. Potential spills from the tanks are protected by containment dikes of compacted earth or steel to hold 110% of the largest tank on site. Currently, the water from each tank is pumped periodically as needed and transported to existing

water-injection disposal wells in the River Bend unit area, or to permitted evaporative disposal sites. XTO disposes of the majority of the produced water (93%) via injection wells, and the remainder via evaporation (U.S. Bureau of Land Management, 2013b).

GASCO Energy (West Tavaputs Plateau Gas Development)

Field development activities: As of June 2012, GASCO's Uinta Basin natural gas development project EIS had been approved by the BLM, allowing for the drilling of nearly 1300 new wells from 575 well pads. GASCO Energy operated 137 wells, including 2 shut-in oil wells and 7 shut-in gas wells, in the Uinta Basin in 2014, distributed between seven different fields mainly in the area between Monument Butte and Natural Buttes fields along the Uintah-Duchesne County line (figure 1.1). The majority of GASCO's wells are in the Pariette Bench (56 wells), Uteland Butte (28 wells), and 8 Mile Flat North (26 wells) fields, with a lesser number of wells in the 8 Mile Flat (11), Gate Canyon (5), Middle Bench (2), and Natural Buttes (1) fields. The 129 producing wells are mainly for gas (113), with only 16 producing oil wells. During 2014, GASCO had started drilling, but not completed, 12 new gas wells, and had approved APDs for another 30 gas wells, 6 oil wells, and 1 water-disposal well. Within its lease holdings, GASCO had drilled and abandoned nine wells, indicating a drilling success rate of nearly 94% of the wells drilled.

In 2014, GASCO's operating wells produced 49,289 BO, 4.495 BCFG, and 466,968 BW through August of that year. In August 2014, GASCO's 136 actively producing wells individually averaged 1.7 BO, 155.9 MCFG, and 16.2 BW per day.

Produced-water management practices: As part of the BLM ROD on the GASCO final EIS (U.S. Bureau of Land Management, 2012b), GASCO had agreed to:

(1) institute an aquifer/groundwater monitoring plan to routinely check for evidence of any contamination from oil and gas development activities over the life of the project;

(2) investigate the use of recycled water for drilling and completion operations;

(3) use a closed-loop drilling system in areas with porous soils over fractured bedrock when drilling through a Drinking Water Source Protection (DWSP) zone or Sole Source Aquifer, or in areas with shallow groundwater; and

(4) limit the new water evaporation facility to 12 pits totaling 78 acres (proposed locations in either section 21, T. 9 S., R. 18 E., SLBL&M, Uintah County, or section 13, T. 4 S., R. 3W., UBL&M, Duchesne County), and five years after the ROD re-evaluating the need for evaporation ponds and possibly then moving to alternate means such as disposal wells.

In July 2013, the BLM approved the permit to drill GASCO's first salt- (produced-) water disposal well, which is to be drilled on an existing well pad in section 20, T. 9 S., R. 19 E., SLBL&M, Uintah County, in Pariette Bench field, Uintah County (figure 9.2). A class II injection-well permit had been received from the EPA for the well, which would dispose produced saline water into sandstone of the Douglas Creek Member in the lower part of the Green River Formation (figures 2.28 and 7.7). The proposed disposal sandstone units would have to have their water tested to see that they contain at least 10,000 mg/L TDS. The water-disposal facilities associated with the well were planned to include two 500-bbl tanks to hold produced water delivered to the site, and containment berms around the tanks to conform to EPA's spill prevention, control, and countermeasure regulations. However, the application for the permit to drill was rescinded as of January 8, 2015, due to lack of activity at the site. Complicating GASCO's decision to use disposal wells instead of evaporation ponds, is the fact that produced water from the Mesaverde Group and Wasatch Formation often has in excess of 50,000 ppm mg/L and contains major scaling constituents of calcium and iron carbonate (U.S. Bureau of Land Management, 2012b). In wells producing from both reservoirs where their waters are mixed, GASCO has been forced to insert a capillary string next to the production string of tubing to allow scale inhibitors to be continuously pumped to the bottom of the wells to provide scale protection throughout the wellbores. According to the BLM (U.S. Bureau of Land Management, 2012b), GASCO has been unable to dispose of its produced waters at other operators' disposal wells due to the other owners' concerns that scale would plug the accepting formations. Before drilling its own disposal well, GASCO has been using either its own Desert Spring evaporation facility (located in section 36, T. 9 S., R. 18 E., SLBL&M, Uintah County), or using other state-approved Uinta Basin commercial disposal facilities, primarily the one operated by Integrated Water Management, LLC (section 30, T. 2 S., R. 4 W., UBL&M, Duchesne County), or various commercial sites operated by LaPoint Recycle and Storage (section 12, T. 5 S., R. 19 E., SLBL&M, Uintah County; temporarily closed as of December 2014), R N Industries (sections 4 and 9, T. 2 S., R. 2 W., UBL&M, Duchesne County), and Western Water Solutions (sections 9 and 10, T. 4 S., R. 1 W., UBL&M, Duchesne County) to dispose of its produced water.

Enervest Operating, LLC (West Tavaputs Plateau Gas Development)

Field development activities: Bill Barrett Corporation (BBC) purchased leases in 2002 on the West Tavaputs Plateau of the southwestern Uinta Basin, which had been originally drilled as early as the 1960s, and discovered new potential in the area around 2005. An EIS for BBC's full field development of 596 new wells on 85 new and 57 prior drill pads was approved by the BLM in July 2010 (U.S. Bureau of Land Management, 2012a). Enervest Operating, LLC assumed ownership of the project from BBC in early 2013 and as of

August 2014 operated 327 gas wells, including 9 shut-in gas wells, 6 that still had no reported production, and 4 disposal wells on the West Tavaputs Plateau (figure 9.2). These wells are in northeastern Carbon County and are predominantly distributed between three different fields: Nine Mile Canyon (197 wells), Peters Point (112 wells), and Stone Cabin (9 wells) (figure 9.2). Only nine wells were listed in 2014 with "undesignated" as a field name. The 308 wells with reported production are all classified as gas wells. In 2014, Enervest had started drilling, but not yet completed, 33 new gas wells, and had approved APDs for another 164 gas wells. Within Enervest's lease holdings, past and present operators have drilled and abandoned 37 wells, indicating a success rate of about 90% of the wells drilled to date.

In August 2014, Enervest's operated wells generated 4144 BO (condensate), 1.831 BCFG, and 48,690 BW for the month. Individually, each of Enervest's 308 actively producing wells averaged 0.4 BO, 191.7 MCFG, and 5.1 BW per day for the month of August 2014.

Future development will consist of multiple wells, up to eight, drilled and completed from a single well pad, in order to minimize the surface disturbance of individual well pads and access roads. This development scheme will also reduce truck traffic in the area for well servicing.

Produced-water management practices: Before October 2008, when the first deep-injection water-disposal well was completed, water production from the current Enervest leases was stored at individual well sites in storage tanks and trucked to commercial disposal operations, such as the RNI disposal site near Roosevelt, Utah, as mentioned in a 2002 annual waste management plan filed with DOGM. Subsequently, more deep-injection water-disposal wells have been completed in the West Tavaputs Plateau area, one in September 2010, and one each in March and October 2013. Although one of these wells initially attempted disposal in the Castlegate Sandstone of the Mesaverde Group (figure 2.13), all now dispose of water in the Wasatch Formation, one of the hydrocarbon-producing formations. To avoid impairing hydrocarbon production from the Wasatch, the deep-injection water-disposal wells are located at least 0.5 mile (0.8 km) outside the structurally controlled producing areas. These disposal areas are structurally downdip from the gas at the top of the anticlinal traps and in the water legs of the reservoirs.

Under the stipulations for full field development provided in the BLM's EIS and ROD (U.S. Bureau of Land Management, 2012a), the field operator is committed to the following:

(1) Groundwater in the 100-year floodplain of the valley bottoms or other sensitive sites within the development area will be protected by using closed-loop drilling techniques for more complete management of drilling and completion fluids.

(2) The amount of road and pad disturbance will be reduced by drilling up to eight wells from a single pad, thereby eliminating 356 pads and 85 miles (137 km) of access roads that would have been required for one well per pad.

(3) Where in-ground pits are used, they will be lined by an impermeable layer to prevent leakage of drilling fluids and the company will have an approved Spill Prevention, Control, and Countermeasure Plan.

(4) Produced water and condensate will be stored in 400-bbl tanks on the well pads and generally connected via pipelines to centralized storage and disposal facilities to avoid most truck traffic and potential leakage at loading and unloading truck transfer points.

(5) Any shallow freshwater (<10,000 mg/L TDS) zones encountered during drilling will be isolated and protected by suitable casing and cement from lower producing horizons, and the company will sample groundwater at three monitoring well sites four times a year to test for any potential leakage from producing wells.

(6) Disposal of produced water will only occur at properly tested, permitted, and inspected company-owned or commercial Class II injection sites.

Newfield Exploration (Monument Butte Oil Field)

Field development activities: As of November 2014, Newfield Exploration operated approximately 3395 oil and gas wells in Monument Butte field area (figure 1.1) and had plans to add an additional 5750 new wells. Development could entail drilling and completion of up to 360 new wells per year until the resource base is fully developed. Under this maximum drilling rate scenario, construction, drilling, and completion of the 5750 new wells would encompass approximately 16 years. The annual rate and total number of wells actually drilled will depend largely on outside factors such as production success, engineering technology, reservoir characteristics, drilling economics, commodity prices, rig availability, and lease stipulations. The anticipated life of an individual well is 20 to 30 years, and the anticipated time it would take for field abandonment and final reclamation is five years. Therefore, the anticipated life of the Monument Butte project could be up to 51 years.

Produced-water management practices: Newfield recycles its produced water through water-treatment plants and then reuses the produced water for EOR waterflood. Produced water is either trucked directly to the water-treatment facilities or initially processed through new centralized Gas-Oil-Separation (GOS) plants before being piped to the water-treatment facilities. Starting in November 2012, Newfield opened its first GOS plant, designed to process up to 30,000 BPD of produced water and oil mixture (emulsion) from more than 200 wells. At the GOS plant, the produced oil is separated and prepared for sale, while the water is sent to the Sand Wash plant for final cleansing and recycling. This GOS facility,

along with an associated gathering system, allows Newfield to collect water and oil from over 200 wells at a single delivery point, and eliminate the need for up to 300 truckloads of produced water per day to the Sand Wash water-treatment plant. The GOS facility reduces volatile organic compounds (VOCs) and nitrogen oxides (NOx) emissions as well as reducing truck traffic in the field.

The Sand Wash water-treatment facility was built in 2010 and commissioned in April 2011. The Sand Wash plant uses two processes for treating produced water that is trucked in or delivered via pipeline from a nearby GOS facility, including (1) conventional gravity-separation technology to handle up to 10,000 BW per day, and (2) technology designed and run by Environmentally Clean Systems (ECS) which uses an electrocoagulation process to treat up to 20,000 BW per day (Diouhy, 2012). Prior to entering the ECS system, Newfield may first run the water through a series of gun-barrel tanks to perform conventional separation of solids and hydrocarbons from the water. The ECS process involves additional cleaning of the water by passing it through tanks containing electrified plates to form ions in the water that attach themselves via electrocoagulation to contaminants, such as Ca, Fe, Ba, Mn, and S, clustering these contaminants into larger bundles of particles that are screened out of the water. Prior to development of its Sand Wash facility, injection facilities did not have the ability to treat pit water, flow-back water from hydraulic fracturing activities, or production water high in iron sulfide. With the completion of its Sand Wash facility in 2011, Newfield now treats produced water, removing oil and gas by-products and removing solids, so it can be re-injected into the oil-producing formation to EOR and also to conserve valuable fresh water resources. Assuming each waterflood well requires 100 BW per day, the Sand Wash facility provides for water treatment and supply for about 200 waterflood wells per day.

In 2014, Newfield completed another water-treatment facility, named Beluga, which employs a different water cleaning system designed and operated by Veolia Water Technologies (2014). The Veolia system combines a multi-flow chemical (alkali) softening and flocculation process with filtration through silicon-carbide ceramic filters (figure 9.8) to prepare the water for recycling in the waterflood EOR process. This system includes softening and removal of oil, grease, and suspended solids and scale formers in a compact, modular design. The flocculated dense solids are removed in a settling zone using lamella plates. Excess solids are intermittently purged from the process for dewatering and subsequent landfill disposal. The solids from the ceramic ultrafiltration unit are continuously recycled back to the crystallization tank of the multi-flow unit, providing seed for further crystal growth. The treated alkaline water is neutralized with acid to prepare it for reuse in the EOR waterflood recovery operations, reducing freshwater demand. Finally, for waterflooding operations, a de-aeration gas stripper removes dissolved oxygen from the treated water, preventing corrosion in the injection piping network in the oil field. Table 9.15 shows Veolia's reported feed water and output processed water quality results. Veolia's trademarked "removal of oil and suspended solids" (ROSS) system has the following treatment characteristics:

- removal of scale formers (hardness, silica, iron, barium, strontium);
- removal of particulates (oil, solids, bacteria, algae, clay);
- high system-recovery rates (>98%), minimizing liquid waste generated;
- thermal resistance of the equipment (up to 210°F); and
- modular, shop-fabricated, pre-piped, pre-wired treatment system.

Preliminary operational results of the new Beluga water-treatment plant, which can process up to 18,000 BPD, are reported by Newfield to have been very positive. Assuming each waterflood well requires 100 BW per day, the Beluga water-treatment facility provides water for another 180 waterflood wells per day.

Following treatment at a water-recycling plant, initial water storage would be at on-site tanks before transfer by pipeline to one of the central water-injection facilities: Ashley, Monument Butte, Jonah, or Beluga for waterflood injection into approved Class II wells to enhance Newfield's EOR secondary oil recovery project. Water pumped from a treatment plant is passed through sock filters before going to a re-injection site.

When the BLM released a ROD at the end of September 2016 for full field development, Newfield was approved to construct up to 12 centralized GOS plants and up to 13 water-treatment plants to allow recycling of produced water for reuse in EOR waterflood operations to cover the water needs for about 2200 approved, Class II, waterflood injection wells, and reduce truck traffic needed to move production fluids within the Greater Monument Butte field area (U.S. Bureau of Land Management, 2016). Construction of four to six water pump stations will also be needed to move the water around the field from production wells to processing and treatment plants, and back to an injection well. Produced water that cannot be cleaned to meet waterflood quality standards will be disposed of at Newfield's Pariette Bench Unit No. 4 disposal well (section 7, T. 9 S., R. 19 E., SLBL&M, Uintah County, API No. 43-047-15681), its sole water-disposal well, or at other State of Utah-approved surface disposal facilities (U.S. Bureau of Land Management, 2016).

Opportunities for Water Reuse in Utah

The greatest opportunities for reuse of produced water is within the petroleum industry itself, and these opportunities are already being used to some extent as explained in the discussions above of the individual Utah petroleum operators' practices. Produced water is reused by Utah gas producers for drilling and well completions, and by Utah oil producers for

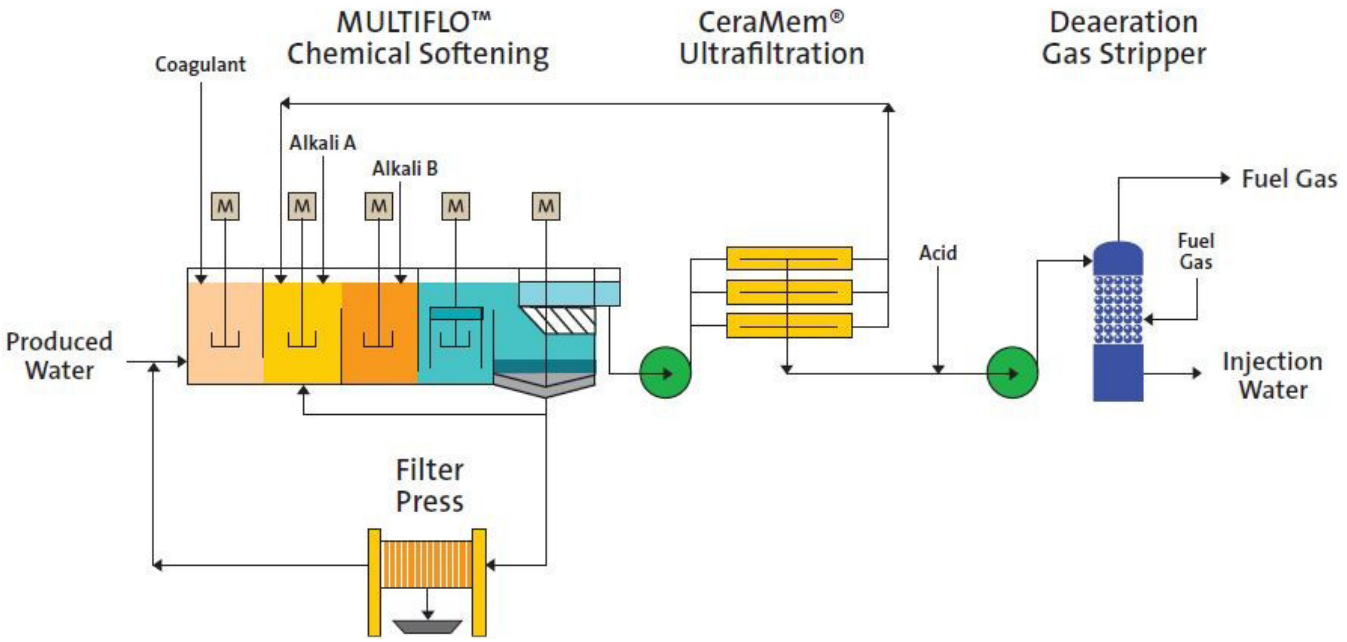

Figure 9.8. *Schematic diagram of the Newfield Beluga plant's Veolia water-treatment process with water moving from left to right; note M = mixer. Multiflo and CeraMem are registered trade names of Veolia Water Solutions and Technologies (source: veoliawaterstna.com/news-resources/information-files/ross-flowback-produced-water.htm webpage accessed October 2014).*

Table 9.15. *Veolia Water Technologies's reported processing performance data for waterflood applications (veoliawaterstna.com/news-resources/information-files/ross-flowback-produced-water.htm webpage accessed October 2014).*

Contaminant	Feed Water	MULTIFLO Effluent	CeraMem Effluent	Deaerator Effluent
Hardness, ppm as $CaCO_3$	1000–5000	< 20	< 20	< 0.5
Total iron, ppm	2–30	< 1.0	< 0.5	< 0.5
Free oil, ppm (>20 µm)	10–300	< 10	< 0.2	< 0.2
Suspended solids, ppm	10–300	< 10	< 0.2	< 0.2
Bacteria, cells/ml	100–9999	100–9999	non-detect	non-detect
Oxygen, ppm	2–8	2–8	2–8	< 0.05

EOR waterflooding operations. However, as has been found in studies elsewhere, more could be done to encourage the sharing of water and treatment options among petroleum companies (Colorado Energy Office, 2014). The Colorado study found the following industry concerns about produced-water reuse that would also be shared by Utah's industry:

(1) the desire for produced-water reuse technologies to be economically practical for energy companies to employ;

(2) the desire for regulatory flexibility in terms of options for produced-water reuse and disposal, particularly in light of the variability in water quality, supply, and demand over the life of a well or field, and from reservoir to reservoir;

(3) the desire for regulatory predictability to enable energy companies to make long-term plans and investments in produced-water sharing and reuse;

(4) the desire to find ways to facilitate the pooling of produced-water supply and demand among smaller operators to allow them to achieve the economies of scale needed to enable produced-water reuse; and

(5) the desire to find economical and environmentally acceptable water storage and transport means to allow operators producing excess water to efficiently meet the needs of operators requiring water.

To address these industry concerns and promote further produced-water reuse will require the future collaboration of industry, state and federal regulators, and the general public.

In addition to the reuse of produced water within the energy industry in the Uinta Basin, there are other wastewater streams that could be reused in petroleum development activities there to reduce the use of freshwater supplies. EOG has proposed making use of some industrial wastewater from the nearby Bonanza electric generation plant for future well drilling and completion operations at its Chapita Wells unit of Natural Buttes field, and other industrial wastewater streams might be available for reuse by Utah's petroleum industry.

Another potential source of wastewater for reuse by the petroleum industry in the Uinta Basin would be seven publicly operated wastewater treatment facilities located in Duchesne and Uintah Counties, which cumulatively processed 30.3 MMBW (1270 million gallons) per year in 2004 (Utah Division of Water Resources, 2005). The list of these facilities and their average annual flow is provided in table 9.16.

The reuse of municipal wastewater by the petroleum industry would likely be considered a Type II reuse, where human exposure is unlikely. Such water is not required to be cleaned to the same level as water used where human exposure is likely. While the TDS content of Type II water is low, Type II water would probably need minor additional petroleum industry treatment to eliminate bacteria that might lead to hydrogen sulfide generation in the reservoir environment. For the municipal wastewater to be reused by the petroleum industry, the following factors would be considered by the State of Utah before approval: (1) the point of discharge must be changed, (2) a change application must be approved if the new water use is inconsistent with the underlying right, and (3) the petroleum industry's reuse of municipal wastewater may be viewed as a consumptive one, which could diminish the amount of water that can be used since it will not be returned to the source (Utah Division of Water Resources, 2005; Western Energy Alliance, 2014). Factor 3 could limit the amount of municipal wastewater available for petroleum industry reuse.

Best Water Handling Practice Recommendations

Based on the discussions above, it appears that the best water handling practices in the Uinta Basin vary depending on the size of the field or unit being developed, whether the product is gas or oil, the completion techniques and well spacing employed in field development, and the reservoir rocks being developed and their varying associated water characteristics, but would typically include Class II injection wells for water disposal where feasible. According to the EPA (CDM Smith, 2012), the best approach to produced-water treatment and management must balance factors such as produced-water quality, simplicity of operations, treatment objectives, and cost. Thus, no single set of best management practices can be advocated or applied across the entire Uinta Basin. The State of Utah's goals in managing the use and disposal of water associated with gas and oil development in the Uinta Basin can be summarized as follows:

(1) Protect the Class I, II, and III water (pristine, drinking water, and limited use classes with less than 10,000 mg/L TDS) from contamination as a result of activities associated with gas and oil development.

(2) Encourage companies to minimize the use of Class I through III waters in oil and gas development.

(3) Encourage companies to reuse water employed or produced in petroleum development activities.

(4) Encourage petroleum company reuse of suitable available wastewater streams, such as power plant or other industrial wastewater and municipal water treatment plant effluent, in petroleum development activities.

The State of Utah strives to protect Class I, II, and III waters through a variety of regulatory efforts administered by DOGM, Utah Division of Water Resources, Utah Division of Water Rights, and UDWQ, as well as companion federal regulatory programs in the BLM and EPA. These regulations control such petroleum development activities as well siting and spacing, well and production facilities construction approval and oversight, production facilities inspection and monitoring, safe handling of petroleum products and waste streams, and proper well abandonment and field reclamation oversight (Ground Water Protection Council, 2009). Such regulations are periodically reviewed and updated to allow for adaptive management as a result of the development of newer or improved best management practices and to respond to the implementation of new technologies, such as the more common recent use of hydraulic fracturing.

Regulatory agencies are encouraging petroleum development companies to reuse drilling wastes such as produced water (Environmental Protection Agency, 2008). However, many of the best management practices are practical only when the developments in an area reach a critical size and implementing centralized water collection, handling, treatment, and reuse or disposal achieve the economies of scale to become cost effective. At the large Greater Monument Butte oil field area, Newfield Exploration has implemented centralized water gathering and treatment facilities that allow most of the produced water to be reused in EOR waterflooding operations, reducing freshwater use by up to 10 MMBW in 2014. At Natural Buttes gas field, Anadarko Petroleum has developed the ACTS program to recover water used in hydraulic fracturing and reduce freshwater use by

Table 9.16. *Publicly operated wastewater treatment plants in Duchesne and Uintah Counties, Utah, and their average annual flow in barrels per year. Source: Utah Division of Water Resources (2005).*

County	Facility	Average Annual Flow
Duchesne	Altamont	519,800
Duchesne	Duchesne	1,823,200
Duchesne	Myton	5,128,300
Duchesne	Neola	605,150
Duchesne	Roosevelt*	4,430,000
Duchesne	Tabiona	85,300
Uintah	Ashley Valley	17,727,850
TOTAL		30,319,600

Note: 1 barrel = 42 gallons

* This facility already uses all of its flow in a land application water reuse project.

over 90%, resulting in a 2014 savings of up to a couple MMB of fresh water used for hydraulic fracturing. Also, EOG plans to minimize freshwater usage in the drilling and completion of new wells at the Chapita Wells unit of Natural Buttes field by only taking 12% of its water needs from freshwater sources, and obtaining the remaining 88% from recycled water from the Bonanza power plant of Deseret Generation and Transmission. Assuming that EOG's future drilling development period spans 15 years, then EOG might use 378,518 bbls of fresh water and 2,775,802 bbls of recycled power plant water annually for field development drilling, again reducing freshwater usage by a few MMB per year. As operators in the larger and more developed areas of the Uinta Basin test and find economic ways to handle and reuse produced water for drilling, completion, or EOR practices, these methods will likely be adopted by smaller operators as their fields grow, or perhaps smaller operators may join together to unitize operations into larger operating areas, and allow economies of scale to permit centralized water treatment and handling to be implemented elsewhere in the basin. At the same time, competition among petroleum service companies that see a growing market in offering cost-effective centralized water treatment, handling, or disposal services will likely lead to reduced costs associated with produced-water management and make these services more widely available to small and large petroleum companies in the Uinta Basin and elsewhere in the U.S.

SUMMARY

The management of produced water associated with petroleum development in the Uinta Basin of Utah can be summarized in the following eleven points.

(1) Produced water management in the Uinta Basin has evolved over time from very little government oversight prior to 1955, to basic efforts at the conservation of resources in the period from 1955 to late 1970, and finally to increasingly detailed and complex regulation since the creation of the EPA in December 1970.

(2) Produced-water volumes from petroleum development in the four-county Uinta Basin study area have increased from 86 to 116 MMB per year from 2008 through 2014.

(3) Current water-management practices used by petroleum companies in the Uinta Basin, in decreasing order of usage, include disposal in deep injection wells, reuse in EOR waterflood, delivery to evaporation ponds for disposal via evaporation, and reuse in hydraulic fracturing.

(4) Disposal of produced water in deep injection wells has increased from 43 to nearly 68 MMB per year from 2008 through 2014; the corresponding number of deep disposal wells has increased over that same period from 56 to 92.

(5) The amount of produced water delivered to commercial and private evaporation ponds has varied from 11.9 to 17.3 MMB over the four-year period for which records were available, from 2010 through 2013, and averaged about 13.7 MMB per year.

(6) The amount of water used in EOR waterflood projects has increased from over 25 to over 44 MMBW per year from 2008 through 2014. With the unitization of 19 smaller waterflood projects into one large Greater Monument Butte unit by Newfield in 2010, the reuse of produced water for EOR was implemented in a large way, allowing Newfield to reuse up to 10 MMB of produced water in 2014 for its waterflood needs. One approach that should be investigated in detail is to transport the excess produced water from the gas fields in the eastern part of the basin for use in waterflooding in the oil fields of the central part of the basin.

(7) Anadarko fully implemented the ACTS technology at its greater Natural Buttes gas operations in 2010, and as of 2014 was claiming it recycled nearly 100% of the water it recovers after the hydraulic fracturing process and reuses it in new well completions, which conserves fresh water and reduces truck traffic. On average this reuse is estimated to involve about 1.5 MMB of flow-back produced water.

(8) As of late 2014, EOG plans to minimize freshwater usage in the drilling and completion of 2808 new wells by only using 12% from freshwater sources, and obtaining the remaining 88% from recycled water from the Bonanza power plant of Deseret Generation and Transmission. Assuming the drilling development period spans 15 years, then EOG could eliminate 2,775,802 bbls of freshwater use annually by substituting recycled power plant water.

(9) The estimated disposition of the 116 MMB of produced water from the four-county study area for 2014 is as follows:

- 68 MMB (58.6%) to disposal wells,
- 24 MMB (20.7%) used for EOR,
- 13.7 MMB (11.8%) delivered to evaporation ponds,
- 1.5 MMB (1.3%) reused in hydraulic fracturing, and
- 8.8 MMB (7.6%) evaporated from ponds over a year to allow for continued delivery of new water.

(10) Regulatory agencies in Utah are encouraging petroleum development companies to reuse drilling wastes such as produced water to reduce freshwater consumption; however, many of the best management practices are practical only when the developments in an area reach a critical size when imple-

menting centralized water collection, handling, treatment, and reuse or disposal achieves the economies of scale to become cost effective. The State of Utah should also look for ways to promote cooperation between oil and gas operators to encourage the use of more produced water for enhanced oil recovery.

(11) Produced water management in Utah is a large and dynamic management challenge that requires a flexible, adaptive regulatory scheme to meet ever-changing conditions and technologies in fields of variable size and with differing product and waste streams.

CHAPTER 10:
CONCLUSIONS AND RECOMMENDATIONS

by

Thomas C. Chidsey, Jr., David E. Tabet, Michael D. Vanden Berg, Craig D. Morgan, Stefan M. Kirby, Peter J Nielsen, Stephanie M. Carney, Robert Ressetar, Rebekah W. Stimpson, and Taylor Boden

CONTENTS

SUMMARY 263
UINTA BASIN RESERVOIRS/AQUIFERS: TRIASSIC-JURASSIC GLEN CANYON GROUP THROUGH TERTIARY GREEN RIVER FORMATION 263
Triassic-Jurassic Nugget and Jurassic Navajo and Entrada Sandstones 263
Cretaceous Cedar Mountain and Dakota Formations 263
Upper Cretaceous Mancos Shale 264
Upper Cretaceous Mesaverde Group 264
Upper Paleocene to Lower Eocene Wasatch/Colton Formation 264
Eocene Green River Formation 264
SUMMARY OF THE COMPILED FLUID GEOCHEMISTRY DATABASE FOR THE UINTA BASIN 264
HANDLING AND MANAGEMENT OF WATER PRODUCED FROM OIL AND GAS RESERVOIRS IN THE UINTA BASIN 265

CHAPTER 10:
CONCLUSIONS AND RECOMMENDATIONS

SUMMARY

The production and disposal of water from oil and gas reservoirs, particularly tight sandstones in the Uinta Basin of eastern Utah, affects the economics of resource development and has recently become a topic of much public debate because produced water is the largest-volume waste stream. Managing produced water can be a significant cost fraction of the value of the gas extracted; thus, there is an economic incentive to minimize this waste stream, and/or generate revenue from treating and reusing produced water in hydrocarbon production or other applications.

Oil and gas fields in the Uinta Basin produced nearly 30 MMBO and 324 BCFG in 2015 from the Tertiary Green River and Wasatch Formations, and several formations in the Upper Cretaceous Mesaverde Group. Nearly 103 MMBW was also produced with these hydrocarbons. The vast majority of the water production was from wells producing in tight-sand reservoirs in the Wasatch and Mesaverde. Balancing the water-use needs associated with Green River waterflood projects in the central part of the Uinta Basin (Monument Butte field trend) and produced-water disposal requirements associated with tight-sand gas development in the eastern part of the basin creates significant material handling challenges to both industry and regulators. These challenges are complicated by an operating environment where many individual producers of varying size exist within a field or the Uinta Basin, each with varying water needs and production, and a production timescale of decades for the basin as wells play out and new ones are completed.

Our study consisted of three major components: (1) compilation and analysis of past and new information on the thickness, structure, depth, lithology, porosity, permeability, water quality, and temperature of all major oil and gas reservoir units and aquifers that store produced water or have the potential for water storage in the Uinta Basin from the Tertiary down through the Upper Triassic–Lower Jurassic Glen Canyon Group, (2) statistical analysis of water production quantity and quality from all oil and gas reservoirs, and (3) evaluation of the existing infrastructure for produced-water management/reuse and recommendations for best management practices. The major conclusions and recommendations of these components are described in the following sections.

UINTA BASIN RESERVOIRS/AQUIFERS: TRIASSIC-JURASSIC GLEN CANYON GROUP THROUGH TERTIARY GREEN RIVER FORMATION

Triassic-Jurassic Nugget and Jurassic Navajo and Entrada Sandstones

- The Upper Triassic–Lower Jurassic Nugget and Lower Jurassic Navajo Sandstone is an excellent potential aquifer for produced-water disposal where less than 10,000 feet (3000 m) in depth; porosity decreases at greater depths. However, there are relatively few Navajo penetrations in the Uinta Basin and the economics for drilling new disposal wells at the required depths are difficult to justify. Old wells that encountered Navajo/Nugget could be re-entered and completed as water-disposal wells.

- The Jurassic Entrada Sandstone is projected to have less than 20 feet (6 m) of porous sandstone throughout much of the basin. The amount of sandstone with 6% usable porosity begins to decrease rapidly below 5000 feet (1500 m) drill depth. There are few penetrations of the Entrada in the deeper part of the basin, but areas of high porosity and permeability could exist, which could either be hydrocarbon bearing or store produced water, depending on the depth and proximity to oil and gas production.

Cretaceous Cedar Mountain and Dakota Formations

- The Cretaceous Cedar Mountain and Dakota Formations are mainly fluvial channel deposits that thicken from less than 25 feet (8 m) in the southwest to over 250 feet (76 m) in the northeast part of the basin.

- A porous sandstone trend is parallel to, but slightly southeast of, the net sandstone thickness trend. Thickness of sandstone with at least 6% porosity is generally less than half of the total sandstone thickness. However, porosity and permeability within the channel sandstones can be highly variable and difficult to predict.

- Channel deposits provide additional stratigraphic traps for hydrocarbons throughout the Uinta Basin. Production can be spotty and volumes highly variable due to the heterogeneity of the lenticular channel deposits. These sandstones have very limited potential for produced-water disposal.

Upper Cretaceous Mancos Shale

- The Mancos Shale is one of the thickest confining units in the Colorado Plateau's aquifers, separating the Glen Canyon through Dakota from the Mesaverde aquifers.
- Gamma-ray logs show that sandstone constitutes less than 1% of the formation except in the west where the Tununk and Blue Gate Members interfinger with the Ferron and Emery Sandstone Members and with the Blackhawk Formation.
- The only produced-water disposal into the Mancos is local injection of water from CBM operations in the Ferron Sandstone Member southwest of the Uinta Basin proper.
- With very low permeability, in the range of 0.05 to 160 nD, the Mancos is likely a poor candidate for produced-water disposal in most of the Uinta Basin. It continues to be a secondary drilling target for shale gas.

Upper Cretaceous Mesaverde Group

- The Tuscher and Farrer Formations in the upper part of the Mesaverde Group make favorable produced-water injection targets. Both formations, especially the Tuscher, have thick, blocky sandstone intervals with good porosity. The Farrer has significant candidate sandstone channels for water disposal but are generally finer grained, thinner, and less massive than the Tuscher channels. We calculated that three sandstone channels in the upper Tuscher, or approximately 40 feet (12 m) of sandstone, would store up to 4.2 MMBW in a 1000-foot (305 m) radius around a well.
- Further subdivision of the sand-rich portions of the Mesaverde Group, into units or facies, would provide a more accurate method to predict high- and low-porosity trends within each formation. Additional studies of the Mesaverde should be conducted to correlate TDS and NaCl waters from laboratory analyses to formation water resistivity from well logs.

Upper Paleocene to Lower Eocene Wasatch/Colton Formation

- The Wasatch/Colton Formation contains sandstones that are candidates for water disposal. However, the thickness and continuity of any sandstone channel are localized and will require long perforated zones and targeted perforations for disposal. Generally higher NGR and PHIA in the Wasatch /Colton suggest favorable conditions for water disposal. The Wasatch is an oil reservoir in the central parts of the basin and would lend itself to water flooding using produced water.
- We suggest two options for disposing produced water from the Mesaverde Group and the Wasatch/Colton Formation. (1) Desalinate produced water to decrease the volume of disposal, and increase re-use in hydraulic fracturing operations, irrigation water, or other surface uses. (2) Inject produced water into sandstone beds of the Mesaverde or Colton/Wasatch either for waterflooding to enhance hydrocarbon production or as waste disposal.

Eocene Green River Formation

- The GRF is a complex lacustrine sedimentary deposit that is up to 7000 feet (2100 m) thick and contains a wide range of lithologies. Main reservoir rocks are typically isolated lenticular sandstones with varying amounts of connectivity. As a result, water chemistry varies significantly both laterally and vertically.
- Water quality in the complex lower GRF varies widely from 650 to 112,000 mg/L TDS. Recharge is mostly from the Wasatch Range to the west, the Douglas Creek arch and Uncompahgre uplift to the east-southeast, and the Uinta Mountains to the north. Groundwater in the lower GRF seems to travel toward the Green River in the central part of the basin, coinciding with an area of higher-TDS water.
- Water quality in the upper GRF also varies widely from 600 mg/L to over 200,000 mg/L TDS. Groundwater in the upper GRF is highly influenced by the location of evaporite mineral deposition, which occurred in three distinct phases and locations.
- The unique Birds Nest aquifer (phase 2 hypersaline zone) in the upper GRF in the eastern part of the Uinta Basin and the area located around the phase 3 hypersaline interval in the western part of the basin, as well as select parts of the lower GRF, serve as excellent produced-water disposal zones since reservoir water already exceeds 10,000 mg/L TDS.

SUMMARY OF THE COMPILED FLUID GEOCHEMISTRY DATABASE FOR THE UINTA BASIN

- Highest TDS tends to correlate with sodium chloride or sodium bicarbonate water types that are typical of the upper and lower Green River, Wasatch/Colton, and Mesaverde units. These samples are predominately produced water with high TDS and may be the result of oil and gas generation processes, long residence time, and/or increased water-rock interaction within these units. Lower TDS values and bicarbonate-water-type areas are typical of the unconsolidated, Uinta–Duchesne River, and Glen Canyon units. These chemistries likely result from a relatively active recharging meteoric groundwater system

within these units where they are near the surface.

- The samples in this database represent a unique regional-scale snapshot of fluid geochemistry across an active petroleum province, including both the shallow meteoric groundwater system and the deeper basin fluid system. Further study and geochemical analysis of these data could yield insight into large-scale fluid evolution in both active petroleum provinces and similar geographic settings elsewhere.

HANDLING AND MANAGEMENT OF WATER PRODUCED FROM OIL AND GAS RESERVOIRS IN THE UINTA BASIN

- Between 2008 and 2014, produced-water volumes from petroleum development in the Uinta Basin study area increased from 86 to 116 MMB per year. Current water-management practices used by petroleum companies in the Uinta Basin for the disposition of the 116 MMB of produced water in 2014 are estimated as follows: 68 MMB (58.6%) to disposal wells, 24 MMB (20.7%) used for EOR, 13.7 MMB (11.8%) sent to evaporation ponds, 1.5 MMB (1.3%) reused in hydraulic fracturing, and 8.8 MMB (7.6%) lost to evaporation.

- Disposal of produced water in deep injection wells has increased from 43 to nearly 68 MMB per year from 2008 through 2014; the corresponding number of deep disposal wells has increased over that same period from 56 to 92. The amount of water used in EOR waterflood projects has increased from over 25 to over 44 MMBW per year from 2008 through 2014. Newfield Exploration reused up to 10 MMB of produced water in 2014 for its waterflood needs at Monument Butte oil field; one approach that should be investigated in detail is to transport the excess produced water from the gas fields in the eastern part of the basin for use in waterflooding in the oil fields of the central part of the basin. The amount of produced water delivered to commercial and private evaporation ponds has varied from 11.9 to 17.3 MMB, and averaged about 13.7 MMB per year.

- Anadarko's ACTS technology at Natural Buttes gas field recycled nearly 100% of the water recovered after the hydraulic fracturing process and reused it in new well completions, which conserves freshwater and reduces truck traffic. On average this reuse is estimated to involve about 1.5 MMB of flow-back produced water. EOG plans to minimize freshwater usage in the drilling and completion of new wells by only using 12% from freshwater sources, and obtaining the remaining 88% from recycled water from the Bonanza power plant of Deseret Generation and Transmission. Assuming the drilling development period spans 15 years, then EOG could eliminate 2,776,000 bbls of freshwater use annually by substituting recycled power plant water.

- Regulatory agencies in Utah are encouraging petroleum development companies to reuse drilling wastes such as produced water to reduce freshwater consumption; however, many of the best management practices are practical only when the developments in an area reach a critical size where implementing centralized water collection, handling, treatment, and reuse or disposal achieves the economies of scale to become cost effective. Produced-water management in Utah is a large and dynamic management challenge that requires a flexible, adaptive regulatory scheme and cooperation within the industry to meet ever-changing conditions and technologies in fields of variable size with differing product and waste streams.

ACKNOWLEDGMENTS

Funding for this project, originally titled *Basin-Scale Produced-Water Management Tools and Options—GIS-Based Models and Statistical Analysis of Shale Gas/Tight Sand Reservoirs and Their Produced-Water Streams*, was provided by the Research Partnership to Secure Energy for America (RPSEA) through the "Small Producer Program," authorized by the U.S. Energy Policy Act of 2005. Partial funding was also provided by the Utah Geological Survey (UGS). Industry partners and contributors (consortium) for the project included the following: Anadarko Petroleum Corp.; EOG Resources, Inc.; Wind River Resources, Inc.; QEP Resources, Inc.; and the U.S. Environmental Protection Agency (EPA). Collaborating regulatory agencies included the Utah Department of Natural Resources (Division of Oil, Gas and Mining; Division of Water Rights; Division of Water Resources), the Utah Department of Environmental Quality, U.S. Bureau of Land Management, and again, the EPA.

We especially thank Kenny Gathings, Kenny Warren, John Kynaston, and Mike Merrill of Anadarko Petroleum for providing access to operator's wastewater facilities in Natural Buttes field and providing valuable best practices information for the project. J.D. Horrocks, Newfield Exploration, provided access to operator's wastewater facilities in Monument Butte field. We also thank Tricia Pfeiffer, Cindy Beeler, and Carol Russell of the EPA's Region 8 office (Denver) for their support. The Utah Division of Oil, Gas and Mining provided information and photographs of produced water facilities and infrastructure in the Uinta Basin. Cheryl Gustin, Jay Hill, and Nikki Simon of the UGS, prepared the many of the figures, tables, and maps.

This report was carefully reviewed by the following: Paul Anderson (Consulting Geologist); Robert Ressetar (retired and formerly with the UGS); Dave Tabet, Mike Lowe, Mike Hylland, Kimm Harty, and Richard Allis (UGS); Kent Perry (RPSEA); and John Terneus (NETL). Their careful reviews and constructive criticism greatly improved the manuscript. Finally, we thank Vicky Clarke, John Good, and the UGS editorial production team for their efforts in producing this publication.

REFERENCES

Allen, J., Si-Young, L., and Potter, S., 2013, Three dimensional geologic model of the eolian Jurassic Navajo Sandstone in central Utah for the evaluation of CO_2 sequestration, *in* Morris, T.H., and Ressetar, R., editors, The San Rafael Swell and Henry Mountains basin—geologic centerpiece of Utah: Utah Geological Association Guidebook 42, p. 223–260.

Anadarko Petroleum Corporation, 2015, Utah fact sheet: Online, http://www.anadarko.com/content/documents/apc/news/Fact_Sheets/Utah_Fact_Sheet.pdf, accessed on April 1, 2015.

Anders, D.E., Palacas, J.G., and Johnson, R.C., 1992, Thermal maturity of rocks and hydrocarbon deposits, Uinta Basin, Utah, *in* Fouch, T.D., Nuccio, V.F., and Chidsey, T.C., Jr., editors, Hydrocarbon and mineral resources of the Uinta Basin, Utah and Colorado: Utah Geological Association Publication 20, p. 53–76.

Anderson, D.S., and Harris, N.B., 2006, Integrated sequence stratigraphic and geochemical resource characterization of the lower Mancos Shale, Uinta Basin, Utah: Utah Geological Survey Open-File Report 483, 130 p.

Anderson, P.B., 1983, Geologic map of the Pine Canyon quadrangle, Carbon County, Utah: Utah Geological and Mineral Survey Map 72, scale 1:24,000.

Anderson, P.B., 2005, Mesaverde gas of southeastern Uinta Basin: Utah Geological Survey Open-File Report 460, 42 p.

Anderson, P.B., Vanden Berg, M.D., Carney, S., Morgan, C., and Heuscher, S., 2012, Moderately saline groundwater in the Uinta Basin, Utah: Utah Geological Survey Special Study 144, 35 p.

Anderson, P.B., Willis, G.C., Chidsey, T.C., Jr., and Sprinkel, D.A., 2010, Geology of Glen Canyon National Recreation Area, Utah-Arizona, *in* Sprinkel, D.A., Chidsey, T.C., Jr., and Anderson, P.B., editors, Geology of Utah's parks and monuments (3rd edition): Utah Geological Association Publication 28, p. 309–347.

Archie, G.E., 1942, The electrical resistivity log as an aid in determining some reservoir characteristics: Journal of Petroleum Technology, v. 5, p. 54–62.

Armstrong, R.L., 1968, Sevier orogenic belt in Nevada and Utah: Geological Society of America Bulletin, v. 79, p. 429–458.

Aschoff, J.L., 2010, Preliminary regional sequence stratigraphic framework and characterization of potential fluvial reservoirs of the upper Mesaverde Group, Uinta Basin, Utah: Utah Geological Survey Open-File Report 569, 43 p.

Asquith, G., and Krygowski, D., 2004, Basic well log analysis: American Association of Petroleum Geologists Methods in Exploration Series No. 16, 244 p.

Benko, K.L., and Drewes, J.E., 2008, Produced water in the western United States—geographical distribution, occurrence, and composition: Environmental Engineering Science, v. 25, no. 2, p. 239–246.

Bereskin, S.R., Taff, D.E., and Ballou, R.L., 1993, Enhanced fracture permeability and unconventional production potential along the Duchesne fault zone, Uinta Basin, Utah [abs.]: American Association of Petroleum Geologists Bulletin, v. 77, p. 1442.

Birgenheier, L.P., McCauley, A., Horton, B., and Ressetar, R., 2015, Chapter 2—geologic setting, *in* Ressetar, R., and Birgenheier, L.P., editors, Cretaceous Mancos Shale,

Uinta Basin, Utah—resource potential and best practices for an emerging shale gas play: Unpublished Utah Geological Survey contract deliverable, prepared for the Research Partnership to Secure Energy for America, award no. 09122-07, p. 2.1–2.14.

Blakey, R.C., and Ranney, W., 2008, Ancient landscapes of the Colorado Plateau: Grand Canyon Association, 156 p.

Bluefield Research, 2014, Water for U.S. hydraulic fracturing—competitive strategies, solutions, and outlook, 2014-2020: Online, http://bluefieldresearch.com/water-for-fracking-2014/, accessed July 1, 2015.

Boden, T., and Tripp, B.T., 2012, Gilsonite veins of the Uinta Basin: Utah Geological Survey Special Study 141, 50 p.

Borer, J., 2003, Day 3—High-resolution stratigraphy of the Green River Formation at Raven Ridge and Red Wash field, NE Uinta Basin—facies and stratigraphic patterns in a high-gradient, high-energy lacustrine system, *in* Keighley, D., Borer, J., Morgan, C., McClure, K., and Griffen, R., editors, Facies asymmetry in alluvial-lacustrine basins—a transect across the Uinta Basin, eastern Utah and western Colorado: Guidebook, Field Trip #4, American Association of Petroleum Geologists Annual Convention, Salt Lake City, May 2003, p. 46–55.

Borer, J., and McPherson, M., 1998, High-resolution stratigraphy of the Green River Formation, Raven Ridge, northeast Uinta Basin: Guidebook, Field Trip #17, American Association of Petroleum Geologists Annual Convention, Salt Lake City, May 1998, 117 p.

Bradley, W.H., 1931, Origin and microfossils of the oil shale of the Green River Formation of Colorado and Utah: U.S. Geological Survey Professional Paper 168, 58 p.

Bredehoeft, J.D., Wesley, J.B., and Fouch, T.D., 1994, Simulations of the origin of fluid pressure, fracture generation, and the movement of fluids in the Uinta Basin, Utah: American Association of Petroleum Geologists Bulletin, v. 78, p. 1729–1747.

Brownfield, M.E., Johnson, R.C., and Dyni, J.R., 2010, Sodium carbonate resources of the Eocene Green River Formation, Uinta Basin, Utah and Colorado, *in* U.S. Geological Survey Oil Shale Assessment Team, Oil shale resources of the Uinta Basin, Utah and Colorado: U.S. Geological Survey Digital Data Series DDS–69–BB, 7 Chapters, pages variable.

Bryant, B., 1990, Geologic map of the Salt Lake City 30′ x 60′ quadrangle, north-central Utah and Uinta County, Wyoming: U.S. Geological Survey Map I-1944, scale 1:100,000.

Bryant, B., 1992, Geologic and structure maps of the Salt Lake City 1° x 2° quadrangle, Utah and Wyoming: U.S. Geological Survey Miscellaneous Investigations Series Map I-1997, 3 sheets, scale 1:125,000.

Bryant, B., 2003, Geologic map of the Salt Lake City 30′ x 60′ quadrangle, north-central Utah and Uinta County, Wyoming: Utah Geological Survey Map M-190DM (digitized from U.S. Geological Survey Map I-1944 [1990]), scale 1:100,000.

Bryant, B., 2010, Geologic map of the east half of the Salt Lake City 1° x 2° quadrangle (Duchesne and Kings Peak 30′ x 60′ quadrangles), Duchesne, Summit, and Wasatch Counties, Utah, and Uinta County Wyoming: Utah Geological Survey Miscellaneous Publication 10-1 DM, 2 plates, scale 1:125,000.

Burchfiel, B.C., Lipman, P.W., and Zoback, M.L., editors, 1992, The Cordilleran orogen—conterminous U.S.: Geological Society of America, Decade of North American Geology, 734 p.

Burton, D., Greenhalgh, B.W., Britt, B.B., Kowallis, B.J., Elliott, W.S., Jr., and Barrick, R., 2006, New radiometric ages from the Cedar Mountain Formation, Utah and the Cloverly Formation, Wyoming—implications for contained dinosaur faunas [abs.]: Geological Society of America Abstracts with Programs, v. 38, no. 7, p. 52.

Campbell, J.A., 1975, Structural geology and petroleum potential of the south flank of the Uinta Mountain uplift, northeastern Utah: Utah Geology, v. 2, no. 2, p. 129–132.

Caputo, M.V., and Pryor, W.A., 1991, Middle Jurassic tide- and wave-influenced coastal facies and paleogeography, upper San Rafael Group, east-central Utah, *in* Chidsey, T.C., Jr., editor, Geology of east-central Utah: Utah Geological Association Publication 19, p. 9–27.

Cashion, W.B., 1967, Geology and fuel resources of the Green River Formation, southeastern Uinta Basin, Utah and Colorado: U.S. Geological Survey Professional Paper 548, 48 p.

Cashion, W.B., and Donnell, J.R., 1974, Revision of nomenclature of the upper part of the Green River Formation, Piceance Creek Basin, Colorado, and eastern Uinta Basin, Utah: U.S. Geological Survry Bulletin 1394–G, 9 p.

Castle, J.W., 1990, Sedimentation in Eocene Lake Uinta (GRF), northeastern Uinta Basin, Utah, *in* Katz, B.J., editor, Lacustrine basin exploration case studies and modern analogues: American Association of Petroleum Geologists Memoir 50, p. 243–263.

CDM Smith, 2012, Guidelines for water reuse—2012: U.S. Environmental Protection Agency Report EPA/600/R-12/618, 9 chapters, 7 appendices, individually paginated.

Chan, M.A., and Pfaff, B.J., 1991, Fluvial sedimentology of the Upper Cretaceous Castlegate Sandstone, Book Cliffs, Utah, *in* Chidsey, T.C., Jr., editor, Geology of east-central Utah: Utah Geological Association Publication 19, p. 95–110.

Chidsey, T.C., Jr., and Laine, M.D., 1992, The fractured Green River and Wasatch Formations of the Uinta Basin, Utah—targets for horizontal drilling, *in* Fouch, T.D., Nuccio, V.F., and Chidsey, T.C., Jr., editors, Hydrocarbon and

mineral resources of the Uinta Basin, Utah and Colorado: Utah Geological Association Publication 20, p. 123–134.

Chidsey, T.C., Jr., Vanden Berg, M.D., and Eby, D.E., 2015, Petrography and characterization of microbial carbonates and associated facies from modern Great Salt Lake and Uinta Basin's Eocene Green River Formation in Utah, USA, *in* Bosence, D.W.J., Gibbon, K.A., Le Heron, D.P., Morgan, W.A., Pritchard, T., and Vining, B.A., editors, Microbial carbonates in space and time—implications for global exploration and production: The Geological Society, London, Special Publication 418, p. 261–286.

Cifelli, R.L., Kirkland, J.I., Weil, A., Deinos, A.R., and Kowallis, B.J., 1997, High-precision $^{40}Ar/^{39}Ar$ geochronology and the advent of North America's Late Cretaceous terrestrial fauna: Proceedings of the National Academy of Science of the United States of America, v. 94, p. 1163–1167.

Cifelli, R.L., Nydam, R.L., Gardner, J.D., Weil, A., Eaton, J.G., Kirkland, J.I., and Madsen, S.K., 1999, Medial Cretaceous vertebrates from the Cedar Mountain Formation, Emery County, the Mussentuchit local fauna, *in* Gillette, D., editor, Vertebrate paleontology in Utah: Utah Geological Survey Miscellaneous Publication 99-1, p. 219–242.

Clark, C.E., and Veil, J.A., 2009, Produced water volumes and management practices in the United States: Argonne National Laboratory, Environmental Sciences Division, Report 09/1, Contract DE-AC02-06CH11357, 59 p.

Clem, K., 1985, Oil and gas production summary of the Uinta Basin, *in* Picard, M.D., editor, Geology and energy resources, Uinta Basin of Utah: Utah Geological Association Publication 12, p. 159–167.

Colburn, J.A., Bereskin, S.R., McGinley, D.C., and Schiller, D.M., 1985, Lower Green River Formation in the Pleasant Valley producing area, Duchesne and Uintah Counties, Utah, *in* Picard, M.D., editor, Geology and energy resources, Uinta Basin of Utah: Utah Geological Association Publication 12, p. 177–186.

Cole, R.D., White, H., and Kirschbaum, M., 2008, Stops 1-4 through 1-10, Thompson Canyon-Sego Canyon, *in* Longman, M.W., and Morgan, C.D., editors, Hydrocarbon systems and production in the Uinta Basin, Utah: Rocky Mountain Association of Geologists and Utah Geological Association Publication 37, p. 417–437.

Cole, R.D., Young, R.G., and Willis, G.C., 1997, The Prairie Canyon Member, a new unit of the Upper Cretaceous Mancos Shale, west-central Colorado and east-central Utah: Utah Geological Survey Miscellaneous Publication 97-4, 23 p.

Colorado Energy Office, 2014, Produced water beneficial use dialogue—opportunities and challenges for re-use of produced water on Colorado's western slope: Report prepared by CDR Associates for the Colorado Energy Office and Colorado Mesa University, 16 p., 2 appendices.

Constenius, K.M., Clark, D.L., King, J.K., and Ehler, J.B., 2011, Interim geologic map of the Provo 30′ x 60′ quadrangle, Salt Lake, Utah, and Wasatch Counties, Utah: Utah Geological Survey Open-File Report 586, scale 1:100,000.

Currie, B.S., 1998, Upper Jurassic–Lower Cretaceous Morrison and Cedar Mountain Formations, NE Utah–NW Colorado—relationships between nonmarine deposition and early Cordilleran foreland-basin development: Journal of Sedimentary Geology, v. 68, p. 632–652.

Currie, B.S., McPherson, M.L., Dark, J.P., and Pierson, J.S., 2008, Reservoir characterization of the Creta¬ceous Cedar Mountain and Dakota Formations, south¬ern Uinta Basin—year two report: Utah Geological Survey Open-File Report 516, 117 p.

Currie, B.S., McPherson, M.L., Hokanson, W., Pierson, J.S., Horman, M.B., Pyden, T., Schellenbach, W., Purcell, R., and Nicklaus, D., 2012, Reservoir characterization of the Lower Cretaceous Cedar Mountain and Dakota Formations, northern Uinta Basin, Utah: Utah Geological Survey Open-File Report 597, 34 p.

Currie, B.S., and Reeder, M.D., 2002, Sequence stratigraphy of the Jurassic Curtis, Summerville, and Stump Formations, Utah-Colorado [abs.]: Geological Society of America Abstracts with Programs, v. 34, no. 6, p. 278.

Currie, B.S., Schwartz, R.K., and Wilcox, W.T., 2005, Sequence stratigraphy of a regional-scale tidal embayment, Upper Jurassic Curtis and Summerville Formations, central Utah [abs.]: Geological Society of America Abstracts with Programs, v. 37, no. 7, p. 141.

Curtice, R., 2015, Chapter 18—best completion practices—review of the Mancos shale-gas wells in Utah, *in* Ressetar, R., and Birgenheier, L.P., editors, Cretaceous Mancos Shale, Uinta Basin, Utah—resource potential and best practices for an emerging shale gas play: Unpublished Utah Geological Survey contract deliverable prepared for the Research Partnership to Secure Energy for America, award no. 09122-07, p. 18.1–18.42.

Dahm, K., and Chapman, M., 2014, Produced water treatment primer—case studies of treatment applications: U.S. Bureau of Reclamation Science and Technology Research Report for Project 1617, 58 p.

Dane, C.H., 1954, Stratigraphic and facies relationships of the upper part of the Green River Formation in Duchesne, Uintah, and Wasatch Counties, Utah: American Association of Petroleum Geologists Bulletin, v. 38, p. 405–425.

Davis, S.J., Dickinson, W.R., Gehrels, G.E., Spencer, J.E., Lawton, T.F., and Carroll, A.R., 2010, The Paleogene California River—evidence of Mojave-Uinta paleodrainage from U-Pb ages of detrital zircons: Geology, v. 38, p. 931–934.

Davis, S.W., Davis, M.E., Lucchitta, I., Hanks, T.C., Finkel, R.C., and Caffee, M., 2001, Erosional history of the Col-

orado River through Glen and Grand Canyons, *in* Young, R.A., and Spamer, E.E., editors, Colorado River origin and evolution—proceedings of a symposium held at Grand Canyon National Park in June 2000: Grand Canyon Association, p. 135–139.

DeCelles, P.G., and Coogan, J.C., 2006, Regional structure and kinematic history of the Sevier fold-and-thrust belt, central Utah: Geological Society of America Bulletin, v. 118, no. 7/8, p. 841–864.

Dickinson, W.R., Fiorello, A.R., Hall, D.L., Monreal, R., Potochnik, A.R., and Swift, P.N., 1989, Cretaceous strata of southern Arizona, *in* Jenney, J.P., and Reynolds, S.J., editors, Geologic evolution of Arizona: Tucson, Arizona Geological Society Digest 17, p. 447–461.

Dickinson, W.R., Lawton, T.F., and Inman, K.F., 1986, Sandstone detrital modes, central Utah foreland region—stratigraphic record of Cretaceous-Paleogene tectonic evolution: Journal of Sedimentary Petrology, v. 56, p. 276–293.

Dickinson, W.R., Lawton, T.F., Pecha, M., Davis, S.J., Gehrels, G.E., and Young, R.A., 2012, Provenance of the Paleogene Colton Formation (Uinta Basin) and Cretaceous-Paleogene provenance evolution in the Utah foreland—evidence from U-Pb ages of detrital zircons, paleocurrent trends, and sandstone petrofacies: Geosphere, v. 8, p. 854–880.

Difley, R., and Ekdale, A.A., 2002, Faunal implications of an environmental change before the Cretaceous-Tertiary (K-T) transition in central Utah: Cretaceous Research, v. 23, p. 315–331.

Diouhy, J.A., 2012, Fracturing water worries prompt cleanup push: Houston Chronicle: Online, http://www.chron.com/business/article/Fracturing-water-worries-prompt-leanup-push-3587007.php, accessed April 1, 2015.

Djebbar, Tiab, and Donaldson, Erle, C., 2012, Petrophysics—theory and practice of measuring reservoir rock and fluid transport properties: Elsevier, 950 p.

Doelling, H.H., 2001, Geologic map of the Moab and eastern part of the San Rafael Desert 30′ x 60′ quadrangles, Grand and Emery Counties, Utah, and Mesa County, Colorado: Utah Geological Survey Map 180, 3 plates, scale 1:100,000.

Doelling, H.H., 2002, Interim geologic map of the San Rafael Desert 30′ x 60′ quadrangle, Emery and Grand Counties, Utah: Utah Geological Survey Open-File Report 404, scale 1:100,000.

Doelling, H.H., 2004, Interim geologic map of the eastern half of the Salina 30′ x 60′ quadrangle, Emery, Sevier, and Wayne Counties, Utah: Utah Geological Survey Open-File Report 438, scale 1:62,500.

Doelling, H.H., Blackett, R.E., Hamblin, A.H., Powell, J.D., and Pollock, G.L., 2010, Geology of Grand Staircase–Escalante National Monument, *in* Sprinkel, D.A., Chidsey, T.C., Jr., and Anderson, P.B., editors, Geology of Utah's parks and monuments (3rd edition): Utah Geological Association Publication 28, p. 193–235.

Doelling, H.H., and Davis, F.D., 1989, The geology of Kane County, Utah—geology, mineral resources, geologic hazards: Utah Geological and Mineral Survey Bulletin 124, 192 p., 10 plates, map scale 1:100,000.

Doelling, H.H., and Kuehne, P.A., 2012, Geologic map of the Short Canyon quadrangle, Emery County, Utah: Utah Geological Survey Map 255DM, scale 1:24,000, 13 p.

Doelling, H.H., Kuehne, P.A., and Kirkland, J.I., 2009, Geologic map of the Willow Springs quadrangle, Sevier and Emery Counties, Utah: Utah Geological Survey Map 237, scale 1:24,000, 14 p.

Dubiel, R.F., 2000, Summary of geology and coal resources of the Blackhawk Formation in the southern Wasatch Plateau, central Utah, *in* Kirschbaum, M.A., Roberts, L.N.R., and Biewick, L.R.H., editors, Geologic assessment of coal in the Colorado Plateau—Arizona, Colorado, New Mexico, and Utah: U.S. Geological Survey Professional Paper 1625-B, 29 p.

Dubiel, R.F., Kirschbaum, M.A., Roberts, L.N.R., Mercier, T.J., and Heinrich, A., 2000, Geology and coal resources of the Blackhawk Formation in the southern Wasatch Plateau, central Utah, *in* Kirschbaum, M.A., Roberts, L.N.R., and Biewick, L.R.H., editors, Geologic assessment of coal in the Colorado Plateau—Arizona, Colorado, New Mexico, and Utah: U.S. Geological Survey Professional Paper 1625-B, 61 p.

Dyer, J., and Donoho, D., 2008, Gas-filled Jurassic Entrada erg-sandstones at Flat Rock field, Uintah County, Utah, *in* Longman, M.W., and Morgan, C.D., editors, Hydrocarbon systems and production in the Uinta Basin, Utah: Rocky Mountain Association of Geologists and Utah Geological Association Publication 37, p. 155–178.

Dyni, J.R., 1976, Trioctahedral smectite in the Green River Formation, Duchesne County, Utah: U.S. Geological Survey Professional Paper 967, 14 p.

Dyni, J.R., 1996, Sodium carbonate resources of the Green River Formation: U.S. Geological Survey Open-File Report 96-729, 39 p.

Dyni, J.R., Milton, C., and Cashion, W.B., Jr., 1985, The saline facies of the upper part of the Green River Formation near Duchesne, Utah, *in* Picard, M.D., editor, Geology and energy resources, Uinta Basin, Utah: Utah Geological Association Publication 12, p. 51–60.

Energy Information Administration, 2015, Oil and gas production ranking by states—2013: Online, http://www.eia.gov/state/rankings/#/series/47.

Estes-Jackson, J.E., Shefte, S.W., and Siguaw, S.G., 2008, Reservoir characterization and development of the Wasatch Formation in the Hanging Rock area, southeastern Uinta Basin, Utah, *in* Longman, M.W., and Morgan, C.D., editors, Hydrocarbon systems and production in

the Uinta Basin, Utah: Rocky Mountain Association of Geologists and Utah Geological Association Publication 37, p. 267–281.

Fisher, D.J., 1936, The Book Cliffs coal field in Emery and Grand Counties, Utah: U.S. Geological Survey Bulletin 852, 104 p.

Fouch, T.D., 1975, Lithofacies and related hydrocarbon accumulations in Tertiary strata of the western and central Uinta Basin, Utah, *in* Bolyard, D.W., editor, Symposium on deep drilling frontiers in the central Rocky Mountains: Rocky Mountain Association of Geologists Guidebook, p. 163–173.

Fouch, T.D., 1976, Revision of the lower part of the Tertiary System in the central and western Uinta Basin, Utah: U.S. Geological Survey Bulletin 1405-C, 7 p.

Fouch, T.D., Lawton, T.F., Nichols, D.J., Cashion, W.A., and Cobban, W.A., 1983, Patterns and timing of synorogenic sedimentation in Upper Cretaceous rocks of central and northeast Utah, *in* Reynolds, M.W., and Dolly, E.D., editors, Mesozoic paleogeography of the west-central United States: Rocky Mountain Section, Society of Economic Paleontologists and Mineralogists, Rocky Mountain Paleogeography Symposium 2, p. 305–336.

Fouch, T.D., Nuccio, V.F., Anders, D.E., Rice, D.D., Pitman, J.K., and Mast, R.F., 1994, Green River (!) petroleum system, Uinta Basin, Utah, USA, *in* Magoon, L.B., and Dow, W.G., editors, The petroleum system—from source to trap: American Association of Petroleum Geologists Memoir 60, p. 399–421.

Fouch, T.D., Nuccio, V.F., Osmond, J.C., MacMillan, L., Cashion, W.B., and Wandrey, C.J., 1992a, Oil and gas in uppermost Cretaceous and Tertiary rock, Uinta Basin, Utah, *in* Fouch, T.D., Nuccio, V.F., and Chidsey, T.C., Jr., editors, Hydrocarbon and mineral resources of the Uinta Basin, Utah and Colorado: Utah Geological Association Publication 20, p. 9–47.

Fouch, T.D., Wandrey, C.J., Pitman, J.K., Nuccio, V.F., Schmoker, J.W., Rice, D.D., Johnson, R.C., and Dolton, G.L., 1992b, Natural gas accumulations in low-permeability Tertiary and Cretaceous (Campanian and Maastrichtian) rock, Uinta Basin, Utah: U.S. Department of Energy, Report No. DE-A121-83MC20422, 81 p.

FracFocus, 2015, A digital chemical disclosure registry: Online, http://fracfocus.org/, accessed various times.

Franczyk, K.J., Fouch, T.D., Johnson, R.C., Molenaar, C.M., and Cobban, W.A., 1990b, Cretaceous and Tertiary paleogeographic reconstructions for the Uinta-Piceance Basin study area, Colorado and Utah: U.S. Geological Survey Bulletin 1787-Q, 48 p.

Franczyk, K.J., Pitman, J.K., and Nichols, D.J., 1990a, Sedimentology, mineralogy, palynology, and depositional history of Upper Cretaceous and lower Tertiary rocks along the Book and Roan Cliffs east of the Green River: U.S. Geological Survey Bulletin 1787-N, 27 p.

Freethey, G.W., and Cordy, G.E., 1991, Geohydrology of Mesozoic rocks in the upper Colorado River basin in Arizona, Colorado, New Mexico, Utah, and Wyoming, excluding the San Juan Basin: U.S. Geological Survey Professional Paper 1411-C, 130 p.

Freethey, G.W., and Stolp, B.J., 2010, Simulation of groundwater flow and solute transport in the Glen Canyon aquifer, east-central Utah: U.S. Geological Survey Scientific Investigations Report 2009-5037, 28 p.

Fryberger, S.G., 1990, Ancient eolian deposits of the Navajo and Weber Sandstones, northeast Utah and Colorado, *in* Fryberger, S.G., Krystinik, L.F., and Schenk, C.J., editors, Modern and ancient eolian deposits—petroleum exploration and production: Society for Sedimentary Geology (SEPM), Rocky Mountain Section Publication, Chapter 19, 12 p.

Gardner, M.H., Cross, T.A., and Levorsen, M., 2004, Stacking patterns, sediment volume partitioning, and facies differentiation in shallow-marine and coastal-plain strata of the Cretaceous Ferron Sandstone, Utah, *in* Chidsey, T.C., Jr., Adams, R.D., and Morris, T.H., editors, Regional to wellbore analog for fluvial-deltaic reservoir modeling—the Ferron Sandstone of Utah: American Association of Petroleum Geologists Studies in Geology 50, p. 95–124.

Graf, W.L., Hereford R., Laity, J., and Young, R.A., 1987, Colorado Plateau, *in* Graf, W.L., editor, Geomorphic systems of North America: Geological Society of America Centennial Special Volume 2, p. 259–302.

Gregson, J.D., Chure, D.J., and Sprinkel, D.A., 2010, Geology and paleontology of Dinosaur National Monument, *in* Sprinkel, D.A., Chidsey, T.C., Jr., and Anderson, P.B., editors, Geology of Utah's parks and monuments (3rd edition): Utah Geological Association Publication 28, p. 161–192.

Groeger, A., and Bruhn, R.L., 2001, Structure and geomorphology of the Duchesne graben, Uinta Basin, Utah, and its enhancement of a hydrocarbon reservoir: American Association of Petroleum Geologists Bulletin, v. 85, p. 1661–1678.

Ground Water Protection Council, 2009, State oil and natural gas regulations designed to protect water resources: U.S. Department of Energy, National Energy Technology Laboratory Report, Contract DE-FC26-04NT15455, 63 p.

Gualtieri, J.L., 1988, Geologic map of the Westwater 30′ x 60′ quadrangle, Grand and Uintah Counties, Utah, and Garfield and Mesa Counties, Colorado: U.S. Geological Survey Map I-1765, scale 1:100,000.

Gualtieri, J.L., 2004, Geologic map of the Westwater 30′ x 60′ quadrangle, Grand and Uintah Counties, Utah, and Garfield and Mesa Counties, Colorado: Utah Geological Survey Open-File Report 441DM (digitized from U.S. Geological Survey Map I-1765 [1988]), scale 1:100,000.

Guerra, K., Dahm, K., and Dundorf, S., 2011, Oil and gas produced water management and beneficial use in the western United States: U.S. Bureau of Reclamation Science and Technology Program Report No. 157, 113 p.

Gwynn, J.W., 1992, The oil well saline-water resources of the Uinta Basin, Utah—their character and distribution, *in* Fouch, T.D., Nuccio, V.F., and Chidsey, T.C., Jr., editors, Hydrocarbon and mineral resources of the Uinta Basin, Utah and Colorado: Utah Geological Association Publication 20, p. 289–308.

Gwynn, J.W., 1995, Resistivities and chemical analyses of selected oil and gas field, water well, and spring waters, Utah: Utah Geological Survey Circular 87, 142 p.

Hamblin, W.K., 2004, Beyond the visible landscape—aerial panoramas of Utah's geology: Provo, Utah, Brigham Young University, 300 p.

Hampson, G.J., 2010, Sediment dispersal and quantitative stratigraphic architecture across an ancient shelf: Sedimentology, v. 57, p. 96–141.

Hanks, T.C., Lucchitta, I., Davis, S.W., Davis, M.E., Finkel, R.C., Lefton, S.A., and Garvin, C.D., 2001, The Colorado River and the age of Glen Canyon, *in* Young, R.A., and Spamer, E.E., editors, Colorado River origin and evolution—proceedings of a symposium held at Grand Canyon National Park in June 2000: Grand Canyon Association, p. 129–133.

Hansen, W.R., 1986, Neogene tectonics and geomorphology of the eastern Uinta Mountains in Utah, Colorado, and Wyoming: U.S. Geological Survey Professional Paper 1356, 78 p.

Hansen, W.R., Rowley, P.D., and Carrara, P.E., 1983, Geologic map of Dinosaur National Monument and vicinity, Utah and Colorado: U.S. Geological Survey Miscellaneous Investigations Series Map I-1407, scale 1:50,000.

Hardwick, C.L., Willis, H.W., and Gwynn, M.L., 2015, Geothermal assessment and modeling of the Uinta Basin, Utah, *in* Vanden Berg, M.D., Ressetar, R., and Birgenheier, L.P., editors, Geology of Utah's Uinta Basin and Uinta Mountains: Utah Geological Association Publication 44, p. 337–353.

Herbst, S.R., and Morris, T.H., 2011, Unexpected reservoir quality sandstone within the mudstone-rich portion of the Middle Jurassic Entrada Sandstone, San Rafael Swell, Utah [abs.]: Geological Society of America Abstracts with Programs, v. 43, p. 610.

Hettinger, R.D., and Kirschbaum, M.A., 2002, Stratigraphy of the Upper Cretaceous Mancos Shale (upper part) and Mesaverde Group in the southern part of the Uinta and Piceance Basins, Utah and Colorado: U.S. Geological Survey Investigative Report I-2764, 21 p.

Hettinger, R.D., and Kirschbaum, M.A., 2003, Stratigraphy of the Upper Cretaceous Mancos Shale (upper part) and Mesaverde Group in the southern part of the Uinta and Piceance Basins, Utah and Colorado, *in* USGS Uinta-Piceance Assessment Team, compilers, Petroleum systems and geologic assessment of oil and gas in the Uinta-Piceance Province, Utah and Colorado: U.S. Geological Survey Digital Data Series DDS–69–B, Chapter 12, 21 p.

Hicks, T.C., Morris, T.H., and Fairbanks, M.D., 2010, Facies analysis of the transitions between subtidal, intertidal, and supratidal zones of the Entrada Sandstone, south-central Utah—a provisional sequence stratigraphic analysis, *in* Carney, S.M., Tabet, D.E., and Johnson, C.L., editors, Geology of south-central Utah: Utah Geological Association Publication 39, p. 317–337.

Hilchie, D.W., 1978, Applied open hole log interpretation: Golden, Colorado, D.W. Hilchie Inc., 161 p.

Hill, B.G., and Bereskin, S.R., editors, 1993, Oil and gas fields of Utah: Utah Geological Association Publication 22, non-paginated.

Hintze, L.F., 1980, Geologic map of Utah: Utah Geological Survey Map M-A-1, 2 sheets, scale 1:500,000.

Hintze, L.F., 1997, Geological highway map of Utah: Provo, Brigham Young University Geology Studies Special Publication 3, scale 1:1,000,000.

Hintze, L.F., and Kowallis, B.J., 2009, Geologic history of Utah: Brigham Young University Geology Studies Special Publication 9, 225 p.

Hintze, L.F., Willis, G.C., Laes, D.Y.M., Sprinkel, D.A., and Brown, K.D., 2000, Digital geologic map of Utah: Utah Geological Survey Map 179DM, scale 1:500,000.

Horton, B.K., 2012, Variability of the Mancos Shale—developing preliminary depositional and sequence stratigraphic models of a developing shale gas play: Salt Lake City, University of Utah, M.S. thesis, 386 p.

Howell, J., and Flint, A., 2005, Tectonic setting, stratigraphy and sedimentology of the Book Cliffs, *in* Coe, A.L., editor, The sedimentary record of sea-level change: New York, The Open University and Cambridge University Press, p. 135–157.

Howells, L., Longson, M.S., and Hunt, G.L., 1987, Base of moderately saline ground water in the Uinta Basin, Utah, with an introductory section describing the methods used in determining its position: Utah Department of Natural Resources Technical Publication 92, 59 p., 2 plates, scale 1:250,000. Also available as U.S. Geological Survey Open-File Report 87-394.

Hunt, C.B., 1956, Cenozoic geology of the Colorado Plateau: U.S. Geological Survey Professional Paper 279, 99 p.

IOGCC and ALL Consulting, 2006, A guide to practical management of produced water from onshore oil and gas operations in the United States: U.S. Department of Energy National Petroleum Technology Office Report, Contract DE-PS26-04NT15460-02, 179 p., 1 appendix.

Jennings, G.R., 2014, Facies analyses and paleogeography of Utah's Entrada Sandstone—traps, tectonic implications and outcrop analog: Provo, Utah, Brigham Young University, M.S. thesis, 66 p.

Johnson, R.C., 2003, Northwest to southeast cross section of Cretaceous and lower Tertiary rocks across the eastern part of the Uinta Basin, Utah, *in* USGS Uinta-Piceance Assessment Team, compilers, Petroleum systems and geologic assessment of oil and gas in the Uinta-Piceance Province, Utah and Colorado: U.S. Geological Survey Digital Data Series DDS–69–B, Chapter 11, 6 p.

Johnson, R.C., Mercier, T.J., Brownfield, M.E., and Self, J.G., 2010, Assessment of in-place oil shale resources in the Green River Formation, Uinta Basin, Utah and Colorado: U.S. Geological Survey Digital Data Series DDS-69-BB, Chapter 1, 153 p.

Johnson, R.C., Nichols, D.J., and Hanley, J.H., 1988, Stratigraphic sections of lower Tertiary strata and charts showing palynomorphs and mollusk assemblages, Douglas Creek arch area, Colorado and Utah: U.S. Geological Survey Miscellaneous Field Studies MF-1997, 2 plates, scale 1:125,000.

Johnson, R.C., and Roberts, S.B., 2003, The Mesaverde total petroleum system, Uinta-Piceance Province, Utah and Colorado, *in* USGS Uinta-Piceance Assessment Team, compilers, Petroleum systems and geologic assessment of oil and gas in the Uinta-Piceance Province, Utah and Colorado: U.S. Geological Survey Digital Data Series DDS–69–B, Chapter 7, 68 p.

Jones, E., and Plink-Björklund, P., 2013, The effects of early Eocene climate change on the composition of fluvial sandstones, Uinta Basin, Utah: American Association of Petroleum Geologists, Search and Discovery article #50880.

Jones, E., and Plink-Björklund, P., 2015, Revisiting the depositional environment and provenance of the Wasatch Formation in the Uinta Basin, Utah—implications for the early Eocene paleogeography of western North America: American Association of Petroleum Geologists, Search and Discovery Article #90216.

Keele, D., and Evans, J., 2008, Analysis of reservoir properties of faulted and fractured eolian thrust-belt reservoirs: Utah Geological Survey Open-File Report 529, 55 p.

Kehew, A.E., 2000, Applied chemical hydrogeology: Upper Saddle River, New Jersey, Prentice Hall, 368 p.

Keighin, C.W., and Fouch, T.D., 1981, Depositional environments and diagenesis of some nonmarine Upper Cretaceous reservoir rocks, Uinta Basin, Utah: Society of Sedimentary Geology Special Publication No. 31, p. 109–125.

Keighley, D., 2015, Phosphatic carbonate shale of the "Bird's Nest saline zone," upper Green River Formation, Uinta Basin, Utah, *in* Smith, M.E., and Carrol, A.R., editors, Stratigraphy and paleolimnology of the Green River Formation, western USA: Syntheses in Limnology 1, p. 251–276.

Keighley, D.G., and Flint, S.S, 2008, Fluvial sandbody geometry and connectivity in the middle Green River Formation, Nine Mile Canyon, southwestern Uinta Basin, *in* Longman, M.W., and Morgan, C.D, editors, Hydrocarbon systems and production in the Uinta Basin, Utah: Rocky Mountain Association of Geologists and Utah Geological Association Publication 37, p. 101–119.

Keighley, D., Flint, S., Howell, J., Anderson, D., Collins, S., Moscariello, A., and Stone, G., 2002, Surface and subsurface correlation of the Green River Formation in central Nine Mile Canyon, SW Uinta Basin, Carbon and Duchesne Counties, east-central Utah: Utah Geological Survey Miscellaneous Publication 02-1, 66 p.

Kelly, J.M., and Castle, J.W., 1992, Red Wash field-U.S.A., Uinta Basin, Utah, *in* Foster, N.H., and Beaumont, E.A., editors, Stratigraphic traps III: American Association of Petroleum Geologists, Treatise of Petroleum Geology, Atlas of Oil and Gas Fields, p. 231–256.

Kirkland, J.I., Lucas, S.G., and Estep, J.W., 1998, Cretaceous dinosaurs of the Colorado Plateau, *in* Lucas, S.W., Kirkland, J.I., and Estep, J.W., editors, Lower and middle Cretaceous terrestrial ecosystems: New Mexico Museum of Natural History and Science Bulletin 14, p. 79–90.

Kirkland, J.I., and Madsen, S.K., 2007, The Lower Cretaceous Cedar Mountain Formation, eastern Utah—the view up an always interesting learning curve, *in* Lund, W.R., and Simon, D.B., editors, Field guide to excursions in southern Utah: Utah Geological Association Publication 35, 108 p.

Kirkland, J.I., Suarez, M., Suarez, C., and Hunt-Foster, R., 2016, The Lower Cretaceous in east-central Utah—the Cedar Mountain Formation and its bounding strata: Geology of the Intermountain West, v. 3, p. 101–228.

Kirschbaum, M.A., and Schenk, C.J., 2011, Sedimentary and reservoir heterogeneity of a valley-fill deposit—a field guide to the Dakota Sandstone of the San Rafael Swell, Utah: U.S. Geological Survey Scientific Investigations Report 2010-5222, 36 p., 1 plate.

Kocurek, G., and Dott, R.H., Jr., 1983, Jurassic paleogeography and paleoclimate of the central and southern Rocky Mountains region, *in* Reynolds, M.W., and Dolly, E.D., editors, Symposium on Mesozoic paleogeography of west-central U.S.: Denver, Colorado, Rocky Mountain Section of Society of Economic Paleontologists and Mineralogists, p. 101–116.

Larson, T.E., and Skold, R.V., 1958, Laboratory studies relating mineral quality of water to corrosion of steel and cast iron: Illinois State Water Survey, Report ISWS C-71, p. 43–46.

Lawton, T.F., 1983, Tectonic and sedimentologic evolution of the Utah foreland basin: Tucson, University of Arizona, Ph.D. dissertation, 217 p.

Lawton, T.F., 1985, Style and timing of frontal structures, thrust belt, central Utah: American Association of Petroleum Geologists Bulletin, v. 69, p. 1145–1159.

Lawton, T.F., 1986, Fluvial systems of the Upper Cretaceous Mesaverde Group and North Horn Formation, central Utah—a record of transition from thin-skinned to thick-skinned deformation in the foreland region, *in* Peterson, J.A., editor, Paleotectonics and sedimentation in the Rocky Mountain region, United States: American Association of Petroleum Geologists Memoir 41, p. 423–442.

Lawton, T.F., Talling, P.J., Hobbs, R.S., Trexler, J.H., Jr., Weiss, M.P., and Burbank, D.W., 1993, Structure and stratigraphy of the Upper Cretaceous and Paleocene strata (North Horn Formation), eastern San Pitch Mountains, Utah—sedimentation at the front of the Sevier orogenic belt: U.S. Geological Survey Bulletin 1787-II, p. 1–33.

Lillis, P.G., Warden, A., and King, J.D., 2003, Petroleum systems of the Uinta and Piceance Basins—geochemical characteristics of oil types, *in* Petroleum systems and geologic assessment of oil and gas in the Uinta-Piceance province, Utah and Colorado: U.S. Geological Survey Digital Data Series DDS-69-B, Chapter 3, 28 p.

Lockley, M.G., Lucas, S.G., Hunt, A.P., and Gaston, R., 2004, Ichnofaunas from the Triassic-Jurassic boundary sequences of the Gateway area, western Colorado—implications for faunal composition and correlations with other areas: Ichnos, v. 11, no. 1, p. 89–102.

Lucas, P.T., and Drexler, J.M., 1975, Altamont-Bluebell—a major naturally fractured and overpressured stratigraphic trap, Uinta Basin, Utah, *in* Bolyard, D.W., editor, Symposium on deep drilling frontiers in the central Rocky Mountains: Rocky Mountain Association of Geologists Guidebook, p. 265–273.

Lucas, S.G., Tanner, L.H., and Heckert, A.B., 2005, Tetrapod biostratigraphy and biochronology across the Triassic-Jurassic boundary in northeastern Arizona, *in* Heckert, A.B., and Lucas, S.G., editors, Vertebrate paleontology in Arizona: New Mexico Museum of Natural History and Science Bulletin 29, p. 83–92.

Lucchitta, I., 1979, Late Cenozoic uplift of the southwestern Colorado Plateau and adjacent Colorado River region: Tectonophysics, v. 61, p. 63–95.

Lucchitta, I., 1989, History of the Grand Canyon and of the Colorado River in Arizona, *in* Jenney, J.P., and Reynolds, S.J., editors, Geologic evolution of Arizona: Arizona Geological Society Digest 17, p. 701–715.

Lyman, S., Mansfield, M., Shorthill, H., Anderson, R., Evans, J., Mangum, C., and Shorthill, T., 2013, Wintertime emissions of hydrocarbons from produced water evaporation facilities, *in* Lyman, S., Mansfield, M., and Shorthill, H., 2013, 2013 Uintah Basin winter ozone and air quality study—final report: Utah State University, Commercialization and Regional Development, Document Number CRD/13.10297B, p. 47–57.

Lynds, R., and Hajek E., 2006, Conceptual model for predicting mudstone dimensions in sandy braided-river reservoirs: American Association of Petroleum Geologists Bulletin, v. 90, no. 8, p. 1273–1288.

Maberry, J.O., 1971, Sedimentary features of the Blackhawk Formation (Cretaceous) in the Sunnyside district, Carbon County, Utah: U.S. Geological Survey Professional Paper 688, 58 p.

Marchetti, D.W., and Cerling, T.E., 2001, Bedrock incision rates for the Fremont River tributary of the Colorado River, 2001, *in* Young, R.A., and Spamer, E.E., editors, Colorado River origin and evolution—Proceedings of a symposium held at Grand Canyon National Park in June 2000: Grand Canyon Association, p. 125–127.

Marino, J.E., 1992, Erg margin and marginal marine facies analysis of the Entrada Sandstone, San Rafael Swell, Utah—implications to hydrocarbon entrapment: Provo, Utah, Brigham Young University, M.S. thesis, 140 p.

Marino, J.E., and Morris, T.H., 1996, Erg margin and marginal marine facies analysis of the Entrada Sandstone—implications to depositional models and hydrocarbon entrapment, *in* Morales, M., editor, The continental Jurassic: Museum of Northern Arizona, Bulletin 60, p. 483–496.

Masters, G.M., and Ela, W.P., 2007, Introduction to environmental engineering and science: Prentice Hall (3rd edition), 720 p.

McCauley, A.D., 2013, Sequence stratigraphy, depositional history, and hydrocarbon potential ofthe Mancos Shale, Uinta Basin, Utah: Salt Lake City, University of Utah, M.S. thesis, 173 p.

McPherson, B.J., and Matthews, V., 2014, Characterization of most promising sequestration formations in the Rocky Mountain Region (RMCCS): Final Technical Report, U.S. Department of Energy DE-FE0001812, 716 p.

McPherson, M.L., Currie, B.S., and Pierson, J.S., 2006, Reservoir characterization of the Cretaceous Cedar Mountain and Dakota Formations, southern Uinta Basin (year 1): Utah Geological Survey Open-File Report 492, 20 p.

Milner, A.R.C., and Kirkland, J.I., 2006, Preliminary review of the Early Jurassic (Hettangian) freshwater Lake Dixie fish fauna in the Whitmore Point Member, Moenave Formation in southwest Utah, *in* Harris, J.D., Lucas, S.G., Spielmann, J.A., Lockley, M.G., Milner, A.R.C., and Kirkland, J.I., editors, Tracking dinosaur origins—the Triassic/Jurassic terrestrial transition: New Mexico Museum of Natural History and Science Bulletin 37, p. 510–521.

Milton, C., Axelrod, J.M., and Grimaldi, F.S., 1954a, New minerals reedmergnerite ($Na_2O•B_3O_3•6SiO_2$) and eitelite ($Na_2O•MgO•CO_2$) associated with leucosphenite, shortite, searesite, and crocidolite in the Green River Formation, Utah [abs.]: Geological Society of America Bulletin, v. 65, p. 1286–1287.

Milton, C., Axelrod, J.M., and Sherwiid, A.M., 1954b, New occurrence of leucosphenite, in oil shale from Utah [abs.]: American Mineralogist, v. 39, p. 337.

Molennar, C.M., and Cobban, W.A., 1991, Middle Cretaceous stratigraphy on the south and east sides of the Uinta Basin, northeastern Utah and northwestern Colorado: U.S. Geological Survey Bulletin 1787, p. P1–P34.

Molina-Garza, R.S., Geissman, J.W., and Lucas, S.G., 2003, Paleomagnetism and paleomagnetostratigraphy of the lower Glen Canyon and upper Chinle groups, Triassic-Jurassic of northern Arizona and northeastern Utah: Journal of Geophysical Research, v. 108, no. B4, p. 1–24.

Morgan, C.D., 2003a, Geologic guide and road logs of the Willow Creek, Indian, Soldier Creek, Nine Mile, Gate, and Desolation Canyons, Uinta Basin, Utah: Utah Geological Survey Open-File Report 407, 79 p.

Morgan, C.D., 2003b, The Bluebell oil field, Uinta Basin, Duchesne and Uintah Counties, Utah—characterization and oil well demonstration: Utah Geological Survey Special Study 106, 95 p.

Morgan, C.D., Chidsey, T.C., Jr., McClure, K.P., Bereskin, S.R., and Deo, M.D., 2003, Reservoir characterization of the lower Green River Formation, southwest Uinta Basin, Utah: Utah Geological Survey Open-File Report 411, 216 p., 28 plates.

Morgan, C.D., McClure, K.P., Bereskin, S.R., and McPherson, M., 2002, A preliminary discussion of fault styles in the southwest Uinta Basin, Utah [abs.]: American Association of Petroleum Geologists, Rocky Mountain Section Meeting Program with Abstracts, p. 33.

Morris, T.H., and Hicks, T.C., 2011, Facies analysis and reservoir characterization of the mudstone-rich portion of the Entrada Sandstone, south-central Utah—emphasis on the Bitter Seep Wash Sandstone at South Salt Wash and Bitter Seep Wash: Utah Geological Survey unpublished report, 110 p.

Morris, T.H., McBride, J.H., and Monn, W.D., 2005, A multidisciplinary approach to reservoir characterization of the Entrada erg-margin gas play, Utah: Utah Geological Survey Open-File Report 459, 52 p.

Morris, T.H., Richmond, D.R., and Marino, J.E., 1991, The Paleocene/Eocene Colton Formation—a fluvial-dominated lacustrine deltaic system, Roan Cliffs, Utah, *in* Chidsey, T.C., Jr., editor, Geology of east-central Utah: Utah Geological Association Publication 19, p. 129–140.

Munroe, J.S., and Laabs, B.J.C., 2009, Glacial geologic map of the Uinta Mountains area, Utah and Wyoming: Utah Geological Survey Miscellaneous Publication 09-4DM, scale 1:100,000.

Myung-Suk, Y., and Cross, A.T., 1997, Palynostratigraphy of Upper Cretaceous-lower Tertiary strata, Price Canyon, Utah: Review of Paleobotany and Palynology, v. 97, p. 53–66.

Narr, W.N., and Currie, J.B., 1982, Origin of fracture porosity—example from Altamont field, Utah: American Association of Petroleum Geologists Bulletin, v. 66, no. 9, p. 1231–1247.

National Petroleum Council, 2011, Management of produced water from oil and gas wells: National Petroleum Council Operations and Environment Task Group Paper 2-17, 32 p.

Nelson, P.H., and Hoffman, E.L., 2009, Gas, water, and oil production from the Wasatch Formation, Greater Natural Buttes field, Uinta Basin, Utah: U.S. Geological Survey Open-File Report 2009-1049, 19 p.

Newman, K.F., and Chan, M.A., 1991, Depositional facies and sequences in the Upper Cretaceous Panther Tongue Member of the Star Point Formation, Wasatch Plateau, Utah, *in* Chidsey, T.C., Jr., editor, Geology of east-central Utah: Utah Geological Association Publication 19, p. 65–76.

Nixon, R.P., 1973, Oil source beds in the Cretaceous Mowry Shale of northwestern interior United States: American Association of Petroleum Geologists Bulletin, v. 57, no. 1, p. 136–157.

Nuccio, V.F., and Condon, S.M., 1996, Burial and thermal history of the Paradox Basin, Utah and Colorado, and petroleum potential of the Middle Pennsylvanian Paradox Formation, *in* Huffman, A.C., Jr., Lund, W.R., and Godwin, L.H., editors, Geology of the Paradox Basin: Utah Geological Association Publication 25, p. 57–76.

Nuccio, V.F., and Roberts, L.N.R., 2003, Chapter 4—Thermal maturity and oil and gas generation history of petroleum systems in the Uinta-Piceance province, Utah and Colorado, *in* Petroleum systems and geologic assessment of oil and gas in the Uinta-Piceance province, Utah and Colorado: U.S. Geological Survey Digital Data Series, DDS-69-B, 39 p.

Osmond, J.C., 1964, Tectonic history of the Uinta Basin, Utah, *in* Sabatka, E.F., editor, Guidebook to the geology and mineral resources of the Uinta Basin—Utah's hydrocarbon storehouse: Intermountain Association of Petroleum Geologists, Thirteenth Annual Field Conference, p. 47–58.

Osmond, J.C., 1985, Reservoir sandstone patterns, Green River Formation, Duck Creek oil field, Uintah County, Utah, *in* Picard, M.D., editor, Geology and energy resources, Uinta Basin of Utah: Utah Geological Association Publication 12, p. 187–192.

Osmond, J.C., 1986, Petroleum geology of the Uinta Mountains–White River uplift, Colorado and Utah, *in* Stone, D.S., editor, New interpretations of northwest Colorado geology: Rocky Mountain Association of Geologists Guidebook, p. 213–221.

Pederson, J.L., and Eddleman, J.L., 2002, Colorado Plateau uplift and erosion evaluated using GIS: Geological Society of America GSA Today, v. 12, no. 8, p. 4–10.

Pederson, J., Karlstrom, K., Sharp, W., and McIntosh, W., 2002, Differential incision of the Grand Canyon related to Quaternary faulting—constraints from U-series and Ar/Ar dating: Geology, v. 30, p. 739–742.

Peterson, F., 1988, Pennsylvanian to Jurassic eolian transportation systems in the western United States: Sedimentary Geology, v. 56, p. 207–260.

Peterson, J.A., 1994, Regional geology of the eastern Great Basin and paleotectonic history of the Railroad Valley area, eastern Nevada, *in* Schalla, R.A., and Johnson, E.H., editors, Oil fields of the Great Basin: Nevada Petroleum Society Special Publication, p. 15–40.

Picard, M.D., 1975, Facies, petrography and petroleum potential of Nugget Sandstone (Jurassic), southwestern Wyoming and northeastern Utah, *in* Bolyard, D.W., editor, Symposium on deep drilling frontiers of the central Rocky Mountains: Rocky Mountain Association of Petroleum Geologists Guidebook, p. 109–127.

Pipiringos, G.N., and O'Sullivan, R.B., 1978, Principal unconformities in Triassic and Jurassic rocks, Western Interior United States—a preliminary survey: U.S. Geological Survey Professional Paper 1035-A, 29 p.

Pitman, J.K., Fouch, T.D., and Goldhaber, M.B., 1982, Depositional setting and diagenetic evolution of some Tertiary unconventional reservoir rocks, Uinta Basin, Utah: American Association of Petroleum Geologists Bulletin, v. 66, no. 10, p. 1581–1596.

Potochnik, A.R., and Faulds, J.E., 1998, A tale of two rivers—Tertiary structural inversion and drainage reversal across the southern boundary of the Colorado Plateau, *in* Duebendorfer, E.M., editor, Geologic excursions in northern and central Arizona: Field Trip Guidebook for Geological Society of America Rocky Mountain Section Meeting, p. 149–173.

Potter, C.J., Tang, R., and Hainsworth, T.J., 1991, Late Paleozoic structure of the southern part of the Uinta Basin, Utah, from seismic reflection data: U.S. Geological Survey Bulletin 1787-V, 18 p.

Ray, R.G., Kent, B.H., and Dane, C.H., 1956, Stratigraphy and photograph-geology of the southwestern part of Uinta Basin, Duchesne, and Uintah Counties, Utah: U.S. Geological Survey Oil and Gas Inventory Map OM 171, 2 plates, scale 1:63,360.

Remy, R.R, 1992, Stratigraphy of the Eocene part of the Green River Formation in the south-central part of the Uinta Basin, Utah: U.S. Geological Survey Bulletin 1787, 79 p.

Ressetar, R., and Birgenheier, L.P., editors, 2015, Cretaceous Mancos Shale, Uinta Basin, Utah—resource potential and best practices for an emerging shale gas play: Unpublished Utah Geological Survey contract deliverable prepared for the Research Partnership to Secure Energy for America, award no. 09122-07, 701 p., 15 appendices, 5 plates.

Ressetar, R., Birgenheier, L.P., and McCauley, A., 2015, Chapter 4—regional correlations and thickness trends, *in* Ressetar, R., and Birgenheier, L.P., editors, Cretaceous Mancos Shale, Uinta Basin, Utah—resource potential and best practices for an emerging shale gas play: Unpublished Utah Geological Survey contract deliverable prepared for the Research Partnership to Secure Energy for America, award no. 09122-07, p. 4.1–4.15.

Rice, D.D, Fouch, T.D, and Johnson, R.C., 1992, Influence of source rock type, thermal maturity, and migration on composition and distribution of natural gases, Uinta Basin, Utah, *in* Fouch, T.D., Nuccio, V.F., and Chidsey, T.C., Jr., editors, Hydrocarbon and mineral resources of the Uinta Basin, Utah and Colorado: Utah Geological Association Publication 20, p. 95–109.

Rider, M., and Kennedy, M., 2011, The geological interpretation of well logs (3rd edition): Scotland, Rider-French Consulting Ltd., 432 p.

Riggs, N.R., and Blakey, R.C., 1993, Early and Middle Jurassic paleogeography and volcanology of Arizona and adjacent areas, *in* Dunne, G., and McDougall, K., editors, Mesozoic paleogeography of the western United States—II: Pacific Section, Society of Economic Paleontologists and Mineralogists, Book 71, p. 347–375.

Roberts, L.N.R., 2003, Structure contour map of the top of the Dakota Sandstone, Uinta-Piceance Province, Utah and Colorado, *in* USGS Uinta-Piceance Assessment Team, compilers, Petroleum systems and geologic assessment of oil and gas in the Uinta-Piceance Province, Utah and Colorado: U.S. Geological Survey Digital Data Series 69-B, Chapter 16, 11 p.

Rose Petroleum, 2015, Mancos operations update—Uinta Basin, Utah: Online, http://www.rosepetroleum.com/press/pressreleases/view/502, accessed July 2015.

Rowley, P.D., Hansen, W.R., Tweto, O., and Carrara, P.E., 1985, Geologic map of the Vernal 1° x 2° quadrangle, Colorado, Utah, and Wyoming: U.S. Geological Survey Miscellaneous Investigations Series Map I-1526, 1 plate, scale 1:250,000.

Ruble, T.E., 1996, Geochemical investigation of the mechanisms of hydrocarbon generation and accumulation in the Uinta Basin, Utah: Norman, University of Oklahoma, Ph.D. dissertation, 268 p.

Ryder, R.T., Fouch, T.D., and Elison, J.H., 1976, Early Tertiary sedimentation in the western Uinta Basin, Utah: Geological Society of America Bulletin, v. 87, no. 4, p. 496–512.

Schamel, S., 2015, Shale oil resource play potential of the Green River Formation, Uinta Basin, Utah: Utah Geological Survey Open-File Report 639, 65 p.

Schlumberger, 2009, Log interpretation charts: Sugarland, Texas, Schlumberger, 310 p.

Schmoker, J.W., Nuccio, V.F., and Pitman, J.K., 1992, Porosity trends in predominately nonmarine sandstones of the Upper Cretaceous Mesaverde Group, Uinta and Piceance Basins, Utah and Colorado, *in* Fouch, T.D., Nuccio, V.F., and Chidsey, T.C., Jr., editors, Hydrocarbon and mineral resources of the Uinta Basin, Utah and Colorado: Utah Geological Association Publication 20, p. 111–122.

Schuh, M.L., 1993, Red Wash, *in* Hill, B.G., and Bereskin, S.R., editors, Oil and gas fields of Utah: Utah Geological Association Publication 22, non-paginated.

Sendziak, K.L., 2012, Stratigraphic architectural and avulsion deposits of a low net sand content fluvial succession—lower Wasatch Formation, Uinta Basin: Golden, Colorado School of Mines, M.S. thesis, 53 p.

Shier, D.A., 2004, Well log normalization—methods and guidelines: Petrophysics, v. 45, p. 268–280.

Smith, A.G., Hurley, A.M., and Briden, J.C., 1981, Phanerozoic paleocontinental world maps: Cambridge University Press, Cambridge Earth Science Series, 102 p.

Smith, J.L., 2004, Investigation of fracture mechanisms in the Duchesne fault zone, Uinta Basin, northeastern Utah—the role of fluid overpressures and other processes: Socorro, New Mexico Institute of Mining and Technology, M.S. thesis, 157 p.

Smith, L.S., 1976, Paleoenvironments of the upper Entrada Sandstone and the Curtis Formation on the west flank of the San Rafael Swell, Emery County, Utah: Brigham Young University Geology Studies, v. 23, pt. 1, p. 113–171.

Spieker, E.M., 1946, Late Mesozoic and early Cenozoic history of central Utah: U.S. Geological Survey Professional Paper 205-D, p. 117–161.

Sprinkel, D.A., 2006, Interim geologic map of the Dutch John 30′ x 60′ quadrangle, Daggett and Uintah Counties, Utah, Moffat County, Colorado, and Sweetwater County, Wyoming: Utah Geological Survey Open-File Report 491, scale 1:100,000.

Sprinkel, D.A., 2007, Interim geologic map of the Vernal 30′ x 60′ quadrangle, Uintah and Duchesne Counties, Utah, and Moffat and Rio Blanco Counties, Colorado: Utah Geological Survey Open-File Report 506, scale 1:100,000.

Sprinkel, D.A., 2009, Interim geologic map of the Seep Ridge 30′ x 60′ Quadrangle, Uintah, Duchesne, and Carbon Counties, Utah, and Garfield and Rio Blanco Counties, Colorado: Utah Geological Survey Open-File Report 549, scale 1:100,000.

Sprinkel, D.A., 2010, Geology of Flaming Gorge National Recreation Area, Utah-Wyoming, *in* Sprinkel, D.A., Chidsey, T.C., Jr., and Anderson, P.B., editors, 2010, Geology of Utah's parks and monuments (3rd edition): Utah Geological Association and Bryce Canyon Natural History Association, p. 285–308.

Sprinkel, D.A., 2014, Interim geologic map of the easternmost part of the Duchesne 30′ x 60′ quadrangle, Duchesne and Wasatch Counties, Utah—year 2: Utah Geological Survey Open-File Report 634, 19 p., scale 1:100,000.

Sprinkel, D.A., in review, Interim geologic map of the Duchesne 30′ x 60′ quadrangle, Duchesne and Wasatch Counties, Utah—year 4: Utah Geological Survey Open-File Report, 2 plates, scale 1:62,500, appendix.

Sprinkel, D.A., Castaño, J.R., and Roth, G.W., 1997, Emerging plays in central Utah based on a regional geochemical, structural, and stratigraphic evaluation [abs.]: American Association of Petroleum Geologists Bulletin Annual Convention, Official Program with Abstracts, v. 6, p. A110.

Sprinkel, D.A., Doelling, H.H., Kowallis, B.J., Waanders, G., and, Kuehne, P.A., 2011a, Early results of a study of Middle Jurassic strata in the Sevier fold and thrust belt, *in* Sprinkel, D.A., Yonkee, W.A., and Chidsey, T.C., Jr., editors, The Sevier thrust belt—northern and central Utah and adjacent areas: Utah Geological Association Publication 40, p. 151–172.

Sprinkel, D.A., Doelling, H.H., Waanders, G., and Kowallis, B.J., in preparation, Stratigraphy, correlation, and paleogeography of Middle Jurassic (Bajocian to Callovian) formations in Utah: Utah Geological Survey Bulletin.

Sprinkel, D.A., Kowallis, B.J., and Jensen, P.H., 2011b, Correlation and age of the Nugget Sandstone and Glen Canyon Group, Utah, *in* Sprinkel, D.A., Yonkee, W.A., and Chidsey, T.C., Jr., editors, The Sevier thrust belt—northern and central Utah and adjacent areas: Utah Geological Association Publication 40, p. 131–149.

Sprinkel, D.A., Madsen, S.K., Kirkland, J.I., Waanders, G., and Hunt, G.J., 2012, Cedar Mountain and Dakota Formations around Dinosaur National Monument—evidence of the first incursion of the Cretaceous Western Interior Seaway into Utah: Utah Geological Survey Special Study 143, 20 p.

Stancel, S.G., Cuzella, J.J., MacMillan, L., and Ragas, A., 2008, Controls on gas production along the southern flank of greater Natural Buttes field—a case study of the Love area, Uinta Basin, Utah, *in* Longman, M.W., and Morgan, C.D., editors, Hydrocarbon systems and production in the Uinta Basin, Utah: Rocky Mountain Association of Geologists and Utah Geological Association Publication 37, p 237–266.

Stanton, R.G., 1976, The paleoenvironment of the Summerville Formation on the west side of the San Rafael Swell, Emery County, Utah: Brigham Young University Geology Studies, v. 23, pt. 1, p. 37–73.

Stearns, D.W., and Friedman, M., 1972, Reservoirs in fractured rocks, *in* King, R.E., editor, Stratigraphic oil and gas fields—classification, exploration methods, and case histories: American Association of Petroleum Geologists Memoir 16, p. 82–106.

Stoddard, T., and McLennan, J., 2015, Chapter 12—log evaluation, *in* Ressetar, R., and Birgenheier, L.P., editors, Cretaceous Mancos Shale, Uinta Basin, Utah—resource potential and best practices for an emerging shale gas play: Unpublished Utah Geological Survey contract deliverable prepared for the Research Partnership to Secure Energy for America, award no. 09122-07, p. 12.1–12.55.

Stone, D.S., 1977, Tectonic history of the Uncompahgre uplift, *in* Veal, H.K., editor, Exploration frontiers of the central and southern Rockies: Rocky Mountain Association of Geologists Guidebook, p. 23–30.

Stone, D.S., 1986, Rangely field summary 2—seismic profile, structural cross section, and geochemical comparisons, *in* Stone, D.S., editor, New interpretations of northwest Colorado geology: Rocky Mountain Association of Geologists Guidebook, p. 226–228.

Stone, D.S., 1993, Tectonic evolution of the Uinta Mountains—palinspastic restoration of a structural cross section along longitude 109° 15′, Utah: Utah Geological Survey Miscellaneous Publication 93-8, 19 p., 3 plates.

Sweeny, J.J., Burnham, A.K., and Braun, R.L., 1987, A model of hydrocarbon generation from type I kerogen—application to Uinta Basin, Utah: American Association of Petroleum Geologists Bulletin, v. 71, no. 8, p. 967–985.

Tänavsuu-Milkeviciene, K., and Sarg, F.J., 2012, Evolution of an organic-rich lake basin—stratigraphy, climate and tectonics—Piceance Creek basin, Eocene Green River Formation: Sedimentology, v. 59, no. 6, p. 1735–1768.

TerraTek, Inc., 1998, Advanced fracture modeling in the Uinta Basin (Utah) for optimized primary and secondary recovery—final report: U.S. Department of Energy, DOE/PC/91008-21, 39 p.

Tiab, D., and Donaldson, E.C., 2011, Petrophysics—theory and practice of measuring reservoir rock and fluid transport properties: Gulf Professional Publishing (3rd edition), 976 p.

Toms, L.C., 2014, Spatial and temporal variations in lacustrine depositional controls from the middle to upper Green River Formation, central and western Uinta Basin, Utah: Salt Lake City, University of Utah, M.S. thesis, 255 p.

Töro, B., and Pratt, B.R., 2015, Characteristics and implications of sedimentary deformation features in the Green River Formation (Eocene) in Utah and Colorado, *in* Vanden Berg, M.D., Ressetar, R., and Birgenheier, L.P., 2015, editors, Geology of Utah's Uinta Basin and Uinta Mountains: Utah Geological Association Publication 44, p. 371–422.

Tripp, B.T., 2004, Gilsonite—an unusual Utah resource: Utah Geological Survey, Survey Notes, v. 36, no. 3, p. 1–3.

Uintah County, 2016, Uintah County, Utah, Rules Chapter 17.140—produced water disposal facilities and evaporation ponds: Online, https://www.municode.com/library/ut/uintah_county/codes/code_of_ordinances?nodeId=TIT17ZO_CH17.140PRWADIFAEVPO, accessed January 31, 2017.

U.S. Bureau of Land Management, 2012a, Greater Natural Buttes Final Environmental Impact Statement FES 12-8: U.S. Department of the Interior, Bureau of Land Management, 9 chapters, individually paginated, 17 appendices.

U.S. Bureau of Land Management, 2012b, Final Environmental Impact Statement—Gasco Uinta Basin Natural Gas Project: U.S. Department of the Interior, Bureau of Land Management, 5 chapters, individually paginated, 19 appendices, and project maps: Online, https://eplanning.blm.gov/epl-front-office/eplanning/legacyProjectSite.do?methodName=renderLegacyProjectSite&projectId=72548, accessed November 8, 2017.

U.S. Bureau of Land Management, 2013a, Finding of No Significant Impact (FONSI) for EOG Resources, Inc. Chapita Wells Unit Liquids Gathering System Phase 1 Project Environmental Assessment BLM-UT-G010-2012-113: U.S. Department of the Interior, Bureau of Land Management, 106 p.: Online, http://digitallibrary.utah.gov/awweb/main.jsp?flag=collection&smd=1&cl=all_lib&lb_document_id=75104&tm=1510167240387, accessed November 8, 2017.

U.S. Bureau of Land Management, 2013b, XTO Energy's River Bend Unit Infill Development Environmental Assessment and Biological Assessment EA Number UT-080-07-772: U.S. Department of the Interior, Bureau of Land Management, 7 chapters, individually paginated, 15 appendices: Online, http://digitallibrary.utah.gov/awweb/guest.jsp?smd=1&cl=all_lib&lb_document_id=75106, accessed November 8, 2017.

U.S. Bureau of Land Management, 2016, Newfield Exploration Corporation Monument Butte Oil and Gas Development Project in Uintah and Duchesne Counties, Utah, Final Environmental Impact Statement UT-G010-2009-0217: U.S. Department of the Interior, Bureau of Land Management, 7 chapters, individually paginated, 9 appendices.

U.S. Environmental Protection Agency, 2004, Evaluation of impacts to underground sources of drinking water by hydraulic fracturing of coalbed methane reservoirs: Environmental Protection Agency, Attachment 4, 10 p.

U.S. Environmental Protection Agency, 2008, An assessment of the environmental implications of oil and gas production—a regional case study, EPA Region 8: U.S. Environmental Protection Agency Sector Strategies Working Draft Report, 4 chapters, 5 appendices, individually paginated.

U.S. Environmental Protection Agency, 2015, U.S. Environmental Protection Agency water –total maximum daily loads (303d): Online, http://water.epa.gov/lawsregs/lawsguidance/cwa/tmdl/index.cfm, accessed April 1, 2015.

U.S. Geological Survey, 2009, Ground water atlas of the United States, chapter C, Colorado Plateaus aquifers: Online,

http://pubs.usgs.gov/ha/ha730/pub/ch_c/C-text.ascii, accessed August 2015.

U.S. Geological Survey, 2014, National Water Information System database: Online, http://waterdata.usgs.gov/nwis, accessed May 14, 2014.

U.S. Geological Survey Oil Shale Assessment Team, 2010a, Oil shale and nahcolite resources of the Piceance Basin, Colorado: U.S. Geological Survey Digital Data Series DDS–69–Y, 7 chapters, pages variable.

U.S. Geological Survey Oil Shale Assessment Team, 2010b, Oil shale resources of the Uinta Basin, Utah and Colorado: U.S. Geological Survey Digital Data Series DDS–69–BB, 7 chapters, pages variable.

Utah Department of Environmental Quality, 2015a, Division of Water Quality, Ground Water Protection Program: Online, http://www.deq.utah.gov/ProgramsServices/programs/water/groundwater/classes.htm, accessed April 1, 2015.

Utah Department of Environmental Quality, 2015b, Division of Water Quality, Water Management Program: Online, http://www.deq.utah.gov/ProgramsServices/programs/water/watersheds/approvedtmdls.htm, accessed April 1, 2015.

Utah Division of Oil, Gas and Mining, 2014, DOGM Live Data website: Online, http://oilgas.ogm.utah.gov/Data_Center/LiveData_Search/well_data_lookup.cfm, accessed March 15, 2014.

Utah Division of Oil, Gas and Mining, 2015, Data research center: Online, http://oilgas.ogm.utah.gov/Data_Center/DataCenter.cfm, accessed July 2015.

Utah Division of Oil, Gas and Mining, 2016a, Oil and gas summary production report by county, December 2015: Online, https://oilgas.ogm.utah.gov/oilgasweb/publications/monthly-rpts-by-cnty.xhtml, accessed March 2016.

Utah Division of Oil, Gas and Mining, 2016b, Application for permits to drill (APD)—by county: Online, http://oilgas.ogm.utah.gov/Statistics/APD_county.cfm, accessed March 2016.

Utah Division of Oil, Gas and Mining, 2016c, Oil and gas summary production report by field, December 2015: Online, https://oilgas.ogm.utah.gov/oilgasweb/publications/monthly-rpts-by-fld.xhtml, accessed March 2016.

Utah Division of Oil, Gas and Mining, 2016d, Oil and gas summary production report by well, December 2015: Online, https://oilgas.ogm.utah.gov/oilgasweb/publications/monthly-rpts-by-well.xhtml, accessed March 2016.

Utah Division of Water Resources, 2005, Water reuse in Utah: Utah Division of Water Resources Report as part of the Utah State Water Plan: Online, https://water.utah.gov/OtherReports/WaterReuse/WaterReuseAA.pdf, accessed November 8, 2017.

Vaill, J.E., and Butler, D.L., 1999, Streamflow and dissolved-solids trends through 1996, in the Upper Colorado River Basin upstream from Lake Powell—Colorado, Utah, and Wyoming: U.S. Geological Survey Water Resources Investigations Report 99-4097, 47 p.

Vanden Berg, M.D., 2008, Basin-wide evaluation of the uppermost Green River Formation's oil-shale resource, Uinta Basin, Utah and Colorado: Utah Geological Survey Special Study 128, 22 p.

Vanden Berg, M.D., 2011, Exploring Utah's other great lake: Utah Geological Survey, Survey Notes, v. 43, no. 2, p. 1–2.

Vanden Berg, M.D., and Birgenheier, L.P., 2017, An examination of the hypersaline phases of Eocene Lake Uinta, upper Green River Formation, Uinta Basin, Utah: Journal of Paleolimnology, DOI 10.1007/s10933-017-9983-x, p. 1-19.

Vanden Berg, M.D., Lehle, D.R., Carney, S.M., and Morgan, C.D., 2013, Geological characterization of the Birds Nest aquifer, Uinta Basin, Utah—assessment of the aquifer's potential as a saline water disposal zone: Utah Geological Survey Special Study 147, 53 p.

Vanden Berg, M.D., Wood, R.E., Carney, S.M., and Morgan, C.D., 2014, Geological characterization of the Uteland Butte Member of the Eocene Green River Formation—an emerging unconventional carbonate tight oil play in the Uinta Basin, Utah [abs.]: American Association of Petroleum Geologists, Rocky Mountain Section, p. 46–47.

Veolia Water Solutions and Technologies, North America, 2014, ROSS™ Technology—Frac flowback and produced water treatment: Online, http://www.veoliawatertech.com/news-resources/datasheets/ross-flowback-produced-water.htm, accessed November 8, 2017.

Verbeek, E.R., and Grout, M.A., 1993, Geometry and structural evolution of gilsonite dikes in the eastern Uinta Basin, Utah, *in* Evolution of sedimentary basins—Uinta and Piceance Basins: U.S. Geological Survey Bulletin 1787-X, 42 p.

Wallace, J., 2012, Baseline water quality and quantity for selected sites in the southeastern Uinta Basin, Utah: Utah Geological Survey Open-File Report 595, 70 p.

Wallace, J., 2015, Groundwater chemistry for shallow alluvial wells and springs in the Uinta Basin, Utah, *in* Vanden Berg, M.D., Ressetar, R., and Birgenheier, L.P., editors, Geology of Utah's Uinta Basin and Uinta Mountains: Utah Geological Association Publication 44, p. 171–188.

Wallace, J., Payne, N., and Emerson, R., 2015, Sensitivity and vulnerability of the aquifers and springs in the Uinta Basin, Utah, to potential contamination associated with energy resource development, *in* Vanden Berg, M.D., Ressetar, R., and Birgenheier, L.P., editors, Geology of Utah's Uinta Basin and Uinta Mountains: Utah Geological Association Publication 44, p. 189–206.

Wanty, R.B., Pitman, J.K., and Fouch, T.D., 1991, Ground¬water chemistry and diagenetic reactions in

Tertiary sandstone of the Green River and Wasatch Formations, Uinta Basin, Utah, *in* Evolution of sedimentary basins—Uinta and Piceance Basins: U.S. Geological Survey Bulletin 1787-X, 21 p.

Weiss, M.P., Witkind I.J., and Cashion W.B., 1990, Geologic map of the Price 30′ x 60′ quadrangle, Carbon, Duchesne, Uintah, Utah, and Wasatch Counties, Utah: U.S. Geological Survey Miscellaneous Investigations Series Map I-1981, scale 1:100,000.

Weiss, M.P., Witkind I.J., and Cashion W.B., 2003, Geologic map of the Price 30′ x 60′ quadrangle, Carbon, Duchesne, Uintah, Utah, and Wasatch Counties, Utah: Utah Geological Survey Open-File Report 198DM (digitized from U.S. Geological Survey Miscellaneous Investigations Series Map I-1981 [1990]), scale 1:100,000.

Wernicke, B., 2011, The California River and its role in carving Grand Canyon: Geological Society of America Bulletin, v. 123, p. 1288–1316.

Western Energy Alliance, 2014, Oil and natural gas exploration and production water sources and demand study—Colorado, Montana, New Mexico, North Dakota, Utah, and Wyoming: Western Energy Alliance report 1302226 prepared by Golder and Associates, 56 p.

White, H., Cole, R., Stancel, S., Lee, C., and MacMillan, L., 2008, "Window" outcrop analogues for Greater Natural Buttes field, Uinta Basin, Utah, *in* Longman, M.W., and Morgan, C.D., editors, Hydrocarbon systems and production in the Uinta Basin, Utah: Rocky Mountain Association of Geologists and Utah Geological Association Publication 37, p. 209–236.

Wilcox, W.T., 2007, Sequence stratigraphy of the Curtis, Summerville, and Stump Formations, Utah and northwest Colorado: Oxford, Miami University (Ohio), M.S. thesis, 108 p.

Willis, G.C., and Biek, R.F., 2001, Quaternary incision rates of the Colorado River and major tributaries in the Colorado Plateau, Utah, *in* Young, R.A., and Spamer, E.E., editors, Colorado River—origin and evolution—proceedings of a symposium held at Grand Canyon National Park in June 2000: Grand Canyon Association, p. 119–123.

Witkind, I.J., 1979, Reconnaissance geologic map of the Wellington quadrangle, Carbon County, Utah: U.S. Geological Survey Miscellaneous Investigations Series Map I-1178, scale 1:24,000.

Witkind, I.J., 1980, Reconnaissance geologic map of the Mounds quadrangle, Carbon and Emery Counties, Utah: U.S. Geological Survey Miscellaneous Investigations Series Map I-1202, scale 1:24,000.

Witkind, I.J., 1988, Geologic map of the Huntington 30′ x 60′ quadrangle, Carbon, Emery, Grand, and Uintah Counties, Utah: U.S. Geological Survey Miscellaneous Investigations Series Map I-1764, scale 1:100,000.

Witkind, I.J., 2004, Geologic map of the Huntington 30′ x 60′ quadrangle, Carbon, Emery, Grand, and Uintah Counties, Utah: Utah Geological Survey Open-File Report 440DM (digitized from U.S. Geological Survey Miscellaneous Investigations Series Map I-1764 [1988]), scale 1:100,000.

Witkind, I.J., and Weiss, M.P., 1991, Geologic map of the Nephi 30′ x 60′ quadrangle, Carbon, Emery, Juab, Sanpete, Utah, and Wasatch Counties, Utah: U.S. Geological Survey Map I-1937, scale 1:100,000.

Witkind, I.J., and Weiss, M.P., 2002, Geologic map of the Nephi 30′ x 60′ quadrangle, Carbon, Emery, Juab, Sanpete, Utah, and Wasatch Counties, Utah: Utah Geological Survey Map M-189DM (digitized from U.S. Geological Survey Map I-1937 [1991]), scale 1:100,000.

Witkind, I.J., Weiss, M.P., and Brown, T.L., 1987, Geologic map of the Manti 30′ x 60′ quadrangle, Carbon, Emery, Juab, Sanpete, and Sevier Counties, Utah: U.S. Geological Survey Map I-1631, scale 1:100,000.

Witkind, I.J., Weiss, M.P., and Brown, T.L., 2007, Geologic map of the Manti 30′ x 60′ quadrangle, Carbon, Emery, Juab, Sanpete, and Sevier Counties, Utah: Utah Geological Survey Map M-212DM (digitized from U.S. Geological Survey Map I-1631 [1987]), scale 1:100,000.

Wood, L.J., and Dutton, S.P., 1999, Sequence stratigra¬phy and reservoir architecture of tide-influenced shoreline systems in the Late Cretaceous Sego Sandstone: Texas Bureau of Economic Geology, Clastic Reservoirs Group Field Trip Guidebook, 132 p.

Wood, R.E., and Chidsey, T.C., Jr., 2015, Oil and gas fields map of Utah: Utah Geological Survey Circular 119, scale 1:700,000.

Wyllie, M.R., Gregory, A.R., and Gardner, G.H.F., 1958, An experimental investigation of the factors affecting elastic wave velocities in porous media: Geophysics, v. 23, p. 459–493.

Yingling, V.L., 1987, Timing and initiation of the Sevier orogeny—Morrison and Cedar Mountain Formations and Dakota Sandstone, east-central Utah: Laramie, University of Wyoming, M.S. thesis, 169 p.

Young, R.G., 1955, Sedimentary facies and intertonguing in the Upper Cretaceous of the Book Cliffs, Utah-Colorado: Geological Society of America Bulletin, v. 66, no. 2, p. 177–202.

Young, R.G., 1973, Depositional environments of basal Cretaceous rocks of the Colorado Plateau, *in* Fassett, J.E., editor, Cretaceous and Tertiary rocks of the southern Colorado Plateau: Four Corners Geological Society Memoir, p. 10–27.

Young, R.A., and Spamer, E.E., editors, 2001, Colorado River—origin and evolution: Grand Canyon Association, symposium volume, 280 p.

Zhang, Y., Gable, C.W., Zyvoloski, G.A., and Walter, L.M., 2009, Hydrogeochemistry and gas compositions of the Uinta Basin—a regional-scale overview: American Association of Petroleum Geologists Bulletin, v. 93, no. 8, p. 1087–1118.

UTAH GEOLOGICAL SURVEY
a division of
Utah Department of Natural Resources

Plate 1
Utah Geological Survey Bulletin 138
Produced Water in the Uinta Basin, Utah: Evaluation of Reservoirs, Water Storage Aquifers, and Management Options

GEOLOGIC UNIT EXPLANATION

QUATERNARY

- Qh — Artificial fill/disturbed
- Qm — Mass wasting deposits
- Qp — Pediment mantle deposits
- Qe — Eolian deposits
- Qg — Gravel deposits
- Qt — Talus deposits
- Qs — Spring/tufa deposits
- Qa — Alluvial deposits
- Qc — Colluvium

QUATERNARY-TERTIARY

- QTa — Older alluvial deposits
- QTp — Older pediment mantle deposits

TERTIARY

- Tv — Tertiary volcanics – undifferentiated
- Tud — Uinta and Duchesne Formations – undifferentiated
- Tgr — Green River Formation
- Twc — Wasatch/Colton Formation
- Tfnc — Flagstaff, North Horn, and Currant Creek Formations – undifferentiated
- T — Tertiary rocks – undifferentiated

CRETACEOUS

- Kmv — Mesaverde Group
- Km — Mancos Shale
- Kmd — Mancos Shale and Dakota Formation – undifferentiated
- Kdcm — Dakota, Burro Canyon, and Cedar Mountain Formations – undifferentiated
- KJcm — Cedar Mountain and Morrison Formations – undifferentiated

JURASSIC

- Jm — Morrison Formation
- Jms — Morrison and Summerville Formations – undifferentiated
- Jscp — Summerville, Curtis/Stump, and Preuss Formations – undifferentiated
- Jcec — Curtis/Stump, Entrada and Carmel Formations – undifferentiated
- Je — Entrada Sandstone
- Ja — Arapien Formation
- Jc — Carmel Formation
- Jn — Navajo Sandstone
- JTrn — Nugget Sandstone
- JTrgc — Glen Canyon Group

TRIASSIC

- Tr — Triassic formations – undifferentiated

PERMIAN, PENNSYLVANIAN, MISSISSIPPIAN

- PPw — Weber Sandstone
- PP — Permian and Pennsylvanian rocks – undifferentiated
- PM — Pennsylvanian and Mississippian rocks – undifferentiated

CAMBRIAN-PRECAMBRIAN

- C — Cambrian rocks – undifferentiated
- Z — Proterozoic and Archean rocks – undifferentiated

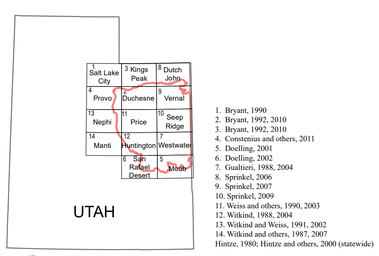

Uinta Basin study area

1:100,000 geology source maps

1. Bryant, 1990
2. Bryant, 1992, 2010
3. Bryant, 1992, 2010
4. Constenius and others, 2011
5. Doelling, 2001
6. Doelling, 2002
7. Gualtieri, 1988, 2004
8. Sprinkel, 2006
9. Sprinkel, 2007
10. Sprinkel, 2009
11. Weiss and others, 1990, 2003
12. Witkind, 1988, 2004
13. Witkind and Weiss, 1991, 2002
14. Witkind and others, 1987, 2007
Hintze, 1980; Hintze and others, 2000 (statewide)

SCALE 1:250,000

5 0 10 MILES

10 0 20 KILOMETERS

Compiled Geologic Map of the Uinta Basin, Utah

UTAH GEOLOGICAL SURVEY
a division of
Utah Department of Natural Resources

Plate 2
Utah Geological Survey Bulletin 138
Produced Water in the Uinta Basin, Utah: Evaluation of Reservoirs, Water Storage Aquifers, and Management Options

A – WEST

Plate 2: West-to-East Cross Section of the Wasatch/Colton Formation and the Mesaverde Group

EAST – A'

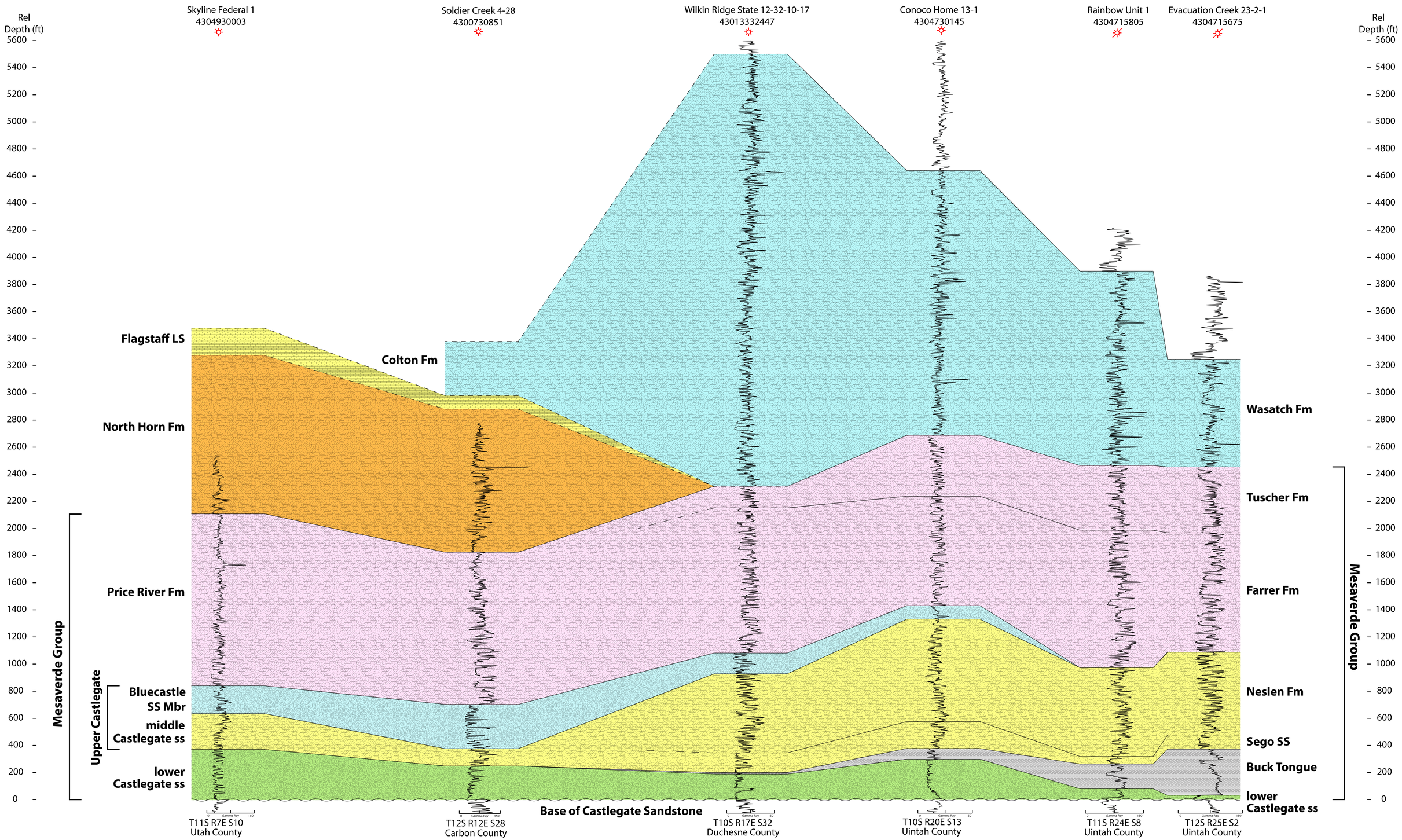

UTAH GEOLOGICAL SURVEY
a division of
Utah Department of Natural Resources

Plate 3
Utah Geological Survey Bulletin 138
Produced Water in the Uinta Basin, Utah: Evaluation of Reservoirs, Water Storage Aquifers, and Management Options

B – NORTH

Plate 3: North-to-South Cross Section of the Wasatch/Colton Formation and the Mesaverde Group

SOUTH – B'

Yellowstone River 1
4301330047

Ute Tribal Kmv 1-28
4301332368

Wilkin Ridge State
12-32-10-17
4301332447

Peters Point Unit
FE 15-6D-13-17
4300731261

Wolf Flat 14C-29-15-19
4304737541

Rattlesnake Canyon 2-12
4301930809

Rel Depth (ft)

5500 5350 5200 5050 4900 4750 4600 4450 4300 4150 4000 3850 3700 3550 3400 3250 3100 2950 2800 2650 2500 2350 2200 2050 1900 1750 1600 1450 1300 1150 1000 850 700 550 400 250 100 0

Colton Fm

Flagstaff LS

North Horn Fm

Price River Fm

Mesaverde Group

Upper Castlegate

Bluecastle SS Mbr

middle Castlegate ss

lower Castlegate ss

Base of Castlegate Sandstone

Wasatch Fm

Tuscher Fm

Farrer Fm

Bluecastle SS Mbr

Neslen Fm

Sego SS

Buck Tongue

lower Castlegate ss

Mesaverde Group

Gamma Ray 0 150

T1N R4W S17
Duchesne County

T4S R3W S28
Duchesne County

T10S R17E S32
Duchesne County

T13S R17E S6
Carbon County

T15S R19E S29
Uintah County

T19S R19E S2
Grand County